NASA Technical Memorandum 79191

30-Centimeter Ion Thrust Subsystem Design Manual

Lewis Research Center

June 1979

NASA

NASA Technical Memorandum 79191

30-Centimeter Ion Thrust Subsystem Design Manual

Lewis Research Center
Cleveland, Ohio

1979

FOREWORD

This publication describes the principal characteristics of the 30-centimeter ion propulsion thrust subsystem and will serve as an aid to solar electric propulsion vehicle designers and users of electric propulsion.

The thrust subsystem defined by this publication was used to focus the thrust subsystem technology program performed for the NASA Office of Aeronautics and Space Technology by the NASA Lewis Research Center.

The document contains functional requirements and descriptions, interface and performance requirements, and physical characteristics of the hardware at both the subsystem and component level.

The contributing authors to this document are:

Robert R. Lovell	Louis Gedeon	Jon C. Oglebay
William H. Hawersaat	Suzanne T. Gooder	Karl F. Reader
James E. Cake	Joseph A. Hemminger	David D. Renz
James F. DePauw	Louis R. Ignaczak	Ronald R. Robson
Edward J. Domino	Edward F. Kramer	Neil D. Rowe
George R. Smolak	Richard J. Krawczyk	Frances J. Shaker
Clifford H. Arth	Erich W. Kroeger	G. Richard Sharp
Robert T. Bechtel	Walter C. Lathem	Clifford E. Siegert
David H. Culp	Joseph E. Maloy	Ralph J. Zavesky
Robert J. Frye		

CONTENTS

		Page
1.0	Introduction	1-1
2.0	Solar Electric Propulsion System Technology Perspective and Design Criteria	2-1
3.0	Thrust Subsystem	3-1
4.0	BIMOD Engine System	4-1
5.0	Thruster	5-1
6.0	Power Processor	6-1
7.0	Gimbals	7-1
8.0	Heat Pipes	8-1
9.0	BIMOD Structure/Thermal Control	9-1
10.0	Interface Module	10-1
11.0	Thruster Controller	11-1
12.0	Power Distribution	12-1
13.0	Propellant Storage and Distribution	13-1
14.0	Interface Module Structure/Thermal Control	14-1

1.0

INTRODUCTION

1.0 Introduction

The 30 cm mercury ion thrust subsystem technology has been developed to provide the low thrust, high specific impulse propulsion capability to satisfy the needs of future planetary and Earth orbital missions. This publication provides a comprehensive description of the thrust subsystem design, hardware, and software that has been developed. The technology program has been sponsored by the NASA Office of Aeronautics and Space Technology and has been conducted at the NASA Lewis Research Center. This document is intended to provide solar electric propulsion (SEP) vehicle designers and users of electric propulsion a complete description of the technology program efforts.

Section 2.0 of the manual provides a perspective of the solar electric propulsion technology and defines the thrust subsystem configuration that has been used to define configuration dependent requirements for the technology elements. These elements include thrusters, power processors, propellant storage and distribution, thruster gimbal system, and thermal control subsystem. Section 2.0 also presents the SEP vehicle design criteria which are applicable to the specific thrust subsystem design.

The organization of the design manual is consistent with the physical architecture of the thrust subsystem. As discussed in Section 2.0, the thrust subsystem comprises BIMOD engine systems and an interface module. The design manual sections have been arranged in a three level tier. Section 3.0, Thrust Subsystem, presents the requirements at the thrust subsystem level. At the subassembly level, the requirements for the BIMOD engine system are stated in Section 4.0 and the requirements for the interface module are stated in Section 10.0. At the component level, Sections 5.0 through 9.0 describe the requirements of the BIMOD elements. Sections 11.0 through 14.0 describe the requirements of the interface module elements.

Each section from 3.0 through 14.0 describes the subject functional requirements, functional description, interface requirements, performance requirements, physical characteristics, development history, and ground support equipment. The design manual thus provides a hierarchy of functional, interface, and performance requirements from the thrust subsystem level to the component level.

For convenience in using this manual, a table of contents and lists of tables and figures are included at the beginning of each section from 2.0 through 14.0.

A wealth of documentation has been produced during the course of the technology program. These include formal NASA publications, contractor final reports, contractor briefing packages, design drawings, software flow charts and programs, and internal memoranda. For the design manual these documents have been placed in two categories. Those documents which are referenced in the text and available for distribution are listed in the subsection Reference Documents of each section. Those documents, such as internal memoranda, drawing packages, and contractor briefing packages are listed in the subsection Applicable Documents Enclosed of each section.

There are four supplements to this design manual which are associated with the applicable documents. The Index Supplement of Applicable Documents contains a listing of all applicable document titles referenced in the design manual and instructions for retrieval of the documents from the other three supplements. The Microfiche Reference Supplement contains those applicable documents suitable for reproduction on microfiche cards. The Microfilm Drawing Supplement contains card framed microfilm design drawings. The Photograph Supplement contains photograph collections.

2.0

SOLAR ELECTRIC PROPULSION

SYSTEM TECHNOLOGY PERSPECTIVE

AND DESIGN CRITERIA

Table of Contents

		Page
2.0	Solar Electric Propulsion System Technology Perspective and Design Criteria	2-3
2.1	Overview	2-4
2.2	Perspective	2-5
2.2.1	Early Research and Facility Development	2-5
2.2.2	SERT I	2-5
2.2.3	SERT II	2-6
2.2.4	The Technology Refinement Phase	2-6
2.2.4.1	Auxiliary Propulsion	2-7
2.2.4.2	Primary Propulsion	2-8
2.2.5	Focused Technology Program	2-9
2.3	Vehicle Level Design Criteria	2-10
2.3.1	Solar Array/Vehicle Articulation	2-11
2.3.2	Structure	2-12
2.3.3	Center of Pressure/Center of Mass Control	2-13
2.3.4	Heavy Component Locations	2-14
2.3.5	Thruster Locations	2-15
2.3.6	Thermal Radiator Location	2-16
2.3.7	Thermal Radiator Area	2-17
2.4	System Features	2-18
2.4.1	Simple Interfaces	2-18
2.4.2	Separate Technologies	2-19
2.4.3	Mission Flexibility	2-19

		Page
2.4.4	Technological Flexibility	2-20
2.5	SEP Focused Technology Program Progress	2-20
2.6	Reference Documents	2-21

FIGURES

2.3-1	Typical Electric Propelled Space Vehicle	2-23
2.3.2	Mariner Encke Spacecraft	2-24
2.3.2-1	SEP Launch Sequence	2-25
2.4-1	SEP Vehicle Major Subsystems	2-26
2.4.3-1	Modularity of Thrust Subsystem	2-27
2.4.3-2	Thrust Subsystem Configurations	2-28
2.4.4-1	Power Processor Modularity	2-29

2.0 Solar Electric Propulsion System Technology Perspective and Design Criteria

2.1 Overview

The information contained in this design manual is intended to facilitate the transfer of electric propulsion technology from the Lewis Research Center to NASA mission centers, industry and potential user agencies. Industrial briefings, workshops and on-site training programs may be required to complete the technology transfer as NASA moves from the research and development phase to the application of electric propulsion technology. NASA OAST and the LeRC are planning to provide the additional necessary support as required to insure the transfer process.

It is crucial that industry, who are to be the manufacturers of the systems employing this technology, be given access to all of the details of the technology. It is also important that the responsible NASA mission centers and the user agencies be given enough of an understanding of the technology so that they can effectively manage it and integrate it into their systems.

The information contained in this design manual is directed toward industry. The manual contains a collection of the latest available documents pertaining to primary electric propulsion within NASA. The documents include heretofore

unpublished design notes, analysis, computer codes, drawings, parts lists, manufacturing and process specifications, photographs, assembly and test procedures, operational software, facility requirements, test plans, test data, and general design information that will enable industry to build this technology into an operational system with known and acceptable risk.

The information contained in this manual was collected and prepared by members of the staff at the LeRC who have been involved in electric propulsion as a team for 20 years.

It is difficult to document the technology that exists in this team as a result of their combined experiences. The next section on perspective is intended to give the reader a chronological overview of the electric propulsion activity in NASA that lead to the currently focused technology program that is described in this design manual. The next section is also intended to give the reader an appreciation for the experience inherent in the Lewis team. In subsequent sections that give requirements, design criteria, and specific designs, there are often no references available. Over the past ten years, a close working relationship has developed between members of the staff of JPL and LeRC. As a result, many of the requirements and

design choices had the benefit of inputs from the user-oriented JPL team and the technology-oriented LeRC team. When the detail design choices were made on the hardware produced in this program, the previous flight experience gained by the LeRC staff were applied. And again many informal discussions were held between members of the staff of JPL and LeRC. Some of these design trade offs may not be well documented in the open literature. The reader is urged to consider the current design carefully before concluding that a design choice might have been non-consequential, arbitrary, or capricious.

2.2 Perspective

2.2.1 Early Research and Facility Development

In 1959, the first electron-bombardment thruster was conceived and tested by members of the staff of the LeRC (reference 2.6.1). In the early 1960's, several facilities were brought on line and the Electric Propulsion Laboratory (EPL) was dedicated to support research and development of electric propulsion (reference 2.6.2).

2.2.2 SERT I

In July 1964, SERT I was launched into a 50 minute ballistic trajectory out of Wallops Island. This spacecraft successfully demonstrated the ability of a mercury electron-bombardment thruster to produce thrust and to neutralize the exhaust beam in the space environment (reference 2.6.3

and 2.6.4). SERT I provided those involved with a great respect for the problems of handling high voltage at high power in the space and vacuum facility environment and the testing of spacecraft utilizing electric propulsion.

2.2.3 SERT II

In February 1970, SERT II was launched into a circular polar orbit. This spacecraft remains operational as of this writing. This spacecraft which was developed, tested, and flown by members of the Lewis staff demonstrated thruster life and provided information on thruster/spacecraft systems interactions. In terms of technology, the SERT II flight provided those involved with an understanding of the systems problems associated with integrating electric propulsion into spacecraft and qualifying it for a space flight (reference 2.6.5). Again, a great respect was gained for producing and handling high voltage at high power levels in the vacuum/plasma environment and the unique testing requirements of electric propulsion.

2.2.4 The Technology Refinement Phase

After the SERT II flight, research and development activities at LeRC proceeded to refine the basic concepts of thrusters and began to concentrate on the required supporting technologies required to firmly establish the technology at the system level. While this basic refinement continues today, there was a growing awareness of the need

to gain user acceptance and technology adoption in the early 70's. As a result, the electric propulsion program was divided into two major parts based on the anticipated use of the technology.

2.2.4.1 Auxiliary Propulsion

There was a perceived need for precision station keeping and attitude control of communication and navigation satellites operating at synchronous orbit. A number of studies had been performed showing the advantages of electric propulsion to perform these functions (reference 2.6.6). The 8cm electron bombardment thruster and its associated propulsion system elements were developed specifically to perform the auxiliary propulsion function. The basic research portion of this program concentrated on thruster life and restart capability to enable 10 year station keeping missions.

User adoption of the 8cm propulsion system has remained elusive. As a final attempt to transfer the 8cm technology, NASA is sponsoring the flight test of a complete auxiliary propulsion system on an Air Force (STP P80-1) flight in early 1981 (reference 2.6.7). A fundamental objective associated with this flight is to have an industrial source for this technology at the conclusion of the flight test. The technology associated with this flight test is not

described in detail in this design manual, because it is covered adequately in the published literature. Although the technology required to develop an operational auxiliary propulsion system is less demanding (low power, low efficiency) for both the thruster and power processors, there are a large number of common elements with the primary propulsion and the reader is urged to study the 8cm literature carefully.

There is a great deal of commonality between many of the ancillary supporting systems for both the primary and auxiliary propulsion programs.

2.2.4.2 Primary Propulsion

The 30cm electron bombardment thrusters and its associated propulsion system elements described in this design manual were developed specifically to support the anticipated requirements of both planetary science and Earth orbital transportation users.

After SERT II, mission planners at JPL began to seriously consider SEP as a candidate propulsion system to perform some of their science missions. Design teams led by Gerpheide and Duxbury of JPL performed the first vehicle level design studies and generated specific propulsion system requirements. At this same time, mission planners at MSFC were considering SEP as a candidate for Earth

orbital missions. They, too, generated technology requirements. The basic technology program at Lewis attempted to satisfy these requirements as the mission planners moved from mission to mission.

In 1973, OAST established a SEP Advanced System Technology (AST) group to coordinate the requirements for primary electric propulsion and focus the technology program. Members of the staff from LeRC, MSFC, and JPL established the common system level design requirements that were to become the basis for the technology program described in this design manual. Before the AST program produced a formalized output, NASA made a decision to reduce the effort in electric propulsion. In 1974, almost all thrust subsystem work was stopped at JPL and MSFC and the basic thrust subsystem technology effort was concentrated at the LeRC.

2.2.5 Focused Technology Program

Until 1974, the primary propulsion technology program at LeRC had concentrated on components. Like the auxiliary propulsion program, the principal emphasis was on the thruster. The thruster technology was aimed at increasing the life and efficiency. The power processing technology was concentrating on reducing weight and increasing efficiency.

Without a clear mission in sight and with total program resources reduced, OAST and LeRC agreed that they would structure a focused technology program aimed at being technology ready for the user Centers in 1979. This program was to look at all of the elements in a thrust subsystem as defined in 3.0. The supporting components were to be developed around the so-called baseline 30cm thruster. Decisions were to be made as to a specific power processor type and thermal control approach, and the elements were to be integrated into the smallest optimum building block above the thruster level. The BIMOD engine system described in 4.0 resulted. As the technology ready program matured, the technology ready date was moved to the end of FY 1980.

The decision to focus the technology ready program around the BIMOD engine system was not apparent at the inception of the program. The attributes of such an approach became apparent as the design alternatives and programmatic advantages were explored. The next sections discuss the vehicle level requirements and system features of the concept.

2.3 Vehicle Level Design Criteria

Why are the thrusters here? Why are the power processors there? Why are the radiators so long? What goes in this

big empty space? These are questions that are asked by almost everyone when they first see the engine system described in section 3.0. The answers to these questions lie in an understanding of the top level vehicle design requirements described below.

The dominant feature of a SEP vehicle is the solar array. Based on packing density of 100 watts per m^2 and an aspect ratio of five to one, then a single wing of a two wing 25Kw array has the dimensions of 5 meters by 25 meters. The vehicle center body on the other hand is typically less than 2 meters in width. Figure 2.3-1 shows the basic vehicle configuration assumed for these studies. When compared with the Mariner Encke Spacecraft proposed by Duxbury in figure 2.3-2, it can be seen that the basic configuration has remained essentially unchanged after innumerable studies of alternate concepts (reference 2.6.8). If we examine these designs, the top level configuration requirements become apparent.

2.3.1 Solar Array/Vehicle Articulation

Requirement: A rotating joint shall be provided through the vehicle center body to provide solar array articulation about the longitudinal axis of each solar array wing.

It can be shown that a single degree of freedom between

the solar array and vehicle center body is necessary and sufficient to allow the solar array face to be sun tracking and to allow the thrust vector to point in any direction in inertial space. By rolling the total vehicle and articulating the solar array shaft with respect to the center body, all of the required thrust beam cone and clock angles can be achieved to perform both planetary and Earth orbital missions.

2.3.2 Structure

Requirement: The structural loads associated with the chemical boost phase of the launch sequence shall be carried in a launch tower or exoskeletal structure capable of being separated from the SEP vehicle during SEP thrusting phases of the mission.

Requirement: The SEP vehicle shall have its mass concentrated near the launch tower pick up points.

The typical launch sequence for SEP shown in figure 2.3.2-1 is: Shuttle launch to low Earth orbit, IUS burn to Earth escape, and SEP separation, deployment and low thrust burn for several years. The launch loads from the Shuttle and IUS are large compared with the micro-g's resulting from the SEP thrusters. The SEP structure need only be strong enough to support launch loads that must be carried through it during the chemical boost phase of

the mission. A launch tower or exoskeletal approach to the structural design gives a 10:1 weight advantage over an approach that carries launch loads through that portion of the structure and remains for the low thrust phase. A further weight savings is enjoyed in the SEP structure if the mass is concentrated near the adaptor tower/vehicle structure pick up points.

2.3.3 Center of Pressure/Center of Mass Control

Requirement: The center of pressure (CP) and center of mass (CM) shall be maintained coincident throughout the flight.

For SEP vehicles, the center of pressure resulting from the solar flux is essentially determined by the solar array. The relatively dense center body determines the center of mass. The center of pressure and center of mass must be coincident in order to avoid steady state disturbance torques. Steady state disturbance torques can be handled in the short run with momentum wheels. But for the typical 25Kw SEP vehicle, the NASA standard momentum wheel will saturate in less than one day for only a few centimeters of CP/CM offset about the pitch axis Planetary missions require periods of "quiet" coast which preclude operating the ion thrusters or any other mass expulsion device that would be required to unload the momentum wheels and maintain attitude control.

A number of potential solutions to this problem exist. The initial design can be controlled but this makes the design peculiar to a given payload. It also requires that the mercury propellant be stored and expended in such a fashion that no center of mass travel is experienced. The center of mass can be controlled actively by placing part of the payload on an Astromast type extension mechanism and moving it in and out to trim the center of mass position. The center of pressure can be controlled by developing reflector vanes either from the center body or from the solar arrays. A method proposed by Jim Stevens from JPL is perhaps the best method. Stevens' method is based on a variable swept wing concept that is implemented with simple flexures and a single jack screw located at the junction of the two solar array wing shafts inside the center body. Stevens' method of wing sweep allows for large variations in the initial CM position and for large CM travel due to asymmetrical consumption of expendables during the mission.

2.3.4 Heavy Component Locations

Requirement: The heavy components and especially the mercury propellant tanks shall be located as near to the location of the solar array shaft axis as possible.

This is a derived requirement from 2.3.2 and 2.3.3.

2.3.5 Thruster Locations

Requirement: The thrusters shall be located as far aft of the solar array shaft axis as possible.

There are three reasons for this requirement. The first reason is to minimize thruster gimbal requirements, the second reason is to insure clearance between the root section of the solar array and the thruster exhaust beam, and the third reason is to maximize the distance between the thrusters and the payload.

The typical outbound mission for SEPS will end up with only a sufficient amount of electrical power to operate one or two thrusters. Since, in general, the thrusters are not pointed through the center of mass when they are all operating or operating in pairs, they must be gimbaled through the center of mass if they are to be operated as singles. When one considers the practical geometry of a vehicle with as many as 10 thrusters, the gimbal angles can become quite large. Moving the thruster aft reduces the required gimbal angle.

The thruster plume is generally considered to be bound by a half cone angle of 55^{o}. When one adds the required gimbal angles mentioned above plus a small amount for attitude control, it becomes apparent that the thruster exhaust plane should be kept aft of the end of the root

section of the solar array. This amounts to 2.5 meters aft of the solar array axis for the 25Kw class vehicle.

The thrusters have inherent characteristics (e.g. EMC, magnetic moments, plume and efflux emissions) that are potentially a source of concern to science payloads. It can be stated that with the thrusters mounted as far aft as possible and with the science mounted as far forward as possible, the interactions will be minimized.

2.3.6 Thermal Radiator Location

Requirement: A sufficient amount of radiator area shall be provided normal to the sun direction to dissipate the waste heat from the SEP power processors.

Since the solar arrays are sun pointing and the arrays are connected to the vehicle center body by a single degree of freedom joint, then there are two sides of the vehicle center body that can act as radiator. They are the sides facing the root sections of the solar array wings.

The question of whether the radiator should be single sided or double sided depends on how one interprets the requirement. If, in fact, the solar arrays are maintained precisely normal to the sun throughout the mission, then a double sided radiator would have a mass advantage over a single sided radiator as proposed in this design manual. However if the vehicle pointing is not held precisely either for

convenience or for improved performance, then the single sided radiator proposed in section 3.0 has distinct functional advantages. For some engine out situations, a "slipped" or "crabbed" flight attitude provides a more optimum thrust vector. For a reacquisition maneuver, when the spacecraft is generally disoriented, at least one radiator side would be non-sun facing. This would allow thruster start up and SEP thrust vectoring for the reacquisition maneuver.

2.3.7 Thermal Radiator Area

Requirement: A sufficient amount of radiator area shall be provided to dissipate the waste heat from the power processors when the vehicle is operating over the required AU range. This is obviously a mission dependent requirement.

The radiator area is fixed by the amount of waste heat and the desired temperature of the electronic components in the power electronics. The temperature of the electronics is determined by the required system reliability, parts type and thermal control characteristics and conduction path characteristics in the electronic packaging. The actual dimensions or aspect ratio of the radiator area is not entirely an independent variable when one considers all of the constraints mentioned above. The width of the radiator can be at least as wide as the minimum center to center

distance between thrusters. This distance, in turn, is governed by the thruster/gimbal clearance requirement. Once the area and width are determined, the length is then determined. For the hardware considered in this design manual, the aspect ratio was about optimum for a 6 thruster SEP vehicle.

2.4 System Features

The top level design requirements discussed in the previous section are independent of the approach selected to develop a SEP vehicle. The requirements must be accommodated in either a highly integrated approach or in a totally modular approach.

When the technology ready program was being formulated, a number of system features were established as goals for the vehicle design point around which the technology program was to be focused. These goals, which are listed below, were based on the cultural heritage and experience of the Lewis team and on their perceptions of user needs. Figure 2.4-1 shows how the SEP vehicle was physically divided into major subsystems of spacecraft (or mission/science module or mission/payload module) thrust subsystem, and solar array. This and lower level architectural design choices were made to satisfy the following goals.

2.4.1 Simple Interfaces

The goal for the thrust subsystem defined above was to have

simple interfaces. The interfaces were to be comparable to a conventional propulsion system. Specifically, the thrust subsystem should be structurally and thermally autonomous, have a simple mechanical (bolt pattern) interface and respond electrically to simple start/stop/gimbal commands. All complex interfaces were to be internalized within their major subsystems.

2.4.2 Separate Technologies

The goal for the thrust subsystem was to separate and internalize all of those technologies peculiar to electric propulsion. This was also the goal for the other two major subsystems. By separating the technologies, the major subsystems could be developed at their own technological pace and could benefit from separate agencies and industries that had specialized expertise.

A feature of this definition of subsystems is that the thrust subsystem can be powered by alternate power sources as they become available.

2.4.3 Mission Flexibility

Figure 2.4.3-1 shows that the thrust subsystem itself is modular. The BIMOD engine system is the fundamental building block of the thrust subsystem in the focused technology program. Although the BIMOD does not have interfaces that are as simple as the thrust subsystem, it does contain most of the high technology associated with

electric propulsion. The use of the BIMOD allows for a wide selection of propulsion options. Figure 2.4.3-2 show the range of options available to satisfy various mission requirements. Still other options using a single BIMOD are obvious.

2.4.4 Technological Flexibility

Figure 2.4.4-1 shows how the modular concept was carried down to the power processor level. The experience of the Lewis team in trying to accommodate technological change into a complex component such as the power processor drove the package design into modules that could be functionally isolated. This also allowed other flexibilities in the manufacturability, testability, and manageability to be enjoyed on the "man sized" modules. Several examples of the benefits of this approach have been realized in the course of building hardware in the technology ready program.

2.5 SEP Focused Technology Program Progress

The degree to which these design goals have been achieved in the selected design approach is subjective. But the early agreement to proceed on the BIMOD engine system as the basic building block for SEP focused technology program has allowed us to make significant progress toward technology readiness. Real problems have been identified and solved. Technology gaps have been identified and changes have been made to strengthen the program. The

program outputs should be invaluable to those responsible for flight hardware development.

2.6 Reference Documents

2.6.1 Kaufman, H. R.: An Ion Rocket with an Electron-Bombardment Ion Source. NASA TN D-585, 1961.

2.6.2 Finke, Robert C.; Holmes, Arthur [illegible]; and Keller, Thomas H.: Space Environment Facility for Electric Propulsion Systems Research. NASA TN D-2774, 1965.

2.6.3 Gold, Harold; Rulis, Raymond J.; Maruna, Frank A., Jr.; and Hawersaat, William H.: Description and Operation of Spacecraft in SERT I Ion Thruster Flight Test. NASA TM X-1077, 1965.

2.6.4 Cybulski, Ronald J.; Shellhammer, Daniel M.; Lovell, Robert R.; Domino, Edward J.; and Kotnik, Joseph T.: Results from SERT I Ion Rocket Flight Test. NASA TN D-2718, 1965.

2.6.5 Rulis, Raymond J.: Design Considerations and Requirements for Integrating an Electric Propulsion System into the SERT II and Future Spacecraft. NASA TM X-52853, 1970.

2.6.6 Lovell, Robert R.; and O'Malley, Thomas A.: Station Keeping of High Power Communication Satellites. NASA TM X-2136, 1970.

2.6.7 Knight, Rodney M.: Planned Flight Test of a Mercury Ion Auxiliary Propulsion System Part II - Integration with Host Spacecraft. NASA TM X-78869, 1978.

2.6.8 Duxbury, John H.: Solar Electric Spacecraft for the Encke Slow Flyby Mission. AIAA Paper 73-1126, November 1973.

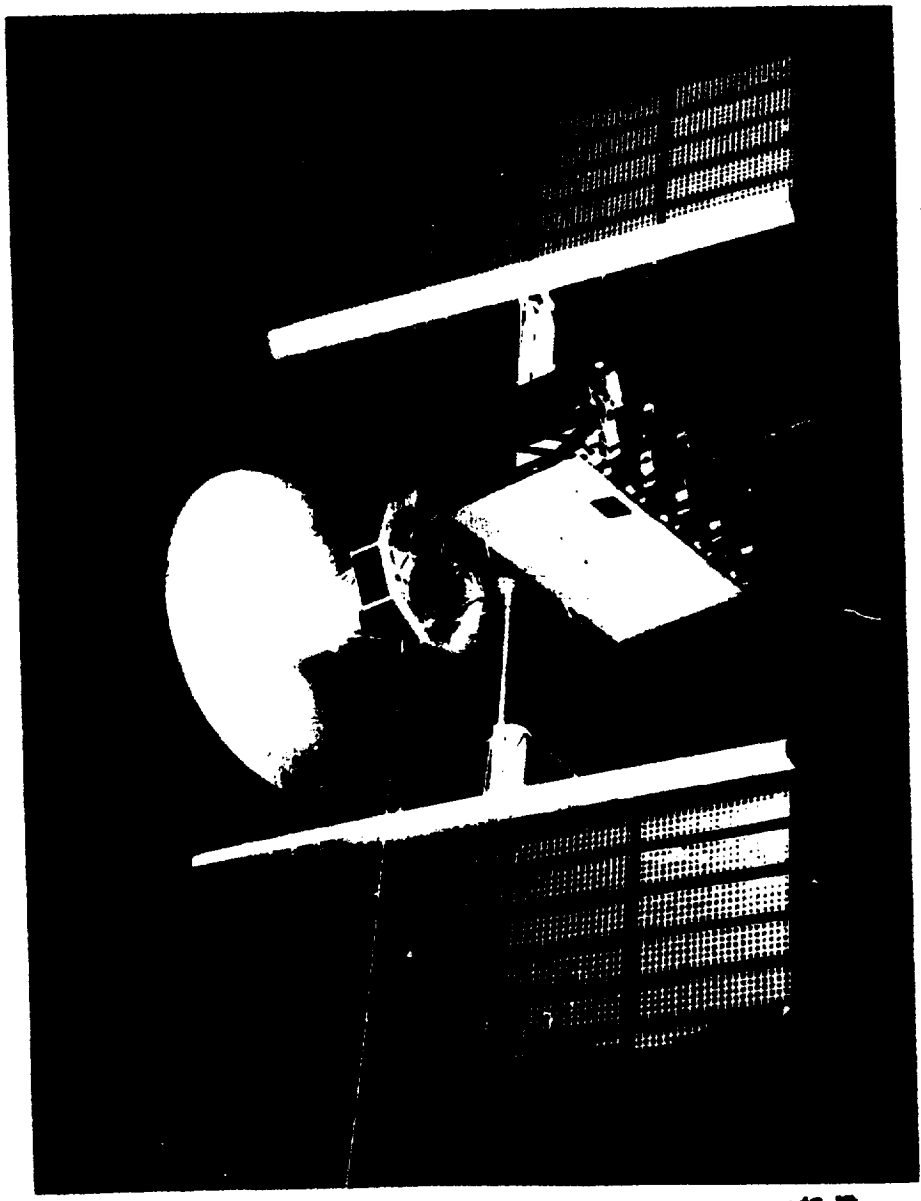

Figure 2.3-1 Typical Electrically Propelled Space Vehicle

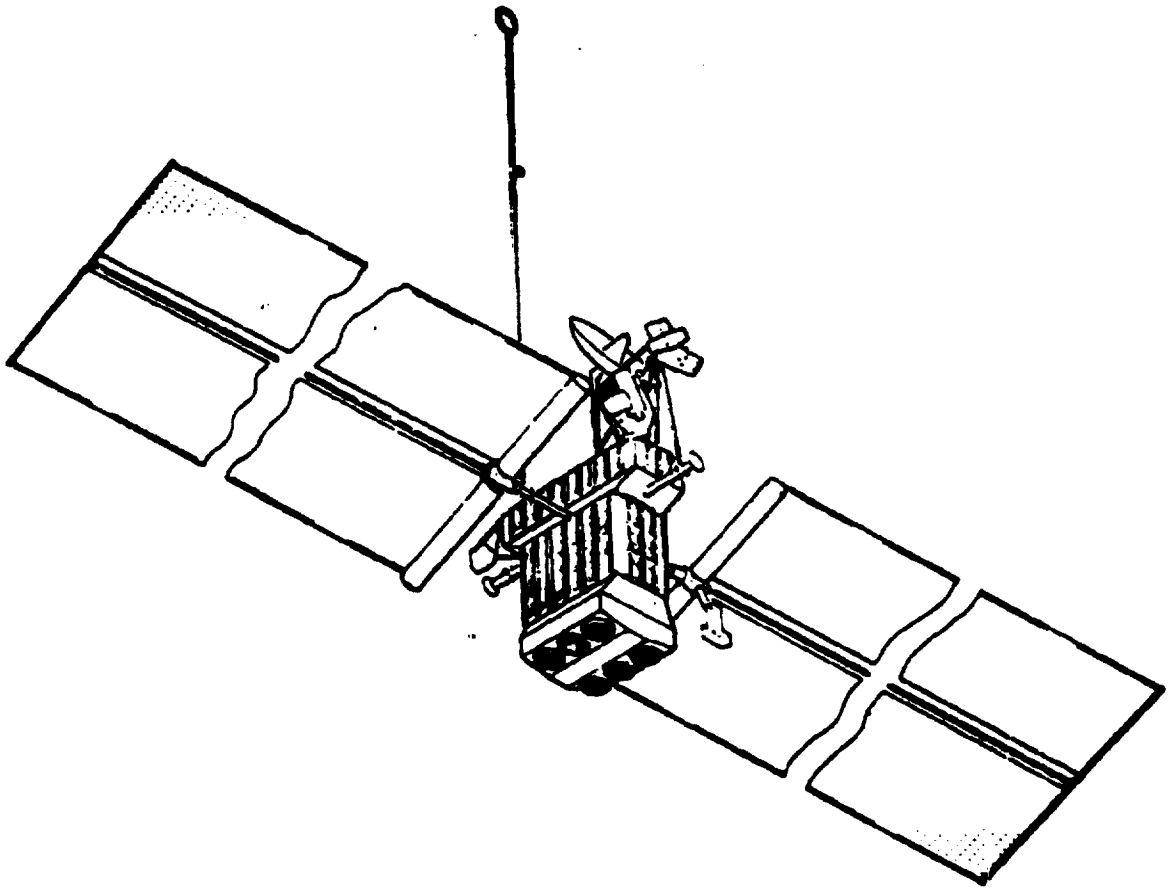

Figure 2.3-2 Mariner Encke Spacecraft

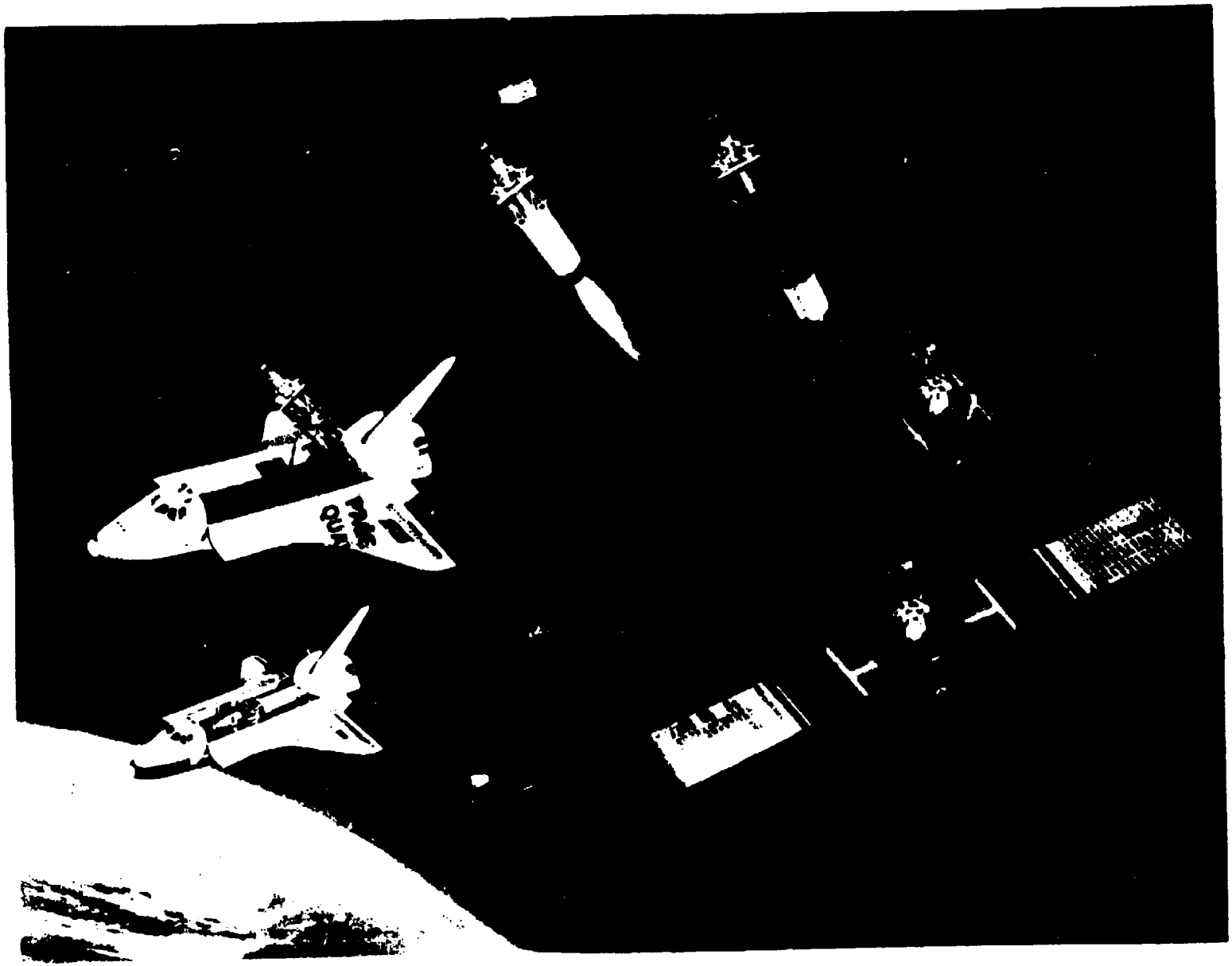

Figure 2.3.2-1 SEP Launch Sequence

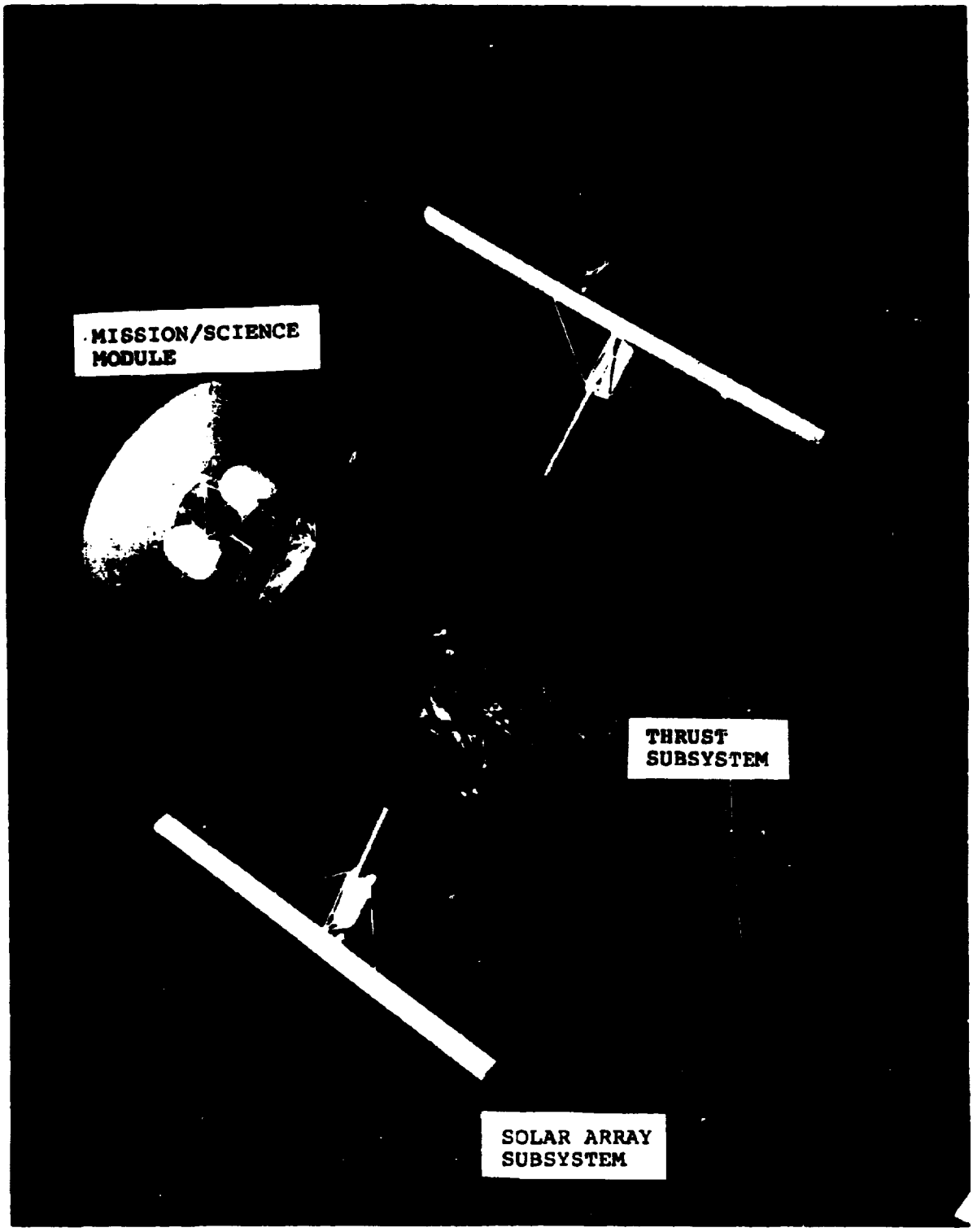

Figure 2.4-1 SEP Vehicle Major Subsystems

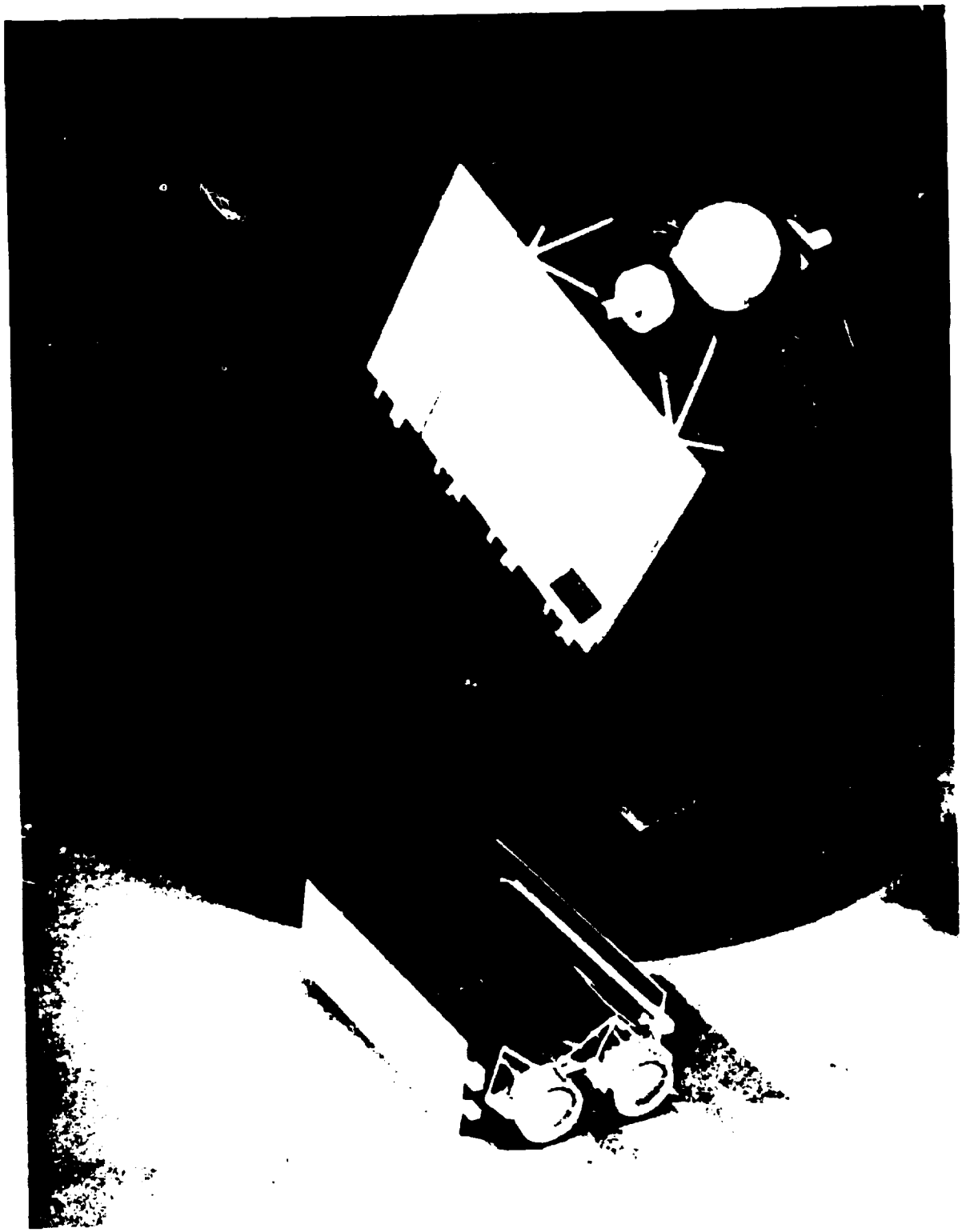

Figure 2.4.3-1 Modularity of Thrust Subsystem

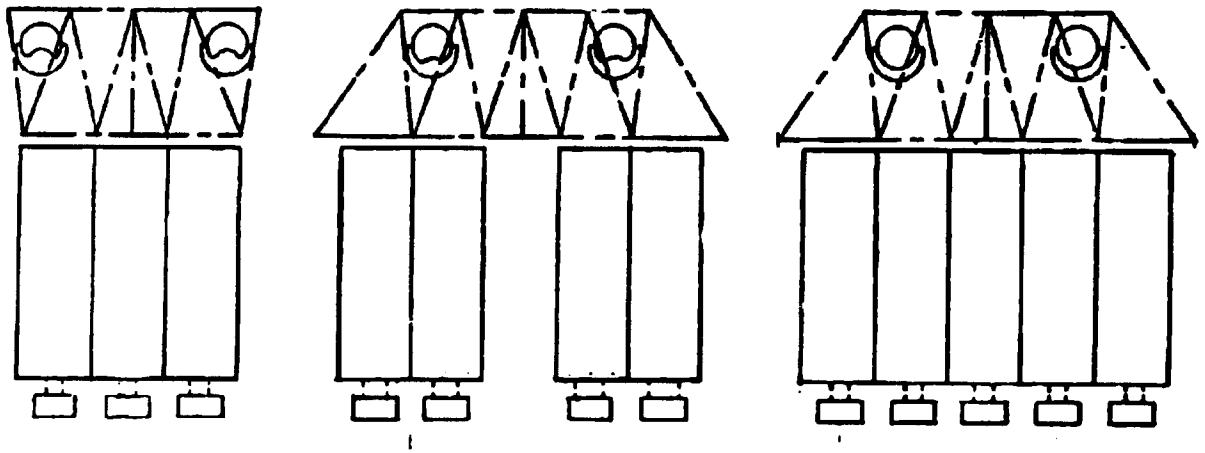

3 BIMOD
- HALLEY FLYBY/TEMPEL 2
- SATURN ORBITER/DUAL PROBE

4 BIMOD
- SOLAR PROBE
- MAGNETO TAIL MAPPING
- SPACE BASED RADAR
- GEOSTATIONARY PLATFORM

5 BIMOD
- ASTEROID MULTIPLE RENDEZVOUS

Figure 2.4.3-2 Thrust Subsystem Configurations

BASIC PACKAGING CONCEPT

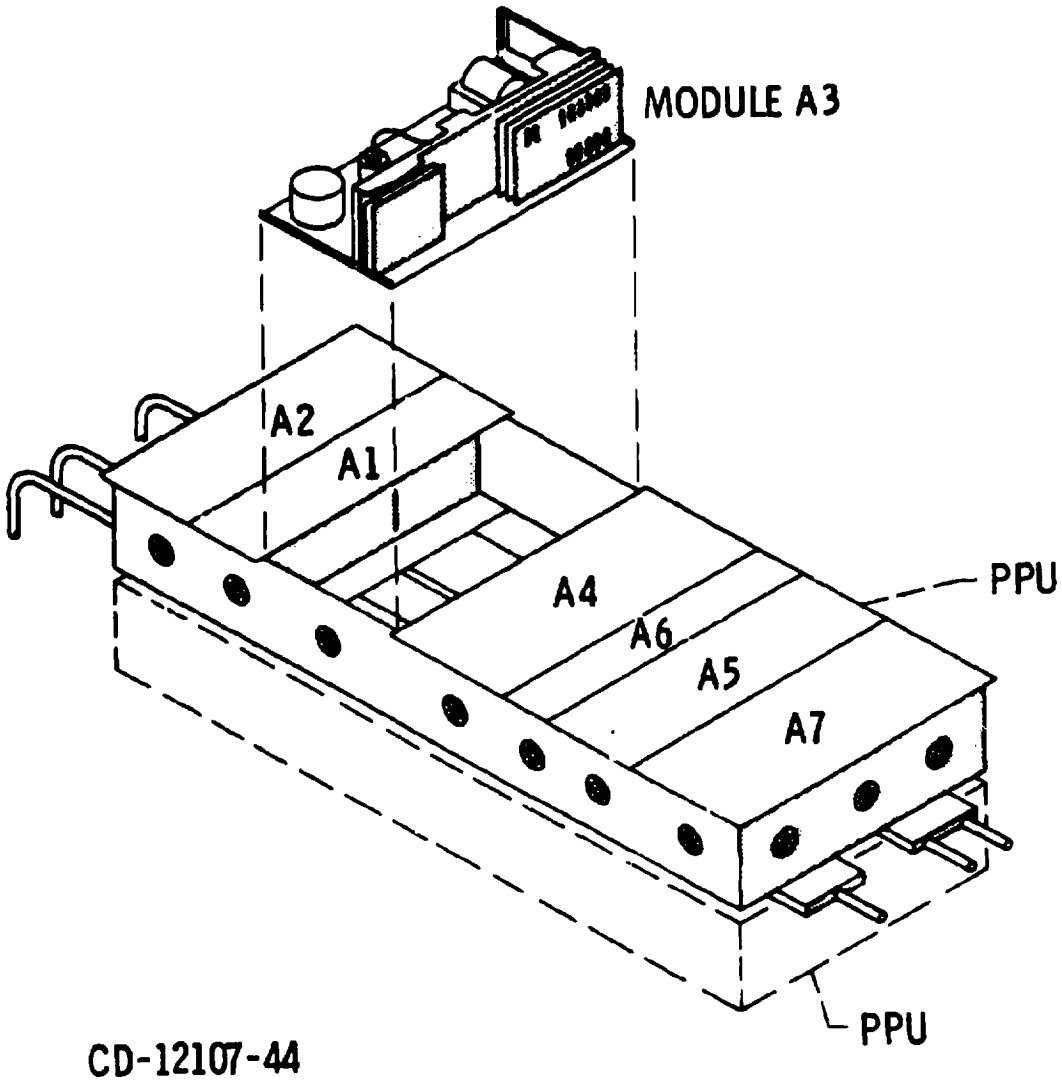

Figure 2.4.4-1 Power Processor Modularity

3.0

THRUST SUBSYSTEM

Table of Contents

		Page
3.0	Thrust Subsystem	3-3
3.1	Reference Documents	3-3
3.2	Functional Requirements	3-4
3.3	Functional Description	3-5
3.3.1	Electrical	3-5
3.3.2	Mechanical	3-7
3.3.3	Thermal	3-8
3.4	Interface Definition	3-8
3.4.1	Electrical	3-8
3.4.1.1	Solar Array Power	3-9
3.4.1.2	Mission Module Battery Bus	3-9
3.4.1.3	Mission Module Computer	3-9
3.4.2	Mechanical	3-10
3.4.3	Thermal	3-10
3.5	Performance Description	3-10
3.5.1	Propulsion	3-10
3.5.1.1.	Thrust Magnitude	3-10
3.5.1.2	Throttling	3-10
3.5.1.3	Startup	3-10
3.5.1.4	Shutdown	3-11
3.5.1.5	Lifetime	3-11
3.5.1.6	Thrust Magnitude Variation	3-11
3.5.2	Thrust Vector Control	3-11
3.6	Physical Characteristics and Constraints	3-11

		Page
3.6.1	Mass	3-11
3.6.2	Power	3-11
3.6.3	Environmental	3-12
3.6.4	Configuration	3-12
3.7	Development History	3-12
3.7.1	Research and Technology	3-12
3.7.2	Advanced Systems Technology Program	3-13
3.7.3	Focused Technology Readiness Program	3-14
3.7.4	System Studies	3-16
3.8	Applicable Documents Enclosed	3-16

TABLES

3.5.1.1-1	Thrust Subsystem Unit Performance	3-18
3.6.1-1	BIMOD Engine System Mass Breakdown	3-19
3.6.1-2	Interface Module Mass Breakdown	3-20
3.6.2-1	Thrust Subsystem Power Requirements (Watts)	3-21

FIGURES

3.3.1-1	Thrust Subsystem Electrical Block Diagram	3-22
3.3.1-2	BIMOD Electrical Block Diagram	3-23
3.3.1-3	Interface Module Electrical Block Diagram	3-24
3.3.2-1	Thrust Subsystem Configuration	3-25
3.3.2-2	BIMOD Engine System	3-26
3.3.3-1	Insulation Blanket Placement	3-27
3.5.1.2-1	Thruster Operating Envelope	3-28

3.0 Thrust Subsystem

3.1 Reference Documents

3.1.1 Masek, T. D.: Solar Electric Propulsion Thrust Subsystem Development. JPL-TR-32-1579, Jet Propulsion Lab, 1973.

3.1.2 Solar Electric Propulsion Multimission Spacecraft, JPL Internal Report 72-442, Jet Propulsion Lab., 1971.

3.1.3 Solar Electric Propulsion Asteroid Belt Mission Study. SD70-21-3, Rockwell International Corp., 1970.

3.1.4 Extended Definition Feasibility Study for a Solar Electric Propulsion Stage Concept Definition. SD73-SA-0132-2-2, Rockwell International Corp., 1973.

3.1.5 Concept Definition and Systems Analysis Study for a Solar Electric Propulsion Stage. SD 74-SA-0176-6, Rockwell International Corp., 1975.

3.1.6 Concept Definition and System Analysis Study for a Solar Electric Propulsion Stage. D180-18553-4, Boeing Aerospace Co., 1975.

3.1.7 Duxbury, J. H.: Solar Electric Propulsion Encke Slow-Flyby 1979 Mission and Spacecraft Description. JPL TM 701-200, Jet Propulsion Lab., 1974.

3.1.8 Duxbury, J. H. and Paul, G. M.: Interplanetary Spacecraft Design Using Solar Electric Propulsion. AIAA Paper 74-1084, October 1974.

3.1.9 Haloy, J. E.; and Sharp, G. R.: A Structural and Thermal Packaging Approach for Power Processing Units for 30-Centimeter Ion Thrusters. AIAA Paper 75-403, March 1975.

3.1.10 Cake, J. E.; Sharp, G. R.; Oglebay, J.C.; Shaker, F.J.; and Zavesky, R. J.: Modular Thrust Subsystem Approaches to Solar Electric Propulsion Module Design. AIAA Paper 76-1002, November 1976.

3.1.11 Sharp, G. R.; Cake, James E.; Oglebay, Jon C.; and Shaker, Francis J.: Mass Study for Modular Approaches to a Solar Electric Propulsion Module. NASA TM X-3473, 1977.

3.1.12 Poeschel, R.L.; and Hawthorne, E.I.; et al: Extended Performance Solar Electric Propulsion Thrust System Study. (Hughes Aircraft Co.) NASA CR-135281, 1977.

3.2 Functional Requirements

1) The thrust subsystem shall provide the thrust required for prime propulsion and attitude control of the vehicle consistent with the solar array power available, the mission specific impulse requirement, and the mission environment.

2) The thrust subsystem shall accept as its input power the unregulated solar array voltage and current and convert this power to provide the twelve regulated power outputs to satisfy ion thruster requirements.

3) The thrust subsystem shall respond to external control required for normal and off normal thruster and power processor operations. These functions shall include executing start sequences, executing throttle sequences, correcting for anomalies, and processing power processor interrupt signals.

4) The thrust subsystem shall have the capability to store

the mercury propellant load sufficient for the mission, to supply the propellant to and array of multiple thrusters over the required pressure range, and to isolate the propellant from the thrusters during the launch environment.

5) The thrust subsystem shall in response to executive level control, provide external disturbance torques to unload the reaction wheels of the attitude and articulation control subsystem.

6) The thrust subsystem shall provide the structural support for its components and subassemblies and shall be capable of sustaining Shuttle/IUS induced loads.

) The thrust subsystem shall maintain its components and ubassemblies within operational and non-operational temperature limits.

3.3 Functional Description

3.3.1 Electrical

The functional block diagram of the thrust subsystem electrical system is shown in figure 3.3.1-1. Unregulated solar array power and regulated mission module power are input to the power distribution unit for distribution to the eight power processors and other thrust subsystem equipment. Each power processor converts the unregulated power outputs to satisfy the load requirements of the 30-cm ion thrusters. Mercury is vaporized by heaters in the thruster and ionized in the discharge chamber via mercury electron bombardment. The mercury

ions drift toward the screen and accelerator grids of the thruster where they are accelerated by the high voltage between these grids and are exhausted at a high velocity, producing thrust.

Control of the vehicle is arranged in three levels. Within the mission module, the mission module computer provides executive level commands to the thrust subsystem. The propulsion section of the mission module computer provides start, stop, and throttle level commands to the thruster controller within the thrust subsystem. The functions of the thruster controller are to execute the stored algorithms to provide the startup, shutdown, or throttling of the thruster designated by the mission module computer. The thruster controller provides command synchronization and clock synchronization to the power processor. In addition to processing telemetry data from the power processors, the thruster controller receives interrupt flags generated by the power processor and takes corrective actions. The third level of control is at the power processor level. The power processor provides the regulation and control of its twelve supplies, generates an interrupt flag for certain out of limit conditions, recycles following thruster arcs, and provides an emergency shutdown.

To perform the attitude control function, the gimbal electronics within the thrust subsystem receives power

signals from the mission module to drive the pair of actuator motors for each thruster gimbal. Angle resolvers on the shaft axes of the gimbals provide direct position information through the gimbal electronics to the mission module computer.

As described in the following sections, the thrust subsystem is divided into two types of subassemblies. These subassemblies are the BIMOD engine systems and the interface module. The electrical block diagram at the BIMOD level is shown in figure 3.3.1-2 and the electrical block diagram for the interface module in figure 3.3.1-3 Sections 4.0 through 7.0 and 10.0 through 12.0 should be consulted for further detail.

3.3.2 Mechanical

The configuration of the thrust subsystem is shown in figure 3.3.2-1. The thrust subsystem comprises four BIMOD engine systems and an interface module. Each BIMOD contains two thrusters and thruster gimbals and two power processors which conduct their waste heat to a common thermal control system (fig. 3.3.2-2). The BIMODs are attached to the interface module at four mounting points as described in Section 4.0. Adjacent BIMODs are attached via struts near the thruster ends of the BIMOD truss.

The interface module contains the two mercury propellant tanks and propellant distribution components, power dis-

tribution unit, thruster controller, and gimbal electronics.

3.3.3 Thermal

The BIMOD engine systems and the interface module are thermally autonomous assemblies. Thermal control for the power processors is provided by the heat pipe/radiator subassemblies of each BIMOD. Insulation blankets are placed between the thrusters and the BIMOD truss to maintain the proper thruster thermal environment and shield the back of the BIMOD radiators from solar illumination (see fig. 3.3.3-1). Insulation blankets are placed on the ends of the thrust subsystem. There are no blankets however between adjacent BIMODs. Section 9.0 should be consulted for further detail on the thermal control for the BIMOD.

The interface module exterior is wrapped with insulation. All thermal blankets on the exterior of the thrust subsystems are constructed to provide protection from meteorite and cometary dust. As described in Sections 10.0 and 14.0, the interface module electronics are mounted to radiators. Supplementary heaters are used to provide the proper thermal environment for the mercury propellant tanks.

3.4 Interface Definition

3.4.1 Electrical

The electrical interfaces between the thrust subsystem and mission module are identified in figure 3.3.1-3.

The thrust subsystem shall maintain isolation of all interface circuits from structure. The thrust subsystem electrical interface shall contain all signal functions at a single interface point, including umbilical functions, if any. The number of interface connectors is TBD, but each connector shall be keyed or sized to prevent improper mating arrangement.

3.4.1.1 Solar Array Power

The solar array configuration unit of the mission module will provide nominal 200 to 400 V dc power to the power distribution unit of the interface module. The battery bus will provide power through eleven separate circuits: Eight circuits to the PDU for the eight power processors; one circuit to the PDU to provide heater power, mercury solenoid valve pulse, and gimbal electronics; and one circuit to each of the thruster controllers.

3.4.1.3 Mission Module Computer

The mission module computer will provide commands to and receive telemetry from the thruster controller and the thruster gimbal electronics in the interface module. The interface to the mission module computer from the thruster controller shall be through a first-in, first-out buffer memory which limits the data transfer rate to TBD bps and provides noise filtering. The buffer memory is connected to the mission module computer bus via a bus adapter unit. The interface from the gimbal electronics is similar to that for the thruster controller.

3.4.2 Mechanical

The thrust subsystem shall be mated to the mission module at the ten mounting points as shown in figure 3.3.2-1, LeRC Drawing CR 622760, Thrust Subsystem Interface Control Drawing (also included in applicable document 3.8.1).

3.4.3 Thermal

The thermal interface between the thrust subsystem and the mission module shall be the multilayer insulation blanket placed across the top of the interface module as shown in figure 3.3.3-1.

3.5 Performance Description

3.5.1 Propulsion

3.5.1.1 Thrust Magnitude

For the solar array power input into the power distribution unit the thrust subsystem shall be capable of producing the nominal thrust and specific impulse in table 3.5.1.1-1 for each of the eight thrusters. Sections 5.0 and 6.0 should be consulted for detailed performance information on the thruster and power processor.

3.5.1.2 Throttling

Each thruster shall be capable of operating over the standard operating envelope identified in figure 3.5.1.2-1.

3.5.1.3 Startup

The thrust subsystem shall be capable of starting the thruster and providing stable operation at 0.75 amp beam current within a nominal time of 43 minutes from start

of thruster preheat.

3.5.1.4 Shutdown

1) The thrust subsystem shall be capable of providing a normal shutdown of the power processor into a standby mode within TBD minutes.

2) The thrust subsystem shall remove a faulted load from the unregulated bus in less than 1 second and from the regulated bus within 0.1 seconds.

3.5.1.5 Lifetime

Each thruster/power processor combination shall be capable of providing operation equivalent to 15 000 hours when operated at 2 amp beam current.

3.5.1.6 Thrust Magnitude Variation

Thrust magnitude errors are TBD.

3.5.2 Thrust Vector Control

The thrust subsystem shall be capable of providing thruster gimbal travel angles of $\pm 35^{\circ}$ about the y-axis and $\pm 16^{\circ}$ about the x-axis as defined in figure 3.3.2-2.

3.6 Physical Characteristics and Constraints

3.6.1 Mass

The estimated mass of the thrust subsystem is 708.7 kg. This includes four BIMODs at 137.5 kg and the interface module at 158.7 kg. A mass breakdown of the BIMOD and interface module is given in tables 3.6.1-1 and 3.6.1-2.

3.6.2 Power

The unregulated and regulated power required of the mission module by the power distribution unit shall not

exceed the estimated values given in table 3.6.2-1.

3.6.3 Environmental

The thrust subsystem shall be compatible with the structural and thermal design criteria identified in Sections 9.0 and 14.0.

3.6.4 Configuration

The configuration of the thrust subsystem is defined by LeRC Drawing CF 638168 (see fig. 3.3.2-1 and applicable document 3.8.1).

3.7 Development History

3.7.1 Research and Technology

Solar electric propulsion technology programs related to the 30 cm thrust subsystem have been on going since the late 1960's. Until the mid-1970's the efforts at LeRC were primarily related to thrusters and power processors. As explained in the development history sections on the thruster and power processor, the 30 cm thruster technology was derived from the SERT II technology. Parallel contract efforts were conducted for bridge inverter and series resonant inverter power processors until 1975. The series resonant inverter approach was first sponsored by the NASA Electronics Research Center (ERC) and also by JPL for the 20 cm thruster before LeRC initiated contracts for the 30 cm power processor breadboards. Documentation for electric propulsion related work conducted by LeRC both in-house and on contract is identified by year in applicable docu-

ment 3.8.2.

In parallel with the component technology at LeRC, JPL had responsibility for solar electric propulsion system technology from the late 1960's to 1975. Reference document 3.1.1 provides a description of that work. Mission and application studies were also conducted by JPL during this time period (see reference documents 3.1.2 and 3.1.3). Also, Marshall Space Flight Center was conducting feasibility studies for a SEP stage (see reference documents 3.1.4, 3.1.5, and 3.1.6).

3.7.2 Advanced Systems Technology Program

The Advanced Systems Technology (AST) program was conducted in 1973 and 1974 by MSFC, JPL, and LeRC. Drawing upon the component and systems technology efforts at the three centers, this activity focused on the definition and integration of SEPS with a planetary spacecraft. The concept of a thrust subsystem evolved during this activity. Most of the SEPS vehicle design drivers discussed in Section 2.0 were recognized and established during the AST Program. In addition to these design criteria, the major outputs of the AST Program were functional, interface, and performance requirements for the thruster and power processor. Reference documents 3.1.7 and 3.1.8 should be consulted for some of the AST results. Trade off studies near the end of the AST program lead to the decision to package the power processor for compatibility with a variable conductance heat

pipe radiator thermal control subsystem (reference document 3.1.9).

3.7.3 Focused Technology Readiness Program

Upon the completion of the AST program in October, 1974, a focused technology readiness program was established by OAST at LeRC. The objective of this program has been to develop the technology for thrusters, power processors, thermal control, propellant system, and thrust vector system. The technology readiness goal is to identify and provide solutions for critical engineering problems such that system performance, interface requirements, and constraints will be defined to the point where application of the technology can be accomplished with known and acceptable risk. A description of the technology program is contained in applicable document 3.8.3.

The system and configuration dependent requirements on the above component technology were specified as a result of the thrust subsystem definition and design process continuing at LeRC since 1975. A thrust subsystem was defined which contained the above technology elements and supporting structure to provide a physical identity. The configuration was governed by the design criteria discussed in Section 2.0. The interfaces were chosen such that they could be simply specified, controlled during the development program, and verified during the test program. The selected thrust subsystem definition and interfaces with the solar array and mission space-

craft internalized all the high technology and functionally interactive elements within the thrust subsystem.

The design process examined various approaches to a thrust subsystem with physical modules containing thruster(s), power processor(s), thermal control, propellant storage and distribution, and thruster gimbals (reference documents 3.1.10 and 3.1.11). The objectives were to create a modular thrust subsystem having six, eight, or ten thrusters. This would yield mission flexibility and enhance the ability to assemble and test the thrust subsystem. The selected configuration, called a BIMOD engine system, is described in Section 4.0. The BIMOD engine system has been under development at LeRC since mid-1976 and represents the highest integration level output from the OAST technology program. As discussed in 4.7, the BIMOD design, power processor package design, and thrust subsystem design were parallel efforts. The BIMOD provided the physical configuration to focus the design and development of the power processors, thermal control system, and thruster gimbal system.

As the BIMOD engine system development has proceeded, thrust subsystem definition studies have continued to refine the interfaces between the thrust subsystem and SEPS and to verify that the thrust subsystem performance and mass meets the mission requirements.

3.7.4 System Studies

The major system studies conducted with JPL and MSFC since the AST program have been the "August Project" during 1977, and the JPL/LeRC Comet/Ion Drive Development Project during 1978. Although the "August Project" was for a higher power and specific impulse system, some of the system design and configuration information was used to refine the thrust subsystem design. Documentation for the thrust subsystem part of this activity is presented in reference document 3.8.2.

During the JPL/LeRC Comet/Ion Drive Development Project, a mission and system design was established for the Halley comet flyby/Tempel 2 rendezvous mission using the BIMOD as a baseline. The results of this study are given in applicable documents 3.8.4 and 3.8.5.

3.8 Applicable Documents Enclosed

3.8.1 Thrust Subsystem Drawing List. NASA Lewis Research Center, May 1979.

3.8.2 Reports and Papers Pertaining to Electrostatic Propulsion. NASA Lewis Research Center staff and contractor reports from 1958 to 1978.

3.8.3 DePauw, James F.: Prime Propulsion Technology Readiness Program. NASA Lewis Research Center, Solar Electric Propulsion Office, July 1978.

3.8.4 Comet/Ion Drive Mission and Flight System Design Report. Volume III-Mission Requirements and Description. Jet Propulsion Laboratory. September 1978.

3.8.5 Comet/Ion Drive Mission and Flight System Design Report. Volume IV-Flight System Requirements and Description. Jet Propulsion Laboratory. October 1978.

Table 3.5.1.1-1 Thrust Subsystem Unit Performance

$P_{PDU\ IN}$, watts	η_{TSS}	I_{SP}, seconds	$THRUST_{TSS\ UNIT}$, millinewtons
3112	.605	3020	129.8
2278	.547	2684	96.8
1756	.492	2492	73.9
1293	.430	2206	53.0
949	.363	1962	37.1

$P_{PDU\ IN}$ = Power distribution unit input power for each power processor/thrusters.

η_{TSS} = Total thrust subsystem efficiency.

$THRUST_{TSS\ UNIT}$ = Thrust output from each thruster.

Table 3.6.1-1 BIMOD Engine System Mass Breakdown

Item	Mass, Kg	Comments
BIMOD Total	137.1	
Power Processors (2)	74.7	Functional Model
Thermal Control	21.0	
Thrusters (2)	20.7	J-Series Includes Mass of Harness to PPU
Thruster Gimbals (2)	6.8	
Truss and Struts	10.1	
Propellant Distribution	0.7	Valves, Field Joints, Lines
Miscellaneous	3.1	

Table 3.6.1-2 Interface Module Mass Breakdown

Entry	Mass, kg
Interface Module Total	158.7
Truss Structure	24.8
Propellant Storage and Distribution	28.2
Thermal Control	9.9
Power Distribution Unit	54.4
Thruster Controller	6.8
Gimbal Electronics	8.0
Harness	26.6

Table 3.6.2-1 Thrust Subsystem Power Requirements (watts)

Item	Mission Mode (One Power Processor/Thrusters)					
	Off	Standby	Preheat	Heat	Min Power	Max Power
Unregulated 200 to 400V						
. Power Processor (each)	2	25	300	375	875	3126
. Voltage Monitor	1	1	1	1	1	1
Regulated 28V						
. Power Processor (each)	--	84	90	95	100	100
. Thruster Gimbals (each)	--	--	--	--	25	25
. Instrumentation*	12	12	12	12	12	12
. Mercury Valves	32	--	--	--	--	--
. Heaters** (BIMOD)	121***	110***	50***	15***	0	0
. Signal Conditioning Circuits	50	50	50	50	50	50
. Propellant Tank** Heaters	19	19	19	19	19	19

* Signal Conditioning Located in Interface Module
** Corresponds to Thermal Cold Case
*** Actual Valve Depends on Resolution of Heater Circuits

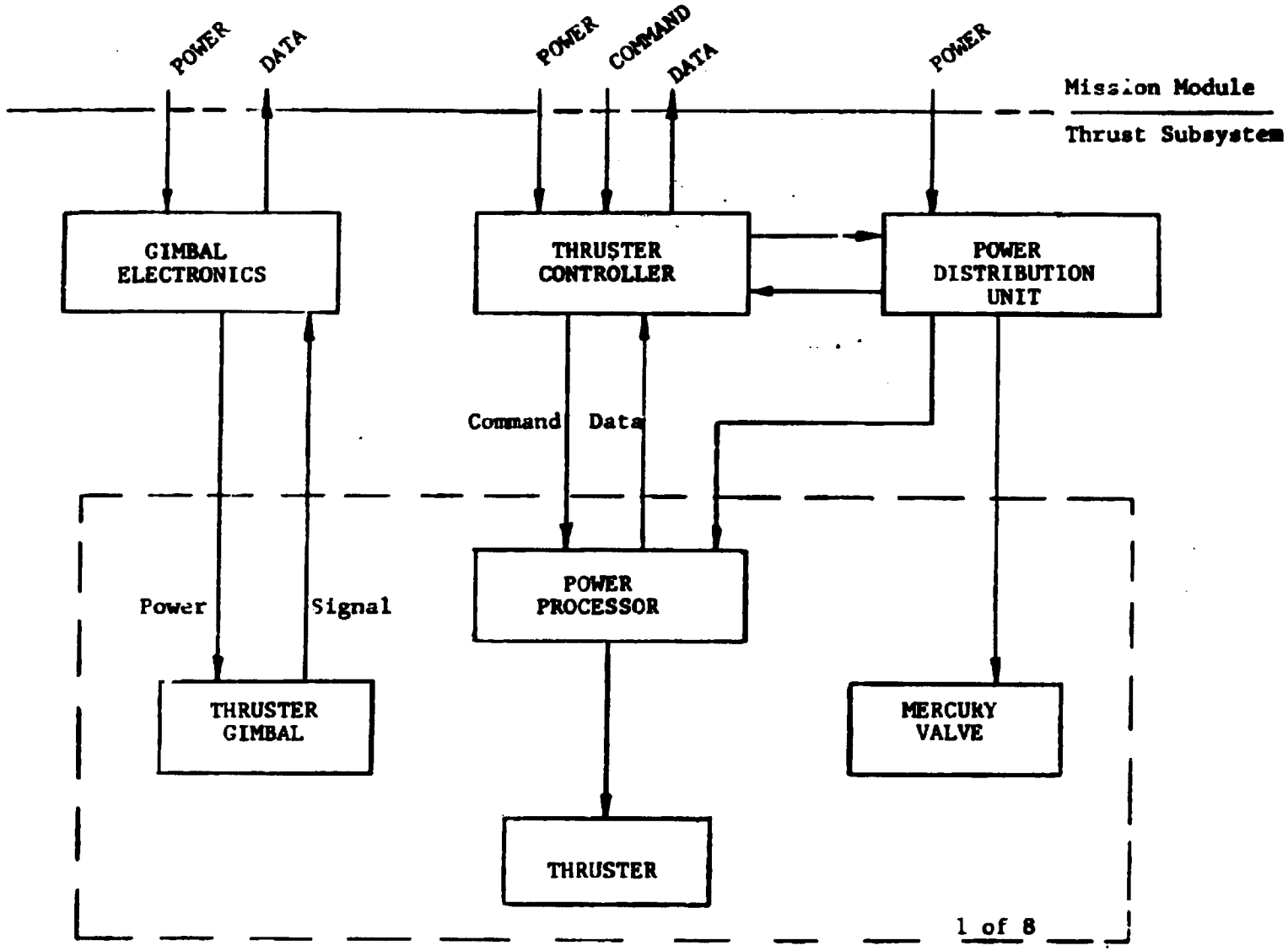

Figure 3.3.1-1 Thrust subsystem electrical block diagram

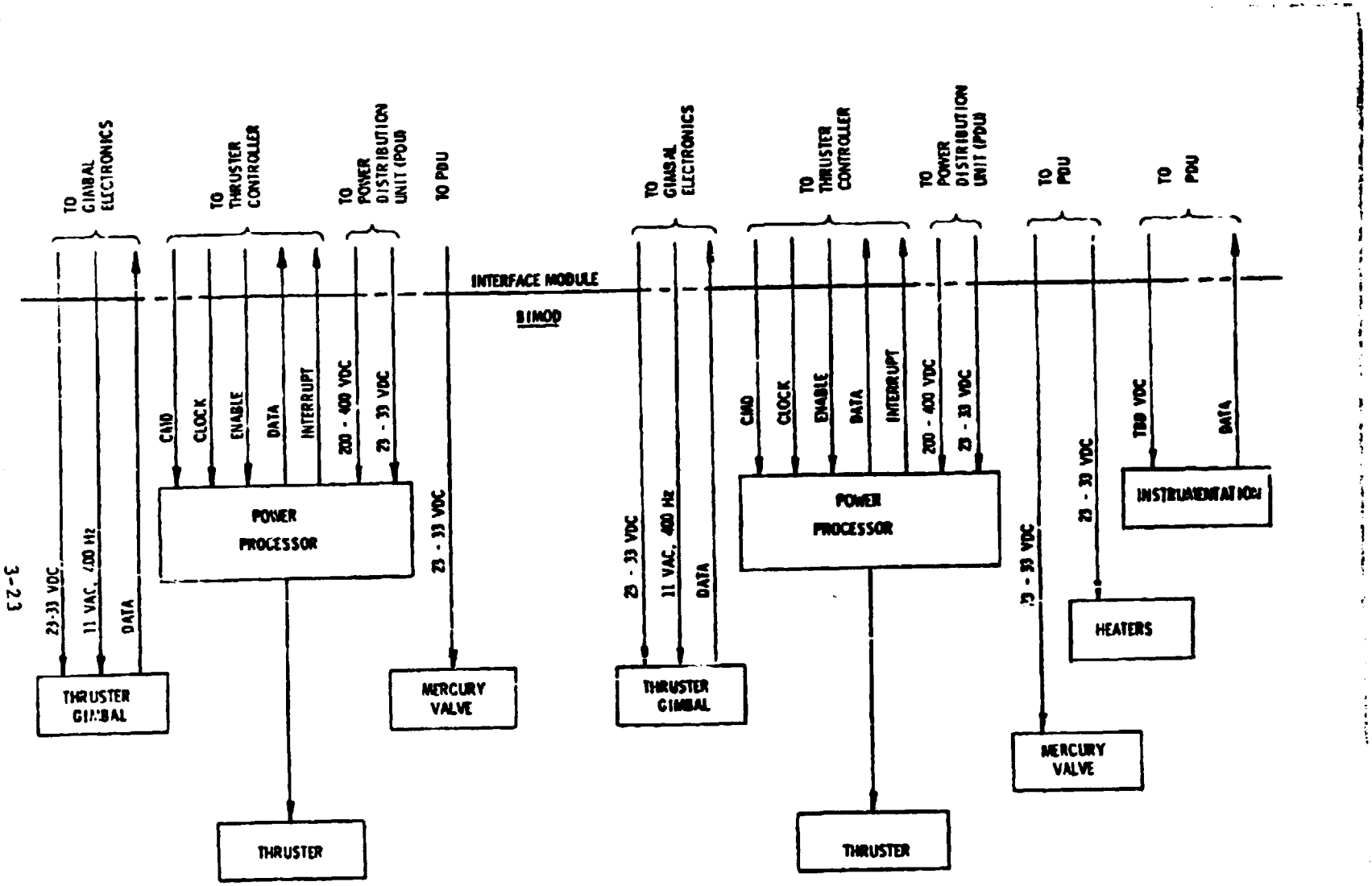

Figure 3.3.1-2 BIMOD Electrical Block Diagram

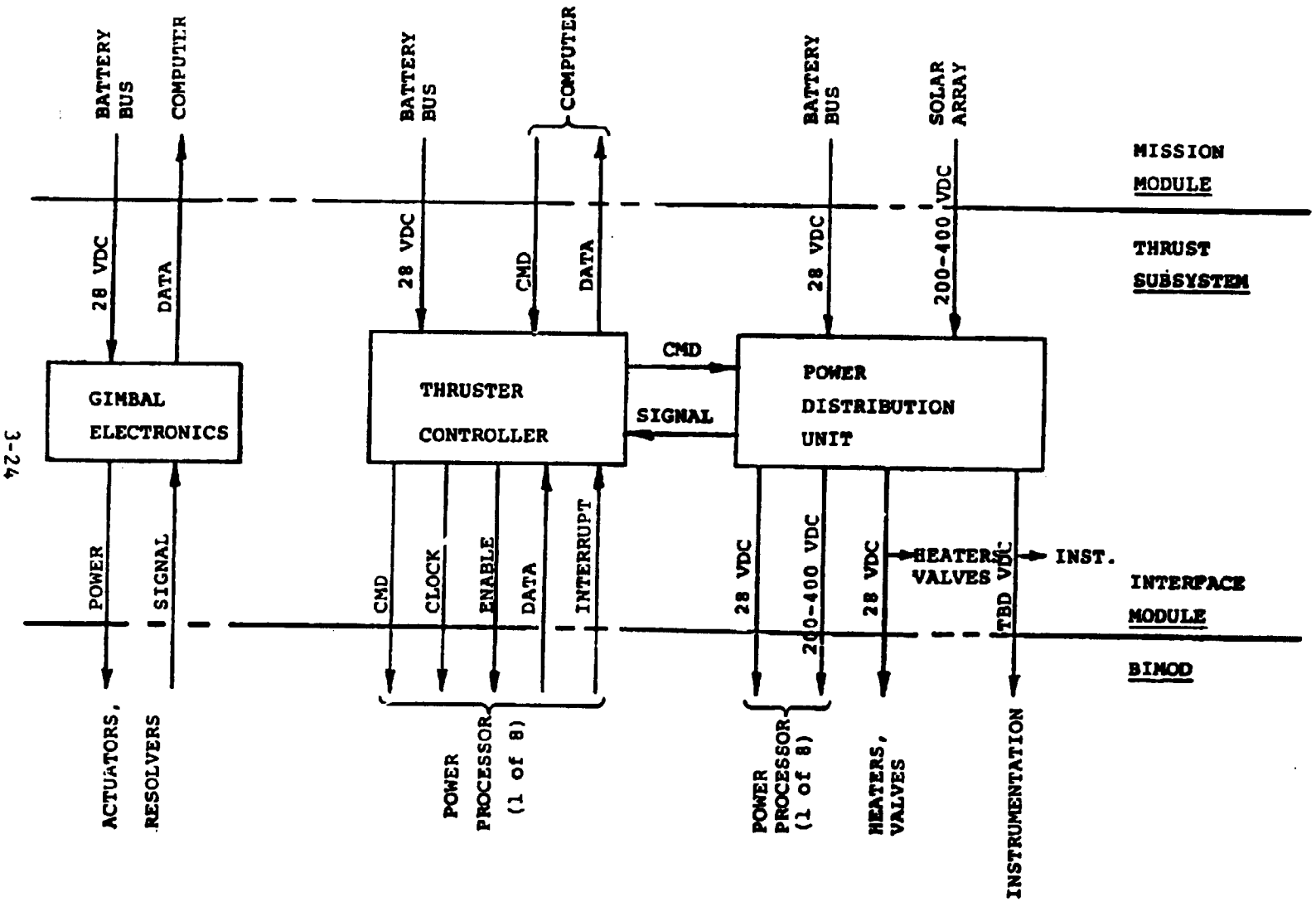

FIGURE 3.3.1-3 INTERFACE MODULE ELECTRICAL BLOCK DIAGRAM

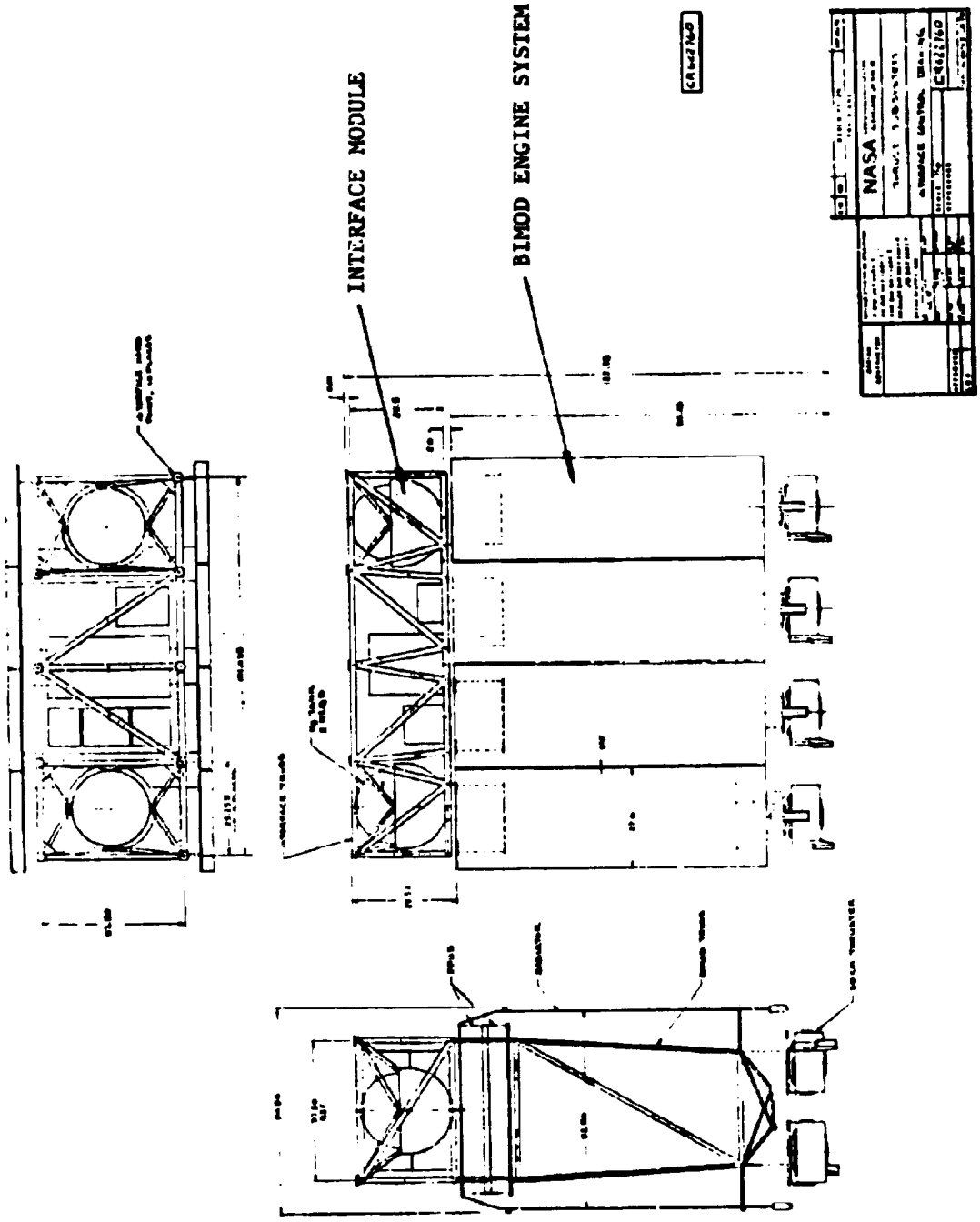

Figure 3.3.2-1 Thrust Subsystem Configuration

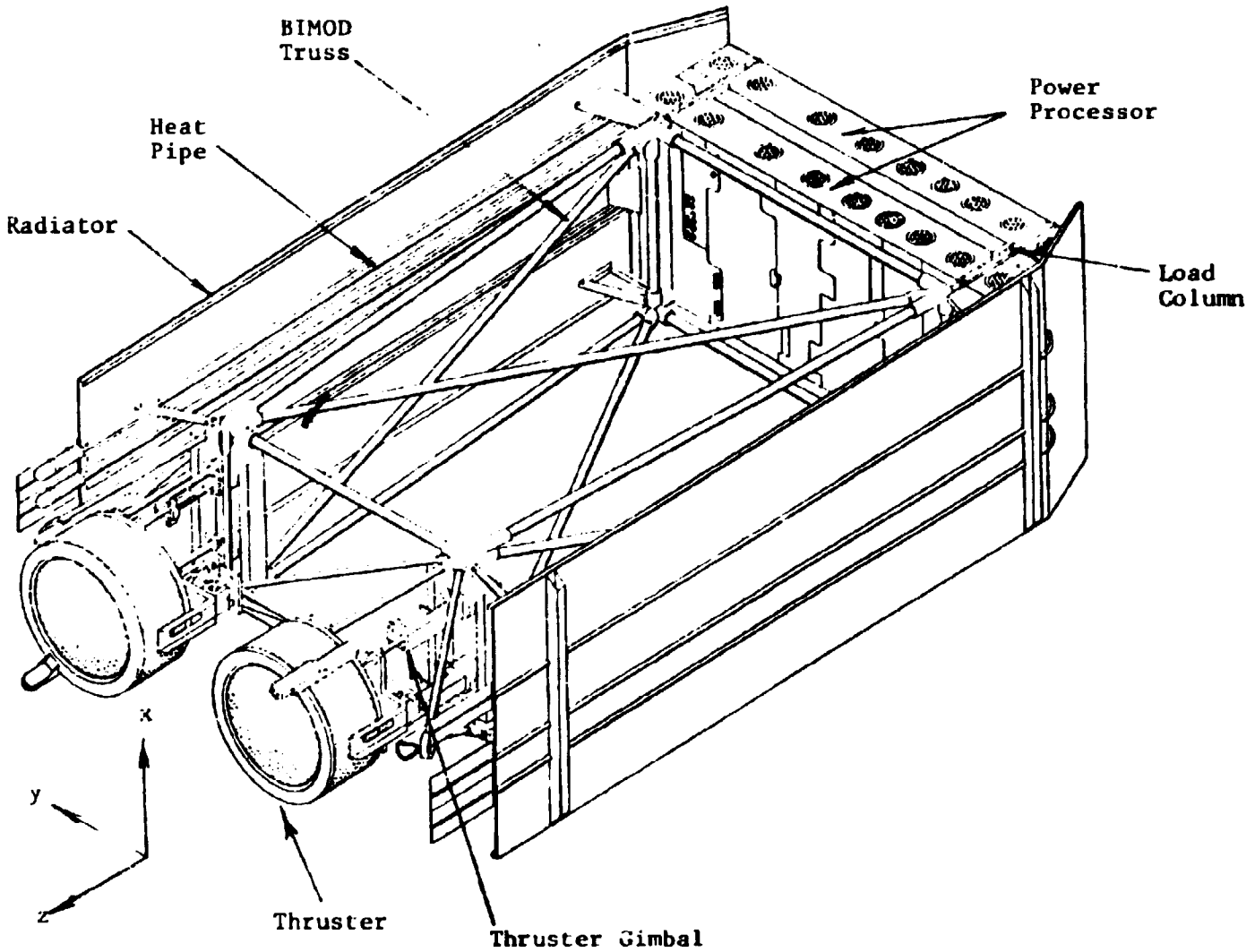

Figure 3.3.2-2 BIMOD Engine System

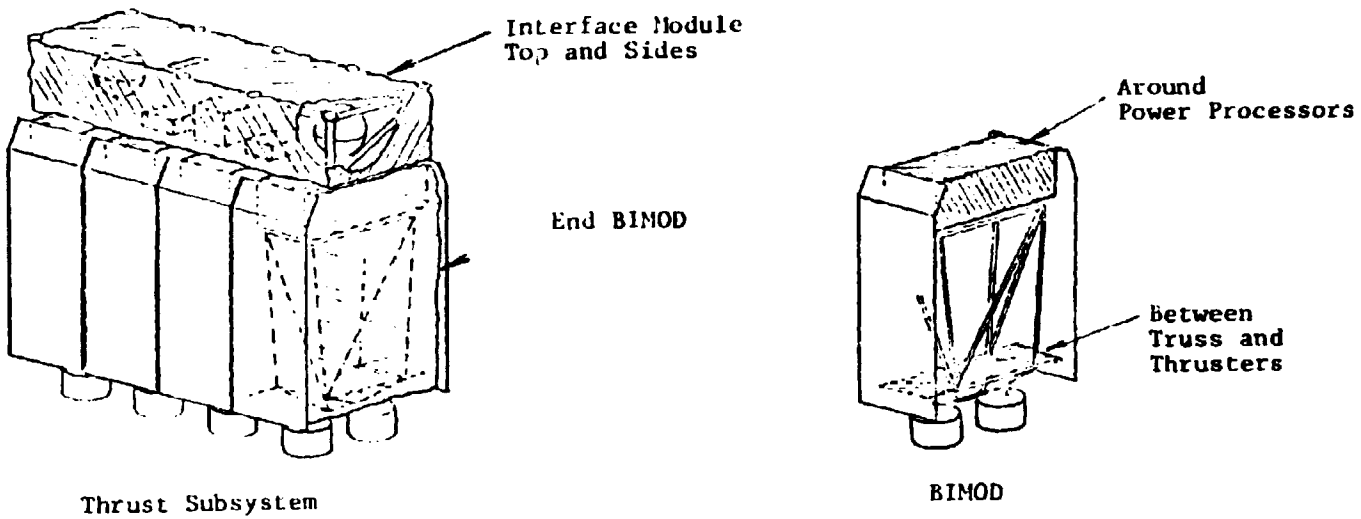

Figure 3.3.3-1 Insulation Blanket Placement

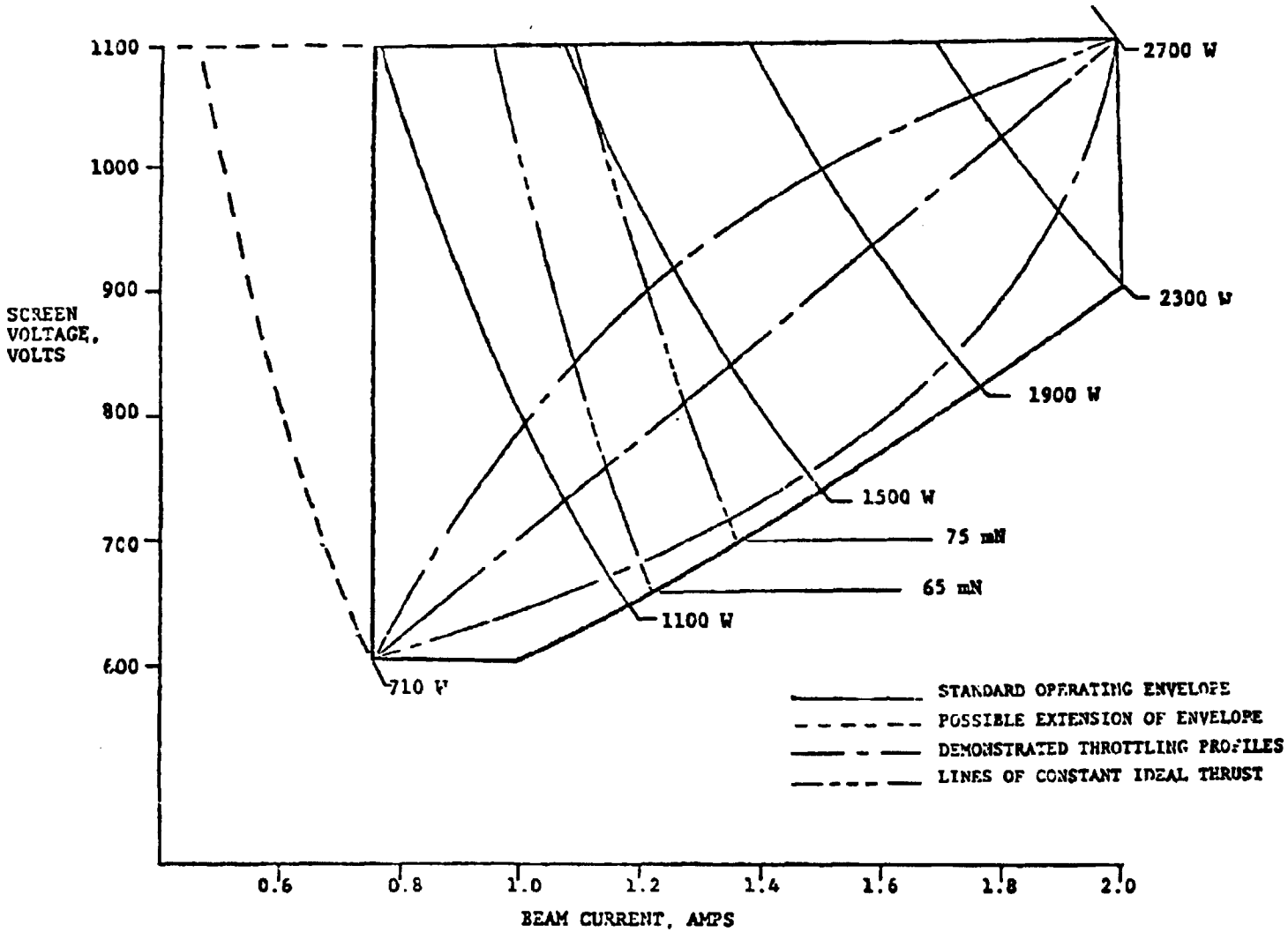

FIGURE 3.5.1.2-1 THRUSTER OPERATING ENVELOPE

4.0

BIMOD ENGINE SYSTEM

Table of Contents

		Page
4.0	BIMOD Engine System	4-5
4.1	Reference Documents	4.5
4.2	Functional Requirements	4-6
4.3	Functional Description	4-7
4.3.1	Electrical	4-7
4.3.1.1	General	4-7
4.3.1.2	Power Processor	4-7
4.3.1.3	Thruster	4-8
4.3.1.4	Thruster Gimbal	4-9
4.3.1.5	Mercury Propellant Valve	4-9
4.3.2	Mechanical	4-10
4.3.2.1	General	4-10
4.3.3	Thermal	4-11
4.3.3.1	General	4-11
4.3.3.2	Power Processor	4-11
4.3.3.3	Thruster/Thruster Gimbal	4-12
4.4	Interface Definition	4-12
4.4.1	Electrical	4-12
4.4.1.1	Power Distribution	4-12
4.4.1.2	Gimbal Electronics	4-13
4.4.1.3	Thruster Controller	4-13
4.4.2	Mechanical	4-13
4.4.3	Thermal	4-14

		Page
4.4.4	Propellant	4-14
4.5	Performance Description	4-14
4.5.1	Propulsion	4-14
4.5.1.1	Thrust Magnitude	4-14
4.5.1.2	Throttling	4-15
4.5.1.3	Startup	4-15
4.5.1.4	Shutdown	4-15
4.5.1.5	Lifetime	4-15
4.5.1.6	Thrust Magnitude Variation	4-16
4.5.2	Thrust Vector Control	4-16
4.6	Physical Characteristics and Constraints	4-16
4.6.1	Mass	4-16
4.6.2	Power	4-16
4.6.3	Environmental	4-16
4.6.4	Configuration	4-16
4.7	Development History	4-17
4.7.1	Background	4-17
4.7.2	Current Program	4-17
4.8	Applicable Documents Enclosed	4-18
4.9	Ground Support Equipment	4-19
4.9.1	Engine System Test Facility	4-19
4.9.1.1	Vacuum Facility Description	4-19
4.9.1.2	Test Hardware Mounting	4-21
4.9.1.3	Test Hardware Accommodations	4-22
4.9.1.4	Utilities	4-23

		Page
4.9.2	Mechanical Ground Support Equipment	4-36
4.9.2.1	Fabrication Fixtures	4-36
4.9.2.2	Test Fixtures	4-36
4.9.2.3	BIMOD Handling and Display Fixtures	4-36
4.9.2.4	Shipping Container	4-36
TABLES		
4.5.1.1-1	BIMOD Thrust Performance	4-37
4.5.1.1-2	J-Series Thruster Performance - Linear Throttle Profile Case	4-38
4.6.1-1	BIMOD Engine System Mass Breakdown	4-39
4.6.2-1	BIMOD Power Requirements (watts)	4-40
4.7.2 1	BIMOD Development and Test Program	4-41
4.9.1.4-1	Test Facility Power System Interlock Levels and Operant Conditions	4-42
4.9.1.4-2	Potential Engine System Test Configurations . .	4-43
FIGURES		
4.3.1-1	BIMOD Electrical Block Diagram	4-44
4.3.2.1-1	BIMOD Engine System	4-45
4.3.3.2-1	Power Processor/Thermal Control Assembly . . .	4-46
4.5.1.2-1	Thruster Operating Envelope	4-47
4.7.2-1	BIMOD Engine System	4-48
4.7.2-2	BIMOD Test Installation	4-49
4.9.1.1-1	Electric Propulsion Laboratory - Tank 6	4-50
4.9.1.1-2	Drawing of Electric Propulsion Laboratory - Tank 6	4-51

		Page
4.9.1.1-3	Bell Jar W-1 on Tank 6	4-52
4.9.1.1-4	Cold Wall Inside the W-1 Bell Jar	4-53
4.9.1.3-1	Three LIMOD Array Mounted on W-1 Support Structure	4-54
4.9.1.3-2	BIMOD Simulator Mounted to W-1 Support Structure	4-55
4.9.1.4-1	Engine System Test Facility Power Flow	4-56
4.9.1.4-2	Solar Array Simulator Functional Diagram	4-57
4.9.1.4-3	Solar Array Simulator Output Circuit Schematic .	4-58
4.9.1.4-4	Solar Array Simulator Reference Circuit Schematic	4-59

4.0 BIMOD Engine System

4.1 Reference Documents

4.1.1 Sharp, G. R.: A Thruster Subsystem Module (TSSM) for Solar Electric Propulsion. AIAA Paper 75-406, New Orleans, LA, 1975.

4.1.2 Cake, J. E.; Sharp, G R.; Oglebay, J. C.; Shaker, F. J.; and Zavesky, R. J.: Modular Thrust Subsystem Approaches to Solar Electric Propulsion Module Design,. AIAA Paper 76-1062, Key Biscayne, Florida, 1976.

4.1.3 Sharp, G. R.; Cake, J. E.; Oglebay, J. C.; and Shaker, F. J.: A Mass Study for Modular Approaches to a Solar Electric Propulsion Module. NASA TM X-3473, 1977.

4.1.4 Finke, Robert C.; Holmes, Arthur D.; and Keller, Thomas A.: Space Environment Facility for Electric Propulsion Systems Research. NASA TN D-2774, 1965.

4.1.5 Kolecki, Joseph C.; and Gooder, Suzanne, T.: Laboratory 15 KV High Voltage Solar Array Facility. NASA TM X-71860, 1976.

4.1.6 Data Systems Development and Operations Branch: Escort - A Minicomputer Based Data Acquisition and Display System Tailored to the Specific Needs of Research Test Facilities at the NASA - Lewis Research Center, Cleveland, Ohio. May 1977.

4.2 Functional Requirements

1) The BIMOD engine system shall convert unregulated solar array power into thrust.
2) The BIMOD engine system shall accept regulated bus power to support its housekeeping functions.
3) The BIMOD engine system shall respond to external control required for normal and off normal thruster and power processor operations. These external control functions shall include executing thruster start, stop, and throttle sequences, correcting for anomalies, and processing power processor interrupt signals.
4) The BIMOD engine system upon external command shall provide two axis gimballing of ion thrusters.
5) The BIMOD engine system shall distribute mercury propellant to the ion thrusters.
6) The BIMOD engine system shall maintain all components within operational and non-operational temperature limits.
7) The BIMOD engine system shall provide structural support for its components and subassemblies.

4.3 Functional Description

4.3.1 Electrical

4.3.1.1 General

The BIMOD electrical system shall be comprised of two power processors, two thrusters, two thruster gimbal systems, and two mercury propellant valves (figure 4.3.1-1).

4.3.1.2 Power Processor

Each power processor shall receive 200 to 400 VDC power from the power distribution unit of the interface module and convert this power to the twelve power supply outputs required to operate a thruster. This conversion shall be accomplished by a silicon controlled rectifier (SCR) series resonant inverter for the screen and accelerator supplies, an SCR series resonant inverter for the discharge supply, and a transistor series resonant inverter with nine output regulators for the remaining supplies. Control of the twelve supplies to execute start, stop, and throttle functions shall be accomplished by set point commands from the thruster controller in the interface module.

Telemetry data shall be obtained by telemetry commands from the thruster controller. The power processor shall automatically control the beam current, discharge voltage, and neutralizer keeper voltage of the thruster by means of feedback control loops.

The power processor shall also receive 23 to 33 VDC power from the power distribution unit for its housekeeping supplies.

Section 6.0 should be consulted for a complete description of the power processor.

4.3.1.3 Thruster

Each thruster shall receive power supplied by its power processor and convert it into thrust. Mercury is vaporized by heaters in the thruster and then ionized in the discharge chamber. The mercury ions drift toward the screen and grid where they are accelerated by the high voltage between the screen and accelerator grids and are exhausted

at a high velocity, producing thrust. Electrons are added to the exhaust beam to neutralize it.

Section 5.0 should be consulted for a complete description of the thruster.

4.3.1.4 Thruster Gimbal

The direction of the thrust vector shall be changed by gimballing the thrusters. Each gimbal shall be driven by two stepper motors and its orientation derived from two resolvers. The gimbals shall be controlled by commands from the mission module computer.

Section 7.0 should be consulted for a complete description of the gimbal.

4.3.1.5 Mercury Propellant Valve

Mercury propellant flow to each thruster shall be turned on and off by a mercury propellant valve. The valve shall be a latching type solenoid valve where pulsing one coil opens the valve and pulsing the other coil closes the valve. It is anticipated that all valves will

be commanded open via ground command at the beginning of the mission and will be left in the open position.

Section 13.0 should be consulted for a complete description of the mercury propellant valve.

4.3.2 Mechanical

4.3.2.1 General

The BIMOD is an integrated assembly of two power processors, two thrusters, two thruster gimbals, a heat pipe/radiator subassembly, and supporting structure. As shown in figure 4.3.2.1-1, the two power processors are mounted to two heat pipe evaporator saddle assemblies. The heat pipes extend to remote space radiators which are attached to the power processors and are supported by an aluminum truss. The base of the truss is mounted to the four columns on the sides of the power processors. The thruster and thruster gimbals are mounted to the far end of the truss. Harnessing and mercury propellant feed lines and valves are supported along the truss.

Section 9.C should be consulted for more detail on the BIMOD structure.

4.3.3 Thermal

4.3.3.1 General

The required temperature environments of the BIMOD components shall be maintained by a combination of variable conductance heat pipes, radiators, multilayer insulation, and heaters.

4.3.3.2 Power Processor

The two power processors are mounted to opposite sides of two heat pipe evaporator saddle subassemblies and are wrapped with a multilayer insulation blanket. An exploded view of figure 4.3.2.1-1 is provided in figure 4.3.3.2-1 which shows the assembly of the power processors and heat pipe saddles. Three heat pipes are embedded in each evaporator saddle, with one heat pipe a redundant pipe. The mounting arrangement of the heat pipes within the saddle allows for heat dissipated from either power processor to be distributed to both heat pipe radiators.

4.3.3.3 Thruster/Thruster Gimbal

Multilayer insulation is placed between the thruster and thruster gimbal motors to provide the proper thermal environment for each and to prevent solar flux from impinging on the back of the radiators.

Section 8.0 should be consulted for more detailed information on the heat pipes and Section 9.0 for the thermal control subsystem.

4.4 Interface Definition

4.4.1 Electrical

4.4.1.1 Power Distribution

The power distribution unit in the interface module will provide the required unregulated and regulated power to operate each BIMOD.

a) The power distribution unit will provide nominal 200 to 400 VDC power to each power processor.

b) The power distribution unit will provide 23 to 33 VDC power to the housekeeping supplies of the power processors and to the mercury propellant valves.

c) The power distribution unit will provide excitation voltages of TBD VDC to the BIMOD temperature and pressure transducers. Transducer outputs signals will be conditioned and formatted by the power distribution unit.

4.4.1.2 Gimbal Electronics

The gimbal electronics in the interface module will provide the drive signals of 23 to 33 VDC to operate the gimbal stepper motors and will provide 11 VAC, 400 Hz power at .05A current to each gimbal angle resolver.

4.4.1.3 Thruster Controller

The thruster controller in the interface module will provide commands to and receive telemetry from each power processor as described in applicable document 4.8.1, Command and Telemetry Codes of Power Processors for the 30cm Ion Thruster.

4.4.2 Mechanical

The BIMOD will be mounted to the interface module truss at the four mounting points as shown on LeRC Drawing CF 638168, BIMOD Thrust Module Interface Control Drawing. (applicable document 4.8.2).

4.4.3 Thermal

A multilayer insulation blanket placed across the top of each BIMOD will assure thermal isolation between the BIMOD and the interface module.

4.4.4 Propellant

Mercury propellant tanks within the interface module will distribute mercury to the ion thrusters through individual distribution lines in the BIMOD. Field joints will be used in the distribution lines between the BIMOD and the interface module.

4.5 Performance Description

4.5.1 Propulsion

4.5.1.1 Thrust Magnitude

The BIMOD shall be capable of providing the nominal thrust and specific impulse as a function of input power listed in table 4.5.1.1-1. The corresponding performance at the thruster and power processor level is listed in table 4.5.1.1-2.

4.5.1.2 Throttling

1) The BIMOD shall be capable of throttling each thruster over the thruster voltage - current envelope identified in figure 4.5.1.2-1.

2) Throttling within this envelope shall be at beam current increments of .1A within 30 seconds and shall be in a direction that does not result in exceeding system input power limits.

4.5.1.3 Startup

The BIMOD shall be capable of starting the thruster and providing stable operation at .75A beam current within a nominal time of 43 minutes from start of thruster preheat.

4.5.1.4 Shutdown

The BIMOD shall be capable of providing a normal shutdown of the power processor into a standby mode within TBD minutes.

4.5.1.5 Lifetime

Each thruster/power processor combination shall be capable of providing operation equivalent to 15,000 hours when operated at 2 amp beam current.

4.5.1.6 Thrust Magnitude Variation

Thrust magnitude errors are TBD.

4.5.2 Thrust Vector Control

The BIMOD shall be capable of providing thruster gimbal travel angles of $\pm 35^{o}$ about the y axis and $\pm 16^{o}$ about the x axis as defined in figure 4.3.2.1-1.

4.6 Physical Characteristics and Constraints

4.6.1 Mass

The estimated mass of the BIMOD is 137.5kg. A breakdown of the BIMOD mass is listed in table 4.6.1-1.

4.6.2 Power

The power required of the power distribution unit by the BIMOD shall not exceed the estimated values given in table 4.6.2-1.

4.6.3 Environmental

The BIMOD shall be compatible with the structural and thermal design criteria identified in Section 9.0.

4.6.4 Configuration

The configuration of the BIMOD is defined by LeRC drawing CF 638168, BIMOD Thrust Module Interface Control Drawing (applicable document 4.6.2)

4.7 Development History

4.7.1 Background

As discussed in Section 3.7, the BIMOD concept was developed in 1975. The concept evolved from an earlier one which integrated a single power processor, thruster, thruster gimbal, heat pipe/radiator/louver thermal control, propellant tank, and structure into a single module (see reference document 4.1.1). Starting in late 1975, a trade-off study was conducted at the engine system level in parallel with the functional model power processor design and thrust subsystem definition activities. The BIMOD was selected in mid 1976 over two competing concepts primarily because of the thermal redundancy inherent in the design. (Reference document 4.1.2 and 4.1.3). There was little difference in mass among the three concepts. Detailed design of the BIMOD continued at a low level through 1977. Procurement and fabrication of long lead items occurred in 1978.

4...2 Current Program

A mass simulation model of the BIMOD has been completed and is ready to enter vibration testing (see figure 4.7.2-1). The mass of the BIMOD simulation model is in close agreement with the mass estimates given in table 4.6.1-1. The live BIMOD will be assembled in July 1979. Upon completion of assembly, the BIMOD will enter a test program which will

1) obtain engineering data on the BIMOD design, performance, and interfaces; and 2) characterize the interfaces that are unique to ion drive. A summary of the test program is given in table 4.7.2-1. A schematic of the test installation for the BIMOD test program is given in figure 4.7.2-2. Further detail may be found in applicable document 4.8.4, BIMOD Test Plan and in Section 4.9.1, Engine System Test Facility.

4.8 Applicable Documents Enclosed

4.8.1 Command and Telemetry Codes of Power Processors for the 30 cm Ion Thruster, Revision 10. NASA Lewis Research Center, Solar Electric Propulsion Office, December 1978.

4.8.2 BIMOD Design Drawing List, NASA Lewis Research Center, May 1979.

4.8.3 BIMOD Ground Support Equipment Drawing List, NASA Lewis Research Center, May 1979.

4.8.4 Ion Drive BIMOD Thrust Module Test Plan. NASA Lewis Research Center, Solar Electric Propulsion Office, November 1978.

4.9 Ground Support Equipment

4.9.1 Engine System Test Facility

The Engine System Test Facility provides the capabilities required to test SEP engine systems under simulated mission conditions for the test configuration identified in figure 4.7.2.2. The facility also includes the capabilities necessary for testing and integrating subsystem elements such as ion thrusters and power processors. These capabilities include vacuum in the 10^{-6} to 10^{-7} torr range, thermal environment from liquid nitrogen temperature to the equivalent thermal input of 1 sun, DC power at 300 $\pm$100 volts and 28 $\pm$5volts, and centralized data collection, processing, and display.

4.9.1.1 Vacuum Facility Description

The Engine System Test Facility is a part of the Electric Propulsion Laboratory of the Lewis Research Center which was designed for testing ion and plasma thrusters, spacecraft and other equipment in simulated space environments. Reference document 4.1.4 details the laboratory as it was configured in 1965. The Laboratory Operations Building houses two space-environment tanks plus auxiliary and test equipment and shop support facilities. The larger of the two tanks - Tank 6 - houses the Engine System Test Facility. This tank, shown in figures 4.9.1.1-1 and 4.9.1.1-2, is 7.6 meters (25 feet) in diameter by 21.3 meters

(70 feet) long. Normal pressure in the tank with thrusters running ranges from $2x10^{-6}$ to $2x10^{-7}$ torr. Reference document 4.1.4 contains detailed information on the tank pumping system, pressure instrumentation, and performance. The test facility currently occupies the largest of the ports, W-1, which is a bell jar 3.1 meters (10 feet) in diameter and 3.1 meters long (figure 4.9.1.1-3). Tank 6 also includes two .93 meter (3 foot) diameter ports for individual thruster operations and a number of small ports for thruster component tests.

The W-1 bell jar is separated from the main tank by a 3.1 meter (10 foot) diameter vacuum gate valve of stainless steel construction. The time required to raise or lower the valve is five minutes. Such isolation (also present on other Tank 6 test facilities) permits rapid test hardware cycling without disturbing other test operations and without the need to bring the main tank to atmosphere. One work-day turn-arounds, including hardware installation and/or removal, are not uncommon.

The W-1 bell jar includes a liquid nitrogen cooled baffle as does the main chamber. The baffle-covered portion of the bell jar wall is shown in cross-section in figure 4.9.1.1-4. With full nitrogen flow to the baffle, test hardware in the bell jar can be cooled to -191°C.

This temperature is limited by the presence of the room temperature W-1 end cap. In addition, an available tungsten iodide lamp bank can be installed in the lower sector of the bell jar to provide the equivalent thermal input of 1 sun (1.4 KW/M).

4.9.1.2 Test Hardware Mounting

In the current configuration, test hardware in the W-1 bell jar is mounted from the 3.1 meter end cap. This arrangement provides convenient access to the hardware when the end cap is in the rolled back position. All test hardware vacuum penetrations - for the electrical harnesses, the mercury propellant feedlines and power processor coolant lines - are carried on a .93 meter (3 foot) flange mounted to the end cap. This arrangement shown in figure 4.9.1.1-3 greatly simplifies the task of moving test hardware into and out of the bell jar and also facilitates hardware check-out and servicing when the end cap is in the rolled-back position. The end cap flange currently contains thirty-seven 10cm (4 inch) flanges which actually carry the penetrations, an arrangement which provides a high degree of flexibility. End cap modifications are currently underway to increase the number of available 10cm flanges to seventy-nine by the addition of a 33cm (13 inch) spool-piece carrying 24 small flanges and a new .93 meter flange with 55 small flanges.

4.9.1.3 Test Hardware Accommodations

In its present configuration, the W-1 bell jar is able to accommodate up to three BIMODs in the flight configuration. Figure 4.9.1.3-1 is a sketch of the end cap in the rolled-back position with a three BIMOD array installed on the supporting frame. As can be seen in the sketch, three BIMODs would fill the cross section of the 3.1 meter bell-jar. The BIMODs would also fill the available bell jar length. In the current test program, the live BIMOD will be located in the center bay. Testing of a thrust subsystem with more than six thrusters or integration testing the interface module in the flight configuration would require modification of the support frame and the facility. Facility modifications could include the addition of spool-pieces to the bell jar.

The W-1 facility presently also includes support fixtures of two types for thrust subsystem component testing. The first is the BIMOD Simulator which is shown in figure 4.9.1.3-2 with two thruster mass models installed and is located in the lower test bay. The Simulator which has the same volume of a live BIMOD consists of a removable

electronic equipment bay and a support truss for two ion thrusters. The equipment bay is 1.6 meters by 1 meter by 0.45 meters and is used for thermal/vacuum integration testing of power processors and thrusters. In addition to thrusters and power processors, the BIMOD Simulator is also a test bed for mercury propellant solenoid valves and thruster gimbal systems. The second type of W-1 test fixture is a simple truss structure for two gimbal-mounted thrusters located in the upper truss bay.

The configuration of the end cap supporting frame is identified in applicable document 4.8.3 as LeRC Drawing CR 622730, Adapter Structure for Three Engine Systems - EPL Tank 6. The BIMOD Simulator is described in applicable document 4.8.3 as LeRC Drawing CR 622740, BIMOD Simulator for EPL Tank 6 Engine System Test Stand.

4.9.1.4 Utilities

The W-1 facility provides the basic utilities necessary for thrust subsystem and subsystem component testing. These utilities include mercury propellant feed systems, power processor cooling systems, DC input power for the power processors, a thruster command system and an automatic data collection and processing system. Other, more specialized utility requirements for specific tests are not presently part of the facility.

1) Propellant System - Each of the propellant systems for the six thrusters contains a single mercury reservoir which is manifolded to provide individual feedlines for the three thruster vaporizers. The reservoir has a capacity of 17 kilograms (38 pounds) which is sufficient for approximately 1100 hours of thruster operation at full power (2 amp beam). For test purposes, each vaporizer feedline includes a calibrated flow tube for measuring propellant flow rates for each thruster vaporizer. Simple line changes at the thruster permits flight-like operation of all three vaporizers from a single propellant feedline.

2) Cooling System - Power Processor cooling for live BIMOD thermal/vacuum testing is furnished by the BIMOD variable conductance heat pipe/radiator system which is described in Section 8. However, for routine BIMOD operation and for individual power processor testing, the use of liquid cooling baths provides greater operating flexibility and simplicity. For this purpose, the power processor heat pipe saddles also contain liquid cooling channels. Available cooling baths can maintain any desired power processor saddle temperature from $-10^{o}C$ to $+50^{o}C$.

3) Input Power - The primary DC power system is required to furnish the power processor input power for BIMOD operation in the Engine System Test Facility The

system must also support testing of individual power processors in the same facility. Each power processor requires a DC input power channel of approximately 3KW at 300 ±100 volts and approximately 100 watts at 28 ±5 volts. (Specific input power requirements are defined in Section 6.0). The power system described below is presently under construction with completion expected in August 1979. The W-1 Primary Power System provides six input power channels. At present, four are independent and two operate from a common power bus. The two-channel bus can be operated in either the bottom-grounded (0 to +V out) mode or as a center-tapped power source. Other power system capabilities include separating the BIMOD single point ground from the facility ground, inserting a solar array simulator into the power train, and potentially using an actual solar array for low output power BIMOD and/or individual power processor testing.

The Primary DC Power System (figure 4.9.1.4-1) consists of power control, grounding control, and system identification/status panels located in the Engine System Test Facility Control Center; DC power supplies, AC and DC control units, and the grounding electronics located in the Power Cage; and the DC Power Patch located

adjacent to the W-1 bell jar. An interlock system is included primarily for personnel protection, but it also provides limited hardware protection.

a) Power Control - The power control panel provides ON/OFF control and output voltage setpoints for each of the six power channels. There are three levels of ON/OFF control. The highest level is provided by a total power system permissive (key lock) and emergency shutdown. This is followed by ON/OFF control of the AC input power to the DC power supplies of each power channel. The final level is the simultaneous application of the 300 volt and the 28 volt power to a power processor. NOTE: the interlock system (see below) exercises pre-emptive control over the power system AC and DC contactors. The output voltages for each power channel are set by potentiometer adjustment on the power panel. The power processor input voltages and currents for each power channel are monitored on a digital panel meter. In addition, the 300 volt line of each power channel includes a current shunt and meter relay for over-current protection.

b) DC Power Supplies - The system DC power is produced by an assemblage of commercial DC power supplies: two Sorenson DCR300-35A supplies (0 to 300 volts, 0 to 5 amps) operated in series for the two-channel, center-tappable bus; four Sorenson DCR6 600-18A supplies (0 to

600 volts, 0 to 18 amps) for the four independent power channels; and six Kepco JQE36-8 supplies (0 to 36 volts 0 to 8 amps) for the 28 volt input power. Any or all of these supplies can readily be paralleled to provide for larger capacity common bus operations. Also, the solar array simulator (see below) can be inserted in the power train of any of the channels, including the two-channel common bus, and still retains the output monitoring and over-current protection of the channel(s). At present, only the two-channel bus power supplies are isolated from facility ground for floating operation. The isolation capability for these two channels is greater than 2 KV. The remaining channels have only the equipment-standard 500 volts input-to-output isolation.

c) Power Patch - All six power channels are terminated at a patch panel located adjacent to the W-1 bell jar. There any channel may be connected to a BIMOD or individual power processor located either in the bell jar for vacuum testing or in one of the air-testing cages. The power patch also provides 300 volt and 28 volt test points for oscilloscope monitoring of the current and voltage waveforms on each power channel.

d) Grounding - In the W-1 test facility, all system elements are tied to a single point ground, analogous to spacecraft common. The bell jar test support fixture

(see Section 4 9.1.3) is subdivided into four electrically isolated elements which are also isolated from the facility. The upper test bay, the center test bay (BIMOD), the lower test bay (BIMOD Simulator), and the support structure. Each of these elements carries its own independent single point ground. Under general test operations, these grounds are tied to the facility ground by normally closed relays. For special test purposes, each single point can be separated from facility ground independently. However, the facility does require special configuration and the interlock system has pre-emptive control for personnel protection. The grounding control panel displays the status of the grounding interlocks and indicates when a single point ground is separated from the facility ground.

e) Interlock System. The normal safety and [illegible] possible [illegible] provided by the interlock system. [illegible] into the system [illegible] to procedures [illegible] of interlock [illegible] entire [illegible] power [illegible] the single [illegible]

cessor. The third level is the permissive for isolating the single point grounds from facility ground. Table 4.9.1.4-1 identifies these various interlock levels and the conditions that invoke them. The status of each interlock is displayed in the Control Center.

f) Identification/Status - In the Control Center, the identification/status panel defines all operational engine systems by thruster number, the location of the power processor supplying that thruster, and the identity of the power channel being used. The engine system identification coding is self-defined (carried in the interconnecting harnesses) and incompletely defined systems are inoperative. Table 4.9.1.4-2 displays the elements available to form the potential engine system configurations by merely selecting one from each column. The panel also displays the operational status of each defined thruster system - interlocks open or closed, power processor on or off, and thruster on or off. The power system configuration (bottom grounded or center-tapped) is also displayed.

g) Solar Array Simulator - A solar array simulator (SAS) is available to serve as the power system identified in figure 4.7.2-2. The maximum power range is from 150 to 7500 watts. This represents an open circuit

C-2

voltage from 50 to 300 volts and a short circuit current from 4 to 36 amps.

The SAS voltage-current characteristics closely simulate that of an actual solar array. Four illuminated solar cells were used in series as the controlled element in the SAS. The illuminated solar cells provide a true solar cell characteristic and permit the option of simulating changes in this characteristic due to variations in solar intensity and/or temperature of the solar array. This is accomplished by changing the illumination and/or temperature of the control cells.

The output impedance of the SAS closely approximates that of an actual solar array. This is indicated by the response time and the dynamic path of the output to a step change in load closely approximating that of an actual solar array.

The functional diagram of the complete circuit is shown in figure 4.9.1.4-2. The output circuit operates as a dissipative voltage regulator which follows the reference input to the open circuit voltage (Voc) adjust control. The reference circuit generates the V-I characteristic curve that drives the output regulator. A voltage across shunt R10 proportional to the current in the output load is applied to the short

circuit current (I_{sc}) adjust control. The I_{sc} adjust control scales this signal and applies it to the input of amplifier AI. AI is a variable load, across the control solar cells, proportional to the current in the output load. Amplifier A2 measures the voltage across the solar cells and provides a reference signal to the output circuit proportional to this voltage. This reference signal corresponds to the required output voltage for the specified load current as defined by the solar array V-I characteristic curve.

The schematic diagram of the output circuit is shown in figure 4.9.1.4-3. Amplifier A3 is an integrator and summing function for the output circuit feedshock loop. The integrator also stabilizes the loop. Amplifier A4 inverts the signal.

The power output consists of four stages of current amplification capable of delivering a load current of 40 amps. Capacitor C8 is used to dampen internal oscillations in these stages.

The present design of the SAS is contained in one standard equipment rack except for the DC power supply. The bottom of the rack contains 40 water cooled transistor modules; 7 driver modules and 33 output

modules. A typical module is shown in figure 4.9.1.4-2. Each module consists of a printed circuit board, a 0.318 cm thick water cooled copper heat sink, and 10 parallel transistors with base and emitter resistors. Each board has a fuse in both the base drive and the emitter output lead. If a transistor fails in a shorted condition, these fuses open and remove that board from the circuit. The system will then continue to operate on the remaining boards. The upper portion of the rack contains the control electronics and indicator lights that identify blown fuses.

The reference circuit schematic diagram is shown in figure 4.9.1.4-4. The four solar cells in series were 0.4 cm by 1.0 cm, N on P, 10 ohm-cm silicon cells with a short circuit current rating of 10mA. The cells were chosen for their low value short circuit current, their representative characteristic curve, and their availability. Any type of solar cell can be used in the circuit, however, Al must be capable of sinking the short circuit current from the cells. The four cells in series provide an open circuit voltage of approximately 2.2 volts. Solar cell illumination is provided by an incandescent DC light source, variable in intensity from zero to

140 mW/cm^2 on the cells. The temperature of the cells is controlled by a variable temperature heatsink. Capacitors C1, C2, and C3 stabilize the SAS.

4) Solar Array - The Electric Propulsion Laboratory houses a 1 KW Solar Array Facility, which is described in reference 4.1.5. This solar array is not tied into the power system at present, but such a tie-in could readily be made. The installed capacity could provide approximately 3.5 amps at a nominal 300 volts - adequate to supply a single power processor operating a thruster at slightly less than a 1 amp beam. A straight-forward expansion of the solar array capacity to about 2 KW would support operation of a single thruster at a 1.5 amp beam or a BIMOD could be operated with both thrusters at the 0.75 amp (1/4 power) beam level.

5) Command System - The W-1 facility includes a thruster command system which is described in Section 11.7. The command system identified in figure 4.7.2 as "thruster control computer" is a precursor to a flight-type thruster controller. The system functions in two modes: manual, in which individual power processor commands are accepted and transmitted as is; and the automatic mode, in which engine system pseudo-commands (such as start-up, throttle, and shut-down) are used to direct computer operation and control of the thrust-

ers. In the automatic mode, the computer also continuously monitors all operating thrusters and will, if necessary, correct off-normal operating conditions, such as low mode, repetitive arcing and neutralizer outages. Both power processor commands and engine system pseudo-commands can be entered either on the Manual Input Unit (in binary) or on punched paper tape (in octal). The paper tapes also specify the times at which the commands or pseudo-commands are to be executed. This feature provides for extended periods of hands-off thruster operations with pre-determined profiles of start ups, throttles, and shut-downs. Thruster operational status and all data available via power processor telemetry are periodically logged by the system. The command system is currently being expanded from three to six command channels. A second stage of expansion will improve the man-machine interface to include English pseudo-commands (rather than binary or octal) and greatly increase the flexibility and speed of telemetry data processing and display.

6) Data System - The W-1 facility has access to an automatic data collection, processing and display system-Escort, which is described in reference 3.8. The test facility interface to the Escort system is the Test Control Computer identified in figure 4.7.2-2. Escort service for W-1 is intended to supplement the data available from the power processor telemetry

systems and to support the data needs of special tests, such as thermal/vacuum testing and interaction testing. There are up to 300 data channels available at present for test data over and above those channels reserved for facility instrumentation. Escort can provide acquired data in either millivolts or in engineering units along with time, date, and test identification information. Parameters derived from the acquired data (for example thrust, specific impulse, and input power) are also readily available on a real-time basis. Escort data is continuously updated and displayed on the Test Control Computer CRT with up to 16 available display formats. Important parameters (15 maximum) can also be displayed on digital panel meters. Hard-copy print-out of the displayed data can be obtained by push-button control or at specified time intervals. The data can also be transmitted to the Lewis Data Collector Facility for recording on legal record tape and/or subsequent central computer processing. Data transmissions to the Facility can be invoked either at predetermined intervals or in response to out-of-limits data.

4.9.2 Mechanical Ground Support Equipment

4.9.2.1 Fabrication Fixtures

1) BIMOD Assembly Fixture, LeRC drawing CF 622763, applicable document 4.8.3.

2) Heat Pipes and PPU Assembly Fixture, LeRC drawing CD 622762, applicable document 4.8.3.

4.9.2.2 Test Fixtures

1) Adapter Structure for Three Engine Systems-EPL Tank 6, LeRC drawing CR 622720, applicable document 4.8.3.

2) BIMOD Simulator for EPL Tank 6 Engine System Test Stand, LeRC drawing CR 622740, applicable document 4.8.3.

4.9.2.3 BIMOD Handling and Display Fixtures

1) BIMOD Display Roll Over Fixture, LeRC drawing CF 622764, applicable document 4.8.3.

2) Portable BIMOD Display Fixture, LeRC drawing CR 622765, applicable document 4.8.3.

3) Off Axis Roll Over Fixture, LeRC drawing CR 622766, applicable document 4.8.3.

4.9.2.4 Shipping Container

1) BIMOD Shipping Container, LeRC drawing CR 622742, applicable document 4.8.3.

Table 4.5.1.1-1 BIMOD Thrust Performance

POWER* BIMOD, WATTS	η BIMOD	I_{SP}, SECONDS	THRUST mN BIMOD
6252	.610	3020	259.6
4579	.552	2684	193.6
3529	.497	2492	147.8
2598	.435	2206	106.0
1907	.368	1962	74.2

η = Total BIMOD efficiency

I_{SP} = Specific impulse

* = Unregulated power defined at output of power distribution unit

Table 4.5.1.1-2 J-Series Thruster Performance - Linear Throttle Profile Case

Set Point	I_{Beam} a	V_{Screen} v	P_{TH} w	η_{TH}	η_{PPU}	η_{Total}	$P_{PPU\ In}$ w	I_{SP} sec	Thrust mN
1	2	1100	2700	.711	.872	.620	3096	3020	129.8
2	1.6	940	1927	.661	.850	.562	2267	2684	96.8
3	1.3	820	1431	.631	.819	.517	1747	2492	73.9
4	1.0	700	1008	.568	.784	.445	1286	2206	53.0
5	.75	600	710	.503	.752	.378	944	1962	37.1

where

P_{TH} = Thruster input pwoer

η_{TH} = Thruster efficiency

P_{PPU} = Power Processor input power

η_{PPU} = Power Processor efficiency

Table 4.6.1-1 BIMOD Engine System Mass Breakdown

Item	Mass, Kg	Comments
BIMOD Total	137.1	
Power Processors (2)	74.7	Functional Model
Thermal Control	21.0	
Thrusters (2)	20.7	J-Series Includes Mass of Harness to PPU
Thruster Gimbals (2)	6.8	
Truss and Struts	10.1	
Propellant Distribution	0.7	Valves, Field Joints, Lines
Miscellaneous	3.1	

Table 4.6.2-1 BIMOD Power Requirements (watts)

Item	Mission Mode (One Power Processor/Thrusters)					
	Off	Standby	Preheat	Heat	Min Power	Max Power
Unregulated 200 to 400V						
. Power Processor (each)	<2	25	300	375	875	3126
Regulated 28V						
. Power Processor (each)	--	84	90	95	100	100
. Thruster Gimbals (each)	--	--	--	--	25	25
. Instrumentation*	12	12	12	12	12	12
. Mercury Valves	32	--	--	--	--	---
. Heaters**	121***	110***	50***	15***	0	0

* Signal Conditioning Located in Interface Module
** Corresponds to Thermal Cold Case
*** Actual Value Depends on Resolution of Heater Circuits

Table 4.7.2-1 BIMOD Development and Test Program

OBJECTIVE 1: Obtain Engineering Data on Ion Drive Propulsion System Design, Performance and Interfaces

- Characterize Non Operating System Parameters
  - Mass Properties
  - Magnetic Properties
- Functional Test to Verify Operation Algorithms and Software Concepts
- Measure Temperature Distribution and Verify Thermal Design
- Vibration Test to Verify Mechanical Design
- Characterize System Performance Over Required Environmental Range
  - Efficiencies
  - Propellant Utilization
  - EMI Signatures
  - Solar Array and Power System
  - Command and Control
  - Ancillary Systems

OBJECTIVE 2: Characterize the Interfaces that are Unique to Ion Drive

- Gross Efflux Effects on Engineering Materials in Line-of-Sight
- Thruster Interactions with Science Instruments and Objectives
- Provide Data for Development and Verification of Analytical Techniques Required to Predict Ion Drive Spacecraft Particle and Field Distributions

Table 4.9.1.4-1 Test Facility Power System Interlock Levels and Operant Conditions

	Pers	Equip
Level 1 - Total System Shutdown and Grounding		
1. Access door to bell jar flange open	X	
2. Power cage door open	X	
3. Power patch access door open	X	
4. Single point ground cables open	X	X
5. Bell jar gate valve closed		X
6. Tank pressure 2X10-5 torr		X
7. Propellant solenoid valves closed		X
Level 2 - Single Power Channel Shutdown		
1. Power processor cage door open	X	
2. Data monitor unit door open	X	
3. Power processor over-temperature		X
4. Thruster computer permit off		X
Level 3 - Ground All Single Point Grounds		
1. Mercury reservoir cage door open	X	
2. Coolant system cage door open	X	
3. Non-floatable equipment connected	X	X

Table 4.9.1.4-2 Potential Engine System Test Configurations

Power Channel	Power Processor Location	Thruster Location
A	A1 - Air Location #1	1 - Lower Bay #1
B	A2 - Air Location #2	2 - Lower Bay #1
C	A3 - Air Location #3	3 - Center Bay #1
D	A4 - Air Location #4	4 - Center Bay #2
E	B1 - Center Bay #1	5 - Upper Bay #1
F	B2 - Center Bay #2	6 - Upper Bay #2
	B3 - Lower Bay #1	D - Load Simulator
	B4 - Lower Bay #2	
	C1 - 3-Inverter BB	

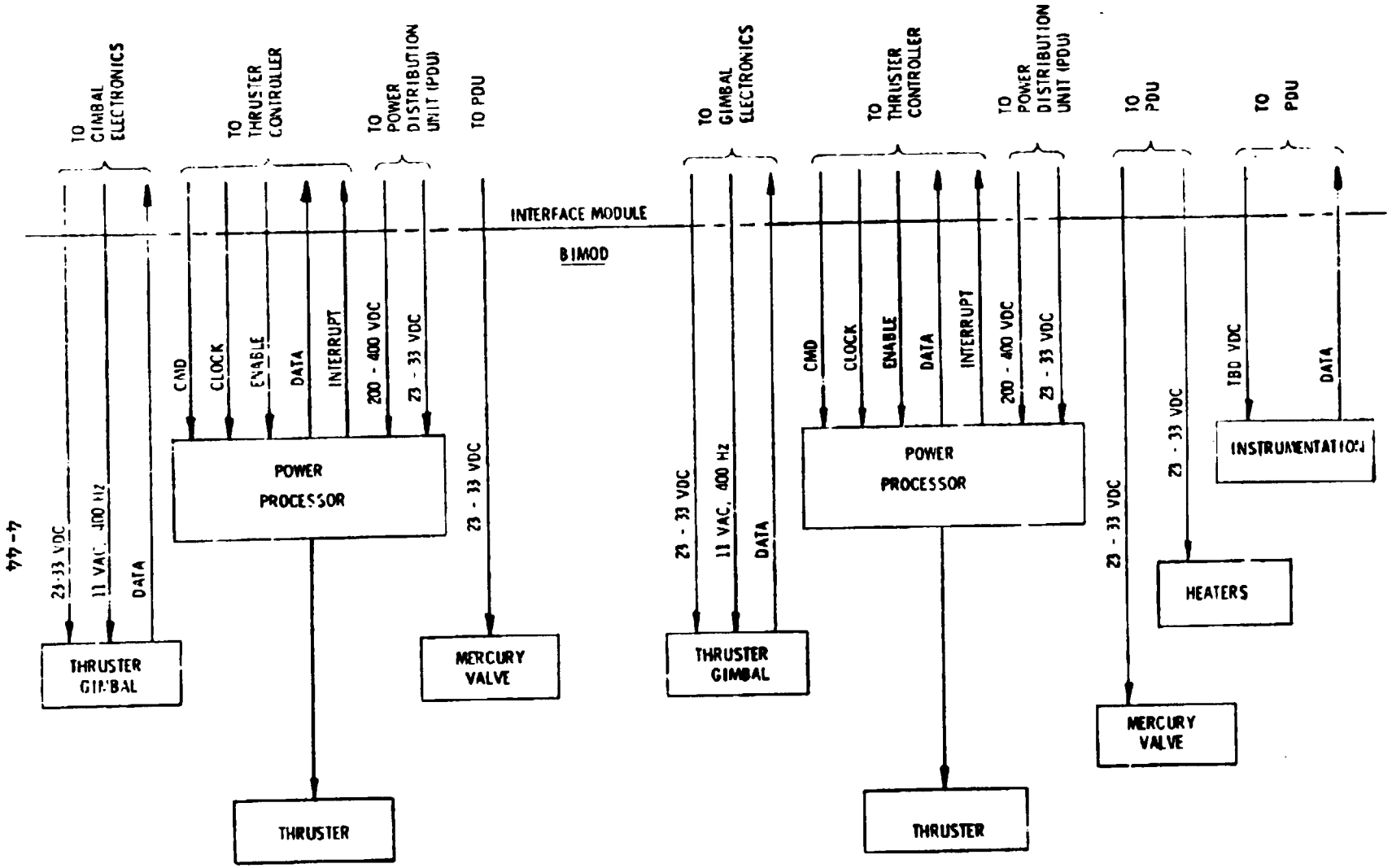

Figure 4.3.1-1 BIMOD Electrical Block Diagram

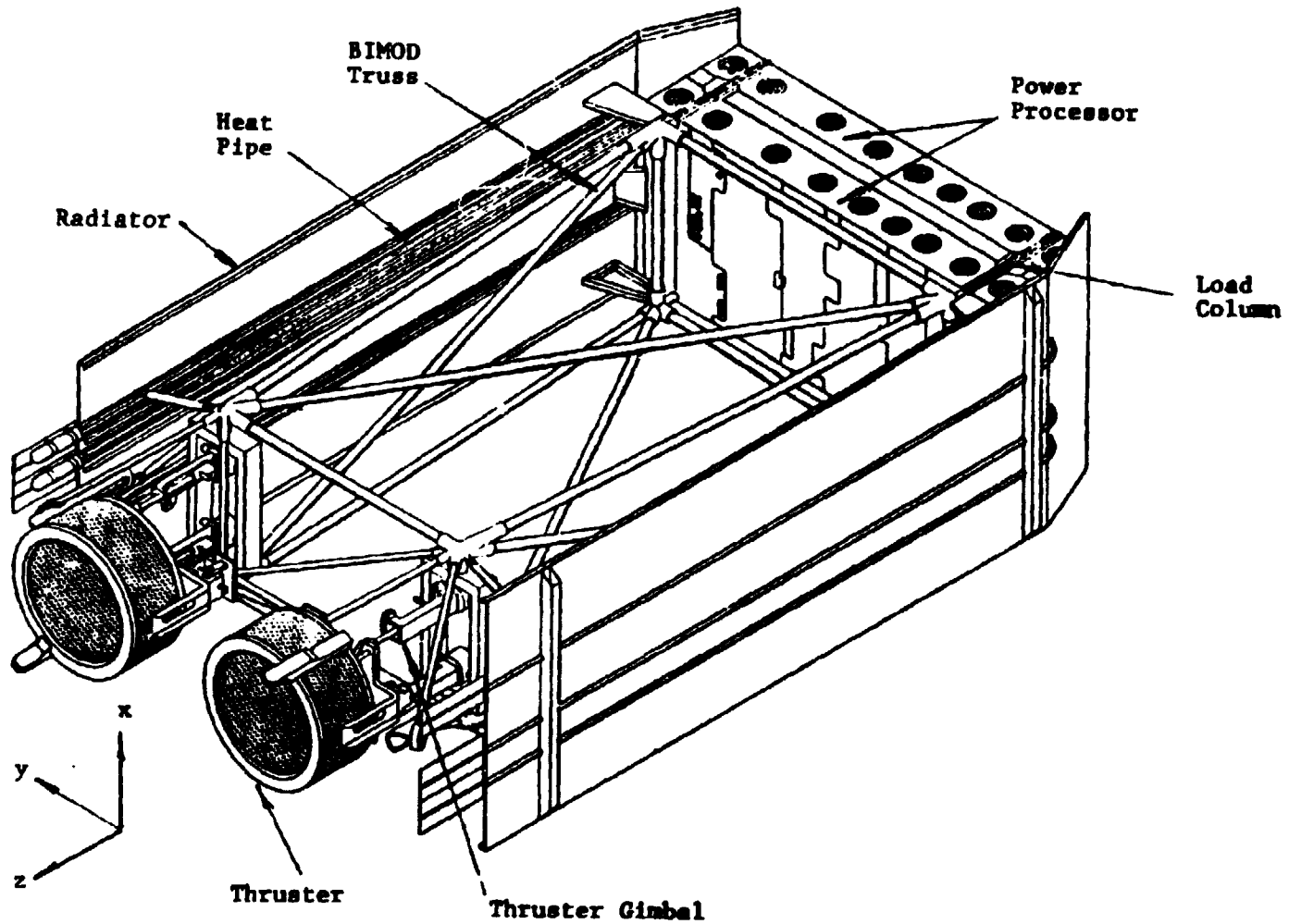

Figure 4.3.2.1-1 BIMOD Engine System

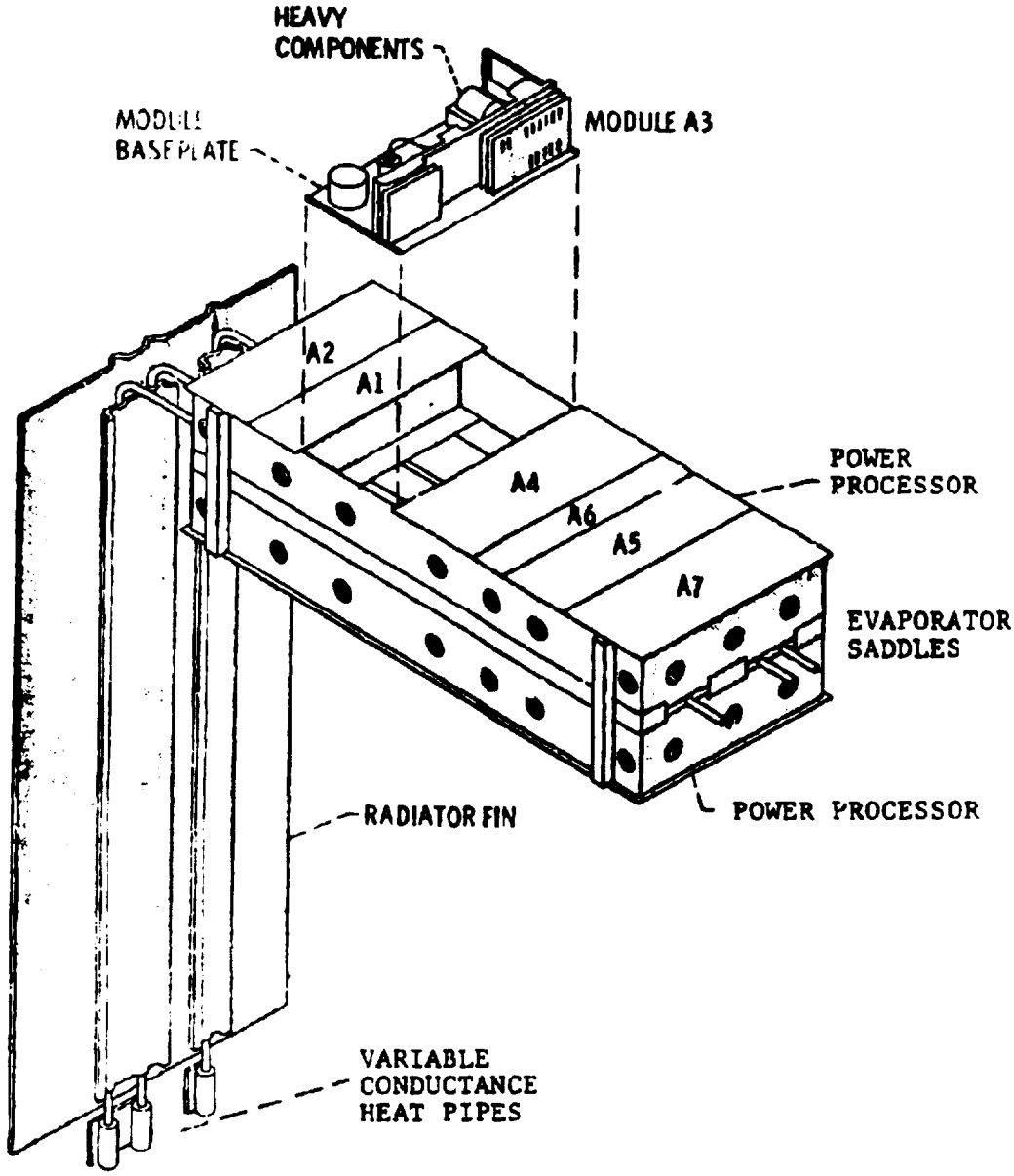

Figure 4.3.3.2-1 Power Processor/Thermal Control Assembly

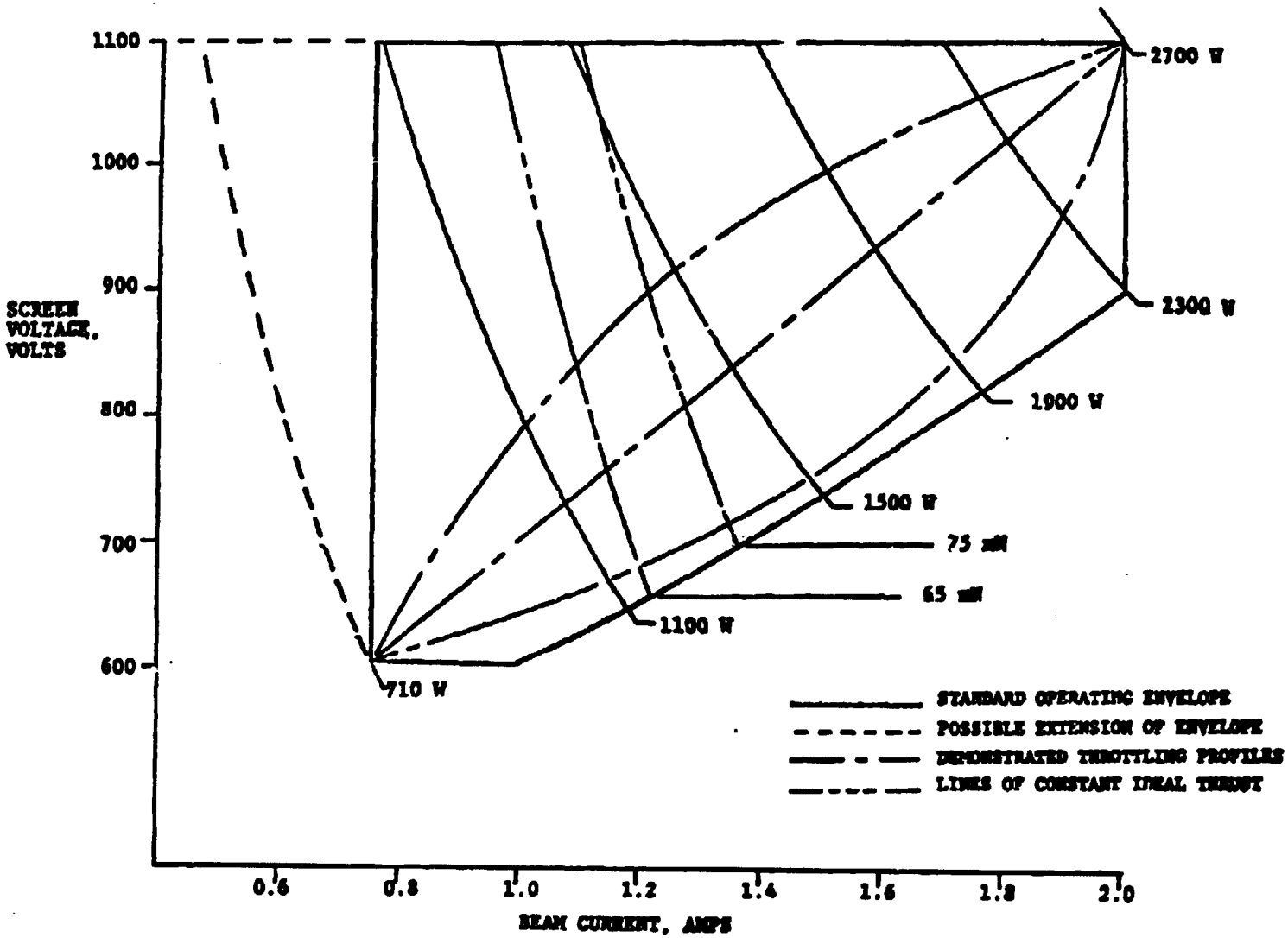

Figure 4.5.1.2-1 Thruster Operating Envelope

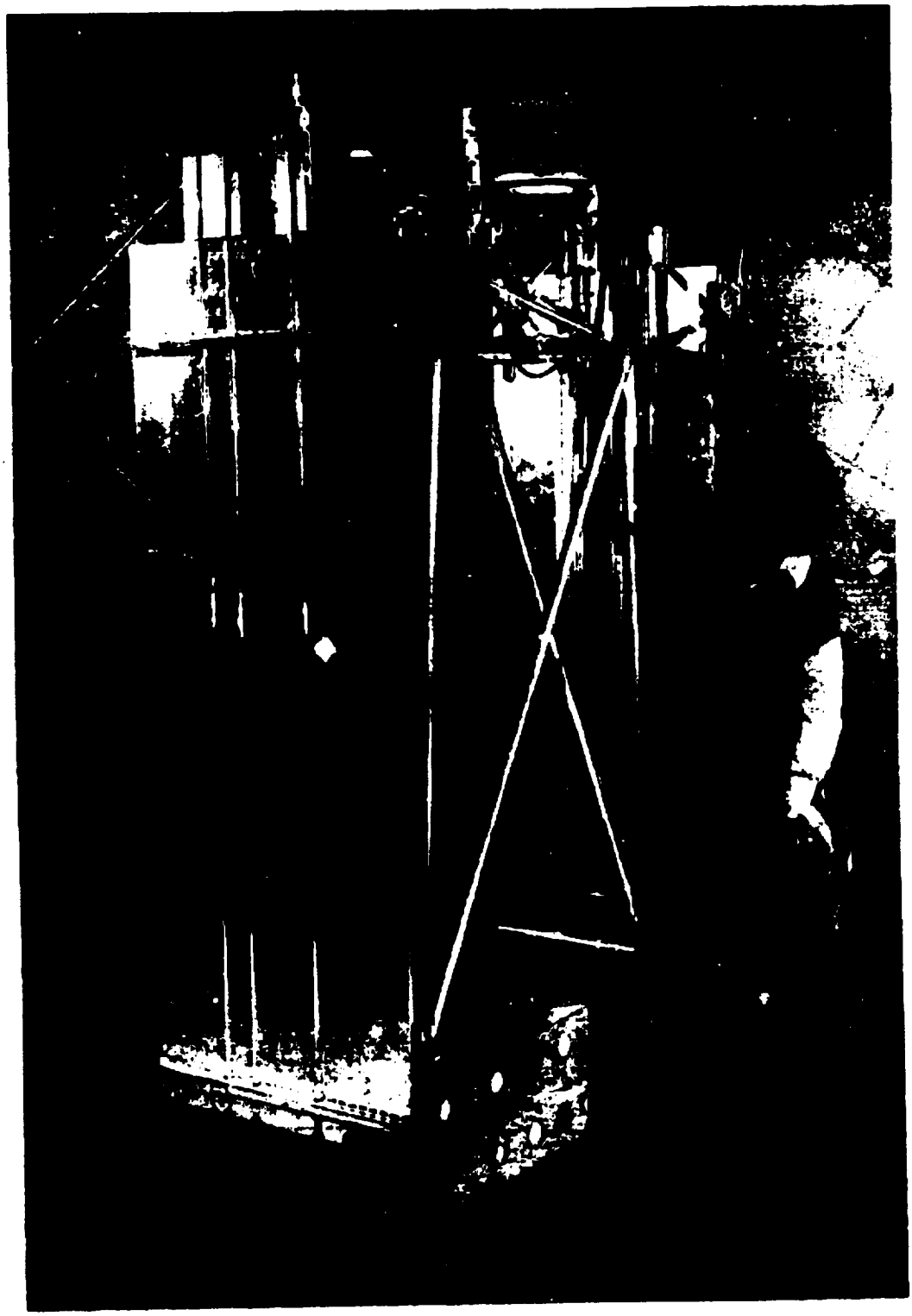

Figure 4.7.2-1 BIMOD Engine System

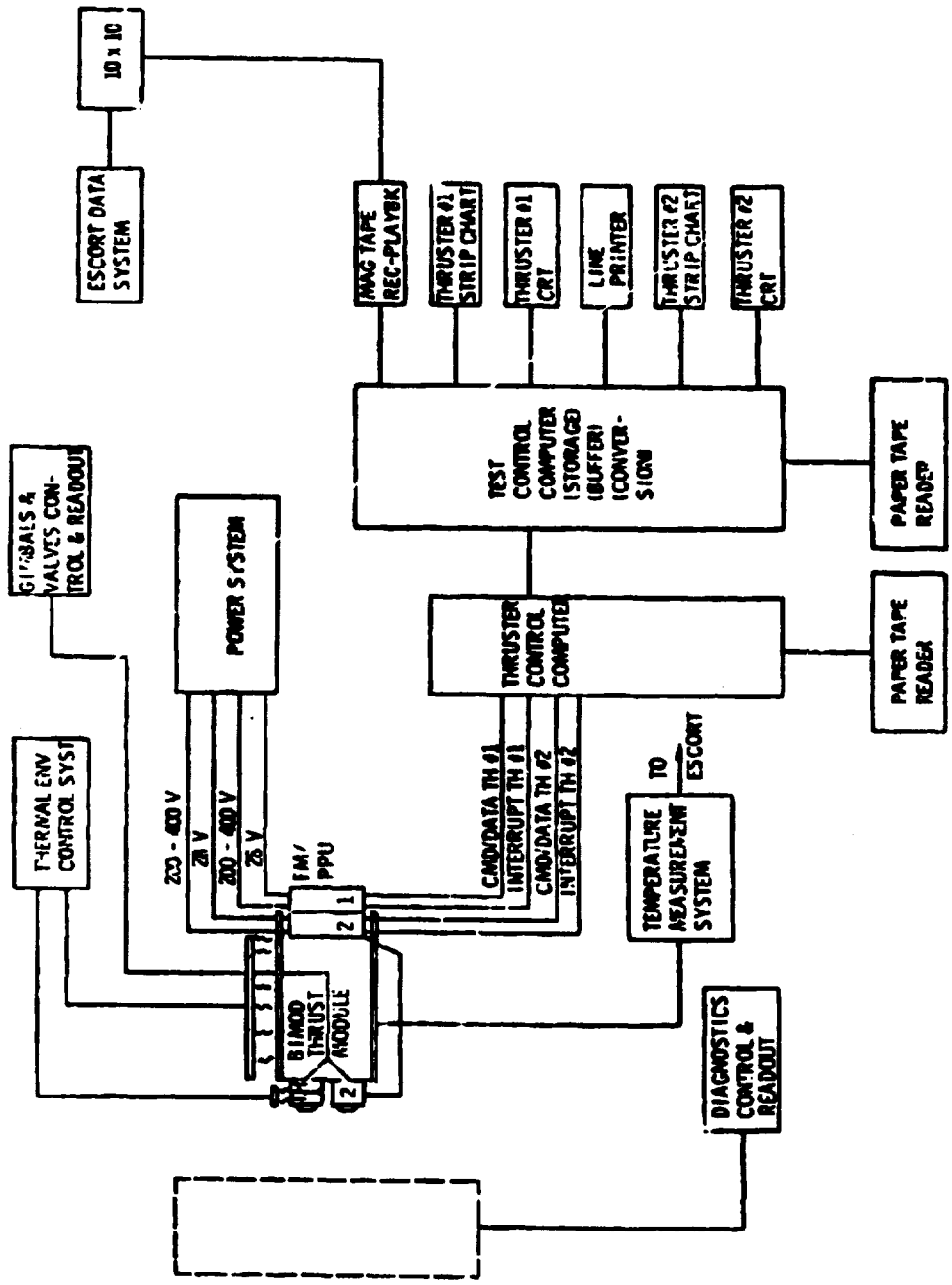

Figure 4.7.2-2 BIMOD Test Installation

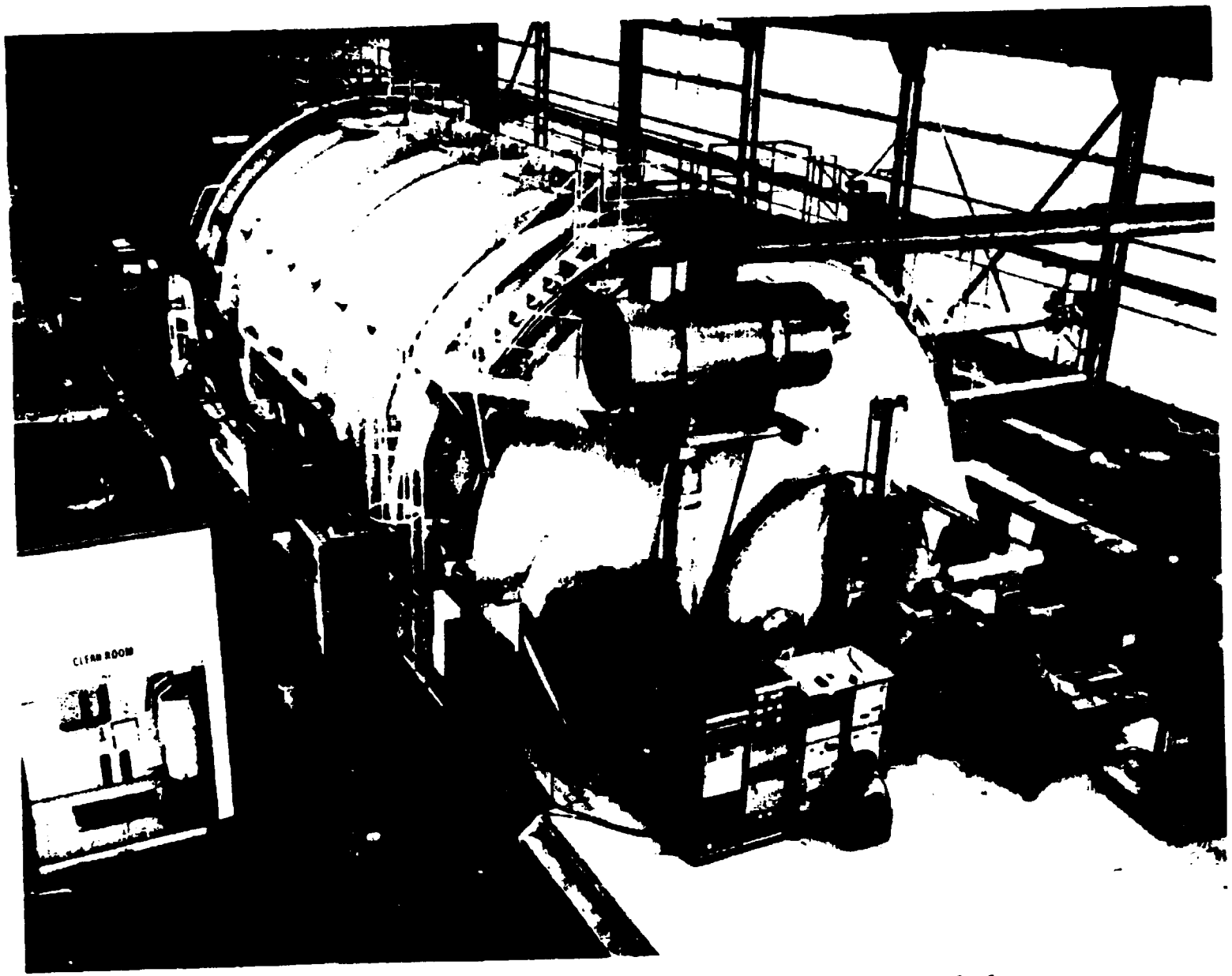

Figure 4.9.1.1-1 Electric Propulsion Laboratory - Tank 6

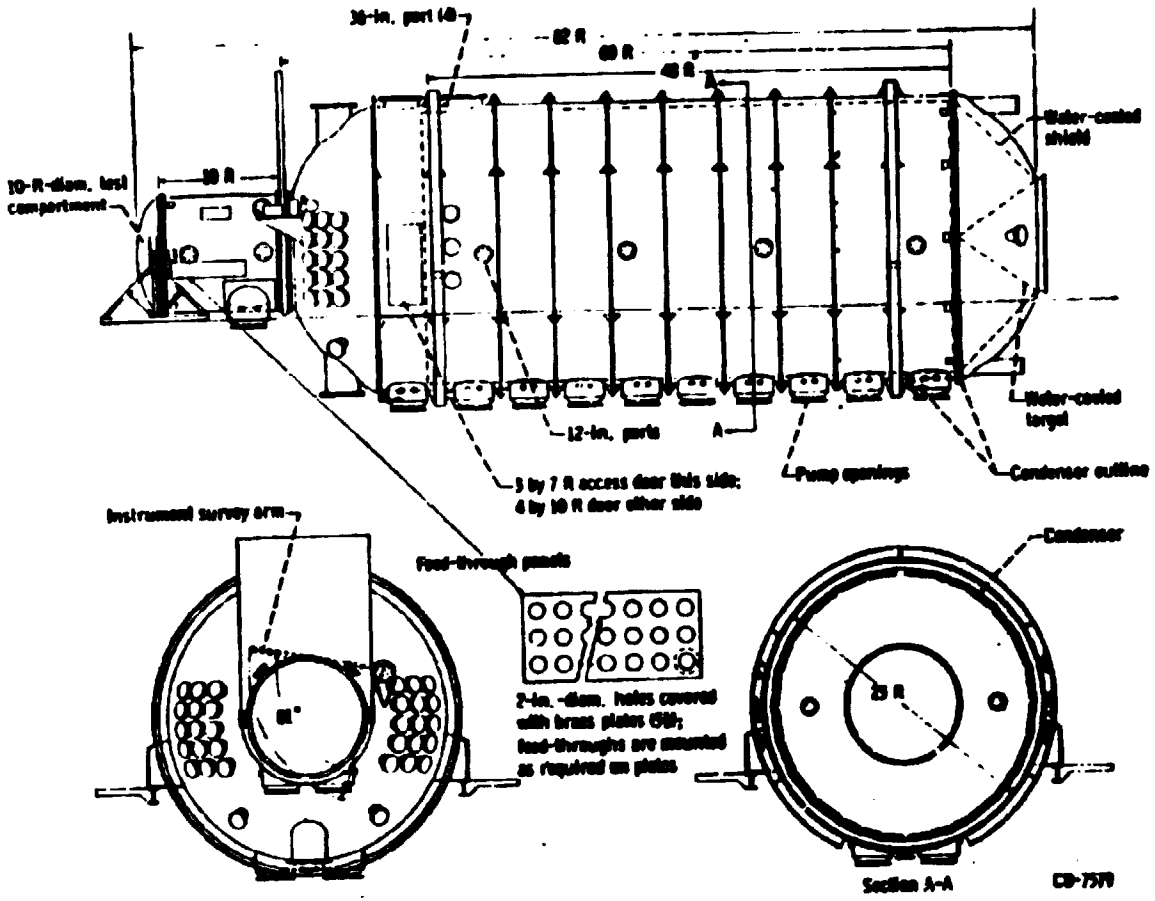

Figure 4.9.1.1-2 Drawing of Electric Propulsion Laboratory - Tank 6

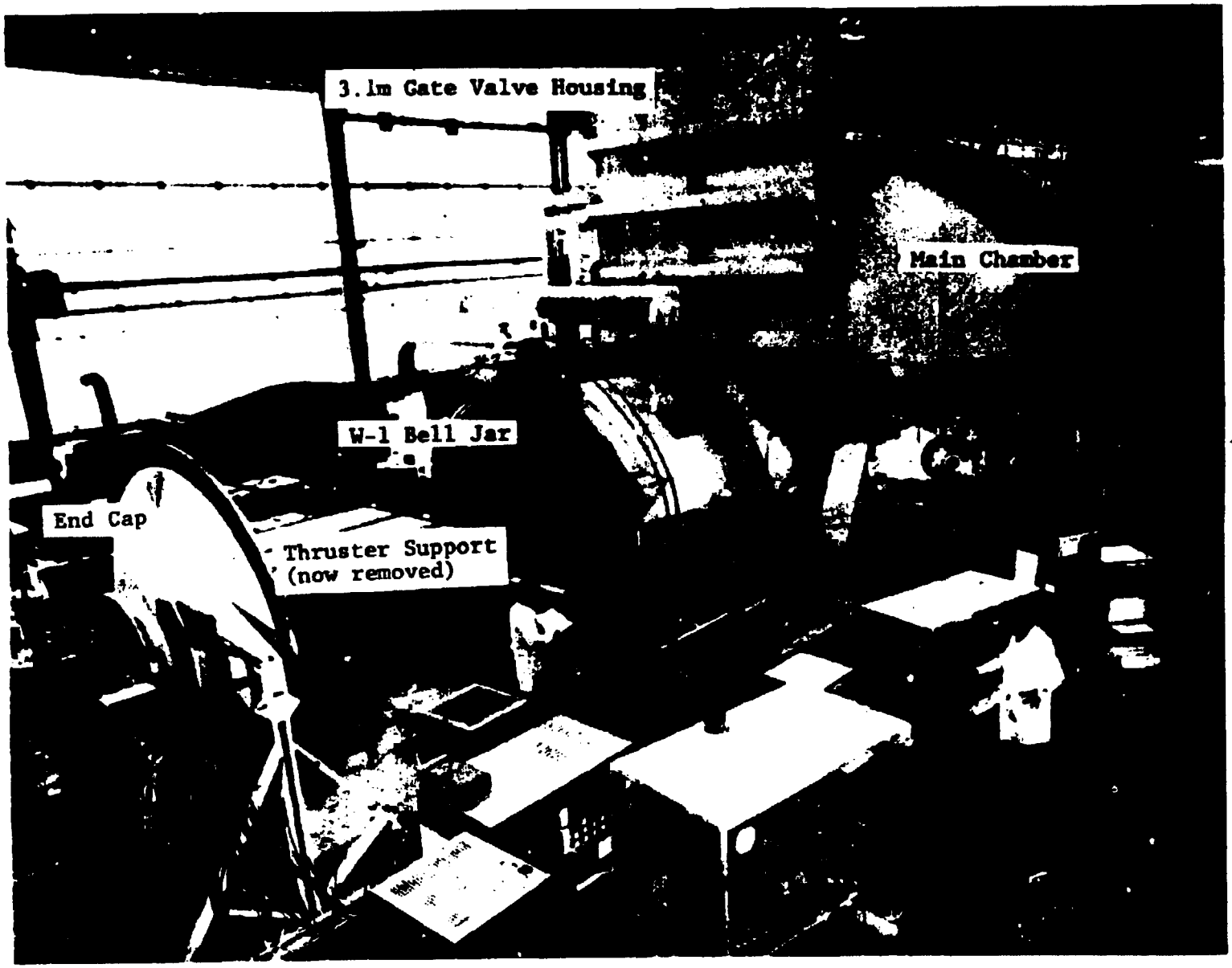

Figure 4.9.1.1-3 Bell Jar W-1 on Tank 6

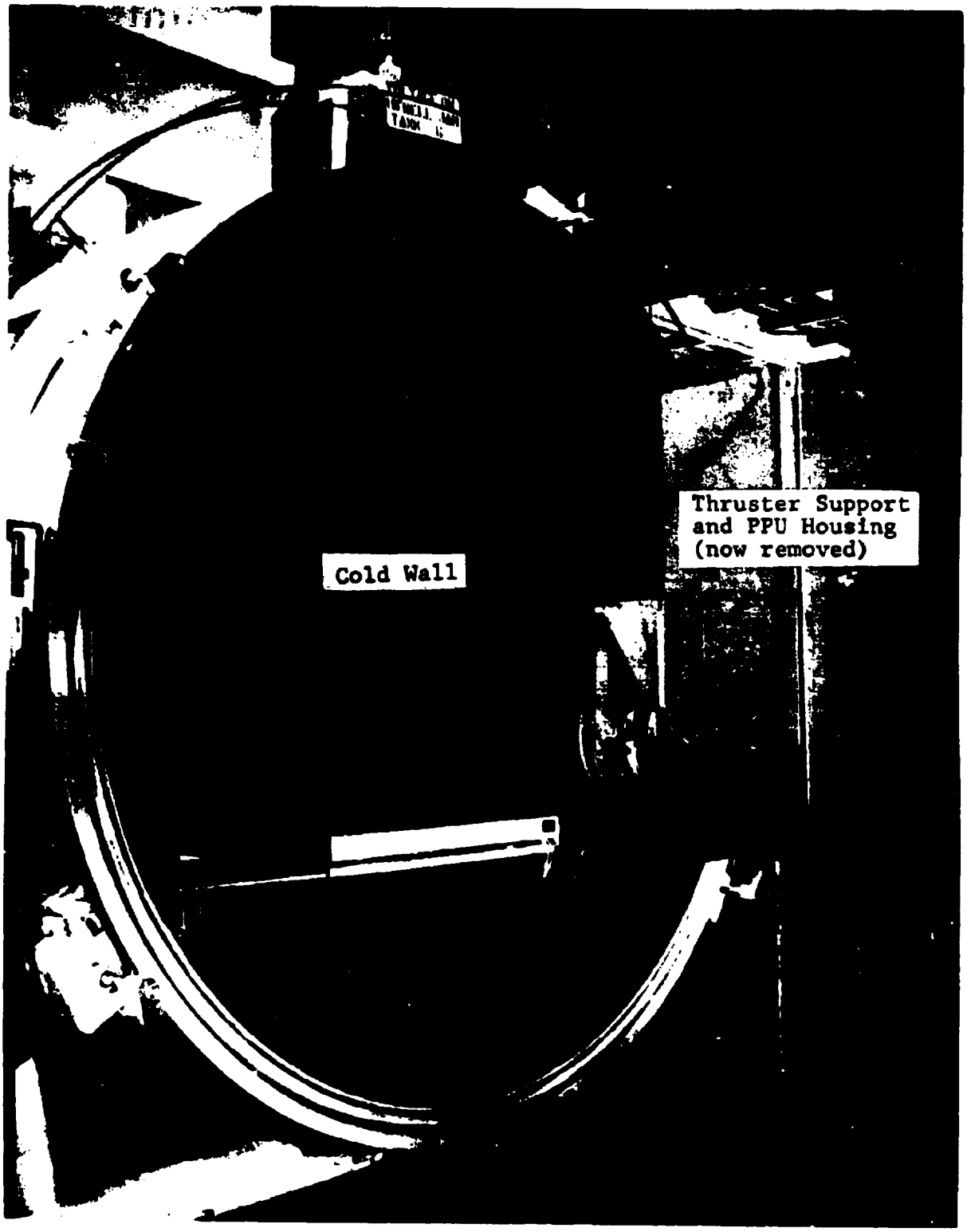

Figure 4.9.1.1-4 Cold Wall Inside the W-1 Bell Jar

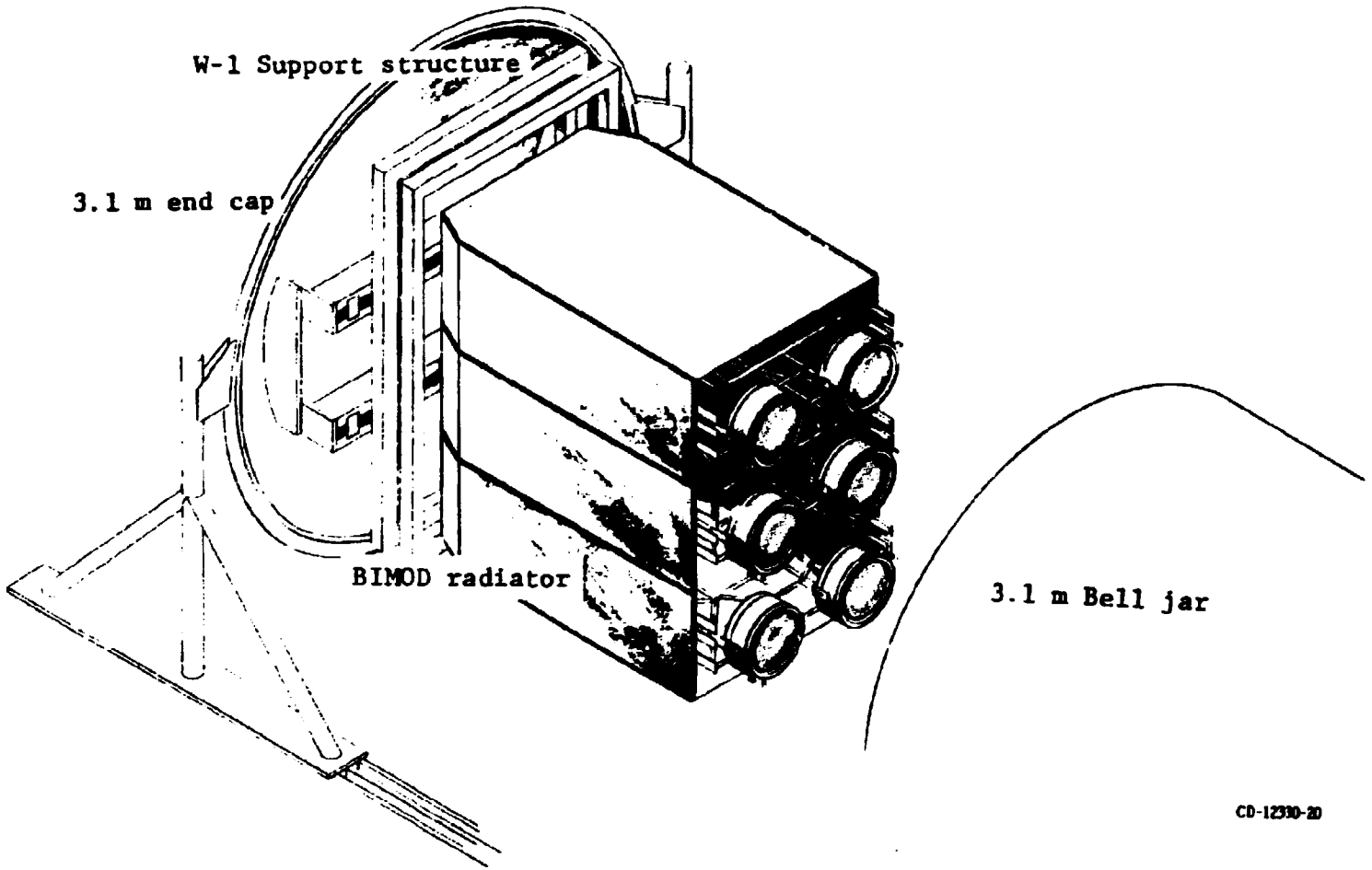

Figure 4.9.1.3-1 Three BIMOD Array Mounted on W-1 Support Structure

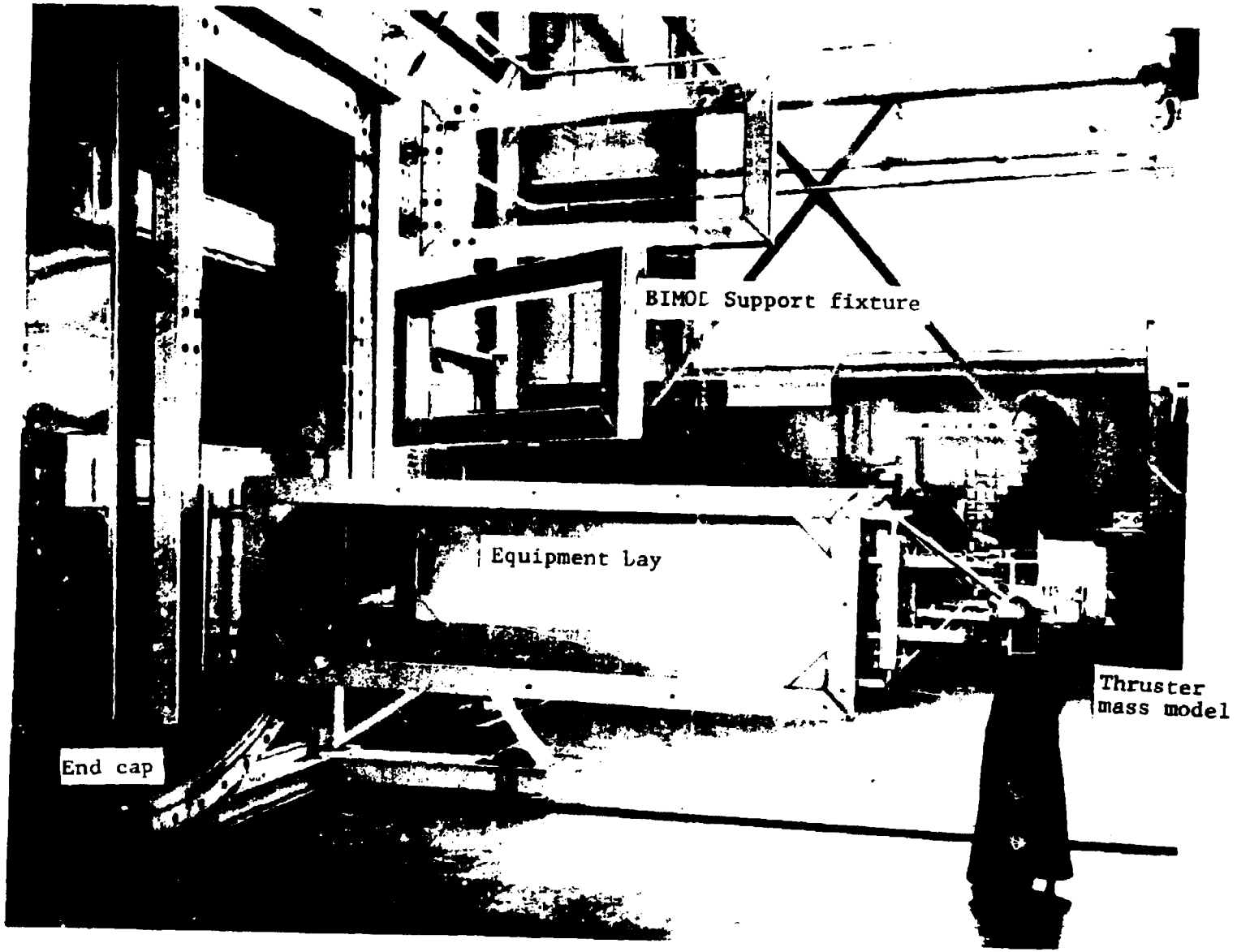

Figure 4.9.1.3-2 BIMOD Simulator Mounted to W-1 Support Structure

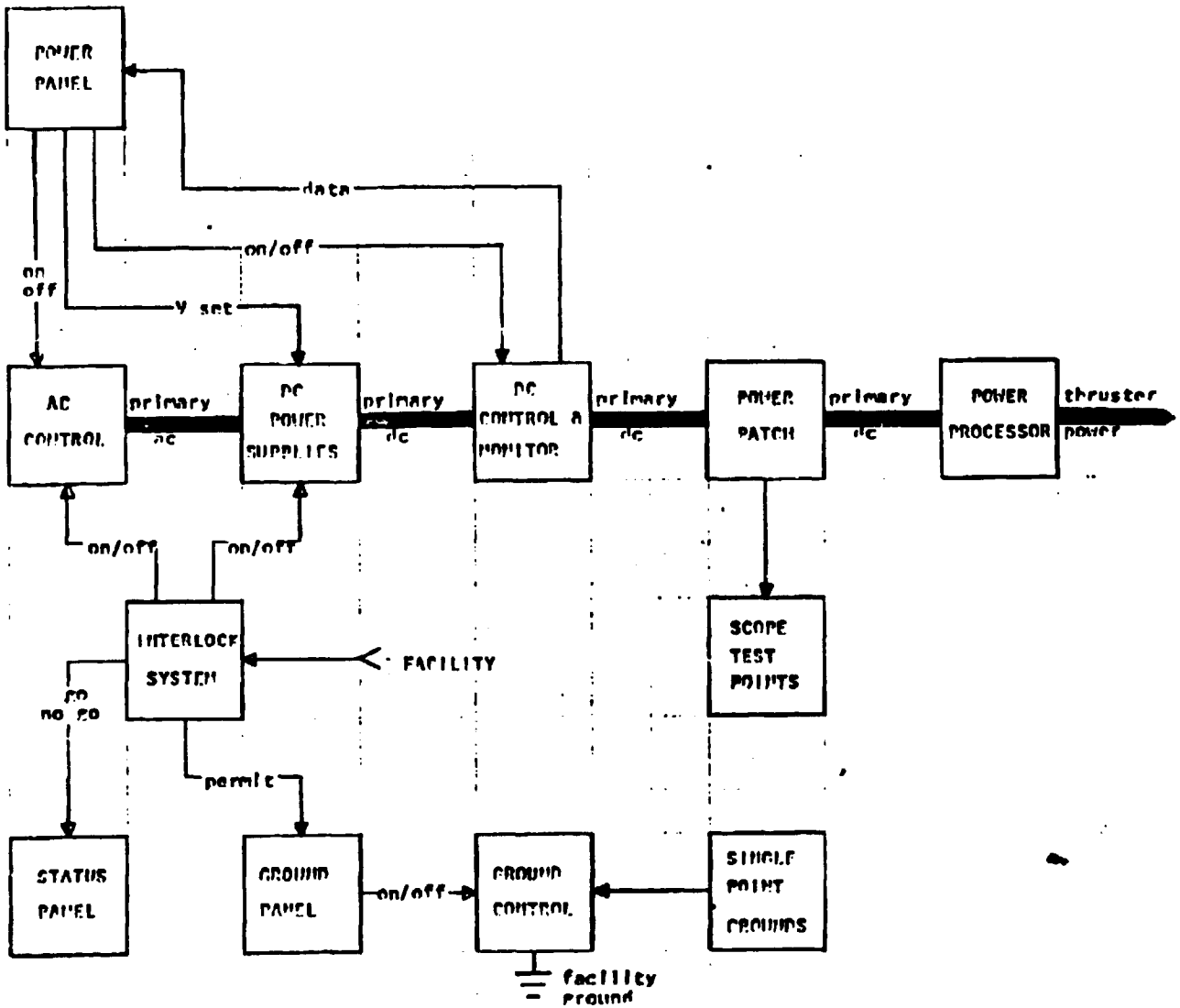

Figure 4.9.1.4-1 Engine System Test Facility Power Flow

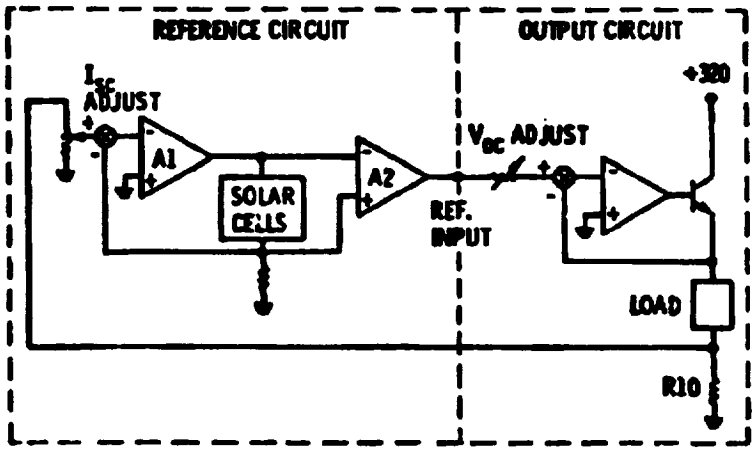

Figure 4.9.1.4-2 Solar Array Simulator Functional Diagram

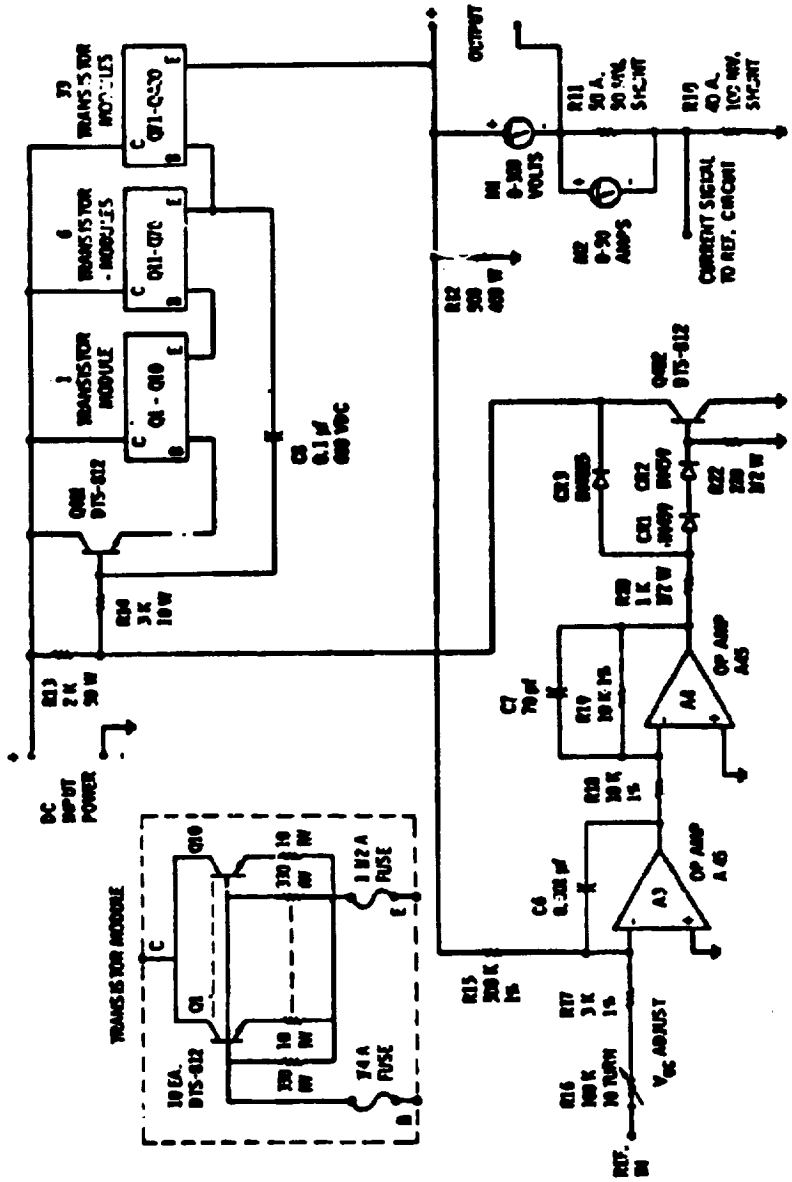

Figure 4.9.1.4-3 Solar Array Simulator Output Circuit Schematic

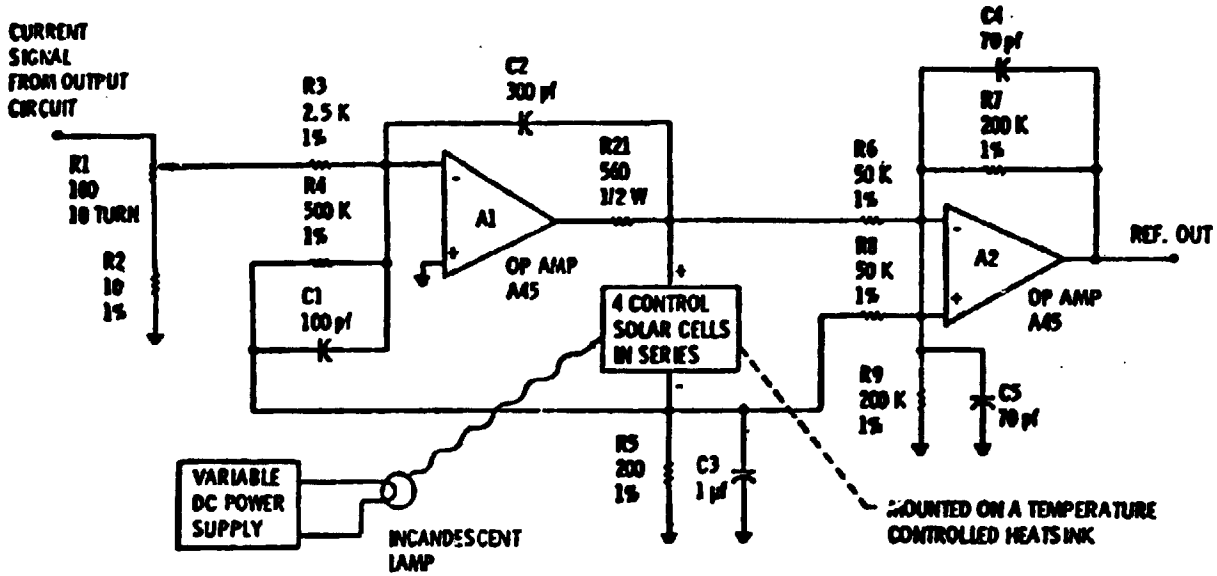

Figure 4.9.1.4-4 Solar Array Simulator Reference Circuit Schematic

5.0

THRUSTER

Table of Contents

		Page
5.0	Thruster	5-4
5.1	Reference Documents	5-4
5.2	Functional Requirements	5-11
5.3	Functional Description	5-12
5.3.1	Electrical	5-12
5.3.1.1	General	5-12
5.3.1.2	Basic Thruster Operation	5-12
5.3.1.3	Parametric Relations	5-14
5.3.2	Mechanical	5-18
5.3.2.1	Main Structure	5-19
5.3.2.2	Discharge Chamber Assembly	5-20
5.3.2.3	Grid System	5-21
5.3.2.4	Isolator Vaporizer Assemblies	5-22
5.3.2.5	Cathodes	5-24
5.3.3	Thermal Description	5-25
5.3.4	Operational Characteristics	5-28
5.3.4.1	Hardware Characteristics	5-28
5.3.4.2	Software Characteristics	5-37
5.3.5	Thruster Lifetime	5-47
5.4	Interface Definition	5-49
5.4.1	Electrical	5-49
5.4.2	Mechanical	5-50
5.4.3	Thermal	5-51
5.4.4	Thruster Induced Environment	5-52

		Page
5.5	Performance Description	5-54
5.6	Physical Characteristics and Constraints	5-56
5.7	Development History	5-57
5.8	Applicable Documents Enclosed	5-63
5.9	Ground Support Equipment	5-64
5.9.1	Electrical Simulator	5-64
5.9.2	Shipping Container	5-64
5.9.3	Dynamic Mass Model	5-64
5.9.4	Ground Power Supply Systems	5-65

FIGURES

5.0-1	Thruster - Exhaust Side	5-68
5.0-2	Thruster - Rearside	5-69
5.3.1.2-1	Basic Thruster Operation	5-70
5.3.1.2-2	Thruster Potential Diagram	5-71
5.3.2-1	Thruster Cross Section	5-72
5.3.2.3-1	Grid System Cross Section	5-73
5.3.2.4-1	Cathode Isolator Vaporizer	5-74
5.3.2.4-2	Main Isolator Vaporizer	5-75
5.3.2.4-3	Neutralizer Isolator Vaporizer	5-76
5.3.2.5-1	Main Cathode	5-77
5.3.2.5-2	Neutralizer Cathode	5-78
5.3.4.1-1	Ion Beamlet Focusing through Grid Aperture	5-79
5.3.4.2-1	Thruster Operating Envelope	5-80
5.3.4.2-2a	Thruster Startup Algorithm	5-81

		Page
5.3.4.2-2b	Thruster Supply Conditions During Startup Phases	5-82
5.3.4.2-3	Low Mode Algorithm	5-83
5.3.4.2-4	Excessive Arcs Algorithm	5-84
5.4.1-1a	Electrical Wiring and Propellant Manifold of Thruster	5-85
5.4.1-1b	Thruster Wire List	5-86
5.4.1-2	Thruster-Power Processor Interconnection Diagram	5-87
5.4.2-1	Thruster Outline and Interfaces	5-88
5.4.3-1	Thruster Heat Balance in BIMOD Installation	5-89
5.5-1	Thruster Performance over Linear Throttle Profile	5-90
5.7-1	Mercury Bombardment Thruster Development History	5-91
5.9.1-1a	Thruster Electrical Simulator - Schematic	5-92
5.9.1-1b	Thruster Electrical Simulator - Specifications	5-93
5.9.3-1	Thruster Mass Models	5-94
5.9.4-1	Lab Power Unit (LPU) Functional Block Diagram	5-95
5.9.4-2	Lab Power Unit (LPU)	5-96

5.0 Thruster

This section describes the 30-centimeter electron bombardment mercury ion thruster. The descriptions and data provided are appropriate to the latest design thruster which is called the "J-Series" thruster. Front and rear side pictures of the thruster are shown in figures 5.0-1 and 5.0-2. The thruster parts list is applicable document 5.8.1. A complete set of drawings is included. Fabrication, assembly and test procedures which supplement the drawings are contained in Hughes Research Labs (HRL) Ion Physics Department (IPD) procedures contained in applicable document 5.8.2.

Functional requirements and a functional description are given in this section along with a description of interfaces and performance. Standard operational sequences are defined. Detail on coding which has been done to convert these algorithms to software is contained in the thruster controller section 11.0.

5.1 Reference Documents

5.1.1 Kaufman, H. R.: One-Dimensional Analysis of Ion Rockets. NASA TN D-261, March 1960.

5.1.2 Kaufman, Harold R.: An Ion Rocket with an Electron-Bombardment Ion Source. NASA TN D-585, 1961.

5.1.3 Cybulski, Ronald J.; Shellhammer, Daniel M.; Lovell, Robert R.; Domino, Edward J.; and Kotnik, Joseph T.: Results from SERT I Ion Rocket Flight Test. NASA TN D-2718, 1965.

5.1.4 Bechtel, Robert T.; and Rawlin, Vincent K.: Performance Documentation of the Engineering Model 30cm Diameter Thruster. NASA TM X-73530, 1976.

5.1.5 HRL Technical Staff: 2.5 kW Advanced Technology Ion Thrusters. NASA CR-134687, 1974.

5.1.6 HRL Technical Staff: 2.5 kW Advanced Technology Ion Thruster Final Report. NASA CR-135076, 1976.

5.1.7 Banks, Bruce; Rawlin, Vince; Weigand, Albert; and Walker, John: Direct Thrust Measurement of a 30cm Ion Thruster. NASA TM X-71646, 1975.

5.1.8 Mirtich, M. J.: The Effects of Exposure to LN_2 Temperatures and 2.5 Suns Solar Radiation on 30-cm Ion Thruster Performance. NASA TM X-71652, 1975.

5.1.9 Mirtich, M. J.: Thermal Environment Testing of a 30-cm Engineering Model Thruster. NASA TM X-73522, 1976.

5.1.10 Oglebay, J. C.: Thermal Analytic Model of a 30-cm Engineering Model Mercury Ion Thruster. NASA TM X-71680, 1975.

5.1.11 Oglebay, J. C.: Comparison of Thermal Analytic Model with Experimental Test Results for 30-centimeter-diameter Engineering Model Mercury Ion Thruster. NASA TM X-3541, 1977.

5.1.12 Mantenieks, Maris A.: Investigation of Mercury Thruster Isolators. AIAA Paper 73-1083, October - November 1973.

5.1.13 Bechtel, Robert T.: A 30cm Diameter Bombardment Thruster with a Variable Magnetic Baffle. AIAA Paper 72-489, April 1972.

5.1.14 Poeschel, Robert L.; and Knauer, W.: A Variable Magnetic Baffle for Hollow Cathode Thrusters. AIAA Paper 70-175, January 1970.

5.1.15 Bechtel, R. T.; Csiky, G. A.; and Byers, D. C.: Performance of a 15cm Diameter, Hollow-Cathode Kaufman Thruster. NASA TM X-52376, 1968.

5.1.16 Bechtel, Robert T.: Component Testing of a 30cm Diameter Electron Bombardment Thruster. AIAA Paper 70-1100, August - September 1970.

5.1.17 Rawlin, V. K.; Banks, B. A.; and Byers, D. C.: Design, Fabrication, and Operation of Dished Accelerator Grids on a 30cm Ion Thruster. AIAA Paper 72-486, April 1972.

5.1.18 Rawlin, Vincent K.: Performance of 30cm Ion Thrusters with Dished Accelerator Grids. NASA TM X-2993, 1974.

5.1.19 Lathem, Walter C.: Ion Accelerator Designs for Kaufman Thrusters. AIAA Paper 69-261, March 1969.

5.1.20 Danilowicz, Ronald L.; Rawlin, Vincent K.; Banks, Bruck A.; and Wintucky, Edwin G.: Measurement of Beam Divergence of 30-Centimeter Dished Grids. NASA TM X-68286, 1973.

5.1.21 Rawlin, V. K.: Sensitivity of 30cm Mercury Bombardment Ion Thruster Characteristics to Accelerator Grid Design. NASA TM-78861, 1978.

5.1.22 Vahrenkamp, Richard P.: Characterisitics of a 30cm Thruster Operated with Small Hole Accelerator Grid Ion Optics. AIAA Paper 76-1030, November 1976.

5.1.23 Rawlin, V. K.; and Pawlik, E. V.: A Mercury Plasma-Bridge Neutralizer. Journal of Spacecraft and Rockets, vol. 5, no. 7, 1968, pp. 814-820.

5.1.24 Bechtel, Robert T.: Performance of a Neutralizer for Electron Bombardment Thruster. AIAA Paper 72-207, January 1972.

5.1.25 Bechtel, R. T.: A Hollow Cathode Neutralizer for a 30cm Diameter Bombardment Thruster. AIAA Paper 73-1052, October - November 1973.

5.1.26 Bechtel, R. T.: Effect of Neutralizer Position on Accelerator Wear for a 30-Centimeter Diameter Ion Bombardment Thruster. NASA TM X-67926, 1971.

5.1.27 HRL Ion Physics Department Staff: Thruster Endurance Test. (Hughes Research Laboratories; NASA Contract NAS3-15523.) NASA CR-135011, 1976.

5.1.28 Collett, C. R.: A 7700 Hour Endurance Test of a 30cm Kaufman Thruster. AIAA Paper 75-366, March 1975.

5.1.29 Power, John L.; and Hiznay, Donna J.: Solutions for Discharge Chamber Sputtering and Anode Deposit Spalling in Small Mercury Ion Thrusters. NASA TM X-71675, 1975.

5.1.30 Mantenieks, M. A.; and Rawlin, V. K.: Studies of Internal Sputtering in a 30cm Ion Thruster. NASA TM X-71654, 1975. (AIAA Paper 75-400, March 1975.)

5.1.31 Collett, C. R.; and Bechtel, R. T.: An Endurance Test of a 900 Series 30cm Engineering Model Ion Thruster. AIAA Paper 76-1020, November 1976.

5.1.32 Mantenieks, Maris A.; and Rawlin, Vincent K.: Sputtering Phenomena of Discharge Chamber Components in a 30cm Diameter Hg Ion Thruster. NASA TM X-735, 1976.

5.1.33 Mirtich, Michael J.: Investigation of Hollow Cathode Performance for 30cm Thrusters. NASA TM X-68298, 1973.

5.1.34 Kerslake, W. R.; Byers, D. C.; Rawlin, V. K.; Jones, S. G.; and Berkopec, F. D.: Flight and Ground Performance of the SERT II Thruster. AIAA Paper 70-1125, August - September 1970.

5.1.35 Kerslake, William R.; and Finke, Robert C.: SERT II Thruster Space Restart. NASA TM X-71651, 1974.

5.1.36 Byers, David C.: A Review of Electron Bombardment Thruster Systems/Spacecraft Field and Particle Interfaces. NASA TM-78850, April 1978.

3.1.37 Reader, P. D.: An Electron-Bombardment Ion Rocket with a Permanent Magnet. AIAA Paper 63-031, March 1963.

5.1.38 Kerslake, William R.: Preliminary Operation of Oxide-Coated Brush Cathodes in Electron-Bombardment Ion Thrusters. NASA TM X-1105, 1965.

5.1.39 Byers, David C.: Performance of Various Oxide-Magazine Cathodes in Kaufman Thrusters. NASA TN D-5074, 1969.

5.1.40 Kerslake, William R.: Design and Test of Porous-Tungsten Mercury Vaporizers. AIAA Paper 72-484, April 1972.

5.1.41 Kerslake, William R.; Byers, David C.; and Staggs, John F.: SERT II Experimental Thruster System. AIAA Paper 67-700, September 1967.

5.1.42 Nieberding, William C.; Lesco, Daniel J.; and Berkopec, Frank D.: Comparative In-Flight Thrust Measurements of the SERT II Ion Thruster. AIAA Paper 70-1162, August - September 1970.

5.1.43 Byers, David C.; and Staggs, John F.: SERT II Flight-Type Thruster System Performance. NASA TM X-52520. 1969.

5.1.44 Jones, Sanford G.; Staskus, John V.; Byers, David C.: Preliminary Results of SERT II Spacecraft Potential Measurements Using Hot Wire Emissive Probes. AIAA Paper 70-1127, August - September, 1970.

5.1.45 Zavesky, Ralph J.; and Hurst, Evert B.: Mechanical Design of SERT II Thruster System. NASA TM X-2518, 1972.

5.1.46 Banks, Bruce: Composite Ion Accelerator Grids. NASA TM X-52425, 1968.

5.1.47 Bechtel, Robert T.; Banks, Bruce A.; and Reynolds, Thaine W.: Effect of Facility Backsputtered Material on Performance of Glass-Coated Accelerator Grids for Kaufman Thrusters. AIAA Paper 71-156, January 1971.

5.1.48 Knauer, W.; Poeschel, R. L.; King, H. J.; and Ward, J. W.: Discharge Chamber Studies for Mercury Bombardment Ion Thrusters. (Hughes Research Laboratories; NASA Contract NAS3-9703.) NASA CR-72440, 1968.

5.1.49 Masek, T. D.; Poeschel, R. L.; Collett, C. R.; and Schnelker, D. E.: Evolution and Status of the

30cm Engineering Model Ion Thruster. AIAA Paper 76-1006, November 1976.

5.1.50 HRL Ion Physics Department Staff: Low Voltage 30cm Ion Thruster Development. (Hughes Research Laboratories; NASA Contract NAS3-16528.) NASA CR-134731, 1974.

5.1.51 Rawlin, Vincent K.; and Mantenieks, Mavis A.: Effect of Background Gases on Internal Erosion of the 30cm Hg Ion Thruster. NASA TM-73803, 1978.

5.1.52 James, E.; Vetrone, R.; and Bechtel, R.: A Mission Profile Life Test Facility. AIAA Paper 78-671, April 1978.

5.2 Functional Requirements

1) The 30-cm thruster is required to condition neutral mercury propellant to provide a neutralized ion beam and generate thrust.
2) The thruster must have sufficient flexibility of control to operate stably at a variety of conditions between the maximum and minimum power levels.
3) The thruster must be capable of throttling over a four to one input power range.
4) The thruster must operate at up to 2.7 kW input power and have specific impulse of at least 3000 seconds.
5) Useful lifetime of 15,000 hours is required.

5.3 Functional Description

5.3.1 Electrical

5.3.1.1 General

Applicable document 5.8.3 contains a general overview of thruster development history and operating principles. References 5.1.1 and 5.1.2 provide a more technical review of principles of operation. The thruster generates thrust by ionizing the mercury propellant in a discharge chamber and accelerating the positively charged ions through a parallel grid accelerator system at one end of the discharge chamber. Electrons are injected into the positive ion beam by a neutralizer downstream of the accelerator grid system to maintain overall charge and current neutrality. The ability to neutralize ion beams in space by this technique was demonstrated by the SERT I flight in 1964 (see reference 5.1.3)

5.3.1.2 Basic Thruster Operation

Basic thruster operation is shown in figure 5.3.1.2-1. Electrons emitted at the cathode travel to the anode. Their path is through the discharge chamber which contains mercury vapor that vaporizer assemblies have produced from the liquid mercury propellant. Ionization occurs when mercury vapor atoms lose an electron after bombardment by these energetic electrons. Ionization efficiency is improved

and controlled by superposition of radial and axial permanent magnetic fields which lengthen the trajectory path of electrons from the cathode to the anode thereby increasing the probability of collision with the mercury atoms. Figure 5.3.1.2-2 is a potential diagram for various thruster elements.

The discharge voltage which produces energetic electrons is normally at a constant 32 V. The discharge chamber is raised to the high positive screen potential of 1100V, thereby providing the potential energy term, eV, shown in figure 5.3.1.2-2.

Extraction of the ion beam from the plasma in the discharge chamber is accomplished by the accelerator grid system, sometimes referred to as the ion optics or ion extraction system. This system consists of two closely spaced, perforated electrodes or grids having a parallel, spherical geometry. The grid nearest the discharge chamber, called the screen grid, is raised to the same high potential as the discharge typically 1100 V. The downstream grid called the accelerator grid is biased to a -300 V potential to aid in beam extraction, provide focusing of the ion beam, and to retard low energy electrons formed outside the thruster in the beam plasma. Otherwise, these electrons would be attracted by the

high positive screen potential.

The resulting plasma ion beam must eventually approach zero potential in order to be decoupled from the thruster (and space vehicle) and produce thrust. Since a small (typically 10 volts) potential difference is required to extract the neutralizing electrons from the neutralizer cathode to the ion beam, the neutralizer itself must operate a some potential below zero potential as shown in figure 5.3.1.2-2. This energy is actually delivered by the screen supply and as a result represents a reduction in ion energy.

5.3.1.3 Parametric Relations

Thruster performance is generally measured in terms of thrust, specific impulse and total efficiency. Equations follow which relate those terms to electrical parameters and propellant flow rate. Additional information is provided in reference 5.1.4.

1) Thrust is the result of rate of change of momentum

$$T = \frac{d}{dt}(MV)$$

where T is thrust

M is mass

V is velocity

$$T = \dot{M}V + M\dot{V}$$

In electric thrusters, the second term is near zero. It can be shown that $\dot{M}$ is a function of beam current (J_b) and that V is a function of accelerating voltage (V_I). The following ideal thrust equation can be derived. It is ideal since it assumes that all ions are singly charged and axial in direction.

$$T_i = 2.0391 \quad J_b \sqrt{V_I}$$

where T_i is ideal thrust (mN)

J_b is beam current (A)

V_I is net accelerating voltage (V)

The constant 2.0391 arises from the following relation:

$$2.0391 = \sqrt{2 \frac{m}{e}} \times 10^3$$

where $\frac{m}{e}$ is the mass to charge ratio for mercury (2.079×10^{-6} kg/coulomb)

Also, $V_I = V_s + V_d - V_n$

where V_s is screen voltage (V)

V_d is discharge voltage (V)

V_n is neutralizer floating potential (V)

Figure 5.3.1.2-2 shows these potentials.

In reality, ideal thrust is not achieved due to existence of doubly charged ions and the fact that the beam diverges somewhat. These factors are determined by methods discussed in references 5.1.5 and 5.1.6. Actual thrust is expressed as follows:

$$T_a = \gamma T_i$$

where γ is thrust reduction factor which varies nearly linearly from 0.95 at 2.0A beam to 0.975 at 0.75A beam. Direct measurement of thrust has been made by a laser interferometer technique described in reference 5.1.7.

2) Specific impulse is the second thruster performance parameter of interest here

$$I_{sp} = \frac{T_a}{\dot{M}_o g}$$

where $\dot{M}_o$ is total propellant mass flow rate. The following expression for specific impulse can be derived:

$$I_{sp} = \frac{100.08\ \gamma\ J_b \sqrt{V_I}}{\dot{m}_o}$$

where $\dot{m}_o$ is propellant mass flow in "equivalent amperes"

$$\dot{m}_o = \left(\frac{m}{e}\right) \dot{M}_o = 2.079 \times 10^{-6}\ \dot{M}_o$$

where $\left(\frac{m}{e}\right)$ is the mass to charge ratio for mercury (kg/coulomb)

$\dot{M}_o$ is mass flow of mercury (kg/second)

The constant 100.08 arises from the following relation:

$$100.08 = \frac{1}{g} \sqrt{2\left(\frac{e}{m}\right)}$$

3) Efficiency is the third performance parameter of interest. For ion thrusters, total efficiency can be expressed as follows:

$$\eta_T = \gamma^2 \eta_u \eta_p$$

where η_u is propellant utilization efficiency

η_p is power efficiency

The utilization efficiency is the ratio of actual beam current to the beam current which could be obtained if each propellant atom were singly ionized and extracted. To maintain consistent dimensions it is necessary to convert mass flow rate from kilograms per second to equivalent changes per second or equivalent milliamps as described above.

$$\eta_u = \frac{J_b}{\dot{m}_o}$$

Power efficiency is the ratio of electrical power which produces thrust (via the beam) to total input power

$$\eta_p = \frac{P_b}{P_t}$$

$$P_b = V_I J_b$$

$$P_t = V_s J_b + V_d J_d + V_a J_a + P_v + P_h + P_k + P_{mb}$$

where V_s is screen voltage (V)

J_b is screen (beam) current (A)

V_d is discharge voltage (V)

J_d is discharge current (A)

V_a is accelerator voltage (V)

J_a is accelerator current (A)

P_v is power required by three vaporizers (W)

P_h is power required by two tip heaters and isolator heater (W) (This term is zero during run phase.)

P_k is power required by two keepers (W)

P_{mb} is power required by the magnetic baffle (W)

Some simplifications lead to a convenient expression of input power during run phase.

Let V_d = 32 volts

$J_d = 6J_b + 2$

V_aJ_a is negligible

$P_h = 0$

$P_v + P_k + P_{mb}$ is approximately 52 watts

Then $P_t = V_sJ_b + 32(6J_b + 2) + 52$

5.3.2 Mechanical

The mechanical design and construction features will be described for the following major subassemblies:

1) Main structure
2) Discharge chamber
3) Grid system
4) Isolator vaporizer assemblies
5) Cathodes

A cross section of the thruster is shown in figure 5.3.2-1. Most of the above subassemblies are shown on this cutaway. For more detail refer to the appropriate drawing numbers which are cited.

5.3.2.1 Main Structure

The loads on a thruster are carried by a cylindrical frame structure shown in figure 5.3.2-1 and drawing D1025324 of applicable document 5.8.1. This cylindrical frame consists of two annular rings supported by 12 box-type columns. The annular rings are channel-shaped sections located both at the backplate of the thruster and at the grid system mounting interface. The rings are designed to carry loads in the transverse direction (in the plane of the ring). They have narrow flanges to resist twisting moments which may occur along the gimbal axis. The flanges also resist in-plane twisting and bending forces which prevail during vibration parallel to the thrust axis. The box-shaped columns between these two rings resist axial and bending forces. Each of the two gimbal mounting brackets are attached to the cylindrical frame through six insulators.

Figure 5.3.2-1 shows that the thruster backplate supports much of the mass of the thruster. The backplate supports the cathode isolator-vaporizer (CIV), main isolator-vaporizer (MIV), propellant distribution,

baffle assembly, and magnets during vibration parallel to the thrust axis. Support for the backplate is provided by a tubular cross structure shown in drawing E1026510 of applicable document 5.8.1. This cross structure is attached to the backplate of the thruster at the outer edges and to the CIV mounting flange in the center as shown in drawing E1025353 of document 5.8.1.

To minimize thruster weight, the entire discharge chamber, including anode, frame support assembly, backplate, outer shell, and gimbal mounts are made of titanium and assembled by tungsten inert gas (TIG) welding and spotwelding methods. The ground screen, rear shield, and perforated outer shield are made of aluminum alloy (type 6061) and the downstream mask is made of titanium.

5.3.2.2 Discharge Chamber Assembly

The prime function of the discharge-chamber assembly of an electron-bombardment ion thruster is to ionize the neutral propellant. The main components of the discharge chamber assembly include the main structure, propellant distribution system, permanent magnets, iron pole pieces, electromagnetic baffle, an electron emitter (cathode), backplate and shield, and an electron collector or anode as shown in

figure 5.3.2-1.

The anode is made from 304L stainless steel wire mesh sintered to a 304L stainless steel backing sheet. The backplate shield is made from 304L stainless steel wire mesh. These mesh materials provide a rough surface to anchor deposited material which has been sputtered from the erosion sites within the discharge chamber. Alinco magnetics are used in 12 axial and 12 radial positions around the sides and backplate of the discharge chamber.

5.3.2.3 Grid System

The grid system structure as shown in figure 5.3.2.3-1 is a critical thruster subassembly in terms of thruster stability, efficiency and lifetime. The grid system is basically a pair of 0.38-mm (0.015-in.) thick molybdenum plates perforated with matching apertures. Screen grid holes are 1.90 mm (0.075 in.) in diameter and accelerator grid holes are 1.14 mm (0.045 in.) in diameter. These grids must be positioned parallel to each other, with about 0.5-mm (0.020-in.) interelectrode spacing.

The screen electrode defines the plasma boundary in the discharge chamber, while the electric field produced between the electrodes accelerates and focuses a beam of positive ions from the plasma

through each pair of screen-accelerator aperatures.

Ion thrusters with dished grids would be subject to significant thrust losses due to the divergence of the ion beam if the hole pattern of screen and accelerator grids were identical. This divergence is a consequence of the relative displacement caused during fabrication in the centerlines of screen grid and accelerator apertures. A change in the aperture center-to-center spacing pattern of one of the electrodes is needed to vector the individual beamlets to provide paraxial trajectories downstream of the grid system. A change of less than 0.5% in the center-to-center aperture spacing is used to converge the beam sufficiently to eliminate such thrust losses. Such a change in spacing is called "compensation" and will be discussed later in section 5.3.4.1.

5.3.2.4 Isolator Vaporizer Assemblies

Three isolator vaporizer assemblies are required to control propellant flow by heating the liquid mercury to produce mercury vapor at a rate required by the thruster. The phase separator used between the liquid and vapor is a sintered porous tungsten disk electron beam welded into a tantalum tube. Heat is supplied by a nichrome heater brazed to the outside of the housing. Such a subassembly is called

a vaporizer.

The vaporizer subassemblies are assembled to isolator subassemblies so that isolator-vaporizer units are replaceable units in a thruster. The isolator function is to provide electrical isolation of the vapor side of the isolator-vaporizer assembly which is at 1100V screen potential from the liquid side which is at ground potential. The isolator for the CIV and MIV assemblies are shown in figures 5.3.2.4-1 and 5.3.2.4-2. The isolators are made up of a series of stainless steel screens spaced apart with ceramics in a ceramic tube such that the minimum Paschen breakdown voltage for mercury vapor is not exceeded. Screen baffles, as used in the cathode and main isolators, are not required in the neutralizer isolator because the voltage level is low. This can be seen in figure 5.3.2.4-3.

The location of the three isolator vaporizer assemblies used in a thruster is shown in figure 5.3.2-1. The CIV as shown in figure 5.3.2.4-1 is mounted on the thruster backplate. Mercury vapor is carried from the CIV to the main cathode via a 1/16 inch stainless steel tube. The vapor enters the discharge chamber through the hollow cathode which will be discussed later.

The MIV provides the majority of the propellant flow to the discharge chamber. The MIV is shown in figure 5.3.2.4-2 It discharges mercury vapor into an annular plenum mounted to the thruster backplate. The plenum distributes the vapor to equalize the mercury density in the discharge chamber.

The neutralizer isolator-vaporizer (NIV) is located in the neutralizer assembly at the outside edge of the thruster. The mercury vapor from the NIV is carried in a tube to the neutralizer cathode as discussed later. The NIV is shown in figure 5.3.2.4-3.

5.3.2.5 Cathodes

Two hollow cathodes are used in the 30-cm thruster. The main cathode is in the discharge chamber and another cathode is in the neutralizer. The main cathode is located at the center of the thruster backplate. The neutralizer cathode is located at the tip of the NIV. The location on the thruster of both of these cathodes is shown in figure 5 3.2-1. A cross section of both of these cathodes is shown in figures 5.3.2.5-1 and 5.3.2.5-2.

A cathode consists of a tungsten tip which is welded into a tantalum tube. A heater is brazed around the tantalum tube. Inside the tantalum tube is a porous tungsten hollow cylinder impregnated with

carbonate compounds containing barium. These compounds lower the work function of electron emitting surfaces and facilitate emission at temperatures consistent with long life. Section 5.3.4.1 describes operation of the cathodes.

5.3.3 Thermal Description

No need for any special thermal control surfaces or devices has been identified and none are included on the thruster subsystem. The thermal dissipation resulting from thruster inefficiency is radiated, mostly through the grid structure to space. Tests have been conducted over a wide range of thermal environments with up to 2.5 suns solar intensity perpendicular to the grid face on both a 400 series (reference 5.1.8) and 700 series thruster (reference 5.1.9). Results of these tests showed only one instance where control of the thruster was lost due to a vaporizer overheating problem. During all the other tests, no apparent thermal problems were encountered and there were no indications of impact on thruster lifetime. The major thermal difference between the tested thrusters and the J-series is that the accelerator (outermost) grid as tested was 43 percent open while the J-series grids are 24 percent open. Analysis has shown that major components of J-series thruster run about 20° C

warmer than the 400 and 700 series test models for a full-power - no-sun case. The interior of the J-series thruster is less susceptible to solar input than previous series due to a smaller percentage of open area of the outermost grid.

Corresponding to the test program cited above, thermal analytic models of the thruster were generated to allow calculation of temperatures for the main parts of the thruster (i.e., anode, engine body, etc.). The results of the analysis compared to test results are reported in reference 5.1.10 for the 400 series tests and in reference 5.1.11 for the 700 series tests. In general, the analytical models predicted operating thruster temperatures within 10° C of the measured values for the main components of the thruster.

As mentioned above, analysis was conducted simulating a J-Series thruster. This was accomplished by modifying the model presented in reference 5.1.11 to account for the reduced open area of the accelerator grids. The specific modifications along with a sample case are presented in applicable document 5.8.4.

5.3.4 Operational Characteristics

5.3.4.1 Hardware Characteristics

The hardware required for thruster operation is divided into four functional groups: 1) propellant feed system, 2) ion production system, 3) ion extraction system, and 4) beam neutralization system.

1) Propellant Feed System - Propellant flow rate is introduced at three locations on the thruster. The bulk of the flow is introduced through the main vaporizer and feed plenum as shown in figure 5.3.2-1. This flow rate is of the same order as the desired beam current so that a 2.0 ampere beam current requires about 2000 milliamps flow. (Flow rates are measured in equivalent mA with the assumption that each neutral atom can become only a singly charged ion). The control of the flow rate is achieved by sensing the beam current and varying main vaporizer heater power to hold the beam constant.

   Some mercury flow is introduced directly through the discharge plasma-bridge hollow cathode. This flow rate is required to form the plasma-bridge for operation of the cathode. It is generally maintained between 85 and 120 equivalent milliamps. The control of this flow rate

is achieved by sensing the discharge voltage and varying the cathode vaporizer power to hold the voltage constant.

The rest of the total flow rate is introduced through the neutralizer cathode. This cathode is also a plasma-bridge hollow cathode. The flow rate is generally maintained between 30 and 50 equivalent milliamps. The control of the neutralizer flow rate is achieved by sensing the neutralizer keeper voltage and varying the vaporizer heater power to keep the voltage constant.

All three vaporizers are functionally the same. A porous tungsten plug is welded into the mercury feed system to act as a phase separator. The liquid mercury immediately behind the plug is heated by a nichrome heater winding. The actual vapor flow through the porous tungsten plug is a function of the mercury vapor pressure and the plug geometry. Thus an increase in heater power will increase the vapor flow rate.

Each vaporizer is designed to operate in the 270° to 320°C range to produce the required flow rates. The range of flow rates at a given

temperature for different vaporizers is controlled by proper selection of the porous tungsten density and area.

Each vaporizer requires its own dedicated power supply in the baseline design.

The propellant feed system incorporates mercury vapor electrical isolators as part of each vaporizer subassembly as shown in figure 5.3.2-1. These permit each vaporizer to operate at ground potential and use the liquid mercury supplied from storage tanks at ground potential. It also permits several thrusters on the same spacecraft to use a single storage and feed system.

The isolators (reference 5.1.12) involve cascading several sections, each of which is capable of withstanding a certain fraction of the total voltage. In each section, dimensions are selected to insure that the voltage drop across the section is less than the Paschen breakdown minimum for mercury vapor. The main and cathode vaporizer isolators are required to stand off the entire beam voltage of up to 1100 V plus margin. The neutralizer vaporizer isolator is

required to stand off only the neutralizer floating potential and therefore is designed for 100 V.

2) Ion Production System - The mercury ions are formed by electron-bombardment inside the discharge chamber. The discharge power supply is operated in a constant current mode. Coarse control of the discharge volt-ampere characteristic is achieved by a solid baffle located downstream of the discharge cathode and shown in figure 5.3.2-1. Fine control of the discharge voltage is maintained at a constant 32 volts by varying the propellant flow rate introduced through the cathode while the discharge current operating set point is selected based on the ion production rate required to provide the beam current desired. In order to increase the ion production efficiency a permanent magnetic field is imposed on the discharge which causes the electrons to spiral out to the anode thereby increasing their length of travel and increasing the probability of an ionizing collision. Further an electromagnetic field is superimposed on the permanent magnetic field in a critical field region. Location of this magnetic field

coil is shown in figure 5.3.2-1. This field further improves the ion production efficiency and also serves to control the cathode to anode electrical impedance. Thus the electromagnetic field can be used to shift the discharge volt-ampere characteristic and voltage-propellant flow rate characteristics to provide optimum control and stability. This becomes useful when throttling over a 4:1 power ratio. Since this electromagnet serves to control the electron flow it is referred to as the magnetic baffle. Detailed discussions of the effects of discharge chamber physical and magnetic geometries on thruster performance can be found in references 5.1.4, 5.1.13 and 5.1.14.

The electron source for the discharge is a plasma-bridge hollow cathode described in Section 5.3.2.5. The hollow cathode concept is required in the ion thruster to provide electron emission more efficiently than thermionic emission alone could provide for required lifetimes. A configuration is needed which shields the emissive surface from direct ion bombardment which would deplete the emissive surface at a rapid rate.

The emitting mechanism within the hollow cathode is not completely understood. However, it is clear that field enhanced thermionic emission (Schottky emission) is a predominate mechanism. Mercury vapor from the CIV flows through the hollow cathode which is emitting electrons from the high temperature emissive material. Electron bombardment of the vapor produces a high density, low potential plasma inside the cylindrical cavity. Plasma conditions are such that although the voltage drop from the plasma to the cavity walls is small, the distance is also very small. High field strengths therefore exist at the surface of the hollow cavity. Field enhanced thermionic emission occurs at temperatures that permit long life operation.

This hollow cathode concept was first used on bombardment thrusters on the SERT II thruster (reference 5.1.15). Because the external power supply is operated in a constant current mode, the plasma sheaths will continuously rearrange themselves to form the necessary impedance "bridge" between the cathode and the external main discharge (reference 5.1.16). These sheaths will actually assume dimensions to maintain a

space charge limited situation. Because the hollow cathode requires the plasma to essentially provide space-charge limited distances, ignition of the discharge without some auxiliary means is extremely difficult. This is due to the relatively low field strengths resulting from the large cathode to anode dimensions. To alleviate this problem, a keeper electrode is placed 0.060 inches downstream of the cathode. This electrode is raised to 400 volts open circuit voltage. Discharge ignition can then be achieved by heating the cathode and low work function material to approximately 1000°C, introducing about 100 equivalent milliamps of mercury flow, and applying the starting voltage to the keeper electrode. The keeper supply is designed to rapidly decrease voltage as the current increases until the final operating voltage of 5 to 10 volts is attained.

Operation of the discharge requires four individual power supplies: the discharge supply, the keeper supply, a magnetic baffle supply, and a cathode tip heater supply.

3) Ion Extraction System - Once the ions are formed, they are extracted and accelerated from the discharge into an ion beam by the ion extraction

system (refs. 5.1.17 and 5.1.18). This system is also referred to as an accelerator grid or an ion optics system. It consists of two perforated, dished electrodes which are maintained at a spacing of 0.50 to 0.75 mm (0.020 to 0.030 in.). The screen electrode has 1.9-mm (0.075-in.) diameter holes and is biased positively and forms one boundary of the discharge chamber. The accelerator electrode has 1.14-mm (0.045-in.) diameter holes and is maintained at a negative potential of -300 volts. Ions are extracted from the discharge plasma through each hole in the screen and accelerated through the matching holes in the accelerator to form ion beamlets as depicted in figure 5.3.4.1-1. Proper focusing of the ions is required to prevent them from striking the accelerator electrode. The factors which affect focusing are the relative values of the electrode voltages, gap to hole diameter ratio, alignment, and ion current through the extraction system (ref. 5.1.19). If too much current is forced on the grid system, a space charge condition will occur which will defocus the ion beamlet and cause direct impingement on the accelerator.

In practice, the hole pattern on the screen grid is intentionally misaligned (reference 2.1.20). The degree of misalignment is greater at the periphery where the curvature of the electrodes makes the beamlet diverge from the thruster axis. This divergence represents a thrust loss. The intentional misalignment distorts the electric field to curve the beamlet back to a direction parallel to the thruster axis and thereby recovering the thrust.

One important electrode parameter which significantly affects performance and discharge voltage is the accelerator hole diameter As will be seen later, the discharge voltage strongly affects thruster lifetime. Thus the present accelerator design incorporates a small hole accelerator grid. This design is discussed in detail in references 5.1.21 and 5.1.22.

4) Beam Neutralization System - The ion beam which is extracted from the discharge chamber must be neutralized. If charge neutrality is not achieved, a space-charge condition will result which will cause ions to return to the accelerator electrode to achieve neutralization. In

practice neutralization is accomplished by the screen supply. A small fraction of the screen energy is used to inject the excess electrons resulting from ionization, originally collected at the discharge anode, back into the ion beam. The neutralizer is also a plasma-bridge hollow cathode and operates in the same manner as the main discharge cathode described previously (references 5.1.23 through 5.1.25). The neutralizer also requires a tip heater supply and a keeper supply.

A primary beam ion has sufficient energy to, if properly focused, overcome the attraction of the negatively biased accelerator. The vast majority of these high energy ions continue on in the beam to provide thrust. However, a few ions undergo a charge-exchange collision. This results in a high energy neutral and low energy ion which is attracted back to the accelerator electrode as impingement current. The level of this current increases as either the ion current and/or the neutral density increase. Thus high neutralizer propellant flow rates and/or poor utilization of main propellant flow rates will result in high accelerator currents which can

be focused on a small portion of the accelerator electrode. This led to significant erosion on the SERT II thruster. However, proper location of the neutralizer relative to the accelerator electrode has reduced neutralizer caused accelerator erosion to acceptable levels (ref. 5.1.26)

5.3.4.2 Software Characteristics

Thruster operation consists of static or steady state operation and dynamic operation which includes startup, throttling, off-normal correction, and shutdown. This section defines the sequence of events and algorithms used to operate thrusters. Section 11.0 on thruster controller describes how these procedures have been implemented in software.

1) Steady State Operation - A steady state operating point is obtained by setting each of the electrical operating parameters and the three vaporizer proportional controller references. The principal parameters to be varied are the screen voltage and beam current since these define the thrust and specific impulse. As discussed in reference 5.1.4, the screen voltage operating envelope is between 600 and 1100 V. The maximum beam current is 2.0 A. The minimum beam current is 0.75 A. For minimum power at 1100 V, the

minimum beam current is 0.46 A. Although operation at low beam currents is possible, operational preferences limit minimum beams to the 0.75 A level. At very low power levels, the discharge losses are low enough that thermal feedback is insufficient to keep isolators and feed system elements warm without adding heaters or purposely making the discharge inefficient to increase losses (dissipation). Also, at very low power levels the discharge is "noisy" and the ability of the power supply system to quench arcs and reestablish a beam is marginal. Operation above 0.75 A eliminates these considerations.

In establishing thruster operation procedures, some attention was paid to the "programability" of the resulting algorithms. The largest factor in an accounting of thruster power is the beam power which produces useful thrust. The next largest factor is the discharge power loss. It is useful to express discharge operating conditions as a simple function of beam conditions. It was decided that the discharge voltage reference should be held at a constant 32 volts for long life operation. The discharge current (anode current) J_d is related to the beam

current J_b by the following relationship:

$$J_d = 6J_b + 2$$

Variations in J_d result in only second order effects on performance. Using this relationship and other approximations discussed in Section 5.3.1.3 and reference 5.1.4, it is possible to express total power as a function of screen voltage and beam current only. Any point within the solid envelope of figure 5.3.4.2-1 is considered an acceptable steady state operating point. This envelope is defined by the lines of $J_b = 0.75$ and $J_b = 2.0$ A and $V_{screen} = 1100$ and 600 V. Note that the high beam current low screen voltage corner of the envelope is cut-off. This line represents the practical maximum beam current for which an ion extraction system can be designed to extract a beam as a function of screen voltage. Note also extension of the envelope below $J_b = 0.75$ A is possible. but is not immediately available without further refinement of operating algorithms.

2) Dynamic Operation - There are many procedures and sequences which will result in thruster startup and operation. The procedures described in the following sections have been selected as

"baseline" procedures for J-series thrusters and have been committed to software for computer control. Baselining algorithms was necessary to allow programming and orderly evaluation and refinement to occur. Because the evaluation process is a lengthy one, changes are not made unless needed. The following sections then are quite specific with regard to thruster operation but it must be pointed out that changes are possible in many areas if applications require them.

a) Startup - The baseline thruster startup algorithm is shown in figure 5.3.4.2-2a and b. It consists of four phases: Preheat High, Preheat Low, Ignition Heat, and Run. A brief description of each phase follows:

The "Preheat-High" phase provides initial heating of main and neutralizer cathodes and main and cathode isolators and feed system prior to startup. The isolator heater power is provided by the discharge supply through the isolator relay. The total isolator heater power is typically 120 watts and is intended to raise feed system temperatures close to those needed prior to initiating propellant flow in a rela-

tively short period of time. This phase is maintained for 18 minutes unless the thruster off time is less than about four hours, in which case the "Preheat-High" time is shortened.

The "Preheat-Low" phase continues cathode and feed system heating prior to turning on propellant flow. However the isolator heater power is reduced by a factor of two to slow the rate of temperature increase This increases the probability of temperatures remaining within the desired temperature window when main propellant flows are initiated. This phase lasts for 17 minutes.

Further, since the neutralizer feed system thermal mass is low, neutralizer tip heater power is sufficient to provide adequate neutralizer temperatures in relatively short times. Thus the neutralizer vaporizer is turned on at the beginning of "Preheat-Low" phase. The vaporizer supply is maintained in closed-loop proportional control at all times

During the "Ignition-Heat" phase, the isolator heater power is turned off and the isolator relay again opened such that the discharge supply

is in normal operation. The cathode vaporizer is turned on in closed loop control and the main discharge is established. This phase lasts for 8 minutes. During this phase, the main vaporizer is off and its temperature is uncontrolled. The main vaporizer flow rate is critical for a good startup. The main vaporizer temperature should generally be 0 to 10° C above the 0.75 A operating temperature of the vaporizer and will cool off by about 10° C in the 8 minutes of this phase.

At the end of this phase, a final check of neutralizer and discharge ignition should be made. If either is not lit, then the algorithm should retreat to the beginning of the "Preheat-Low" phase for a second pass through "Preheat Low" and "Ignition Heat". If this final check is negative the second time, the startup should be terminated and the thruster allowed to cool down before any restart attempts. This is shown in the flow diagram of figure 5.3.4.2-2a.

The "Run" phase involves the turn on of the screen and accelerator high voltages and extraction of the ion beam.

If low mode or excessive arcing results, the appropriate off-normal algorithms shown in figure 5.3.4.2-3 or 5.3.4.4 should be employed. If the discharge goes out the algorithm should retreat to the beginning of the "Preheat-Low" phase as above.

b) Throttling - Throttling is changing from one steady state operating point to another during the run phase. Throttling must be done in a prescribed manner to maintain control during the transition and to prevent off-normal conditions. This is achieved by observing proper sequencing and timing of set point changes to allow for thermal lags in the system response. Only five operating points need be changed for throttle. They are 1) the beam current reference, 2) discharge current, 3) magnetic baffle current, 4) screen voltage, and 5) neutralizer keeper voltage reference. All other set points are fixed during the run phase. A general discussion of throttling is presented in reference 5.1.4. Since operation at too low a discharge-to-beam current ratio results in low mode, changes in the above parameters should be made in order 1 to 5 when throttling down

and in reverse order when throttling up. The abnormal operating conditions are described in detail in a later section.

Changes during throttling should not be made in greater than 0.1 A beam current increments or 100 V screen voltage increments. Changes should be made at 30 second or greater intervals to provide adequate time for proportional control loops to respond and temperatures to equilibrate.

Consideration of mission parameters dictates the selection of a throttling profile. For example, the ideal specific impulse (see Section 5.3.1.3) is a function only of screen voltage. The line on figure 5.3.4.2-1 corresponding to 1100 V screen voltage represents an ideal specific impulse of 3350 sec. Likewise, screen voltage of 900 V corresponds to 3035 sec and screen voltage of 600 V corresponds to 2490 sec. The ideal thrust is a function of both beam current and screen voltage. Two typical constant ideal thrust lines for 65 and 75 millinewtons are shown in the figure. A throttling profile near the top of the envelope will provide a high specific impulse as the expense of thrust, while

moving along a line of constant power towards the lower half of the envelope will increase thrust at the expense of specific impulse.

Throttling has been demonstrated for the three profiles of figure 5.3.4.2-1 as well as for constant voltage lines of 1100, 900, 800, 700, and 600 V within the envelope and lines of constant beam current equal to 0.75, 1.0, 1.3, 1.6, and 2.0 A within the envelope. Therefore, it is possible by combining various profiles to generate virtually any throttling profile within the envelope which mission considerations might dictate.

A "standard" throttling profile for the 30 cm thruster is the linear screen voltage-beam current relation shown in figure 5.3.4.2-1.

$$V_s = 400\ J_b + 300$$

This so-called "standard" was adopted as it was simplest to code and it fulfilled the requirement to throttle over a 4:1 power range. It need not be adhered to rigidly if there is advantage to the mission by throttling over another profile within the bounds described above.

Specific values of magnetic baffle current and

neutralizer keeper voltage as a function of beam current are determined for each thruster during the thruster acceptance test.

c) Off-Normal Correction - The two most common off-normal conditions are low mode and excessive high voltage arcing. These usually result from improper throttling or start-up or other perturbation. Low mode is a condition resulting from excessive main propellant flow. The high density of neutral mercury atoms change the characteristic of the discharge such that the beam actually decreases with further increases in flow rate. This causes loss of control since the proportional control loop continually attempts to increase beam current by increasing vaporizer flow and that only succeeds in driving the main flow rate to the limit determined by thermal equilibrium of the feed system. Since this condition results in very low utilization efficiency, it is accompanied by a high accelerator impingement current. Correction of this condition is accomplished by turning off the main vaporizer until control of propellant flow is reestablished as shown in figure 5.3.4.2-3. Increasing the discharge voltage set point serves to increase

stability of control loops and hastens the ionization and extraction of the excess neutrals in the discharge chamber.

Excessive high voltage arcing is also generally caused by excessive flow. The correction of this condition is to turn off the high voltage and main vaporizer until neutral densities are sufficiently reduced. This algorithm is shown in figure 5.3.4.2-4.

It should be noted that proper timing and checks must be added to these algorithms to insure that operation is not trapped in a continuous loop if the algorithm should fail.

d) Shutdown - Shutdown of the thruster is accomplished by merely throttling down to the lowest point on the throttling profile and turning off all power supplies.

5.3.5 Thruster Lifetime

Thruster life limiting factors can be discussed on the basis of two types of areas within the discharge chamber. First are erosion sites where sputter phenomena remove material and cause wearout. The second consideration is deposition sites where the sputtered material is deposited at a rate exceeding

the sputter rate for that site. Sputter erosion of various discharge chamber surfaces is discussed in references 5.1.27 and 5.1.28. The most critical of these surfaces is the discharge side of the screen electrode since it is thin to begin with and its geometry effects ion extraction performance. Deposition sites are also of concern since sputtering of erosion sites results in thin deposited metallic films on non-sputtered surfaces. These films build to a thickness where they begin to peel off or spall (references 5.1.27 through 5.1.30). The resulting flakes are then free to move about within the discharge chamber and cause electrical shorting.

These phenomena were noted in the 10,000 hour life test described in reference 5.1.27. Short and long term testing (references 5.1.29, 5.1.31, and 5.1.32) indicated covering of deposition surfaces with wire mesh to be an effective preventive of deposition spalling. This wire mesh provides a rough surface for deposited material to lock into as it builds up. These results primarily influenced the physical design of the discharge chamber components.

The primary factors that influence sputter rates were found to be beam current (ion density) and

discharge voltage (ion energy).

The beam current operating point is obviously dictated by mission requirements, however selection of the 32 volt operating point for the discharge voltage is dictated primarily by sputter erosion rates. Since lower voltages result in lower sputter rates, the lowest discharge voltage consistent with performance requirements was chosen.

Results of both component and thruster testing for both 30 cm and SERT II systems indicate that other factors such as cathode emissive mix depletion, accelerator electrode erosion, and so forth, are not critical life-limiting factors. (See refs. 5.1.27, 5.1.31, 5.1.33 through 5.1.35).

5.4 Interface Definition

5.4.1 Electrical

The electrical interface between the thruster and the power processor outputs is the wiring harness. This harness grouped in two bundles, attached to the thruster, is shown in figure 5.4.1-1a and the accompanying wire list of figure 5 4.1-1b. The wires are terminated at the power processor end with loop type crimp-on connectors designed to fit over a #10 screw type terminal

The wire list also shows three Chromel-Alumel (type K) thermocouples included in the harness. It is intended that these vaporizer thermocouples be used only for ground testing and would be suitably terminated without thruster disassembly and would not be used for flight.

An interconnection drawing of the thruster/power processor is shown in figure 5.4.1-2. That figure includes an isolator heater supply (PS-4). In reality that supply is not used in the baseline algorithms described in section 5.3.4.2. The discharge supply is used to provide isolator heat.

5.4.2 Mechanical

Mechanical interface details and outline dimensions of the thruster are shown in figure 5.4.2-1. It shows that the thruster is supported at four locations. Two mounting points are located 180° apart on the thruster sides. These are referred to as gimbal mounting pads. The two remaining points are located on the backside of the thruster on the ground screen. (For the gimbal side see section 7.4.2).

The standard electrical harness for the thruster is contained in two bundles 12 feet long located as shown in figures 5.4.2-1 and 5.4.1-1a. That standard

length of cable is adequate to reach the power processor terminations in the BIMOD configuration.

The mercury feed line connection is located on the backside of the thruster ground screen as shown in figures 5.4.2-1 and 5.4.1-1a. (For mercury feed line side see section 1.3.4.2.) The feed-line can be connected to the thruster without removing the ground screen. Either of two different mainfolds can be mounted to the thruster. The type intended for flight has a single mercury feed tube. The type used for preliminary thruster testing has separate feed tubes for each of the three vaporizers so that individual flow rates can be measured.

5.4.3 Thermal

The thermal interfaces of the thrusters consist of an insulation blanket placed between the radiators behind the thrusters, the mounting of the thrusters with the structure, adjacent thrusters, and the space environment.

A simplified heat balance for a thruster and its interfaces is shown in figure 5.4.3-1.

Past analyses assume that the heat transfer through the insulation blanket is zero as shown in the sketch and that the heat conducted through the

supports (Q_c) is zero.

The solution of the heat balance depends on many variables such as view factors, optical properties, radiating area, etc. Analytical results have been generated for a thruster operating at full-power (i e., 2 amp beam current). These results can be found in applicable document 5.8.5.

The insulation blanket temperature varies from -87° C to 409° C depending on the solar flux, blanket spacing, and the optical properties of the blanket. Although not presented in the results, the temperature of the main body of the thruster (designated thruster body in sketch) varies from 198° C to 323° C depending on the solar flux, blanket spacing, and the optical properties of the blanket.

5.4.4 Thruster Induced Environment

An interface area exists between propulsion device effluents and other space vehicle systems. The particle and field efflux from ion thrusters and its impact on space vehicle systems has been the subject of many studies and publications. Reference 5.1.36 identifies many of the publications in this area and classifies them with regard to analytical or experimental type, ground or space location,

thruster size and propellant.

Thruster efflux can be classified in the following five categories: 1) Nonpropellant particles which are primarily sputtered metal - most of which travels in straight lines from sputter sites. 2) Neutral propellant particles which are emitted at low energy from the thruster and also travel in straight lines from the thruster. Occasionally a high energy neutral particle will be produced by a collision of a low energy neutral propellant atom with a high energy beam ion. 3) Beam ions which are highly energetic and travel straight away from the thruster after being accelerated by the ion optics from the discharge chamber plasma. 4) Low energy plasma which is produced by charge exchange reactions of the high energy beam ions and the neutral propellant. Unlike the previously mentioned particles, the trajectories of the low energy plasma particles are strongly affected by local electromagnetic fields. 5) Field effluxes which are the static and dynamic magnetic fields of the thruster and electromagnetic fields from optical to very low frequencies.

The thruster efflux identified above has potential to affect many spacecraft systems such as solar

arrays, thermal control, optical sensors, communications, science instruments, structures and materials and space vehicle potential control. All of these considerations are summarized more completely in reference 5.1.36. A major emphasis of the BIMOD test program is to characterize and assess the impact of effluents from a single and multiple thruster arrays. Multiple thruster testing is important since efflux from "n" thrusters is not in many cases simply the superposition of "n" single-thruster effluxes.

5.5 Performance Description

Thruster performance can be totally described in terms of thrust, specific impulse, and total thrust efficiency, as a function of thruster input power. The exact values of these parameters depends on the specific operating points chosen in the operating envelope of figure 5.3.4.2-1. If the beam is operated at the maximum voltage at the expense of beam current for a given input power, the specific impulse will be maximized, but the thrust will be minimized. Operating at the maximum beam current to screen voltage ratio (as determined by the ion extraction system performance) will maximize the thrust to power ratio, but minimize the specific impulse.

At high beam currents, the power efficiency represents a larger loss than the propellant utilization efficiency. However, the utilization decreases more rapidly with beam current at the lower beam current values and becomes the predominant factor in total efficiency.

However, in general, the actual difference in any of these parameters over the entire range of input power is less than 10 percent. Any operating point within the envelope of figure 5.3.4.2-1 is considered an acceptable steady state operating point. Therefore, constant voltage and constant beam current throttling profile between the 2700 and 710 watt lines are acceptable operating profiles. This affords a great deal of flexibility in mission profile selection.

The performance curves for the linear profile shown in figure 5.3.4.2-1 are shown in figure 5.5-1. These curves represent serial number J-1 thruster data and show improved performance over the data of reference 5.1.4. This is due to the improved extraction system design. A first order approximation of the effect of throttling profile on thruster performance can be made using the combined data of

figure 5.5-1 and reference 5.1.4.

5.6 Physical Characteristics and Constraints

1) Mass - The thruster mass as measured on thruster J-4 is 10.37 kg (22.8 lb). That mass includes 1.45 kg (3.2 lb) of cable.

2) Power - Input power required from the power processor is 710 to 2700 watts depending on operating point. Section 5.3.4.2 contains a discussion of how power level varies with throttle point.

3) Volume - Thruster volume is 26,130 cubic centimeters (1595 cu in.) based upon the outline dimensions of figure 5.4.2-1.

4) Environment - Vibration environmental requirements for the thruster are contained in applicable document 5.8.6. Thermal environmental limits are as follows Temperatures are defined as bulk temperature of main structure baseplate.

a) Nonoperating Survival (dry) - Ultimate temperatures have not been determined.

b) Nonoperating Survival (with mercury in lines) - Reference 5.1.9 documents successful thruster operation after cold soak to -90° C.

High temperature limits have not been determined but would be in excess of operating values below.

Feed line temperature must not be raised if the feed line valve has been closed with mercury in the line.

c) Operating Range - Thruster operation is possible above -39° C - the freezing point of mercury.

High temperature (without application of heater power) should be limited to +250° C so vaporizer heater control is maintained.

5) Packaging - No unusual packaging requirements exist.

5.7 Development History

The development of the electron bombardment mercury ion thruster is well documented in the literature Figure 5.7-1 shows pictorially the development history at NASA-LeRC. Tests of a 10 cm thruster were conducted by Kaufman (ref. 5.1.2) as early as 1959. These first lab thrusters utilized simple solenoidal electromagnetic fields, hot wire filament cathodes and neutralizers, and "steam" operated propellant systems that were "boilers" in the truest sense. Since the primary concern regarding electric propulsion in the early days was the ability to effectively neutralize an ion beam in space, the first efforts were directed towards developing a flight thruster for use on the SERT I spacecraft

(figure 5.7.1 and reference 5.1.3).

Parallel efforts were being conducted to improve thruster and system performance, lifetime, and weight by use of permanent magnetic fields (ref. 5.1.37), oxide coated cathodes (refs. 5.1.38 and 5.1.39) and electrically controlled, variable flow porous tungsten propellant vaporizers (ref. 5.1.40). These efforts made possible the SERT II mission, intended to demonstrate extended operation of mercury ion thrusters in space (refs. 5.1.34, 5.1.35, and 5.1.41 through 5.1.45). Parametric investigations of discharge chamber and permanent magnetic field variations eventually increased thruster efficiencies. The use of the plasma bridge hollow cathode neutralizer improved neutralization efficiency and lifetime (refs. 5.1.23 through 5.1.25) The adaption of this type cathode to the main discharge further enhanced lifetime and, since chemical contamination and absorption was not nearly as critical as with the oxide coated cathode, greatly simplified ground testing, handling, and storage. With the exception of the ion extraction system, the SERT II thruster represents the summation of various technologies which are still in use on the 30-cm thruster today.

The SERT II spacecraft contained two thrusters. The first thruster operated for a total of 2000 hours before a grid-to-grid short apparently terminated its test. The second thruster operated for 3800 hours, compared to the mission goal 4300 hours before the same type failure occurred. These shorts were attributed to extensive localized ion erosion of the accelerator electrode in the area of the neutralizer location (ref. 5.1.35). This problem was subsequently addressed in the SERT II and the 30-cm thrusters with the resulting repositioning of the neutralizer further away from and directed more downstream from the accelerator (ref. 5.1.26). This modification has eliminated this life limiting factor.

After the shutdown of the SERT II thrusters, the spacecraft continued to orbit for several years with a portion of each 90 minute orbit in the earth's shadow. In 1973, the spacecraft was repowered and the discharges of both thrusters re-lit (ref. 5.1.35). One thruster also has successfully produced an ion beam. Tests with the SERT II spacecraft are continuing.

Even before the launch or SERT II in 1970, research into higher thrust to power systems was underway.

Since this goal requires a lower beam voltage and higher beam current, initial emphasis was placed on improving the ion extraction system using the same analytical techniques which were perfected during the SERT II program (ref. 5.1.19). One concept involved the use of a single composite, glass-coated grid, but this design proved to be dependent on sputtered material from the test facility and was abandoned (ref. 5 1.46 and 5.1.47). Eventually, a technique of hydroforming the grids and then chemically etching the apertures proved to provide excellent mechanical integrity under the thermal load of the discharge at span to gap ratios of about 600-to-1 along with good beam extraction performance (ref. 5.1.17 and 5.1.18)

At the same point in time, the Hughes Research Labs of Malibu, CA were contracted to perform plasma studies of mercury bombardment thrusters (ref. 5.1.48). From 1967 through 1973 the status of the 30-cm thruster was one of continued redesign in order to improve performance, lifetime, and vibration capabilities (ref. 5.1.49). By 1973 however, the thruster design had taken shape in the form of the 700 series thruster. Thruster S/N 701 was committed to a 10,000-hour life test (ref. 5.1.27 and 5.1.28) and thruster S/N 702

was vibrated (ref. 5.1.50). The vibration test resulted in the need for slight structural modifications resulting in the 800 series thruster. Subsequent 10 000-hour life test results indicated internal sputtering to be the primary life limiting factor Extensive testing at Lewis identified and verified modifications for these problems and led to the evaluation of the 900 series thruster. This thruster was committed to life test (ref. 5.1.31).

The test was terminated after 4200 hours due to an electrical harness short. When the thruster was removed from the vacuum facility to modify the harness, diagnostic measurements of thruster wear areas were made. Screen grid erosion was more than predicted and the required 15 000-hour lifetime could not be met.

After intensive investigation, the reason for the erroneous prediction of wear rate was discovered. Pretest wear rates were determined in a LeRC vacuum facility at the equivalent of 2×10^{-6} torr. It was discovered that sputter phenomena (thus wear rate) are a function of tank pressure and background gases. At higher pressures, oxides and nitrides of the base metal were being sputtered rather than the base

metal molybdenum itself. This penomena is documented in reference 5.1.51.

It was known from previous technology work that reducing the size of the holes in the accelerator grid would permit operating the thruster at lower discharge voltage to reduce screen grid erosion without loss of performance. That was the major change involved in moving from 900 to J-series identification although several minor changes to simplify fabrication were made at the same time. A thruster design review was conducted by Hughes Research Labs in February 1978 under Lewis Contract.

One J-series thruster (J1) is currently in long term test at Xerox EOS (ref. 5.1.52) under Lewis contract. This test is a thruster design verification test scheduled for completion in July 1979. Subsequent J-series thrusters (J2 through J8) will be sent to the Xerox EOS facility and to the Hughes life test facility where they will be evaluated. Two J-thrusters will be included in the BIMOD test program. Both of the contracted test facilities mentioned have frozen mercury target facilities to minimize the effect of back sputtered facility material. A description of the BIMOD test program is

included in section 4.0.

As the thruster hardware configuration became established, fabrication and test phases began. Increased emphasis was placed on integrating the thruster with the power processors and defining necessary control algorithms. In 1977, these components were combined with a control computer to provide a total system for test. From these tests has evolved a total system control package which is currently being tested at the Xerox EOS facility and will form the basis of control methods for flight use.

5.8 Applicable Documents Enclosed

5.8.1 Thruster Parts List. (Hughes Research Laboratory.)

5.8.2 Fabrication, Assembly and Test Procedures 37 (IPD's) for 30cm Thrusters.

5.8.3 Ion Propulsion for Spacecraft. NASA Lewis Research Center, 1977.

5.8.4 Modifications of the 30cm Thruster Thermal Model to Account for "Shag" grids (J-Series Thruster), NASA Lewis Research Center Internal Memorandum, April 1979.

5.8.5 Oglebay, Jon C.: Thermal Analysis of 30cm Ion Thruster, NASA Lewis Research Center Internal Memorandum, March 1978.

5.8.6 Test Requirements Document for J-Series Thruster.

5.9 Ground Support Equipment

5.9.1 Electrical Simulator

The electrical simulator is an array of resistors sized to handle the power requirements of a thruster. Resistances which are fixed on a thruster can be simulated by fixed resistors or by variable resistance potentiometers. The potentiometers can be useful for documenting power supply characteristics. The discharge and beam supply loads usually require variable loads simulated by discrete resistors which can be switched-in sequentially or high power carbon pile potentiometers. A schematic of a typical electrical simulator is shown in figure 5.9.1-1.

5.9.2 Shipping Container

Recent 30 cm thrusters have been shipped in standard wooden shipping containers. No special design effort was made and no container documentation exists. Serious consideration should be given to permanent containers for shipping and storage of flight hardware.

5.9.3 Dynamic Mass Model

Two mass models of the thruster can be seen in figure 5.9.3-1. The mass model thruster is fabricated from aluminum. It is only a weight mass simulation, the moments of inertia nor the dynamic response of the thruster were not simulated. The major elements

of the mass model were placed as lumped mass to closely simulate the inertias. The thruster is primarily of sheet metal construction, and it was impossible to simulate the dynamic response. In sheet metal construction, the masses are low and do not couple any significant loads to the gimbal or structure. The thruster gimbal mounting pads are identical to the actual thruster, and the two stand-offs that mount the bottom of the thruster to the gimbal mounting frame were simulated.

5.9.4 Ground Power Supply Systems

There are presently four different designs of power processors used to support thruster testing. They are 1) the two inverter thermal vacuum breadboard (TVBB). 2) the three inverter technology breadboard. 3) the electrical prototype power processor (EP/PPU). and 4) the lab power unit (LPU). All are capable of operating the present "J" series thruster. The first three power supplies are precursor breadboards to the Functional Model Power Processor (FM/PPU) and use SCR series resonant inverters for the main power stages. The TVBB and three inverter power processors each have manual control panels, but have the capability of pre-selection of all set points required for each phase of thruster start-up. They also have

pre-setable set points for up to 15 different thruster throttle operating points (see section 5.3.4.2). These two units have accrued well over 20 000 hours of thruster operation. The EP/PPU incorporates the same electrical design as the FM/PPU and is operable by either a manual input panel, or directly from a computer.

The LPU is functionally equivalent to the FM/PPU, but housed in four standard equipment racks with interconnecting cables. It consists of programmable laboratory type power supplies, signal conditioning amplifiers, A to D and D to A converters in three of the racks while the fourth rack contains the command and control logic and a continuous data display on digital panel meters. The LPU can operate an ion thruster in a direct manual mode with potentiometer adjustment of all power outputs or it can duplicate PPU operation under control of the thruster controller.

The LPU requires a three-phase, 208V input of about 10KW. The output connectors are two "MS 3102" type connectors. The computer control interface is through an "MS 3102" type connector while the 28V power is through an "MS 27508" connector as on the

FM/PPU. For personnel safety, the LPU has interlocks on all doors and power connectors. All ground power supply systems are fully protected for unattended operation. Figure 5.9.4-1 is a block diagram for the LPU and figure 5.9.4-2 is a picture of the unit.

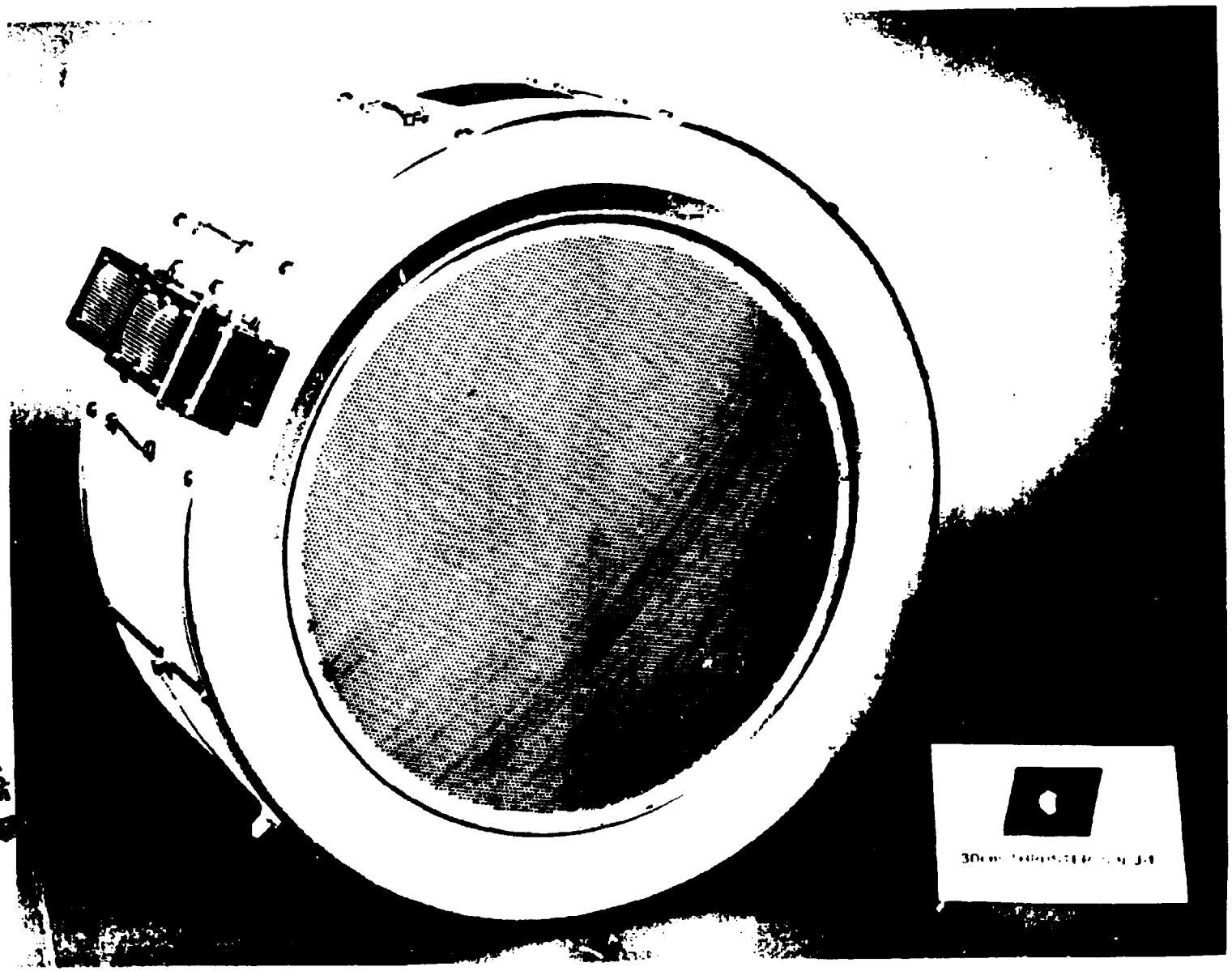

FIGURE 5.0-1 Thruster - Exhaust Side

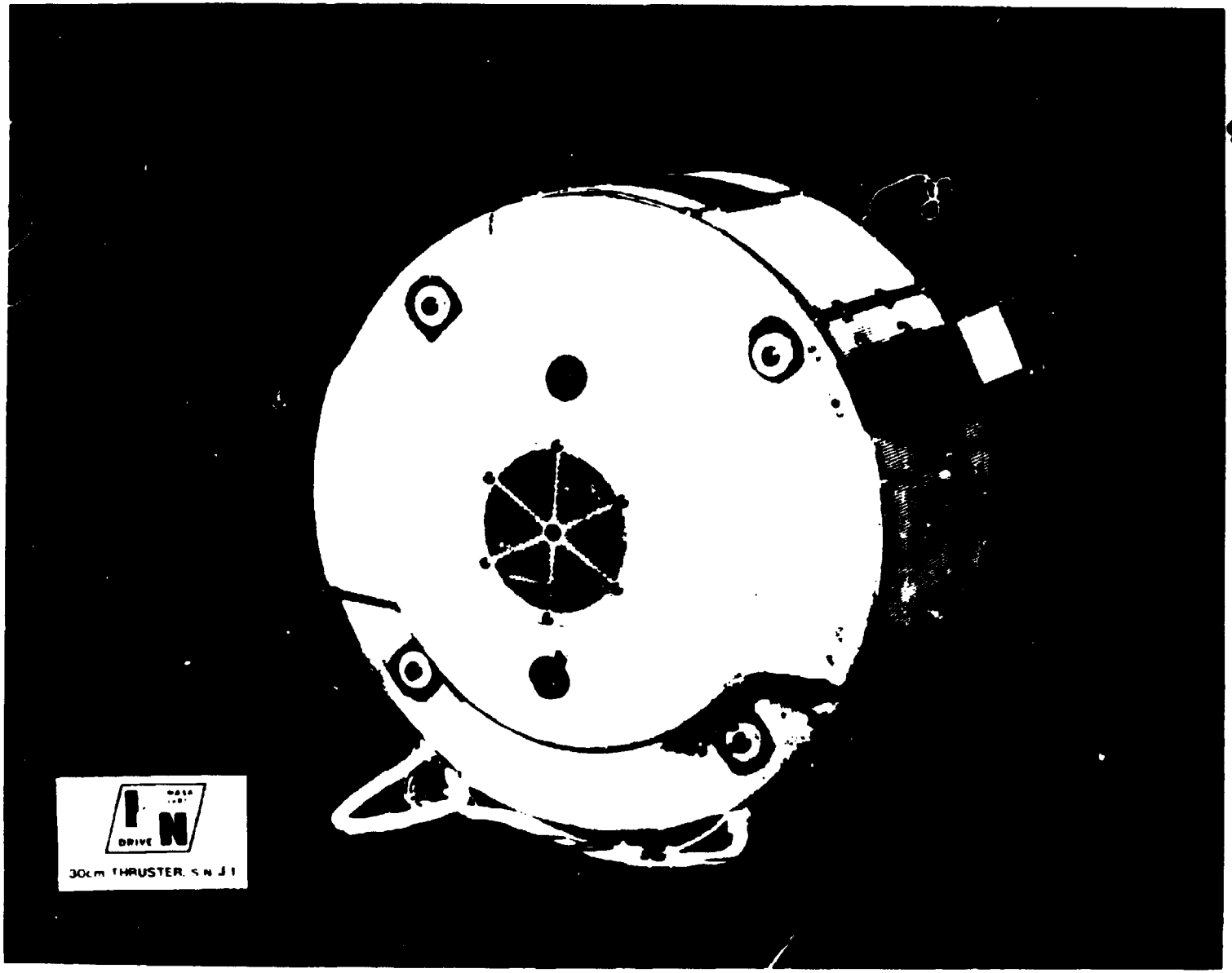

FIGURE 5.0-2 Thruster - Rearside

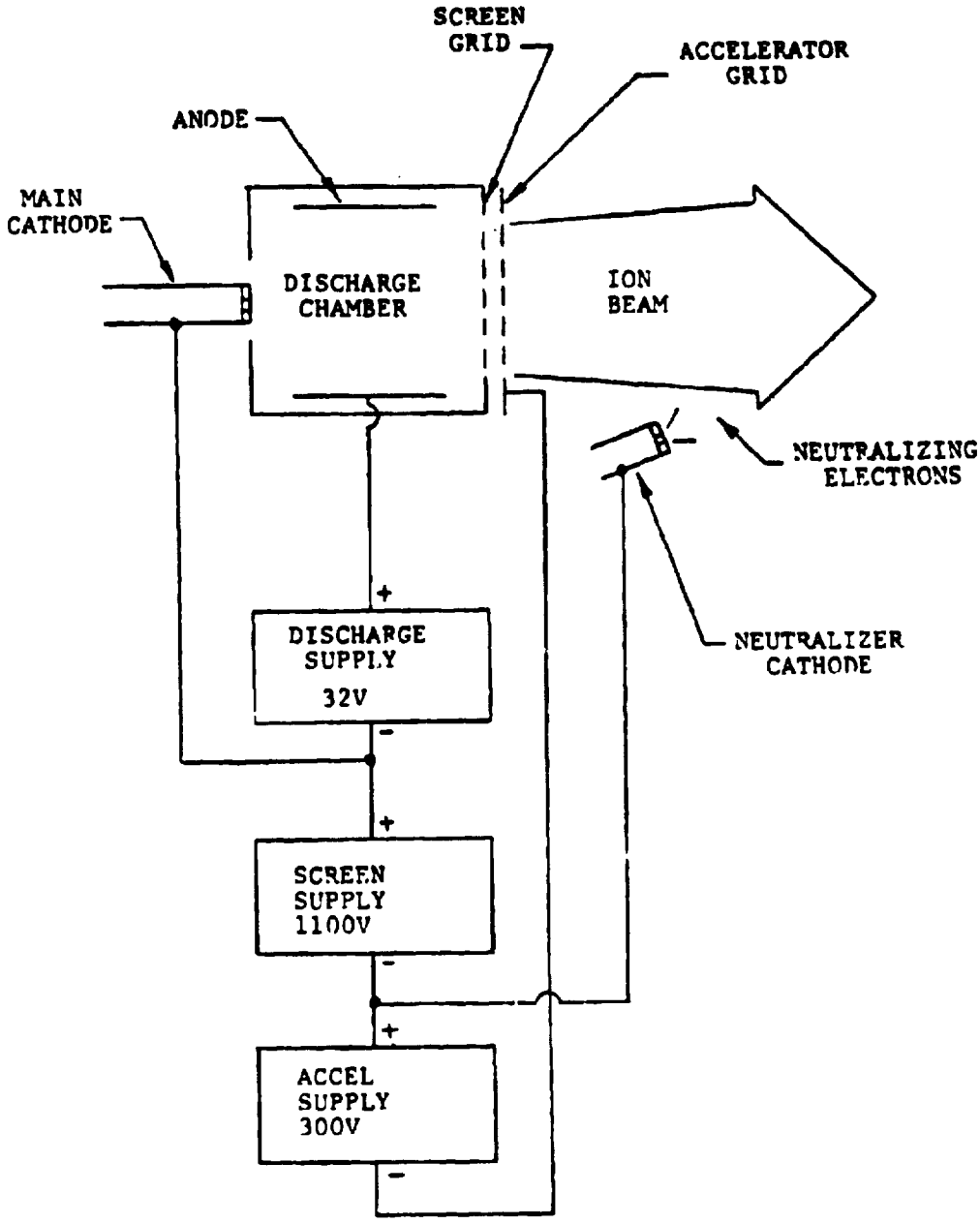

FIGURE 5.3.1.2-1 - BASIC THRUSTER OPERATION

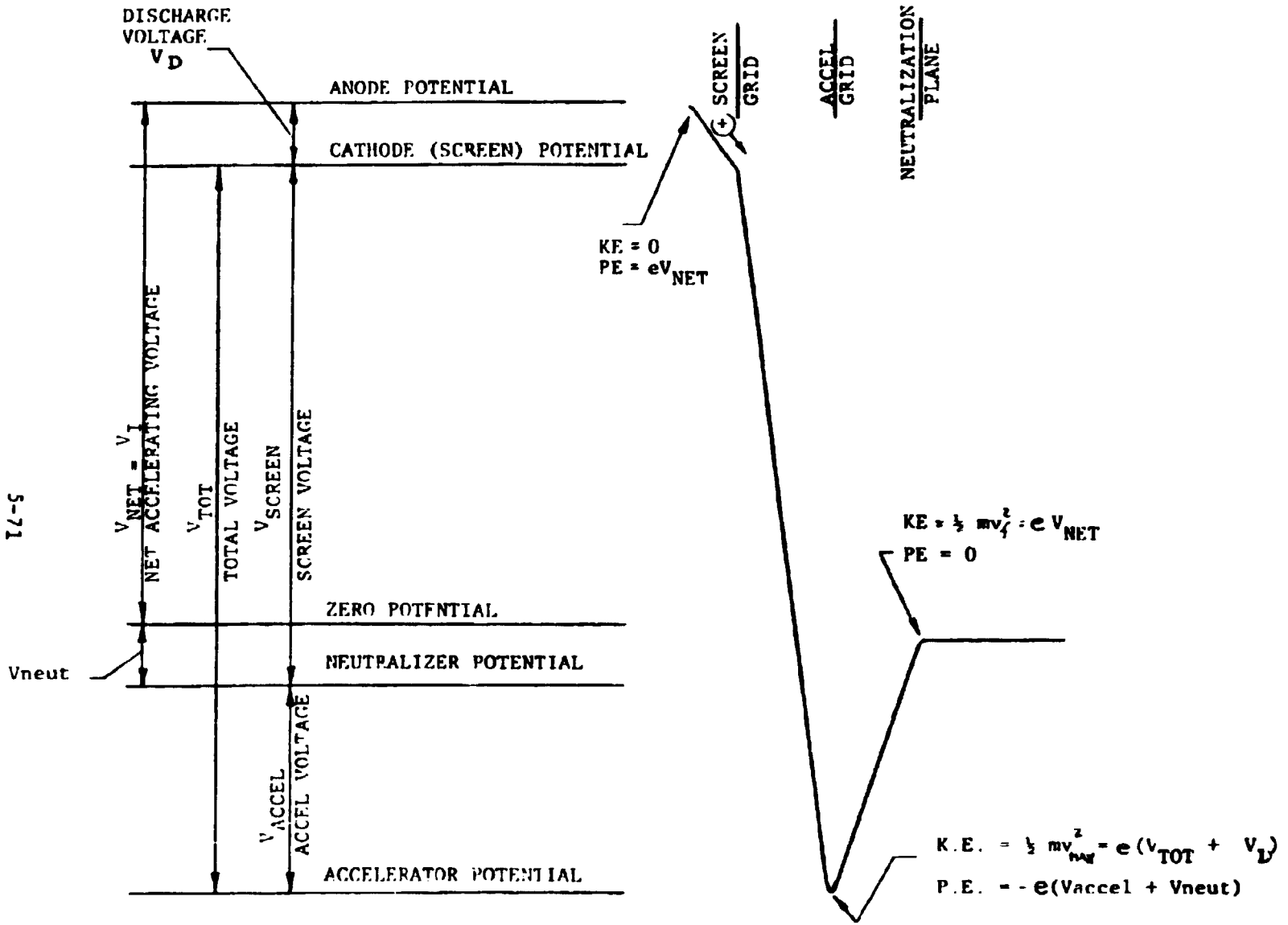

FIGURE 5.3.1.2-2 - THRUSTER POTENTIAL DIAGRAM

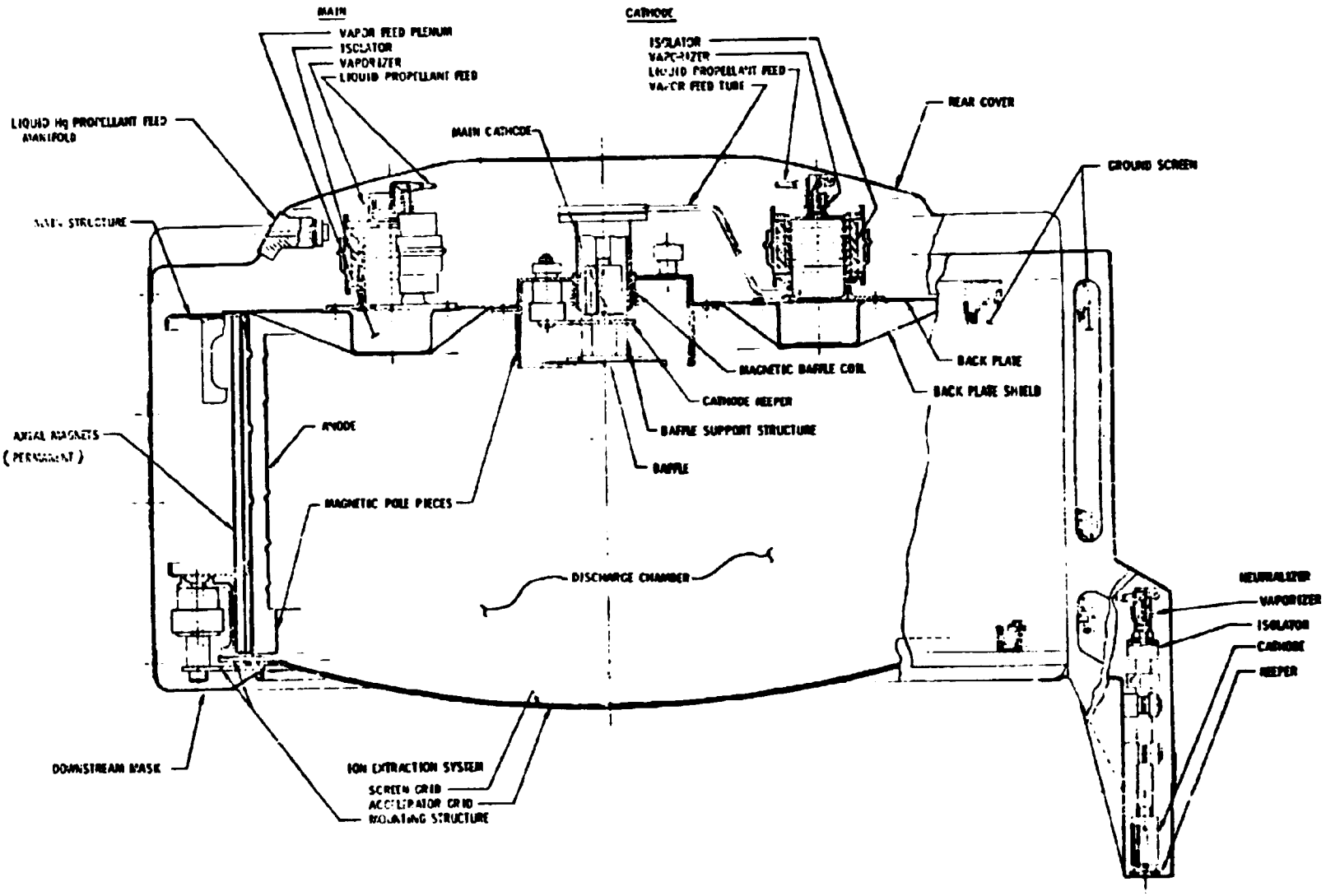

Figure 5.3.2-1
Thruster Cross Section

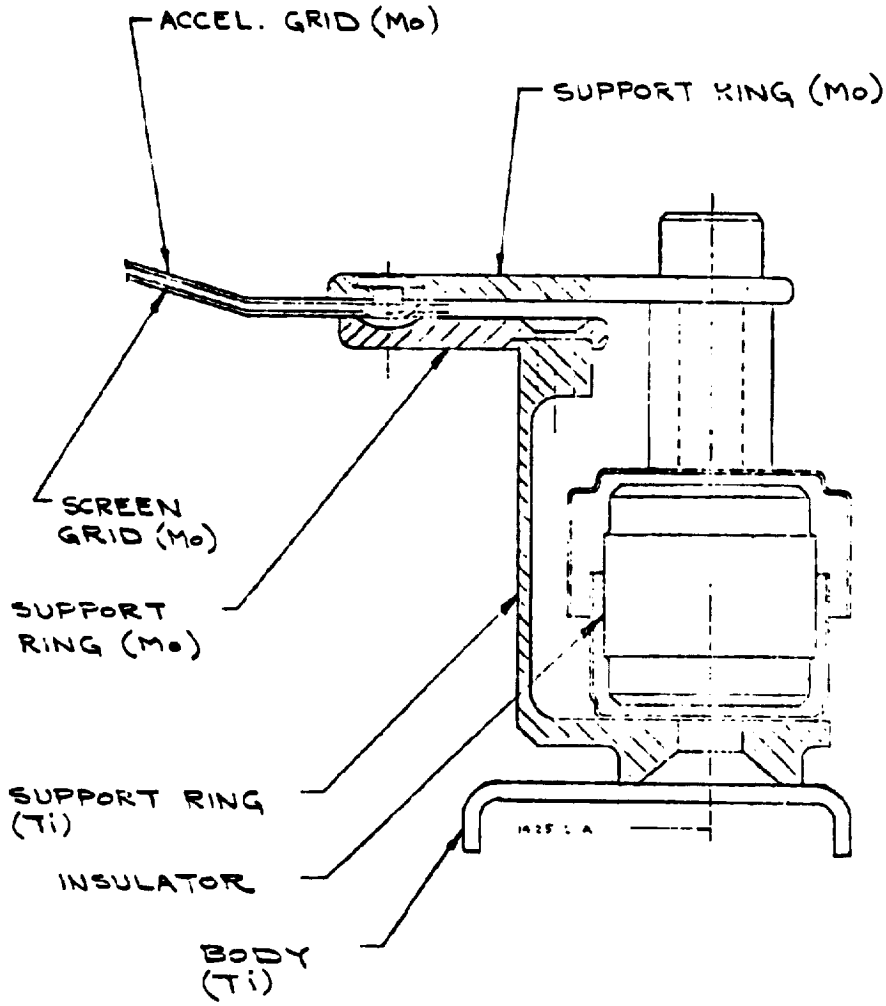

FIG. 5.3.2.3-1
GRID SYSTEM CROSS SECTION

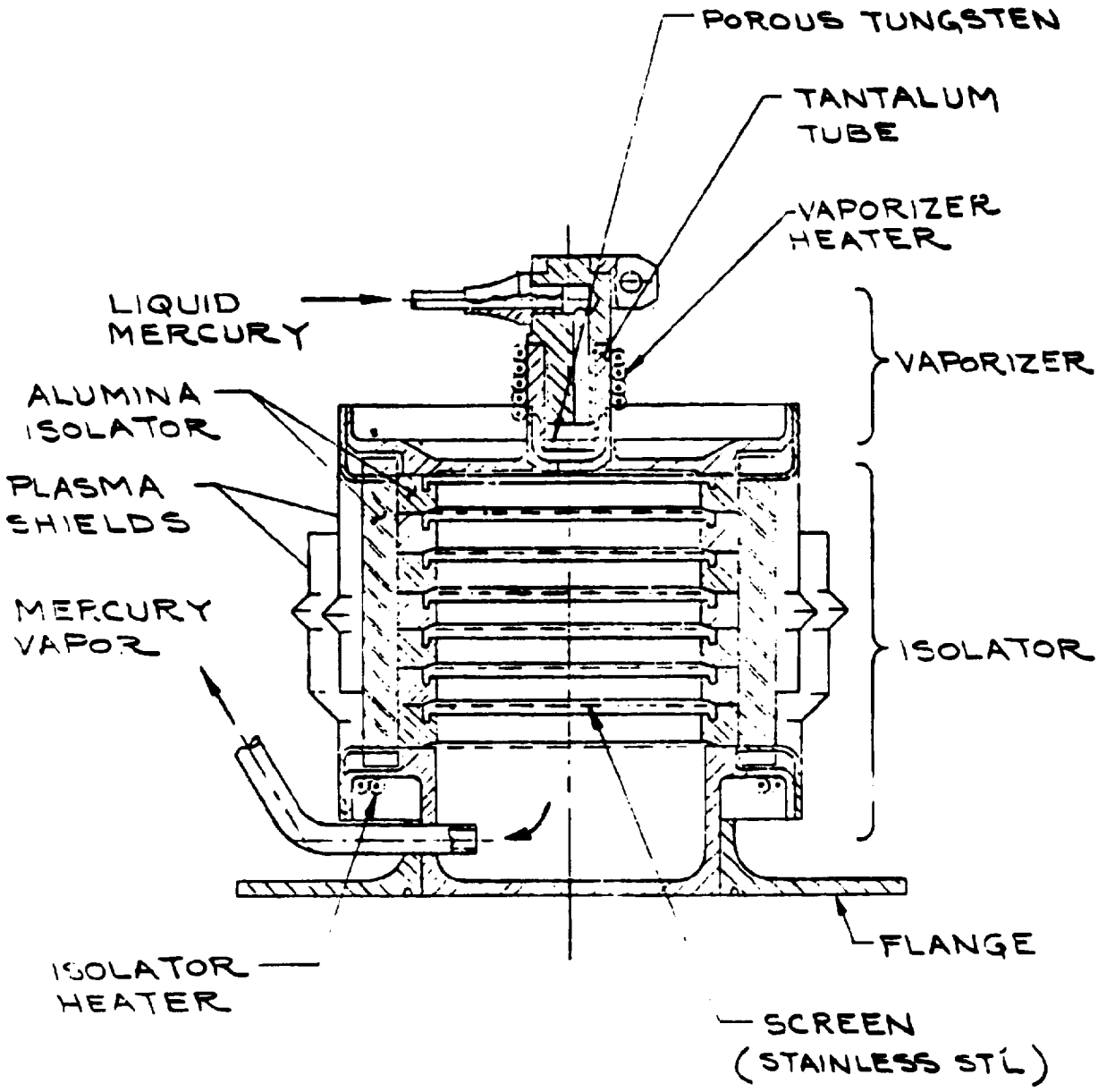

FIG. 5.3.2.4-1
CATHODE ISOLATOR VAPORIZER

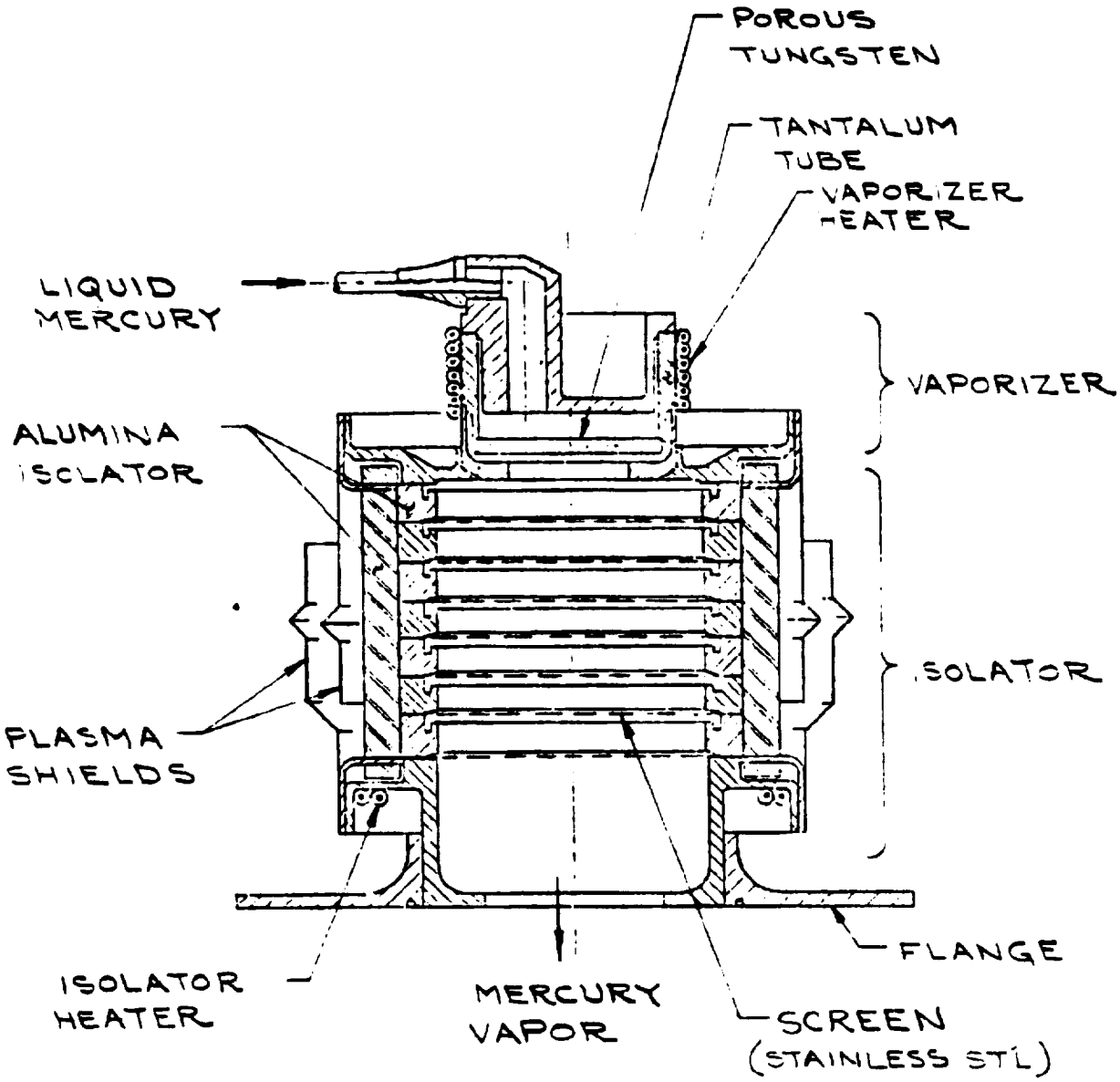

FIG. 5.3.2.4-2
MAIN ISOLATOR VAPORIZER

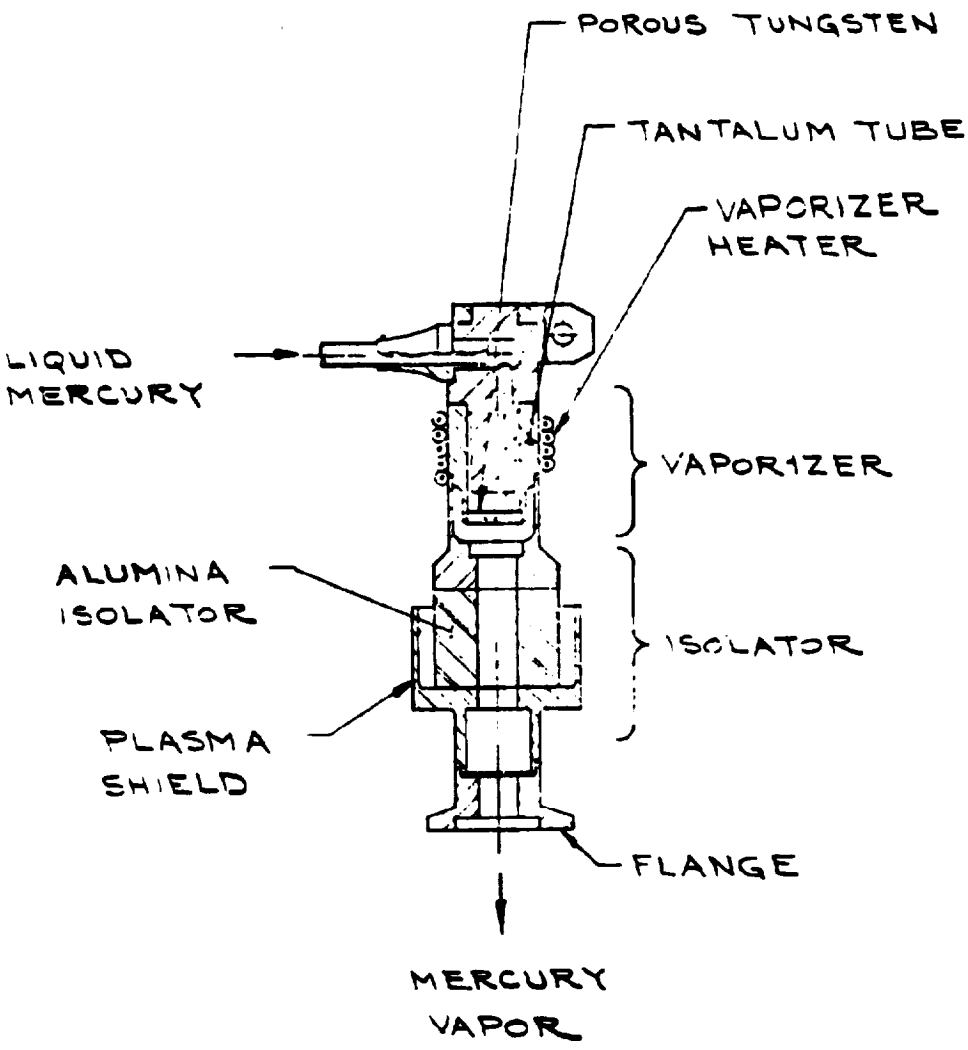

FIG. 5.3.2.4-3

NEUTRALIZER ISOLATOR VAPORIZER

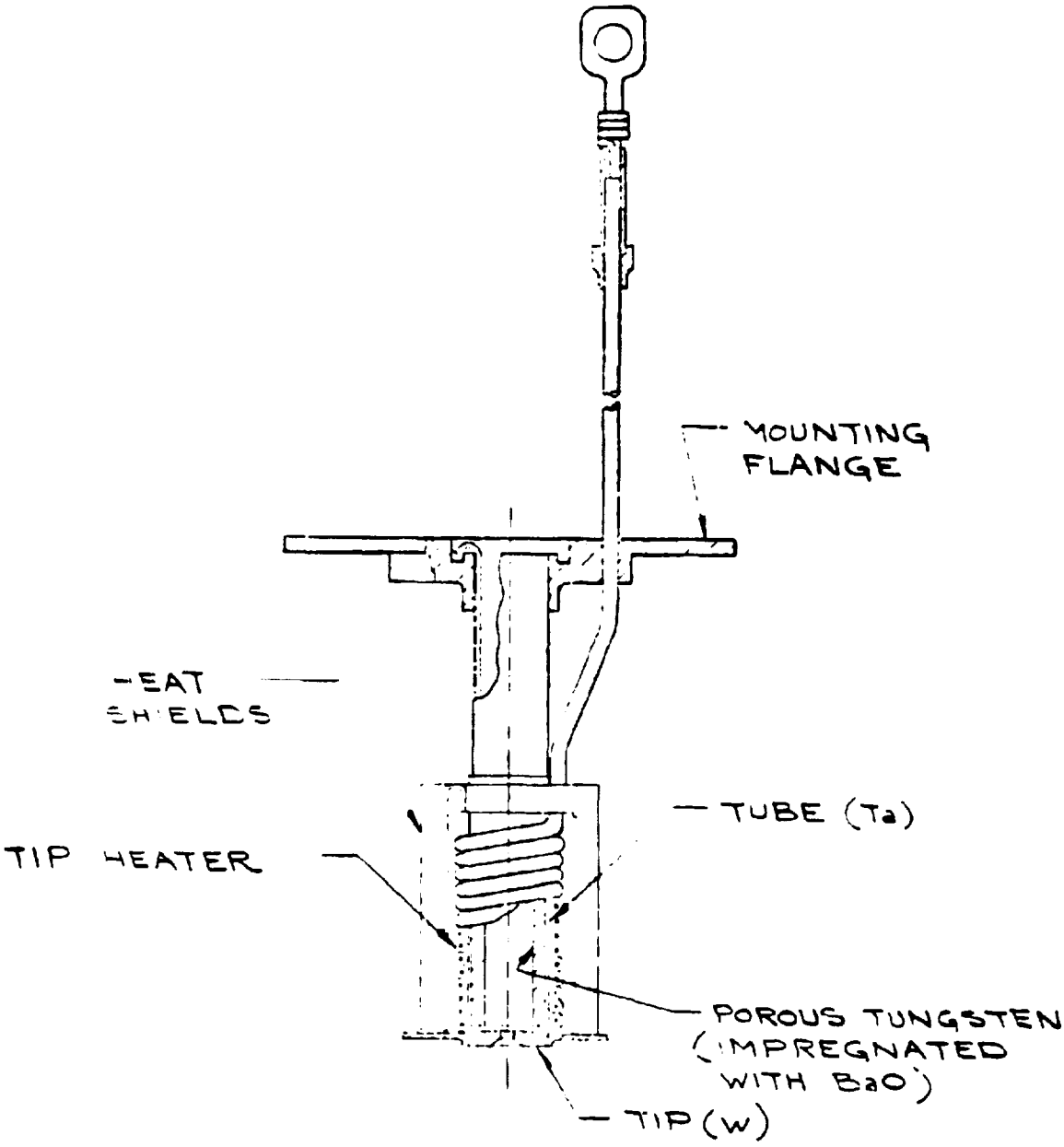

FIG. 5.3.2.5-1
MAIN CATHODE

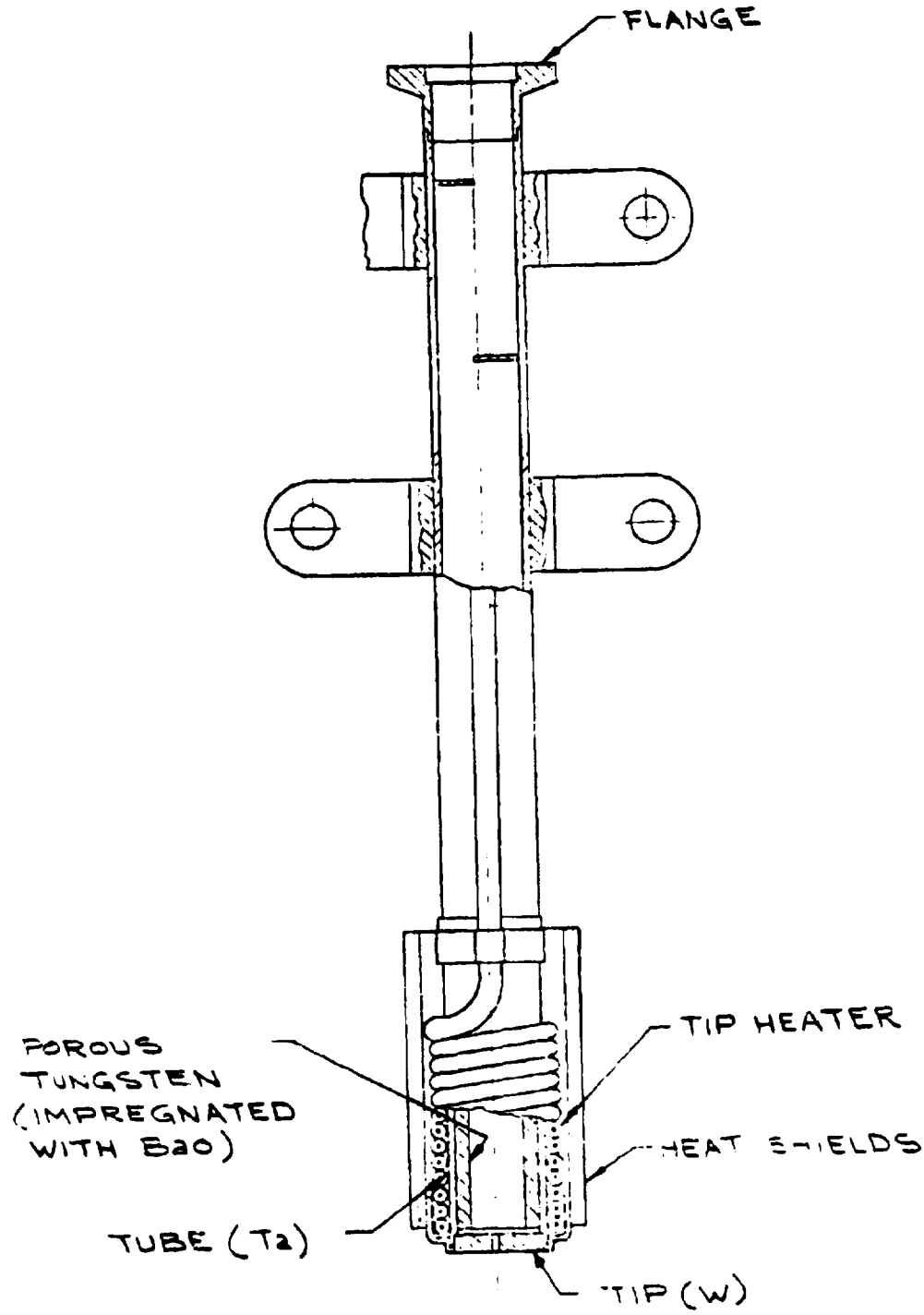

FIG. 5.3.2.5-2
NEUTRALIZER CATHODE

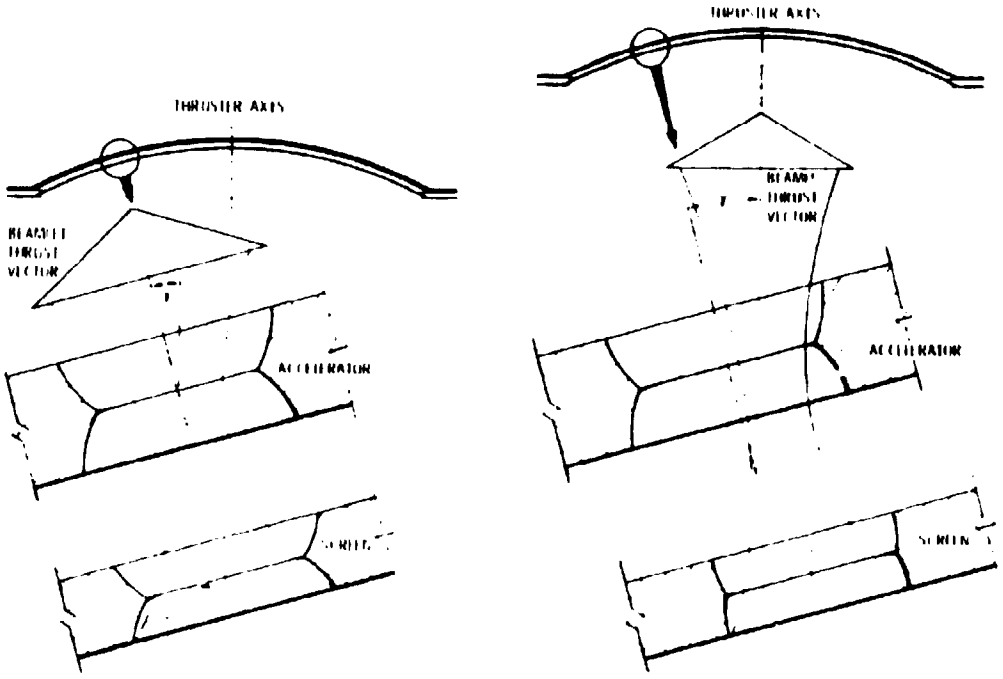

FIGURE 5.3.4.1-1 ION BEAMLET FOCUSING THROUGH GRID APERATURES

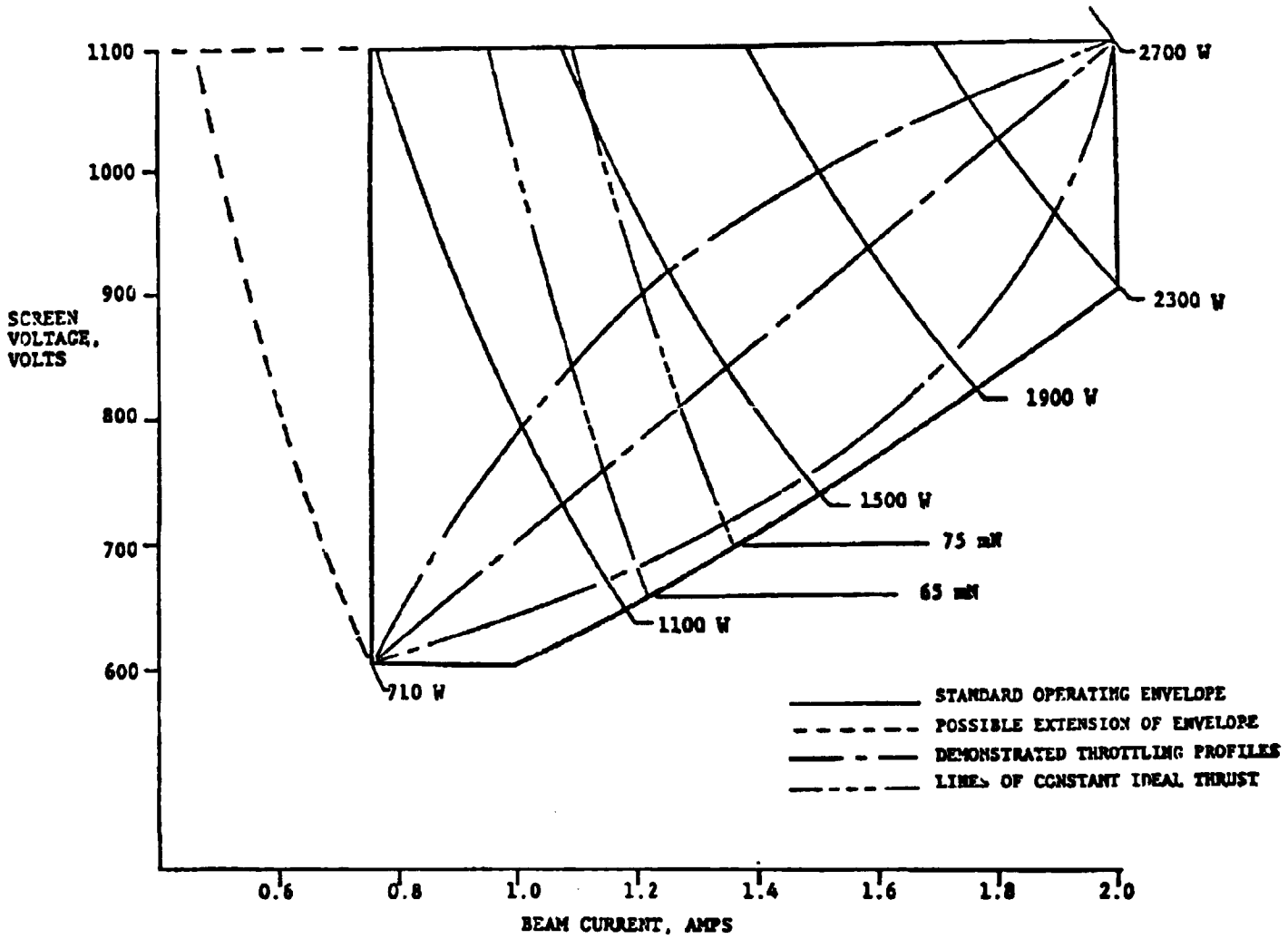

FIGURE 5.3.4.2-1 THRUSTER OPERATING ENVELOPE

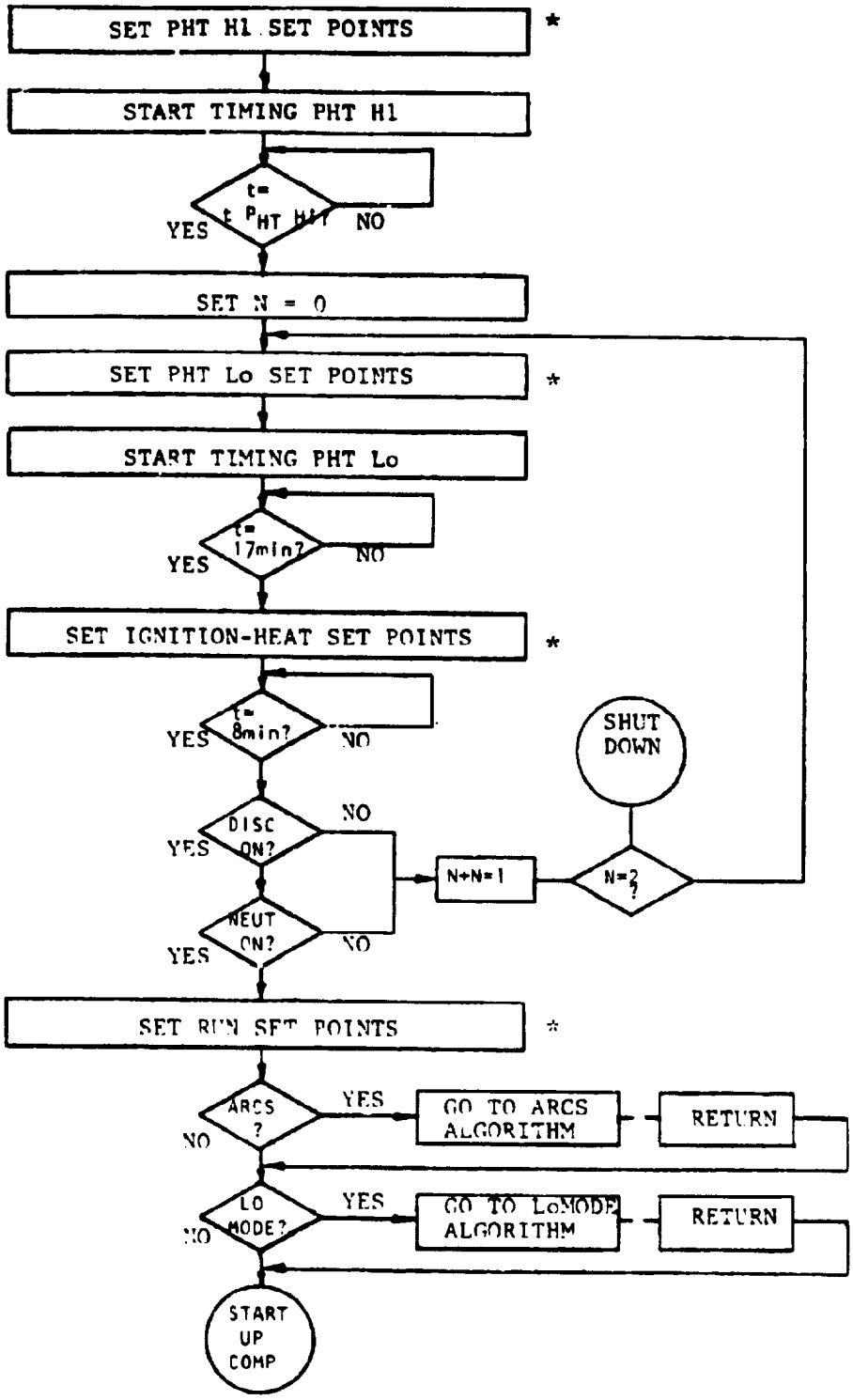

FIGURE 5.3.4.2-2a THRUSTER START-UP ALGORITHM
*See Figure 5.3.4.2-2b

PHASE	MAIN VAP I_1	CATH VAP I_2	NEUT VAP I_6	CATH TIP I_3	NEUT TIP I_5	NEUT KPR I_7	NEUT KPR SET V_{7s}	CATH KPR I_8	DISCH/ISOL HTR I_{9_H}	DISCHARGE I_9	DISCHARGE SET V_{9s}	SCREEN/ACCEL (Hi Voltage) $V_{11/10}$	BEAM SET J_{BS}	MAG BAFFLE I_{12}
Off							Off							
Preheat Hi	Off	Off	Off	4.25/0*	4.0/0*	On	17V	On	7.0	X	X	Off	X	Off
Preheat Lo	Off	Off	2A	4.25/0	4.0/0	On	17V	On	5.0	X	X	Off	X	X
Ignition-Heat	Off	2A	2A	4.25/0	4.0/0	On	17V	On	X	6.5	36V	Off	X	1.5A
Run	1.5A	2A	2A	4.25/0	4.0/0	On	15V	On	X	6.5	32V	600/300	.75	1.8A

*Current at Hi value if corresponding discharge is not lit and at zero if it is lit.

Figure 5.3.4.2-2b Thruster Supply Conditions During Startup Phases

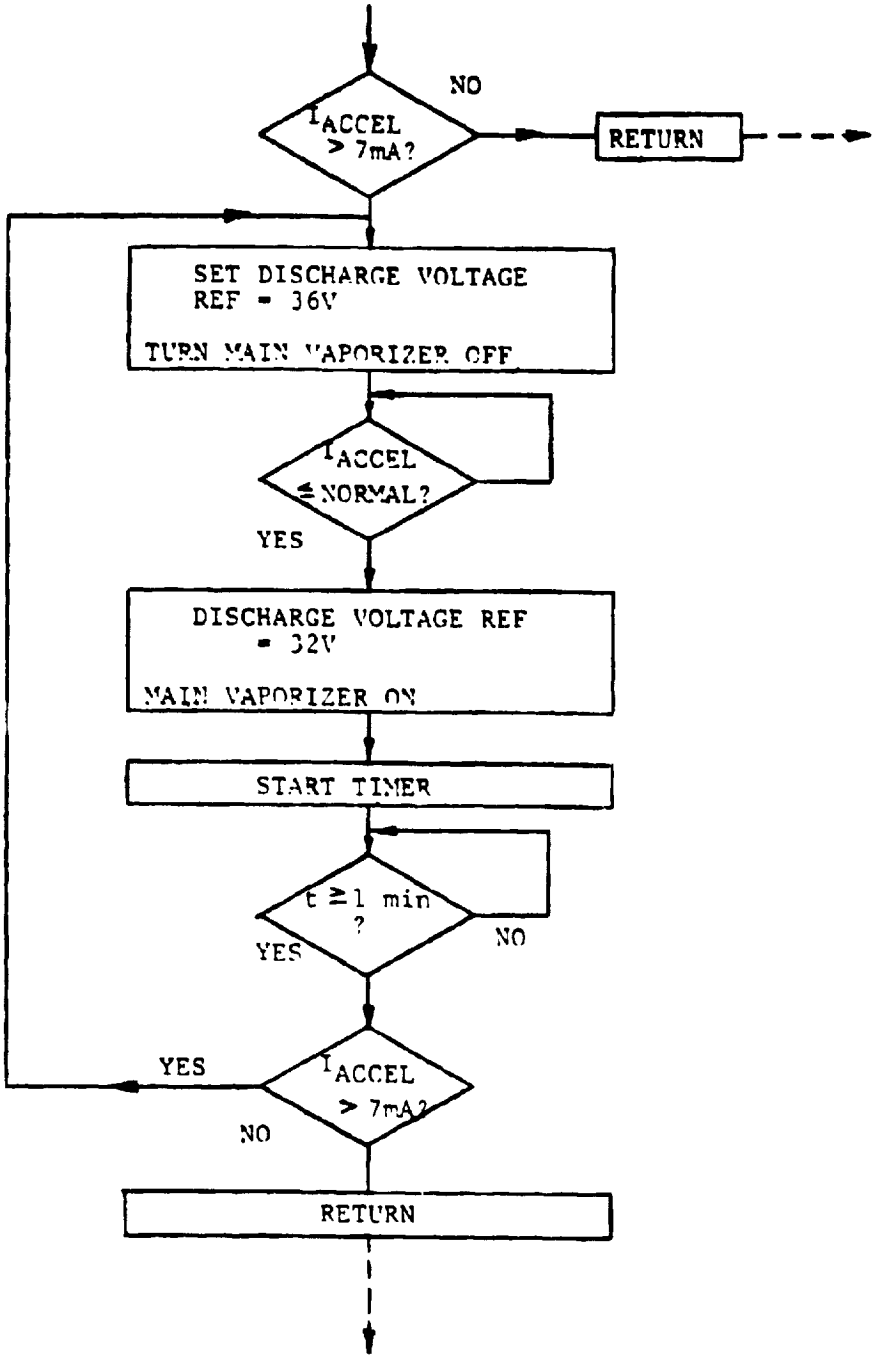

FIGURE 5.3.4.2-3 LOW MODE ALGORITHM

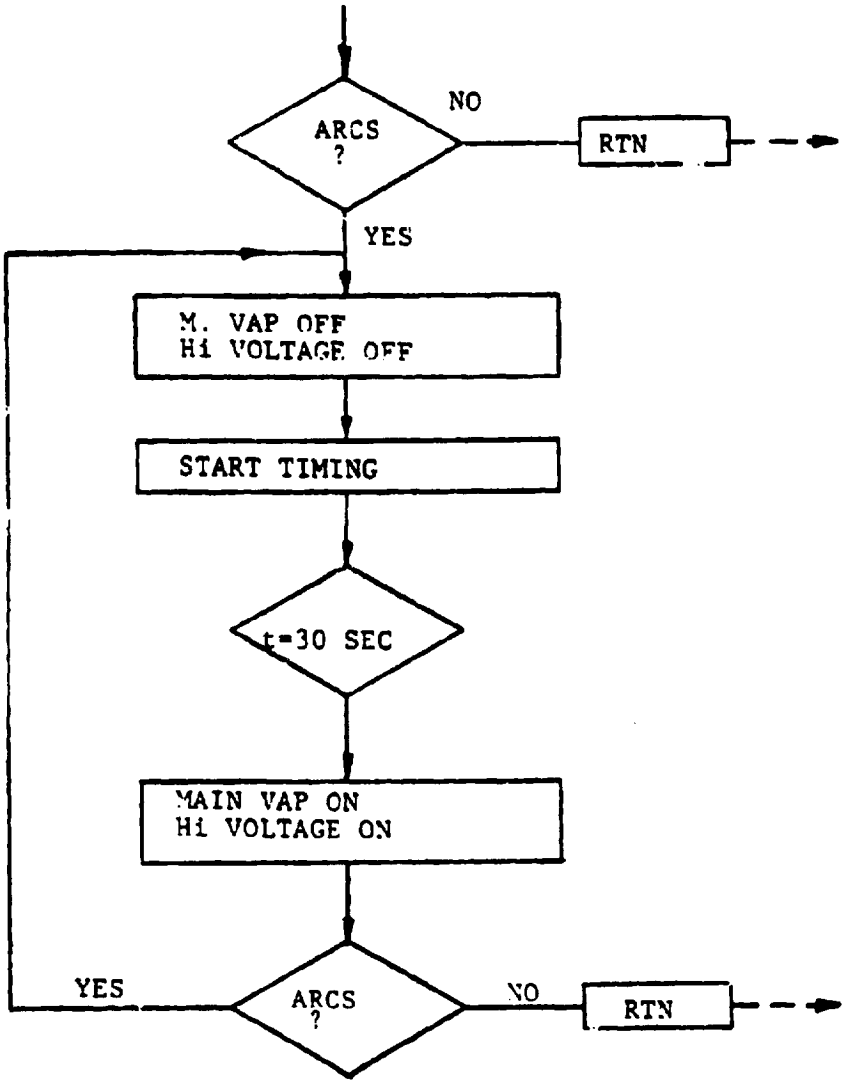

FIGURE 5.3.4.2-4 EXCESSIVE ARCS ALGORITHM

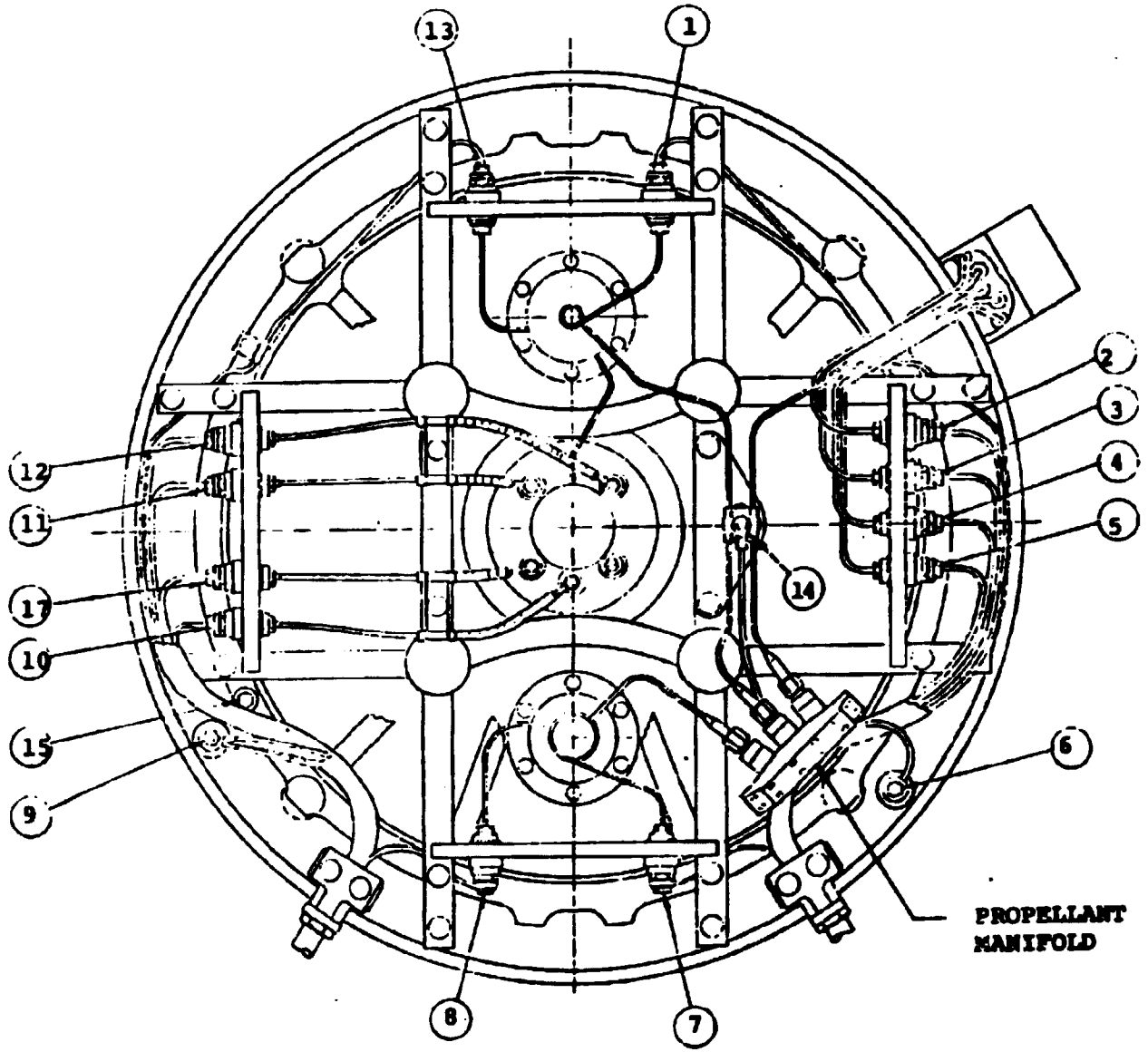

Figure 5.4.1-1a - ELECTRICAL WIRING AND PROPELLANT MANIFOLD OF THRUSTER
(Excluding Platinum Resistance Temperature Sensors)

TERMINAL NO.	TERMINATION	AWG NO.	WIRE NO.
1	Cathode Vaporizer	16	1
2	Neutralizer Keeper	16	2
3	Neutralizer Heater	16	3
4	Neutralizer Vaporizer	16	4
5	Neutralizer Common	16,16	5A,5B
6	Accelerator	20	6
7	Main Vaporizer	16	7
8	Main Isolator	16	8
9	Discharge (Anode)	16,16,20	9A,9B,9P
10	Cathode Heater	16	10
11	Cathode Keeper	20	11
12	Magnetic Baffle (Outer)	16	12
13	Cathode Isolator	16	13
14	Vaporizer Return	16	14
15	High Voltage Return	16,16,20	15A,15B,15P
16	Sensor Common	20	16
17	Mag Baffle (Inner)	16	17
18	Main Vaporizer Sensor	20	18
19	Cathode Vaporizer Sensor	20	19
20	Neutralizer Vaporizer Sensor	20	20
21(-) 22(+)	Main Vaporizer Thermocouple		21(-), 22(+)
23(-) 24(+)	Cathode Vaporizer Thermo-couple		23(-), 24(+)
25(-) 26(+)	Neutralizer Vaporizer Thermo-couple		25(-), 26(+)

Figure 5.4.1-1b Thruster Wire List

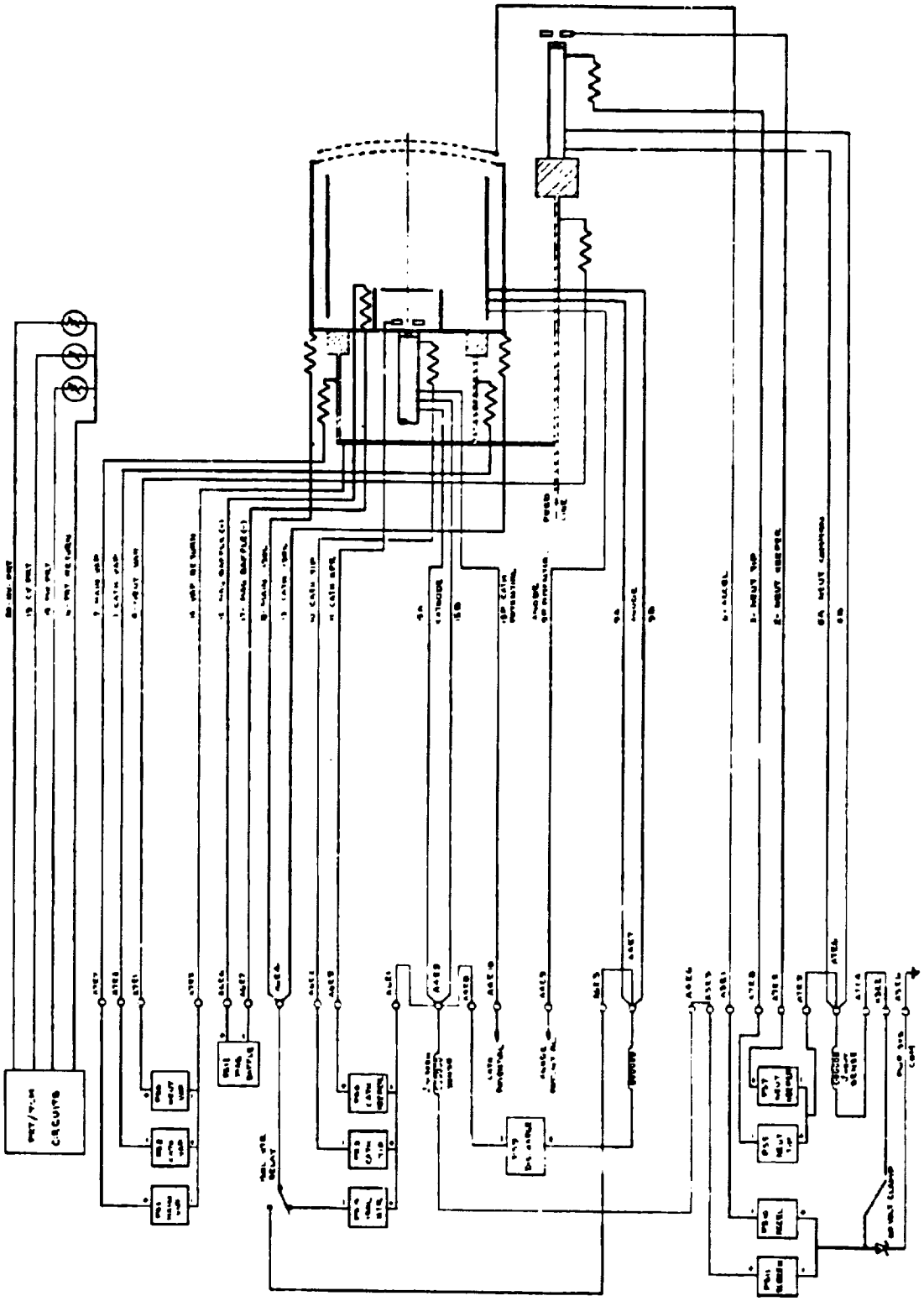

Figure 5.4.1-2 Thruster-Power Processor Interconnection Diagram

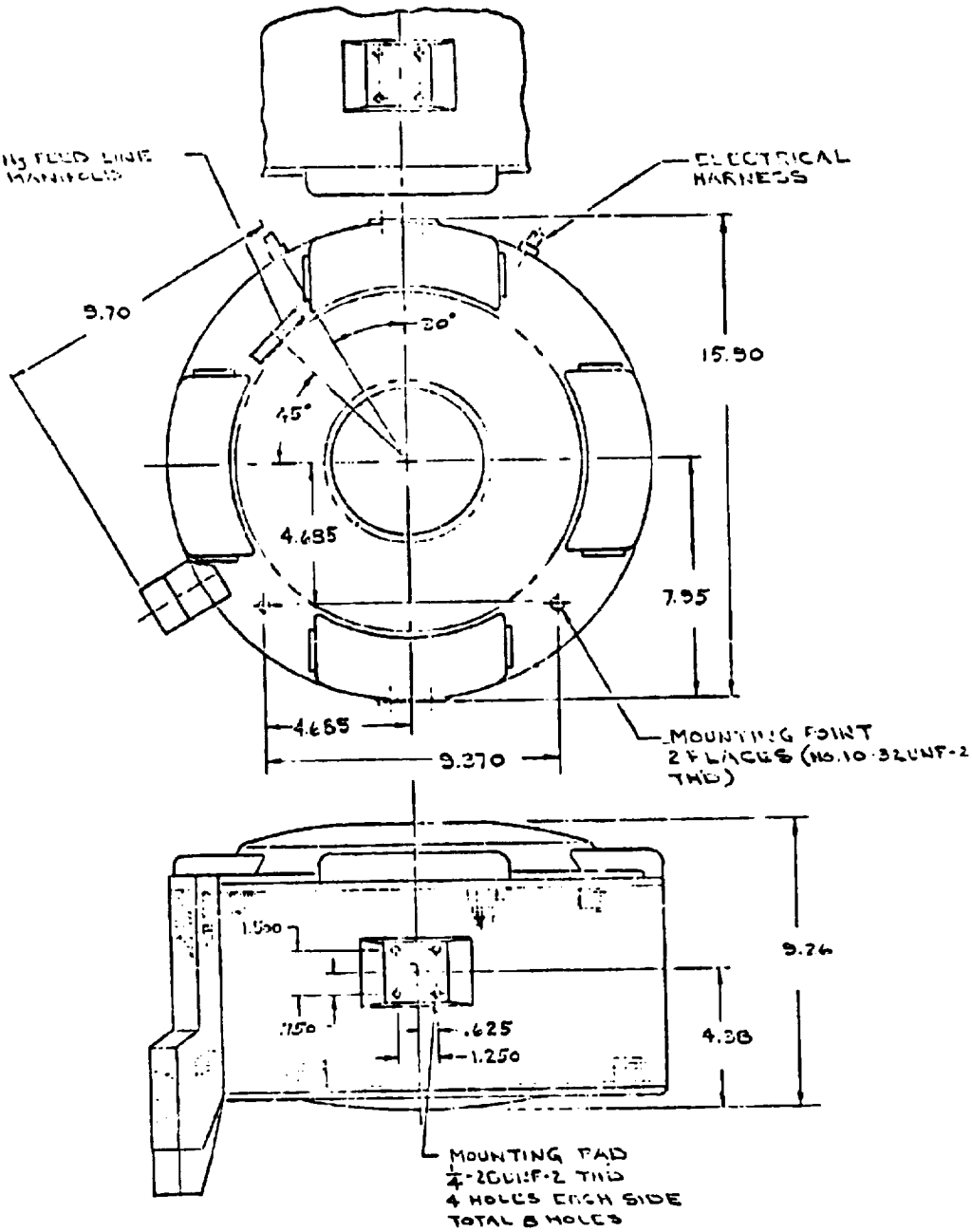

FIGURE 5.4.2-1
THRUSTER OUTLINE & INTERFACES

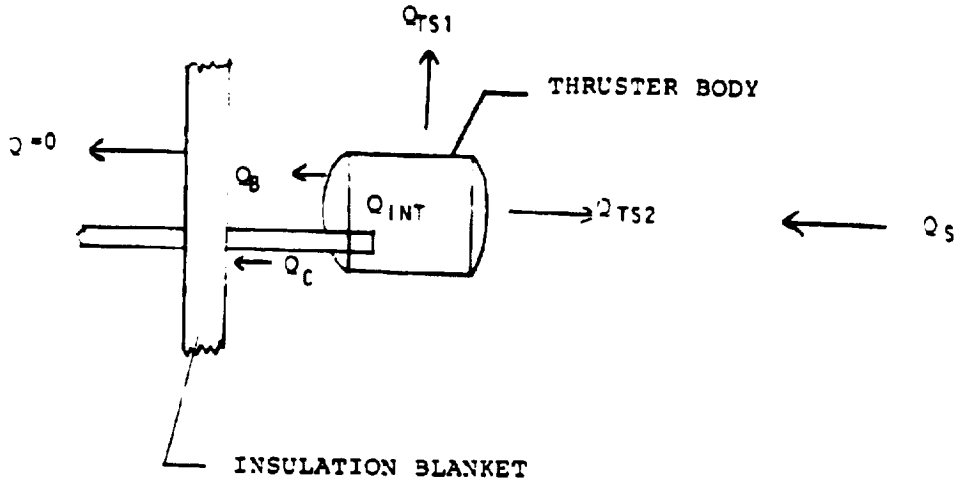

$$Q_{INT} + Q_S = Q_C + Q_B + Q_{TS1'} + Q_{TS2}$$

where

Q_{INT} = Internal heat generated in thruster

Q_S = Solar flux absorbed by the thruster

Q_C = Heat conducted from thruster through its supporting structure

Q_B = Heat transferred between rear of thruster and insulation blanket

Q_{TS1} & Q_{TS2} = Heat transferred between the thruster and environment

FIGURE 5.4.3-1 - THRUSTER HEAT BALANCE IN BIMOD INSTALLATION

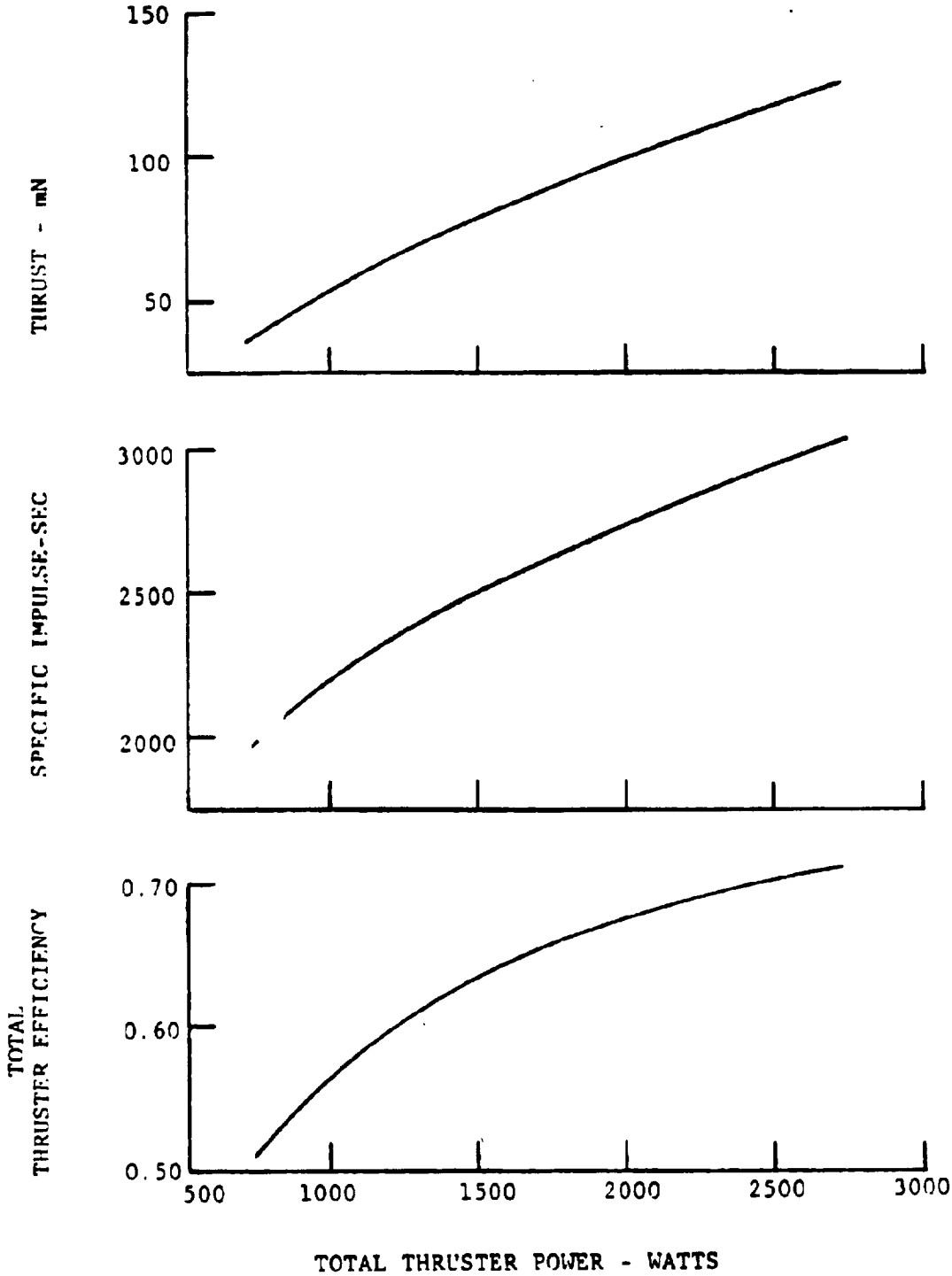

FIGURE 5.5.-1 THRUSTER PERFORMANCE OVER LINEAR THROTTLING PROFILE (FIGURE 8.3.4.2-1)

LEWIS RESEARCH CENTER

MERCURY BOMBARDMENT THRUSTER DEVELOPMENT

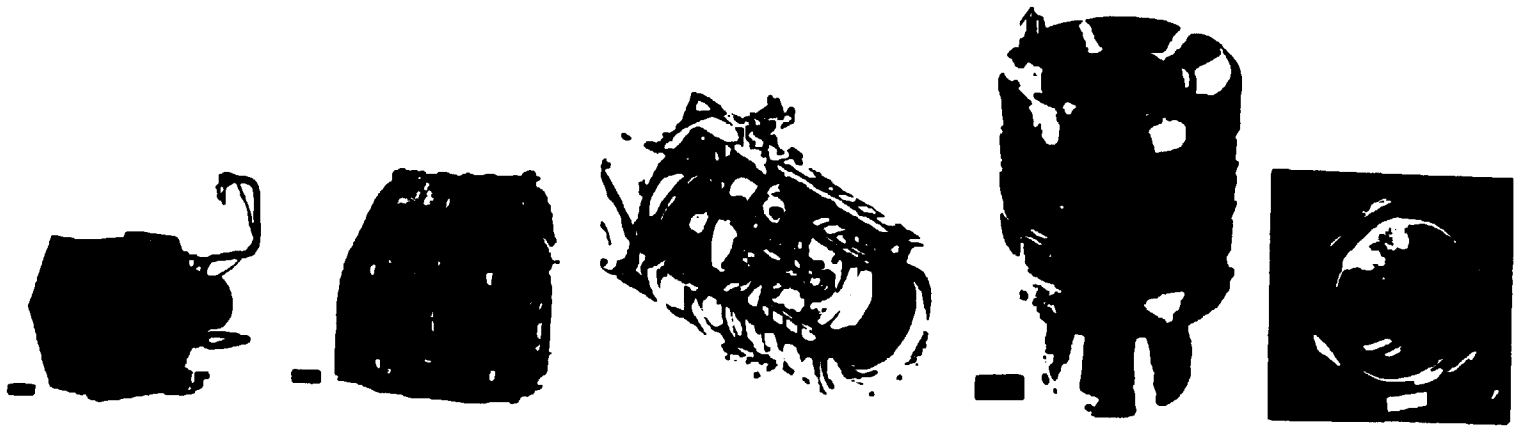

	1959 FIRST THRUSTER	1964 SERT I	1970 SERT II	1976 SIT-8 EM THRUSTER	1976 30-cm EM THRUSTER	1978 30-cm J SERIES THRUSTER
DIAM, cm THRUST, mN POWER, kW I_{sp}, sec	10 4 0.4 5000	10 25 1.5 4000	15 28 0.85 4200	8 5 0.125 2800	30 130 2.6 3000	30 130 2.7 3000
	LAB MODEL DEMO FEASIBILITY OF IDEA	31 min FLIGHT PROVED NEUT IN SPACE SHORT DESIGN LIFE	5½ MON FLT OPERATION 1ST USE OF HOLLOW CATH	MODULAR SIZES 2.5 TO 20 mN 5000 CYCLES DEMO	DISHED GRIDS LOWER I_{sp} GIVES HIGH T/P LARGER T, AT SAME P LOSS	LIFETIME IMPROVE-MENTS INCORPORATED "SMALL HOLE" ACCEL GRID

Figure 5.7-1 Mercury Bombardment Thruster Development History

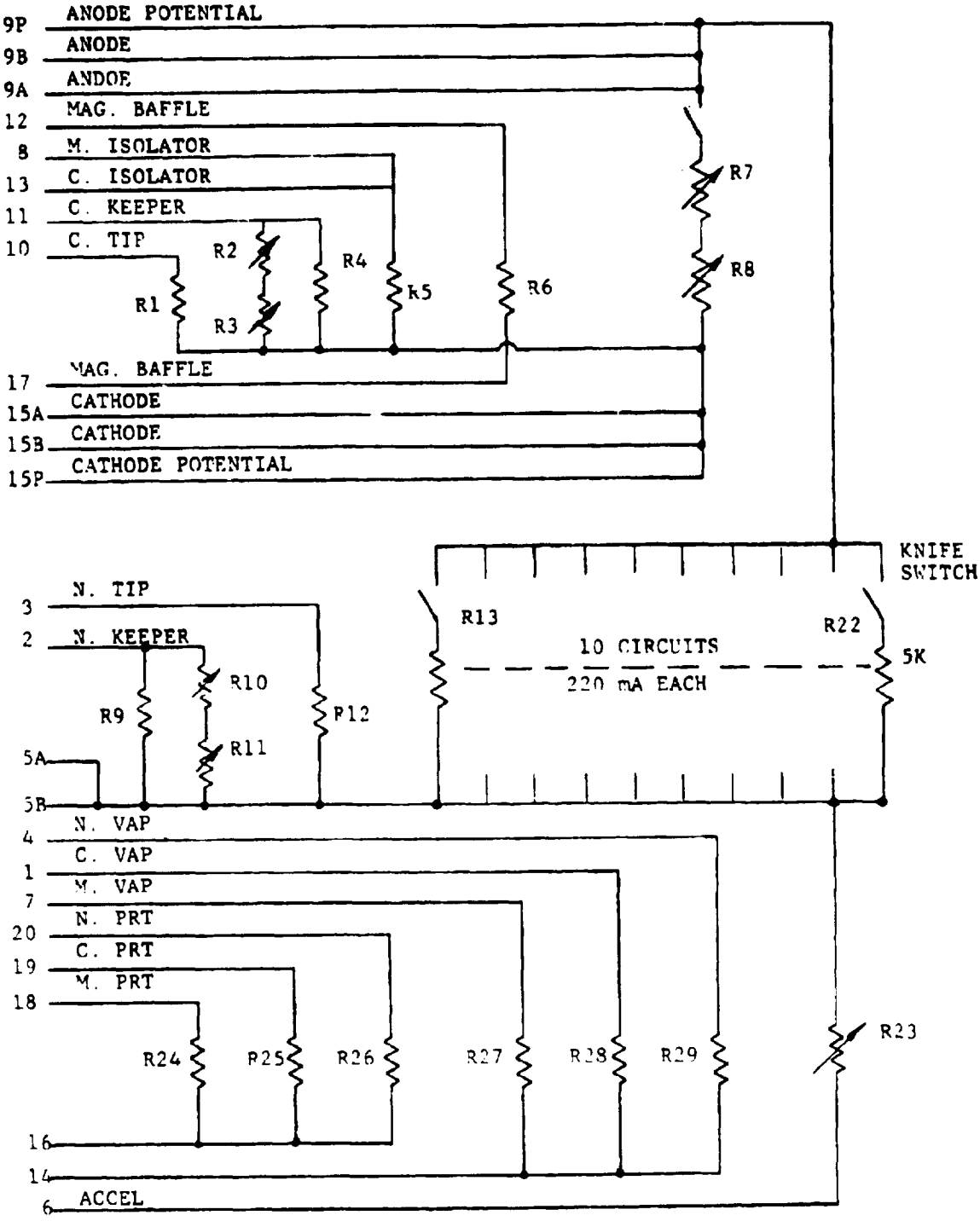

FIGURE 5.9.1-1a THRUSTER ELECTRICAL SIMULATOR - SCHEMATIC

RESISTOR		OHMS	MAX POWER
R1	Cathode Tip	3	100W
R2	Cathode Keeper-Coarse	0-750	20W
R3	Cathode Keeper-Fine	0-25	20W
R4	Cathode Keeper-Bleed	50K	5K (500V)
R5	Main & Cathode Isolator	2.5	250W
R6	Magnetic Baffle	0.5	25W
R7	Discharge - Coarse	0-35	1000W
R8	Discharge - Fine	0-2	600W
R9	Neut. Keeper - Bleed	50K	5W (500V)
R10	Neut. Keeper - Coarse	0-750	20W
R11	Neut. Keeper - Fine	0-10	20W
R12	Neut. Tip	3	100W
R13		5K	400W (1100V)
	Beam	(each)	(each)
R22			
R24	Main Vap - Platinum Res. Temp.	100	0.1
R25	Cath Vap - Platinum Res. Temp.	100	0.1
R26	Neut Vap - Platinum Res. Temp.	100	0.1
R27	Main Vap	6.8	30
R28	Cathode Vap	3.4	40
R29	Neut Vap	3.4	40

Figure 5.9.1-1b - Thruster Electrical Simulator - Specifications

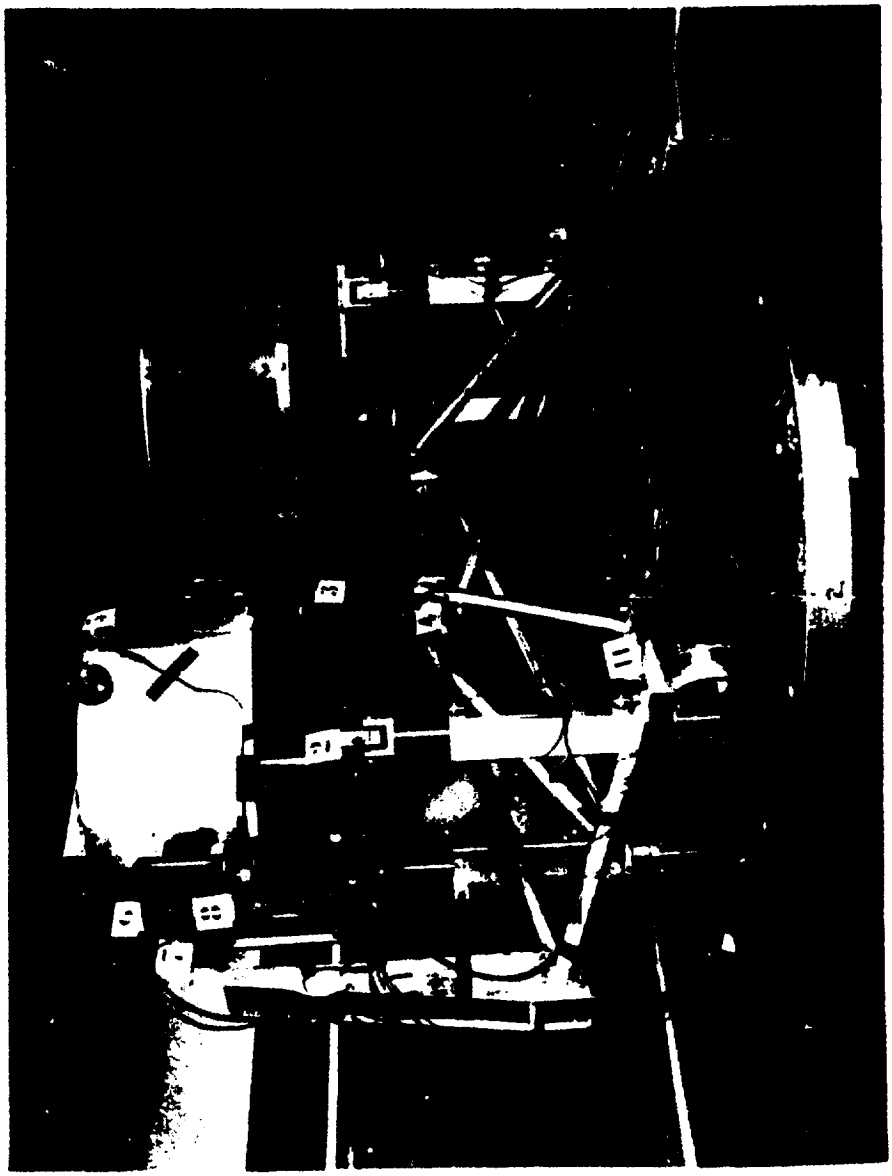

Figure 5.9.3-1 Thruster Mass Models

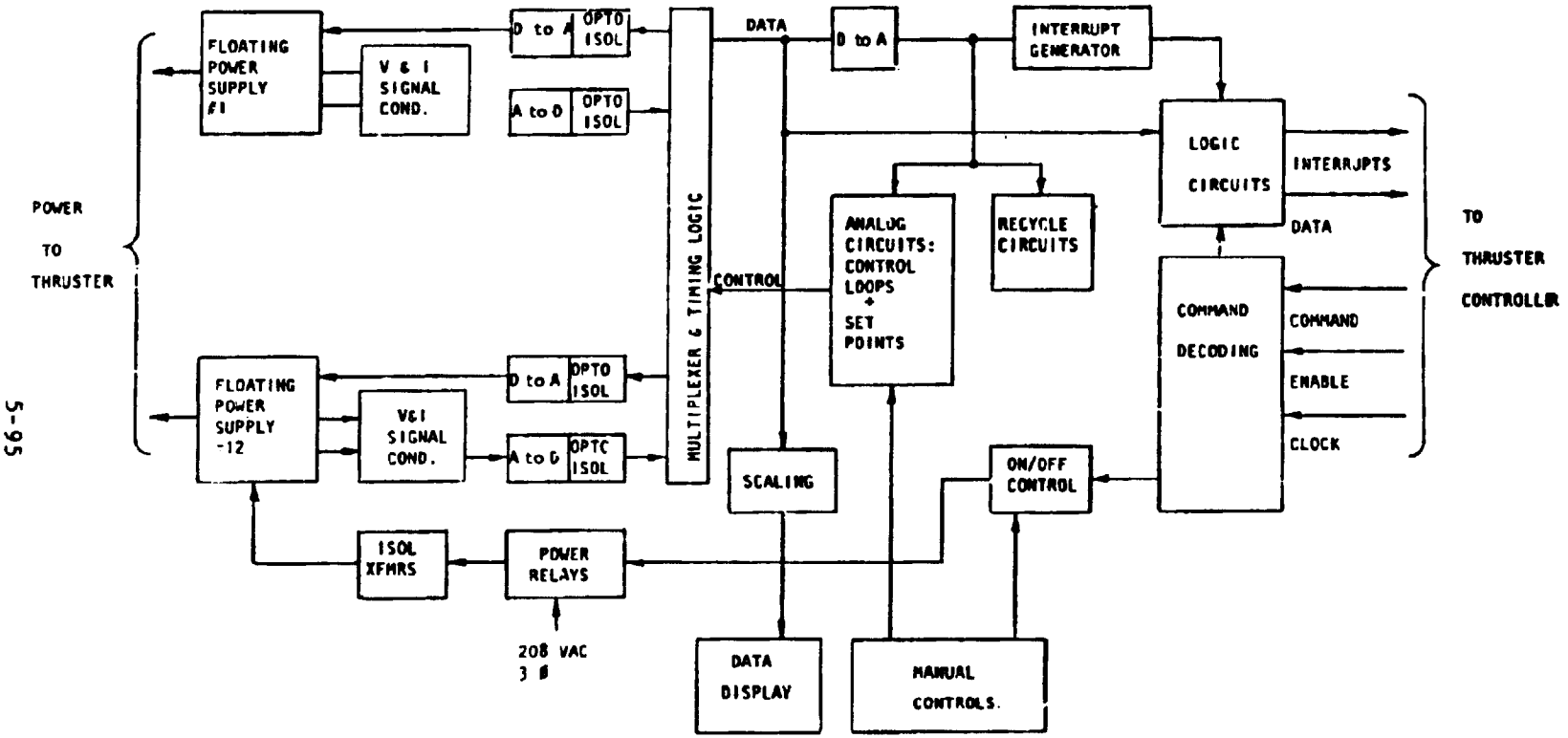

Figure 5.9.4-1 LAB POWER UNIT FUNCTIONAL BLOCK DIAGRAM

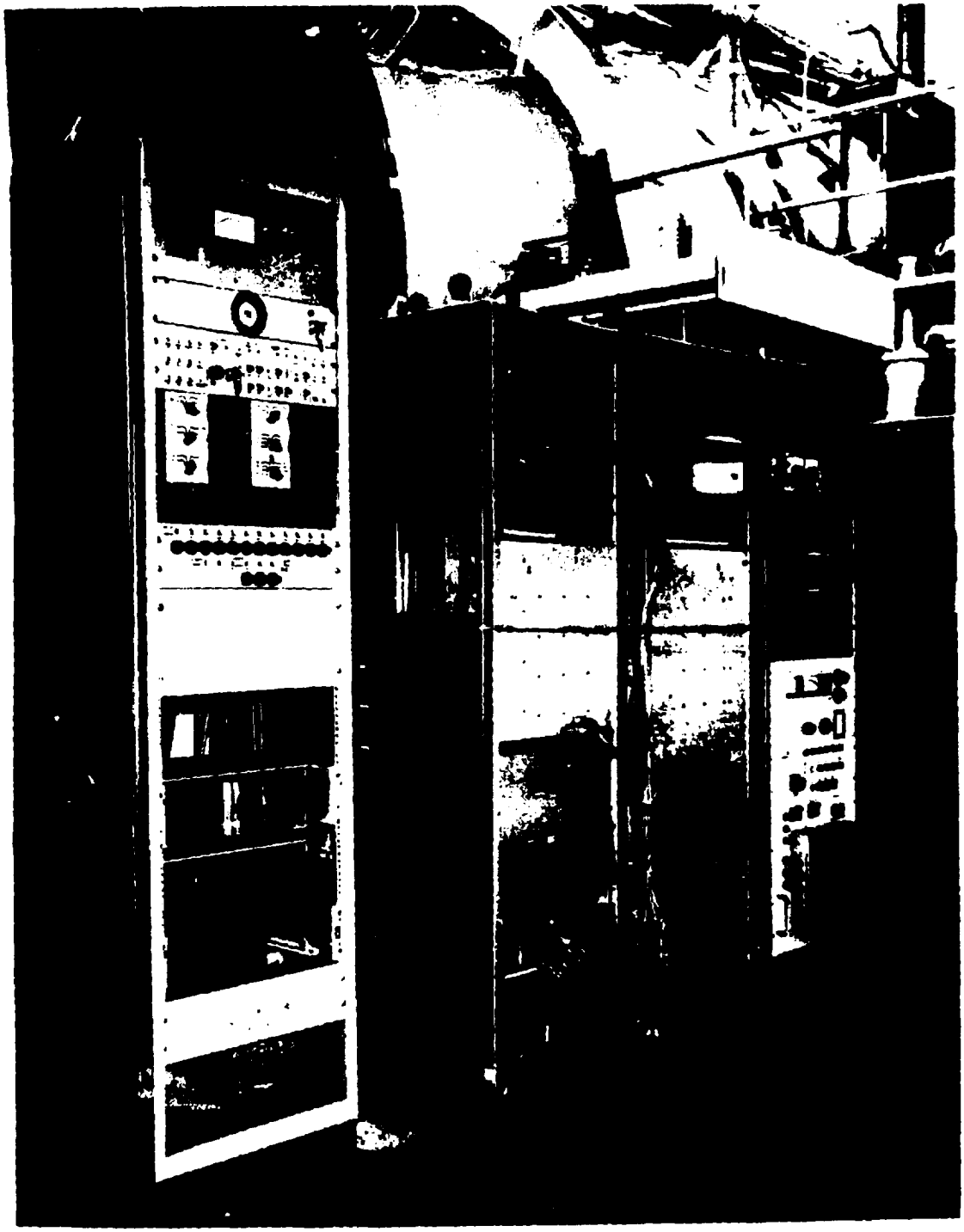

Figure 5.9.4-2 Lab Power Unit (LPU)

6.0

POWER PROCESSOR

Table Of Contents

		Page
6.0	Power Processor	6-4
6.1	Reference Documents	6-4
6.2	Functional Requirements	6-5
6.3	Functional Description	6-6
6.3.1	Electrical	6-6
6.3.2	Mechanical	6-10
6.3.3	Thermal	6-12
6.4	Interface Definition	6-15
6.4.1	Electrical	6-15
6.4.1.1	Input Power	6-15
6.4.1.2	Processor/Controller	6-16
6.4.1.3	Thruster	6-16
6.4.1.4	Temperature Sensors	6-17
6.4.1.5	Grounding	6-17
6.4.2	Mechanical	6-17
6.4.3	Thermal	6-17
6.4.3.1	Multilayer Insulation	6-17
6.4.3.2	Bonding	6-18
6.4.3.3	Mechanical	6-18
6.5	Performance Description	6-18
6.5.1	Input Power	6-19
6.5.2	Command Format	6-20
6.5.3	Telemetry	6-21
6.5.4	Output Power	6-21

		Page
6.5.5	Electromagnetic Interference	6-22
6.5.6	Efficiency	6-23
6.5.7	Shorts, Overloads, Transient. Recycle Tests	6-24
6.6	Physical Characteristics and Constraints	6-24
6.6.1	Dimensions	6-25
6.6.2	Volume	6-25
6.6.3	Center of Mass	6-25
6.6.4	Mass	6-25
6.6.5	Power Profile	6-25
6.6.6	Outgassing	6-25
6.6.7	Grounding	6-26
6.6.8	Identification Marking	6-26
6.6.9	Packaging	6-26
6.6.10	Location and Mounting	6-27
6.7	Development History	6-27
6.7.1	Electrical	6-27
6.7.2	Mechanical	6-31
6.8	Applicable Documents Enclosed	6-32
6.9	Ground Support Equipment	6-35
6.9.1	Power Processor Controller	6-35
6.9.2	Power Processor Simulator	6-36
6.9.3	Thruster Dummy Load and Test Console	6-38
6.9.4	Procedures	6-39

Page

TABLES

6.5.3-1 Telemetry Ranges and Accuracies.....6-41

6.5.4-1 FM/PPU Output Requirements.....6-42

6.5.6-1 PPU Efficiency Characteristics.....6-43

6.6.4-1 PPU Mass Breakdown.....6-44

6.9.4-1 FM/PPU Test Procedures.....6-45

FIGURES

6.3.1-1 Power Processor Block Diagram.....6-47

6.3.1-2 Basic Series Resonant Inverter.....6-48

6.3.1-3 Block Diagram Interface Unit, PPU Commands, Control and Protection System.....6-49

6.3.2-1 FM/PPU Assembly Photograph.....6-50

6.4.1-1 Power Processor Interface Diagram.....6-51

6.4.1-2 FM/PPU Thruster Power Interface.....6-52

6.4.1-3 PPU Grounding Diagram.....6-53

6.6.3-1 FM/PPU Center of Mass.....6-54

6.6.5-1 FM/PPU Power Profile.....6-55

6.6.10-1 BIMOD Thrust Module Co-Ordinate System.....6-56

6.9.1-1 Power Processor Controller Schematic.....6-57

6.0 Power Processor

6.1 Reference Documents

6.1.1 Biess, J.J.; Inouye, L.Y.; and Schoenfeld, A.D.: Electric Prototype Power Processor for a 30-cm Ion Thruster. (TRW DSSG, Redondo Beach, CA.) NASA CR-135287, 1978.

6.1.2 Biess, J.J.; and Frye, R.J.: Electrical Prototype Power Processor for the 30 cm Mercury Electric Propulsion Engine. AIAA Paper 78-684, April 1978.

6.1.3 Maloy, J.E.; and Sharp, G.R.: A Structural and Thermal Packaging Approach for Power Processing Units for 30-cm Ion Thrusters. NASA TM X-71686, March 1975.

6.1.4 Solar Electric Propulsion (SEP) Dual Shear Plate Packaging Design. JPL-701-204, Jet Propulsion Lab, Pasadena, CA, 1974.

6.1.5 Sharp, G.R.; Gedeon, L.; and Oglebay, J.C.: A Mechanical Thermal and Electrical Packaging Design for a Prototype Power Management and Control System for the 30-cm Mercury Ion Thruster. NASA TM X-78862, 1978.

6.1.6 Biess, J.J.; and Inouye, L.Y.: Power Processor for a 30-cm Ion Thrusters. (TRW Systems Group, Redondo Beach, CA.) NASA CR-134785, 1974.

6.1.7 Biess, J.J.; Inouye, L.Y.; and Schoenfeld, A.D.: Extended Performance Electric Propulsion Power

Processor Design Study. (TRW DSSG, Redondo Beach, CA.) NASA CR-135357 and CR-135358, 1977.

6.1.8 Herron, B.G.: Development of a 30-cm Ion Thruster Thermal Vacuum Power Processor. AIAA Paper 76-991, November 1976.

6.1.9 Herron, B.G., et al: 30-cm Ion Thruster Power Processor. (Hughes Research Laboratories, Malibu, CA.) NASA CR-135401, 1978.

6.2 Functional Requirements

1) The power processor shall accept as its input, unregulated solar array power and condition this power to provide the twelve regulated power outputs to satisfy ion thruster operation requirements.
2) The power processor shall provide telemetry signal conditioning for power processor input parameters, operating parameters and status, and thruster operating parameters and status.
3) The power processor shall receive regulated 28 volt power to provide startup control and standby status/telemetry information.
4) An external computer will send commands and receive data from the power processor. The power processor shall verify, decode, and execute commands for thruster startup, throttling,

shutdown and anomaly correction, and for power processor/thruster status and telemetry.

5) The power processor shall sense for critical thruster/power processor out-of-limit conditions, and depending on the condition sensed, shall either: (1) initiate corrective action, (2) generate a flag so that the external computer will provide action, or (3) shutdown the power process/thruster.

6) The power processor shall be designed to meet the sine, random, and static acceleration levels specified in applicable document 6.8.1.

7) The power processor shall dissipate all internally generated heat through the power processor baseplate mounted heat pipes. Junction temperatures for solid state components shall operate at less than 110° C. High reliability for solid state components shall be maintained by limiting mounting surface temperature to 75° C.

Preliminary requirements for the electrical prototype (E/P) power processor are referenced in applicable document 6.8.2.

6.3 Functional Description

6.3.1 Electrical

The FM/PPU electrical circuitry is contained in a

seven module assembly. This modular approach allowed for a logical division of circuitry that facilitates testing and permits high voltage, high power, and noise sensitive circuitry to be isolated. A block diagram of the power processor (PPU) circuitry and its module allocation is shown in figure 6.3.1-1.

The first, or A1 module, contains the input filter for the solar array power, the 28 volt converter that supplies the internal control electronics power, and the telemetry signal conditioning oscillator. The input filter uses a special swinging inductor filter design that provides the necessary current ripple attenuation. The input filter feeds the three series resonant inverters used in the PPU. These are: (1) the Beam Inverter, for the screen and accelerator supplies, (A3 module), (2) the Discharge Inverter (A4 module), and (3) the Multiple Output Inverter (A5 module), which supplies power for nine low power output supplies (A6 and A7 modules).

The beam and discharge series resonant inverters use thyristor power switches and operate at a resonant frequency of 20 kHz. Figure 6.3.1-2 presents a basic schematic of the series resonant

inverter power stage used for the DC-AC power inversion. The power stage includes two power switching thyristors (SCR1 and SCR2), two shunt power diodes (CR1 and CR2), the series resonant tank (L1, L2, C1 and C2), and the output transformer and its associated output rectifiers and filtering. When the power thyristor SCR1 is turned on, a sinusoidal current flows through the power thyristor, the resonant tank (L1, C1 and C2) and the output power transformer T. On the alternate half cycle, thyristor SCR2 is turned on. The sinusoidal current waveform in the power switching devices allows for high frequency operation without the associated turn-on and turn-off switching losses commonly found in other power conversion circuits. Also during abnormal output loading conditions such as thruster arcing, the series resonant LC tank limits the instantaneous peak current flowing through all the power components and thereby provides inherent component overstress protection.

The multiple output inverter is also a half bridge series resonant inverter, but uses transistors as the power switches and operates at a resonant frequency of 50 kHz. The higher frequency operation of this inverter permits minimal weight magnetics

and output stage filtering. This inverter provides the current source for nine series-connected, transformer coupled output stages. These output stages are contained in the A6 and A7 modules. A6 contains those supplies that are referenced to the high voltage screen output (up to +1100 volts) and A7 contains those that are referenced to neutralizer common or spacecraft common (as previously shown in figure 6.3.1-1).

All power outputs of the three inverters mentioned have individual control electronics to provide output regulation, overload protection, on-off control, and commandable operational set points or references.

The A2 module contains the digital interface unit and the PPU command, protection and control sections. The digital interface unit provides the interface between the power processor and a computer. High speed serial data from the computer is processed by the digital interface unit and controls the overall operation of the PPU. PPU telemetry data and off-normal PPU/thruster operation signals are processed by this module and transmitted to the computer to allow monitoring of the thrust system operation. A block diagram of this module is shown in figure 6.3.1-3.

and information regarding the digital commands and their format is contained in applicable document 6.8.3. Reference 6.1.1 and applicable document 6.8.4 provide a detailed description of the power processor.

6.3.2 Mechanical

The power processor (PPU) has been structurally designed to support its own mass during the launch environment as well as act as the foundation for the rest of the BIMOD. The PPU structure has been designed so that no electrical component has a vibration resonance below 200 Hz (applicable document 6.8.15). The overall first mode resonance in the Z axis (thrust axis) occurs at 120 Hz; a frequency that is between the point at which the sine vibration cuts off and the random vibration builds up to full level.

The PPU structure is designed for a nominal combined static and dynamic acceleration of 72 g's for all axes. A structural analysis is included in applicable document 6.8.14. The main structure is comprised of seven cross beam modules (fig. 6.3.2-1) Each cross beam is machined from a solid block of 6060-T6 aluminum alloy to get reliable thermal conduction throughout the structure. A zirconium-magnesium alloy

(ZK60AT5) was also considered and would have been more weight efficient, but was rejected on cost grounds (applicable document 6.8.16). High heat dissipation or heavy components are mounted on the module base plate which is bolted to the heat pipe evaporator saddles. The lighter components are mounted to the cross beam webs between the base plate and the upper flange. All other components such as integrated circuits, capacitors, resistors, etc. are mounted on Printed Circuit Boards (PCB's). To remove the dissipated heat, the PCB's were mounted to aluminum picture frames. These frames are mounted to the cross beam base plate. Aluminum spacers and bolts tie the edges and central portion of the PCB's to the cross beam webs for structural integrity.

The heat pipe evaporator saddles are bolted to the cross beam base plates and are the structural backbone of the PPU's in the BIMOD configuration, as well as providing good heat transfer from the module base plate to the heat pipes. The heat pipe saddles also transfer the shear loads from the cross beams of the upper PPU to the cross beams of the lower PPU so that the upper and lower cross beams become one very deep shear beam.

The long 0.040 inch thick magnesium sides of the PPU are the most highly stressed for the thrust (Z) axis launch environment. The thickness of these sides was the major factor for determining the 120 Hz first mode Z axis resonance. This resonance could be shifted by small changes in the side thickness.

The BIMOD truss cantilever loads are transferred to the interface truss through columns attached to the sides of the PPU near the corners. The structural stability of these columns is enhanced by the PPU sides and cross beam webs, thus allowing the use of lightweight columns. NASA drawings CF 63700, CF 637010, and CF 637011 are the main PPU assembly drawings. A complete PPU drawing list is shown in applicable document 6.8.5.

6.3.3 Thermal

Temperature measurements made during electrical testing of the electrical prototype power processor (EP/PPU) showed that many hot spots existed. A thermal model was assembled (applicable document 6.8.8). The results showed that many areas within the power processor would be operating at temperatures much higher than desired.

90° C. Heat dissipating components mounted on the web section were located near the base.

Each printed circuit board has an aluminum frame 7.6-mm (0.030-in) wide and 1.59-mm (0.062-in) thick, to aid in the transfer of heat to the module base plate. Electronic components dissipating 0.020 watts or more were mounted next to the frame and cemented to the copper foil that extended from under the frame. Components that must be electrically insulated are first mounted on BeO pads. The copper foil 7.6 mm wide extends around the perimeter of the printed circuit board making direct contact with the frame. The aluminum frame and the circuit board are riveted together at each location of a heat dissipating component. Components dissipating 0.100 watts were placed at the bottom of the frame near to the module base plate; the lower heat dissipators were placed at the top of the frame.

The standoffs, that are required to attach the printed circuit board to the web section, are used to transfer heat. The printed board is cut away at the location of each standoff to the frame. The threaded aluminum standoffs make contact with the frames. Metal to metal contact is made from the foil under the electronic component through the

standoff to the web. One or two standoffs are required for the center of the printed circuit boards. They are used to transfer heat from components dissipating 0.050 watts or less; copper foil connects the component to the standoff.

Three ounce copper foil was used on the surface facing the frame; the other side has two ounce copper foil. The entire board was conformal coated with Solithane 113.

Applicable documents 6.8.10 and 6.8.11 detail the procedures and the results of the thermal vacuum testing.

6.5 Interface Definition

6.4.1 Electrical

The functional power processor interfaces are shown in figure 6.4.1-1. They consist of (1) the input power, solar array and regulated 28 volts, (2) the computer interface, input and output lines, and (3) the thruster interfaces, power leads and temperature measurements.

6.4.1.1 Input Power

1) The unregulated solar array input voltage shall be between 200 and 400 volts d.c. The maximum voltage (solar array open circuit voltage) shall not exceed 425 volts. The maximum nominal power

will not exceed 3200 watts. A single connector for two power leads and a ground reference lead is required. Since the power processor electrically isolates the input power, the ground reference may be at any potential within the input voltage range (e.g., the solar array could be grounded on the low side, or center tapped).

2) The FM/PPU also requires approximately 100 watts of 28±5 volts d.c. power. A single connector for two power leads and a ground reference lead is required. The 28 volts power is also electrically isolated in the power processor.

6.4.1.2 Processor/Controller

The power processor/ ontroller interface requires a single connector for five circuits; command, data, enable, clock and PPU off-normal flag. These circuits are typically twisted shielded pairs. A description and specifications for the signals on these lines is contained in applicable document 6.8.3.

6.4.1.3 Thruster

The thruster interface consists of twenty power leads. The twenty thruster power leads, shown in figure 6.4.1-2, are hard wired to the various power processor modules. The voltage, current and power levels for this interface are given in Table 6.5.4-1.

6.4.1.4 Temperature Sensors

The three temperature sensors each require a twisted, shielded pair, and a single connector for all three circuits.

6.4.1.5 Grounding

The grounding philosophy is illustrated in figure 6.4.1-3. All grounds shown shall be referenced to a single common point.

6.4.2 Mechanical

The two identical Power Processors, when bolted back to back against common heat pipe saddles, become essentially a rectangular box 1.17 m (3.84 ft) long by 0.49 m (1.61 ft) wide by 0.32 m (1.05 ft) high. The heat pipes protrude from the small ends. A clearance of 3.2 cm (1.26 in.) must be allowed for the electrical harnesses and connectors on the upper and lower surfaces of the box. The Power Processors are fastened in the interface truss on the BIMOD truss by the eight #10-32 bolts shown on the BIMOD interface Control Drawing (CF 638168). The mating structural flanges must be kept to the dimensions shown on the drawing in order to avoid interference with the PPU lids.

6.4.3 Thermal

6.4.3.1 Multilayer Insulation

The thermal interface between the PPU and the sur-

roundings (except for the PPU base plate) consists of multilayer insulation blankets. An opening exists between blankets for the PPU nearest the thrusters to allow for outgassing of the PPU's.

6.4.3.2 Bonding

RTV 566 is used at the interface between the module base plate and the heat pipe evaporator saddle to enhance heat transfer by filling in voids.

6.4.3.3 Mechanical

Four rows of bolts are used to assemble the PPU to each heat pipe evaporator saddle. Where possible, the spacing between bolts was set at a maximum of 3.8 cm (1.5 in.).

6.5 Performance Description

The measurable parameters that are necessary to meet the functional requirements of the PPU are:

1. Input Power
2. Command Format
3. Telemetry
4. Output Power
5. Electro-Magnetic Interference (EMI)
6. Efficiency
7. Shorts, Overloads, Transient, Recycle Tests

The information provided herein is the result of in-house testing on the Functional Model Power Processor (FM/PPU) that was packaged, fabricated

and tested at LeRC. Extensive information on the Engineering Prototype Power Processor (EP/PPU) is provided by the documents referenced in section 6.1. The EP/PPU and FM/PPU share a common electrical design. Test of FM/PPU SN #1 was performed with a thruster load bank (applicable document 6.8.6). FM/PPU SN #1 also accumulated about 1300 hours of vacuum operation with an ion thruster. A thermal vacuum test was also performed on FM/PPU SN #1, the results of which are detailed in applicable document 6.8.7.

FM/PPU SN #1 has been shipped to Xerox-EOS for participation in a Mission Profile Life Test. To date (April 3, 1979) FM/PPU has accumulated an additional 200 hours of vacuum operation for a total of 1500 hours.

6.5.1 Input Power

The input power requirements for the FM/PPU are:

1. Input Voltage: 200 to 400 V dc main bus
   3 kW @ 2.0 amp beam
2. Input Voltage: 23 to 33 V dc control bus
   100 W @ 2.0 amp beam

The FM/PPU was successfully operated over the voltage range of 28 $\pm$ 5 V dc. Some problems were encountered in operations over the entire 200 to 400 V dc range of the 400 V dc bus. Below 210 V dc, a

condition known as latchup occasionally occurred were both A4 module SCR's conducted simultaneously. This is not considered a major problem but one that can be remedied by minor control adjustments.

6.5.2 Command Format

The command control requirements for the FM/PPU are:

1. Format - Serial Pulse Code Modulation - NRZ
2. Logic Levels - 4.1 volts or greater for a logic "1"
   0.5 volts or less for a logic "0"
3. Parity - ODD
4. Command Word Length - 16 bits
5. Echo Back Word Length - 24 bits
6. Bit Rate - Variable, 1 KBPS to 10 KBPS
7. Priority Interrupts - Six
   a. High Accelerator Current
   b. Low Screen Voltage
   c. Beam Current Out of Limits
   d. Solar Array Input Voltage Out of Limits
   e. Excessive Arcs
   f. Neutralizer Failure
8. The above specifications were met during Performance Acceptance Testing (PAT) (applicable document 6.8.7).

Detailed information on the command codes, formats, and interfaces is contained in applicable document 6.8.3.

6.5.3 Telemetry

Telemetry for the FM/PPU consists of 28 seven bit digitally coded channels. Telemetry channels are only transmitted upon receipt of the appropriate interrogation command. The telemetry channels, their range, and accuracy are shown in table 6.5.3-1. During FM/PPU performance acceptance testing, the repeatability, stability, and accuracy of the telemetry was within specification. During module testing some analog channels (prior to digitizing) indicated significant ripple due to the 2 KHz magnetic amplifier isolation scheme that is used. This ripple will be reduced on future units by the addition of low pass filtering. Calibration curves for FM/PPU SN #1 are shown in applicable document 6.8.3.

6.5.4 Output Power

The FM/PPU contains the twelve power supplies required to power an ion thruster. These FM/PPU output requirements are listed in table 6.5.4-1.

The requirements for FM/PPU, SN #1 were met during performance acceptance testing at an input voltage of 300 V dc.

Test results for the EP/PPU at various input levels and loads are detailed in reference 6.1.1.

FM/PPU in-house LeRC testing successfully demonstrated the following functional operations with a 30-cm thruster:

1. Neutralizer keeper ignition
2. Neutralizer keeper-neutralizer vaporizer control loop
3. Cathode keeper ignition
4. Discharge ignition
5. Discharge voltage - cathode vaporizer control loop
6. Magnetic baffle operation
7. High voltage application to accelerator and screen
8. Beam current regulation from 0.5 to 2.0 amps
9. Stable thruster operation
10. Recovery from internal engine arcs
11. Shutdown of ion engine

6.5.5 Electromagnetic Interference

Electromagnetic Interference (EMI) for the FM/PPU will be done in accordance with NASA specifications (applicable document 6.8.9).

At the time of writing this manual, the FM/PPU EMI testing contract is being negotiated with R&B Enterprises of Plymouth Meeting, PA. Testing is expected to begin in the Fall of 1979.

Electromagnetic interference tests were performed on the 30-cm EP/PPU so that baseline information would be available to spacecraft system engineers to conduct interaction studies for spacecraft subsystems and scientific experiments.

Two basic sets of tests were formed:

1. Conducted narrowband and broadband interference with the power processor and ion engine operating at the 2 amp beam current level.

2. Radiation and conducted narrowband and broadband interference with the power processing operating with an ion engine load simulator in an electromagnetic compatibility screen room.

The results of the above testing on the EP/PPU are shown in reference 6.1.1 and applicable document 6.8.20.

6.5.6 Efficiency

The efficiency of the FM/PPU was measured during performance acceptance testing. Efficiency for the FM/PPU and EP/PPU were specified at 88% at a 2.0 amp thruster beam. The efficiencies for both the FM/PPU and EP/PPU at 300 V dc input voltages and a 1.0 and 2.0 amp beam are shown in table 6.5.6-1. Additional testing of FM/PPU's is currently under-

way and the data will be published when available. Additional efficiency information on the EP/PPU is available in reference 6.1.1.

6.5.7 Shorts, Overloads, Transient, Recycle Tests

Some transient, recycle, overload, and shorting tests were performed on the PM/PPU's but no quantitative data are available. In-house testing is still underway and test results will be published on completion of the testing. Detailed test results on the EP/PPU are available in reference 6.1.1.

6.6 Physical Characteristics and Constraints

This section defines the physical characteristics and constraints of the Power Processor Subsystem. Items to be specified here are:

1. Dimensions
2. Volume
3. Center of Mass
4. Mass
5. Power Profile
6. Outgassing
7. Grounding
8. Identification Marking
9. Packaging
10. Location and mounting

6.6.1 Dimensions

Dimensions of the PPU are 114.93 cm (45.25 in.) L, 45.97 cm (18.10 in.) W, 15.24 cm (6.0 in.) H.

6.6.2 Volume

Volume of the PPU is 80 518 cm^3 (4914 $in.^3$).

6.6.3 Center of Mass

Center of mass is shown in figure 6.6.3-1.

6.6.4 Mass

Mass of the PPU is 37.53 kg (82.75 lbs.). The detailed mass breakdown is shown in table 6.6.4-1.

6.6.5 Power Profile

The power profile for pre-heat and three levels of beam current is shown in figure 6.6.5-1.

6.6.6 Outgassing

The outgassing design criteria for the PPU shall be such that one square cm of venting area is required for 1000 cubic cm volume. A total of 18 screen vent holes (9 per side) provide the vent paths. Each hole is 4.7625 cm (1.875 in) in diameter and covered with a 150 mesh stainless steel screen. The 150 mesh screen provides a 37.4% open area for venting to space. With a PPU volume of 80 518 cm^3, a venting area of 80.5 cm^2 is required. The design provides a venting area of about 120 cm^2 thus providing a margin of about 50%.

6.6.7 Grounding

The grounding philosophy for the PPU is illustrated in figure 6.4.1-3. The grounding philosophy includes:

1. Isolation of the 200 to 400 V dc bus
2. Isolation of the 28 V dc bus
3. Isolation of the thruster
4. Isolation of spacecraft computer control box
5. Isolation of digital interface unit
6. Isolation of PPU commands
7. Isolation of PPU telemetry conditioning

6.6.8 Identification Marking

The identification marking for each module is located on top of each crossbeam near the connectors. The identification marking for the PPU is located at the center of the A2 module end.

6.6.9 Packaging

Modular packaging techniques were used in the design of the PPU. The PPU is comprised of seven modules fastened together by side skins, overlapping cover plates and the heat pipe saddles. Details of the construction techniques are shown in the appropriate assembly drawings listed in applicable document 6.8.5.

6.6.10 Location and Mounting

The location and mounting of the PPU in relation to the BIMOD structure are illustrated in figure 6.6.10-1. Mounting details are shown in the appropriate assembly drawings listed in applicable document 6.8.5

6.7 Development History

6.7.1 Electrical

The baseline LeRC Functional Model Power Processor (FM/PPU) is the most current power processor hardware available. The electrical design of the FM/PPU is identical to the Electrical Prototype Power Processor (EP/PPU). The EP/PPU is an electrical brassboard produced under a LeRC contracted effort with TRW, Inc. Defense and Space System Group from mid-1975 through 1976 (references 6.1.1 and 6.1.2). The objective of the EP/PPU effort was to design, fabricate, and test a power processor that would meet electrical specifications typical of a flight mission. The EP/PPU was designed to incorporate an integrated modular packaging approach, although no detailed flight type structural or thermal analysis was performed under this contract. The subsequent FM/PPU effort used the EP/PPU electrical design and further refined the packaging by optimizing packaging density.

FM/PPU was designed for flight structural, thermal, and environmental requirements (references 6.1.3 and 6.1.5). The EP/PPU contract also provided the electronic parts (commercial equivalents of Hi-Rel parts), and flight type magnetics sufficient to fabricate five FM/PPU's. The EP/PPU has undergone several thousand hours of thruster testing, including vacuum operation with a thruster. Conducted EMI tests were performed on the EP/PPU while operating a thruster, and radiated emission tests were performed with a thruster load bank (reference 6.1.1 and applicable document 6.8.20).

Prior to the EP/PPU effort, there were three 30-cm thruster power processor breadboard programs between 1972 and early 1975. These were the Hughes Thermal Vacuum Breadboard (TVBB)(references 6.1.8 and 6.1.9), and the TRW Thermal Vacuum Breadboard (reference 6.1.6), and the TRW Three Inverter Breadboard. The Hughes TVBB design uses a uniquely driven, transistor full bridge inverter power stage and was tested on a 30-cm ion thruster in both ambient and thermal vacuum environments. The TRW TVBB and Three Inverter utilize series resonant thyristor (SCR) half bridge inverter power stages. Both of these units underwent thruster integration

testing and the TRW TVBB saw limited thermal vacuum operation. In February, 1975, a management decision was made to pursue the SCR series resonant inverter power processor as the baseline design. To date, the TRW TVBB and Three Inverter power processors have accrued a total of over 20 000 hours of thruster operation (with no power component failures). During this time, these two power processors were used extensively for thruster/power processor development and characterization, and for numerous parametric, optimization, interaction, and control studies. The results of this work established the thruster/power processor voltage, current, set points, and interface requirements; the high voltage recycle procedure; the critical interrupt parameters and their magnitudes. It also baselined the thruster startup, throttle, and shutdown algorithms; and the control requirements, particularly the main, cathode and neutralizer control loops. This data has been incorporated in the EP/FM power processor electrical design. Also, several minor electrical design changes have occurred as a result of EP/FM power processor testing.

Since the FM/PPU design, there have been two contracts to investigate the techniques to further the

baseline FM/PPU performance. The first contract, the Extended Performance Electric Propulsion Power Processor Design Study (reference 6.1.7), was to compare and evaluate concepts for improving the performance and increasing the power output of the power processor to as high as 10 kW. This study was initiated to support a possible 1985 Halley Comet rendezvous mission, and was conducted by TRW DSSG from May through October, 1977.

The most recent contracted effort is the Improved Power Processor Design Study, or the "79 Breadboard." This effort furthers the designs and data base in the extended performance design study. This was done by incorporating updated thruster requirements to optimize power supply sizing, performing trade-off studies and updating electrical components (e.g., CMOS logic). It also included incorporating a microprocessor, refining the power stage and control logic, performing stability analysis and performing a power processor reliability assessment. This contract that started in October, 1978, with TRW DSSG will extend until 1980 and produce an updated electrical brassboard power processor.

6.7.2 Mechanical

From 1972 to 1974, a number of FM/PPU packaging concepts were considered in the course of a joint program with the JPL, the MSFC, and the LeRC. Most of these concepts utilized direct radiation to space through louvers for thermal control. The two earliest competing concepts had the electrical components either bolted directly to the radiators or bolted to the webs of the crossbeams, sandwiched between two plates (reference 6.1.4). In 1974, a study as conducted (applicable document 6.8.4) that showed an all heat pipe thermal control system would be most weight efficient for the large heat dissipations anticipated. The dual shear plate approach was then modified by enlarging one flange of the cross beam enough to accommodate the heavy or high heat dissipating components. The flange was then bolted directly to the heat pipe saddles. That approach eventually evolved into a packaging arrangement for two PPU's bolted to a common redundant heat pipe system in order to further reduce structural and thermal control system mass. Additional background and technical information is provided in applicable documents 6.8.17 through 6.8.31.

6.8 Applicable Documents Enclosed

6.8.1 Sharp, G. R.: Functional Model/Power Processing Unit Test Requirements Document. SSPD-01-04-0076. Vibration of FM/PPU S/N 2 to Qualification Levels. 1978.

6.8.2 Exhibit "A." Statement of Work. Electrical Prototype/Power Processor Unit for a 30-cm Ion Thruster. (NAS3-19730.) July 1975.

6.8.3 Command and Telemetry Codes of Power Processors for the 30-cm Ion Thruster. Revision 10. NASA Lewis Research Center, December 1978.

6.8.4 Maloy, J.E.; and Sharp, J.R.: A Structural and Thermal Packaging Approach for Power Processing Units for 30-cm Ion Thrusters. NASA TM X-71686, 1975.

6.8.5 FM-PPU Drawing List.

6.8.6 Ignaczak, L.R.: 30 cm PPU Dummy Load and Test Console (DL/TC) Operating Instructions. July 1977.

6.8.7 Siegert, C.E.: Electrical Performance of FM/PPU 1 During Thermal Vacuum Testing. February 1979.

6.8.8 Description and Results of the Solar Electric Propulsion System (SEPS) Functional Model Power Processor Unit (FM/PPU) Thermal Model. NASA Lewis Research Center Memorandum to Record, April 1979.

6.8.9 Renz, D.D.: Specification for Electromagnetic Interference Test for a 30-cm Ion Thruster Power Management and Control System, Specification 3-759182, November 1978.

6.8.10 Thermal Vacuum Testing of FM/PPU April-May, 1978. NASA Lewis Research Center Memorandum, June 1978.

6.8.11 Functional Model/Power Processing Unit Thermal Vacuum Test Procedure.

6.8.12 Makovec, R.J. and Reid, D.: Power Processor Simulator Operator's Manual. 1978.

6.8.13 FM/PPU Card and Module Test Procedure.

6.8.14 FM/PPU Structural Analysis

6.8.15 FM/PPU Electrical Component and Printed Wiring Board Vibrational Natural Frequency Calculations.

6.8.16 FM/PPU Materials Comparison for Cross Beam Modules.

6.8.17 FM/PPU Photographs, P.C. Boards, Modules, and FM/PPU.

6.8.18 EP/PPU Electrical Stress Analysis. Volume 1 - Modules A1 through A5.

6.8.19 EP/PPU Electrical Stress Analysis. Volume 2 - Modules A6 and A7.

6.8.20 Electromagnetic Interference Test Report for the EP/PPU. (Systems Environment Associates, Report TRS 4051 for TRW Systems Group.) January 1977.

6.8.21 EP/PPU Magnetics Specifications.

6.8.22 Electrical Prototype/Power Processor Unit, Final Design Review. (TRW Systems Group; NAS3-19730.) 1976.

6.8.23 Electrical Prototype/Power Processor Unit, Final Design Review, Appendix A - Schematics. (TRW Systems Group; NAS3-19730.) 1976.

6.8.24 Electrical Prototype/Power Processor Unit, Final Design Review, Appendix B - Parts List. (TRW Systems Group; NAS3-19730.) 1976.

6.8.25 Electrical Prototype/Power Processor Unit, Final Design Review, Appendix C - Electrical Stress Analysis. (TRW Systems Group; NAS3-19730.) 1976.

6.8.26 Electrical Prototype/Power Processor Unit, Final Design Review, Appendix D - Component Sizes. (TRW Systems Group; NAS3-19730.) 1976.

6.8.27 Electrical Prototype/Power Processor Unit, Final Design Review, Appendix E - Reliability Analysis. (TRW Systems Group; NAS3-19730.) 1976.

6.8.28 Extended Performance Electric Propulsion Power Processor Design Study. Preliminary Design Review. Volume I - Program Summary. (TRW Systems Group; NAS3-20403.) 1977.

6.8.29 Extended Performance Electric Propulsion Power Processor Design Study. Preliminary Design Review. Volume II - Detailed Results. (TRW Systems Group; NAS3-20403.) 1977.

6.8.30 Design Study for Improved Ion Thruster Power Processor. Task I - Design Update. Volume I - Summary of Results. (TRW Systems Group; NAS3-21746.) 1979.

6.8.31 Design Study for Improved Ion Thruster Power Processor. Task I - Design Update. Volume II - Schematics and Parts Lists. (TRW Systems Group; NAS3-21746.) 1979.

6.9 Ground Support Equipment

6.9.1 Power Processor Controller

The Power Processor Controller (PPC) is a device designed, developed, and fabricated at LeRC to generate PPU commands for testing an FM/PPU prior to thruster integration testing. The PPC has been designed to manually simulate the functions of a thrust subsystem computer. Specifically, the PPC will:

1. Transmit and acknowledge all command functions
   a. Power supply ON/OFF commands
   b. Power supply address and set point discrete commands
   c. Beam current set point commands
   d. Discharge current set point commands
   e. Magnetic baffle set point commands
   f. Screen voltage set point commands
   g. Telemetry measurement commands

2. Provide a PPU, telemetry output display in binary and decimal form. Display and identify interrupt identification signals transmitted by the PPU.

a. High accelerator current

b. Low screen voltage

c. Beam current out of limit

d. Input voltage out of limit

e. Excessive arcs

f. Neutralizer failure

3. Provide single transmission of any command.

4. Provide repetitive transmission of any command.

5. Provides a pseudo-memory of PPU configuration based on present display representing last command transmitted.

6. Provides a variable address capability to test the command user field word in the PPU. The PPC is a standard 19 inch rack mounted unit that is powered by 60 cycle, 110-120 V ac power. Figure 6.9.1-1 is a schematic diagram of the PPC. An instruction manual is not available at this time.

6.9.2 Power Processor Simulator

The Power Processor Simulator (PPS) is a device designed, developed and fabricated at LeRC to simulate, as closely as possible, all functions of an EM/PPU. Specifically, the PPS will:

1. Receive and acknowledge by visual display all command functions which a PPU must respond to:

   a. Power supply ON/OFF commands

   b. Supply address and set point discrete commands

   c. Beam current reference setting commands

   d. Discharge current reference setting commands

   e. Magnetic baffle current reference setting commands

   f. Screen voltage reference setting commands

   g. Telemetry measurement commands

2. Provide a selectable (0 to 127) telemetry measurement count output in response to telemetry measurement request commands.

3. Identify illegal commands which a PPU could not decode.

4. Check the parity of the input pulse train to confirm that it is in odd parity, which is the proper form.

5. Check for the proper user command code in input pulse train.

6. Initiate an interrupt signal identical to those issued by a PPU.

   a. High accelerator current

   b. Low screen voltage

   c. Beam current out of limit

d. Input voltage out of limit

e. Excessive arcs

f. Neutralizer failure

7. Provide echo-back signals

8. Acknowledge a recycle signal

9. Confirm that the external power supplies can provide about 10 amps at 300 V and 5 amps at 28 V while remaining within the 180 to 420 V and 23 to 33 V range, respectively.

The PPS is a portable device weighing approximately 35 pounds. A resistive load bank is provided that is used to verify 6.9.2 Step 9 above. The resistive load bank is also portable and weighs approximately 20 pounds. A PPS manual (applicable document 6.8.12) contains a description, schematic diagrams, operating instructions, illustrations, and photographs of the unit.

6.9.3 Thruster Dummy Load and Test Console

The thruster Dummy Load and Test Console (DL/TC) is a device that provides loads, instrumentation, and a simulated solar array power supply for power processor testing. The DL/TC also provides arc and short circuit simulation between PPU outputs, output to ground for selected supplies. The function of the DL/TC is twofold:

1. To provide the power source, loads, and metering for PPU testing only.

2. To provide a power source and metering for PPU/Ion thruster testing.

Each of the above functions are accomplished by jumper cables appropriately patched on a rear panel.

Two types of loads are used in the DL/TC. High voltage loads consist of power triodes with variable grid bias controls to control load current. All other loads consist of one or more additive decade stages of fixed resistors. Protective circuitry for meters and other circuitry is provided for arc and short circuit testing. Digital and analog displays are provided for easy readout. A DL/TC manual (applicable document 6.8.6) contains a description, photographs and operating instructions for the unit.

6.9.4 Procedures

Computerized test procedures have been developed to assist engineers and technicians in checking the FM/PPU's. Procedures have been developed at the P.C. board and module level (applicable document 6.8.13), plus a Performance Acceptance Test Procedure (PAT) along with a Data Package for recording data. These procedures provide a step

by step procedure for performing a test, along with expected values and limits. Table 6.9.4-1 lists all the procedures.

TABLE 6.5.3-1

TELEMETRY RANGES AND ACCURACIES

CHANNEL		RANGE	ACCURACY % of F.S.
J_B (J11)	Beam Current	0-2.56A	3
V_1 (V11)	Net Accelerating Voltage	0-1280V	3
J_E (Jg)	Discharge Current	0-15A	3
V_1 (Vg)	Discharge Voltage	0-50V	3
V_G	Neutr. Common/S/C/Common Voltage	0-100V	3
J_A (J10)	Accelerator Current	0-50MA	3
V_{NK} (V7)	Neutr. Keeper Voltage	0-50V	3
J_{MB} (J12)	Mag. Baffle Current	0-6.4A	5
V_A (V10)	Accelerator/S/C/Common Voltage	0-650V	5
J_{NK} (J7)	Neutr. Keeper Current	0-4A	5
J_{NE}	Neutr. Emmission Current	0-2.56A	3
J_{SA}	PPU Input Current	0-20A	5
V_{SA}	PPU Input Voltage	0-450V	5
J_{CV} (J2)	Cathode Vaporizer Current	0-2A	5
J_{NV} (J6)	Neutr. Vaporizer Current	0-2A	5
J_V (J1)	Main Vaporizer Current	0-2A	5
J_{CK} (J8)	Cathode Keeper Current	0-1.28A	5
V_{CK} (V8)	Cathode Keeper Voltage	0-50V	5
J_{NT} (J5)	Neutr. Heater Current	0-10A	5
J_{CT} (J3)	Cathode Heater Current	0-10A	5
J_{HTR} (J4)	Isolator Heater Current	0-10A	5
V_{NT} (V5)	Neutr. Heater Voltage	0-20V	5
V_{CT} (V3)	Cathode Heater Voltage	0-20V	5
T_{MV}	Main Vaporizer Temperature	To 400°C	TBD
T_{CV}	Cathode Vaporizer Temperature	To 400°C	TBD
T_{NV}	Neutr. Vaporizer Temperature	To 400°C	TBD
Interrupt Status		Digital word indicating cause of interrupt	
Recycle Count		digital word equal to number of recycles	

TABLE 6.5.4-1

FM/PPU OUTPUT REQUIREMENTS

SUPPLY	MAXIMUM RATING E VOLTS	MAXIMUM RATING I AMPS	MAXIMUM RATING P WATTS	STATIC LOAD REGULATION %	STATIC LOAD RIPPLE % PP
Main Vaporizer	14	2	28	5	5
Cathode Vaporizer	10	2	20	5	5
Cathode Heater	20	4.4	8.8	5	5
Isolator Heater	10	2.5	25	7	7
Neutralizer Heater	20	4.4	88	5	5
Neutralizer Vaporizer	10	2	20	5	5
Neutralizer Keeper (1000 V Boost)	25	3	75	5	2
Cathode Keeper (1000 V Boost)	25	1	25	5	2
Magnetic Baffle	4	5	20	5	5
Discharge	50	14	700	1	2
Accelerator	500	.10	50	5	5
Screen	1100	2.1	2310	3	1

TABLE 6.5.6-1 PPU EFFICIENCY CHARACTERISTICS

SET POINT	I BEAM	I SCREEN	P I	PLANNING VALUE (EP/PPU)	FM-1	FM-2	FM-3
1	2.0	1100	2700	.872	.870	.876	.869
2	1.6	940	1927	.850	.854	.847	.841
3	1.3	820	1431	.819	.822	.824	.814
4	1.0	700	1008	.784	.789	.788	.779
5	0.75	600	710	.752	.747	.743	.730

TABLE 6.6.4-1

PPU MASS BREAKDOWN

COMPONENT	MASS	
Module A1	5.31 KG	(11.71 lbs)
Module A2	3.53 KG	(7.79 lbs)
Module A3	8.36 KG	(18.44 lbs)
Module A4	5.99 KG	(13.20 lbs)
Module A5	2.29 KG	(5.04 lbs)
Module A6	3.45 KG	(7.60 lbs)
Module A7	4.64 KG	(10.24 lbs)
Legs (4)	0.38 KG	(0.83 lbs)
Sides (4)	1.04 KG	(2.30 lbs)
Power Harness	0.16 KG	(0.35 lbs)
Signal Harness	0.63 KG	(1.32 lbs)
Lids	1.04 KG	(2.30 lbs)
Hardware	0.51 KG	(1.13 lbs)

TABLE 6.9.4-1

FM PPU TEST PROCEDURES

PC BOARD PROCEDURES

A1A3 - 28 VDC Converter
A2A1 - Digital Interface
A2A2 - Digital Interface
A2A3 - Digital Interface
A2A5 - PPU Commands
A2A6 - PPU Commands
A2A7 - PPU Commands
A2A8 - PPU Control and Protection
A2A9 - PPU Control and Protection
A2A10 - PPU Control and Protection
A2A11 - PPU Control and Protection
A2A12 - PPU Control and Protection
A2A13 - Telemetry
A2A14 - Constant Current Thermistor Supply

A3A2 - Accelerator Regulator
A3A3 - SCR Firing Network - Screen Supply
A3A4A - Series Inverter Control Logic
A3A4B - Series Inverter Control Logic
A3A5 - Screen Regulator
A3A6 - A3 Telemetry

A4A3 - SCR Firing Network - Discharge Supply
A4A4A - Series Inverter Control Logic - Discharge
A4A4B - Series Inverter Control Logic - Discharge
A4A5 - V9 Regulator - Discharge
A4A6 - A4 Telemetry

A5A2 - Transistor Drive Network - Multiple Inverter
A5A3A - Series Inverter Control Logic
A5A3B - Series Inverter Control Logic
A5A4 - Multiple Inverter Regulator
A5A5 - Ramp Generator

TABLE 6.9.4-1(Concluded)

A6A5 - V3 Cathode Heater Regulator
A6A6 - V4 Isolator Heater Regulator
A6A7 - Cathode Keeper Regulator
A6A8 - Magnetic Baffle Regulator
A6A9 - A6 Telemetry
A6A10 - A6 Module Reference Board

A7A6 - Main Vaporizer Regulator
A7A7 - V2 Cathode Vaporizer Regulator
A7A8 - V6 Neutralizer Vaporizer Regulator
A7A9 - V5 Neutralizer Heater Regulator
A7A10 - V7 Neutralizer Keeper Regulator
A7A11 - A7 Telemetry
A7A12 - (A7A6, A7A9) Reference
A7A13 - A7A7 Reference
A7A14 - A7A8 $V_{(NK)}$ Reference
A7A15 - (A7A8, A7A10), References

MODULE PROCEDURES

A1 Test Procedure - 28 VDC Converter, Input Filer, TLM Oscillator
A2 Test Procedure - Digital Interface, PPU Commands, PPU Control & Protection
A3 Test Procedure - V11 Output and Series Resonant Inverter-Screen Supply
A4 Test Procedure - Series Resonant Inverter - Discharge Supply
A5 Test Procedure - Transistor Drive Network - Multiple Inverter
A6 Test Procedure - (V3, V4, V8, and V12) Outputs
A7 Test Procedure - (V1, V2, V5, V6, and V7) Outputs

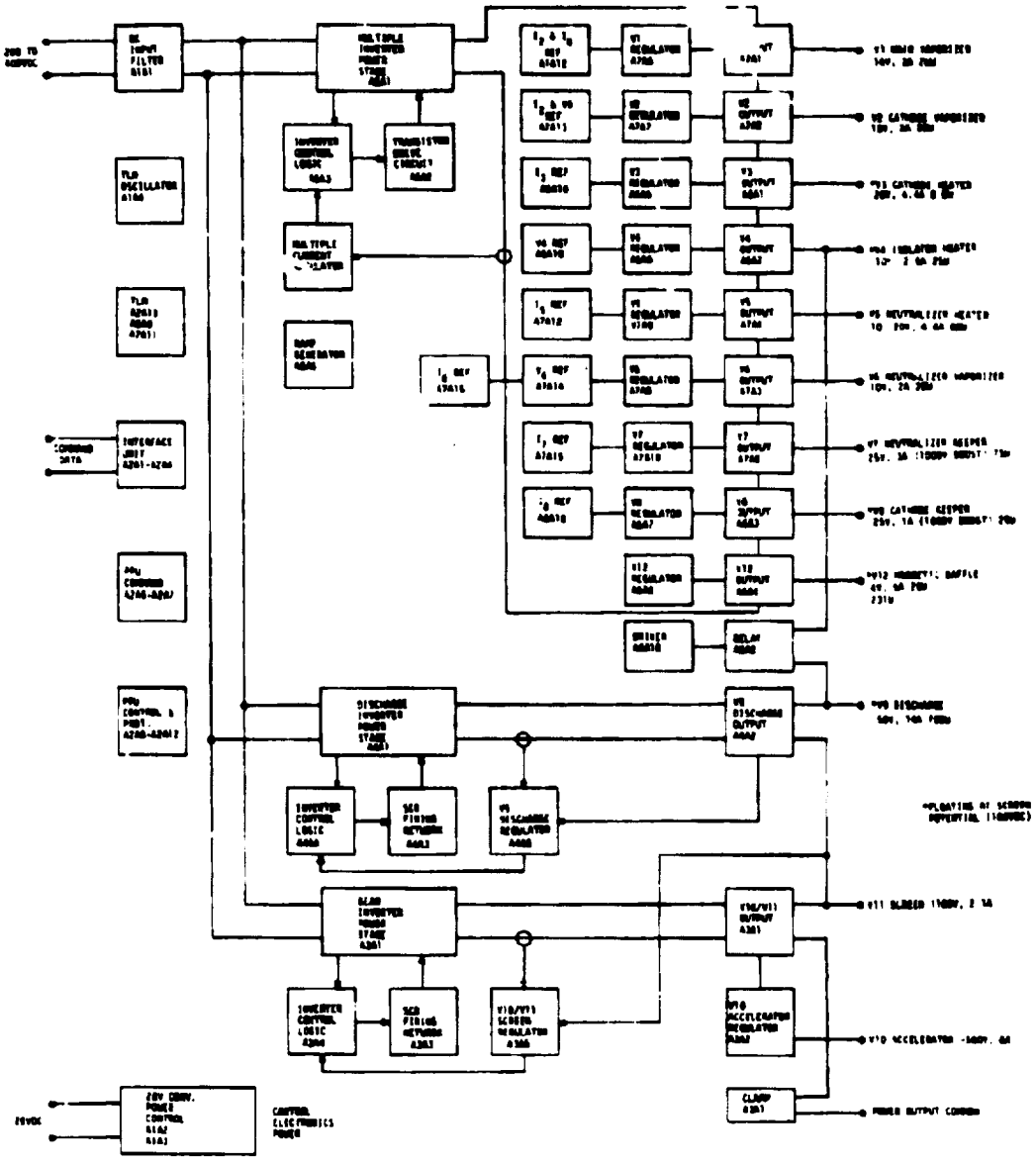

LEGEND: AXAY
X = module no. (1 through 7), Y = subassembly no. (1, 2---n)

FIGURE 6.3.1-1 POWER PROCESSOR BLOCK DIAGRAM

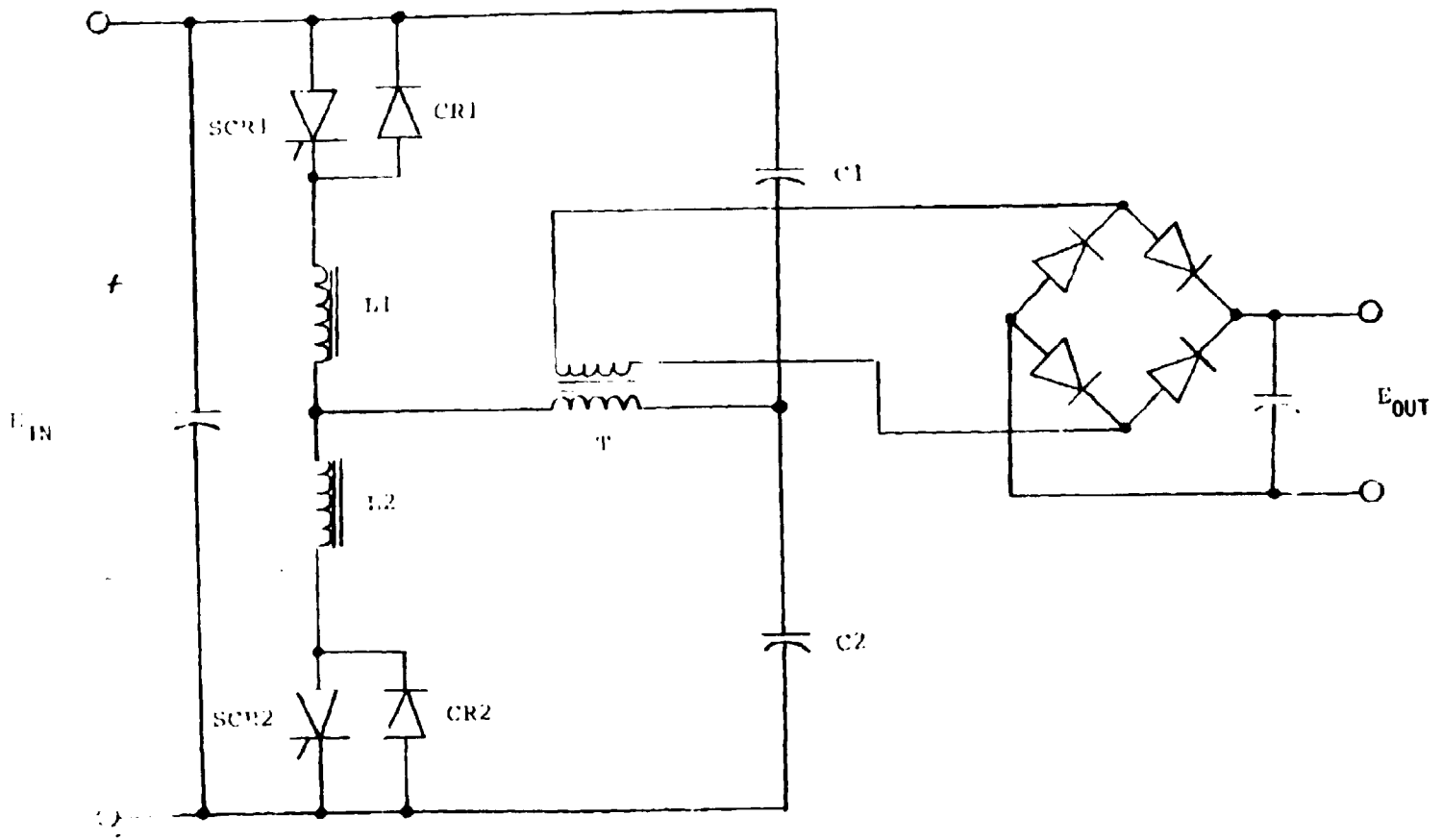

FIGURE 6.3.1-2 BASIC SERIES RESONANT INVERTER

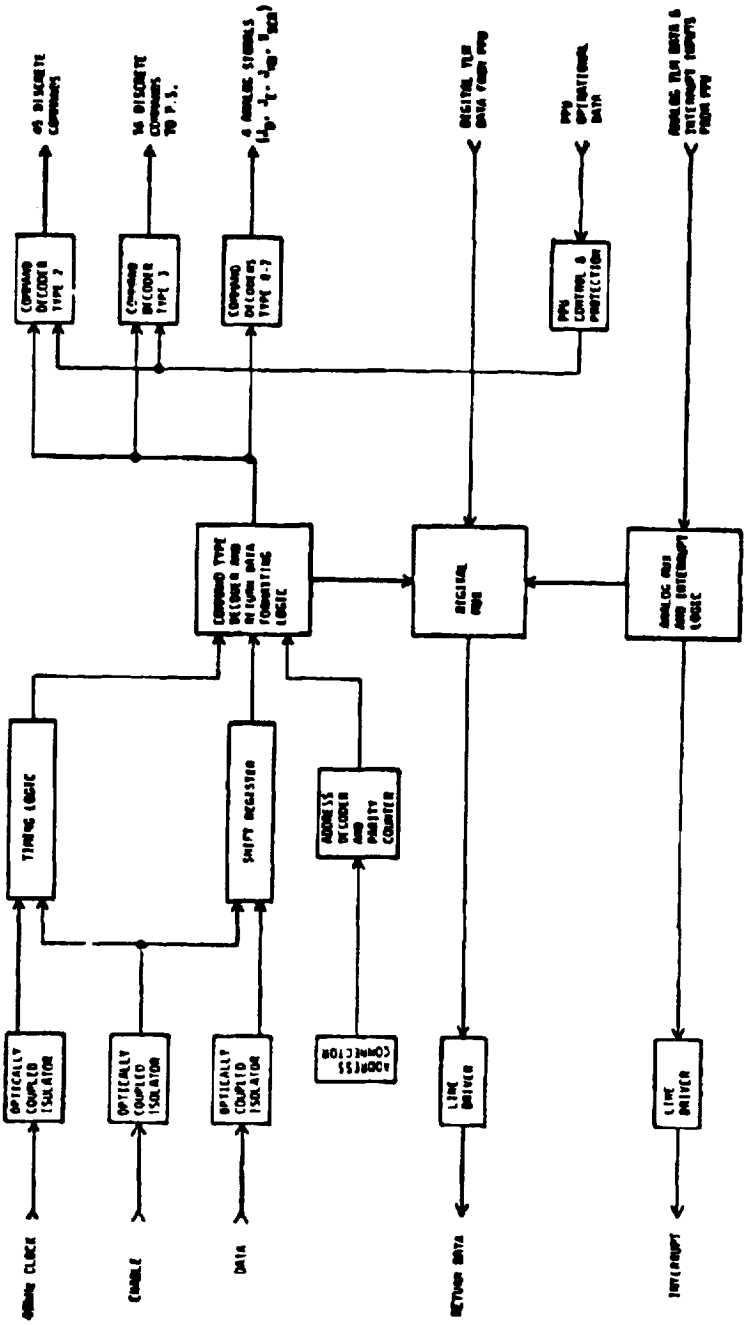

FIGURE 6.3.1-3 BLOCK DIAGRAM INTERFACE UNIT, PPU COMMANDS, CONTROL AND PROTECTION SYSTEM

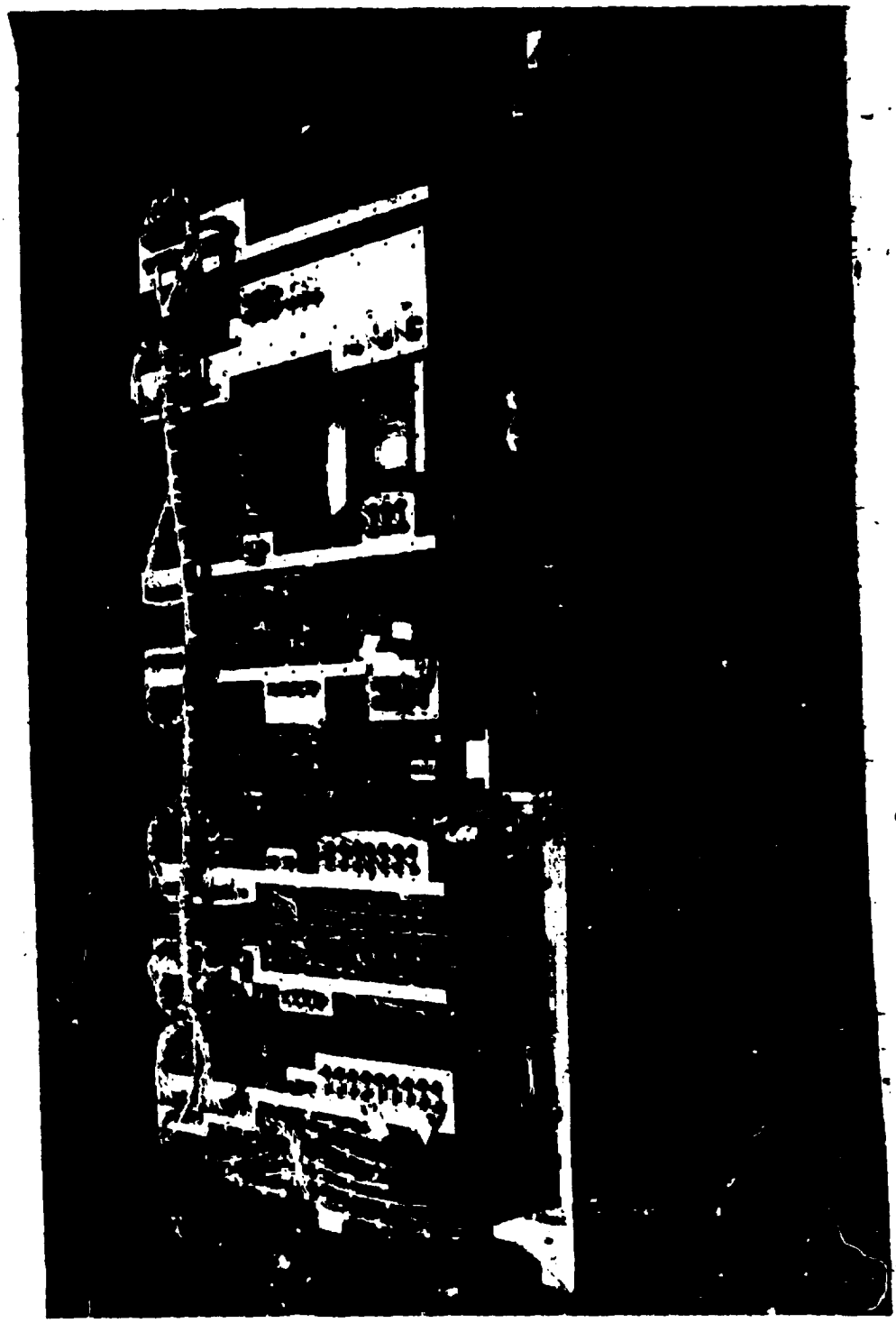

FIGURE 6.3.2-1 FM/PPU Assembly Photograph

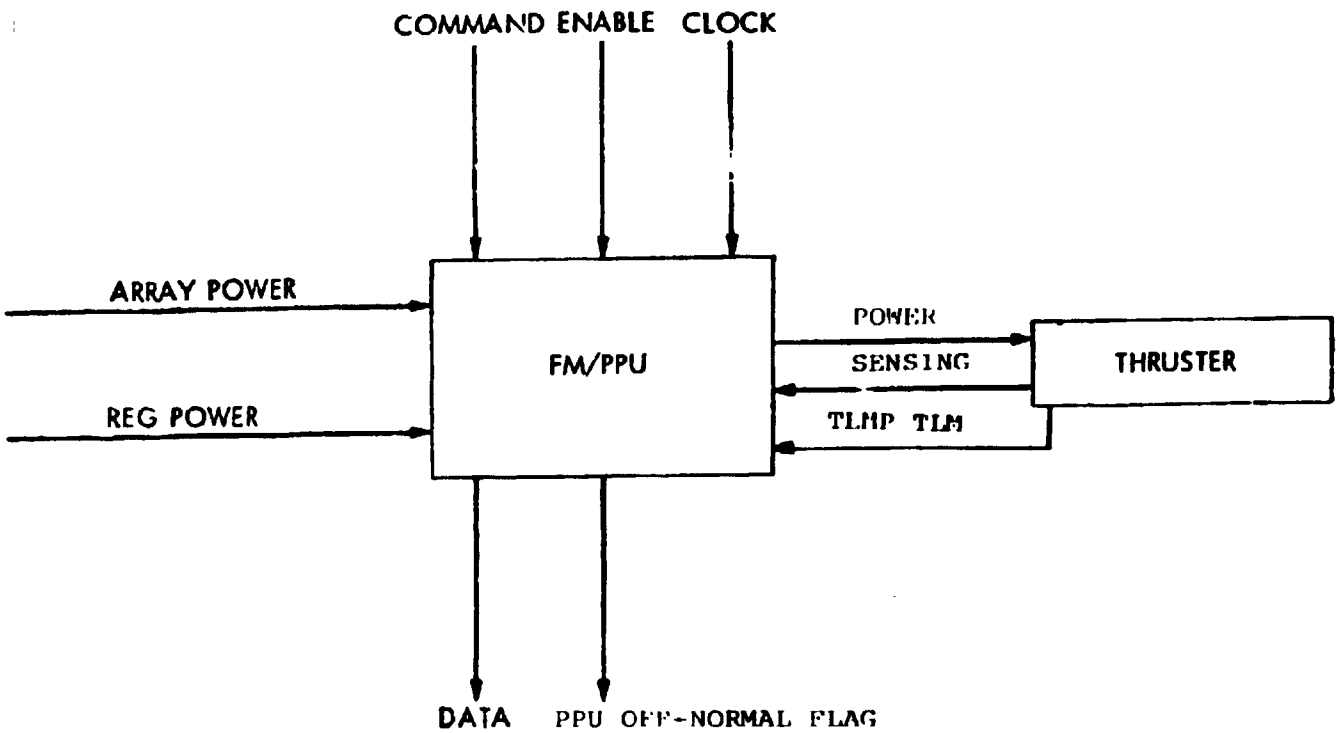

FIGURE 6.4.1-1 POWER PROCESSOR INTERFACE DIAGRAM

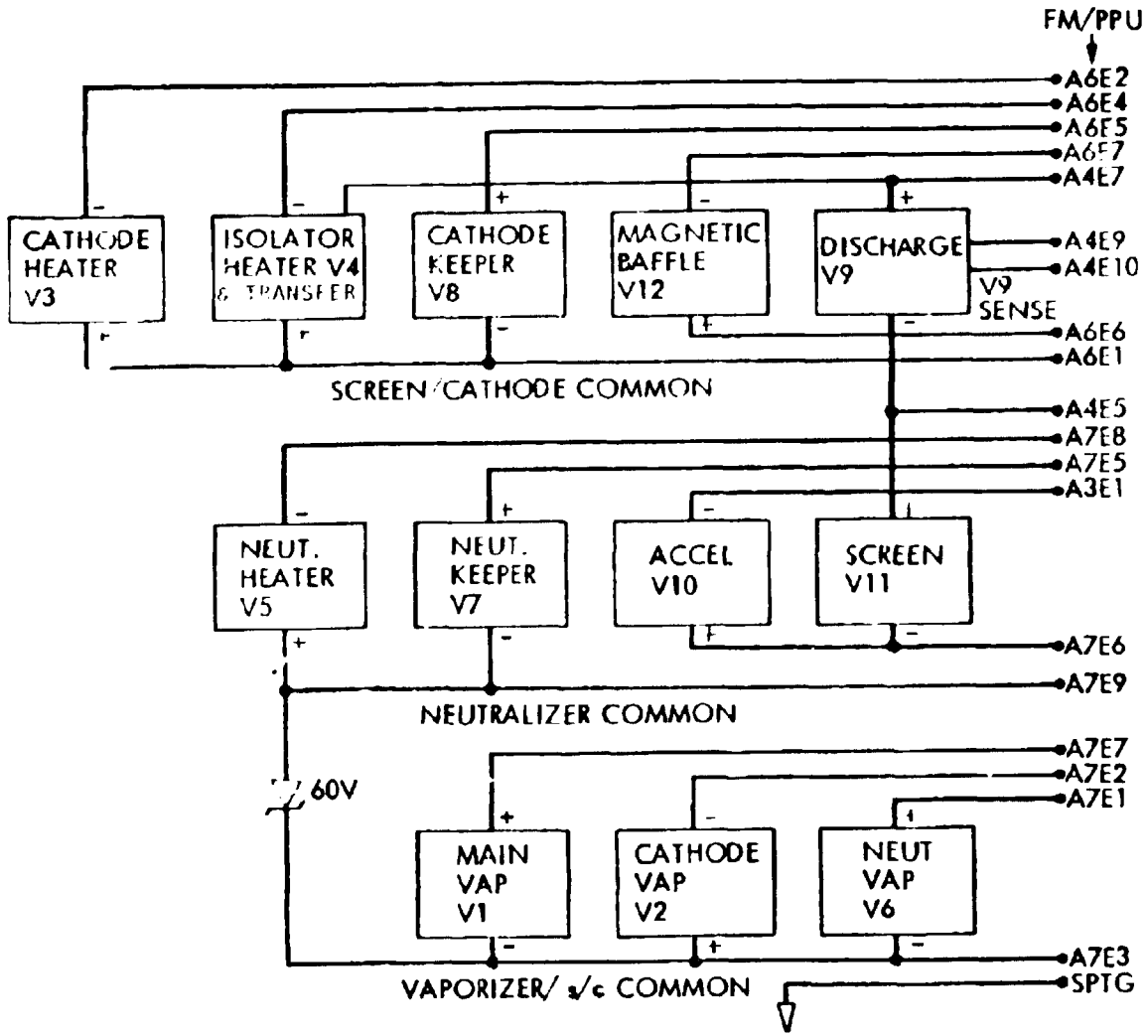

FIGURE 6.4.1-2 PM/PPU-THRUSTER POWER INTERFACE

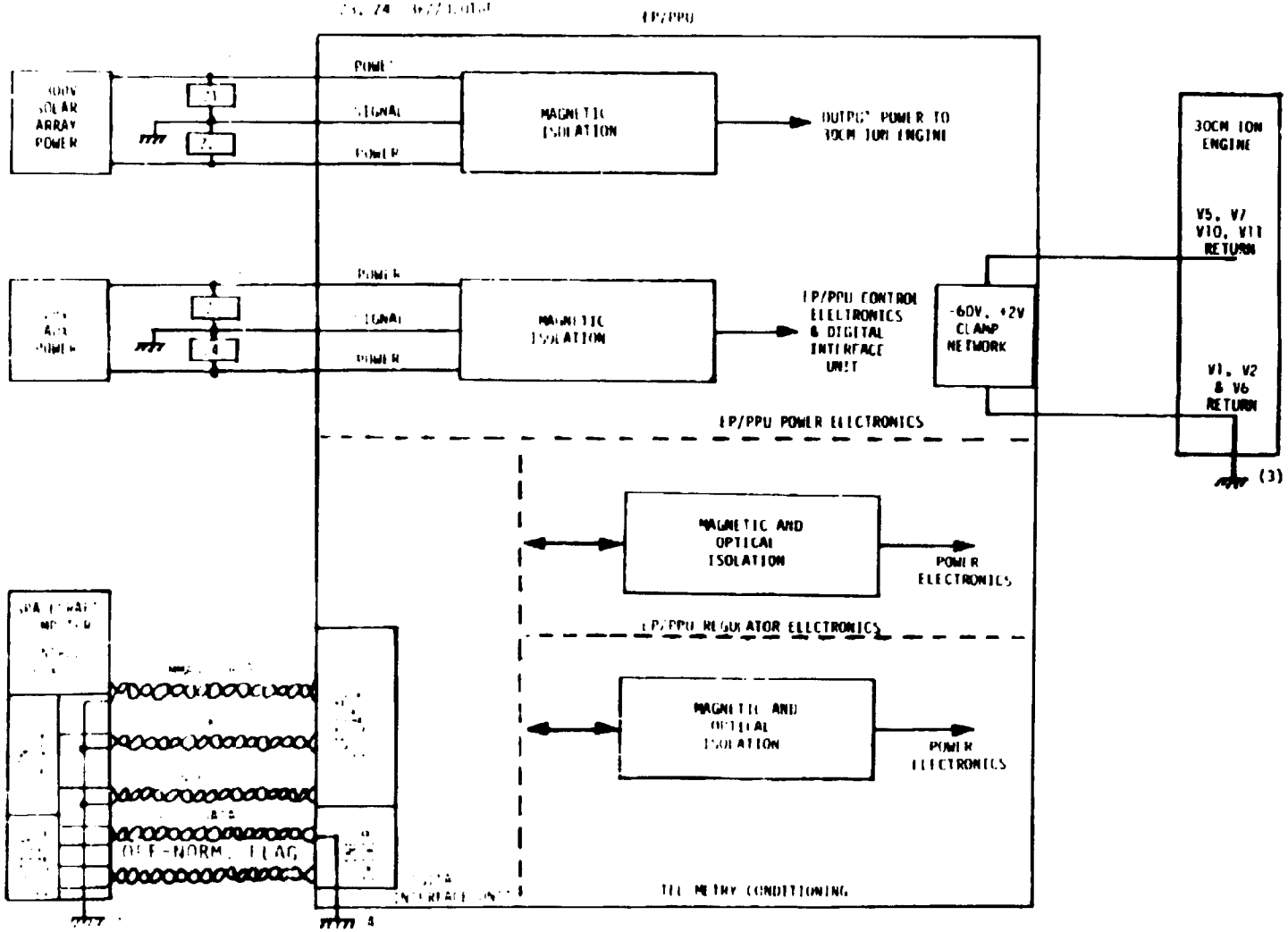

FIGURE 6.1.1-3 PPU GROUNDING DIAGRAM

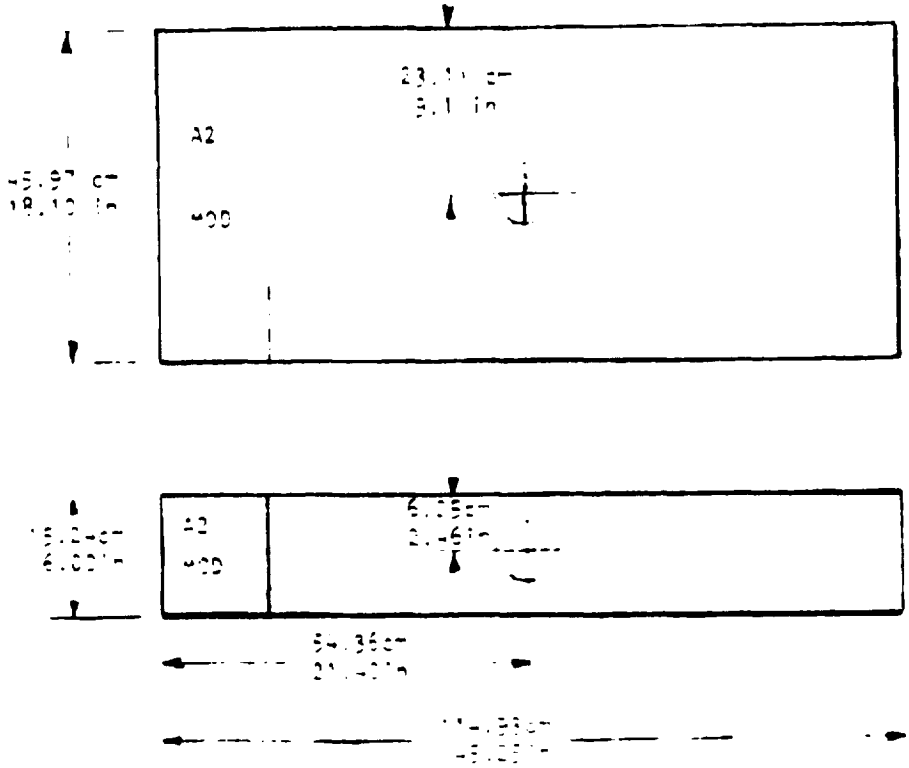

FIGURE 6.6.3-1

SW SEQ CENTER OF MASS

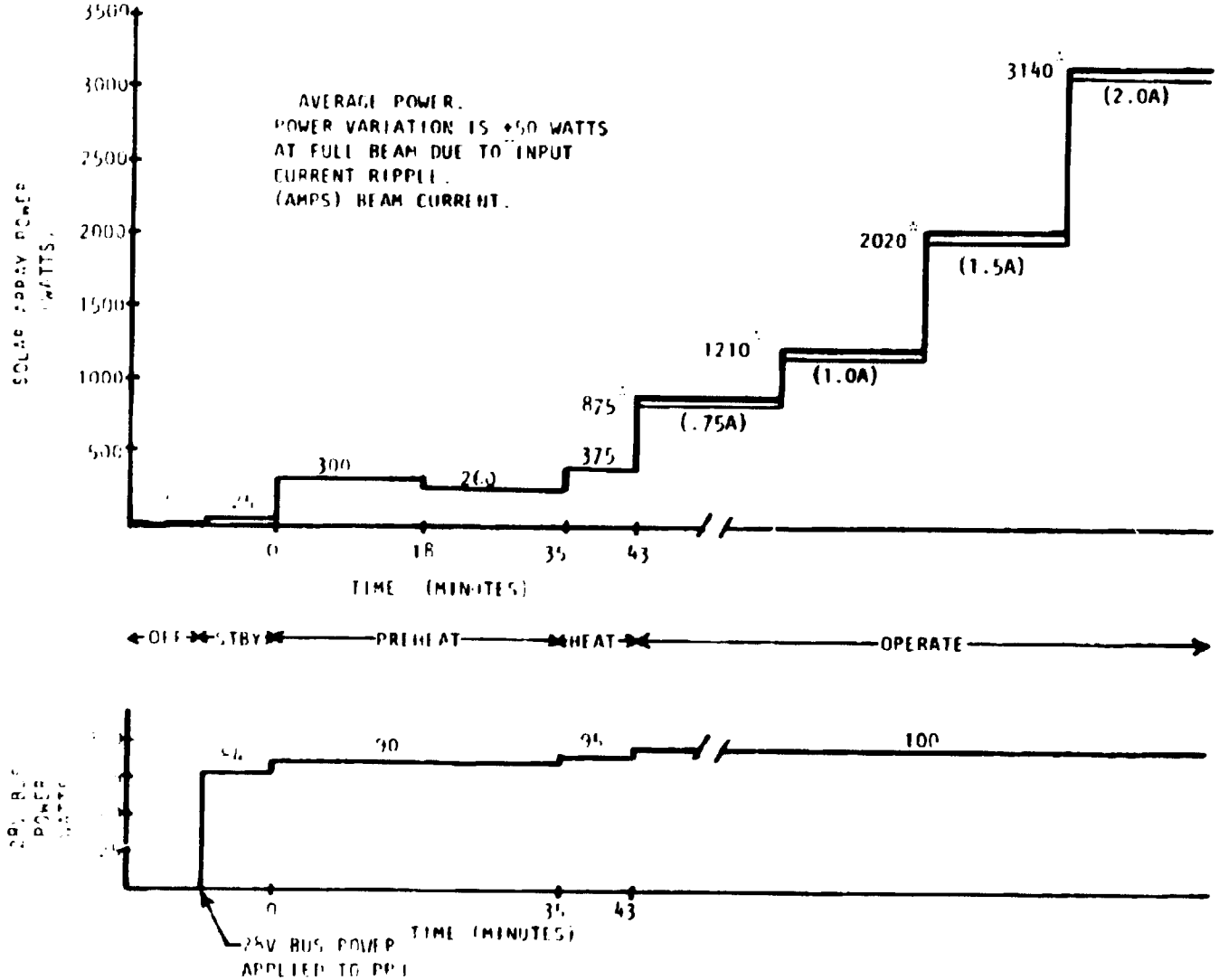

FIGURE [illegible] EM/PPU POWER PROFILE

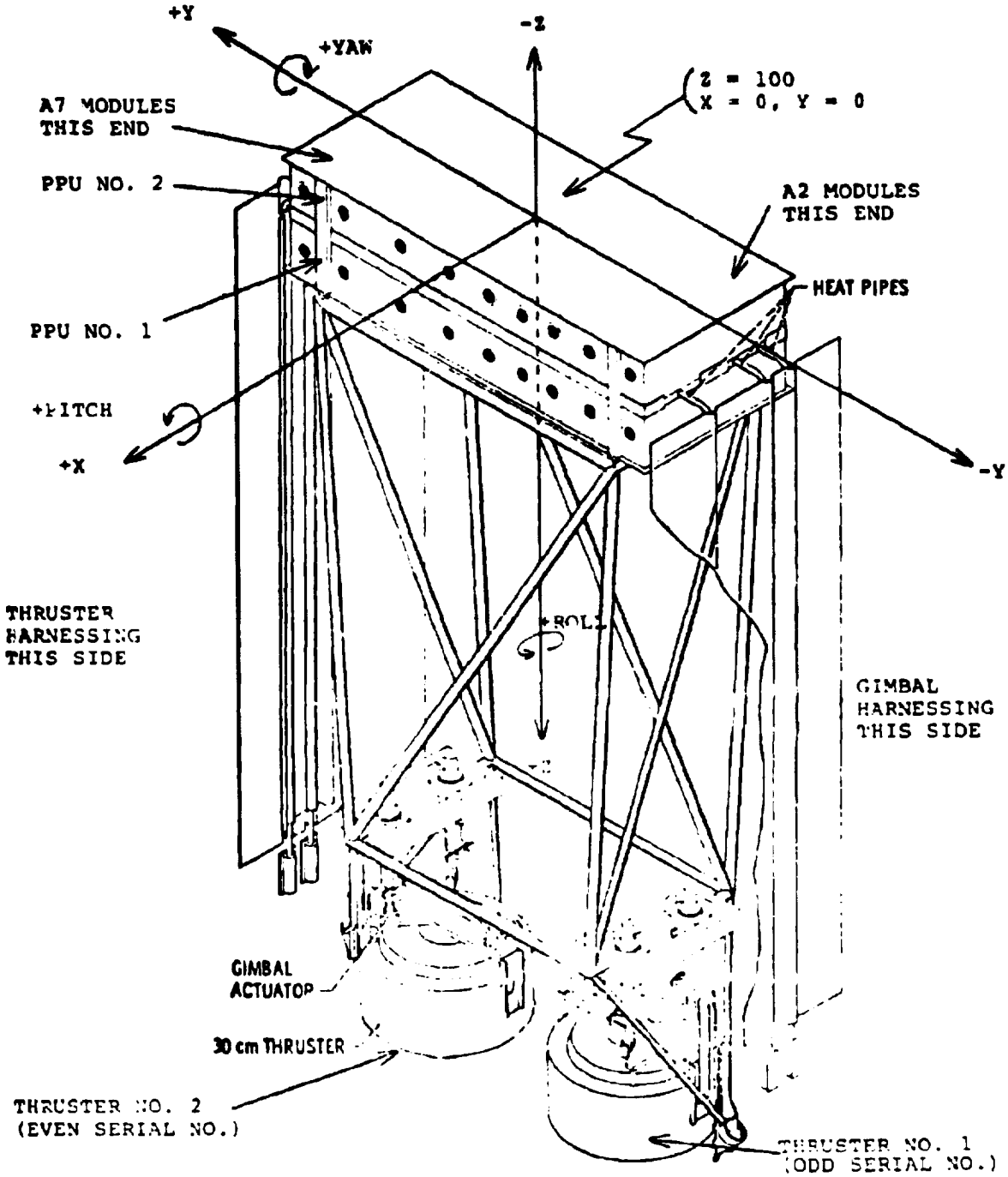

FIGURE 6.6.10-1 [illegible] Thrust Module Co-ordinate System

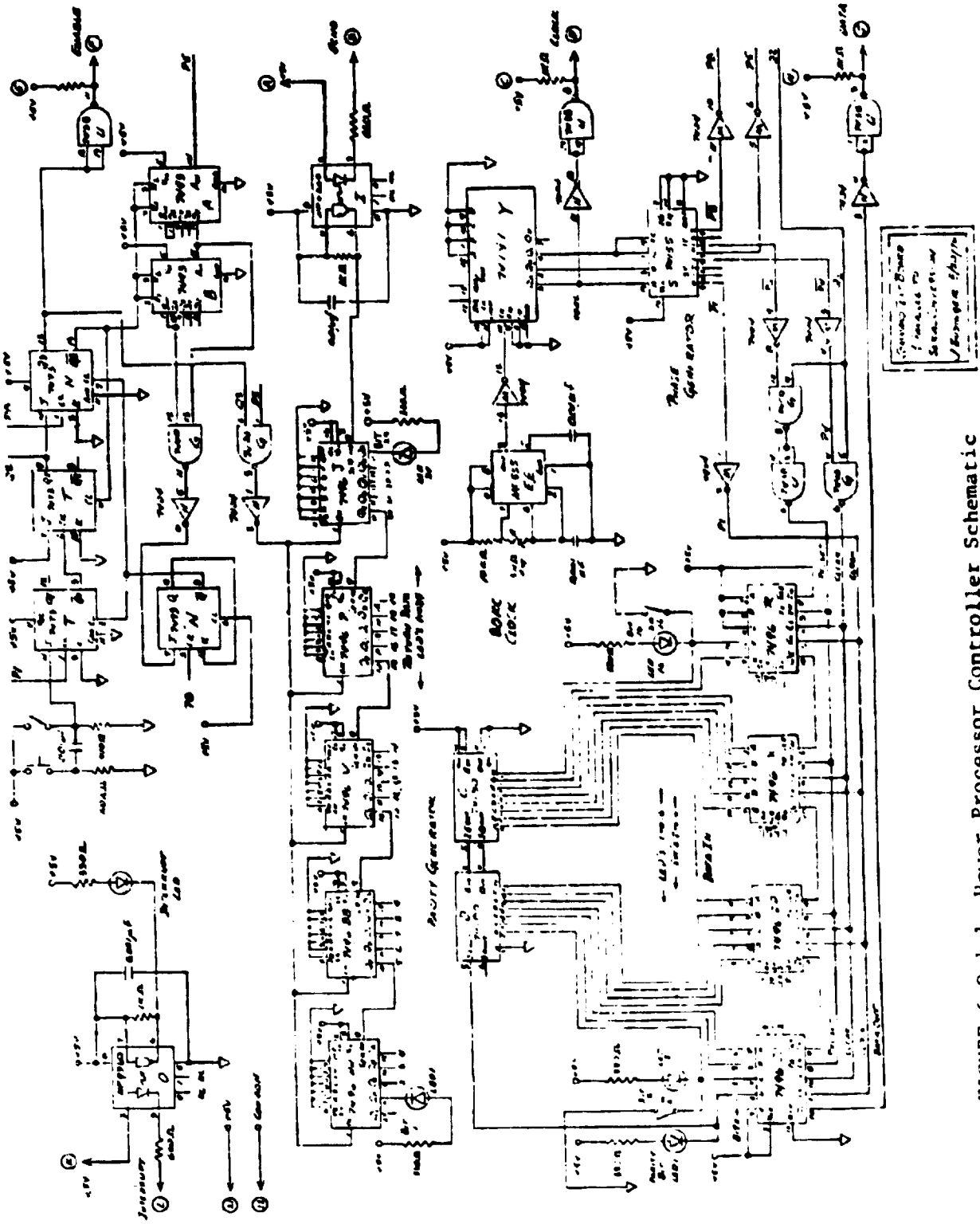

FIGURE 6.9 1-1 Power Processor Controller Schematic

7.0

GIMBALS

Table of Contents

		Page
7.0	Gimbals	7-4
7.1	Reference Documents	7-4
7.2	Functional Requirements	7-4
7.3	Functional Description	7-5
7.3.1	Electrical	7-5
7.3.2	Mechanical	7-6
7.3.3	Thermal	7-8
7.4	Interface Definition	7-9
7.4.1	Electrical	7-9
7.4.2	Mechanical	7-11
7.4.3	Thermal	7-12
7.5	Performance Description	7-12
7.5.1	Angular Travel	7-12
7.5.2	Slew Rate at 400 PPS of the Motor	7-14
7.5.3	Torque at 400 PPS of the Motor	7-14
7.5.4	Power Consumption	7-14
7.5.5	Capable of Deep Space Operation	7-14
7.5.6	Life	7-15
7.5.7	Duty Cycle	7-15
7.5.8	Locked Position Power	7-15
7.5.9	Alignment	7-15
7.5.10	Temperature	7-15
7.5.11	Storage in Space	7-15
7.5.12	Operation with the Thruster	7-16

		Page
7.5.13	Operation in a One "G" Field	7-16
7.5.14	Gimbal Motor Specifications	7-16
7.5.15	Gimbal Motor Gear Train Specifications	7-16
7.5.16	Gimbal Actuator	7-17
7.5.17	Gimbal Feedback Sensor Characteristics	7-17
7.5.18	Environmental Testing	7-17
7.6	Physical Characteristics and Constraints	7-18
7.6.1	Mass	7-18
7.6.2	Size	7-18
7.6.3	Harness	7-18
7.7	Development History	7-18
7.8	Applicable Documents Enclosed	7-19
7.8.1	30-cm Ion Engine Gimbal System Drawings	7-19
7.9	Ground Support Equipment	7-19
7.9.1	Gimbal Control Electronics	7-19
7.9.2	Miscellaneous	7-22
TABLE		
7.5.18-1	Gimbal System Vibration Levels	7-23
FIGURES		
7.3.2-1	Gimbal System/Thruster Interface, BIMOD Configuration	7-24
7.3.2-2	BIMOD Gimbal System	7-25
7.3.3-1	Thruster End of the BIMOD	7-26
7.4.1-1	Gimbal Electrical Interface Drawing	7-27
7.4.2-1	Thruster Interface Drawing	7-28

		Page
7.4.3-1	Major Heat Flow Paths of the Structure, Gimbals, and Thrusters	7-29
7.5.1-1	Maximum Envelope Capability of the Gimbal System	7-30
7.5.1-2	Gimbal Angles	7-31
7.5.18-1	Gimbals During Vibration Testing	7-32
7.5.18-2	Gimbals During Vibration Testing	7-33
7.5.18-3	Gimbals During Vibration Testing	7-34
7.7-1	Ion Auxiliary Propulsion System	7-35
7.7-2	Ion Auxiliary Propulsion System Thruster Gimbal Assembly	7-36
7.9.1-1	Gimbal Control Block Diagram	7-37

7.0 Gimbals

This section describes the gimbal system that has been designed to meet the anticipated requirements of the 30-cm thruster (reference 7.1.1). The gimbal control and position indication system is also described.

7.1 Reference Documents

7.1.1 Cake, James E.; Sharp, G. Richard; Oglebay, Jon C.; Shaker, Francis J.; and Zavesky, Ralph J.: Modular Thrust Subsystem Approaches to Solar Electric Propulsion Module Design. NASA TM X-73502, 1976.

7.1.2 Zavesky, Ralph J.; and Hurst, Evert B.: SERT II Gimbal System. NASA TM X-2427, 1971.

7.1.3 Banks, B. A.: 8-cm Mercury Ion Thruster Systems Technology. NASA TM X-71611, 1974.

7.1.4 Herron, B. G., et al.: Engineering Model 8-cm Thruster System. AIAA/DGLR Paper 78-646, April 1978.

7.2 Functional Requirements

The functional requirements of the gimbal system are to:

1) Provide for the mounting of a 30-cm thruster to the structure of the bimodular thrust system (BIMOD).
2) Direct the thrust vector of the 30-cm thruster in two axes to enable attitude control and spacecraft orientation control.

3) Provide an angular readout system that relates the position of the thruster beam vector with respect to the axes of the BIMOD.

7.3 Functional Description

7.3.1 Electrical

The gimbal is driven by two three-phase variable reluctance stepping motors. Two phases of the motor are energized at a given time and stepping is accomplished by de-energizing one of the energized windings and energizing the de-energized winding at the same time. The direction that the motor steps, clockwise or counterclockwise, is determined by which energized winding is de-energized.

The angular position of the gimbal is indicated by means of two resolvers (one for each axis). The resolver is a transformer with two rotating secondary windings that are oriented 90° with respect to each other. These secondary windings are rotated with respect to the primary winding by the shaft of the resolver. Rotation of the secondary windings varies their coupling coefficient with respect to the primary winding. The magnitude of the output voltage from one of the secondary windings is proportional to the sine of the shaft angle, and the magnitude of the output voltage from the other secondary winding is proportional to

the cosine of the shaft angle. If the primary voltage is

$$V_p = A \sin \omega t$$

then the secondary voltages are the following:

$$V_{S1} = AB \sin \theta \sin (\omega t + \phi)$$

$$V_{S2} = AB \cos \theta \sin (\omega t + \phi)$$

where A and B are constants, θ is the shaft angle, and ϕ is a constant phase shift between the primary and secondary windings. The magnitudes of the output voltages are

$$\text{magnitude of } V_{S1} = AB \sin \theta$$

$$\text{magnitude of } V_{S2} = AB \cos \theta$$

Therefore,

$$\theta = \arcsin \frac{\text{magnitude of } V_{S1}}{AB}$$

$$\theta = \arccos \frac{\text{magnitude of } V_{S2}}{AB}$$

The stepping motors are prevented from overdriving the gimbal by four limit switches. There are two limit switches for each motor, one for each direction of travel. These limit switches must be incorporated into the drive circuitry for the stepping motors.

7.3.2 Mechanical

Figure 7.3.2-1 shows the conceptual gimbal system in a BIMOD configuration. Figure 7.3.2-2 is a photograph of the BIMOD gimbal system attached to a vibration fixture and with a dummy model thruster on one

gimbal. The gimbal parts are iridited and show up in gold. Extending or retracting of the two linear actuators in conjunction with angular rotation of the cross pin hinge or gimbal pivot provides the thruster gimballing in two mutually orthogonal axes. When the linear actuators are both extended, rotation takes place about the X axis in a -θ direction. When both actuators are retracted, gimbal rotation is in a +θ direction. Differential movement of the actuators, one extended and one retracted, causes angular rotation, θ about the Y axis. The actuators and the cross pin hinge attach the thruster mounting frame to the BIMOD structure. The thruster mounting frame consists of a Y-shaped thruster mounting bracket, two side mounting pads, and two ground screen mount standoffs. The thruster is mounted to the side mounting pads, and the two ground screen mount standoffs. The two jackscrew type actuators are driven by a stepper motor-gearhead assembly. The actuators have a universal joint at both ends for angular compliance. Switches limit the length of linear travel which controls the angular travel limits of the gimbal. A guide pin that is attached to the thruster mounting frame rides in the slot of a support bracket that is mounted to the lower BIMOD truss. This guide pin is used for lateral support.

One advantage of this system is the result of favorable geometry. The arrangement of the actuators, cross pin hinge and the guide pin provides stiffness in all directions eliminating the need for pin puller restraints during launch, while allowing the two degrees of required gimbal movement. The stiffness in all directions is not a function of gimbal position. The static and dynamic loads are carried in the Z-direction by the two actuators and the cross pin hinge, in the Y-direction by the thrust washers in the cross pin hinge, and in the X-direction by the cross pin hinge, the guide pin, and the guide pin bracket.

The angular position of the gimbal system is continuously monitored by an angle indicator system that consists of two resolvers. These resolvers are attached to the cross pins of the hinge and provide direct readout of the and gimbal angles.

The propellant for the thruster is carried across the gimbal interface by a flexible propellant feed line shaped like a coiled spring tube.

7.3.3 Thermal

The location of the gimbals with respect to the thrusters and aft insulation of the BIMOD is shown in figure 7.3.3-1. As of April 1979 there has been

no extensive thermal analysis done on this system. It may be required to maintain some components (e.g., resolver and motor) within certain temperature limits depending on the environment to which they are subjected. If so, thermal control shall be provided by coatings, additional multilayer insulation and/or supplementary heaters. The amount and location are to be determined (TBD).

7.4 Interface Definition

7.4.1 Electrical

1) Stepping motor:

Singer-Kearfott variable reluctance stepping motor number CR4 0192 039

158:1 gearhead, number CR2 0391 070

Power: 28V dc, 8.3 watts

Winding Resistance: 220 ohms

Amps per phase: 0.13

Stepping rate: 400 Hz nominal

700 Hz maximum

Phase sequence for counter clockwise rotation:

Step/Winding	A	B	C
1	ON	ON	OFF
2	OFF	ON	ON
3	ON	OFF	ON

2) Resolver:

Singer-Kearfott number CM4 1093 009

Resolver is brushless

Input voltage: 11.8 V ac maximum, 400 Hz sine wave

Input current: 0.050 amps maximum

Input power: 0.090 watts maximum

Input impedance: 103 + j197 ohms

Output voltage: 10.62 V ac maximum

Transformer ratio: 0.90

The resolver can be operated at lower input voltages (and hence lower power) with an equivalent drop in output signal level.

3) Limit Switches:

Form: SPDT

Rating: 115 V ac, 5 amps
28 V dc, 2 amps

4) Number of wires:

4 per stepping motor	- 8
6 per resolver	-12
2 per limit switch	- 8
2 shields	- 2
Total number of wires	30 per gimbal

5) The gimbal electrical interfaces are shown in figure 7.4.1-1.

7.4.2 Mechanical

The thruster to gimbal installation is specified in figure 7.4.2-1 and NASA Drawing CF 637900. The thruster is mounted to the gimbal by the two gimbal mounting pads, and two standoffs. NASA Drawing CF 637900 shows that parts 3 and 4 mount to the thruster at the gimbal pads, and two parts 22 mount to the thruster ground screen on the bottom of the thruster. The feed line is attached to the back of the thruster at the manifold shown on figure 7.4.2-1.

The gimbal to structure installation is specified in NASA Drawing CF 637900 and the associated detailed parts. The interface points are: (1) the cross pin trunions, parts 8 and 10, (2) the bearings of the actuator rings, parts 30 and 37, (3) the support pin and the support parts 5 and 6, and (4) the base of the spring feed line, part 16. The detailed parts drawings can be used to obtain specific mounting dimensions.

The gimbal axes are the same as the designated spacecraft axes. They are shown on figure 7.3.2-1.

The gimbal system must overcome the added torque caused by the wiring harness and the feed lines. The coiled feed line additional torque is negligible. A test to determine the torque due to the harness has been planned, but the torque values are TBD.

7.4.3 Thermal

The thermal interfaces of the gimbal system include the insulation blanket placed between the radiators behind the thrusters, the mounting of the gimbal system with the structure, adjacent gimbals and thrusters, and the space environment. A schematic showing the major heat flow paths is shown in figure 7.4.3-1. As of April 1979 no detailed thermal analysis has been done on the gimbal system. If analysis of the gimbal system indicates that insulation and/or heaters are required to maintain the components within an acceptable range, they shall be added as required. Any insulation to be added shall be constructed in the same manner as that shown in table 9.3.2-1.

7.5 Performance Description

7.5.1 Angular Travel

The angular limits of the gimbal system as previously stated are

$= \pm 35^{o}$ minimum

$= \pm 15^{o}$ minimum

The total envelope that can be used with the present gimbal system has been plotted using the output of the resolvers (see fig. 7.5.1-1). The envelope limits are controlled by the maximum travel of the actuators. Any position within the envelope can be reached by

commanding the desired α and β angle inputs. Assuming that the resolver zero positions can be aligned with the known beam vector of the thruster, figure 7.5.1-1 then represents the maximum envelope capability of movement of the beam vector.

The angular travel is limited by the actuator linear travel and the relationships of the actuators to the cross pin hinge. By changing the distance between actuators the α angle can be varied, and by changing the distance between the actuators and the cross pin hinge, the β angle can be varied. The limitations are: (1) large angles could not be obtained because of mechanical interference, and (2) structural support of the system is required during the launch environment. It would be possible to achieve gimbal angles up to 50° in an α direction and up to 25° in a β direction with minor geometry changes.

The equation that relates the angle γ with the rotation angles α and β is given by the following equation:

$$\gamma = \arccos \frac{\cos \beta \cos \alpha}{\sqrt{\cos^2 \alpha \sin^2 \beta + \cos^2 \beta}}$$

β = rotation about the X-axis

α = rotation about the Y-axis

γ = the angle that the thrust vector makes with Z-axis (see fig. 7.5.1-2.)

7.5.2 Slew rate at 400 PPS of the Motor

a direction = 6.13°/minute

b direction = 2.67°/minute

7.5.3 Torque at 400 PPS of the Motor

a direction with two actuators operating = 25 ft-lb

b direction with two actuators operating = 62 ft-lb

Several 30-cm gimbal system variables could affect the operational characteristics. The pulsing rate of the stepper motor can be varied in order to change the slew rate of the system. The gear reduction ratio of the motor could also be changed up to a point where the minimum torque required to move the gimballed thruster is reached. The torque limitation is the requirement to be able to move the gimballed thruster in a one "g" environment in any attitude of the system.

7.5.4 Power Consumption

8.3 watts/actuator maximum, 0.1 watts/resolver maximum.

7.5.5 Capable of Deep Space Operation

All bearing and thrust bearings are Vespel polyimide plastic self-lubricating material. The female member or nut of the gimbal actuator is also Vespel. The only lubricant required would be in the bearings of the motor, in the bearings and gears of the gearhead and the bearings of the resolvers. The lubricant

will be either ion plated or sputter deposited MoS_2.

7.5.6 Life

TBD, but has been designed for a minimum of 5000 cycles of total travel of the actuator. Limited travel around a particular point could extend the actuations to 100,000.

7.5.7 Duty Cycle

The maximum duty cycle is determined by the temperature rise of the motor in vacuum. This is still TBD, because the thermal vacuum test on a system has not been completed.

7.5.8 Locked Position Power

The gimbal does not require any power to maintain the thrust vector in any fixed position.

7.5.9 Alignment

The gimbal system is capable of repeatable alignment within $\pm 0.10^{\circ}$ of true position within the operating envelope.

7.5.10 Temperature

The gimbal motor and the resolver running temperature extremes are -65° C to $+125^{\circ}$ C. Non-operating survival temperature extremes are -TBD$^{\circ}$ C to +TBD$^{\circ}$ C.

7.5.11 Storage in Space

The system is capable of a minimum of 15 years storage life in space, with or without operation. The allowable space environment is TBD.

7.5.12 Operation with the Thruster

The gimbal is also capable of changing the direction of the thrust vector while the thruster is operating.

7.5.13 Operation in a One "G" Field

The system is capable of operating in any attitude in a one "g" field with a 9.1 kg thruster installed. This requirement was brought about by unknown requirements of attitude during the testing phase of a thrust module. Gimbal angle constraints may arise from the requirement for compatability with testing other components such as heat pipes, or mercury targets in a vacuum.

7.5.14 Gimbal Motor Specifications

Manufacturer - Singer Company, Kearfott Division

Type - Variable reluctance stepper motor size 11

Stepping angle/pulse - 15^{o} pulse

Number of phases - three

Maximum stepping rate - 700 steps/sec

Total power input - 8.3 watts

Voltage - 28 volts

Operating speed - 400 steps/sec

Torque at 400 steps/sec - 0.3 in-oz

7.5.15 Gimbal Motor Gear Train Specifications

Manufacturer - Singer Company, Kearfott Division

Size - 11 (compatible with the motor)

Ratio - 158:1

7.5.16 Gimbal Actuator

Pitch of the jack screw - 13 threads/inch

Total linear travel - 4.50 ± 0.06 inches (tentative)

Stiffness - 0.005 max. inches of tolerance clearance stackup is allowed in the direction of travel of the actuator.

Backlash - the actuators are anti-backlash due to the jack screw principle.

7.5.17 Gimbal Feedback Sensor Characteristics

Type - Resolver - Singer - Kearfott type CM4 1093 C09 Size 8.

Resolution - Infinite, accuracy of present unit is 9 minutes, should be able to obtain a unit with 3-minute accuracy, if necessary.

7.5.18 Environmental Testing

The gimbal system was designed to carry a thruster load of 91 kg.

The system was vibration tested to one "g" sine input to identify the natural frequency of the system. See figures 7.5.18-1, 7.5.18-2, and 7.5.18-3.

The vibration levels have been selected in anticipation of flying for shuttle flight applications. The gimbal system will be vibrated to the specifications in table 7.5.18-1.

7.6 Physical Characteristics and Constraints

7.6.1 Mass

The weight of one gimbal system including two resolvers is 3.4 kg. The flight weight of the gimbal electronics is TBD, but is anticipated to about 1 kg.

7.6.2 Size

The dimensions of the gimbals are defined by the gimbal drawings (applicable document 7.8.1). The size of the flight gimbal electronics unit is TBD.

7.6.3 Harness

The harness for controlling the gimbals is TBD because the position of the control electronics is TBD.

7.7 Development History

The SERT II gimbal system is described in reference 7.1.2. This reports the performance of the only known thruster gimbal system flown to date. The SERT II spacecraft was launched February 3, 1970. The gimbal design was similar to that of a Hooke universal joint. It consisted of an inner and outer ring, four bearings, two gimbal mounts, and two linear actuators. This configuration is not inherently stiff, and two pin pullers were used for additional support during launch.

Because the reliability of the pin pullers is always questionable, and once they are fired they cannot be relatched, a geometry was investigated that would

allow the required two degrees of freedom and have three degrees of dynamic stability. Pin Pullers would not be required.

NASA developed such a gimbal system for the 8-cm thruster (ref. 7.1.4). The conceptual gimbal is described in reference 7.1.3. The 8-cm thruster system, including the gimbal is shown in figures 7.7-1 and 7.7-2. An auxiliary propulsion system will be flown on the United States Air Force STP P 80-1 flight in late 1981. The ion auxiliary propulsion system will consist of two 8-cm thruster systems and associated diagnostics.

The geometry used for the 8-cm gimbal system was extended to the 30-cm gimbal system. The linear actuators, cross pin hinge, support pin, and even the coiled feed line are similar.

7.8 Applicable Documents Enclosed

7.8.1 Gimbal System Drawing List. NASA Lewis Research Center.

7.9 Ground Support Equipment

7.9.1 Gimbal Control Electronics

This section is a functional description of a control system that has been successfully developed for control of a gimbal. It is presently implemented with transistor logic (TTL) for ground based applications, but

a flight-type complementary metal-oxide-semiconductor (CMOS) design of the same concept is in the preliminary design stages.

The gimbal control electronics receives a 10 bit binary digital word (9 magnitude bits plus sign) from the spacecraft for each axis angle (and). These are words A and B (see fig. 7.9.1-1). These words are stored in latches and held until updated by new words received from the spacecraft. The spacecraft interface is TBD. These two words provide the controller with gimbal angle information. The actual angles of the gimbal are derived from the two resolvers. The information from the resolvers is in analog form and is converted to 10 bit binary digital words (9 magnitude bits plus sign) by an analog to digital converter. This converter is multiplexed between the two resolvers and its output is stored in two latches (words C and D). Word A from the spacecraft and word C from the resolvers are compared in a digital comparitor as are words B and D. Based on whether A is greater than, less than, or equal to C, and whether B is greater than, less than, or equal to D, the stepping motor drive logic determines which, neither, or both stepping motors should be driven and in which direction. The stepping motors will continue to drive

until C is equal to A and D is equal to B. The information from the resolvers is updated and stored in latches C and D at a 200 Hz rate. Limit switches prevent overdriving of the gimbal mechanism should the controller receive a word to go to an angle larger than can be accommodated. A 28 volt power is applied to the stepping motors only during the time they are actually stepping in one direction or the other. The stepping motors step at a 400 Hz rate, and the resolvers use a 10 volt peak to peak, 400 Hz sine wave for excitation.

The gimbal controls for two thrusters (a BIMOD) could be incorporated into one unit and all four resolvers could share one analog to digital converter. This would reduce the electronics required, but might adversely affect the reliability of the overall system.

The 10 bit binary digital word used in this system is a linear representation of the sine curve between minus 35 degrees and plus 35 degrees, and intersects the sine curve at minus 30 degrees, zero degrees, and plus 30 degrees. This linear representation must be taken into account when the spacecraft generates a word to send to the gimbal control electronics. However, this linear representation greatly simplifies

the electronic circuitry and hence saves on weight, power, and parts count, and increases the reliability.

7.9.2 Miscellaneous

An assembly and vibration test fixture has been manufactured. It is used to assemble gimbals, and in conjunction with gimbals, it is used as the fixture to dynamically test thrusters.

Two gimbal control units have been designed and built. They are presently in a breadboard state, but flight packaging has been considered.

TABLE 7.5.18-1 Gimbal System Vibration Levels

SINUSOIDAL VIBRATION QUALIFICATION

TEST LEVELS FOR ALL AXES

Sweep Rate: 3.0 Oct/Min

Frequency	Level
5 - 10.5	0.8 in d.a.
10.5 - 2000	4.5 g,0 to peak

GAUSSIAN RANDOM VIBRATION QUALIFICATION

TEST LEVELS FOR ALL AXES

Time: 12 sec/axis

Frequency	Power Spectral Density	g's RMS
20 Hz	.00054	
20-150 Hz	+9db/Oct	
150-600 Hz	.225	
600-2000 Hz	-9db/Oct	13.1
2000 Hz	.0061	

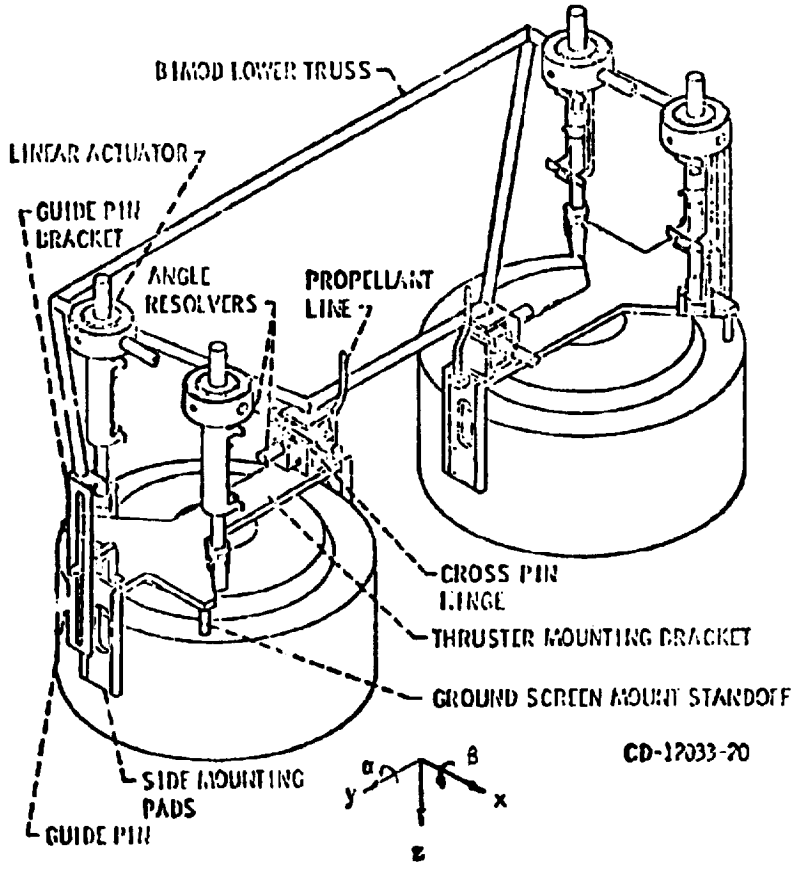

FIGURE 7.3.2-1 Gimbal system/thruster interface; BIMOD configuration.

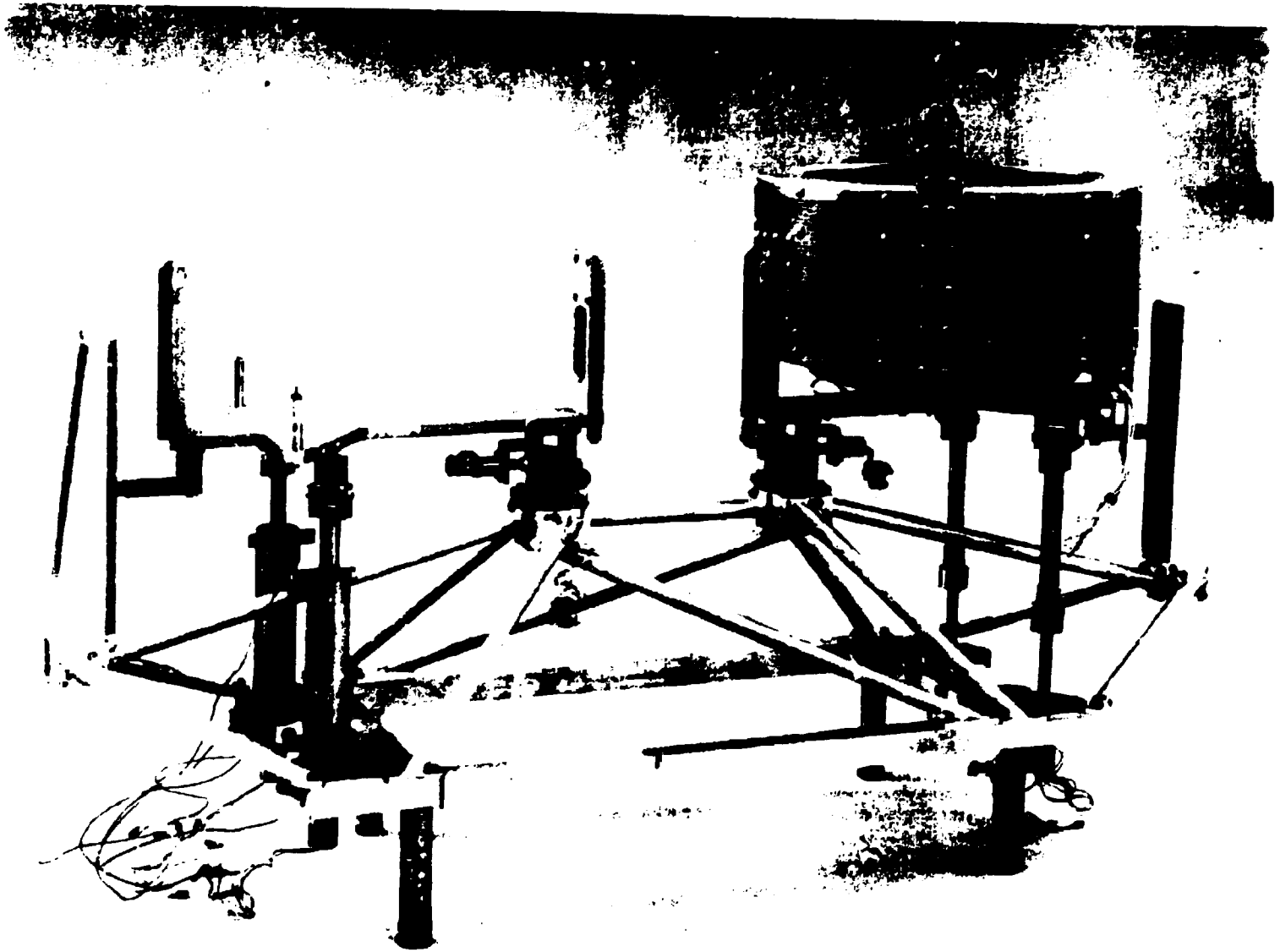

FIGURE 7.3.2-2 BIMOD GIMBAL SYSTEM

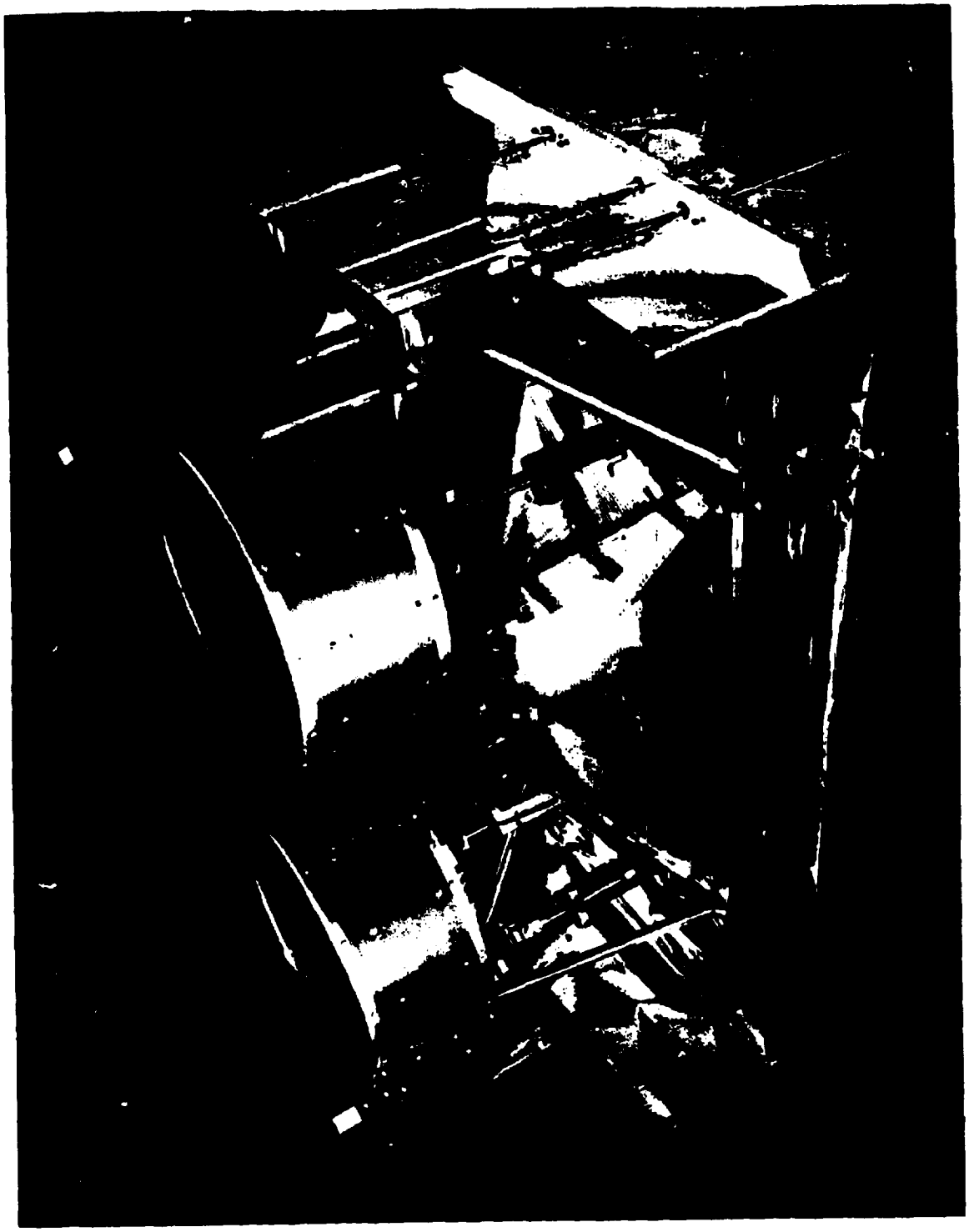

FIGURE 7.3.3-1 Thruster End Of The BIMOD

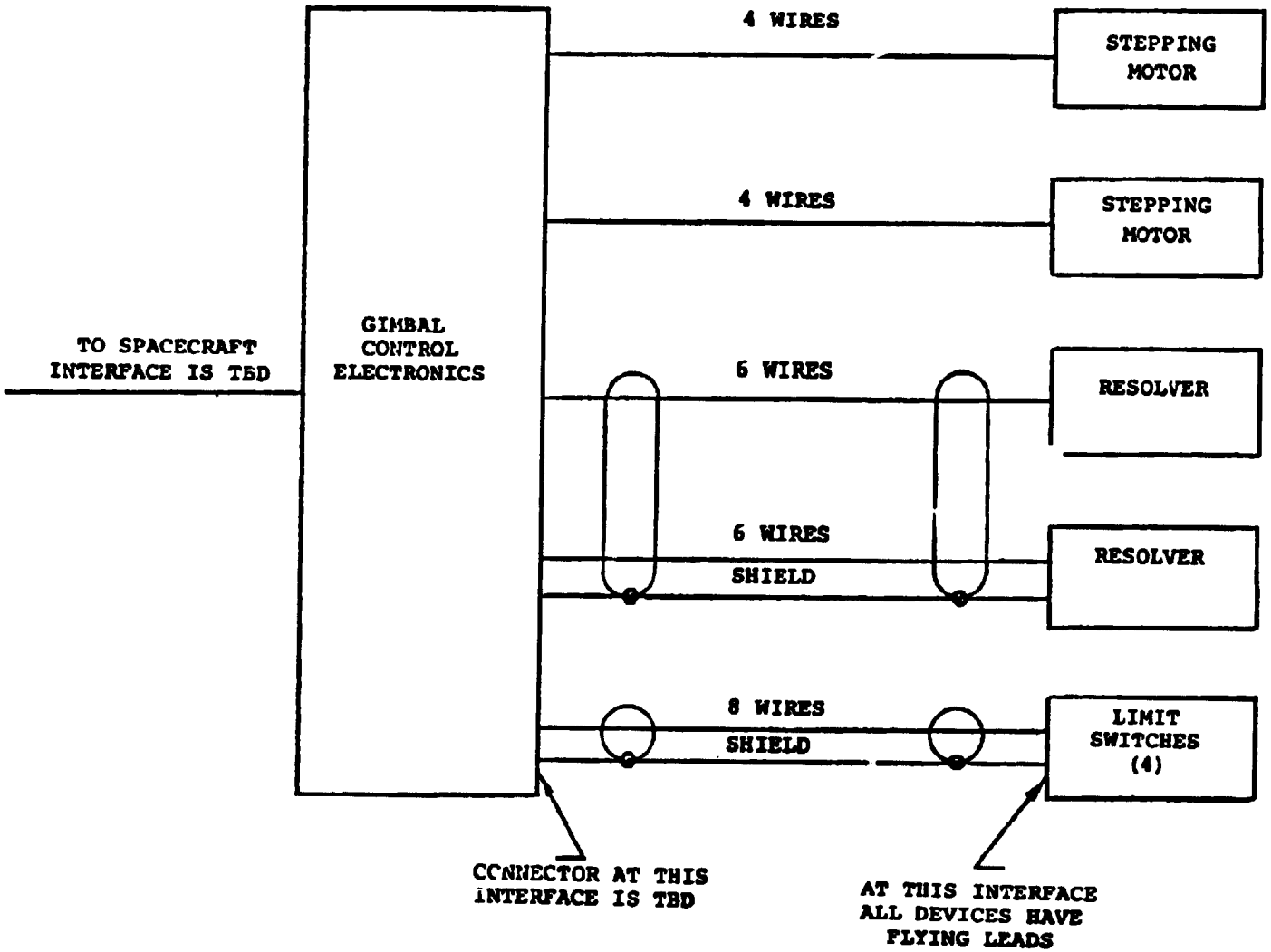

FIGURE 7.4.1-1 GIMBAL ELECTRICAL INTERFACE DRAWING

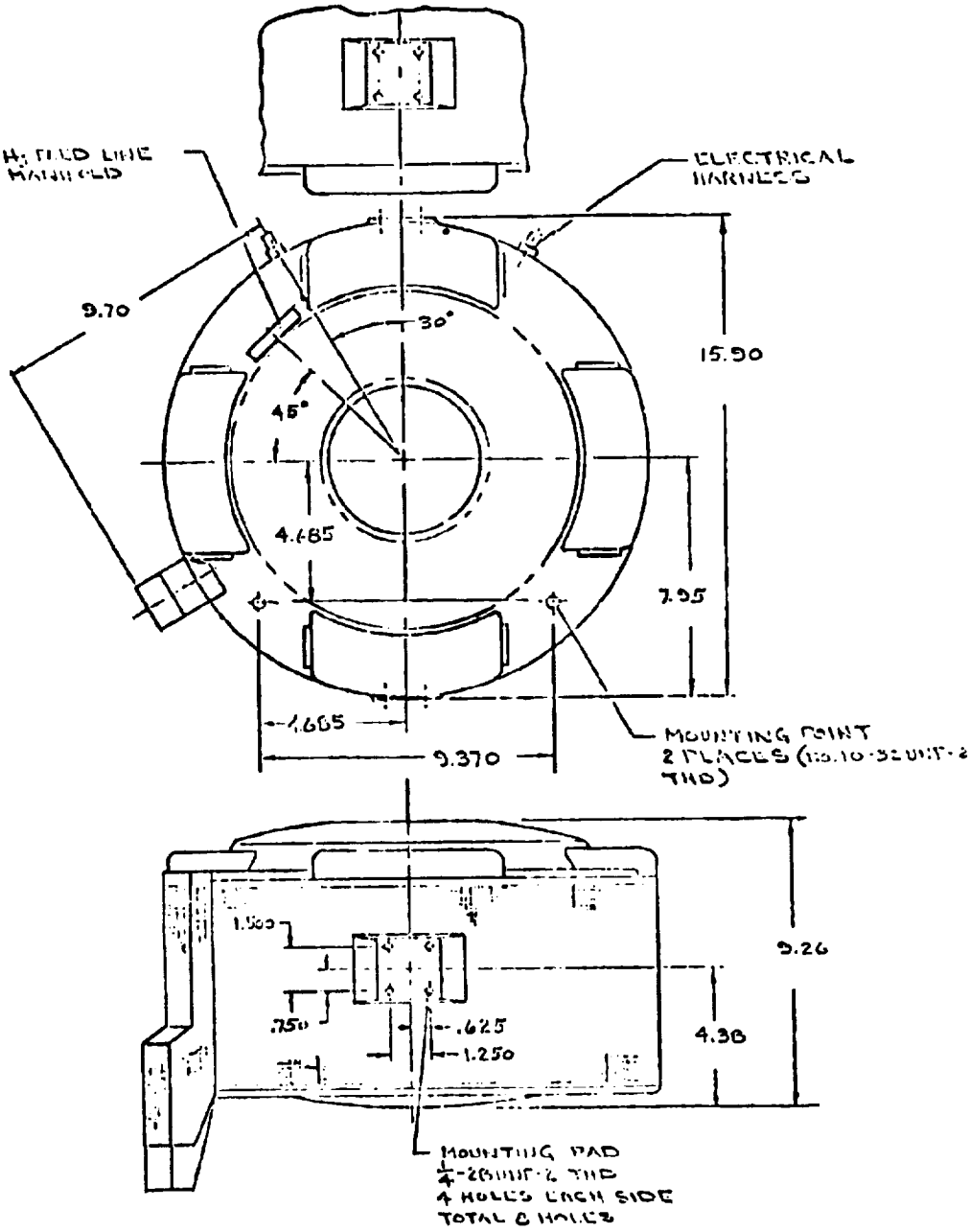

FIGURE 7.4.2-1 THRUSTER INTERFACE DRAWING

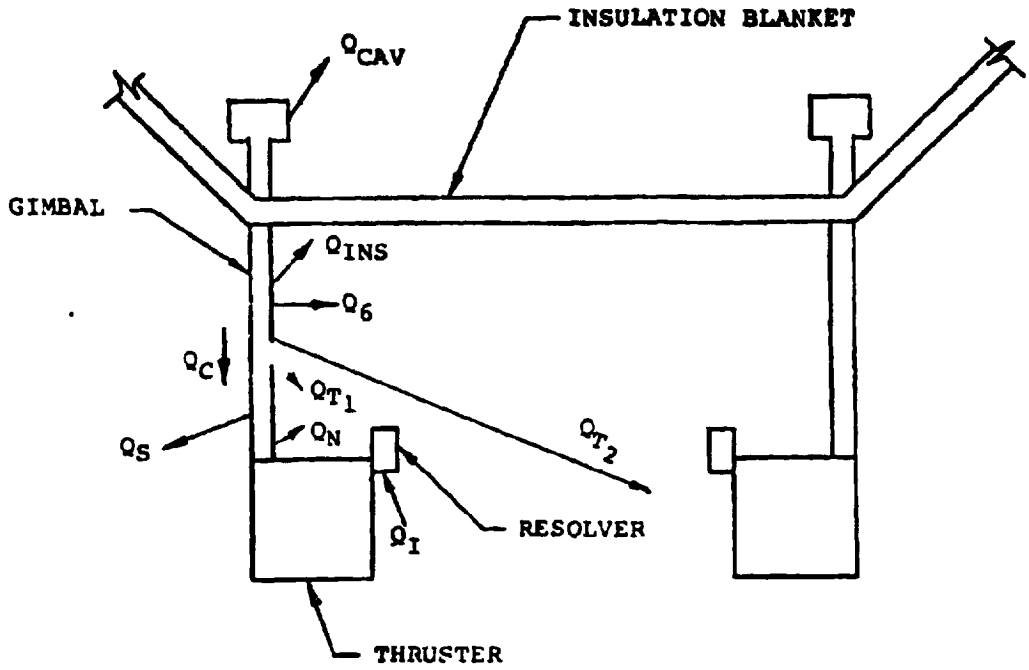

Q_{CAV} = radiation heat transfer between the gimbals and BIMOD cavity

Q_{INS} = radiation heat transfer between the gimbals and the rear insulation blanket

Q_C = conductive heat transfer between the gimbal and thruster

Q_6 = radiation heat transfer between adjacent gimbals

Q_{T_1} & Q_{T_2} = radiation heat transfer between the gimbals and thruster

Q_I = internal heat generated by the resolvers

Q_N = radiation heat transfer between the gimbals and the resolvers

Q_S = radiation heat transfer between the gimbal and the space environment

FIGURE 7:4.3-1 MAJOR HEAT FLOW PATHS OF THE STRUCTURE, GIMBALS, AND THRUSTERS

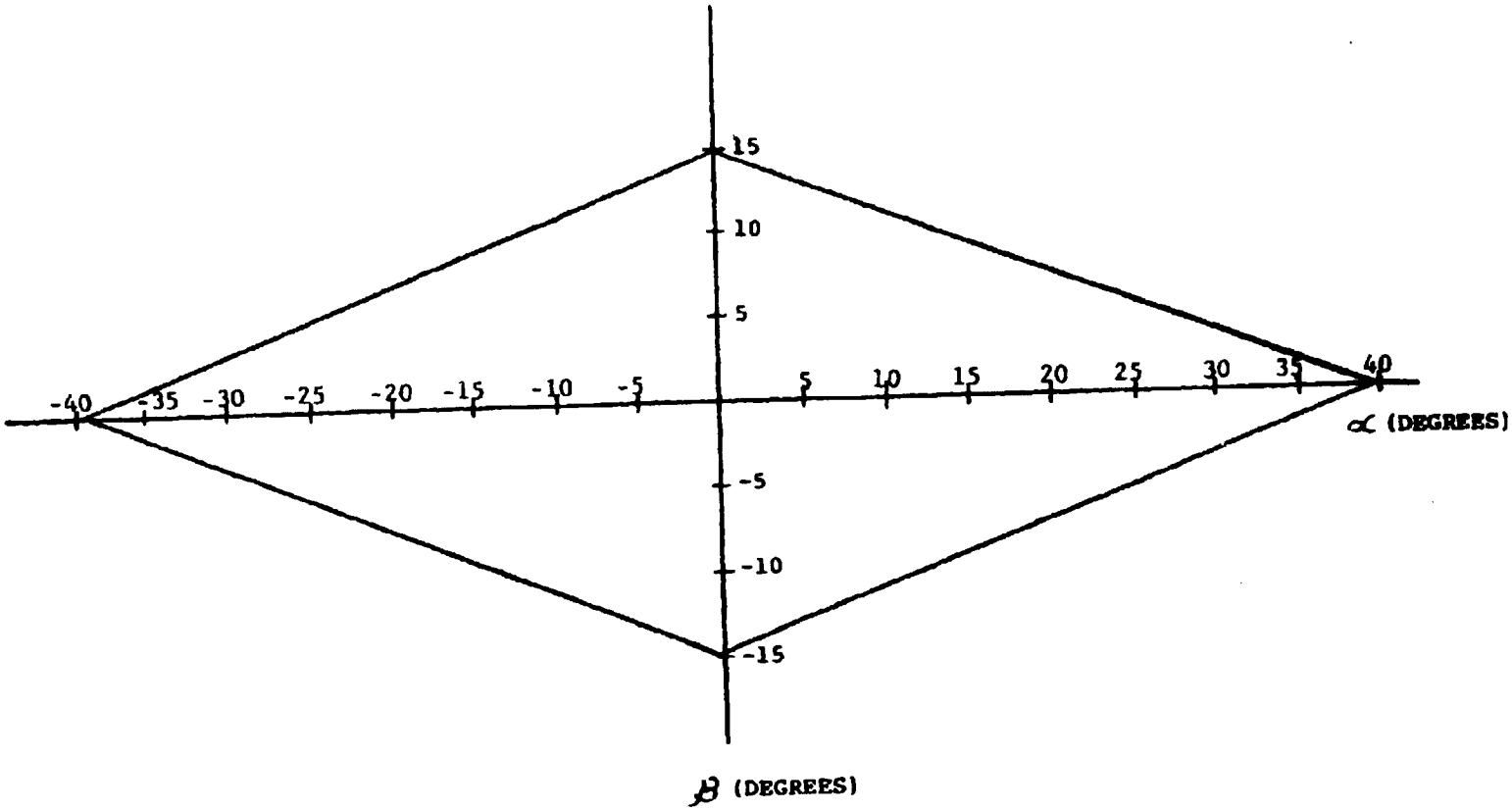

FIGURE 7.5.1-1 MAXIMUM ENVELOPE CAPABILITY OF THE GIMBAL SYSTEM

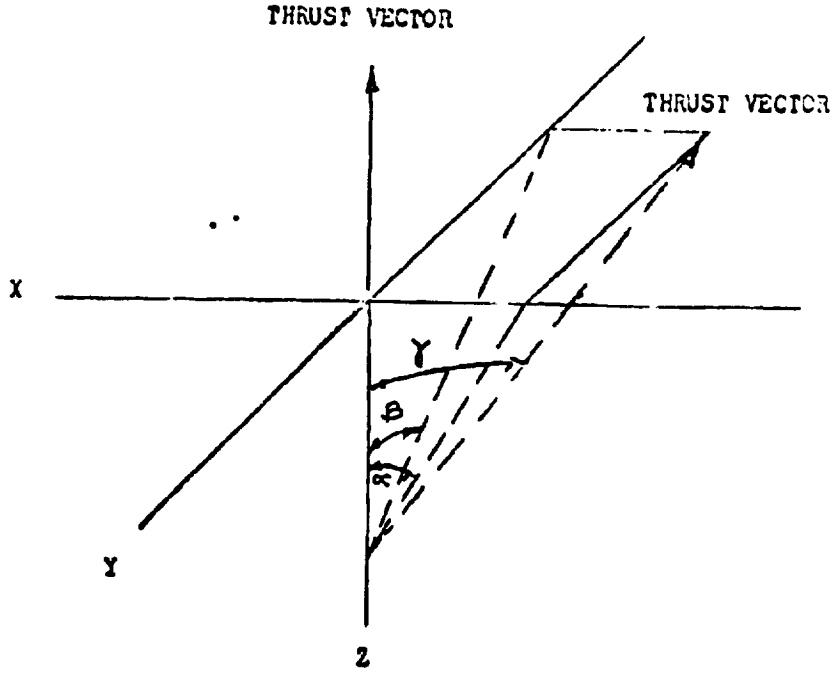

FIGURE 7.5.1-2 GIMBAL ANGLES

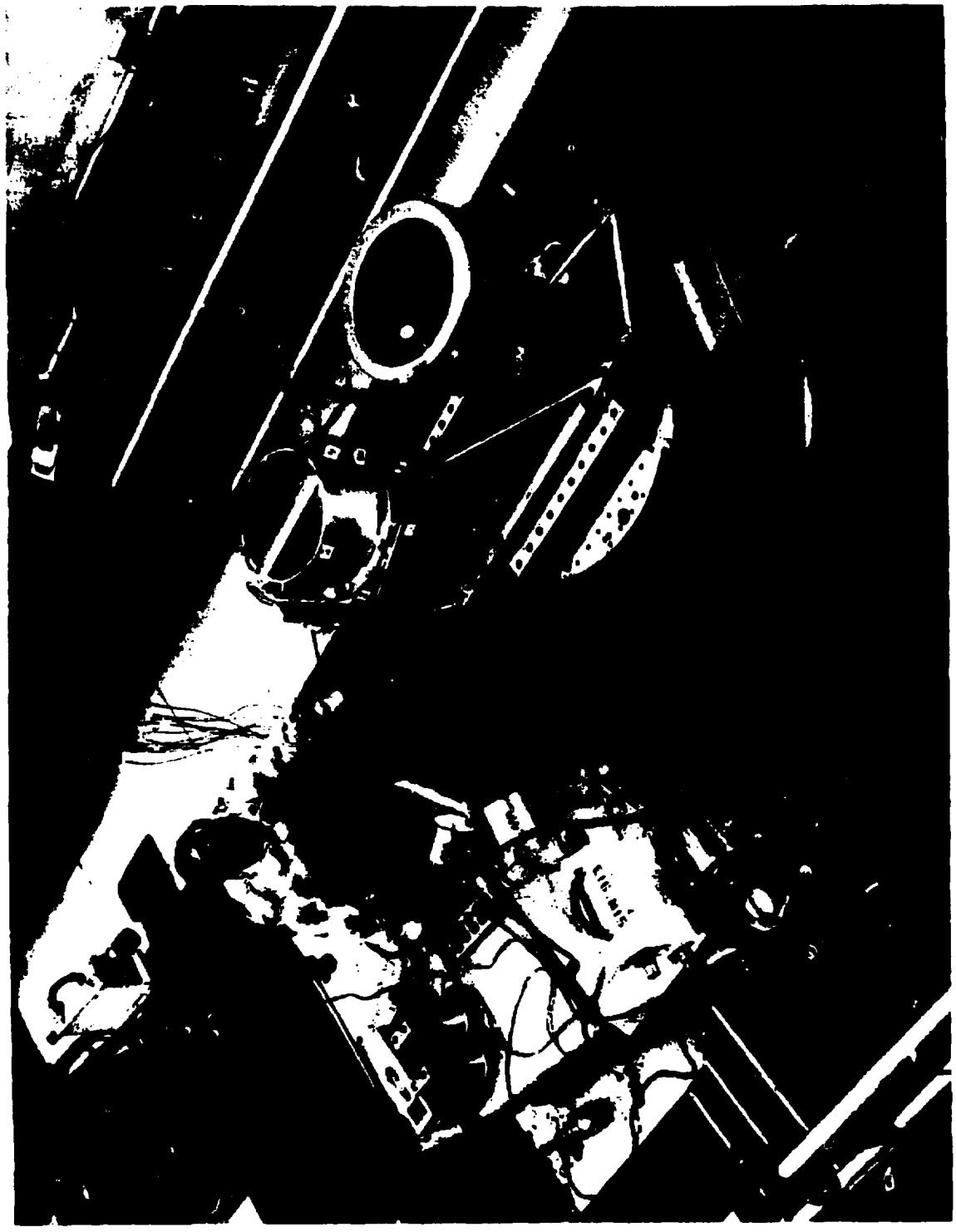

FIGURE 7.5.18-1 Gimbals During Vibration Testing

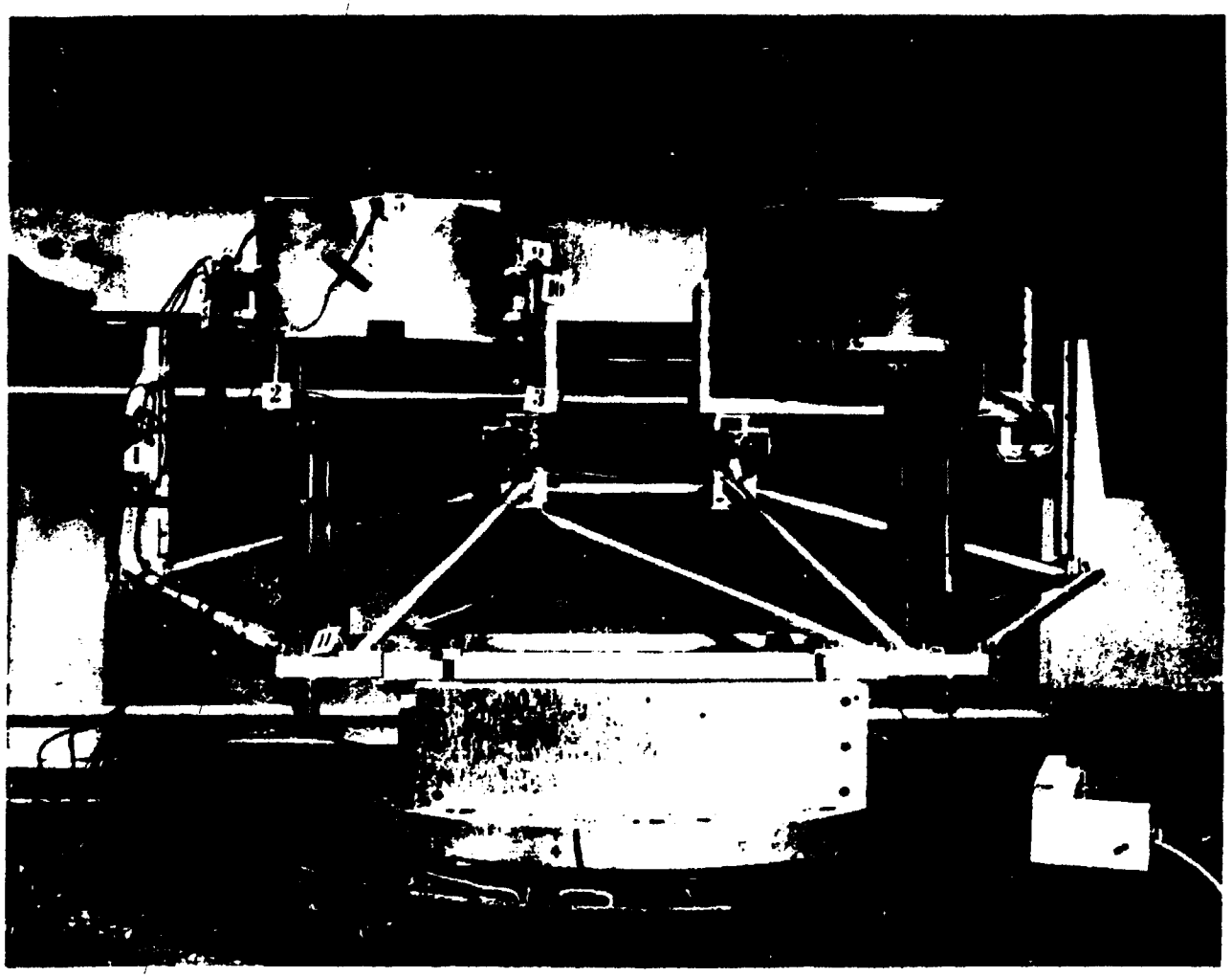

FIGURE 7.5.18-2 Gimbals During Vibration Testing

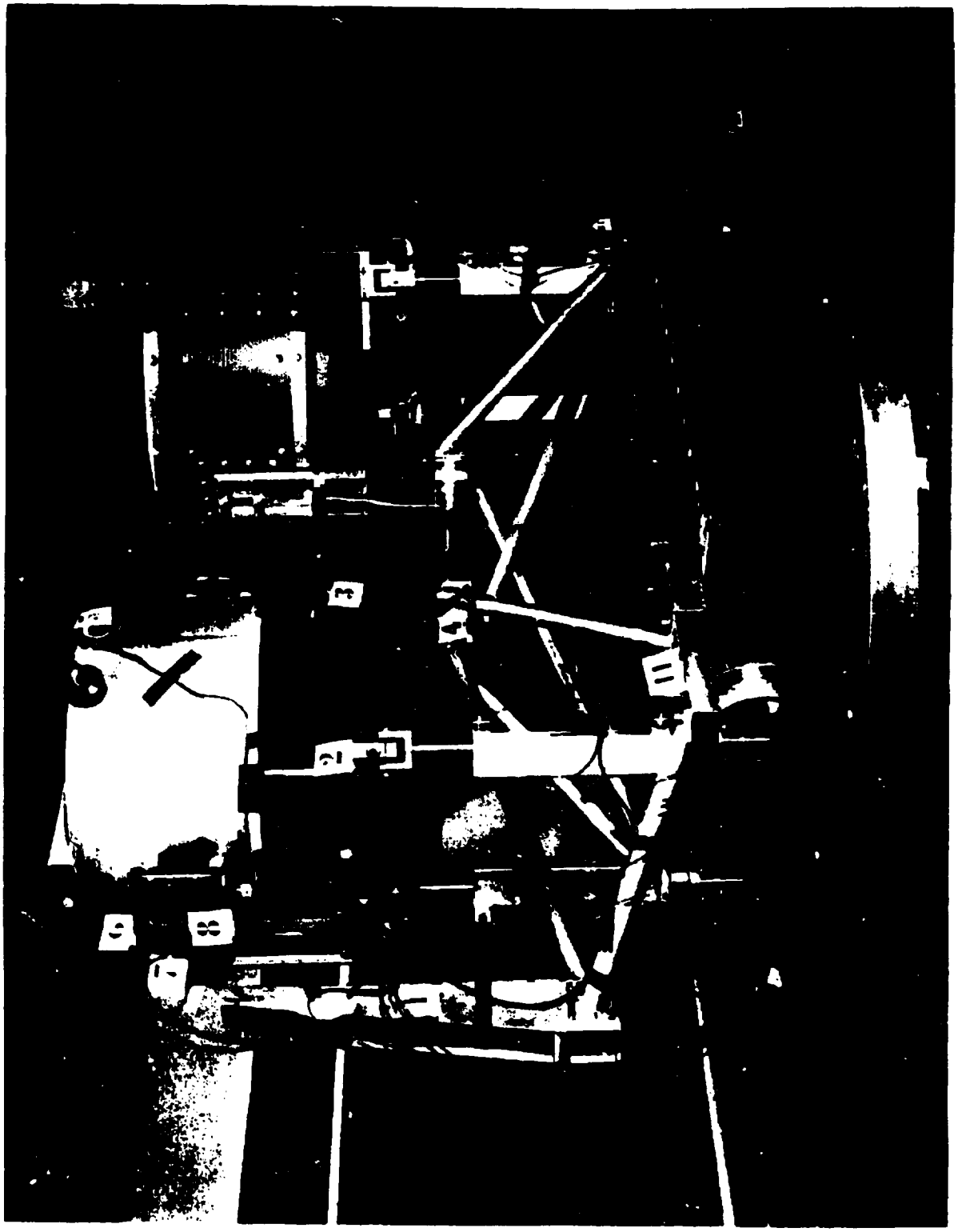

FIGURE 7.5.18-3 Gimbals During Vibration Testing

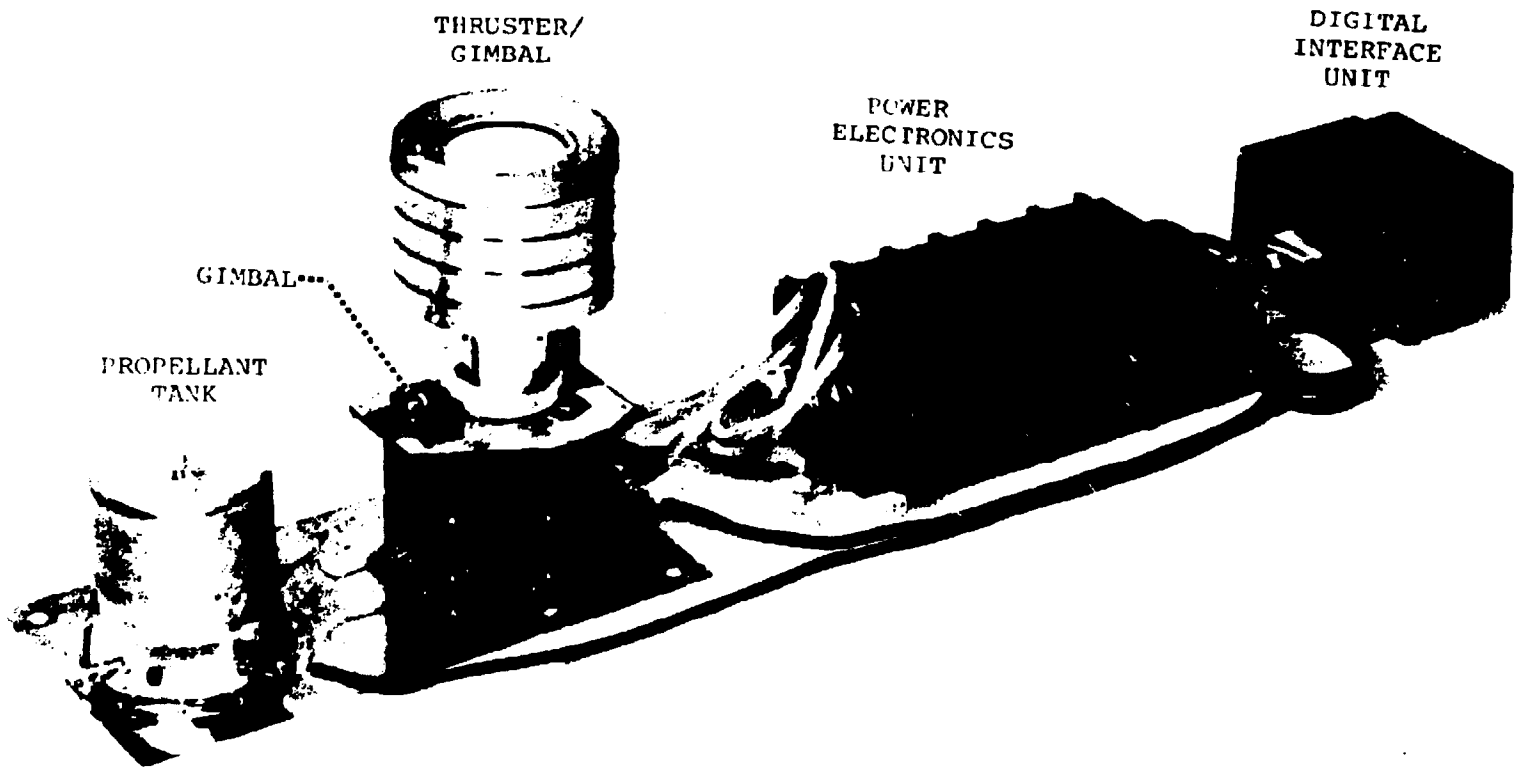

FIGURE 7.7-1 Ion Auxiliary Propulsion System

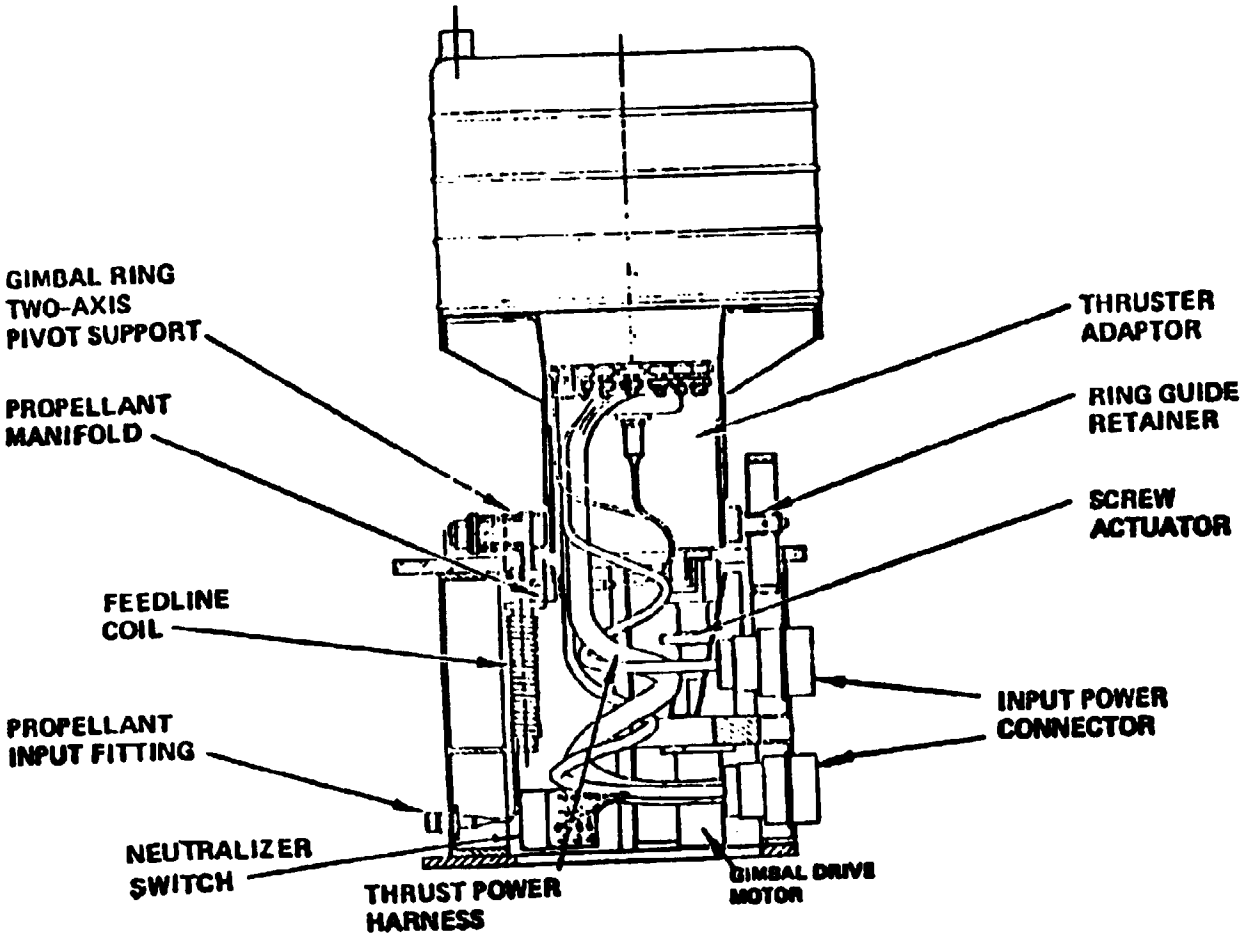

FIGURE 7.7-2 Ion Auxiliary Propulsion System
Thruster Gimbal Assembly

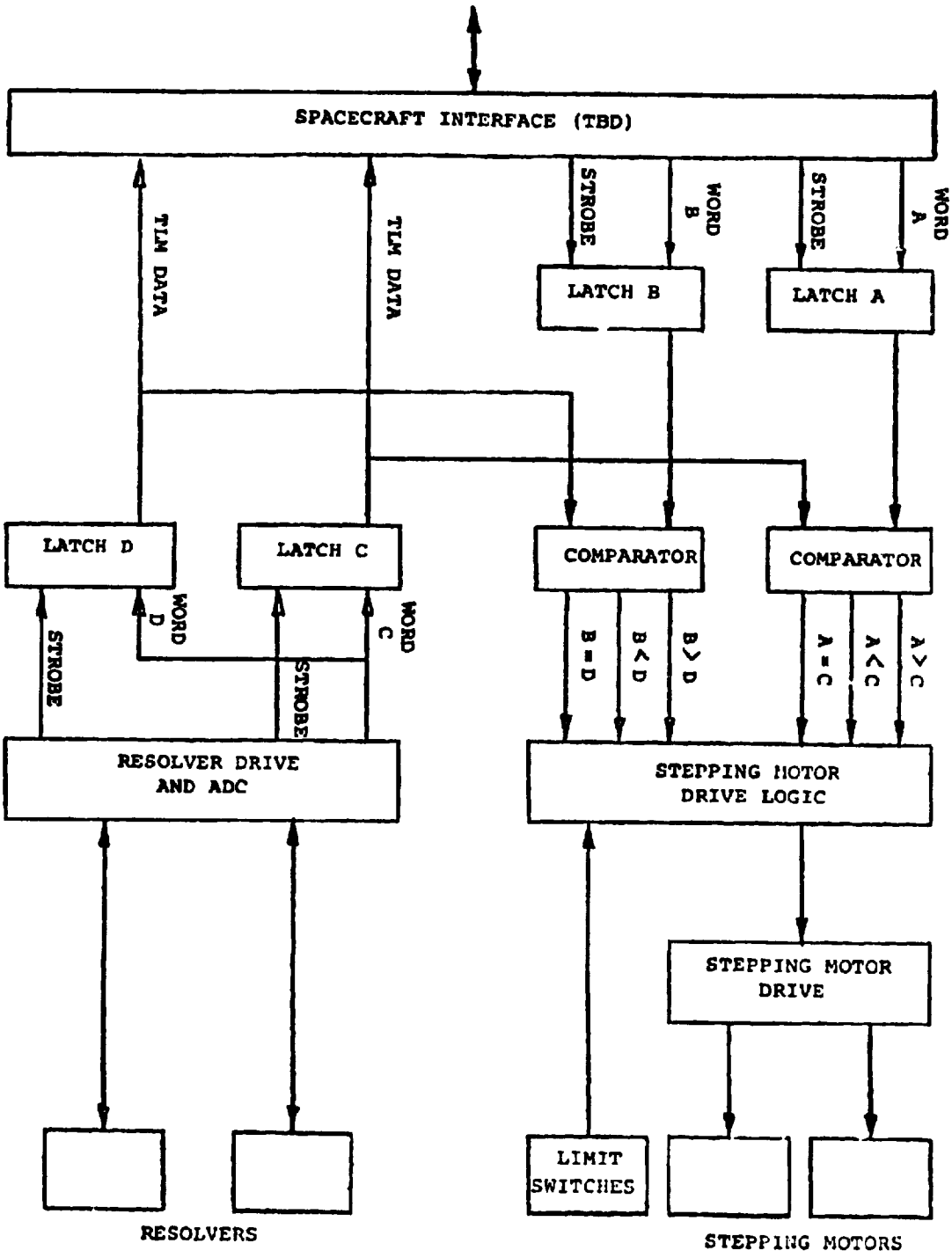

FIGURE 7.9.1-1 GIMBAL CONTROL BLOCK DIAGRAM

8.0

HEAT PIPES

Table of Contents

		Page
8.0	Heat Pipes	8-7
8.1	Reference Documents	8-7
8.2	Functional Requirements	8-10
8.2.1	Mechanical	8-10
8.2.2	Thermal	8-11
8.2.3	Reliability	8-12
8.3	Functional Description	8-13
8.3.1	Mechanical	8-13
8.3.1.1	Tube Envelope	8-14
8.3.1.2	Tube Interior-Wall Grooves	8-14
8.3.1.3	Slab Wick	8-14
8.3.1.4	Arteries	8-15
8.3.1.5	Gas Reservoir	8-15
8.3.1.6	Priming Foil and Cap	8-15
8.3.1.7	Working Fluid	8-15
8.3.1.8	Control Gas	8-16
8.3.2	Thermal	8-16
8.3.2.1	Tube Envelope	8-16
8.3.2.2	Tube Interior-Wall Grooves	8-17
8.3.2.3	Slab Wick	8-17
8.3.2.4	Arteries	8-17
8.3.2.5	Gas Reservoir	8-17
8.3.2.6	Priming Foil and Cap	8-18

		Page
8.3.2.7	Working Fluid	8-18
8.3.2.8	Control Gas	8-19
8.3.3	Operational Characteristics	8-19
8.3.3.1	Evaporator Section	8-19
8.3.3.2	Adiabatic Section	8-21
8.3.3.3	Condenser Section	8-21
8.3.3.4	Gas Reservoir	8-22
8.4	Interface Definition	8-23
8.4.1	Mechanical	8-23
8.4.2	Thermal	8-24
8.5	Performance Description	8-25
8.6	Physical Characteristics and Constraints	8-26
8.7	Development History	8-27
8.7.1	Materials Compatibility and Processing Procedures	8-28
8.7.2	Artery Wicking Systems	8-29
8.7.3	Working Fluid and Control Gas Properties	8-31
8.7.4	Gravitational Effects	8-33
8.7.5	Local Heat Flux Limitations	8-34
8.7.6	Computer Modeling	8-35
8.7.7	System Considerations	8-35
8.7.8	Design Alternatives	8-36
8.8	Applicable Documents Enclosed	8-37
8.9	Ground Support Equipment	8-38

		Page
8.9.1	Acceptance and Characterization Tests	8-38
8.9.1.1	Structural Support Equipment.	8-38
8.9.1.2	Thermal Control Equipment	8-38
8.9.1.3	Thermal Instrumentation	8-39
8.9.2	BIMOD Tests	8-39
8.9.2.1	Auxiliary Cooling Tubes	8-39
8.9.2.2	Tilting Feature of BIMOD Support Fixture.	8-39

TABLES

8.3.2.7-1	BIMOD Heat Pipe Gas and Liquid Inventory.	8-40
8.3.3.2-1	Properties of Typical Heat Pipe Envelope and Wicking Materials	8-40
8.4.1-1	Heat Pipes and Saddles Plating Sequence and Procedure Numbers	8-41
8.4.1-2	Maximum Reheating Times for the Forming of Heat-Treatable Alloys at Various Temperatures	8-41
8.5-1	SEP Heat Pipe Thermal Capacity Test Results	8-42
8.5-2	Turn-on and Full-on Temperatures of SEP Heat Pipes.	8-43
8.6-1	Physical Details of CTS and SEP Variable Conductance Heat Pipe Systems	8-44
8.7-1	Configuration and Details of Heat Pipes Flown on Sounding Rocket Test Flight	8-46
8.7-2	CTS Heat Pipes Gas and Liquid Inventory	8-47
8.7-3	CTS Heat Pipes Thermal Capacity Test Results.	8-47

Page

8.7-4 CTS Heat Pipes Control Range Test Results 8-47

8.7.3-1 Properties of Typical Heat Pipe Working Fluids. . 8-48

FIGURES

8.2.2-1 Total Thermal Resistance of Heat Pipe (Exterior Evaporator Surface to Exterior Condenser Surface). 8-49

8.3.1-1 Schematic of SEP BIMOD Thermal Control System . . 8-50

8.3.1.4-1 Heat Pipe Artery Locations in CTS and SEP Designs 8-51

8.3.1.7-1 Vapor Pressure versus Temperature for Several Heat Pipe Fluids. 8-52

8.3.2.4-1 Effect of Artery Depriming on Thermal Transport Capability of CTS-Type Heat Pipes 8-53

8.3.2.7-1 Liquid Transport Capability versus Temperature for Several Heat Pipe Fluids. 8-54

8.3.2.7-2 Zero-g Figure of Merit versus Temperature for Several Heat Pipe Fluids. 8-55

8.3.2.7-3 One-g Figure of Merit versus Temperature for Several Heat Pipe Fluids. 8-56

8.3.2.7-4 Heat Transport Capability versus Operating Temperature Range for Various Heat Pipe Working Fluids. 8-57

		Page
8.3.2.8-1	Effect of Control Gas on the Temperature Profile of a Variable Conductance, Gas-Filled Heat Pipe.	8-57
8.3.3-1	Illustration of the Operation of a Gas-Filled, Variable Conductance Heat Pipe.	8-58
8.4.1-1	TRW Sketch of SEP BIMOD Heat Pipe Module Assembly.	8-59
8.5-1	Illustration of the Effect of Gravity on the Thermal Transport Capability of a Heat Pipe . . .	8-60
8.5-2	Temperature Profile of SEP Development, 0.070-Inch Artery Heat Pipe Showing Varying Sink Conditions.	8-60
8.7-1	Temperature Distribution Along Ames Slab Wick A During Rocket Flight Heat Pipe Experiment	8-61
8.7-2	Artery Thermistor Voltage and Power Profile for Ames Slab Wick A During Rocket Flight Heat Pipe Experiment	8-61
8.7-3	Temperature Distribution Along Ames Slab Wick B During Rocket Flight Heat Pipe Experiment	8-62
8.7-4	Artery Thermistor Voltage and Power Profile for Ames Slab Wick B During Rocket Flight Heat Pipe Experiment	8-62

		Page
8.7-5	Location of Variable Conductance Heat Pipe System (VCHPS) on the Communications Technology Satellite (CTS).	8-63
8.7-6	Illustration of Components of CTS Variable Conductance Heat Pipe System.	8-64
8.7-7	Physical Dimensions of CTS Variable Conductance Heat Pipe System.	8-65
8.7-8	Performance of CTS Heat Pipes Fabricated by TRW.	8-66

8.0 Heat Pipes

8.1 Reference Documents

8.1.1 Farber, B.; Golden, D. S.; Marcus, B.; and Mock, P.: Transmitter Experiment Package for the Communications Technology Satellite. (TRW Defense and Space System Group; NASA Contract NAS3-15839.) NASA CR-135035, 1977.

8.1.2 Mock, P. R.; Marcus, B. D.; and Edelman, E. A.: Communications Technology Satellite: A Variable Conductance Heat Pipe Application. AIAA Paper 74-749, July 1974.

8.1.3 Stipandic, E. A.; Gray, A. M.; and Gedeon, L.: Thermal Design and Test of a High Power Spacecraft Transponder Platform. AIAA Paper 75-680, May 1975.

8.1.4 Eninger, J. E.; Luedke, E. E.; and Wanous, D. J.: Flight Data Analysis and Further Development of Variable Conductance Heat Pipes, Research Report No. 1. (TRW Systems Group.) NASA CR-137782, 1976.

8.1.5 Eninger, J. E.; Edwards, D. K.; and Luedke, E. E.: Flight Data Analysis and Further Development of Variable Conductance Heat Pipes, Research Report No. 2. (TRW Systems Group.) NASA CR-137953, 1976.

8.1.6 Edwards, D. K.; Fleischman, G. L.; and Marcus, B. D.: Theory and Design of Variable Conductance Heat Pipes: Steady State and Transient Performance Research Report No. 3. (TRW Systems Group.) NASA CR-114530, 1972.

8.1.7 Marcus, B. D.; Edwards, D. K.; and Anderson, W. T.: Variable Conductance Heat Pipe Technology Research Report No. 4. (TRW Systems Group.) NASA CR-114686, 1973.

8.1.8 Anderson, W. T.; Edwards, D. K.; Eninger, J. E.; and Marcus, B. D.: Variable Conductance Heat Pipe Technology Final Research Report. (TRW Defense and Space Systems Group.) NASA CR-114750, 1974.

8.1.9 Marcus, B. D.: Theory and Design of Variable Conductance Heat Pipes. (TRW Systems Group.) NASA CR-2018, 1972.

8.1.10 Tower, L. K.; and Kaufman, W. B.: Accelerated Life Tests of Specimen Heat Pipe from Communications Technology Satellite (CTS) Project. NASA TM-73846, 1977.

8.1.11 Edelstein, F.: Heat Pipe Manufacturing Study: Final Report. (Grumman Aerospace Corp.; NASA Contract NAS5-23156.) NASA CR-139140, 1974.

8.1.12 Saaski, E. W.: Investigation of Bubbles in Arterial Heat Pipes. (McDonnell Douglas Astronautics Co.) NASA CR-114531, 1972.

8.1.13 Saaski, E. W.: Investigation of Arterial Gas Occlusions. Final Report. (McDonnell Douglas Astronautics Co.) NASA CR-114731, 1974.

8.1.14 Eninger, J. E.: Menisci Coalescence as a Mechanism for Venting Non-Condensable Gas from Heat Pipe Arteries. AIAA Paper 74-748, July 1974.

8.1.15 Marcus, B. D.; and Fleischman, G. L.: Diffusion Freeze-out in Gas-Loaded Heat Pipes. ASME 72-WA/HT-33, Nov. 1972.

8.1.16 Marcus, B. D.: CTS TEP Thermal Anomalies - Heat Pipe System Performance. (TRS Defense and Space Systems Group.) NASA CR-159413, 1977.

8.1.17 Alexovich, R. E.; and Curren, A. N.: Thermal Anomalies of the Transmitter Experiment Package on the Communications Technology Satellite. NASA TP-1410, 1979.

8.1.18 Kelleher, M. D.: Effects of Gravity on Gas-Loaded Variable Conductance Heat Pipes. (Naval Postgraduate School Report, NPS-69KK77031.) March 1977.

8.1.19 Eninger, J. E.; and Edwards, D. K.: Excess Liquid in Heat-Pipe Vapor Spaces. AIAA Paper 77-748, June 1977.

8.1.20 Eninger, J. E.; and Edwards, D. K.: Computer Program Grade II for the Design and Analysis of Heat Pipe Wicks. (TRW Systems Group.) NASA CR-13795, 1976.

8.1.21 Antoniuk, D.; and Luedke, E. E.: CTS-Type Variable Conductance Heat Pipes for SEP FM/PPU Final Report. (TRW Defense and Space Systems Group; NASA Contract NAS3-21130.) NASA CR-159550, 1978.

8.1.22 Eninger, J. E.: Graded-Porosity Heat Pipe Wicks. AIAA Paper 76-480, July 1976.

8.2 Functional Requirements

The functional requirements of the heat pipes used in the BIMOD configuration can be separated into the following three categories: mechanical, thermal, and reliability.

8.2.1 Mechanical

Mechanical functional requirements include the following:

1) A maximum weight per heat pipe of 1.39 kg (3.06 lb).
2) Adequate strength of the heat pipe envelope to withstand the internal pressure of the operating fluid and the body loads to which it would be subjected during acceleration and vibration environments. Structurally, the heat pipes are not required to carry any other external loads.
3) Dimensions to fit the BIMOD configuration, which includes:
   a) A 114.778-cm (45.188-in.) long evaporator section at which the heat dissipated by the power processing units (PPU's) is input to the heat pipe.
   b) A 13.635-cm (5.368-in.) long adiabatic section, which includes a 90^{o} bend and which serves to isolate the PPU's and radiators when the heat pipes are in their OFF mode.

c) A 182.88 cm (72.00-in.) long condenser section at which the transported heat is transferred to the BIMOD radiators.

d) A 1.27-cm (0.50-in.) outside diameter, which is required as a result of the 1.585-cm (0.624-in.) spacing between the PPU heat rejection surfaces in the BIMOD configuration.

4) Mechanical configuration to allow for operating the heat pipes in a one-g environment during various types of ground testing.

8.2.2 Thermal

Thermal functional requirements, which are of primary significance in the selection of the heat pipes used, include the following:

1) Heat transport capacity per heat pipe ranging from 220 watts or more when its evaporator temperature is 50^{o} C (122^{o} F) or less to 1 watt or less when its evaporator temperature is 10^{o} C (50^{o} F) or less.

2) An effective sink temperature of -75^{o} C (-102^{o} F) for the heat pipe condenser and gas reservoir radiators. The factors which were used to determine this effective sink temperature were based on the use of a BIMOD in a particular spacecraft configuration and in a deep space environment. These factors are shown in the memorandum included as applicable document

8.8.3, "SEP FM/PPU Thermal Control System Design Summary," dated November 1, 1977.

3) An overall (refer to fig. 8.2.2-1) thermal resistance of 0.044° C/watt (0.08° F/watt) or less. This thermal resistance is characteristic of Communications Technology Satellite (CTS) heat pipe (FM-006 system) operation and is considered to be applicable to the BIMOD configuration.

4) Material properties which are not affected by thermal cycling or expected extremes of operating temperature.

8.2.3 Reliability

Reliability requirements include the following:

1) One redundant heat pipe for each of the two BIMOD system radiators. The 50% redundancy increases system reliability considerably by allowing for the failure of two heat pipes per BIMOD configuration without significantly affecting the overall system thermal performance. These failures could be permanent (e.g., due to latent manufacturing defects such as weld leaks, impurities which cause generation of additional noncondensable gases by breaking down the methanol, etc.) or reversible (primarily the result of artery depriming).

2) Compatibility of wall and wick materials with the working fluid. This is necessary to prevent failures due to:

a) Breakdown of the working fluid, either by direct reaction, catalytic reaction between the fluid and wick or fluid and envelope, or due to the presence of impurities in the fluid, wick, or envelope.

b) Decomposition of the wick, either by chemical corrosion, physical deterioration because of the dynamic action of the fluid, or electrolytic action caused by dissimilar metals.

c) Decomposition of the heat pipe envelope, especially due to a corrosive external environment.

3) A heat pipe reliability factor which will provide a system mission lifetime of four years.

8.3 Functional Description

8.3.1 Mechanical

The mechanical configuration of the heat pipes is designed primarily to support its thermal performance. The heat pipes are not used as BIMOD structural members. The heat pipes connect the evaporator saddles, which are bolted to the PPU baseplate, to the condenser saddles, which are bolted to the radiators. A conceptual schematic of the overall heat pipe mechanical configuration

is shown in figure 8.3.1-1. Applicable document 8.8.4 lists the heat pipe system detailed mechanical drawings.

The operation of the heat pipes is affected by their mechanical environment. Shock or vibration of sufficient intensity can cause the maximum allowable wicking stresses to be exceeded and the arteries will deprime when the heat pipes are under a thermal load. Similarly, tilting the heat pipes so the returning fluid has to work against a one-g field will cause the arteries to deprime when fluid head height and the heat pipe thermal load are large enough.

The mechanical function of each component can be summarized as follows:

8.3.1.1 Tube Envelope

The heat pipe tube envelope provides containment for the working fluid and control gas. It also provides structural support for the heat pipe slab wick, arteries, priming foil and cap, and gas reservoir.

8.3.1.2 Tube Interior-Wall Grooves

The interior-wall grooves provide capillary-flow paths for the working fluid between the tube interior walls and the diametral slab wick.

8.3.1.3 Slab Wick

This slab wick is the primary flow path for condensed

working fluid from the tube wall grooves to the arteries. It also provides a secondary capillary return flow path for condensed working fluid from the condenser to the evaporator section.

8.3.1.4 Arteries

The arteries are the primary capillary return flow path for condensed working fluid from the condenser to the evaporator section. Figure 8.3.1.4-1 shows the location of the arteries on the slab wick and in the tube cross-section for both the BIMOD and CTS designs.

8.3.1.5 Gas Reservoir

The gas reservoir provides for storage of the control gas when the heat pipes are working in their operating temperature range.

8.3.1.6 Priming Foil and Cap

The priming cap, which has a priming foil welded over a window cut in it, is welded to the evaporator end of an artery. The holes in, and the thickness of, the priming foil, as well as the cap I.D., are sized to permit gas and vapor bubbles in the arteries to vent to the vapor space during artery priming at a rate much faster than is possible by bubble diffusion through the liquid in the artery wall screen holes.

8.3.1.7 Working Fluid

Methanol has the required wetting and surface tension

properties to provide adequate return capillary flow of the condensed fluid in the slab and artery wick structures. The operating vapor pressure (fig. 8.3.1.7-1) of methanol is very low, resulting in minimal stress in the containment structure. This helps to minimize weight.

8.3.1.8 Control Gas

The helium in the nitrogen/helium gas mixture used (90%/10%) allows for leak detection of a sealed heat pipe following manufacture.

8.3.2 Thermal

The thermal function of each heat pipe component can be summarized as follows:

8.3.2.1 Tube Envelope

This is the primary heat flow path to and from the working fluid. In the ideal case, it should have a high thermal conductivity and a small thickness in the evaporator and condenser sections to minimize thermal resistance. To minimize heat transfer from the evaporator to the condenser when the heat pipe is in the OFF mode, however, the adiabatic section of the heat pipe should have a low thermal conductivity, a small thickness, and a long length. The use of stainless steel for the entire envelope compromises only the high thermal conductivity requirement in the evaporator and condenser sections. This compromise has little effect on the overall

thermal resistance, as is evident from the experience with the CTS heat pipes.

8.3.2.2 Tube Interior-Wall Grooves

Besides providing capillary-flow paths for the working fluid between the tube interior walls and the diametral slab wick, they also increase the surface area for transferring heat from the walls to the working fluid.

8.3.2.3 Slab Wick

The flow of the condensed working fluid through this component of the wicking structure contributes 20-30% of the heat transfer capacity of the heat pipe.

8.3.2.4 Arteries

The flow of the condensed working fluid through these components of the wicking structure contributes 70-80% of the heat transfer capacity of the heat pipe. Various forces can cause one or both of the arteries to deprime, however, which reduces artery fluid flow to zero and reduces heat pipe heat transfer capacity to 20-30% of the full rated capacity. (Fig. 8.3.2.4-1 illustrates this response for one of the CTS heat pipes.)

8.3.2.5 Gas Reservoir

When the heat pipes are working in their operating temperature range, the control gas is compressed into this component and a temperature-dependent length of the condenser section, thereby limiting the length of the con-

denser section which is transferring heat to its respective radiator. The smaller the reservoir-to-condenser volume ratio, the smaller the operating temperature range will be.

8.3.2.6 Priming Foil and Cap

These components contribute to the thermal function of the heat pipes by eliminating one cause of artery depriming, that due to the accumulation of control gas bubbles in the arteries.

8.3.2.7 Working Fluid

From a thermal standpoint, methanol was chosen as the preferred heat pipe working fluid for a number of reasons:

1) As is indicated in figures 8.3.2.7-1 through 8.3.2.7-3, methanol heat transport capacity increases as its operating temperature rises in the temperature range required for PPU operation. This is desirable because it reduces the possibility of a thermal-runaway condition which might result from a PPU defect causing higher-than-normal heat dissipation, a heat pipe artery depriming, etc.
2) As is indicated in figure 8.3.2.7-4, the freezing point of methanol is very low, allowing for lower radiator operating temperatures.

3) Methanol's coefficient of expansion is negative during freezing. This permits the methanol to freeze without causing structural damage to the heat pipe.

4) The amount of working fluid used is governed primarily by the ability of the heat pipe arteries to prime in one-g. The volumes of methanol used in the solar electric propulsion (SEP) heat pipes are noted in table 8.3.2.7-1.

8.3.2.8 Control Gas

The nitrogen/helium gas mixture used (90%/10%) has an average molecular weight similar to methanol vapor. This eliminates potential working fluid/control gas stratification problems which would affect the heat transfer performance of the heat pipes. Figure 8.3.2.8-1 shows the effect of the presence of control gas in the heat pipe on its temperature profile during operation. The mass of control gas affects the "turn-on" and "full-on" temperatures of the heat pipes. The control gas masses used in each heat pipe are shown in table 8.3.2.7-1.

8.3.3 Operational Characteristics

The operation of the heat pipes is shown schematically in figure 8.3.3-1. The heat pipe components function as follows:

8.3.3.1 Evaporator Section

During PPU operation, the evaporator saddle temperature

rises and heat is conducted into the tube walls and to the working fluid in the interior wall grooves. As the fluid evaporates, it is replaced by capillary action through the grooves from the slab wick. The working fluid vapor is forced to the condenser end of the heat pipe by a pressure differential resulting from the difference in temperature at opposite ends of the heat pipe (fig. 8.3.2.8-1).

A limiting heat flux occurs when the amount of working fluid being supplied through the interior wall grooves is not adequate to support the rate of evaporation. At this point, a "local" (or "partial") "dryout" (or "burnout") occurs. This local dryout condition is indicated by a local rise in temperature (over the working fluid vapor temperature, which is reflected in the adiabatic section of the heat pipe).

A further limiting heat flux occurs when the amount of working fluid being supplied through the slab wick is not adequate to support the rate of evaporation. At this point, depriming of one or both arteries causes an overall heat pipe "dryout" (or "burnout") condition, in which the evaporator temperature rises to a point where other heat transfer paths and mechanisms act in parallel with the heat pipes to bring the evaporator temperature to a

steady-state level. This new equilibrium temperature generally would cause the PPU electronic components to exceed their maximum safe operating temperature.

8.3.3.2 Adiabatic Section

The working fluid vapor passes through this section on its way from the evaporator to the condenser. Minimum heat transfer takes place in this section, since (1) it is not attached to a conduction heat source or a radiator surface, and (2) it is generally constructed of a low thermal conductivity material (table 8.3.3.2-1) such as stainless steel. Its purpose is to minimize the heat leak from the PPU's to the radiators when the PPU's are not operating and, therefore, the heat pipes are in their OFF mode. The temperature of the adiabatic section wall is generally considered to be the same as the working fluid vapor temperature.

8.3.3.3 Condenser Section

When the working fluid vapor reaches this section, it condenses on the cooler heat pipe walls. The heat is conducted to the BIMOD radiator to which the heat pipe is attached, where it is radiated to space. The condensed fluid is drawn by capillary action through the grooves in the tube walls to the slab wick and then to the wire mesh arteries. The fluid is returned, through capillary action by both the slab wick and the two ar-

teries, to the evaporator section for re-evaporation.

8 3.3.4 Gas Reservoir

When a gas-filled variable conductance heat pipe begins to operate, the non-condensible control gas is swept to the condenser end of the heat pipe and fills the gas reservoir and a portion of the condenser section. No working fluid circulation occurs in these gas-blocked volumes and, therefore, no heat transfer takes place by condensation of the working fluid. As the evaporator temperature rises, the partial pressure of the working fluid rises, which causes the control gas to be compressed into a smaller volume and opens a greater length of the condenser section to heat transfer from the working fluid to the condenser radiating surface. At its design operating temperature of 50^{o} C (122^{o} F), each heat pipe is designed to transport 220 (or more) watts to its radiator when its entire control gas charge is compressed into just the gas reservoir volume.

The temperature of the gas reservoir also affects the gas-blocked length of the condenser. The temperature of the gas reservoirs on these heat pipes will be passively controlled by a small radiator attached to it, rather than actively controlled by a feedback controlled electric heater. The heat pipe design conditions call for a

gas reservoir effective sink temperature of -75° C (-102° F).

8.4 Interface Definition

8.4.1 Mechanical

The evaporator sections of the heat pipes are soldered to the aluminum saddles using (1) a four-step plating process on both the aluminum saddles and the stainless steel heat pipes (plating sequence and procedure numbers are included in table 8.4.1-1), and (2) a 60/40 tin-lead, soft-solder (Federal Spec. QQ-S-571; melting range = 183° C (361° F) to 190° C (374° F)). The soldering procedure places limits on (1) total and individual void areas in the solder joint (X-rays of soldered joints show total void areas less than 10% of the total contact area), and (2) the time the 6061-T6 aluminum saddles are maintained in the solder melting temperature range. (Table 8.4.1-2 shows the temperature-versus-time constraints.)

The evaporator saddles are bolted to the functional model power processor unit (FM PPU) cross beams with a thin layer of room temperature vulcanizing (RTV) 566 in the interface. Two saddles are required, each containing three heat pipe evaporator sections, as shown in figure 8.4.1-1. Each saddle half has nut plates fas-

tened to it. Also, a small rectangular tube is soldered to each saddle half. Water will be circulated through these tubes for cooling the PPU when the heat pipes orientation makes them inoperable during ground tests.

The condenser ends of the heat pipes are mechanically attached to their respective radiators. Both the 0.020-in.-thick radiator and the longitudinal radiator stiffeners are formed to enclose the condenser sections of the heat pipes. Thin layers of RTV 566 are used for both the heat pipe-to-condenser saddle interfaces and the condenser saddle-to-radiator interfaces. Number 2 machine screws attach the stiffeners/saddles to the radiator.

8.4.2 Thermal

The BIMOD heat pipes interface with the PPU's through the evaporator saddles and directly with their respective radiators. The 1.27-cm (0.5-in.) diameter heat pipe provides 457.94 cm^2 (70.98 $in.^2$) of heat input area over its 114.78-cm (45.188-in.) evaporator length and 726.66 cm^2 (113.10 $in.^2$) of heat discharge area over its 182.88-cm (72.00-in.) condenser length. The internal evaporation and condensing areas are 377.50 cm^2 (58.51 $in.^2$) and 601.49 cm^2 (93.33 $in.^2$) respectively, taking into account the area blocked by the slab wick

edges. At the specified 220 watt capacity per heat pipe, these areas give average internal heat fluxes of 0.583 watt/cm^2 (3.760 watts/$in.^2$) in the evaporator section and 0.366 watt/cm^2 (2.360 watts/$in.^2$) in the condenser section. Based on an estimated maximum heat dissipation of 410 watts per PPU, the local maximum heat flux for the evaporator section, which is influenced by the proximity of the highest heat-dissipating components in the PPU A-3 module, has been estimated from analysis and test data to be approximately 0.603 watt/cm^2 (3.891 watts/$in.^2$). The local maximum heat flux in the condenser section is close to the average flux, varying only according to the temperature distribution encountered along the length of the heat pipe radiator.

8.5 Performance Description

TRW fabricated seven heat pipes in providing the six required for the first "live" BIMOD assembly. TRW's MULTI-WICK program indicated that the individual heat pipe performance in zero-g could be approximated in one-g by tilting the heat pipe so the evaporator end is 0.762 cm (0.30 in.) higher than the condenser end. Figure 8.5-1 shows a sample curve of the effect of tilt on heat pipe performance. For the SEP heat pipe configuration, 0.762 cm (0.30-in.) head represents a 0.229° (or 13.75') tilt angle.

Figure 8.5-2 shows two temperature response curves obtained during testing on one of the SEP development heat pipes. In particular, it shows the effect of sink temperature on heat pipe performance. Following fabrication, each heat pipe was put through functional acceptance tests by TRW. The results are summarized in tables 8.5-1 and 8.5-2.

8.6 Physical Characteristics and Constraints

Physical dimensions are shown in table 8.6-1 and figure 8.4.1-1. At full power (410 watts dissipated by each PPU), the heat pipes will operate at 50° C (122° F) or lower with the entire 1.83 meters (72 in.) length of condenser section being effective. Heat pipes having a 14,000 watt-in. capacity are required. Should an artery or arteries not prime, power has to be reduced to allow the arteries to prime or the system may be allowed to operate at a higher than 50° C (122° F) temperature.

The PPU will not be operating for extended periods, at which time the radiator and condenser section of the heat pipes will drop to below -98° C (-144° F), the freezing point of methanol. To prime the heat pipe, the condenser section will be heated to above -98° C (-144° F) before power is applied to the PPU. Heaters will be located on the radiator next to the heat pipes and heaters will also be on the reservoir fins.

At 10^{o} C (50^{o} F), the heat pipes will be turned off. The only heat transferred to the radiator from the PPU will be that due to conduction through the heat pipe metal walls (<1 watt).

The adiabatic sections of the heat pipe will be thermally insulated. The reservoirs will be insulated with multi-layer insulation (MLI) from any direct or indirect heat. A fin on the reservoir will view space to maintain a cold reservoir.

8.7 Development History

The heat pipes used in the BIMOD configuration are a gas-filled, variable conductance type which have had flight experience: (1) in the International Heat Pipe Experiment (IHPE) sounding rocket test in 1974, and (2) on the Transmitter Experiment Package (TEP) of the Communications Technology Satellite (CTS), which has been operating successfully since its launch in January 1976.

The physical configuration and details of the two heat pipes flown in the sounding rocket tests are indicated in table 8.7-1. They were subjected to approximately 6 minutes of zero-g and helped to verify the capability of TRW's artery priming foil to successfully perform the venting of non-condensable gas, which is necessary for successful priming of the artery with working fluid.

Figures 8.7-1 through 8.7-4 summarize the flight data, showing the temperature distribution along the slab wicks, the power applied to the evaporator heaters, and the voltage indicated on the artery thermistor (which was used to indicate successful artery priming) for both heat pipes.

References 8.1.1, 8.1.2, and 8.1.3 provide the details of the CTS heat pipe application. The location of the heat pipe assembly on the CTS spacecraft is shown in figure 8.7-5. The various components and dimensional details of the CTS heat pipe system are shown in figures 8.7-6 and 8.7-7. Other physical property data is shown in tables 8.7-2 and 8.6-1. Figures 8.7-8(a) through (e) and tables 8.7-3 and 8.7-4 summarize the heat transfer capacity and control temperature response data resulting from the post-fabrication verification tests performed on the 15 heat pipes that TRW built for the CTS program.

In addition to the flight experience using this heat pipe design, there has been a history of component technology developments (refs. 8.1.4 through 8.1.9). This history can be summarized as follows.

8.7.1 Materials Compatability and Processing Procedures

Studies in this area have been supported by:

1) An ongoing life test on CTS VCHPS FM-006 assembly. This system has been successfully operating in excess of 34,720 hours (3.96 yrs) at a power input of 150 watts and a nominal operating temperature of 52° C (125° F).

2) Accelerated life tests on a sample, short CTS heat pipe. The results of these tests are reported in reference 8.1.10.

3) Early TRW material compatibility tests and studies involving generation of non-condensable gases in heat pipes, as indicated in reference 8.1.8. Applicable documents 8.8.1 and 8.8.2 show Lewis-authored studies which were performed prior to launch of CTS and which evaluated the gas-generation potential of the CTS heat pipes. Reference 8.1.11 is a good summary reference on manufacturing problems.

8.7.2 Artery Wicking Systems

Studies in this area included:

1) Resolving manufacturing difficulties resulting from the necessity of bending the heat pipes, and therefore the wire-mesh arteries, in some designs. It was found that, to prevent crimping of an artery during bending, the wires had to be oriented at a 45° bias to the artery centerline. For long heat pipes, this requirement forced the development of an

artery splice technique because the length of individual artery sections was limited by the width of available, commercially produced wire mesh. Material size limitations also resulted in the development of a splicing technique for the metal felt slab wick used in the CTS-type heat pipe designs.

2) Venting non-condensable gas bubbles from the working fluid in arteries. Many literature references can be found in this area (e.g., refs. 8.1.12 and 8.1.13). TRW developed a patented venting technique (ref. 8.1.14) using a "priming foil," which is part of the artery wall on the evaporator end of the heat pipe. The thickness of the foil, and the diameter of the holes placed in it, are sized so that the menisci which form on the surfaces of the working fluid film that covers the holes contact each other, causing the film to break. This allows the gas bubbles being transported in the working fluid to be vented out of the arteries into the surrounding vapor space.

3) Increasing the artery diameter to increase the fluid return capability of the arteries. Limitations were encountered in that increasing the artery size also increased the head height to which an artery had to prime in a one-g environment. This negative effect could be compensated for, to some degree, by placing

the artery closer to the bottom of the heat pipe wall. However, if the artery touches the wall at any location, it won't prime. The defined separation distance is limited by the manufacturing tolerance in placing the arteries in the heat pipe cross-section.

4) Overall wick design. When compared with other wick designs, that used in the CTS-type design provides a low thermal resistance along with the high pumping capacity of the artery configuration. This is done by separating the evaporation and condensation areas from the primary fluid return passages, thereby making them more efficient. And placement of the arteries low in the cross-section improves one-g operating capabilities.

8.7.3 Working Fluid and Control Gas Properties

Studies in this area included:

1) Effects of working fluid properties (table 8.7.3-1) on artery priming. Early work on arterial, variable conductance heat pipes using high-vapor-pressure working fluids showed that they suffered instability problems which would lead to artery depriming under high thermal loads. This is one of the disadvantages of using ammonia in arterial heat pipes.

2) Freezeout of working fluid through diffusion into the below-freezing, gas-blocked region of the heat pipe

(e.g., ref. 8.1.15). TRW performed tests and studies in this area as part of the CTS program. The conclusions indicated a large time constant for this phenomenon and, therefore, it should not be a problem with the working fluid and control gas used in these heat pipes.

3) Formation of control gas bubbles in arteries during thawing of frozen working fluid. This has been tentatively identified as the probable cause for the artery depriming which led to the four CTS thermal anomalies experienced in 1977. Control gas absorbed by the working fluid is entrapped during freezing and is released when thawing occurs. If the heat pipe is under load, the bubbles that form in the arteries can result in the artery depriming because the priming foil can't vent the gas fast enough. The problem is a statistical one because depriming would be a function of how many bubbles were produced, whether they combine into larger ones, and the thermal loading condition on the heat pipe, which could affect the rate at which the bubbles are brought to the evaporator end of the heat pipe. The rate of formation of bubbles would be affected by the thermal environment, including changes in the heat pipe evaporator loading condition, solar im-

pingement on radiator surfaces, and so forth. If this phenomenon checks out as the cause, the obvious solution to prevent future anomalies would be to insure that all of the heat pipe working fluid is thawed prior to subjecting the heat pipe to a thermal load. Heaters mounted on the condenser section of the heat pipe would be activated and the working fluid taken to a temperature above its freezing point. The heaters would be turned off prior to activating the equipment which provides the thermal load for the heat pipe, thus reducing the power requirements for the overall system. A report on TRW's initial anomaly investigation work is included in reference 8.1.16. The physical description of the anomalies is included in reference 8.1.17. TRW in continuing work in this area under contract NAS3-21740.

8.7.4 Gravitational Effects

Gravity is a major consideration because of the necessity of performing ground tests prior to launch in a spacecraft application. References 8.1.18 and 8.1.19 touch on the effect of gravity on the performance of gas-loaded variable conductance heat pipes.

1) When the working fluid and control gas have widely

differing molecular weights, strange temperature distributions can result.

2) Much research has been done in the area of the effect of tilt on a heat pipe's thermal performance. Gravitational forces reduce or enhance the fluid return capability of the heat pipe, depending on its orientation. Figure 8.5.1 illustrates the results of this behavior.

3) The heat pipe configuration and wick design must allow for being able to test the heat pipe in a one-g environment, preferably at thermal transport levels approximating zero-g transport capability.

8.7.5 Local Heat Flux Limitations

Local heat flux limitations are governed primarily by the design of the wicking structures in the heat pipe. Local heat fluxes can be reduced by improving the temperature-averaging capability of the structures through which the heat is brought in and out of the heat pipes. This consideration is especially important in heat pipes with diametral slab wicks, which result in two separated vapor-flow channels. If more heat enters the heat pipe on one side than on the other, as occurs in the BIMOD configuration when one PPU is on and the other is off, the location of the front between the working fluid vapor and the control gas can vary in each passage. This would

cause a strange temperature distribution and/or potential control problems. The heat pipe saddles in the BIMOD configuration were specially designed to provide a more uniform heat distribution around the heat pipes under all PPU operating conditions.

8.7.6 Computer Modeling

In addition to development of physical hardware, there has been much computer modeling effort involved in this heat pipe design. TRW's GRADE (ref. 8.1.20), GASPIPE and MULTIWICK computer programs have been useful tools in the design of these heat pipes. In addition, a "CTS Heat Pipes/South Panel" model was evaluated using the SINDA Thermal Analyzer program. This model is being updated to provide thermal analysis support for TRW's efforts in investigating the cause(s) of the CTS thermal anomalies.

8.7.7 System Considerations

The CTS-type heat pipe design was selected for the BIMOD configuration because it provides a high heat-transfer capacity/heat-pipe-weight ratio, superior to that of other known designs for the diameter, length, and thermal response properties specified. Its improved performance is a product of a TRW IR&D effort and a development effort (ref. 8.1.21) conducted as Phase I of TRW's contract to fabricate the first set of these heat

pipes used on a BIMOD assembly. Besides those noted above, other design factors that were evaluated for this system included cost, ease of integration, and system expansion flexibility. Thermal control system tradeoff studies indicated heat pipes, and especially those with the improved CTS-type capability, reduced system weight while reducing system costs and are easily integrated into the BIMOD configuration. The system can be easily expanded by increasing heat pipe length and, therefore, radiator size. This would have to be traded off against requirements for redundancy, number of heat pipes, etc., however.

8.7.8 Design Alternatives

Other heat pipe designs have been evaluated for possible substitution for, or improvement of, the CTS design. TRW has developed metal felt wicks which have a variable porosity between the evaporator and the condenser ends of a heat pipe (ref. 8.1.22). This design improves the fluid return capability of felt wicks by a factor of about three. Advantages of this design include:
(1) Potential elimination of arteries and, therefore, the uncertainty resulting from the bi-stable operating modes of artery heat pipes. This would permit using working fluids such as ammonia and, therefore, lighter envelope materials, such as aluminum. Aluminum/ammonia

heat pipes can be fabricated with a stainless steel adiabatic section, minimizing OFF-mode heat transfer through this region and minimizing thermal gradients in the walls of the evaporator and condenser sections. (2) The heat pipes made with just a variable porosity wick would be easier to manufacture and would, therefore, be cheaper in cost. Even with these advantages, however, a heat pipe with just a variable porosity wick still cannot perform thermally as well as one with the arterial design. One possible improvement of the CTS-type design could be the substitution of the regular slab wick with one of variable porosity, thereby increasing heat pipe capacity in the deprimed-arteries mode.

8.8 Applicable Documents Enclosed

8.8.1 Tower, L. K.: Decomposition Reaction of Methanol in CTS Pipe. NASA Lewis Research Center Internal Memorandum, no date.

8.8.2 Gas Generation in CTS VCHPS. NASA Lewis Research Center Internal Memorandum, June 1975.

8.8.3 SEP FM/PPU Thermal Control System Design Summary. NASA Lewis Research Center Internal Memorandum for Record. November 1977.

8.8.4 Heat Pipe Drawing List. NASA Lewis Research Center.

8.9 Ground Support Equipment

8.9.1 Acceptance and Characterization Tests

Special equipment to support these tests was designed to provide for simple, flexible, and accurate test operations.

8.9.1.1 Structural Support Equipment

Hardware from the BIMOD assembly fixture (a Multi-Purpose Assembly and Test Stand), two CTS heat pipe system test stand frames (welded and flat structures), and auxiliary attachment hardware were combined to form a support frame with leveling screws on its legs and a tilting top (adjustable with one threaded rod) to which the heat pipes are attached during testing.

8.9.1.2 Thermal Control Equipment

Two evaporator heater assemblies, three condenser cooling saddle assemblies, three gas reservoir heater assemblies, and three gas reservoir cooling jackets provided for thermal input and output for the heat pipes. Electric resistance heaters were used on the heater assemblies. When required, a water/glycol solution (provided from a constant temperature bath) or cold gaseous nitrogen (GN_2) (provided from a storage bottle and passed through a heat exchanger coil in a liquid nitrogen (LN_2) thermos or dewar) was used in the condenser cooling

saddles. The cold GN_2 was also used in the gas reservoir cooling jackets.

8.9.1.3 Thermal Instrumentation

Copper constantan thermocouples were used to measure the thermal response of the heat pipes. (Temperature-responsive liquid crystal material has also been used successfully to locate the working fluid/control gas interface of an operating variable conductance heat pipe.)

8.9.2 BIMOD Tests

8.9.2.1 Auxiliary Cooling Tubes

Copper, rectangular tubes were soldered into the evaporator saddles along with the heat pipes. A water/glycol solution from a constant temperature bath will be used to cool the PPU's when the heat pipes are in a non-functioning orientation or environment.

8.9.2.2 Tilting Feature of BIMOD Support Fixture

The tilt of the heat pipes in the BIMOD configuration can be adjusted remotely during thermal-vacuum testing as a result of a feature built into the BIMOD Support Fixture.

Table 8.3.2.7-1 BIMOD Heat Pipe Gas and Liquid Inventory.

HEAT PIPE	GAS LOAD (10^{-6} LB-MOLES)	LIQUID LOAD (CC)
1 thru 7	6.00	140

Table 8.3.3.2-1 Properties of Typical Heat Pipe Envelope and Wicking Materials.

Material	Condition	Thermal Conductivity K $\left(\frac{\text{Btu-ft}}{\text{hr-ft}^2\text{-}^\circ\text{F}}\right)$	Yield Stress Sy $\left(\text{psi}\right)$	Density ρ $\left(\text{lb/cu in}\right)$	Specific Heat C_p $\left(\text{Btu/lb}^\circ\text{F}\right)$	Thermal Stress Parameter Ks $\left(\frac{\text{Btu-lb}}{\text{hr-}^\circ\text{F}}\right)$	Stress Weight Parameter S/ρ $\left(\text{inch}\right)$	Thermal Response $t/C_p\rho$
Aluminum (6061)	T6 Annealed	98	40 x 10^3 8 x 10^3	9.8 x 10^{-2}	23 x 10^{-2}	39.6 x 10^3 7.9 x 10^3	4 x 10^5 .8 x 10^5	44
Copper (OHFC)	Hard Annealed	226	40 x 10^3 10 x 10^3	32.3 x 10^{-2}	9.2 x 10^{-2}	90.4 x 10^3 22.6 x 10^3	1.2 x 10^5 .3 x 10^5	34
Stainless Steel (304)	Hard Annealed	9.4	75 x 10^3 35 x 10^3	29 x 10^{-2}	12 x 10^{-2}	7.1 x 10^3 3.3 x 10^3	2.5 x 10^5 1.2 x 10^5	28
"Monel" (K-500)	Hard Annealed	10.1	90 x 10^3 40 x 10^3	32 x 10^{-2}	10 x 10^{-2}	9.1 x 10^3 4.0 x 10^3	2.8 x 10^5 1.3 x 10^5	31

Table 8.4.1-1 Heat Pipes and Saddles Plating Sequence and Procedure Numbers.

Item	Process	Procedure Number
Aluminum saddles	1. Double zincate.	-------
	2. Copper strike.	MIL-C-14550
	3. Copper plate.	MIL-C-14550, Class 2
	4. Tin plate.	TRW PR 6-18-4
Stainless steel pipes	1. Nickel strike.	QQ-N-290
	2. Copper plate.	TRW PR 6-33-3
	3. Tin plate.	TRW PR 6-18-4

Table 8.4.1-2 Maximum Reheating Times for the Forming of Heat-Treatable Alloys at Various Temperatures.*

Temperature	2014-T6	2024-T81	2024-T86	6061-T6	7075-T6
500°F	No	No	No	No	No
450°F	To temp.	5 min	5 min	5 min	No
425°F	To temp	15 min	15 min	15 min	To temp
400°F	5-15 min	30 min	30 min	30 min	5-10 min
375°F	30-60 min	1 hr	1 hr	1-2 hr	30-60 min
350°F	2-4 hr	2-4 hr	2-4 hr	8-10 hr	1-2 hr
325°F	8-10 hr			50-100 hr	2-4 hr
300°F	20-50 hr	20-40 hr	10-20 hr	100-200 hr	10-12 hr

* Under these conditions of time and temperature, the losses in strength as a result of reheating generally will not exceed about 5 per cent. It is to be understood that these are maximum accumulated times of reheating and that, in most cases, equal formability will be obtained with shorter periods of heating.

Table 8.5-1 SEP Heat Pipe Thermal Capacity Test Results. (Elevation of 0.3 inch; adiabatic temperature = 1225 °F; effective length of pipes = 66 inches)

Heat Pipe Number	Configuration	Power Held (Watts)	Power at Groove Dryout (Watts)	Power at Burnout (Watts)	Power Factor (Watt-Inches)
1	1	220	---	230	14,520
2	2	270	310	None; stopped	17,820
3	1	220	---	230	14,520
4	1	220	260	None; testing stopped at 300 watts	14,520
5	2	280	290	300	18,480
6*	2	>150	150	175	9,900
7	2	300	220	320	19,800

* Performance below specification.

Table 8.5-2 Turn-on and Full-on Temperatures of SEP Heat Pipes.

Module Configuration	Heat Pipe Number	Temperature (°F)	
		Turn-on	Full-on
A	1	103	123
	2	103	121
	4	105	126
B	3	100	124
	5	100	125
	7	105	126

Table 8.6-1 Physical Details of CTS and SEP Variable Conductance Heat Pipe Systems.

CHARACTERISTIC	CTS VCHPS	SEP BIMOD VCHPS
Function	Control temperature of TEP OST and PPS (in parallel with South Panel)	Control temperature of PPU's in BIMOD configuration
Number of heat pipes	Three per spacecraft	Three per PPU, or six per BIMOD
Thermal		
System capacity	196 watts min at $T_e \geq 50°C$ (122°F) and <3 watts at $T_e < 10°C$ (50°F)	410 watts per PPU at $T_e \geq 50°C$ (122°F) and <3 watts per PPU at $T_e < 10°C$ (50°F)
Heat pipe capacity	Nom. 150 watts min at $T_e \geq 50°C$ (122°F) and <1 watt at $T_e < 10°C$ (50°F)	220 watts min at $T_e \geq 50°C$ (122°F) and <1 watt at $T_e < 10°C$ (50°F)
Heat pipe power factor	7500 watt-inches	14,000 watt-inches
Temp. control range	21-48°C (70-118°F)	33-47°C (91-117°F)
Max. eff. sink temp.		-75°C (-102°F)
Tubes		
Material	304 stainless steel, fully annealed (σ_y = 35,000 psi; σ_u = 75,000 psi)	SAME
Cross-section	0.500 OD x 0.028 wall	SAME
Internal threads	100 TPI, 0.005 deep, 40° included angle	SAME
Free vol/length ratio	.1027 in^3/in	SAME
	#1 / #2 / #3	
Total length	68.00 / 74.86 / 79.78	122.556
Evap. section length	22.00 / 22.00 / 22.00	45.188
Adiab. section length	3.70 / 3.70 / 3.70	5.368
Cond. section length	42.30 / 49.16 / 54.08	72.000
Effective length $((L_e+L_c)/2)+L_a$	35.85 / 39.28 / 41.74	63.962
Reservoirs		
Material	304 stainless steel	SAME
Configuration	Spun hemispherical cap with 1.75 OD cylindrical center section	SAME
Free volume	8.22 in^3	SAME

Table 8.6-1 (continued) Physical Details of CTS and SEP Variable Conductance Heat Pipe Systems.

CHARACTERISTIC	CTS VCHPS	SEP BIMOD VCHPS
Wicks		
Material	304 stainless steel	SAME
Reservoir wick	0.020 thick (spot-welded to interior walls)	SAME
Tube wick	0.050 thick (interference fit across dia. of tube; one splice required	SAME
Arteries		
Material	316 stainless steel	304 stainless steel
Cross-section	0.063 ID x $(150)^2$ mesh (0.0026 dia. wire)	0.070 ID x $(150)^2$ mesh (0.0026 dia. wire); one splice required
Priming foils		
Material	304 stainless steel	SAME
Cross-section	0.063 ID x 0.0005 wall with 0.010 dia. holes	0.081 ID x 0.00027 wall with 0.006 dia. holes
Attachment	Spot-welded to end of arteries and diametral wick	Welded over window in end-cap; end-cap welded to end of artery.
Working fluid		
Material	Methanol (Spectrophotometric grade)	SAME
Freezing point	-98°C (-144°F)	
Boiling point	65°C (149°F)	
Control gas		
Material	90% nitrogen, 10% helium (research grade)	SAME
Evaporator saddles		
Material	6061-T6 aluminum alloy	SAME
Fabrication method	Extruded	Machined or extruded
Attachment	60-40 tin/lead solder (following Cu/Ni/Sn plating)	SAME
Condenser saddles		
Material	6061-T6 aluminum alloy	SAME
Fabrication method	Extruded	Formed sheet (also serves as radiator stiffeners)
Attachment	60-40 tin/lead solder (following Cu/Ni/Sn plating)	RTV-566 and bolts to radiator

Table 8.7-1 Configuration and Details of Heat Pipes Flown on Sounding Rocket Test Flight.

Tube (304 stainless-steel):
- Length - 36 inches
- Outside diameter - 0.5 inches
- Wall thickness - 0.028 inches
- Internal threads - 100 per inch

Slab-wick (304 stainless-steel X-13 felt metal):
- Thickness - 0.050 inches
- Fiber diameter - 0.00085 inches
- Porosity - 84%

Arteries (304 stainless-steel 150-mesh screen):
- Inside diameter - 0.063 inches
- Height from bottom of slab wick - 0.170 inches

Priming foils (304 stainless-steel):
- Thickness - 0.0005 inches
- Diameter of holes - 0.01[illegible] inches
- Hole spacing in row - 0.032 inches
- Row spacing - 0.075

Active length { 1.50 inches for Configuration X-2 / 0.375 inches for Configuration X-1

Hole pattern { 17° spirals for Configuration X-2 / straight for Configuration X-1

Thermistor (Veco, part No. J2A7):
- Bead diameter - .013 inches
- Leads - .001 inch platinum
- Resistance at 25°C - 2000 Ω

Flight heat sink: aluminum block 12" x 1.32" x 1.32"

Flight heater: 10 inches long and beginning 2 inches from the evaporator end

Flight thermistor locations:

Thermistor No.	Distance from evaporator end
1	2.5 inches
2	6
3	9.5
4	18
5	24
6	30
7	36
8	on heat sink
9	on heat sink

NOTE: On one of the flight heat pipes (slab wick A) thermistor No. 6 did not function properly.

Table 8.7-2 CTS Heat Pipes Gas and Liquid Inventory.

HEAT PIPE	GAS LOAD (10^{-6} LB-MOLES)	LIQUID LOAD (CC)
1	3.94	89
2	4.83	94
3	5.76	98

Table 8.7-3 CTS Heat Pipes Thermal Capacity Test Results.

ASSEMBLY	HEAT PIPE NO./CAPACITY (WATTS)		
	-1	-2	-3
001	175	175	155
002	155	155	165
004	185	125	165
005	165	145	165
006	165	125	155

Table 8.7-4 CTS Heat Pipes Control Range Test Results.

HEAT PIPE	SPEC TURN-ON TEMPERATURE RANGE (°F)	TEST TURN-ON TEMPERATURE (°F)				
		S/N001	S/N002	S/N004	S/N005	S/N006
D315260-1	88 ± 4	89	90	87	86	83*
D315260-2	94 ± 4	93	92	91	90	89*
D315260-3	100 ± 4	97	99	97	96	95*

*Out-of-spec temperatures acceptable since S/N001 is life test unit only.

Table 8.7.3-1 Properties of Typical Heat Pipe Working Fluids.

FLUID	BOILING POINT	MELTING POINT	DENSITY		VISCOSITY		SURFACE TENSION	LATENT HEAT	SPECIFIC HEAT	HEAT OF FUSION	CRITICAL FLUX
			LIQUID	VAPOR	LIQUID	VAPOR					
	F (deg) C (deg)	F (deg) C (deg)	lb/cu ft g/cm³	lb/cu ft g/cm³	cps cs	cps cs	dyne/cm	Btu/lb cal/g	Btu/lb °F cal/g °C	Btu/lb cal/g	w/sq in w/cm²
Freon 12 (CCl_2F_2)	- 21.6 - 29.8	- 252 - 156	92.6 1.48	0.385 0.00533	0.37 0.249	0.0127 2.01	16.6	71.04 39.47	0.21 0.21		138 21.5
Ethyl Chloride (CH_3CH_2Cl)	54 12.27	- 218 - 138.7	56.0 0.896	0.1872 0.0030	0.30 0.328	0.0093 3.1	20.30	163.9 90.55	0.36 0.36		203 31.5
Acetone (CH_3COCH_3)	133 56.6	- 139 - 95	48 0.77	0.135 0.0022	0.6 0.78	0.0085 3.68	17.4	224 124.5	0.55 0.55*	42 23.4	218 35.8
Methanol (CH_3OH)	148.5 64.68	- 144 - 97.8	49.8 0.798	0.0766 0.0012	0.34 0.43	0.0135 11.15	22.6	473 262.8	0.606 0.466	28.8 16.4	268 87
Hexafluoro-benzene (C_6F_6)	178 80.2	39.2 3.8	100 1.62	0.402 0.0064			21.4	73 40.6	0.265 at 24C 0.265	26.6 14.66	131 20.4
DC-200(R) - 66 CS	212 100	80 - 87.7	47.6 0.763	0.075* 0.001*	0.45 66 at 25C	0.01* 10.0*	15.9 at 25C	95.8 52.4	0.504 0.504		74 11.6
Dowtherm-E(R)	362 177.76	0 - 18	70.8 1.127	0.269 0.0046	0.335 0.337	0.01093 2.36	37 at 25C	119.1 66.3	0.411 0.411	38 21.1	182 28
Dowtherm-A(R)	495.8 257.7	53.6 12	53.78 0.864	0.2495 0.00399	0.27 0.316	0.0183 2.59	40 at 25C	126 71.3	0.524 0.524	42.2 23.4	172 26.7
CP-69(R)	585.8 307	- 85 - 65	80* 0.81	0.25* 0.004	0.25* 0.32	0.01* 2.5	41 at 20C	120.5 67			162* 25
Water (H_2O)	212 100	32 0	60 0.9604	0.0573 0.0006	0.2838 0.799	0.0125 20.9	72 at 25C	970 539.55	1.0 1.0	144 79.71	793 109
Ammonia (NH_3)	- 28.1 33.34	- 107.9 77.7	42.5 0.681	0.0552* 0.000708 at 0C	0.25 0.367	0.0079	42.41	587.99 326.44	1.07 1.07	142.6 79.4	446 59.1

NOTES:
1. ALL VALUES GIVEN AT THE BOILING POINT UNLESS OTHERWISE NOTED
2. ESTIMATED OR APPROXIMATE VALUE INDICATED BY AN ASTERISK

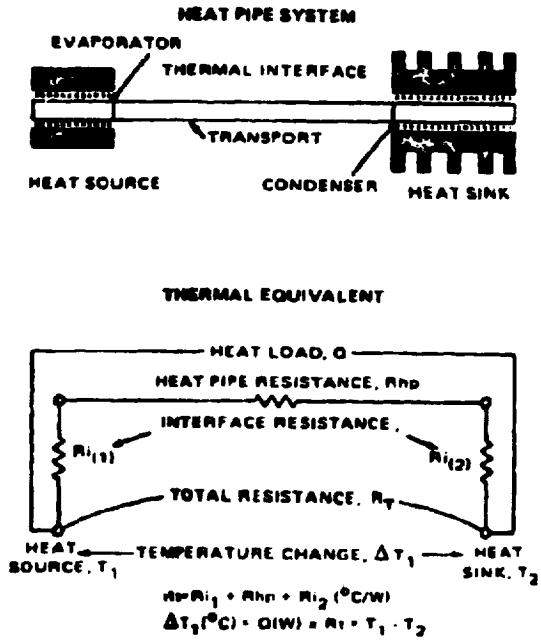

Figure 8.2.2-1 Total Thermal Resistance of Heat Pipe (Exterior Evaporator Surface to Exterior Condenser Surface).

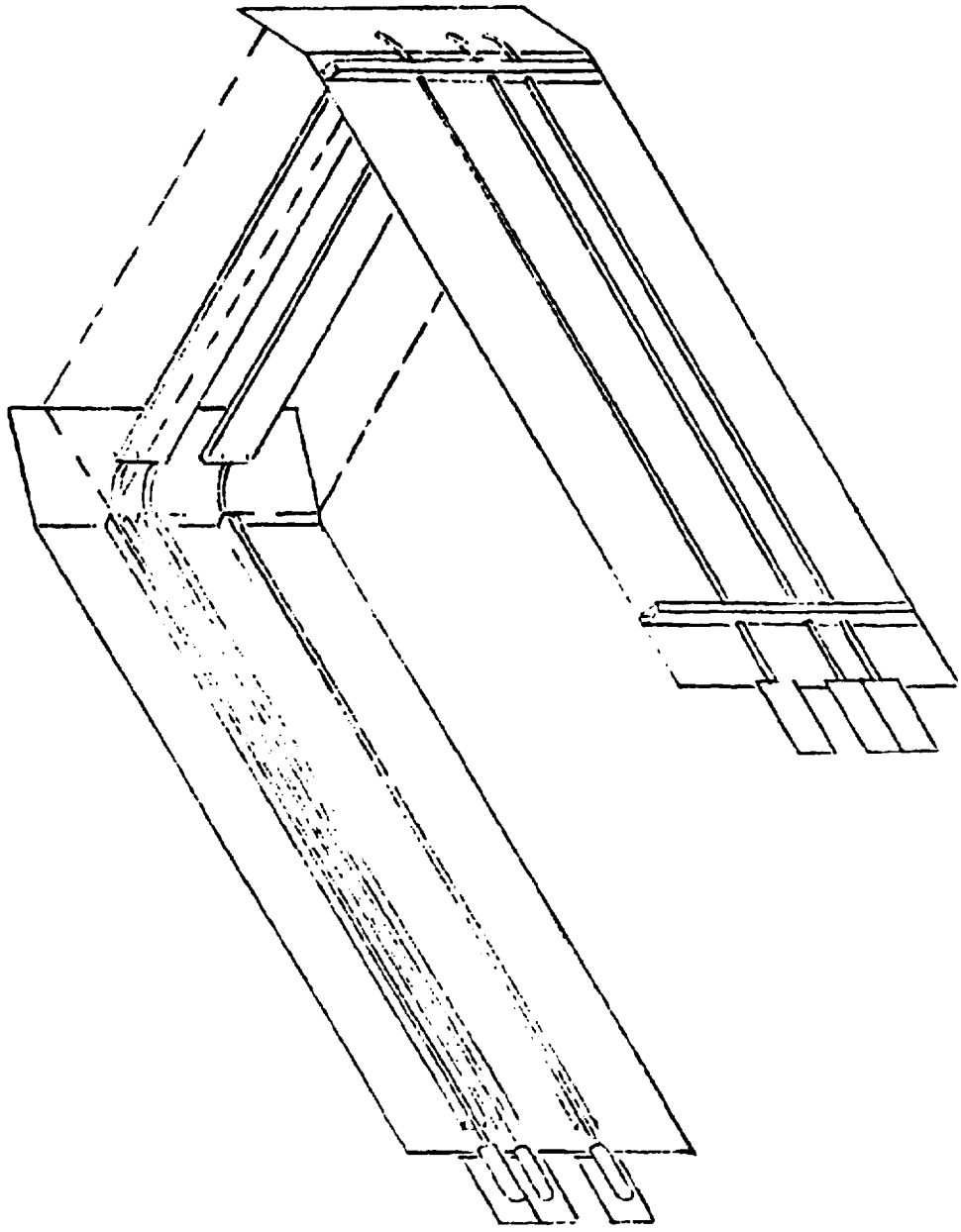

Figure 8.3.1-1 Schematic of SEP BIMOD Thermal Control System.

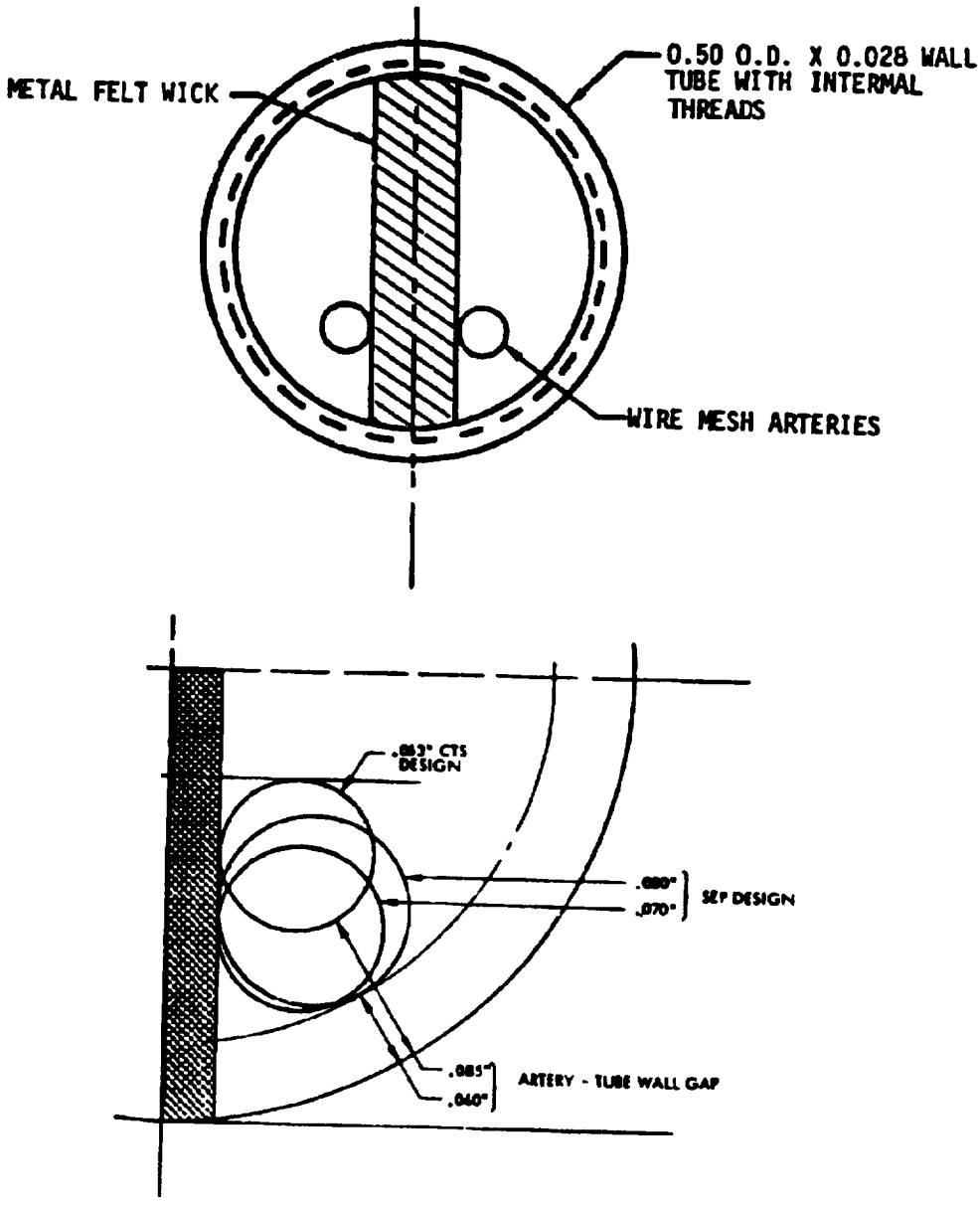

Figure 8.3.1.4-1 Heat Pipe Artery Locations in CTS and SEP Designs.

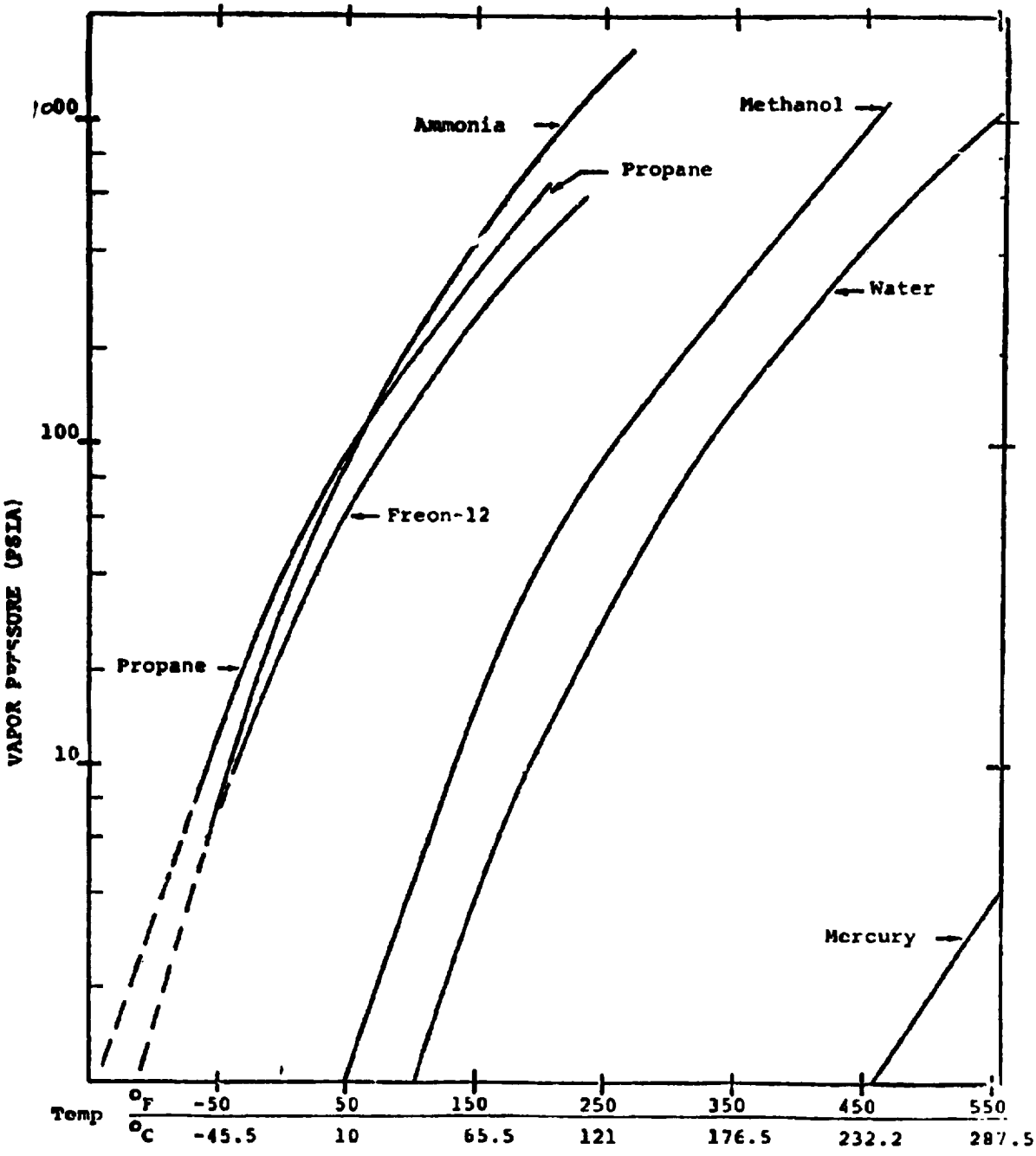

Figure 8.3.1.7-1 Vapor Pressure versus Temperature for Several Heat Pipe Fluids.

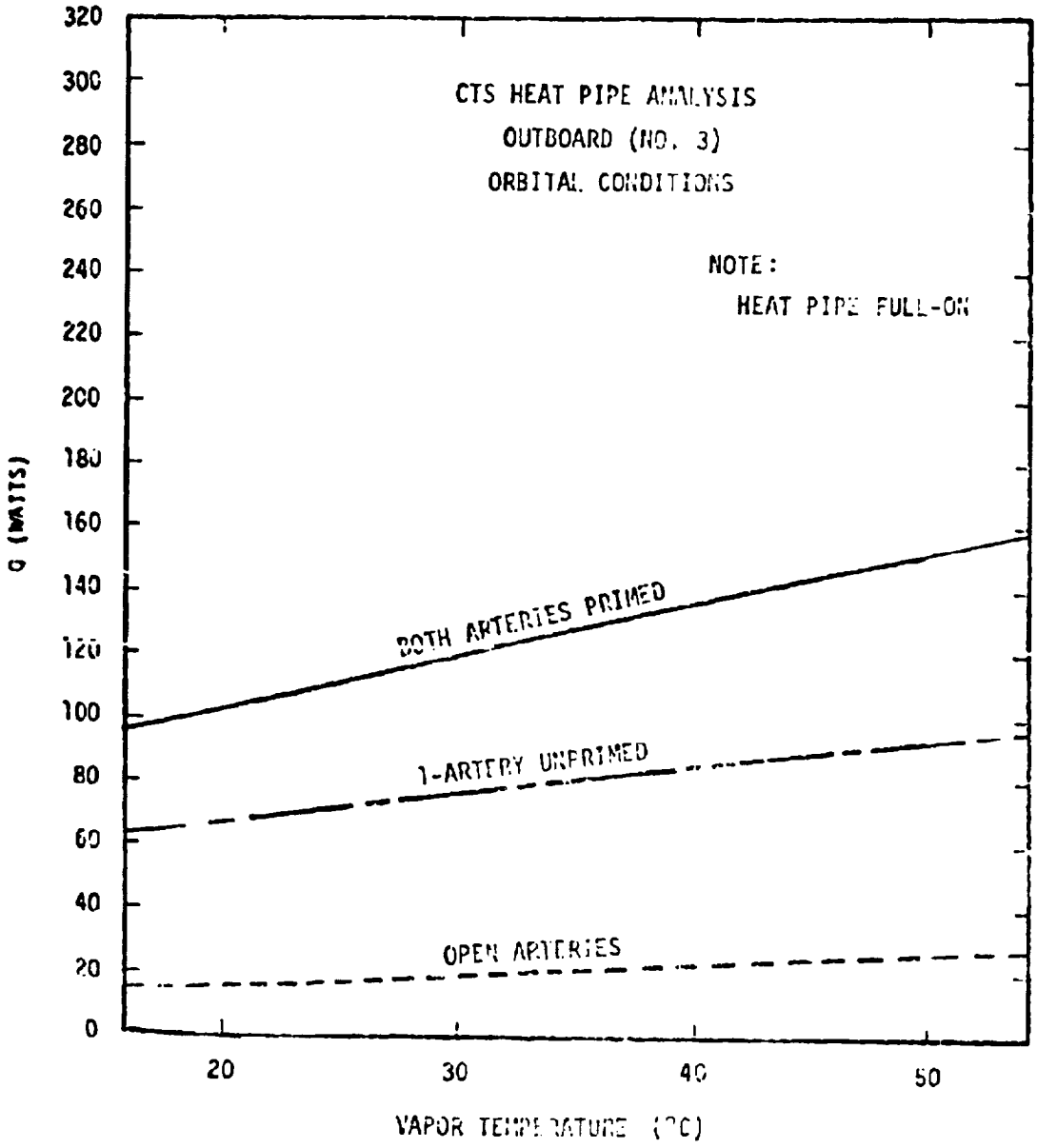

Figure 8.3.2.4-1 Effect of Artery Depriming on Thermal Transport Capability of CTS-Type Heat Pipes.

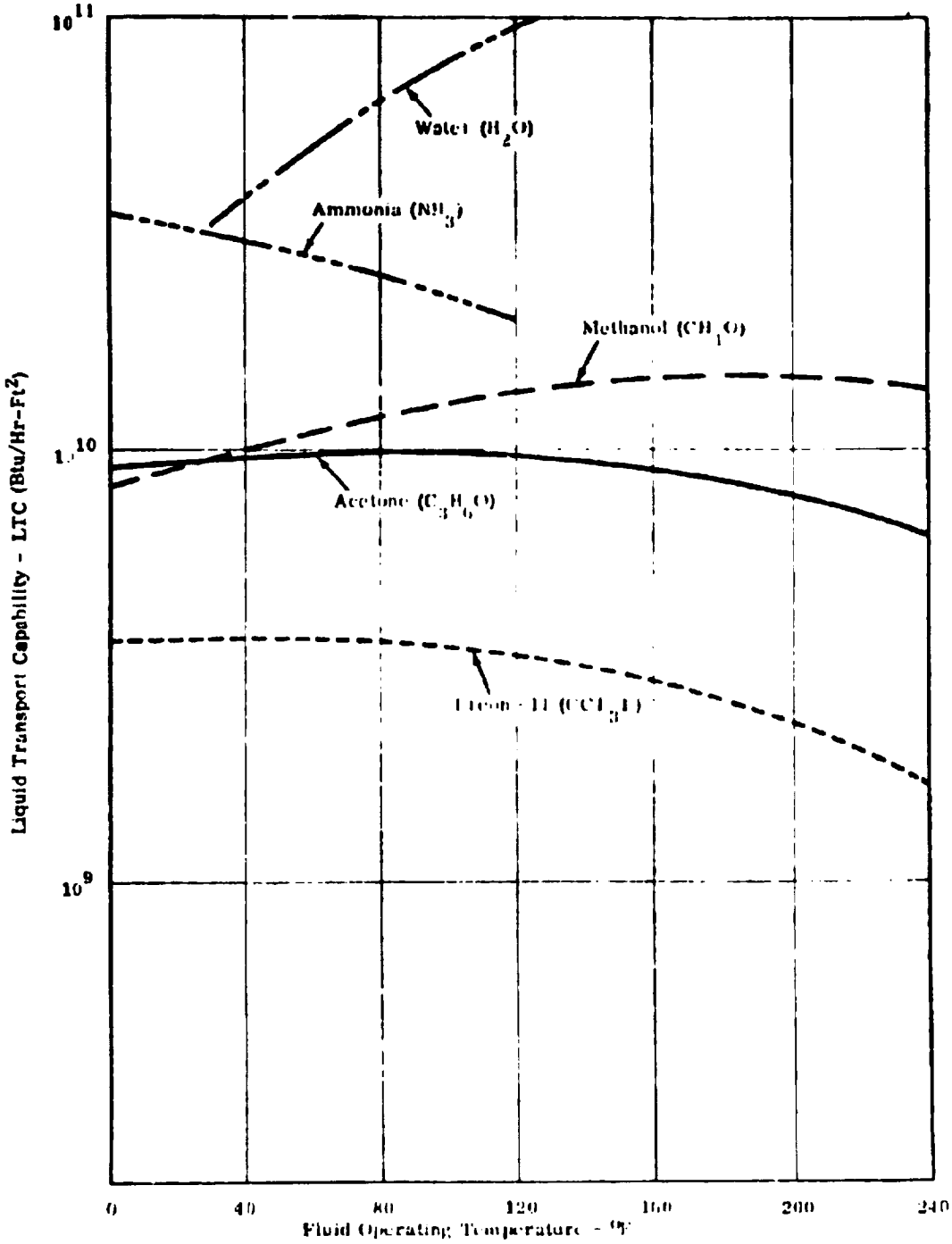

Figure 8.3.2.7-1 Liquid Transport Capability versus Temperature for Several Heat Pipe Fluids.

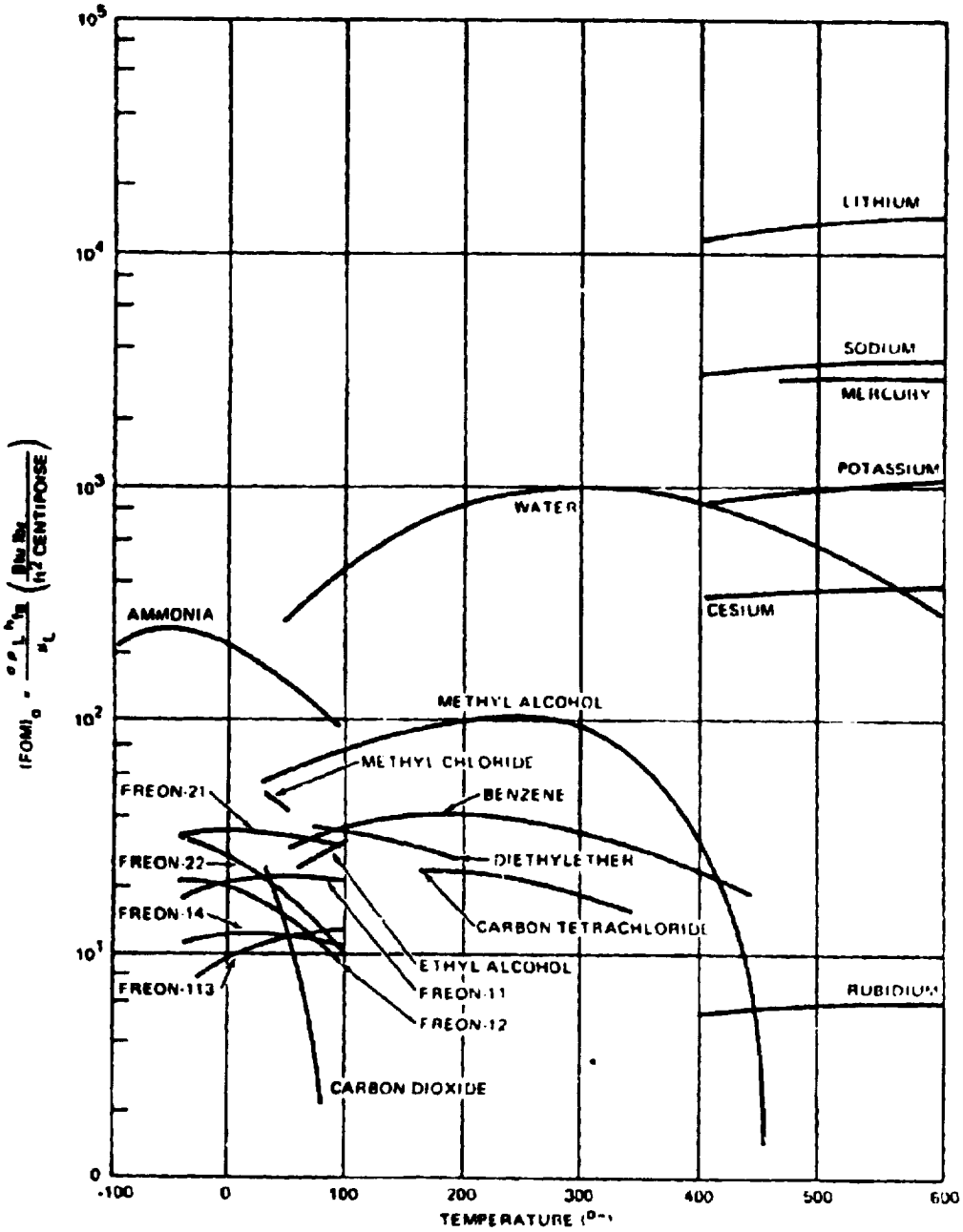

Figure 8.3.2.7-2 Zero-g Figure of Merit versus Temperature for Several Heat Pipe Fluids.

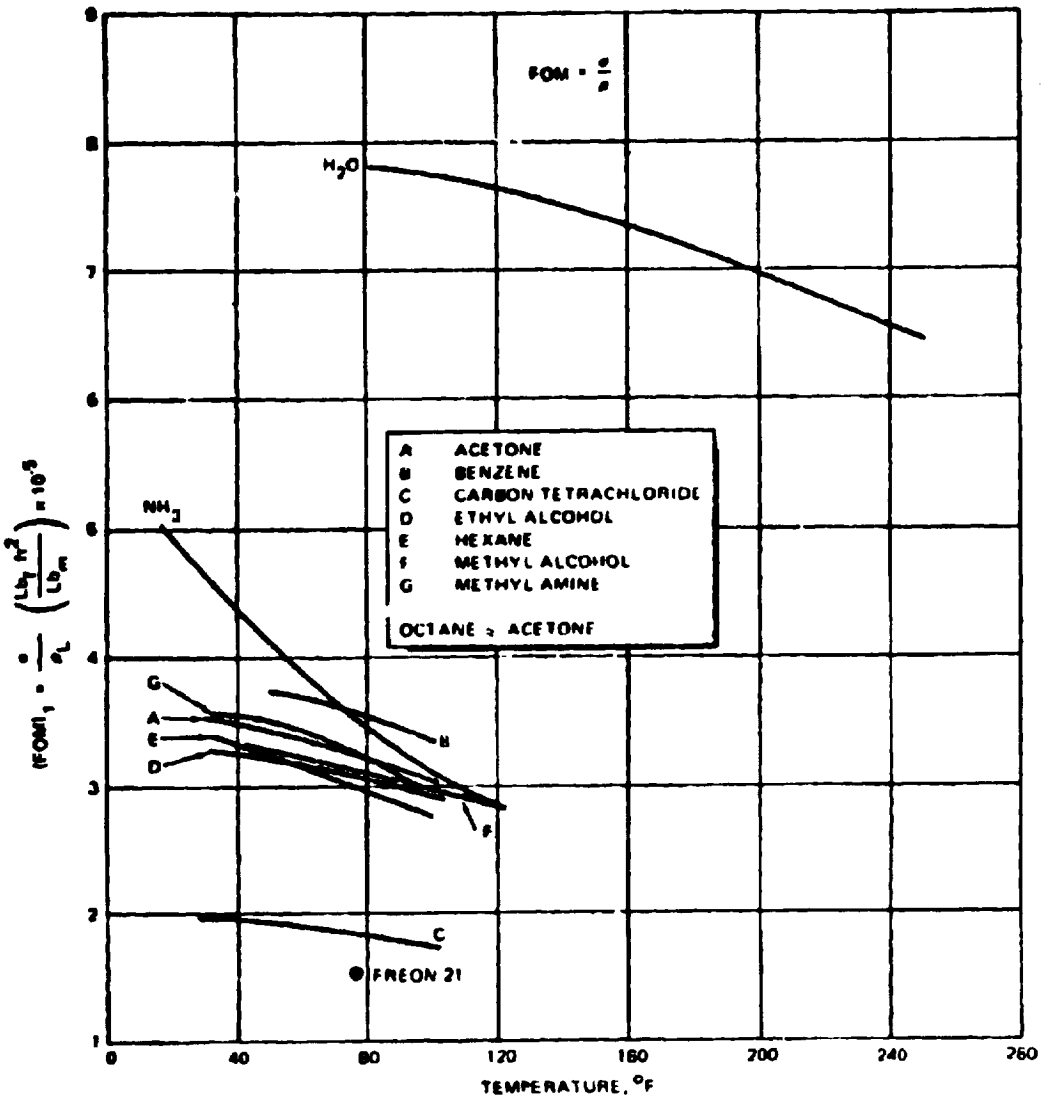

Figure 8.3.2.7-3 One-g Figure of Merit versus Temperature for Several Heat Pipe Fluids.

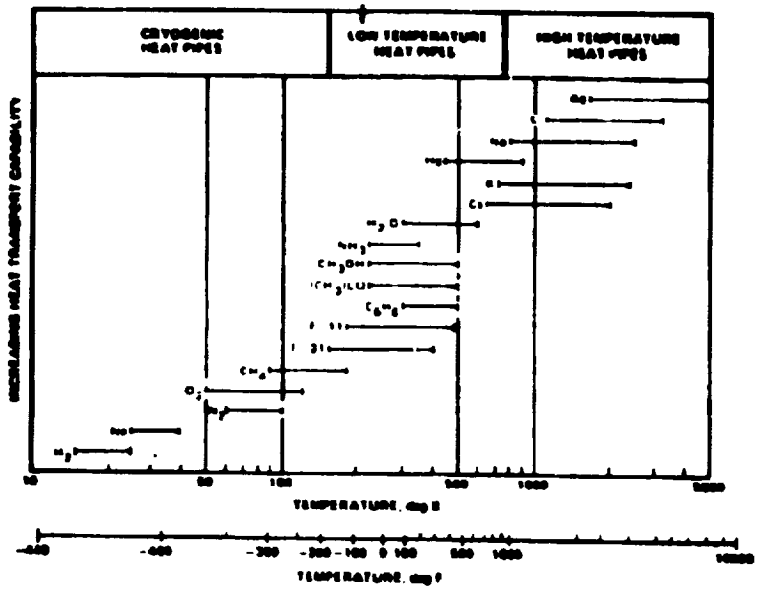

Figure 8.3.2.7-4 Heat Transport Capability versus Operating Temperature Range for Various Heat Pipe Working Fluids.

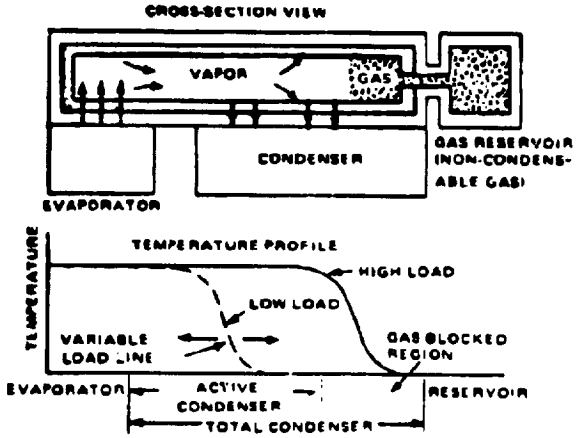

Figure 8.3.2.8-1 Effect of Control Gas on the Temperature Profile of a Variable Conductance, Gas-Filled Heat Pipe.

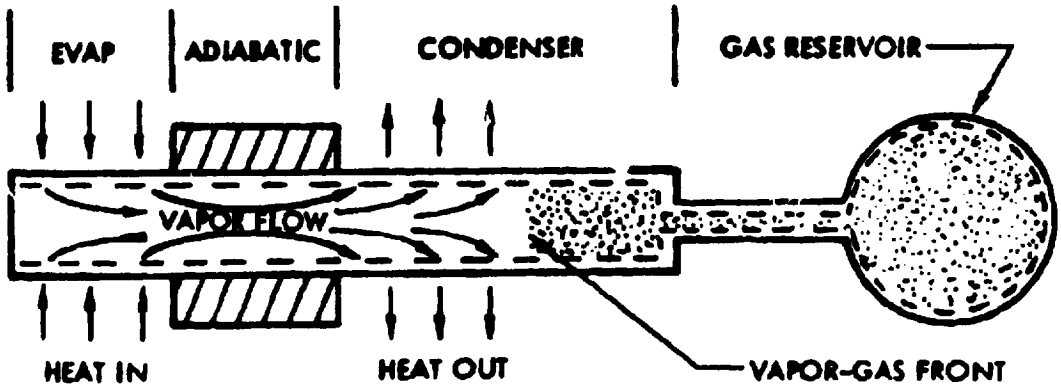

Figure 8.3.3-1 Illustration of the Operation of a Gas-Filled, Variable Conductance Heat Pipe.

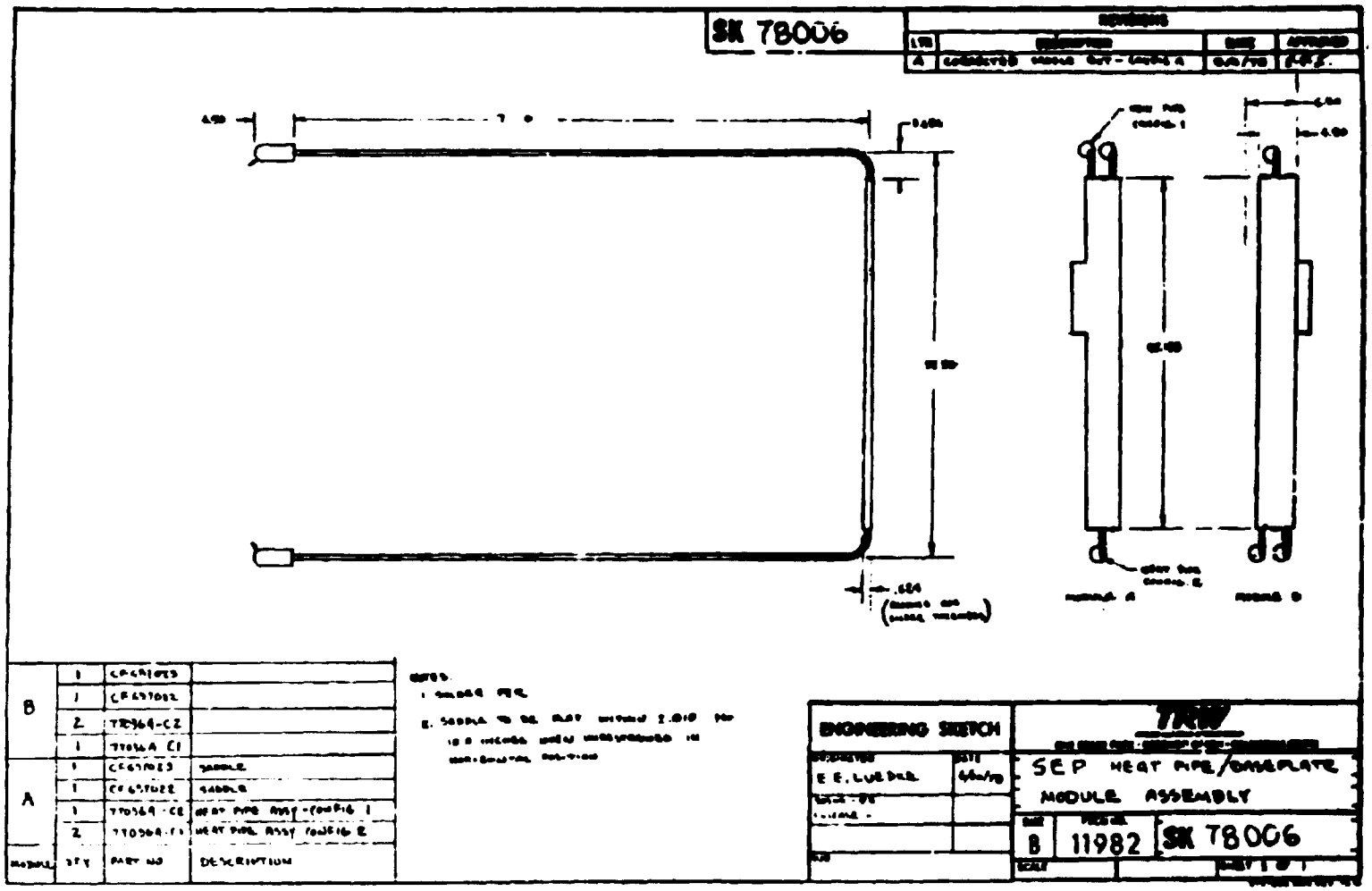

Figure 8.4.1-1 TRW Sketch of SEP BIMOD Heat Pipe Module Assembly.

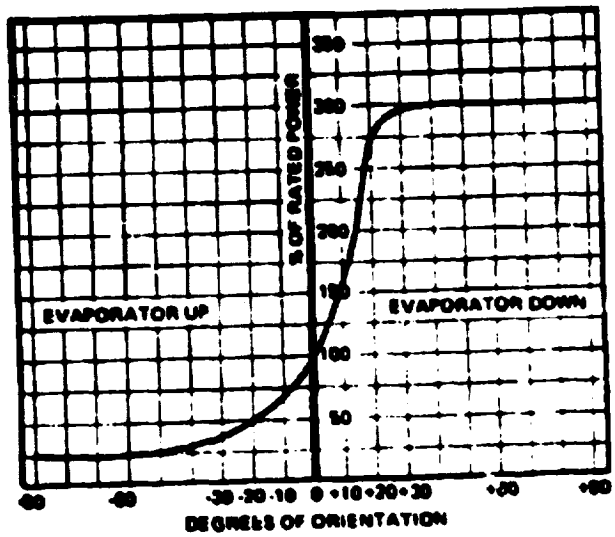

Figure 8.5-1 Illustration of the Effect of Gravity on the Thermal Transport Capability of a Heat Pipe.

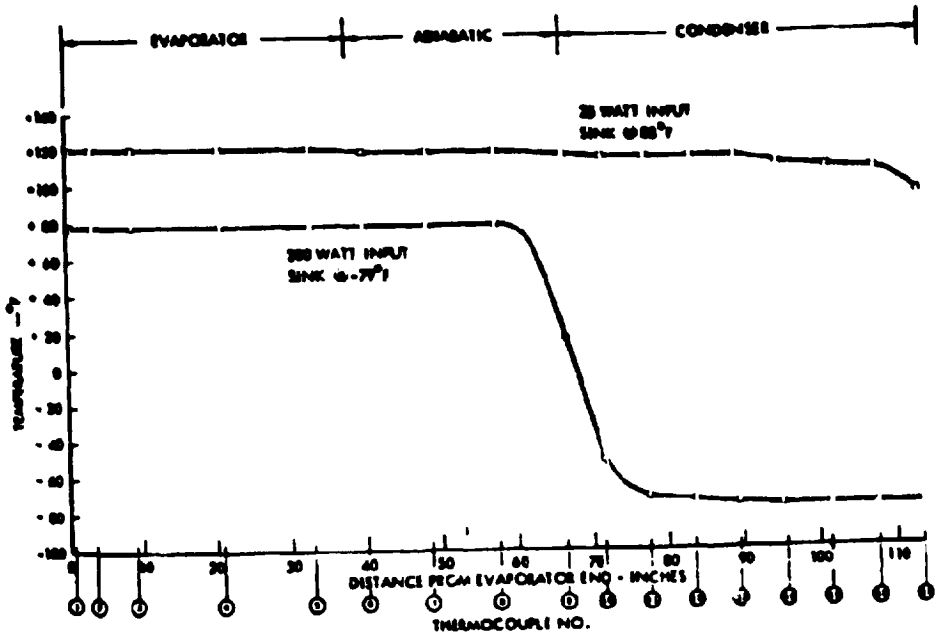

Figure 8.5-2 Temperature Profile of SEP Development, 0.070-Inch Artery Heat Pipe Showing Varying Sink Conditions.

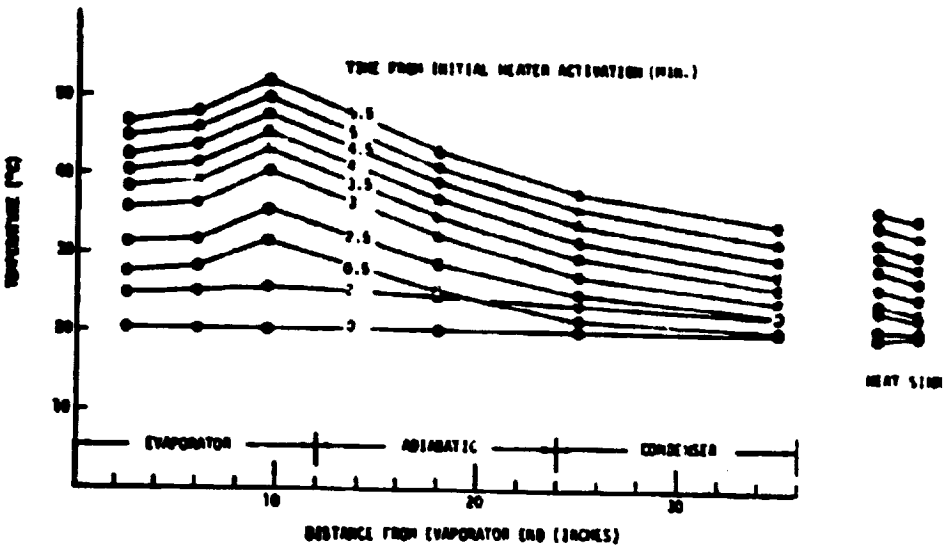

Figure 8.7-1 Temperature Distribution Along Ames Slab Wick A During Rocket Flight Heat Pipe Experiment.

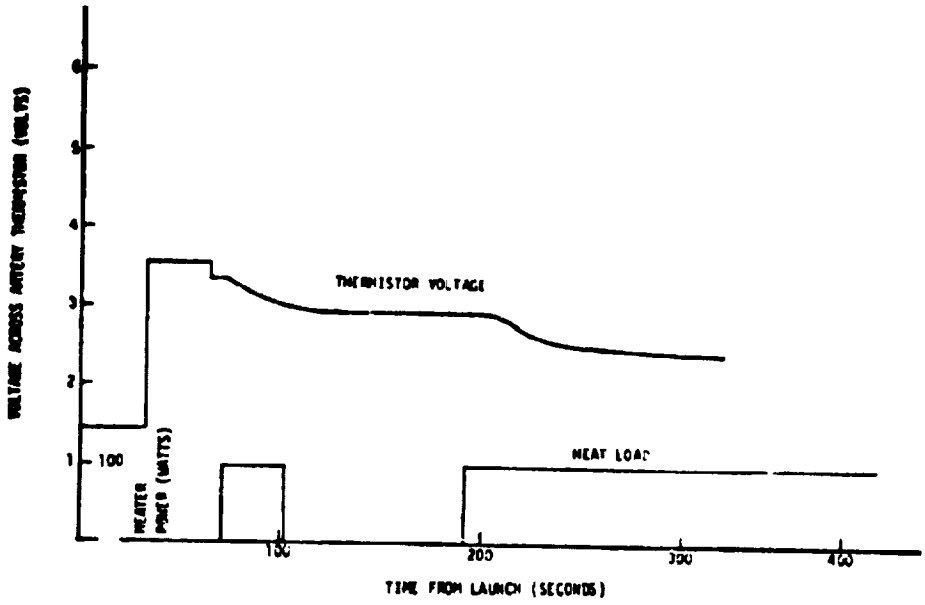

Figure 8.7-2 Artery Thermistor Voltage and Power Profile For Ames Slab Wick A During Rocket Flight Heat Pipe Experiment.

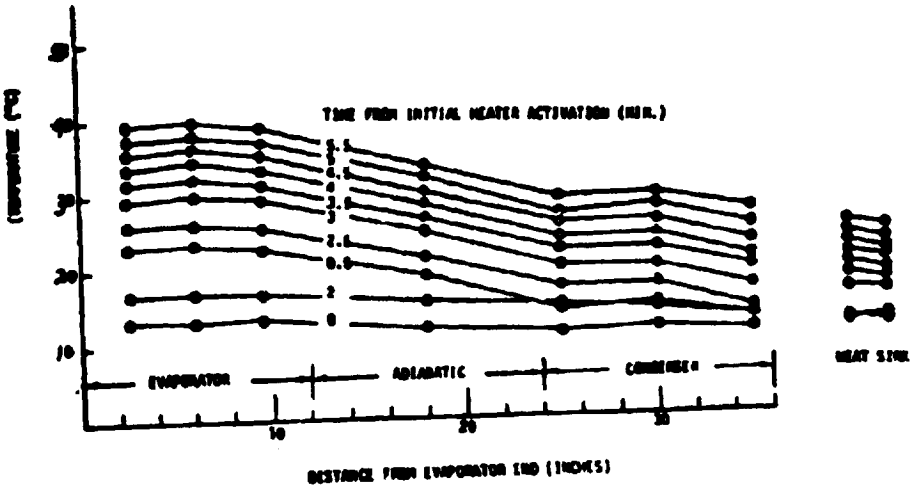

Figure 8.7-3 Temperature Distribution Along Ames Slab Wick B During Rocket Flight Heat Pipe Experiment.

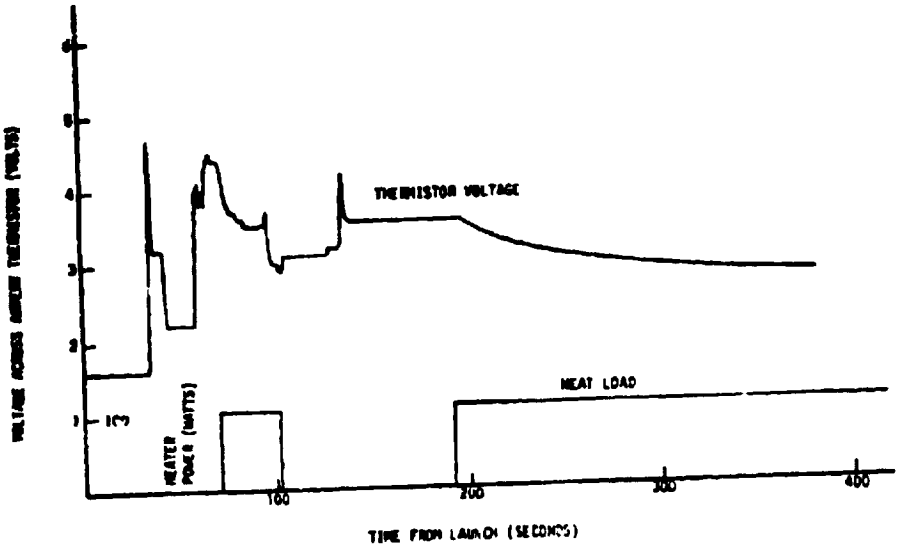

Figure 8.7-4 Artery Thermistor Voltage and Power Profile For Ames Slab Wick B During Rocket Flight Heat Pipe Experiment.

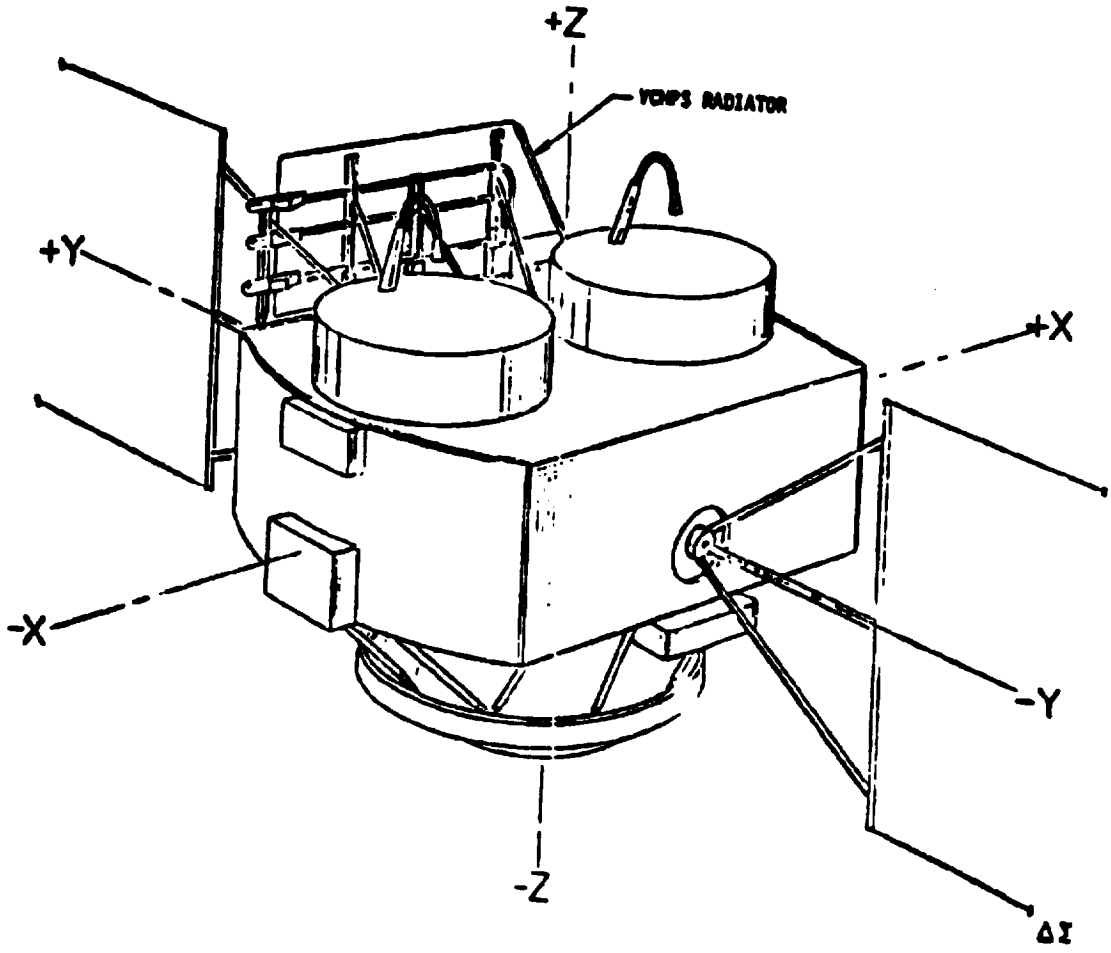

Figure 8.7-5 Location of Variable Conductance Heat Pipe System (VCHPS) on the Communications Technology Satellite (CTS).

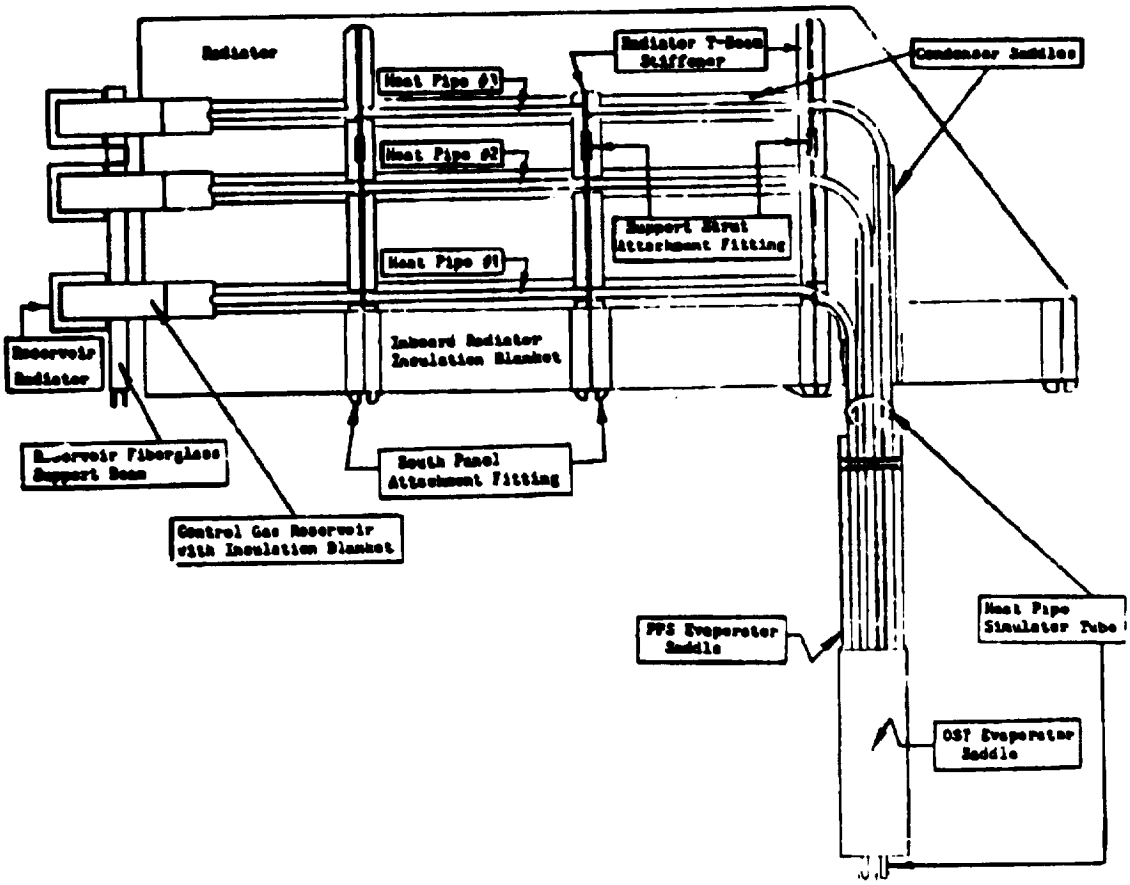

Figure 8.7-6 Illustration of Components of CTS Variable Conductance Heat Pipe System.

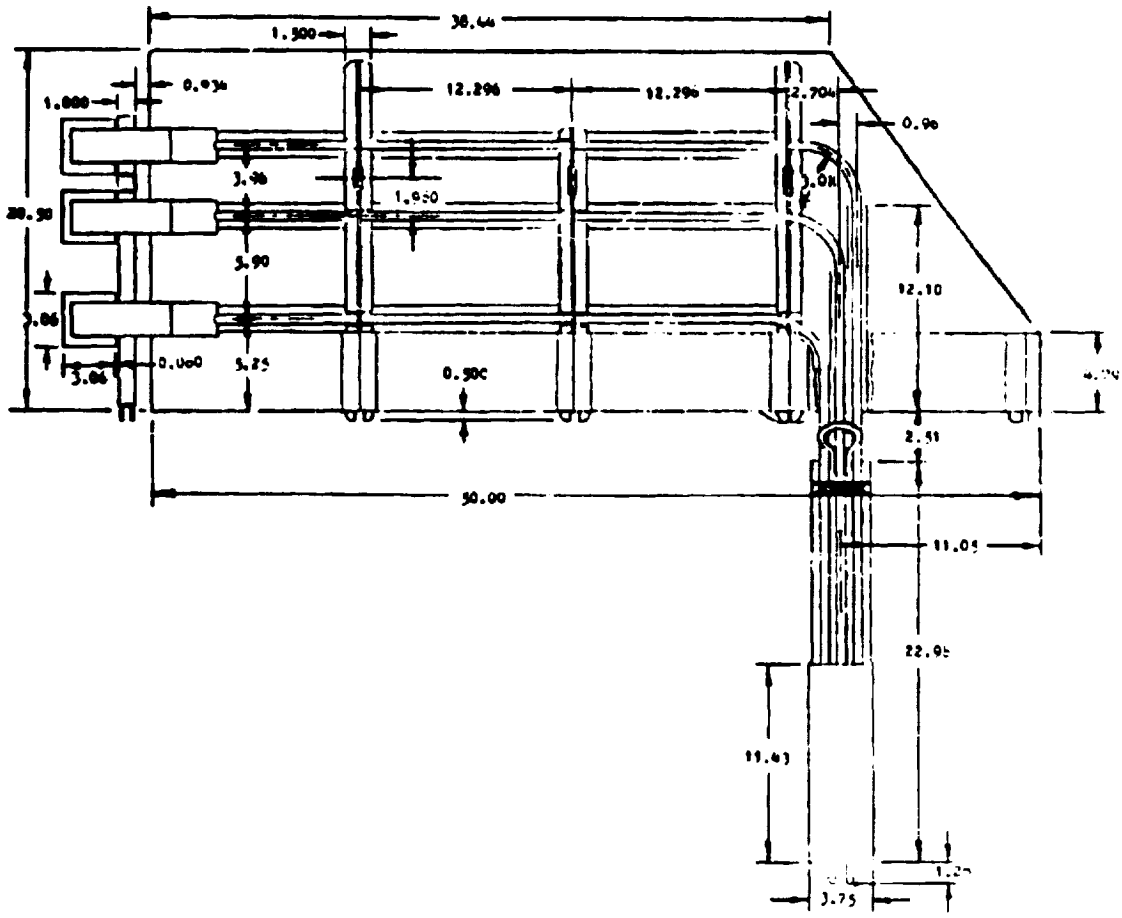

Figure 8.7-7 Physical Dimensions of CTS Variable Conductance Heat Pipe System.

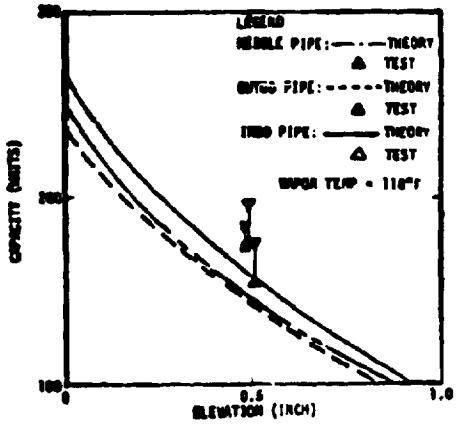

(a) VCHPS EM-001.

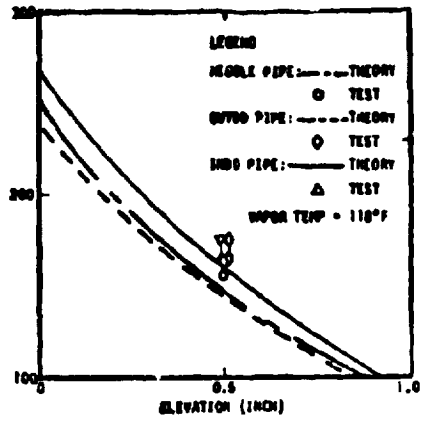

(b) VCHPS EM-002.

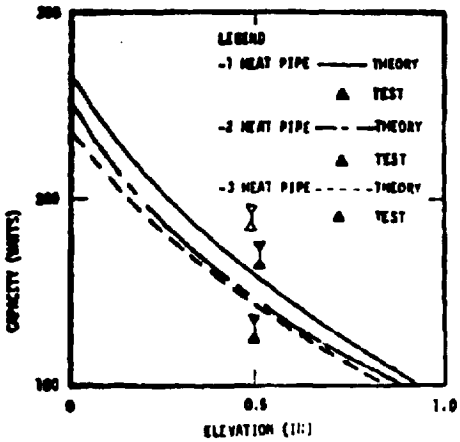

(c) VCHPS [illegible]4.

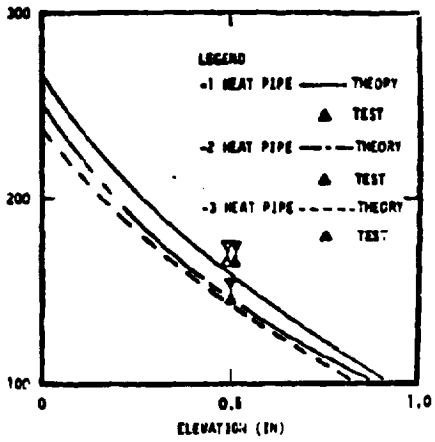

(d) VCHPS FM-005.

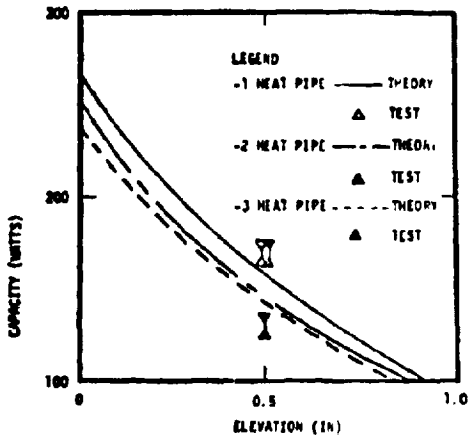

(e) VCHPS FM-006.

Figures 8.7-8

Performance of CTS Heat Pipes Fabricated by TRW.

9.0

BIMOD STRUCTURE/THERMAL CONTROL

Table of Contents

		Page
9.0	BIMOD Structure/Thermal Control	9-3
9.1	Reference Documents	9-3
9.2	Functional Requirements	9-3
9.3	Functional Description	9-5
9.3.1	Mechanical	9-5
9.3.2	Thermal	9-6
9.4	Interface Definition	9-8
9.4.1	Mechanical	9-8
9.4.2	Thermal	9-9
9.5	Performance Description	9-9
9.6	Physical Characteristics and Constraints	9-10
9.7	Development History	9-10
9.8	Applicable Documents Enclosed	9-16
9.9	Ground Support Equipment	9-16
TABLES		
9.3.2-1	Materials for Space Exposed Multilayer Insulation Blankets	9-17
9.6-1	BIMOD Engine System Masses	9-18
9.6-2	BIMOD Thermal System Masses	9-19
9.6-3	BIMOD Structural Masses	9-20
FIGURES		
9.3.1-1	Power Processor/Heat Pipe Structure	9-21
9.3.1-2	BIMOD Isometric	9-22
9.3.1-3	BIMOD Mass Simulation Model	9-23

Page

9.3.2-1 BIMOD Thermal Control Schematic.....9-24

9.7-1 Parametric Study of Radiator Fin Weight and Thickness Versus Radiating Capacity.....9-25

9.0 BIMOD Structure/Thermal Control

9.1 Reference Documents

9.1.1 Sharp, G.R.; Cake, J.E.; Oglebay, J.C.; and Shaker, F.J.: Mass Study for Modular Approaches to a Solar Electric Propulsion Module. NASA TM X-3473, 1977.

9.1.2 Farber, B.; Goldin, D. C.; Marcus, B.; and Mock, P.: Transmitter Experiment Package for the Communications Technology Satellite. (TRW Defense and Space Systems Group.) NASA CR-135035, 1977.

9.1.3 Spacelab Payload Accommodation Handbook, SLP/2104, Issue No. 1, Rev. No. 1, July 1978.

9.1.4 Sharp, G.R.: A Thruster Subsystem Module (TSSM) for Solar Electric Propulsion. NASA TM X-71683, 1975.

9.1.5 Maloy, J.E.; Sharp, G.R.: A Structural and Thermal Packaging Approach for Power Processing Units for 30 cm Ion Thrusters. NASA TM X-71686, 1975.

9.1.6 Sharp, G.R.; Gedeon, L.; Oglebay, J.C.; Shaker, F.J.; and Siegert, C.E.: A Mechanical, Thermal and Electrical Packaging Design for a Prototype Power Management and Control System for the 30 cm Mercury Ion Thruster. NASA TM X-78862, 1978.

9.1.7 DePauw, J.R.; Reader, K.F.; and Staskus, J.V.: Test Program for Transmitter Experiment Package and Heat Pipe System for the Communications Technology Satellite. NASA TM X-3455, 1976.

9.2 Functional Requirements

The bimodular (BIMOD) structure is designed to withstand

quasi-static accelerations of 10g's in the z direction (thrust) and 6 g's in the x and y directions. These load factors, which represent ultimate load factors, are conse. tively assumed to act simultaneously. In addition, the load factors are assumed to include the dynamic transient effects of the space transportation system/interim upper stage STS/IUS system as well as the dynamic response of the TSS mounted on the payload adaptor structure as given in reference 9.1.1. The complete static and dynamic (free vibration) analysis of the BIMOD is given in applicable document 9.8.1

Dynamically the BIMOD is designed to have a minimum resonant frequency 15 Hz when individually cantilevered from its power processor attachment points. This minimum frequency was established to preclude or minimize dynamic coupling between the BIMODs and the combined STS/IUS/SEPs system.

The BIMOD thermal control system is required to radiate to space all the waste heat (410 watts each) generated by its two power processors when operating at full power. The thermal control system is also required to maintain survival level temperatures for the power processors, propellant feed lines and the full length of the heat pipes at a minimum expense of heater power during non-operating conditions. Both of these requirements are imposed over a space environment ranging from 0.3 A. U.

to 3.0 A.U.

9.3 Functional Description

9.3.1 Mechanical

The two power processors (PPU) of the BIMOD are mounted back to back (fig. 9.3-1-1) against the heat pipe evaporator saddles which serve as the structural backbone of the power processor structure. When bolted back-to-back the power processors become one large fully enclosed rectangular box capable of resisting all tensile, compressive, bending, shear and torsional loads that may be imposed by the BIMOD truss attachment brackets (applicable document 9.8.2). The BIMOD truss resultant tensile, compressive and bending loads are carried to the interface module by four short columns that are integral with the long sides of the power processor box structure (fig. 9.3.1-2). However, the main function of the sides of the power processor is to support the ends of the individual cross beam modules of the power processors (fig. 9.3.1-1).

The PPU ends of the BIMOD radiators are rigidly attached to the PPUs by fiberglass shear panels and fiberglass angles which are designed to limit the application of dynamic or static acceleration loads to the heat pipes (applicable document 9.8.3). At the thruster end of the BIMOD the radiators are attached to the BIMOD aluminum truss by struts. These struts will allow longitudinal and lateral expansion and contraction of the thermal

control radiator/heat pipe condenser system while restricting radiator side sway and twisting (fig. 9.3.1-3).

The main functions of the BIMOD aluminum truss are to support the thrusters and the thruster ends of the heat pipe radiators. The thruster end of the truss is designed to be integral with the thruster gimbal system. Thus, the thruster launch acceleration loads applied in the X axis (fig. 9.3.1-2) are absorbed at one end of the thruster by a thruster pin which intersects a wishbone part of the truss in its structural plane when the thrusters are in the launch configuration (with their thrust axes parallel - see Section 7.3.2).

NASA drawing CR 638185 is the top BIMOD assembly drawing. A complete list of BIMOD drawings can be found in applicable document 9.8.4.

9.3.2 Thermal

The BIMOD thermal control subsystem (fig. 9.3.2-1) consists of multilayer insulation (MLI) blankets, variable conductance heat pipes, heat pipe radiators and supplementary heaters. Two power processors are mounted to opposite sides of a common heat pipe evaporator saddle and are wrapped with an MLI blanket. The MLI blanket consists of 20 layers of ¼ mil crinkled aluminized Kapton with an outer layer of 5 mil aluminized Kapton. The required temperature environment for the power processors is maintained by methanol-stainless steel heat pipes

(reference 9.1.2) and supplementary heaters. The supplementary heaters are required to maintain the component's minimum temperatures in a non-operating mode at distant A.U.. Each PPU dissipates 410 watts operating at full power with an efficiency of 87%. The minimum capacity for each variable conductance heat pipe is 220 watts. Two sets of three heat pipes (fig. 9.3.1-3) are embedded in the heat pipe evaporator saddle with one pipe in each set being a redundant pipe. The mounting arrangement of the heat pipes within the heat pipe evaporator saddle allows for heat dissipated from either PPU or both PPUs to be distributed to both heat pipe radiators of a BIMOD.

To size each radiator, the following assumptions were used: (1) the radiator has a view factor to the solar array of 0.05 and to space of 0.95, (2) there is no solar flux incident on the radiator, (3) the emittance of both the solar array and the radiator is 0.8 (silvered teflon on radiator), (4) the radiator dissipates heat at 50° C, and (5) the radiator is 0.020-inch-thick aluminum. Figure 9.3.1-2 shows the heat pipe radiator configuration along with its dimensions (69 cm wide by 183 cm long). In order to keep the variable conductance heat pipe working fluid, methanol, above its freezing point of -93° C, strip heaters are mounted in line with the heat pipes on the back side of the radiators.

In order to provide meteoroid and cometary dust particle protection, as well as prevent solar flux from impinging on the back of the radiators, MLI is also placed on the ends of the BIMOD perpendicular to the radiators and along the bottom of the BIMOD behind the thrusters (fig. 9.3.1-3). The composition of these MLI blankets is given in table 9.3.2-1.

The propellant feed lines are located in the BIMOD structural cavity. Thermal control is provided by a combination of isolation, insulation, and heaters to prevent freezing of the mercury.

The thrusters are exposed to both solar flux and to deep space. In order to provide thermal control for the thrusters in a non-operating mode with no solar flux, heaters are placed on the engine body of each thruster to prevent them from becoming too cold.

9.4 Interface Definition

9.4.1 Mechanical

The mechanical interfaces of the BIMOD occur at both ends of the BIMOD. At the thruster end the BIMOD is attached to adjacent BIMODs by struts. The only purpose of these struts is to prevent contact between adjacent heat pipe radiators during the launch acceleration environment.

The BIMOD is attached to the interface truss by eight

#10-32 high strength bolts. Two bolts are located at the end of each power processor side column. NASA Drawing CF 638168 gives complete details of the BIMOD envelope dimensions, structural attachment bolt pattern, and allowable flange sizes.

9.4.2 Thermal

The thermal interface at the power processor end of the bimod consists of a MLI blanket wrapped around the power processor as discussed in Section 9.3.2. The blankets provide thermal control of the power processors as well as providing autonomy of the power processors from the interface module and the BIMOD cavity.

The radiators, the MLI blankets perpendicular to the radiators at each end of a BIMOD and the insulation blankets between the radiators behind the thrusters provide the thermal interfaces between the BIMOD and the space environment.

9.5 Performance Description

The BIMOD structural/thermal system has not, as of March 20, 1979, been exercised as a system. However, the heat pipes have been individually tested (see Section 8.0) and do possess sufficient capacity to meet the thermal requirements of the power processors with two of six of the BIMOD heat pipes being fully redundant.

Although the BIMOD assembly has not been vibrated, the power processor (Section 6.3.2) has survived prototype

qualification vibration levels which were taken as one and one-half times the flight levels for Spacelab hard point mounted components independent of mass loading (see ref. 9.1.3).

Both vibration qualification and thermal vacuum qualification tests are planned in the near future for the live BIMOD (see Section 4.7). The gimbal system (Section 7.5) was also vibrated to these levels without damage.

9.6 Physical Characteristics and Constraints

The physical size of the BIMOD is 2.53 m tall by 0.69 m wide on the radiator face by 1.39 m deep. NASA Drawing CF 638168 contains a description of the envelope and protruding parts of the BIMOD.

The overall mass of the BIMOD is 137.5 kg. Table 9.6-1 gives a mass breakdown of the major BIMOD systems. The mass of the BIMOD thermal control system is 21.0 kg and a breakdown of that mass can be found in table 9.6-2. The total mass of the BIMOD structure is 10.1 kg. A detailed breakdown can be found in table 9.6-3

The BIMOD, is designed to withstand the functional requirements outlined in Section 9.2.

9.7 Development History

The BIMOD structural/thermal design is the culmination of an effort at developing a modular thrust subsystem that was begun in 1974. The earliest result was a

thrust module that contained one thruster with its own propellant tank and one power processor with thermal control by a combination of direct radiation from the PPU face through louvers and utilizing heat pipes for the remaining heat (see ref. 9.1.4).

The use of individual propellant tanks and feed systems for each thruster was not weight efficient and was thus dropped. The use of PPU's with thermal control by both louvers and heat pipes was not as efficient as heat pipes alone (see refs. 9.1.5 and 9.1.6). Also, thermal redundancy of heat pipes with individual PPU's was difficult to provide without incurring weight penalties. Because of these deficiencies the BIMOD concept was initiated in 1975.

The structural analysis of the BIMOD and the complete TSS was accomplished by using the Automated Multi-Stage Substructuring (AMSS) capability of NASTRAN (applicable document 9.8.5). Because of its modularity, this feature of NASTRAN proved to be very efficient in performing both static and dynamic (free vibration) analysis of the complete system. Each of the major components of the TSS (i.e., BIMOD, Interface Module, Heat Pipe Radiators, etc.) was first analyzed using the conventional NASTRAN formulation to determine preliminary design sizes. After preliminary sizing of the structural members in these substructures, the AMSS feature of NASTRAN was used to

assemble the components into a TSS and check the complete system, both statically and dynamically. The stage configuration could readily be changed by adding or deleting BIMODs with a minimum of time and effort by using this technique.

In addition to the development history of the overall BIMOD thermal/structural system there is a history of development of specific thermal/structural components.

1) Heat Pipes - Heat pipe development history is covered in Section 8.7.

2) Evaporator Saddles

a) Configuration Evaluation - One configuration had the saddles bolted around the heat pipes evaporator sections, with RTV-566 in the interface joints. Although it provided the flexibility to be able to easily replace heat pipes, it was rejected due to weight and manufacturing cost consideration. Another configuration had the saddles serve as the actual evaporator section envelope. This concept was rejected because of manufacturing and assembly difficulties and cost considerations. The configuration chosen uses a soft-solder joint between the heat pipes and saddles.

b) Solder Joint - The solder joint used on the BIMOD has flight history on the CTS heat pipe, on which both evaporator and condenser sections used soldered saddles. To evaluate the effects of thermal stresses in the solder joint caused by differential expansion between the stain-

less heat pipes and aluminum saddles, TRW performed a series of thermal cycling tests on samples of saddle/pipe solder joints. As indicated in reference 9.1.2, the joints successfully withstood this environment.

Assembly techniques have also undergone development efforts. At Lewis, samples were soldered in vacuum to determine if solder void area could be reduced. Results are still being evaluated. Also, a special soldering fixture was developed which provided both normal and lateral compression during soldering (this was necessary because of the saddle cross-section used) and which had a fast temperature-rise response (which was necessary to minimize the time the aluminum saddles spent at high temperature.)

Another solder joint reliability question considered was the potential deterioration of the solder joint due to amalgamation of the solder with mercury originating at the thruster. Although a catastrophic failure appears unlikely (the exposed joint areas are small and the mercury which would come in contact with it would probably not be a bulk amount), the potential problem could be eliminated by coating the exposed surfaces with a conformal coating of some type.

c) Saddle Cross-section Evaluation - During fabrication

of the SEP heat pipes, TRW pointed out that the BIMOD configuration put an asymmetric thermal load on the heat pipe when only one PPU was operating because of the simple evaporator saddle design being used. A thermal analysis was performed, and the saddle redesigned, to improve distribution of the heat from each PPU to both sides of the heat pipe slab wick. (See applicable document 9.8.6, and NASA Drawing CF 637022, Parts 13 and 14).

3) Condenser Saddles

a) Configuration Evaluation - The initial configuration considered for the condenser saddles was the same as CTS, with the same saddle cross-section and a soldered joint. Evaluation of the radiator design, however, resulted in a condenser saddle design which is dual purpose -- it not only helps carry the thermal load from the heat pipes to the radiator but also serves as a radiator stiffener along the length of the heat pipe. The final weight/unit length is comparable to the CTS design. RTV-566 is used as the interface material and the saddle is attached to the radiator with no. 2 machine screws.

b) RTV Joint - A thin layer of RTV-566 is used as the interface material to improve thermal conduction through the joint. The pot life following mixing of the catalyst with the base material is 30 to 45 minutes. Procedures and tooling design concepts developed for applying the

the CTS radiators to the heat pipe condenser saddles are being applied to assembly of the BIMOD radiator within the above time limitation. In addition, means of extending the RTV pot life are also being investigated.

4) Radiators

a) Thickness Evaluation - The initial configuration considered used a 0.040-inch radiator, similar to the CTS radiator. A study was performed to evaluate the effect of radiator thickness on radiator efficiency. Some of the results are summarized in figure 9.7-1. The SEP radiator is 0.020-inch thick, cutting the weight/unit area in half. A short radiator extension helped to compensate for the loss of thermal efficiency.

b) Material Evaluation - Thermal conductivity also affects radiator efficiency. Aluminum alloy 1100-H14 was substituted for the 6061-T6 used on CTS. Although alloy 1100-H14 is less strong mechanically the strength is adequate.

c) Thermal Coating - Silvered-teflon is being used on the emitting surface of the radiator. It has a history of space applications (including CTS). In addition, its durability has been tested in ground, temperature-cycling tests (ref. 9.1.7). Also, surface charging of the material, which is of especial significance in synchronous orbit, was investigated during the CTS program. Electrically conducting adhesive materials were tested,

one of which was used on the CTS radiator.

9.8 Applicable Documents Enclosed

9.8.1 Olex, Mark; and Zimpfer, Dennis: BIMOD Truss Analysis, August 1977.

9.8.2 Sharp, G.R.: Stress Analysis of BIMOD Tower to FM/PPU Attachment Bracket, May 1979.

9.8.3 Sharp, G.R.: Heat Pipe Condenser Support Vibration Calculations, May 1979.

9.8.4 BIMOD Assembly and Detail Drawing List. NASA Lewis Research Center.

9.8.5 Smallowitz, J.M.: The NASTRAN Structural Analysis of a Solar Electric Propulsion Module.

9.8.6 Thermal Analysis of FM/PPU Heat Pipe Saddle Designs. NASA Lewis Research Center Internal Memorandum January 1978.

9.9 Ground Support Equipment

See Section 4.9

Table 9.3.2-1 Materials for Space Exposed Multilayer Insulation Blankets

* ½ mil scrimmed Kapton with 1 mil black conductive coating on one side (outer layer)
* 1 mil double aluminized dimpled mylar
* 1 mil double aluminized flat mylar
* 1 mil double aluminized dimpled mylar
* 3 layers of 2 mil Tedlar
* 15 layers of ¼ mil double aluminized mylar separated by Dacron net
* 1 mil double aluminized Teflon

Table 9.6-1 BIMOD Engine System Masses

Description	Mass, kg (lb)
1. Functional Model/Power Processors with External Structure (2)	74.7 (164.7)
2. Thermal Control System	21.0 (46.3)
3. Thrusters (2) with Electrical Processors	20.7 (45.6)
4. Thruster Gimbal Systems (2)	6.8 (15.0)
5. BIMOD Structural Mass	10.1 (22.3)
6. Propellant Distribution	0.7 (1.5)
7. Miscellaneous (Gimbal Harness, Miscell. hardware, , RTV, etc.)	3.5 (7.7)
Total	137.5 (303.1)

Table 9.6-2 BIMOD Thermal System Masses

Description	Mass, kg (lb)
1. Radiators	4.17 (9.20)
2. Radiator Saddles	1.68 (3.71)
3. Radiator Saddle Hardware	0.31 (0.69)
4. Heat Pipes	7.56 (16.66)
5. Multilayer Insulation	1.81 (3.98)
6. Radiator Coating	0.44 (0.98)
7. Heat Pipe Evaporator Saddles	3.68 (8.12)
8. RTV at Evaporator Saddles	0.20 (0.44)
9. RTV at Radiator Saddles	0.20 (0.43)
10. Radiator Support Structure	
a. At FM/PPU	0.29 (0.64)
b. At Thruster	0.21 (0.46)
c. Radiator Support Heat Sections	0.32 (0.70)
11. Evaporator Saddle Solder	0.17 (0.38)
Total	21.04 (46.39)

Table 9.6-3 BIMOD Structural Masses

Description	Mass, kg (lb)
BIMOD Truss	9.7 (21.4)
BIMOD Truss to FM/PPU Attach Brackets	0.3 (0.6)
BIMOD to BIMOD Attach Struts	0.1 (0.3)
Total	10.1 (22.3)

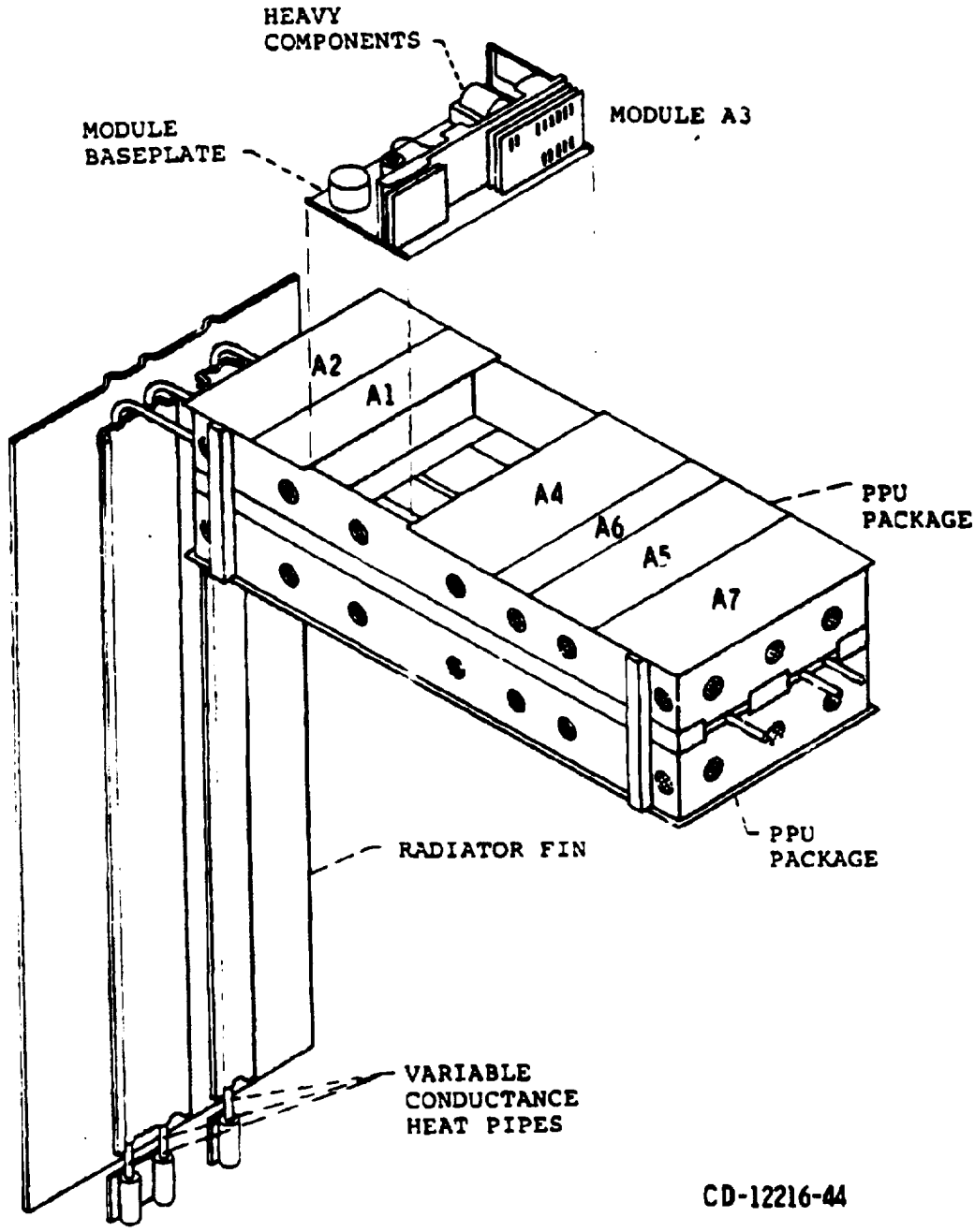

9.3.1-1 Power Processor/Heat Pipe Structure

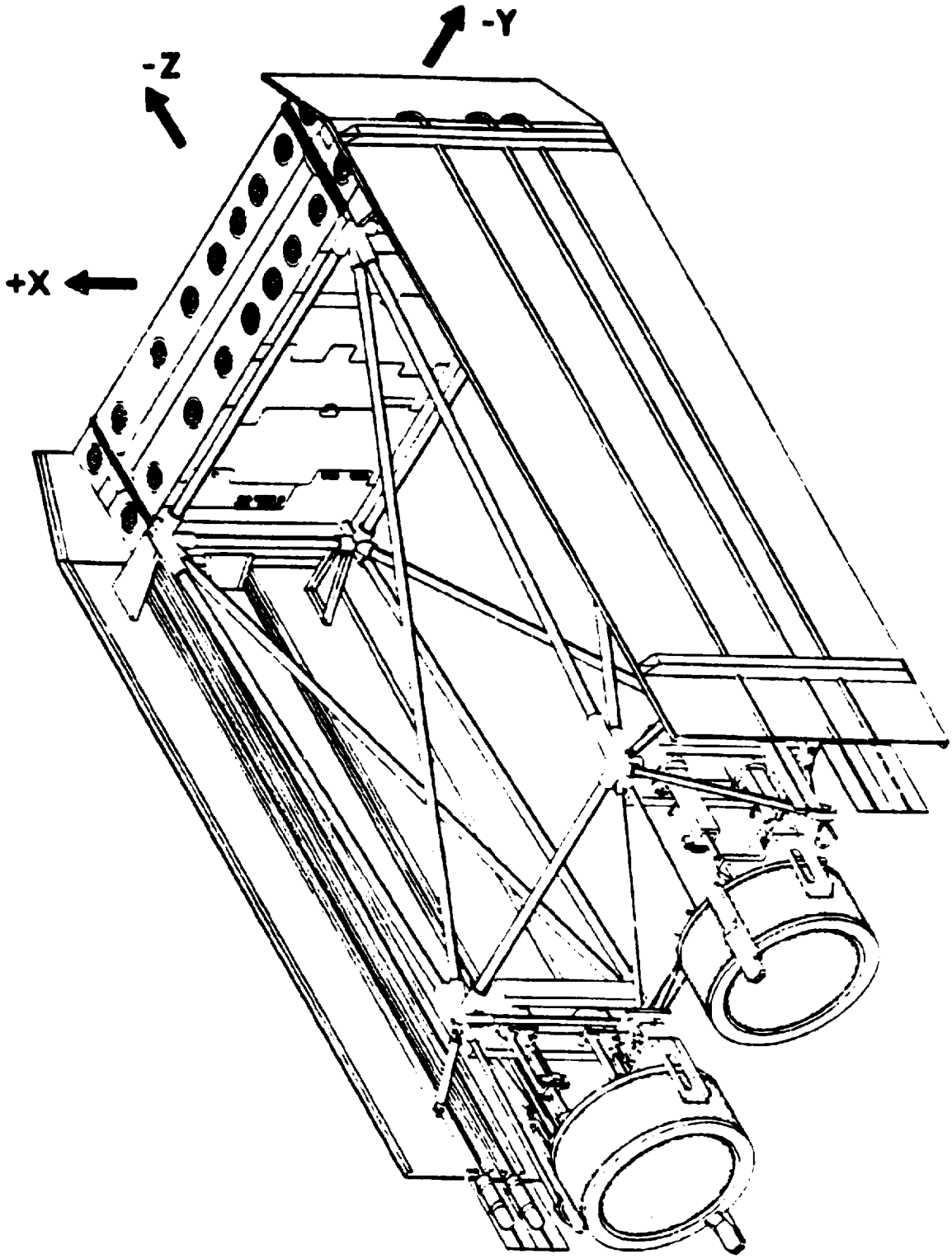

FIGURE 9.3.1-2 BIMOD ISOMETRIC

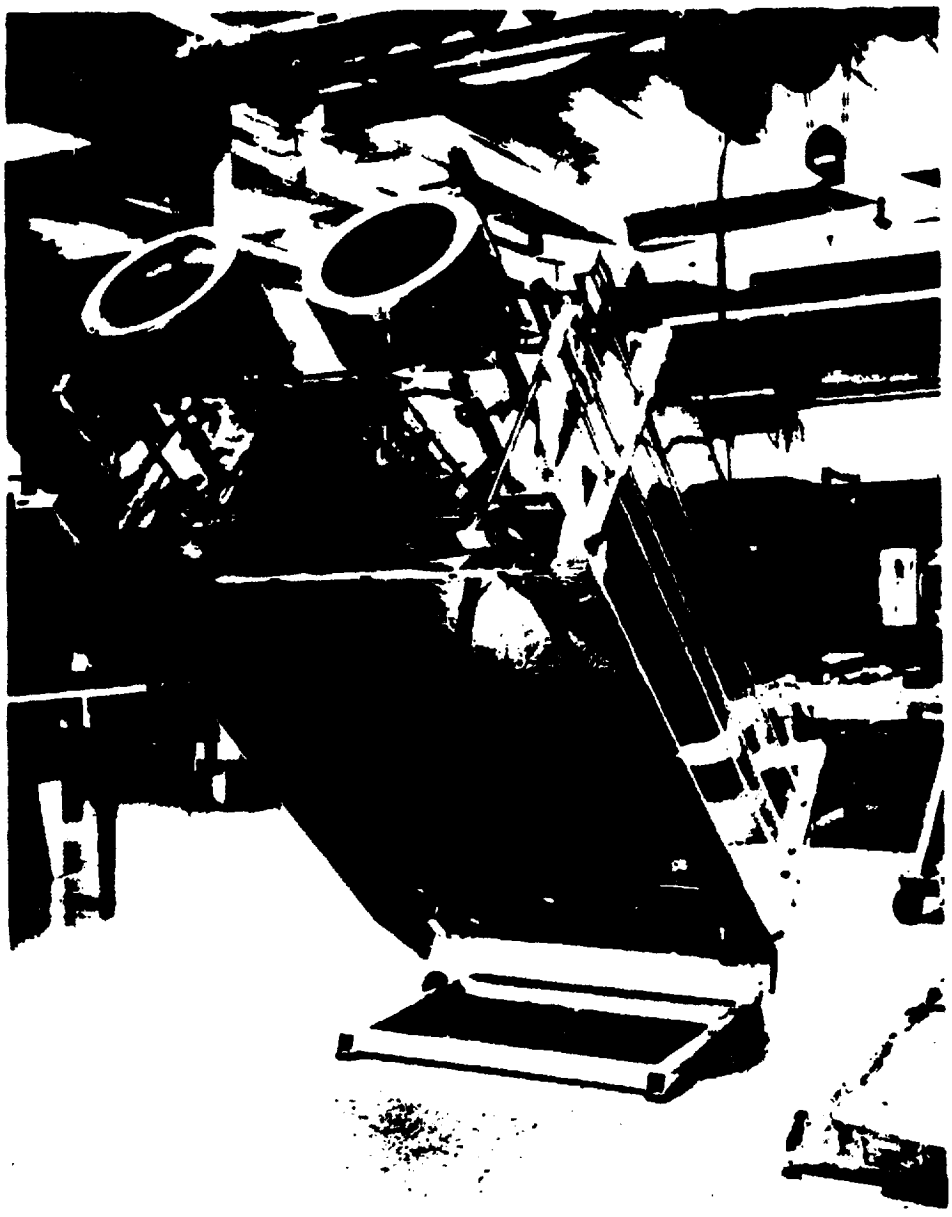

Figure 9.3.1-3 BIMOD Mass Simulation Model

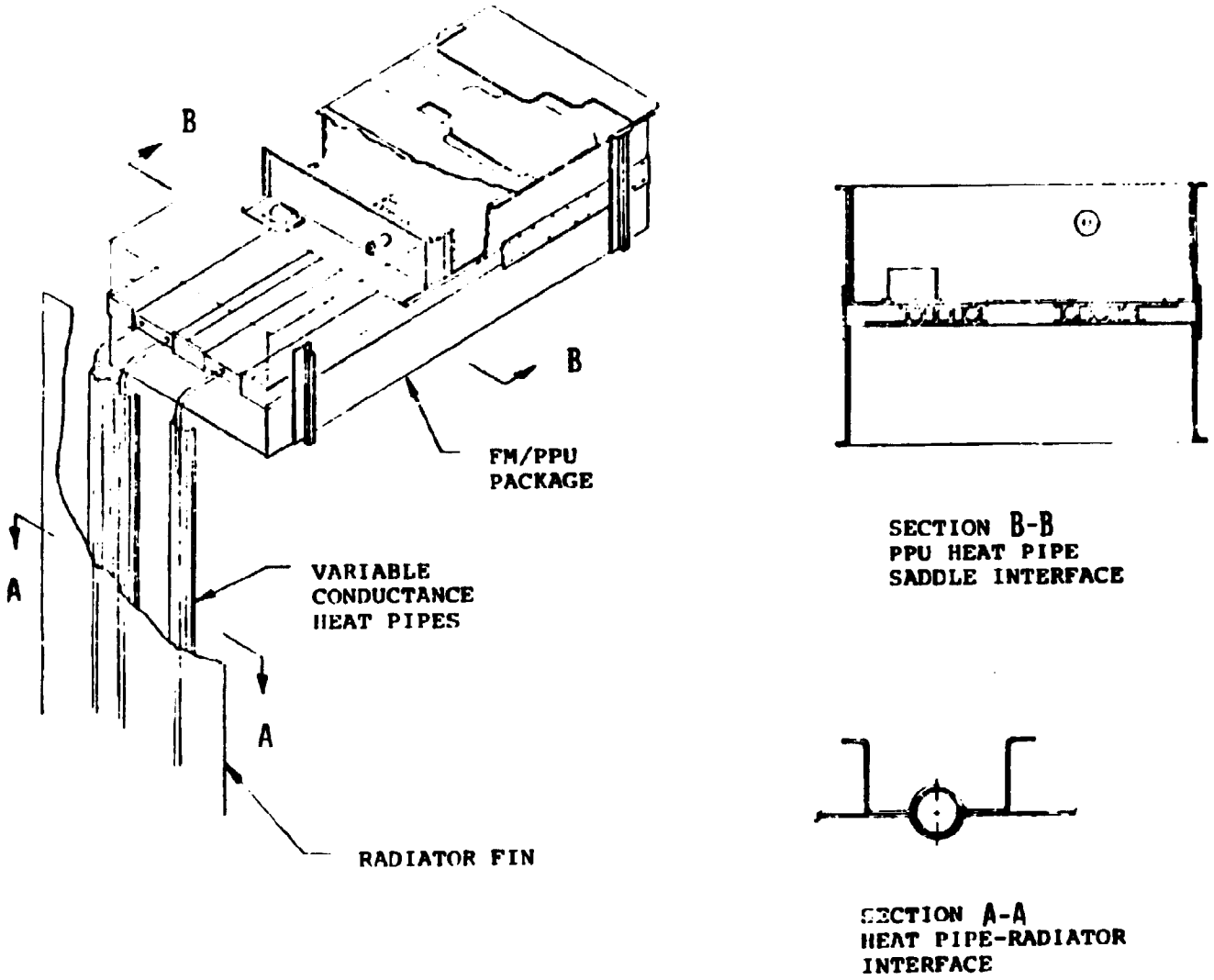

Figure 9.3.2-1 BIMOD Thermal Control Schematic

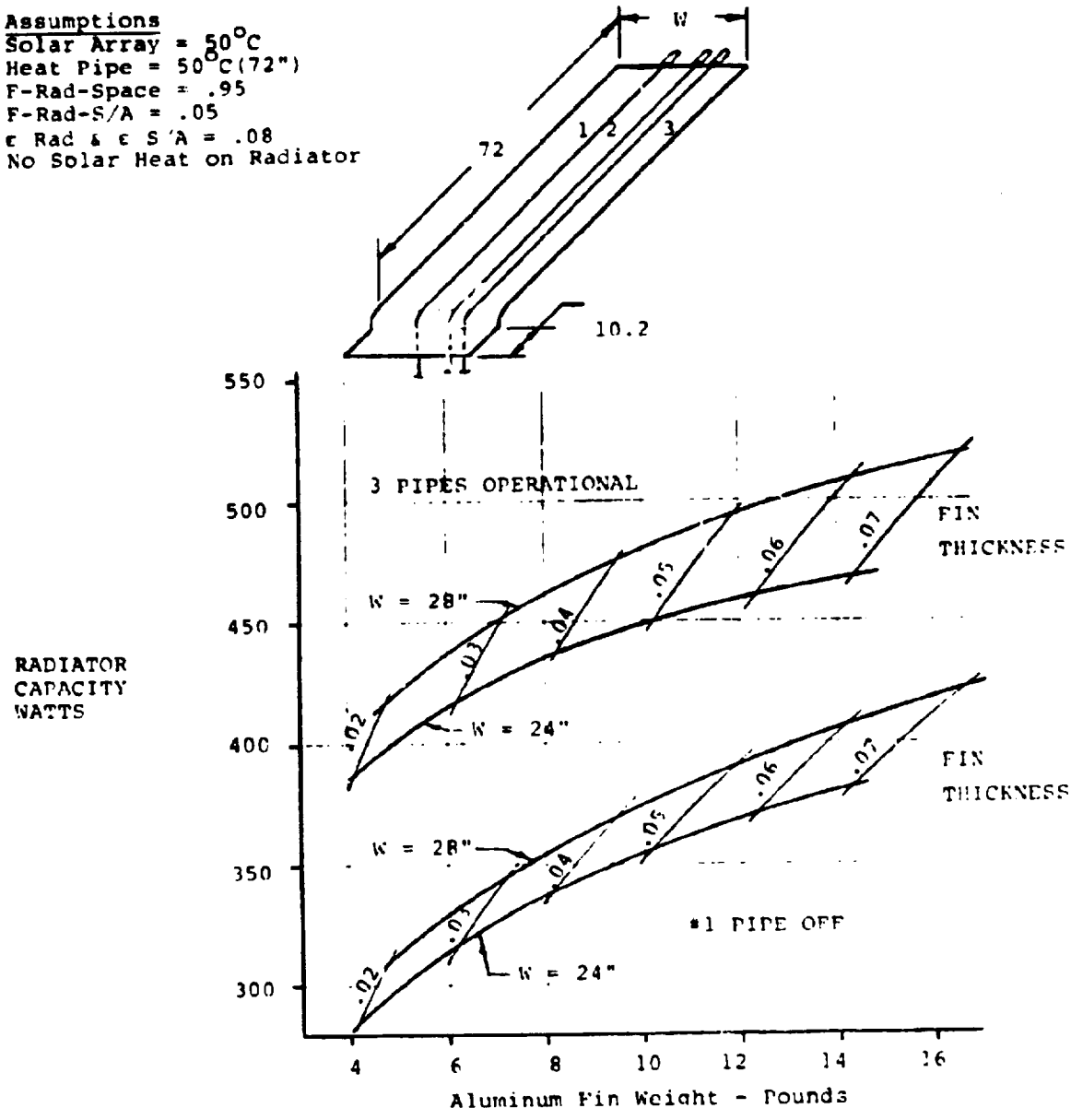

TOTAL RADIATOR WEIGHT = ALUMINUM FIN WEIGHT + SUPPORT STRUCTURE AND HARDWARE

Figure 9.7-1 Parametric Study of Radiator Fin Weight and Thickness vs Radiating Capacity

10.0

INTERFACE MODULE

Table of Contents

		Page
10.0	Interface Module	10-3
10.1	Reference Documents	10-3
10.2	Functional Requirements	10-3
10.3	Functional Description	10-4
10.3.1	Electrical	10-4
10.3.1.1	General	10-4
10.3.1.2	Thruster Controller	10-4
10.3.1.3	Power Distribution Unit	10-5
10.3.1.4	Thruster Gimbal Electronics	10-6
10.3.2	Mechanical	10-6
10.3.3	Thermal	10-7
10.4	Interface Definition	10-7
10.4.1	Electrical	10-7
10.4.1.1	Solar Array Power	10-7
10.4.1.2	Mission Module Battery Bus	10-7
10.4.1.3	Mission Module Computer	10-8
10.4.2	Mechanical	10-8
10.4.3	Thermal	10-9
10.4.4	Propellant	10-9
10.5	Performance Description	10-9
10.6	Physical Characteristics and Constraints	10-9
10.6.1	Mass	10-9
10.6.2	Power	10-9
10.6.3	Environmental	10-10

		Page
10.6.4	Configuration	10-10
10.7	Development History	10-10
TABLES		
10.6.1-1	Interface Module Mass Breakdown	10-12
10.6.2-1	Power Distribution Unit Power Requirements . .	10-13
FIGURES		
10.3.1.1-1	Interface Module Electrical Block Diagram . . .	10-14
10.3.2-1	Thrust Subsystem Interface Control Drawing . .	10-15

10.0 Interface Module

10.1 Reference Documents

None

10.2 Functional Requirements

1) The interface module shall serve as a power, control, structural, and thermal interface between the mission module and the BIMOD engine systems of the thrust subsystem.

2) The interface module shall receive power from the mission module and distribute power to the interface module equipment and BIMOD engine systems.

3) The interface module shall be capable of clearing thrust subsystem load faults on the solar array power busses.

4) The interface module shall receive commands from the mission module and upon command decoding shall either transmit the command or enter preprogrammed sequences to command the interface module equipment or BIMOD engine systems.

5) The interface module shall receive data from the interface module equipment and BIMOD engine systems, and shall either transmit this data upon request to the mission module or employ in the control of the thrust subsystem.

6) The interface module shall provide the structural interface between the mission module and thrust subsystem, shall provide a direct load path from the BIMOD engine systems to the mission module, and shall provide structural support for the interface module components.

7) The interface module shall provide a thermal interface between the mission module and thrust subsystem and shall maintain the interface module components within operational and nonoperational temperature limits.

10.3 Functional Description

10.3.1 Electrical

10.3.1.1 General

As shown in figure 10.3.1.1-1, the interface module electrical equipment shall include a thruster controller, power distribution unit, and gimbal electronics.

10.3.1.2 Thruster Controller

1) The thruster controller shall receive executive level commands from the mission module that are required to start, throttle, and shut down the thruster. The controller contains the thruster algorithms described in Section 5.0, Thruster and discussed in detail in Section 11.0, Thruster Controller. The controller implements these algorithms into appropriate commands

and transmits the set point commands, reference commands, and telemetry requests to the power processors. The controller monitors the operation of each thruster/power processor combination and provides corrective action in response to abnormal operation conditions indicated by interrupt flags generated by the power processor.

2) The thruster controller returns telemetry requested by the mission module computer of all thrust subsystem equipment.

3) The thruster controller controls the application and removal of 200 to 400 V dc power to the power processors and the 28 V dc regulated power to the power processors, mercury propellant valves, and thrust subsystem heaters.

10.3.1.3 Power Distribution Unit

The power distribution unit shall accept 200 to 400 V dc power and 28 V dc power from the mission module and distribute this power to the interface module equipment and BIMOD engine systems as commanded by the thruster controller. The power distribution unit provides switching of 28 V dc power for the power processors, mercury valves, and heaters. The power distribution unit provides for clearing of load faults on the 200 to 400 V dc bus. Signal conditioning for and formatting data from

thrust subsystem temperature and pressure transducers is performed by the power distribution unit.

Section 12.0 should be consulted for further detail.

10.3.1.4 Thruster Gimbal Electronics

The thruster gimbal electronics shall generate the drive signals for the thruster gimbal motors and shall format position data from the gimbal angle resolvers as required for transmission to the mission module computer.

10.3.2 Mechanical

The interface module truss shall be an aluminum tubular structure which provides a ten point mounting interface with the mission module on one side and mounting for each of the four BIMOD engine systems on the other side (see figure 10.3.2-1). The BIMOD loads are carried directly through the truss members to the mission module attachment points. The length and width of the structure is determined by the area required to attach the four BIMOD engine systems. The height is determined by the mercury propellant tank size.

The two mercury tanks are suspended by aluminum tubes which are tied directly to the mission module mounting points. The interface module also contains the mercury propellant manifolds, lines, valves, and pressure and temperature sensors as described in Section 13.0.

10.3.3 Thermal

The required temperature environments of the interface module components are maintained by a combination of multilayer insulation, passive radiators, and heaters. The multilayer insulation is wrapped around the entire interface module. The power distribution unit and gimbal electronics are mounted to passive radiators interior to the interface module cavity. The thruster controller is mounted to a passive radiator exposed to space. Heaters are employed on the propellant tanks.

10.4 Interface Definition

10.4.1 Electrical

The electrical interfaces between the interface module equipment and the BIMOD engine systems are defined in Section 4.4 and summarized in figure 10.3.1.1-1.

10.4.1.1 Solar Array Power

The solar array configuration unit of the mission module will provide nominal 200 to 400 V dc power at up to 125 amps to the power distribution unit. Harness from the mission module to terminals on the power distribution unit shall be carried as part of the interface module.

10.4.1.2 Mission Module Battery Bus

The mission module battery bus will provide 28 V dc power to the power distribution unit of the interface

module. The battery bus will provide power through eleven separate circuits: Eight circuits to the PDU for the eight power processors; one circuit to the PDU to provide heater power, mercury solenoid valve pulse, and gimbal electronics; and one circuit to each of the thruster controllers.

10.4.1.3 Mission Module Computer

The mission module computer will provide commands to and receive telemetry from the thruster controller and the thruster gimbal electronics in the interface module. The interface to the mission module computer from the thruster controller shall be through a first-in, first-out buffer memory which limits the data transfer rate to TBD bps and provides noise filtering. The buffer memory is connected to the mission module computer bus via a bus adapter unit. The interface from the gimbal electronics is similar to that for the thruster controller.

10.4.2 Mechanical

The mechanical interface between the interface module and the individual BIMODs is defined in Section 4.4.2. The interface module will be mounted to the mission module at the ten mounting points as shown in figure 10.3.2-1, LeRC Drawing CR 622760, Thrust Subsystem Interface Control Drawing.

10.4.3 Thermal

The thermal interface between the interface module and the BIMODs will be the multilayer insulation blanket placed across the top of each BIMOD. The interface between the interface module and the mission module will be the multilayer insulation blanket placed across the top of the interface module.

10.4.4 Propellant

The mercury propellant interface between the interface module and the BIMODs is defined in Section 4.4.4.

10.5 Performance Description

The performance of the interface module equipment is discussed in the following major sections: 11.0, Thruster Controller; 12.0, Power Distribution; 13.0, Propellant Storage and Distribution; and 14.0, Structure/ Thermal.

10.6 Physical Characteristics and Constraints

10.6.1 Mass

The estimated mass of the interface module is 158.7 kg. A breakdown of the interface module masses is listed in table 10.6.1-1.

10.6.2 Power

The power required of the solar array bus and mission module battery bus by the power distribution unit of the interface module shall not exceed the estimated values

listed in table 10.6.2-1. The power required of the mission module battery bus by the thruster controller(s) is TBD.

10.6.3 Environmental

The interface module shall be compatible with the structural and thermal design criteria identified in Section 14.0.

10.6.4 Configuration

The configuration of the interface module is defined by LeRC drawing CR 622760, Thrust Subsystem Interface Control Drawing, figure 10.3.2-1.

10.7 Development History

Design trades for the interface module have been conducted as part of the thrust subsystem definition and design effort since late 1975. One of the major trades conducted has been to consider a separate propellant tank for each thruster, a single common tank for all thrusters, or two common tanks for all thrusters. The first option was rejected because of the possibility of having to pump mercury from one tank to another should a failure occur in any element of a tank, power processor, thruster chain. The two common tank configuration was chosen over the single common tank approach because the total interface module structure mass favored the two-tank approach.

Another major trade was in the power interface. Concepts previous to the present design showed the shaft axis of the solar arrays attached to the interface module at a solar array drive mechanism. The interface module distributed solar array power to both the mission module and the thrust subsystem. Also, the interface module provided its own regulated power. In the present design, the solar array interface is with the mission module and the interface module receives both unregulated and regulated solar array power from the mission module. This simplifies the mechanical and electrical interfaces with the mission module. Also, functional duplication is reduced because only the mission module provides regulated power.

Another major design trade concerned the mechanical interface with the launch adapter tower. Early concepts showed that this mechanical interface was between the interface module and the launch adapter. In the present design, the launch adapter is attached to the mission module, thereby simplifying the interfaces between the thrust subsystem and the vehicle.

Table 10.6.1-1 Interface Module Mass Breakdown

Entry	Mass, kg
Interface Module Total	158.7
Truss Structure	24.8
Propellant Storage and Distribution	28.2
Thermal Control	9.9
Power Distribution Unit	54.4
Thruster Controller	6.8
Gimbal Electronics	8.0
Harness	26.6

Table 10.6.2-1 Power Distribution Unit Power Requirements*, Watts

Item	Off	Min Power	Max Power
Unregulated 200 to 400 VDC			
. Voltage Monitor	1	0	1
. BIMOD Input	(see table 4.6.2-1)		
Regulated 28 VDC			
. Signal Conditioning Circuits	1	TBD	50
. Propellant Tank Heaters	0	19	19
. BIMOD Input	(see table 4.6.2-1)		

* Measured at input terminals

FIGURE 10.3.1.1-1 INTERFACE MODULE ELECTRICAL BLOCK DIAGRAM

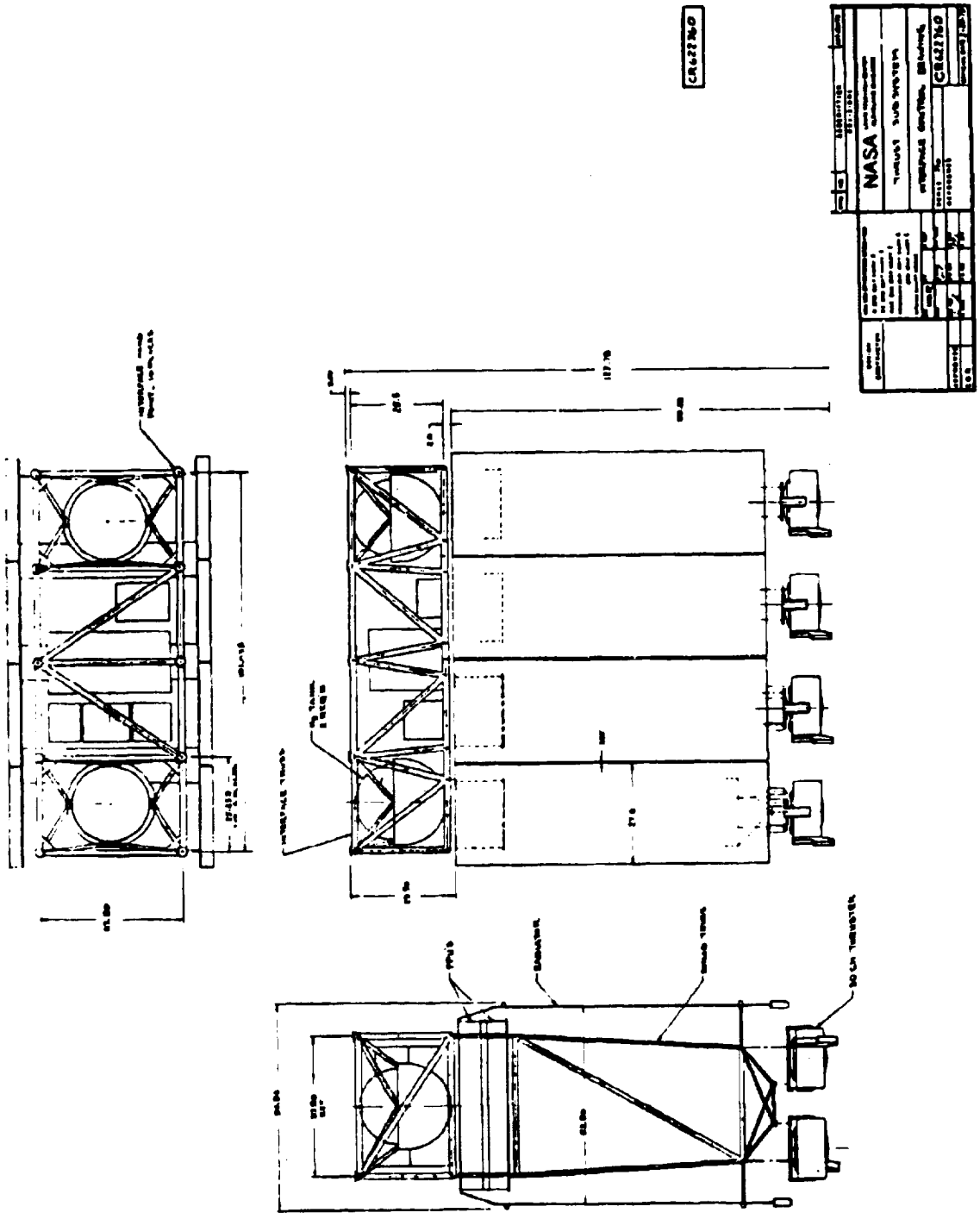

Figure 10.3.2-1 Thrust Subsystem Interface Control Drawing

11.0

THRUSTER CONTROLLER

Table of Contents

		Page
11.0	Thruster Controller	11.3
11.1	Reference Documents	11-6
11.2	Functional Requirements	11-6
11.3	Functional Description	11-9
11.3.1	Electrical	11-9
11.3.1.1	Controller Concept Description	11-9
11.3.1.2	Control Software Development	11-16
11.3.1.3	System Software Description	11-19
11.3.1.4	Thruster Control Software	11-27
11.3.1.5	Utility Routines	11-35
11.3.2	Mechanical	11-40
11.3.3	Thermal	11-40
11.4	Interface Definition	11-40
11.4.1	Electrical	11-41
11.4.1.1	Thruster Power Processing Unit	11-42
11.4.1.2	Spacecraft Telemetry, Command, and Control	11-43
11.4.1.3	Mercury Propellant Feed System	11-45
11.4.1.4	Power Distribution Unit	11-46
11.4.2	Mechanical	11-47
11.4.3	Thermal	11-47
11.5	Performance Description	11-47
11.6	Physical Characteristics and Constraints	11-48
11.7	Development History	11-48

		Page
11.8	Applicable Documents Enclosed.	.11-50
TABLES		
11.3.1.4-1	Pseudocommand Function Codes	.11-52
11 3.1.4-2	Thruster Status Codes.	.11-53
11.3.1.4-3	Allowable Pseudocommands as a Function of Thruster Status.	.11-54
11.3.1.4-4	STCHK Checks and Actions	.11-55
11.3.1.4-5	Thruster Operational Parameter Values and Status for STARTUP Phases.	.11-56
11.3.1.4-6	Reaction to PPU Off-Normal Flags	.11-57
FIGURES		
11.0-1	Space Vehicle Computer Control Heirarchy . . .	.11-60
11.3.1.1-1	Thruster Controller Conceptual Block Diagram.	.11-61
11.3.1.1-2	Each PPU/Computer Interface Interconnection . .	.11-62
11.2.1.1-3	Digital Word Structure	.11-63
11.3.1.2-1	Algorithm/Software Development System.	.11-64
11.3.1.2-2	PPU Interface Hardware/Software Driver Full Return Word.	.11-65
11.3.1.3-1	Basic Software Organization.	.11-66
11.3.1.4-1	Thruster Control Software Functional Block Diagram.	.11-67

11.0 Thruster Controller

Operation of a single ion thruster requires control of several voltages and currents through operational phases of preheat, ignition, operation, throttling etc. Algorithms for these control functions are described in Section 5.3.4.2. Implementation of these algorithms to control several thrusters simultaneously requires computer control. Control of space vehicle thrusters via ground computer is impractical due to the data rates and the transmission time delays that prevail in proposed planetary missions. Thruster control must be accomplished on-board the space vehicle.

This section describes progress that has been made in understanding the thruster control function. A space vehicle computer control heirarchy shown in figure 11.0-1 is proposed. It indicates the thruster controller controlling the several power processor-thruster systems in response to direction from a vehicle control computer. Information flow between the space vehicle computer and the thruster controller is ordinarily restricted to an executive level of detail such as instructions to operate certain thrusters at certain power and specific impulse levels, etc.

Development of flight-type thruster controller hardware and software has not begun. An understanding of software requirements has been gained through operation of two major test tasks of the Technology Readiness Program described in applicable document 11.8.1. The Mission Profile Life Test (MPLT) program to evaluate electric propulsion components in long term tests requires computer control of three thrusters simultaneously in ground test. The BIMOD test program described in applicable document 11.8.2 requires computer control of at least two thruster systems. The discussion of hardware and software contained in this section represents the state of knowledge acquired by preparing for and starting those test programs.

Details of these programs including flow charts and program listings are contained in applicable document 11.8.3. In addition to detailed programs developed to conduct test programs, some preliminary system studies have been done which treat the thruster control task in a general way.

This section (11.0) covers thruster operation and control only. Functions and requirements not necessary for this purpose are not discussed. The controller concept used in Sections 3.0 and 10.0 of this design

manual uses a more integrated approach which includes the following functions in the controller:

1) Power processor temperature monitoring and control.
2) Radiator and heat pipe temperature monitoring and control.
3) Mercury propellant tank pressure monitoring.
4) Mercury tank and propellant feed system temperature monitoring and control.
5) Control of solar array bus switching and fault clearing for the power processing units.
6) Solar array bus monitoring and telemetry.
7) Engineering telemetry digitization and processing.

In addition the system designer might choose to expand the controller to include:

1) Gimbal drive electronics.
2) Gimbal position command interface and processing.
3) Gimbal position readout electronics.
4) Gimbal position telemetry interface.
5) Other housekeeping and initialization functions.

However, none of these functions (no matter how essential for the operation of the thruster, power processors, and gimbals) is required for the implementation of the thruster control algorithms and anomaly correction techniques which have been developed and so they are

not discussed here.

11.1 Reference Documents

11.1.1 Extended Performance Solar Electric Propulsion Thrust System Study. (Hughes Space and Communications Group) NASA CR-135281, 1977.

11.1.2 SERT C Project Study. NASA TM X-71508, 1974.

11.1.3 Ward, J. W.: Application of a Minicomputer to the Control and Testing of Ion Propulsion Systems. AIAA Paper 73-1080, October 1973.

11.1.4 Low, C. A. Jr.: Digital Computer Control of a 30 cm Mercury Ion Thruster. AIAA Paper 75-380, March 1975.

11.1.5 Power, J. L.: Planned Flight Test of a Mercury Ion Auxiliary Propulsion System. I - Objectives, Systems Descriptions, and Mission Operations. NASA TM-78859, 1978. Also AIAA Paper 78-647, April 1978.

11.1.6 Power, J. L.; and Rotnem, J. O.: Operation of a Small Mercury Ion Thruster System in a Simulated Stationkeeping Mode, Using a Microprocessor, AIAA Paper 76-995, November 1976.

11.2 Functional Requirements

1) The thruster controller shall provide complete operational control for all ion thrusters in the system.

2) For any of the ion thrusters it controls, the thruster controller shall cause the following

operations to be performed in response to external commands:

a) Start the thruster

b) Throttle the thruster operating power level to any one of TBD (tentatively 100) points within its operating range.

c) Shutdown the thruster

d) Precondition thruster cathode tip and thruster neutralizer tip for operations.

e) Start and operate the thruster neutralizer only.

3) The thruster controller shall pass through to the power processing units (PPU) controlled, any designated thruster setpoint commands, reference commands, and telemetry requests. It shall return the requested telemetry data.

4) The thruster controller shall provide corrective action in response to abnormal operating conditions in the thrusters and their associated power processing units.

5) The thruster controller shall monitor the operation of the thrusters and associated power processing units.

6) The thruster controller shall control the application and removal of 28v power to the thruster

power processing units, thus providing overall on/off control to them.

7) The thruster controller shall be the sole communication channel to the thruster power processing units. It shall generate properly coded commands and transmit them to the PPUs in the correct format. It shall receive telemetry and status information from the PPUs and process the off normal flag generated by the PPUs.

8) The thruster controller shall control the operation of the solenoid valves in the mercury propellant feed system.

9) The thruster controller shall provide the sole command and telemetry interface between the thruster system and the remainder of the spacecraft.

10) The thruster controller shall return properly formatted telemetry information to the spacecraft.

11) Upon request, the thruster controller shall return full telemetry information concerning its own operation and the operation of any of the thrusters and thruster PPUs.

12) The thruster controller shall provide for the in-flight programming or replacement of its control algorithms to allow workaround for thruster or thruster PPU abnormalities.

13) The thruster controller shall accept status information concerning the solar array bus voltage applied to each thruster PPU.

11.3 Functional Description

11.3.1 Electrical

11.3.1.1 Controller Concept Description

Figure 11.3.1.1-1 is a conceptual block diagram of the thruster controller. It has four functional elements; an interface to the spacecraft telemetry, command, and control system(s), an interface to the thruster power processing units, an interface to the power distribution unit, and the control computer itself. Each of the interfaces will be discussed separately in this section. The functioning of the control computer will be described in sections 11.3.1.2 through 11.3.1.5. Requirements for redundancy, error correction, and failure detection arising from reliability considerations are not discussed.

1) Communications Interface with Spacecraft - The details of the communications interface to the spacecraft telemetry, command, and control system and associated control computer processing requirements are TBD as they are strongly dependent on the spacecraft design. The basic functions of the communications interface are (1) to receive suitably coded commands directed to the thruster

controller to flag their presence to the control computer and (2) to return telemetry and status information to the spacecraft. Commands received will either be directed to the control computer itself for the initiation of the various controlled operations or passed through to allow direct control of the thruster PPUs, the mercury propellant system valves, or the 28 V dc supply to the thruster PPUs. The communications interface will cause the control computer to initiate return of properly formatted telemetry data (in one or more selectable formats) and return that telemetry and status information as required.

Upon receipt of properly coded requests via the communications interface, the thruster controller will return to the spacecraft specific telemetry and status information from any of the thruster PPUs through the communications interface. In addition, detailed status information from the control computer software and playback of selected portions of the control computer memory will be made to the spacecraft via the communications interface.

The communications interface will input data from

the spacecraft for the reprogramming of selected portions of the control computer memory. Using this method, control constants will be changed to compensate for changes in thruster or thruster PPU operating characteristics. In addition it will be possible to work around some failures by reprogramming the control algorithms themselves.

The communications interface will also obtain time information from the spacecraft master clock and provide a seconds clock to the control computer for use in the sequencing of control operations.

2) Communications Interface with Thruster Power Processing Units - The power processor interface handles all transmission of command, telemetry, and status information between the control computer and the individual thruster PPUs. The power processor interface will select which power processor is to be commanded and activate its command bus; it will generate suitable parity for the transmitted commands; it will check for transmission and interpretation errors and abort execution if an error is detected; it will monitor the power processor off-normal flag line; and it will return telemetry data and transmission error and off-normal flag information to the control

computer. A schematic of the interface currently being used in the development systems is shown in applicable document 11.8.4.

Applicable document 11.8.5 contains a document entitled "Command and Telemetry Codes of Power Processors for the 30 cm Ion Thruster." This document contains detailed information on the interface between the individual thruster PPUs and the power processor interface, including timing, level, format, and a complete listing of all commands and their associated codes. A brief explanation of the interface will be given here for completeness.

Figure 11.3.1.1-2 shows the basic electrical interface for one thruster PPU. It is composed of five signal pairs optically isolated on the receiving end. The command sync line operates at four times the bit rate. The command enable line serves two functions; (1) it provides synchronization at the beginning of a command transmission sequence and (2) it aborts execution of the command currently being processed if it goes "low" before the end of command processing. The command line transmits coded commands and telemetry requests to the

thruster PPU in a serial digital format. The digital data line echoes back the command or telemetry request as it is clocked into the thruster PPU. The command echo is followed by execution information and telemetry data if requested. The line labeled "interrupt" is the thruster PPU off-normal flag line. It goes high when certain off-normal conditions described in applicable document 11.8.5 are detected by the power processor.

Figure 11.3.1.1-3(a) shows the basic transmission format for commands to the thruster PPUs. The bits are numbered in the order transmitted. Bit one is a parity bit which will be generated by the power processor interface. Bits 2 through 11 contain the command information from the control computer. Bits 12 thru 16 contain a unique thruster PPU address, also supplied by the control computer.

The power processor interface will transmit the first 16 bits to the selected thruster PPU and the power processor will echo them back to the power processor interface which will compare them on a bit by bit basis. If there is an error in transmission, the power processor interface will drop the enable line to its "low" state and abort

command execution. The sequence of operations now varies depending on whether an executable command or telemetry request was sent to the thruster PPU. If a command is to be executed by the power processor at bit time 24, bit 18 is set to "one". If a command was not sent to the power processor the power processor interface will drop the enable line to abort execution. If a telemetry request will be processed by the power processor beginning at bit time 18, bit 17 is set to "one" by the thruster PPU. If a telemetry request was not transmitted, the power processor interface will drop the enable line to its "low" state to abort execution.

The thruster PPU returns seven bits of digitized telemetry data or status flags beginning at bit time 18. The power processor interface will receive this data, append suitable error flags, and return the resulting data word to the control computer. The thruster PPU off-normal flag will be sampled each time a command is transmitted to the power processor and returned to the control computer as a flag bit in the return word. The detailed level of error checking will be performed because the control computer must, at all times, know the

exact status of each thruster PPU to negate potential damage to the thruster or power processor.

3) Power Distribution Unit Interface - The details of the power distribution unit interface in figure 11.3.1.1-1 are also discussed in section 12.0. This interface will permit the control computer to switch the individual thruster PPU on and off by controlling their 28 V dc housekeeping supply. This allows the thruster controller a backup control in the event of failures in the power processors on their command buses (power processors are shutdown to await higher level intervention) and allows the thruster controller to switch the individual thruster PPU to a known initialized state by cycling their 28 V dc housekeeping supply. In addition, this interface will permit the control computer to always be aware of the current status of the 28 volt supply to all power processors and so will prevent the possibility of false failure shutdowns.

The power distribution unit interface will allow the thruster controller to control all mercury propellant feed solenoid valves in the system. This will insure that propellant is always available to the operating thrusters and will allow

the control computer to be constantly aware of the valve status. In addition this will permit the thruster controller to implement certain reconditioning algorithms for thruster and neutralizer cathode/isolator/vaporizer assemblies which may require the removal of propellant feed temporarily.

The power subsystem interface will also return status information on solar array bus switching to the control computer on request. This will assure that no attempt will be made to start a thruster using an unpowered power processor, allow proper sequencing of solar array and 28 V dc housekeeping, and prevent the generation of false failure returns. (An unpowered thruster PPU looks like a failed power processor to the thruster controller.)

11.3.1.2 Control Software Development

The control computer shown in figure 11.3.1.1-1 will operate the thrusters using the thruster control techniques and algorithms embedded in software which has been developed and operated successfully on a minicomputer based software development system. This software is currently undergoing additional refinement and long term test evaluation. Of necessity, the development system provides a gross simulation of the ill-defined communications and power

distribution unit interfaces of figure 11.3.1.1-1. The simulation is obtained by simplified hardware and by software utility and driver routines. The complete development system, hardware and software, is fully described in applicable document 11.8.3.

A schematic diagram of the PPU communications interface is provided in applicable document 11.8.4. The PPU communications interface operates essentially as described in section 11.3.1.1 but parity is generated by the software. Figure 11.3.1.2-2 shows the return word from the communications interface. Bits 0 through 7 are a pass through of the power processor return bits. The power processor off-normal flag is passed through in the bit 8 position. If a transmission or interpretation error is detected, bits 9 through 11 are set by the hardware to indicate the type of error. If any of bits 8 through 11 is set, bit 15 is also set to permit easy software checking for their presence.

The computer I/O interface card at I/O select code 17 (octal) provides 16 relay contact closures which are processed through the 28 volt power/alarm control panel to provide shutdown control for the 28 V dc housekeeping supply to each of the thruster PPUs.

Another contact closure is used to provide a shutdown alarm.

The seconds clock provides time in seconds in the form of 8 BCD digits upon request. The clock time is input at I/O select codes 21 and 22 (octal). The clock time is displayed on the clock display panel via I/O select codes 21 and 22 (octal). The command display panel operating through I/O select code 20 (octal) is used to display the last command transmitted by the computer in binary format. The data in the clock display and the command display are interfaced to an adding machine tape type printer which is used to log all commands transmitted. Real thruster PPU commands (for pass through as well as "pseudocommands" (requests for initiation of computer automatic control operations) and data printing requests are entered into the manual command panel in binary format.

An optical paper tape reader is used to enter programs, data, and preset command sequences. Teletypes or Decwriters are used for data logging, status printing, and diagnostic and error message printing. The computer's front panel "switch register" is also used to provide a variety of initialization and operational inputs and diagnostic requests to the running software.

11.3.1.3 System Software Description

Figure 11.3.1.3-1 provides an overview of the software system. The system now operates three thrusters simultaneously but is expandable to eight or more thrusters with a minimum of changes. All data, control constants, flags, and calibration constants necessary for thruster operation and control (with the exception of timers) are stored in a large common block in high memory. The thruster control routines are written in a form which is independent of the thruster being controlled (except for timing functions). They obtain the information required for thruster operation from a special operational common block which is loaded with the proper data each time the thruster control routines are called.

1) Common Block - The overall layout of the common area is shown to the left of figure 11.3.1.3-1.
   a) PPU-Status Block - The first major section in the common area stores the last command for each type and/or subtype sucessfully transmitted to each of the thruster PPUs.
   b) Thruster Blocks - The third, fourth, and fifth segments of common are the individual thruster common blocks. All are identical. They start off with a series of identifiers, flags, and

variables used in the overall system operation. This is followed by a block of flags and variables used for the actual thruster control operations. Then there is a set of control constants (labeled "Thruster Constants") used to establish time sequences, define setpoints, etc. The last section of the thruster common blocks contains the power processor telemetry and reference command calibrations.

c) Operational Common - The second segment in common is called "Operational Common" and is the portion of common actually used by the thruster control routines. The first section in this segment contains flags and variables which are only used during a given pass through the thruster control routines and which do not have to be preserved. The second section is loaded word for word with the contents of the "Thruster Flags and Variables" portion of one of the thruster common blocks. Only this section is restored to the thruster common block after a pass through the thruster control routines. The third section of operational common is loaded with the various thruster

constants from one of the thruster common blocks word for word. The last section of operation common, "Selected PPU Calibration Constants" is loaded with those thruster PPU calibrations needed by the thruster control routines.

d) Command/Time Buffer and Miscellaneous - The second last segment of common contains storage for variables used by the various utility routines. The last segment is a buffer used to store commands or pseudocommands for automatic execution when the time associated with each command or pseudocommand has passed. Before any operations commence, the various constants are loaded into the common block. This loading specifies the hardware arrangement and "thruster addresses" to be used.

2) Main Control Sequence Loop - The center portion of figure 11.3.1.1-1 shows in simplified form the main control sequence loop.

a) Hardware and Software Permit Flags - An understanding of the control sequence requires a knowledge of two "permit flags" associated with each thruster, a hardware permit flag and a software permit flag. The hardware

permit flag may be set up during initialization to allow operation of a particular power processor/thruster combination. If it is on, 28 V dc housekeeping may be applied to the power processor. It is reset by the software during certain failure conditions (and the 28 V dc housekeeping removed) as a final protective shutdown. No normal software operation or pseudo-command will reset the hardware permit flag to allow thruster control operations. The software permit flag is turned on and off during the normal operations by two special pseudo-commands and may be turned off following loss of control situations which do not indicate a hardware failure. This permit flag allows an effective software lockout for a given power processor/thruster combination during normal operations.

The hardware permit flag is a permissive which when reset prevents operation of equipment which should not be operated. It can only be set manually. It can be reset manually or by software to prevent the use of hardware which is either inoperative or suspected of being defective.

The software permit flag is a permissive which when reset terminates all software operations with a given power processor/thruster combination. It is set by a special pseudocommand only. It is reset by pseudocommand to provide an "off" state in which extraneous commands from the command/time buffer or manual command panel are rejected. It is reset by software to stop further operations following loss of control situations which do not necessarily indicate hardware failure.

b) Main Control Sequence Loop Overview - As the title states, this is an overview section. Complete detail is contained in applicable document 11.8.3.

Referring to figure 11.3.1.3-1, operations commence at the entry point MPLTS. First there is an initialization process which allows setting of the hardware clock, printout of the identifiers for the thruster common blocks loaded, and setting of the hardware permit flags. The thruster flags and variables portions of the thruster common blocks for those thrusters whose hardware permit status has changed are then initialized. Application of

28 V dc housekeeping to the permitted power processors then occurs.

If desired, actual control operations then begin. The routine FLOOP is called which first updates the clock subroutine and all seconds timers and thruster run hours timers as appropriate.

Control operations start with the power processor/thruster combination associated with the first thruster common block and continue for the remaining power processor/thruster combinations in sequence. First the hardware permit flag is checked. If it is off, all further processing for that thruster is skipped. The software permit flag is checked and if it is "off" the new command flag and new command locations in common are checked for a "software permit on" pseudocommand. If the pseudocommand is found, the software permit flag is set "on" to allow thruster control processing to occur during the next pass through the main sequence loop. If both the hardware and software permit flags are on, thruster control processing will occur.

First, the routine STASH is called to load the operational common block with data from the thruster common block associated with the power processor/thruster combination currently being serviced. The thruster control subexecutive routine SEXEC is then called and the required thruster control operations are performed. The routine STASH is called again to restore the thruster flags and variables portion of operational common block (which quite possibly has been changed) to the current thruster common block. This operation is then repeated until all power processor/thruster combinations have been serviced.

Next, the hours timers for each power processor/thruster combination are set to run or stop depending on the current status of each combination. The manual command input panel is checked for the presence of a new command input. If present, the command or pseudocommand is placed in the appropriate thruster common block new command location and the associated new command flag is set. A check is made for the presence of a command/time tape containing commands or pseudocommands to

be executed automatically in the future at the times designated. If a tape is present, the next record is read from the tape and placed in the command/time buffer. Unless there has been a manual command input during this pass through the loop, the command/time buffer is checked for the presence of a command whose time has come. If found, the command is placed in the new command location in the thruster common block for the power processor/ thruster addressed and the associated new command flag is set.

Then the required data logging functions are performed. Either a telemetry scan is taken, a line of the data page is printed, or there is no operation. Finally, the flow returns to MPLTS where certain diagnostic functions may be performed. The loop repeats indefinitely as long as operation continues.

All operations take place sequentially and no interrupts are used. For input/output operations the software waits a specified time for the completion of the operation and either makes an error return or simply continues

depending on which is appropriate. Communication with the power processors, timing, command input, command display, command generation, command decoding, message and data printing etc. are handled by a series of utility routines which are distinct from the thruster control routines.

11.3.1.4 Thruster Control Software

Figure 11.3.1.4-1 shows diagramatically how the thruster control subroutines are accessed by the main program sequence loop. This section provides a general discussion of thruster control and anomaly correction software subroutines developed for use in current thruster test programs. Software details (flowcharts and listings, etc.) are provided in document 11.8.3.

The single most difficult task encountered during software development was to meet all of the timing requirements of the various control and correction algorithms for three thrusters running simultaneously. Additional refinements will be required to adapt the software to a system of eight or more thrusters. A description of the thruster control subroutines follows.

1) SEXEC - Thruster Sub-Executive Routine - SEXEC is called once for each active thruster every time around the main program sequence loop (FLOOP).

FLOOP provides a pseudocommand function code for each new command and sets a new command flag. SEXEC takes appropriate action depending on current thruster status. Refer to the following tables:

Table 11.3.1.4-1 Pseudocommand Function Codes

Table 11.3.1.4-2 Thruster Status Codes

Table 11.3.1.4-3 Allowable Pseudocommands as a Function of Thruster Status

SEXEC first checks a continuation flag (set and cleared by TCSCR) to see if the previous pseudocommand function has been completed. If not finished, the new command is saved in a wait queue. If finished, the new command is passed to TCSCR and the new command flag is cleared. TCSCR is called only if the continuation flag is set or a new command is waiting.

A second function for SEXEC is to call STCHK on a regular basis to monitor thruster conditions. The call to STCHK is programmed to occur at 5 sec intervals but the interval can be longer if there are delays anywhere in the program loop (e.g., a function being performed on one or more thrusters which requires more than 5 sec to implement). On

return from STCHK, SEXEC then turns control back to the main program.

2) TCSCR - Thruster Command Sequence Control Routine

When called by SEXEC, TCSCR initiates action to implement the function defined by the code passed to it (see table 11.3.1.4-1). In most cases TCSCR calls other subroutines to send commands or implement functions (i.e., throttle and shutdown) but TCSCR controls the timing and program flow for a full start which involves four major phases: a) Preheat High, b) Preheat low, c) Ignition/Heat, and d) Beam On (or run). The subroutines which implement the functional pseudocommands are PRCON for preconditioning, CMBLK for thruster startup, THROT for throttling, and STOP for thruster shutdown. These subroutines are described later. TCSCR also calls corrective action subroutines in response to problems detected by PPINT or STCHK. These include FIXIT to handle PPU off-normal conditions detected by PPINT, LOMOD and NTLMR which deal with main discharge low mode and neutralizer low mode respectively when detected by STCHK. These subroutines are also discussed later in this section.

3) STCHK - Thruster Status Checking Routine - STCHK

monitors certain thruster operational parameters looking for off-normal conditions. In some instances minor corrective actions are taken by STCHK but more typically, if STCHK detects a problem, it sets appropriate flags so that TCSCR can take corrective action on the next program loop. Table 11.3.1.4-4 lists the checks made during the various thruster status conditions, explains the purpose of the checks and notes action taken if any.

4) PRCON - Precondition Main and Neutralizer Cathode Tips - PRCON is a subroutine which controls the preconditioning of the emissive surfaces of the cathode and neutralizer tips. The procedure involves a timed high level heat phase, a timed cool down phase, a timed low level heat phase, and a final timed cool down phase. Heat levels and times are specified in the software common block. The only allowable functional pseudocommand during this activity is a shutdown (see table 11.3.1.4-3).

5) CMBLK - Transmit Selected Command Blocks - CMBLK is a subroutine which when called by TCSCR transmits one of five predefined blocks of commands. These are used to set up the various phases of a thruster startup. Table 11.3.1.4-5 shows the supply current and voltage values and on/off switch

status (0 for Off, + for On) for the four major phases of a startup sequence.

a) CMBLK (1) sets up the high level preheat phase for the neutralizer (STATUS = 2). This block is also used for the start neutralizer only pseudocommand (STATUS = 55).

b) CMBLK (2) sets up the high level preheat phase for the main discharge chamber (STATUS = 2) and is used with CMBLK (1).

c) CMBLK (3) sets up the ignition/heat phase which establishes the discharge in the main chamber and stabilizes temperatures before turning on high voltages.

d) CMBLK (4) is used to retreat to the low preheat phase if the main discharge and/or the neutralizer discharge is not lit at the end of ignition/heat timing phase. Only one retreat is allowed. On the second loop the thruster is shutdown.

e) CMBLK (5) sets up appropriate conditions for operation at low beam level and turns on the high voltage supply.

6) <u>THROT - Throttling Routine</u> - THROT, when called by TCSCR, will control throttling of the beam current to the requested setpoint. Five parameters

are varied during throttling. They are beam current, J_B, discharge current, J_E, screen electrode voltage, V_I, magnetic baffle current, J_{MB}, and neutralizer keeper voltage, V_{NK}. J_B is throttled in maximum increments of 0.1A until desired setpoint is reached. The appropriate values of J_E, J_{MB} and V_I are calculated assuming a linear relationship between each of them and J_B. V_{NK} is changed somewhat differently. Three values are defined in the thruster common block and used in different J_B ranges. A new throttle command will be accepted during throttling and if necessary direction of throttle will be changed and throttling will continue until last requested point is reached.

7) <u>STOP - Control Thruster Shutdown</u> - STOP, when called by TCSCR, implements a controlled thruster shutdown. If the beam current is not already at the low limit, a throttle is invoked before turning off the supplies. As an exception, if the thruster is in an off-normal condition and the correction routine decides the thruster must be shutdown, a special flag is set and the throttle is skipped. Also, in some extreme cases, the software permit will be turned off as a protective

measure.

8) PPINT and FIXIT - Detect and Correct Off-Normal Conditions - PPINT and FIXIT are very closely related in their functions. Table 11.3.1.4-6 lists the PPU off-normal conditions which they handle. The table also shows the actions taken by the two subroutines. The off-normal conditions are listed in priority order (i.e., the order in which PPINT will initiate corrective action). Subroutine FIXIT continues corrective action on a specific condition as directed by PPINT. If PPINT detects a condition of higher priority it suspends current action and initiates action on the new condition. No off-normal condition is ignored (except high accelerator current which is handled by another routine), because the off-normal flags are not cleared unless conditions are corrected or the thruster is shutdown. After the higher priority problem is fixed, PPINT returns to the lower priority problem for which corrective action was suspended.

9) LOMOD - Correct Main Discharge Low Mode Condition - LOMOD is called by TCSCR to correct a problem in the main discharge commonly called low mode (low beam current mode). The condition occurs when excess mercury flow through the main vaporizer

causes a point to be reached where the normally positive slope of the beam current versus flow curve goes through an inflection point and becomes a negative slope. Being on the negative side of the slope is called a "low mode" condition. In this condition the accelerator current, J_A, increases very rapidly as the flow increases. STCHK (11.3.1.4-3) uses J_A to detect the condition. LOMOD corrects the problem in the following general way. The main vaporizer is turned off to allow the flow to decrease. At the same time the discharge voltage is increased to prevent the cathode vaporizer control loop from driving the cathode flow too high. When J_A is back to normal, the main vaporizer is turned back on and the discharge voltage reduced. A shutdown is initiated if the condition still exists after a prescribed time and/or number of correction cycles.

10) NTLMR - Corrects Neutralizer Discharge Low Mode - The basic algorithm is under development and thus no reportable software is available.

11) ERROR - Handles PPU Command Transmission Errors - ERROR is called by PPUIO if a software or hardware error flag is set in the PPU during command transmission. ERROR initiates a shutdown immediately

on any software error but allows up to 10 hardware errors in any one hour period before shutdown.

12) TIMER - General Purpose Timing Routine - TIMER is a general purpose subroutine used for timing various phases of startup, low mode correction, etc. It resets and starts the timer and informs the calling routine when the time requested has elapsed. The software timer is kept updated by a system utility routine which monitors the system hardware clock.

13) MESSG and STPRT - Printing of Message and Status Information - MESSG and STPRT are utility subroutines which provide information to the operator which allow determination of the status and previous history of the PPU and thruster. Currently this information is printed on the operator's data logger. Other routines, of course, supply additional information to supplement the general information provided by MESSG and STPRT. These routines are especially important because they reflect the type of information which the thruster controller must provide in some appropriate form to the spacecraft controller and/or ground control.

11.3.1.5 Utility Routines

This section discusses some of the utility routines

which are important for an understanding of the software implementing the thruster control algorithms. Only a brief description is given to illustrate the types of functions provided. Routines concerned with conversion and printing of alphanumeric data, data logging, command/time buffer and tape servicing, command logging and similar functions are not included. The routines presented here handle timing, manual command input, pseudocommand decoding, command generation, communications with the power processors, conversion of telemetry returns and reference commands, and the generation of telemetry averages.

1) CLOCK and FCLCK - Clock Driver - CLOCK handles input and conversion of the time in seconds from the hardware clock. "Current software time" is a double precision integer variable (32 bits) representing the time in seconds. CLOCK may be called in two modes. In the first mode the value of "current software time" is simply returned. In the second the hardware clock is interrogated and following the return, the eight BCD digits are converted to double precision binary and used to update "current software time". If the value of the time from the hardware clock is less than the value of "current software time" or if there is no

response from the hardware clock, the value of current software time remains unchanged. The value of current software time is returned to the calling program.

2) UPSEC and FUPSC - Software Timers - UPSEC provides 24 second timers to a maximum value of 32,766 seconds. In the reset mode the routine stores as a negative double precision number the value of current software time (from CLOCK following an update) in the designated timer start value location. In the read mode the routine obtains a value for current software time from CLOCK (updated) and adds the negative start value for the designated timer. This value is then returned as the current timer value.

3) WOMAN - Command Input - WOMAN handles the input of commands and data control words from the manual command panel. A parameter in the call is set to minus one if there has been a command or pseudo-command input operation. It is set to plus one if there has been no successful command or pseudo-command input operation, if there was a data control word input operation or if there was no input operation. If a manual command input is present, it is first decoded to determine whether it is a

command/pseudocommand or data control word. If it is a data control word, it is placed in the data control flag location in common and processing terminates. If it is a command/pseudocommand, the new command flag is the appropriate thruster common block is tested to see if there is an unprocessed command waiting. If one is waiting, it is checked to see if it came from the manual command panel ("new command time" zero) or from the command/time buffer. If it came from the buffer, it is restored to the buffer along with its associated time. The new command is placed in the thruster new command location, the new command flag is set, and the new command time is set to zero. A message is then printed and the flow returns to the calling program.

4) DCODE - Command Decoding - DCODE examines commands, pseudocommands and data control words and returns a series of parameters which characterize the command. Data control words are differentiated from other inputs. If the input is not a data control word, a command status number is returned. For operational pseudocommands this number is the "thruster status number" from the control software corresponding to the status required by the pseudocommand. Inputs which are not recognized as data

control words or valid pseudocommands are presumed to be power processor commands. If the input is a throttle pseudocommand, a parameter is set to the throttle point number.

5) KOMND - PPU Command Generation - KOMND performs the following functions: it accepts requests for command generation as two decimal numbers; it generates the corresponding command bit pattern; it appends the proper thruster address code for the power processor/thruster combination currently being serviced; it calls PPUIO and transmits the command it has generated; it examines the return from PPUIO for errors and PPU off-normal flags; if an error is detected, it prints an error message and calls the error routine, ERROR; if an off-normal flag is detected, it interrogates the power processor "interrupt status" register, prints a message, and then calls the "interrupt" routine PPINT; as appropriate it loads stripped power processor return data, the PPUIO full return words, and an interrupt flag into operational common; and returns to the calling program.

6) PPUIO - PPU I/O Driver - PPUIO is the power processor communications interface driver routine. When called, PPUIO first generates correct parity

for the command. Next an attempt is made to compute a storage address for the command in the power processor status blocks at the start of common. If none can be computed, an error return is made.

The command is now transmitted to the power processor. If a transmission or interpretation error occurs, the command is retransmitted up to a maximum of five times. All error flag bits are then returned and processing stops. If the command is successfully transmitted in one of the five tries, the command is stored in one of the thruster status blocks at the beginning of common. If the command was a telemetry request, an immediate return is made. If the command was a setpoint, reference, or on/off command, it is printed on the command/time printer and then a return is made to the calling program.

11.3.2 Mechanical

This item is to be determined because flight-type hardware design has not been done.

11.3.3 Thermal

This item is to be determined because flight-type hardware design has not been done.

11.4 Interface Definition

11.4.1 Electrical

The thruster controller has interfaces with the following equipment:

1) Thruster power processing units for the transmission of commands and telemetry requests to these units and the return of telemetry and status information.
2) Spacecraft telemetry, command and control system(s) for the receipt of commands, reprogramming of the control computer, receipt of time information, and the return of telemetry, status, and program loading information.
3) Mercury propellant feed system for the control of mercury propellant valves (probably via the power subsystem) and possibly for the measurement of propellant tank pressure to allow determination of propellant use rates and possibly the diagnosis of possible propellant feed problems.
4) The power distribution system for (a) the on/off control of 28 V dc housekeeping to the thruster power processing units, (b) possible return of power processor 28 V dc housekeeping status information, (c) return of status information on the thruster power processing unit solar array bus switching, and (d) the supply of housekeeping power to the thruster controller itself.

These interfaces will be examined in greater detail in the following sections. Since hardware has not been designed, specific information is not available in many areas.

11.4.1.1 Thruster Power Processing Unit

The thruster controller distributes commands to the power processors on an individual basis. To be compatible with present power processor designs, the command and response format must be that described in detail in applicable document 11.8.5. The thruster controller should perform both a transmission verification (echo check) and an interpretation verification and abort execution if either check is failed by dropping the enable line. The command bit rate shall be TBD (tentatively 10kc). The interface shall process all commands listed in the document mentioned above.

The allowed power processor address codes and their power processor/thruster assignment are to be determined. The present development system and software uses addresses assigned uniquely to each power processor serial number. System analysis may later show that addresses should be assigned to specific thruster physical locations on the flight vehicle or be defined by some other determining factor.

The thruster controller shall meet all signal level and timing requirements specified in Appendix A to applicable document 11.8.5. The minimum command transmission rate shall be TBD (tentatively 100 commands per second).

11.4.1.2 Spacecraft Telemetry, Command, and Control

The thruster controller receives all commands and returns all telemetry concerning thruster operations via this interface. The spacecraft should provide the capability for storing timed command sequences of up to TBD commands (tentatively 250) and causing the thruster controller to execute these commands as required. The option shall be provided for stopping the sequence should any command fail to execute.

The interface will provide for the following general commands:

1) Start designated thruster.
2) Throttle designated thruster to any one of TBD (tentatively 100) points.
3) Shutdown designated thruster.
4) Precondition designated thruster.
5) Start and operate neutralizer of designated thruster.
6) Additional status control commands.

In addition the telemetry, command, and control system will process and the thruster controller will receive and pass

through to the designated power processor/thruster combination all power processor commands shown in applicable document 11.8.5. Responses from the power processors arising from such commands are returned by the thruster controller via the telemetry, command, and control system.

The thruster controller will format and return telemetry to the telemetry, command, and control system at the following rates:

Low Cruise	TBD bits per seconds
High Cruise	TBD bits per second
Initial Start	TBD bits per second
Malfunction	TBD bits per second

The rates shall be selectable on command from the telemetry, command, and control system. In addition the thruster controller will return the status information to the telemetry, command, and control system upon receipt of a suitably coded request.

Upon command the thruster controller will accept reprogramming from the spacecraft central computer or ground via this interface. Ground reprogramming will be possible at the following rates:

High rate	TBD bits per second
Low rate	TBD bits per second

Upon command the thruster controller will read out

selected portions of its memory for transmission to the ground at the following rates:

High rate	TBD bits per second
Low rate	TBD bits per second

The thruster controller command word format is to be determined.

The bit rate shall be TBD bits per second. High signal level shall be TBD. Low signal level shall be TBD. The thruster controller shall return telemetry with a format to be determined.

The thruster controller shall accept timing information from the telemetry, command, and control system suitable for the generation of a clock having a one second resolution.

11.4.1.3 Mercury Propellant Feed System

The thruster controller will control all solenoid valves in the mercury feed system (probably via the power subsystem). If latching valves are used, information on the status of each valve will be returned to the thruster controller. Information on the pressure in all mercury propellant tanks should be available to the thruster controller. (The physical form of this interface is dependent on the overall design, so signal levels, pulse lengths, etc. are all TBD.)

11.4.1.4 Power Distribution Unit

This interface involves three separate functional areas as follows:

1) The thruster controller will control the application and removal of the 28 V dc housekeeping voltage for all thruster power processing units. If a latching system is used, information on the status of the housekeeping supplies for all power processors should be available to the thruster controller. If power to the thruster controller is interrupted, if volatile memory is lost, or if computer logical flow is lost, all 28 V dc housekeeping must be removed from all thruster power processing units immediately. (The physical form of this interface is dependent on the overall design so signal levels, pulse widths, etc. are TBD.)
2) The status of the solar array bus supplied to each thruster power processing unit should be continuously available to the thruster controller. (The physical form of this interface is dependent on the overall design and so signal levels, format, etc. are TBD.)
3) The thruster controller will receive operating power from the power subsystem. Voltage levels, power levels, etc. are TBD. Upon application of power the thruster controller will start in a

predictable fashion; no actions will be taken effecting a power processor until suitable commands are received via the telemetry, command and control system interface.

11.4.2 Mechanical

This item is to be determined because flight-type hardware design has not been done.

11.4.3 Thermal

This item is to be determined because flight-type hardware design has not been done.

11.5 Performance Description

Because hardware has not yet been developed, performance description is not applicable. Following are major performance requirements.

1) Under absolute worst case conditions with all thrusters operating the maximum time to complete one circuit of the main control sequence loop shall not exceed TBD seconds. (Tentatively 20 seconds.)
2) Under normal, stable, beam on operating conditions the status of each power processor/thruster combination shall be monitored at least once every TBD seconds. (Tentatively 5 seconds.)
3) Timers available in the control computer shall time to at least 16,383 seconds with an accuracy

of plus or minus 5% of reading.

4) The thruster controller shall be capable of operating TBD thrusters simultaneously. (Tentatively 8 thrusters.)

5) The thruster controller shall be capable of starting TBD thrusters simultaneously. (Tentatively 2 thrusters.)

6) Under absolute worst case conditions the thruster controller shall initiate corrective action following a low to high transition of any power processor unit off-normal flag line within TBD seconds. (Tentatively 20 seconds.)

7) The area available for alternate programming in the control computer memory shall be at least TBD words. (Tentatively half the area used for thruster control algorithms, flags, variables, and constants.)

11.6 Physical Characteristics

This item is to be determined because flight-type hardware design has not been done.

11.7 Development History

It has long been recognized that hardware performing the functions of the thruster controller would be required for the operation of a system of ion thrusters in a flight application. However, the thruster controller is not in as mature a state of development as

the other components of a functional ion thruster system. There are various reasons for this lag: (1) the necessity for firmly defining the characteristics and control requirements of the other system components before the thruster controller can be defined; (2) the necessity for assembling multiple thrusters and power processors, the facilities to operate them simultaneously, and the control hardware to permit the development of tested control techniques and control algorithms; and (3) the fact that the thruster controller serves to provide a number of interface functions which are dependent on overall space vehicle design and mission strategy.

A few preliminary studies of the characteristics of a thruster controller have been made as part of larger system studies. They are contained in references 11.1.1 and 11.1.2. Applicable document 11.8.6 summarizes the results of a series of consultations between LeRC and JPL on the subject. Some previous efforts were devoted to the development of digital control techniques for the thrusters and power processors as described in references 11.1.3 and 11.1.4. Reference 11.1.5 and 11.1.6 report work of this type which has been done on smaller 8 cm thrusters.

The development of multiple thruster control techniques and thruster control algorithms was begun at the LeRC in the early 70's and has continued to the present. For the current tested software package (which is a continuation of the work of C. A. Low) the first automatic startup and shutdown of a thruster occurred in November, 1977. Throttle and anomaly correction capabilities were added to produce the first complete software package in June 1978. The software has been undergoing long term evaluation testing since August 1978 as part of the Mission Profile Life Test at XEROX/EOS in Pasadena. Debugging, refinement, and documentation activities are continuing through the present. Extensive multithruster tests are planned as part of the BIMOD tests which are scheduled to start later this year at Tank 6, LeRC.

11.8 Application Documents Enclosed

11.8.1 DePauw, J. F.: Prime Propulsion Technology Readiness Program. NASA Lewis Research Center, July 1978.

11.8.2 Edkin, R. A.: Ion Drive BIMOD Thrust Module Test Plan. NASA Lewis Research Center, Solar Electric Propulsion Office, November 1978

11.8.3 Kramer, E. H.; and Lathem, W. C.: Developmental Multi-Thruster Control System NASA Lewis Research Center, April 1979.

11.8.4 Kramer, E. H.: 30 cm PPU/HD 2100 Computer Parallel/ Serial Interface and Timing Circuits. NASA Lewis Research Center, July 1977.

11.8.5 Command and Telemetry Codes of Power Processors for the 30 cm Ion Thruster. December 1978.

11.8.6 Koerner, T. W.: Preliminary Assessment of Functional Requirements of the Ion Drive Controller and Interfacing Subsystems. Jet Propulsion Lab Interoffice Memorandum, July 1978.

TABLE 11.3.1.4-1 PSEUDOCOMMAND FUNCTION CODES

Function Code	Function:
110	Manual command - transmit immediately
120	Software Permissive - OFF (Prohibits further commands)
1	Full Start - automatically implements functions 2-9
2	Preheat High - sets up high level preheat conditions
4	Preheat Low - reduces heat level to isolators
6	Ignition/Heat - sets up conditions to obtain plasma discharge
9	Beam On - turns accelerating voltage on, etc.
55	Starts neutralizer only
66	Preconditions cathode and neutralizer tips
70	Manual control -disables status checking and off normal correction routines
77	Throttles to requested beam power level
99	Shutdown thruster
550	Turns thruster off leaving neutralizer lit (TBD)
750	Returns control to software from manual control (Enables status checking and correction routines)

TABLE 11.3.1.4-2 THRUSTER STATUS CODES

Status Code	Description
00	Thruster off
01	Full start initiated (Phases 2-9 controlled by subr. TCSCR)
02	Preheat high commands transmitted
03	Timing preheat high phase
04	Preheat low commands transmitted
05	Timing preheat low phase
06	Ignition/heat commands transmitted
07	Timing ignition/heat phase and checking for main discharge ignition
08	Timing ignition/heat phase (main discharge lit)
09	Beam on commands transmitted, status set to 75 and control turned over to subroutine STCHK
20	Correcting neutralizer out
22	Beam current out of limits
23	Screen voltage out of limits
24	Correcting for excessive grid arcing
44	Correcting neutralizer lomode condition
45	Timing for neutralizer correction algorithm
55	Neutralizer only starting (or running)
66	Preconditioning cathode and neutralizer tips
70	Manual control mode (software algorithms disabled)
75	Normal run mode
77	Throttling
88	Correcting main lomode condition
97	No throttle shutdown
98	No throttle shutdown, software permit off
99	Throttle to lowest beam, shutdown

TABLE 11.3.1.4-3 ALLOWABLE PSEUDOCOMMANDS AS A FUNCTION OF THRUSTER STATUS

STATUS CODES	1	2	4	6	9	55	66	70	77	99	550*	750**
0	X	X				X	X			X		
1, 2			X					X		X		
3			X					X		X		
4				X				X		X		
5				X				X		X		
6					X			X		X		
7								X		X		
8								X		X		
9								X		X		
20								X		X		
22								X		X		
23								X		X		
24								X		X		
44								X		X		
45								X		X		
55	X	X						X		X		
66										X		
70										X		X
75								X		X	X	
77								X		X		
88								X		X		
97 (NA)												
98 (NA)												
99 (NA)												

NOTES:

*PSEUDOCOMMAND 550 TURNS OFF THRUSTER LEAVING NEUTRALIZER LIT, REINITIALIZES APPROPRIATE FLAGS AND TIMERS AND SET STATUS TO 55.

**PSEUDOCOMMAND 750 ASSUMES THRUSTER IS RUNNING NORMALLY AND SETS STATUS TO 75. CAUTION! COMMAND IS INTENDED AS RETURN FROM MANUAL CONTROL MODE (70) WHEN OPERATOR IS SURE THRUSTER IS RUNNING NORMALLY. USE WITH DISCRETION.

TABLE 11.3-1.4-4 STCHK Checks and Actions
(In order of occurrence in program)

CHECK	DURING STATUS CODES	PURPOSE OF CHECK	ACTION TAKEN
o NA	70	NA	NA
o Arbitrary Telemetry Command	20-24	Detect new PPU off normal flags	NA-PPUIO sets up software PPU off normal flags for later examination by STCHK
o Neutralizer Keeper Current	2-9, 20-24, 44-45, 55, 75, 77, 88, 99	Is neutralizer lit?	If lit and status ≤ 7 turn neutralizer vaporizer heater on (first time only)
o Neutralizer Tip Heater Current	(same)	Is tip heater in right mode (depends on whether neutralizer is lit) ?	If not, reset set point
o Main Discharge Current	8-9, 20-24, 44-45, 75, 77, 88, 99	Is main discharge lit?	NA (used with next check)
o Cathode Tip Heater Current	(Same)	Is tip heater in right mode (depends on whether main discharge is lit) ?	If not, reset setpoint
o Accelerator Current	22, 44-45, 75, 77	Is main discharge in lomode condition?	If so, save current command. If not complete, set status to 88 (lomode correction), and return to SEXEC
o PPU off Normal Flags	44-45, 75, 77, 88	Take care of "saved" off normal flags not previously handled	Call subroutine PPINT which checks to see if condition still exists and initiates appropriate action
o Neutralizer Vaporizer Heater Current	75 (and only if all PPU off normal flags are clear)	Is neutralizer discharge in lomode condition?	If so, set status to 44 (neutralizer lomode correction)and return to SEXEC

TABLE 11.3.1.4-5 Thruster Operational Parameter Values & Status for Startup Phases

	High Preheat			Low Preheat			Ignition/Heat			Beam On		
SUPPLIES AND INTERLOCKS	SW	J	V	SW	J	V	SW	J	V	SW	J	V
Main Vaporizer Heater	0			0			0			+	1.5 PC	
Cathode Vaporizer Heater	0			0			+	2.0 PC		+	2.0 PC	
Cathode Tip Heater	+	4.2		+	*		+	*		+	*	
(Isolator Heater Enable)	+			+			0			0		
Neutralizer Tip Heater	+	4.0		+	*		+	*		+	*	
Neutralizer Vaporizer Heater	0	2.0 PC		+	2.0 PC		+	2.0 PC		+	2.0 PC	
Neutralizer Keeper	+	2.4	17	+	2.4	17	+	2.4	17	+	1.8	**
(Neutralizer Keeper Interlock)	0			0			0			+		
Cathode Keeper	+	1.0		+	1.0		+	1.0		+	1.0	
Main Discharge	+	7.0	36	+	5.0	36	+	**	36	+	**	32
Accelerator Electrode(-)	0		300	0		300	0		300	+		300
Screen Electrode (+)	0			0			0			+		**
Magnetic Baffle	0			0			+	**		+	**	
Beam Current								**			**	
(Isolator Heater Switch)	+			+			0			0		

* Cathode and neutralizer tip heater settings depend on status of discharges (lit or not lit)

** Software selectable and to some extent thruster dependent

TABLE 11.3.1.4-6 Reaction to PPU Off-Normal Flags

OFF NORMAL	DURING STATUS CODES	ACTION BY PPINT	ACTION BY FIXIT
o Solar Array Input Volts Out of Limits	o All but 70, 98	a) Immediate Shutdown b) Turn off 28 volts c) Turn off Hardware Permit	No action
	o 70, 98	No action	No action
o Neutralizer Failure	o 1-9, 55, 66, 70, 98	No action	No action
	o 99	Set status = 98	No action
	o 21-24, 44-45, 75, 77 88, 97	a) Check parameters b) If in limits turn H.V. and vaporizer supplies on c) If out of limits: c1) send corrective commands c2) start 40 sec timer c3) save current command if unfinished c4) set status code = 20 c5) turn control over to FIXIT	No action
	o 20	No action	a) Check parameters until 40 seconds up b) If back in limits return to normal operation (restore saved command) c) If out of limits at end of time retreat to low preheat (set status = 4)

(Continued)

OFF NORMAL	DURING STATUS CODES	ACTION BY PPINT	ACTION BY FIXIT
o Excessive Arcing	o 1-9, 55, 66, 70, 98	No action	No action
	o 99	Set status = 98	No action
	o 20-23, 44-45, 75, 77, 88, 97	a) Turn H.V. and main vap. off b) Start 60 second timer c) Save current command if unfinished d) Set status = 24 e) Turn control over to FIXIT	No action
	o 24	No action	a) At end of 60 seconds turn H.V. & main vap. back on b) Check for arcing c) If clear return to normal operation (restore saved command) d) If still excessive turn H.V. and main vap. off and restart 60 second timer e) If excessive arcs continue through 5 on/off cycles initiate shutdown (set status = 98)
o Beam Current Out of Limits	o All but 75	No action	No action
	o 75	a) Check first for lomode - if true take no action b) If not in lomode set status = 22 c) Turn control over to FIXIT	No action
	o 22	No action	a) Send corrective commands b) Time for 60 seconds c) Check J_B against limits d) If in limits return to normal operation (set status = 75)

(Continued)

TABLE 11.3.1.4-6 (Concluded)

OFF NORMAL	DURING STATUS CODES	ACTION BY PPINT	ACTION BY FIXIT
			e) If out of limits initiate shutdown (set status=98)
o Low Screen Voltage	o All less than 75 (except 23)	No action	No action
	o 98	No action	No action
	o 75, 77, 88, 97, 99	a) save current command if not finished b) set status = 23 c) turn control over to FIXIT	No action
	o 23	No action	a) Send corrective commands b) Check V_I against limits c) If in limits return to normal operation (set status = 75 or restore saved command) d) If out of limits initiate shutdown (set status = 98)
High Accelerator Current	o All	No action	No action

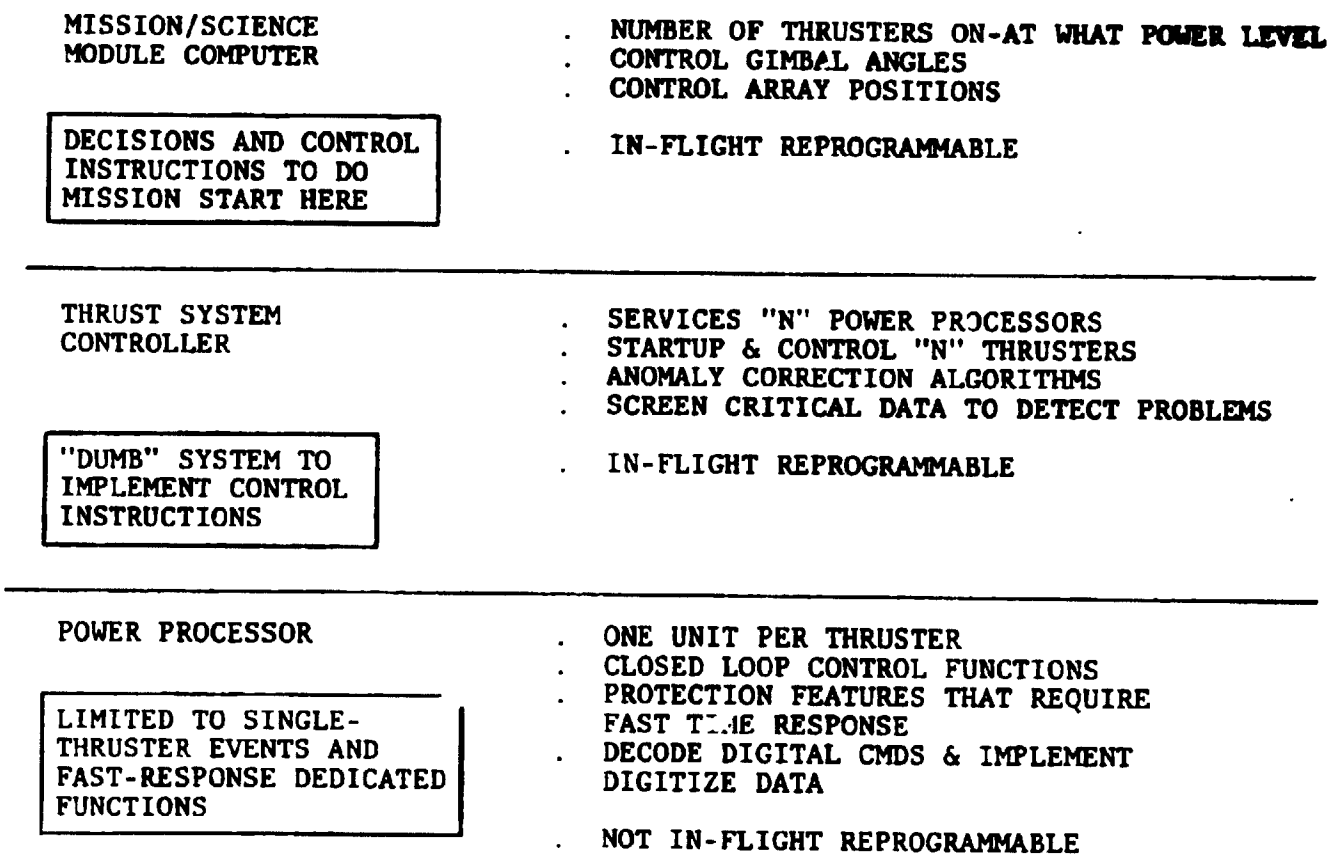

Figure 11.0-1 Space vehicle computer control heirarchy

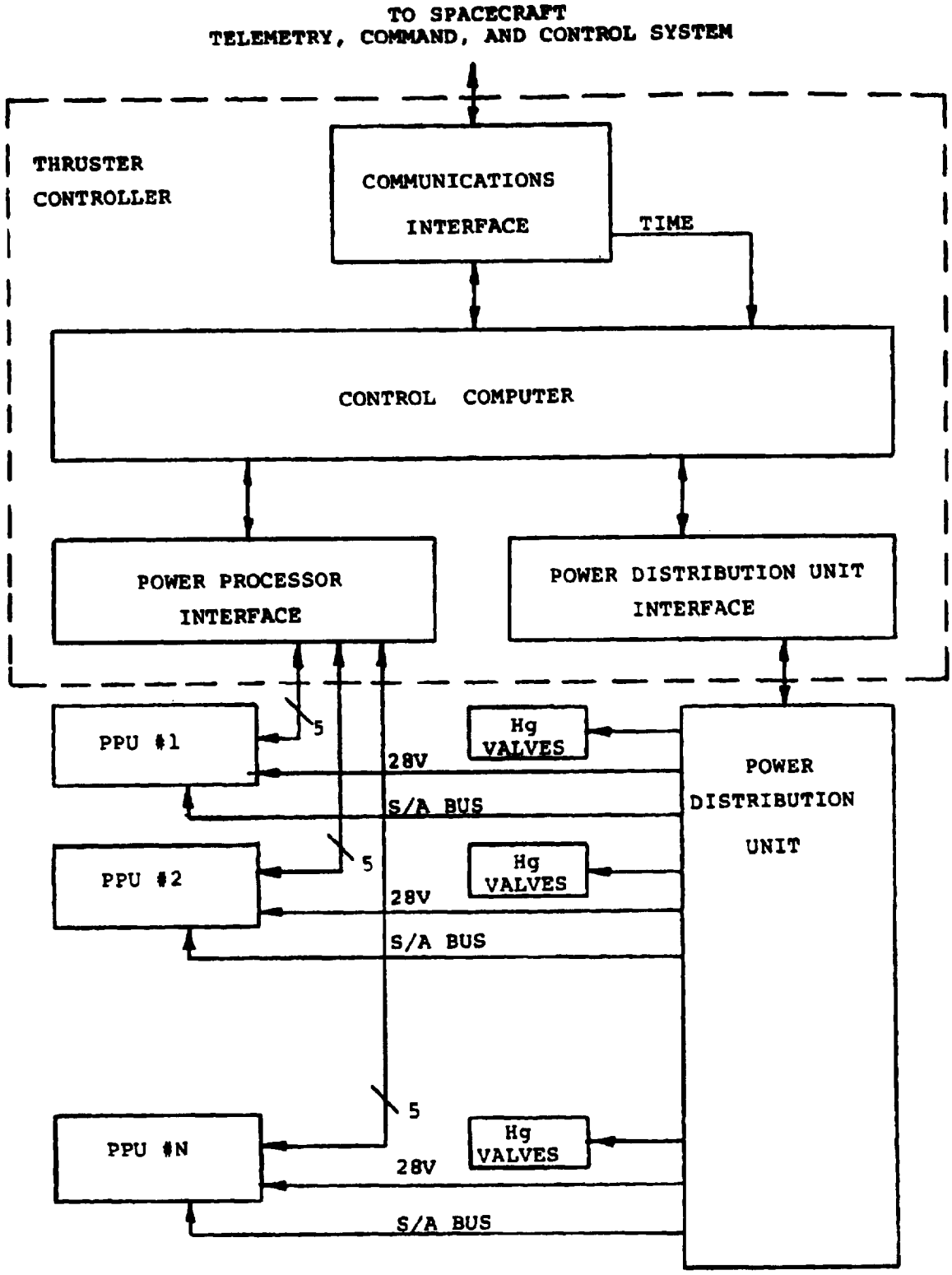

Figure 11.3.1.1-1 Thruster Controller Conceptual Block Diagram

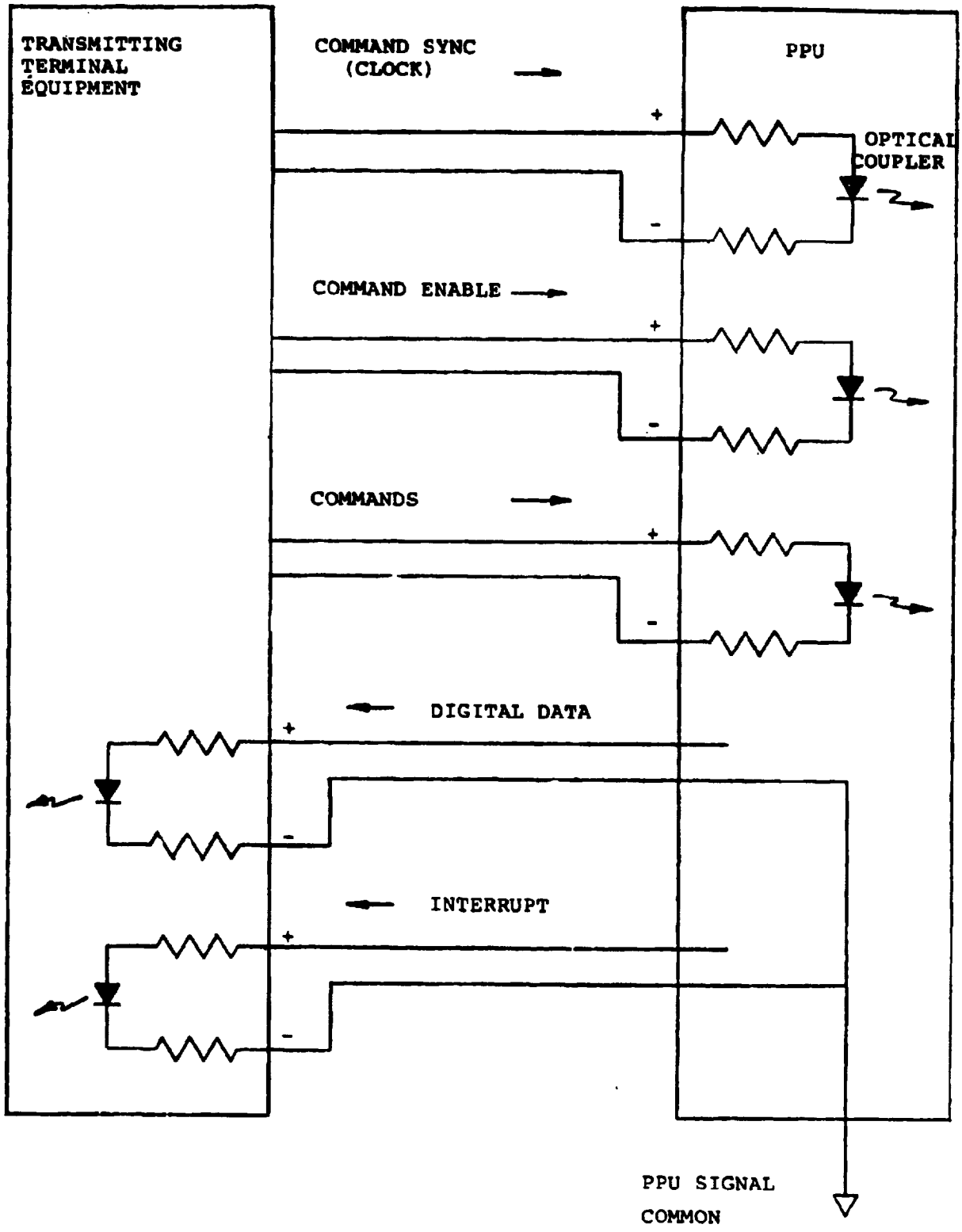

Figure 11.3.1.1-2 Each PPU/Computer Interface Interconnection

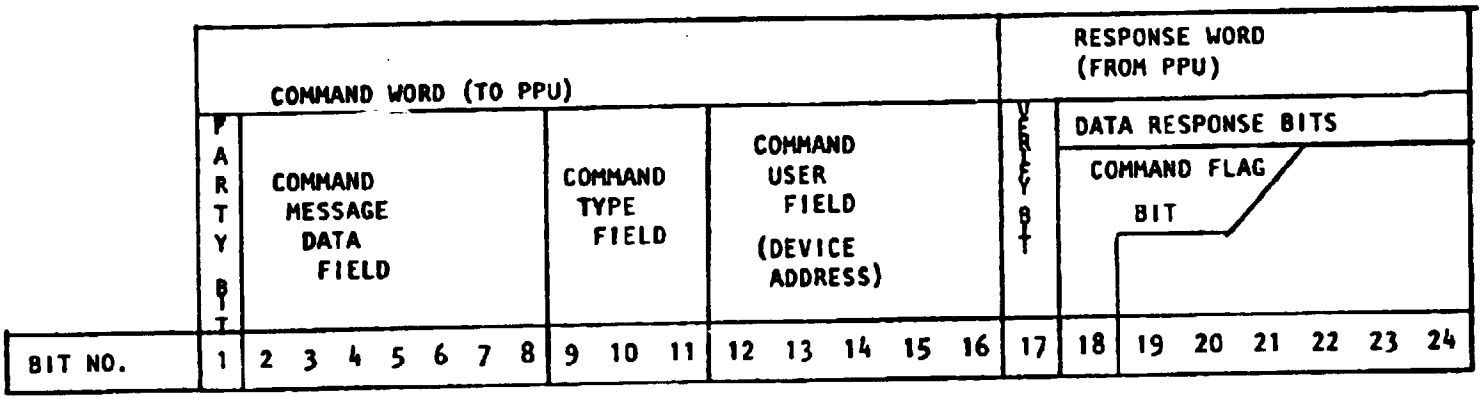

a. Definition of Bits to/from PPU

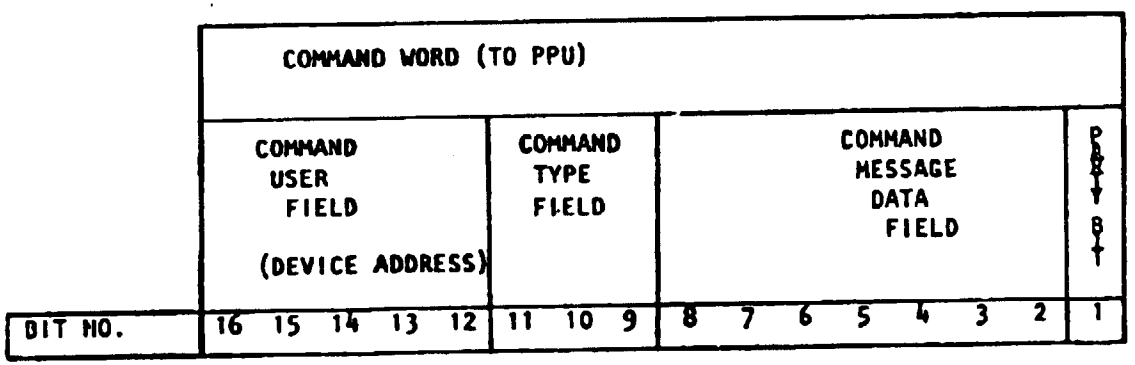

b. Definition of command bit order as used in software

Figure 11.3.1.1-3 Digital word structure

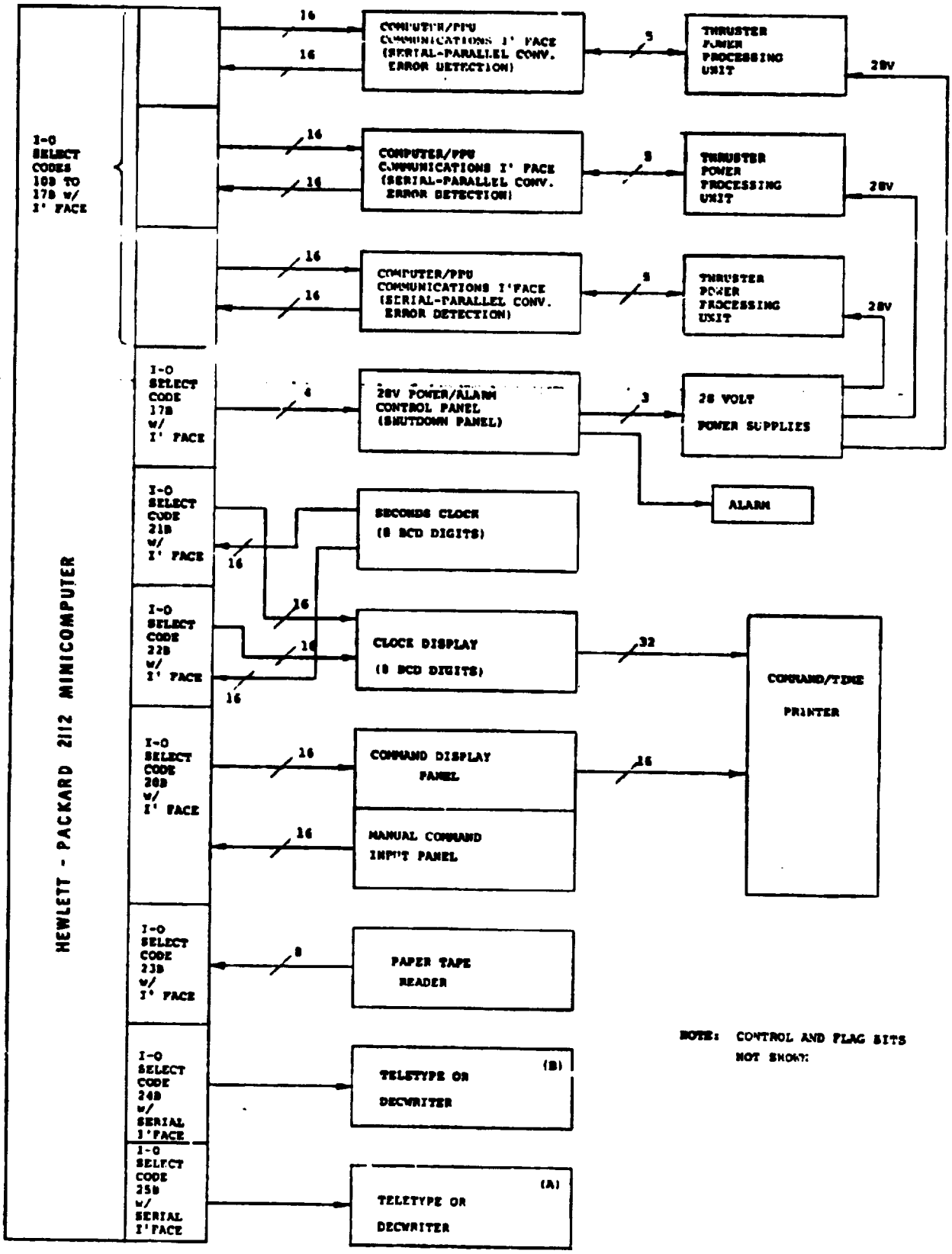

FIGURE 11.3.1.2-1, ALGORITHM/SOFTWARE DEVELOPMENT SYSTEM

	Type of Command or Telemetry Request or Condition Sent to PPU to Cause Return.	Bit Number	Interrupt Status Telem. Request	Off Norm. Flag Hi.	Telemetry Request	PPU Command
Data, Off Normal Flags, Execution Verification flags, Generated by Thruster Power Processing Unit.	Not Used	0	0	X	X	0
	Neutralizer Out (Low Jnk, High Vg)	1	*	* X	X	0
	Excessive Arcs	2	*	* X	X	0
	Input Voltage Out of Limit	3	*	* X	X	0
	Beam Current Out of Limit	4	*	* X	X	0
	Screen Voltage Out of Limit	5	*	* X	X	0
	Accelerator Current Above limit	6	*	* X	X	1
	Telem. Verify Bit	7	1	I	1	0
	PPU Off Normal	8	0	1	0	0
Error Condition Flags Generated By PPU Interface Hardward or by Software Driver Routine.	No Command Verify Bit Returned	9	0	0	0	X
	No Telem. Verify Bit Returned	10	X	X	X	0
	Hardware Echo Error	11	X	X	X	X
	Not Used	12	0	0	0	0
	Invalid Command, Software Error	13	X	X	X	X
	No I-O Flag Bit, PPU Interface Fail.	14	X	X	X	X
	Error Flag Bit, Set if any of bits 8-14 set.	15	X	X	X	X

X - Value as appropriate; for bits 8 thru 15 condition indicated flagged by "one" state.

* - For interrupt status telemetry request indicated conditions flagged by "one" state.

I - Not effected by type of command transmitted, value as determined by other conditions.

Figure 11.3.1.2-2 PPU Interface Hardware/Software Driver Full Return Word.

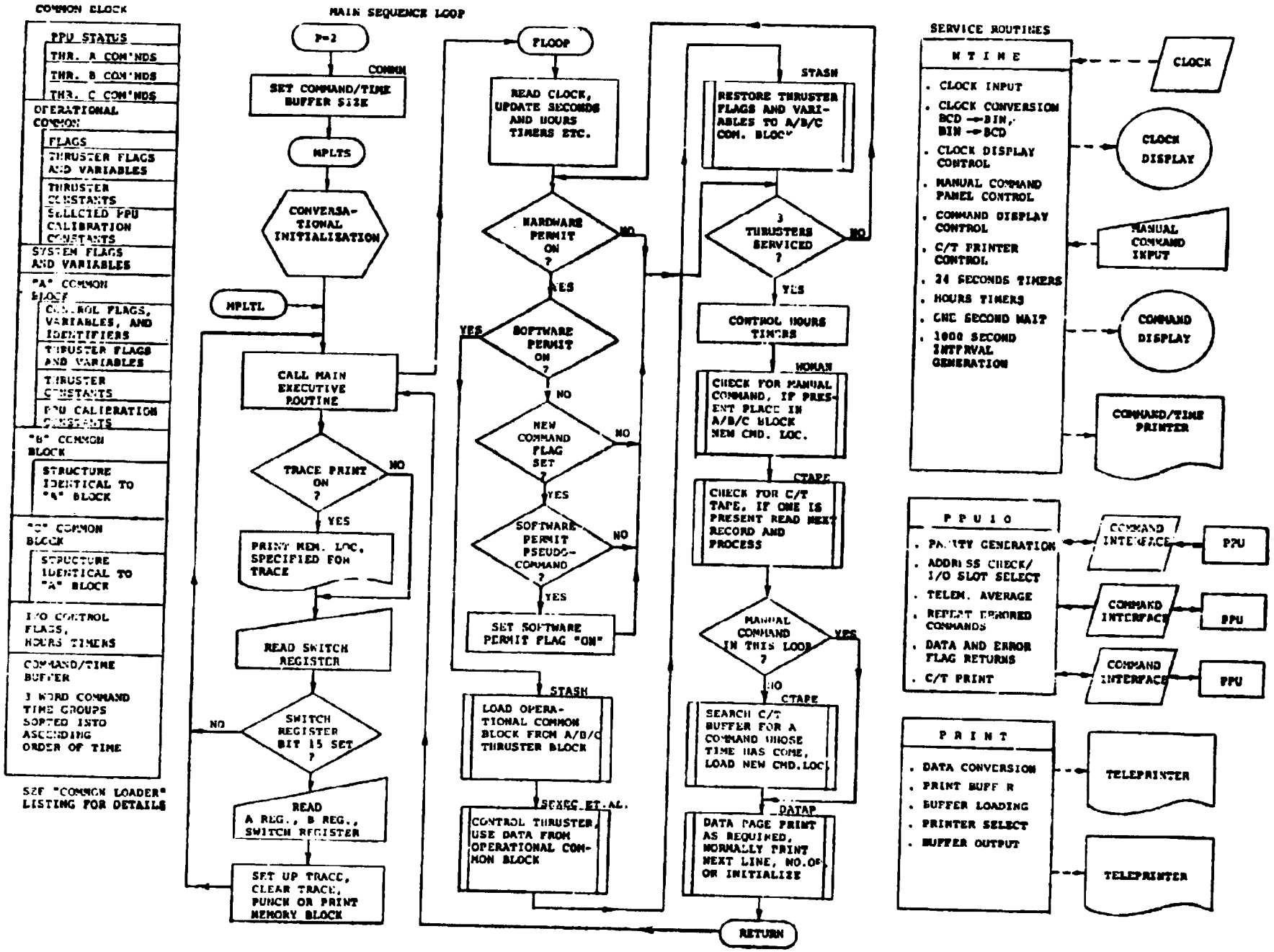

Figure 11.3.1.3-1 Basic Software Organization

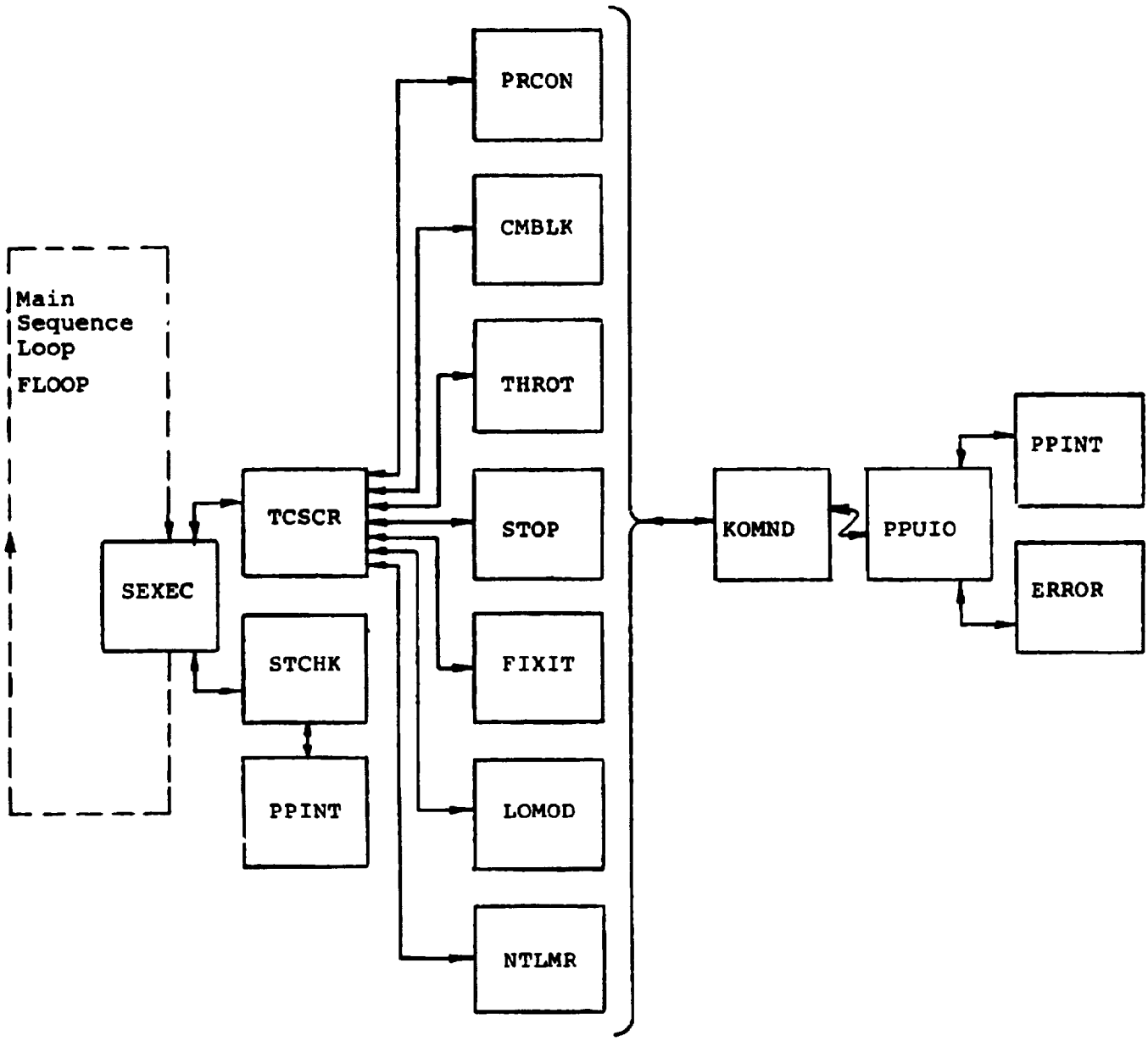

Figure 11.3.1.4-1 Thruster Control Software
Functional Block Diagram

12.0

POWER DISTRIBUTION

Table of Contents

		Page
12.0	Power Distribution	12-2
12.1	Reference Documents	12-2
12.2	Functional Requirements	12-2
12.3	Functional Description	12-2
12.3.1	Electrical	12-2
12.3.2	Mechanical	12-5
12.3.3	Thermal	12-5
12.3.4	Operational Characteristics	12-6
12.4	Interface Definition	12-7
12.4.1	Electrical	12-7
12.4.1.1	Solar Array Interface	12-8
12.4.1.2	Regulated Bus Interface	12-8
12.4.1.3	Thruster Controller Interface	12-9
12.4.1.4	PPU Unregulated Bus Interface	12-9
12.4.1.5	PPU Regulated Bus Interface	12-9
12.4.1.6	Auxiliary Loads	12-10
12.4.2	Mechanical	12-10
12.4.3	Thermal	12-11
12.5	Performance Description	12-11
12.6	Physical Characteristics and Constraints	12-12
12.7	Development History	12-12
12.8	Applicable Documents Enclosed	12-12

FIGURE

12.3.1-1	Power Distribution Unit - Functional Block Diagram	12-13

12.0 Power Distribution

12.1 Reference Documents

None.

12.2 Functional Requirements

1) The PDU shall provide solar array power to each PPU upon command.

2) The PDU shall provide independent 28 volt power from the mission module battery bus to each PPU upon command.

3) The PDU shall provide fault clearing and isolation between each PPU and the solar array.

4) The PDU shall provide sensors for monitoring configuration and performance within the Thrust Subsystem (TSS) power system.

5) The PDU shall provide power to the TSS heaters and valves upon command.

6) The PDU shall interface with the TSS controller for data and command functions.

7) The PDU shall provide overload protection on all low voltage power circuits.

8) The PDU shall provide other power as required by units within the TSS.

12.3 Functional Description

12.3.1 Electrical

The functional block diagram (fig. 12.3.1-1) indicates the main elements of the PDU and its interfaces.

The primary power is the solar array bus which is brought in to terminals. This bus is maintained within 200 to 400 volts by reconfiguration of the array modules external to the TSS. Both sides of the solar array are isolated from spacecraft ground while the center tap could be kept at S/C ground.

The solar array bus power switch is a quad-redundant configuration of high power hybrid switches. The primary function is to clear the solar array bus in the event of a PPU input fault. Each switch consists of a motor driven switch in parallel with high power transistors. The switch is in development stage at this time.

The solar array power is provided to each PPU through series redundant relays. Switching may be provided on both sides of the PPU input power lines to isolate any faults that may unbalance the solar array-spacecraft potential. These relays are not intended to provide fault clearing nor hot switching of PPU input power. Thus a hybrid switch would not be necessary for this application.

The function of the precharge converter is to provide low level fault detection current after the bus power switch has opened. The converter also provides cur-

rent to charge the PPU input filter before reclosing the bus power switch, thus preventing transient overloading of the solar array. At normal solar array bus voltages the converter draws minimal power in the unloaded condition.

The 28 volt power is provided to each PPU through a parallel redundant relay and fuse. These are maintained as separate circuits from the battery bus in the mission module to minimize transients to other PPU's in the event of a 28 V fault in one PPU.

The 28 V power from the mission module also provides power switching to actuate latching solenoid valves in the PS&D system and the BIMOD feed lines, power the gimbal electronics and, in the present concept, power the BIMOD heaters as required. If the heaters are to operate from the solar array bus, hybrid switches may be required.

Logic level command signals to solid state drivers transfer the relays and switches within the PDU. Options are to have the thruster controller output a logic level signal for each switching function within the PDU or for the PDU to decode command words from the controller. Solid state switches and current limiting could be used for the 28 volt power

switching but present additional circuit and heat sink complexity.

The voltage and current sensors distributed within the PDU allow monitoring and diagnosis of TSS performance. These sensors are powered from the 28 volt bus and provide an analog output. Other instrumentation such as temperatures and pressures, within the interface module and each BIMOD will require signal conditioning. All analog data channels would then require multiplexing and A to D conversion to generate an input to the thruster controller. Depending on the total number of channels this instrumentation signal processing could be done in the PDU or in a separate signal conditioning unit.

12.3.2 Mechanical

The weight estimate for all components and wiring within the PDU is estimated at 45 pounds.

The size and layout is TBD although there may be some advantage to integrating the solar array bus with the interface module structure.

12.3.3 Thermal

The operating temperature limits are presently specified as -30° C to $+55^{\circ}$ C.

No dissipation has been established for any internal

components but the total dissipation should be less than 50 watts.

12.3.4 Operational Characteristics

The operational characteristics of the PDU can be explained by reference to the functional block diagram (fig. 12.3.1-1).

The hybrid power switch in the solar array input line is normally closed and the PPU input relays are also normally closed thus applying solar array power to all PPU inputs and keeping the input filters charged. For non-operating conditions, the PPU 28 volt switch is open, thus disabling the PPU. In this mode each PPU draws about two watts from the solar array bus. When the 28 volt power is applied to the PPU, in the standby mode, it draws about 25 watts from the solar array bus. As each PPU is enabled, BIMOD heaters will be switched off to minimize the load on the 28 volt bus.

Variations in thrust level will move the operating point along the solar array characteristic curve. An abnormal event such as loss of peak power tracking capability (external to the TSS) or a PPU input fault could cause the operating point to exceed the knee of the solar array curve thus causing the array voltage to collapse. This second condition would be sensed

within the PDU and after a time delay, either directly or through the thruster controller, cause the hybrid power switch to open the solar array bus thus clearing the fault. The 23 volt power would then be removed from all PPU's. If a permanent fault exists it will be detected by the limited short circuit current of the precharge converter. Opening the PPU power relays will then isolate the failed PPU. The PPU power relays would be reclosed to check if the fault had cleared, as would be the case for a PPU-SCR "latch-up". If the fault was still present, the PPU would be removed from the bus and remain off line.

The precharge converter now charges the input filters of the PPU's. The hybrid power switch can now be closed without causing a transient due to filter inrush current. The PDU is again ready to support thruster operation.

12.4 Interface Definition

12.4.1 Electrical

Electrical interfaces to the mission module consist of unregulated solar array power, regulated housekeeping power, commands to the ion drive controller, and signal lines to the mission module data system. Electrical interfaces to the BIMODs consist of thermal heater power, valve control lines, gimbal electronics, independent circuits for each 200 to 400 volt unregulated bus power input, independent cir-

cuits for each PPU regulated bus input, and thrust subsystem temperature, pressure, and power system monitors.

The thrust subsystem power distribution shall provide for maintaining electrical isolation from spacecraft structure for all interface power, TLM, and command lines.

12.4.1.1 Solar Array Interface

Unregulated solar array power is provided to the thrust subsystem from the solar array reconfiguration unit. The positive side of the solar array power is redundantly fed to hybrid contactors in the thrust subsystem interface module by pair of power cables. The load side of the contactors is connected to a positive array bus bar. The negative side of the array is directly fed to a negative array bus bar in the thrust subsystem interface module by a pair of power cables. All terminations are on stud connections.

12.4.1.2 Regulated Bus Interface

Regulated bus power is provided to the thrust subsystem from the mission module battery bus. A total of nine independent circuits consisting of a pair of No. 16 AWG wires each (power and return) are fed into the interface module. One circuit is dedicated

to each PPU and the remaining circuit powers the thrust subsystem housekeeping functions, (signal conditioning, relay driver, current sensors). Independent circuits are employed to provide PPU power circuit isolation so that a fault on one PPU regulated bus input would be less likely to undervoltage the remaining units.

12.4.1.3 Thruster Controller Interface

The mission module interface with the thruster controller consists of a clock signal, data line and a command line, and a regulated bus power feed. Each PPU interfaces with the thruster controller with the following circuits: interrupt line, data line, clock, enable and command circuits.

12.4.1.4 PPU Unregulated Bus Interface

The positive array bus bar in the interface module is wired to the power relays providing unregulated array power to each PPU. The negative array bus bar is wired directly to each PPU providing the return for the unregulated array power. The PPU unregulated bus relays are series redundant to assure isolation of a faulted load from the bus.

12.4.1.5 PPU Regulated Bus Interface

Each PPU regulated bus input is provided by parallel redundant standard power relays. Fusing is used to provide fault isolation on the battery supported

regulated bus. The regulated bus power and return lines for each PPU are carried as separate circuits back to the battery bus in the mission module. This reduces the charge that a surge on one PPU input could induce as undervoltage condition in the remaining thrust subsystem mission module loads.

12.4.1.6 Auxiliary Loads

Standard 28 V power relays (latching) are used to power the following circuits from the regulated bus by command from the thruster controller; BIMOD heaters, propellant solenoid valves, transducers, signal conditioning circuits, and telemetry formatting circuits.

12.4.1.7 Telemetry Interfaces

All thruster data is passed to the mission module by the thruster controller. A separate signal conditioning and formatting circuit provides thrust subsystem housekeeping parameters (temperatures, pressures, power system status, etc.) directly to the mission module data system. These parameters are also made available to the thruster controller for monitoring of thrust subsystem status.

12.4.2 Mechanical

The power distribution unit and the signal conditions circuits in the thrust subsystem interface module may be housed in a common or separate enclosure (TBD)

that will require mounting in the interface module. Preference for separate enclosures is driven by the different functions to be performed and possible incompatibility problems that could be minimized. The signal conditioning and control circuits could be housed in an enclosure of less than 0.5 cubic foot with a weight of less than 10 pounds. The 28 V power distribution hardware could be housed in an enclosure of less than 1.0 cubic foot with a weight of less than 45 pounds. The high power contactors (hybrid switch) and the PPU unregulated bus power relays would be mounted on an open plate that could form a structural element of the interface unit. Estimated weight for the components on this plate is 25 pounds.

12.4.3 Thermal

The power distribution unit and signal conditioning circuits in the thrust subsystem interface module contain active devices which dissipate heat and will require a controlled ambient temperature. The total heat dissipated is TBD but will be less than 50 watts. Required operating temperature range is from -30 to +55° C.

12.5 Performance Description

Not applicable.

12.6 Physical Characteristics and Constraints

The physical characteristics and constraints for the PDU have not been established and will be determined at a later date.

12.7 Development History

The history of the PDU is generally centered around the development of switchgear capable of handling high power, in the range of 25 kW. Other relays, switches, transistors, etc. found in the PDU are standard components already developed and qualified for space application. However, the switch to handle 200 to 400 V dc at 25 kW does not exist. It will have to be scaled upwards or developed specifically for use in the PDU.

A Westinghouse contract exists for a development of a 25 kW switch, and other companies, such as Hartman, Kinetics and Ward-Leonard have shown an interest in developing the switch. Others in the field like Teledyne, Potter & Brumfield, Cutler-Hanmer, Leach, Clare, ITT Jennings, Kilovac, and Babcock have the capability, but have shown no interest.

12.8 Applicable Documents Enclosed

None.

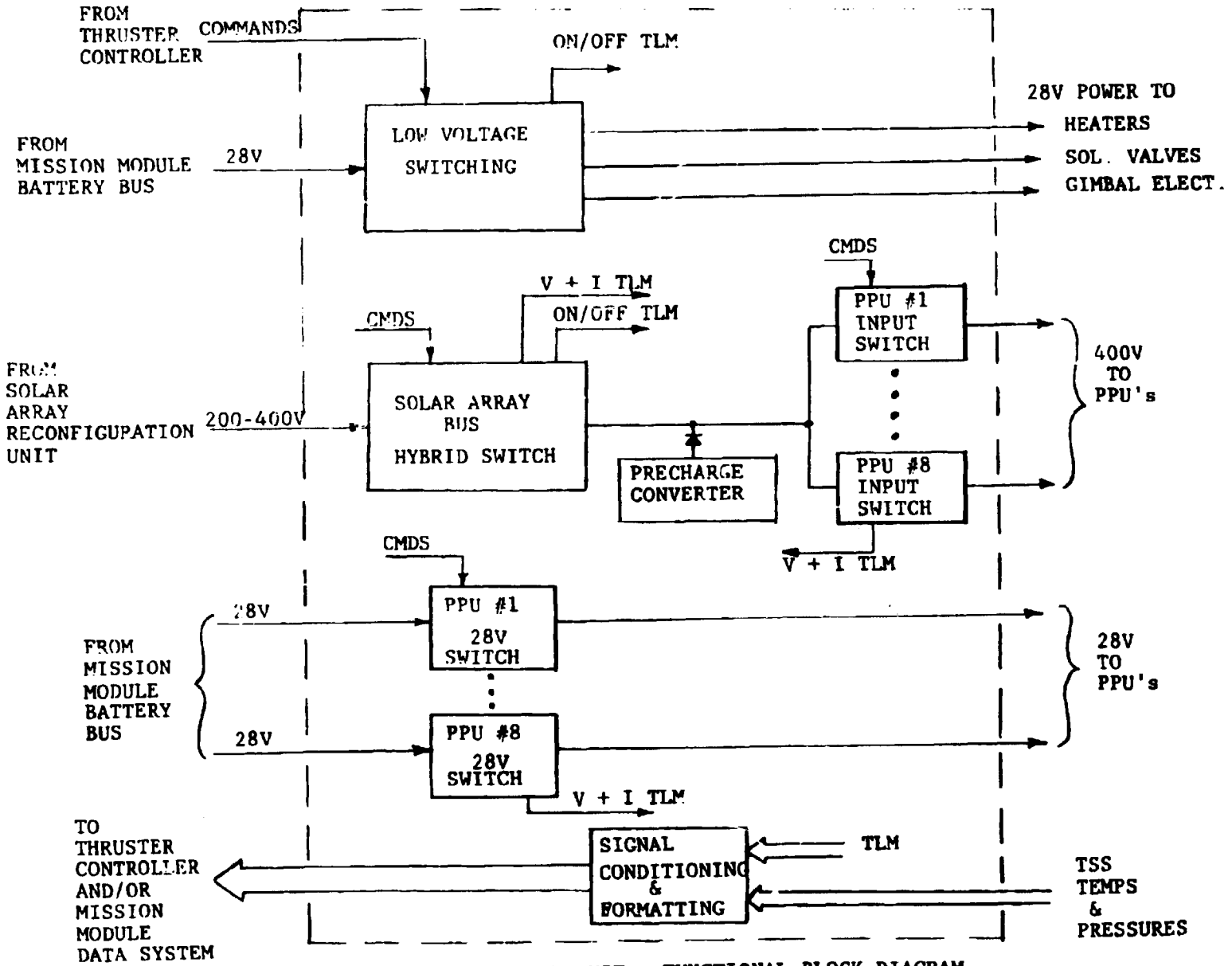

POWER DISTRIBUTION UNIT - FUNCTIONAL BLOCK DIAGRAM
FIGURE 12.3.1-1

13.0

PROPELLANT STORAGE AND DISTRIBUTION

Table of Contents

		Page
13.0	Propellant Storage and Distribution	13-5
13.1	Reference Documents	13-5
13.2	Functional Requirements	13-5
13.3	Functional Description	13-5
13.3.1	Electrical	13-5
13.3.2	Mechanical	13-7
13.3.2.1	Storage Tank	13-7
13.3.2.2	Valves	13-8
13.3.2.3	Instrumentation	13-8
13.3.2.4	Distribution System	13-9
13.3.3	Thermal	13-10
13.3.4	Operational Characteristics	13-11
13.4	Interface Definition	13-11
13.4.1	Electrical	13-11
13.4.2	Mechanical	13-12
13.4.3	Thermal	13-13
13.5	Performance Description	13-13
13.5.1	Materials Compatibility	13-13
13.5.2	Mercury Purity	13-14
13.5.3	Mercury Slosh Dynamics	13-16
13.5.4	Two Tank System	13-16
13.5.5	Off-Loading The Tank	13-16
13.5.6	System Utilization	13-18
13.5.7	Tank Configuration	13-18
13.5.8	Tank Stress Calculation	13-19

		Page
13.5.9	Fill Valves	13-20
13.5.10	Solenoid Latching Valve	13-21
13.5.11	Pressure Transducer	13-23
13.5.12	Temperature Transducer	13-23
13.5.13	Field Joint	13-24
13.5.14	Fill and Drain Procedure	13-25
13.5.15	Cleaning Procedure	13-25
13.6	Physical Characteristics and Constraints	13-25
13.7	Development History	13-26
13.8	Applicable Documents Enclosed	13-28
13.9	Ground Support Equipment	13-29

TABLES

13.4.2-1	PS&D System Components	13-30
13.6-1	Component Weights	13-32
13.6-2	Tank Weight, Mercury Weight, Mass Fraction	13-33
13.6-3	Tank Size Versus Mercury Weight	13-34
13.6-4	Dual Tank System Weight Breakdown	13-35

FIGURES

3.3-1	BIMOD, PSD, Thruster System Schematic - Dual Tank System	13-36
3.3-2	BIMOD, PSD, Thruster System Schematic - Single Storage Tank	13-37
3.3.2-1	SERT II Tank Design	13-38
3.3.2-2	91 Kg Mercury Capacity Propellant Tank	13-39
3.3.2-3	Mercury Propellant Tank	13-40

Page

13.4.1-1 Electrical Interface Diagram.....13-41

13.4.2-2 Mercury Storage Tank.....13-42

13.4.2-3 Temperature Transducer.....13-43

13.4.2-4 Nitrogen Fill Valve (Closed).....13-44

13.4.2-5 Nitrogen Fill Valve (Open).....13-45

13.4.2-6 Pressure Transducer.....13-46

13.4.2-7 Pressure Transducer In-Line Mount.....13-47

13.4.2-8 Mercury Fill and Drain Valve (Open).....13-48

13.4.2-9 Mercury Fill and Drain Valve (Closed).....13-49

13.4.2-10 Main Manifold.....13-50

13.4.2-11 Solenoid Latching Valve.....13-51

13.4.2-12 Flexible Gimbal Line.....13-52

13.4.2-13 "Y" Fitting for Mercury Feed Line.....13-53

13.4.2-14 Shoulder and Nut (Field Joint).....13-54

13.4.2-15 Coupling (Field Joint).....13-55

13.5.5-1 Fill Fraction and Reservoir Pressure at 80° C vs. Loading Temperature.....13-56

13.5.7-1 Electro Optical Systems Tank Design.....13-57

13.5.10-1 Electrical Schematic of the Solenoid Latching Valve Connector.....13-58

13.5.10-2 Mercury Control Valve Intrusion Test Configuration.....13-59

13.5.10-3 Latching Valve Test Results.....13-60

13.5.12-1 Half-Bridge Voltage Output vs. Temperature for Various ISO-CURVE Thermistors.....13-61

Page

13.5.13-1 Design Attributes of Resistoflex Fittings.....13-62

13.7-1 Ion Auxiliary Propulsion System.....13-63

13.0 Propellant Storage and Distribution

This section describes the propellant storage and distribution system that has been designed to meet the requirements of the 30-cm thruster and a wide variety of missions that would utilize the 30-cm thrusters.

13.1 Reference Documents

13.1.1 Lestingi, J.; and Zavesky, R. J.: Constrained Sloshing of Liquid Mercury in a Flexible Spherical Tank. AIAA Paper 78-670, 1978.

13.1.2 Zavesky, R. J.; and Hurst, E.B.: Mechanical Design of SERT II Thruster System. NASA TM X-2518, 1972.

13.2 Functional Requirements

The functional requirements of the propellant storage and distribution system are: (1) to store the required mercury for the lifetime of the mission, (2) to isolate the propellant from the thruster during launch so that the dynamic environment does not have a detrimental effect on the operation of the thruster, and (3) to supply the propellant to the thruster within a pressure range that satisfies the requirements of the thruster.

13.3 Functional Description

The baseline propellant storage and distribution system is shown in figure 13.3-1. The baseline system contains two propellant tanks. Figure 13.3-2 illustrates a single tank for comparison.

13.3.1 Electrical

The propellant storage and distribution electrical sys-

tem is shown in Figure 13.3-1 and consists of the solenoid-operated latching valves, the pressure transducers, and the temperature transducers.

The solenoid latching valves are off during launch, such that the propellant is in the line up to these valves. Operation of the solenoid latching valves to the "on" condition will open these valves to the manifold and distribute the propellant through the interface structure to the bimodular engine systems (BIMOD). Within each BIMOD there are two solenoid latching valves, one for each thruster. When these valves are activated to the "on" condition, the propellant will flow to the three vaporizers within the thruster.

The pressure transducers as shown in figure 13.3-1 are located in the line connecting the two propellant storage tanks, and on the manifold that distributes the propellant to the four BIMODs. These two pressure transducers are to be "on" at all times when operating voltage is available.

The temperature transducers as shown in figure 13.3-1 are located on the two propellant storage tanks. These two transducers, which actually are resistive thermistors, are to be "on" at all times when operating voltage is available.

13.3.2 Mechanical

The following discussion covers the functional role of each component of the propellant storage and distribution system.

13.3.2.1 Storage Tank

The storage tank design is a derivative of the design approach employed by the Space Electric Rocket Test Two (SERT II) system (figure 13.3.2-1). The tank design is a passive nitrogen blowdown system. The mercury is contained in a spherical shell. An elastomeric bladder separates the mercury propellant from the pressurized nitrogen gas. The tank contains an internal metal liner which supports the bladder during the launch environment, thus minimizing the sloshing effects. The perforated liner holes permit the pressurized gas to pass through the liner and move the bladder. A tank with a capacity of 91 kg of mercury is shown in figure 13.3.2-2.

The volume of mercury is determined by the mission requirements. Some missions may not require the full sphere of mercury propellant. A storage tank of the same outside dimensions can be employed and the shape of the bladder support liner need only be changed (Figure 13.3.2-3) for the required volume of mercury. This concept minimizes slosh effects during the launch environment.

The nitrogen gas volume is designed for an initial pressure of 50 psia when the tank is full of mercury

and 15 psia when the tank is empty. These pressures are dictated by the requirements of the thruster vaporizers. The upper pressure limit of 50 psia was determined from the intrusion pressure of the porous tungsten that is used for vaporizer flow control. The lower limit is determined by the partial pressure of mercury. The liquid to vapor interface must be retained at the liquid side of the plug; therefore, the propellant system must supply mercury at a higher pressure than the partial pressure of mercury at the operating temperature of the vaporizer. A safety factor of 2:1 has been employed on both pressure requirements.

13.3.2.2 Valves

The nitrogen and mercury fill valves are identical to the flight proven SERT II hardware. They will be used to fill and drain the system. The redundant mercury solenoid latching valves are used to isolate the mercury from the thrusters during the launch environment. Mercury will be contained in the system up to the two redundant solenoid latching valves during launch. A solenoid latching valve is in each thruster feed line close to each thruster. This valve will only be used to isolate a malfunctioning thruster.

13.3.2.3 Instrumentation

The pressure transducer is mounted in the mercury line close to the tank. Pressure changes are used to determine the amount of mercury used over a period of time.

The temperature of the tank, and specifically the temperature of gas, must also be monitored because it has the largest variational effect on the system pressure.

Another pressure transducer is mounted at the manifold. It is used to monitor the pressure and verify that mercury has been distributed to the thrusters after the isolation valve has been opened. Another fill and drain valve is also placed in the system at this point, in order to purge the system, and properly load and unload the mercury.

The temperature transducer is mounted to the propellant tank wall, and will be used to monitor the mercury and nitrogen pressurant temperature.

13.3.2.4 Distribution System

The manifold distributes the mercury to the BIMODs or thrusters.

The flexible gimbal line is a coiled spring tube which complies with the movement of gimbals. Field joints are used in the appropriate places such as at the valves, and across structures. Tubing will vary from 1/8-inch diameter for the tubing on the tank side of the manifold, to 1/16 inch diameter tubing on the thruster side. The 1/8-inch diameter tubing is required to evacuate the system during the filling operation. The 1/16-inch tubing is more than adequate for mercury flow, and is used

to keep the propellant utilization high because of the small mercury volume in tubes and components. The 1/16-inch diameter tubing in the flexible gimbal line is easier to flex than the 1/8-inch tubing.

All materials in contact with the mercury have been flight tested on SERT II for nine years. The pressures of both feed systems on SERT II have been monitored during the lifetime of the flight. The decrease in pressure has been directly related to utilization of the mercury.

13.3.3 Thermal

The required thermal environment(s) for the propellant storage and distribution system shall be maintained by a combination of multilayer insulation and supplementary heaters.

The propellant feed lines shall be located inside the BIMOD cavity and between the aft insulation of the BIMOD and the thrusters. In a non-operating mode at distant astronautical units (A.U.), it will be required to wrap the feed lines with multilayer insulation and supplementary heaters to prevent the freezing of mercury. The amount of heater power required is to be determined (TBD).

The propellant storage system shall be located in the interface module along with other components. Previous analyses of the interface module indicate that the storage

system temperature limits can be maintained with the assistance of approximately 15 watts of supplementary heating for each propellant tank.

13.3.4 Operational Characteristics

The present propellant storage tank has a capacity of 1000 kg of mercury. The tank is designed to operate at 50-psia nitrogen pressure at the beginning of the flight, and at 15 psia when all of the mercury in the tank has been expelled.

13.4 Interface Definition

13.4.1 Electrical

The electrical interface definitions as referred to in the functional description (section 13.3.1) are as shown in figure 13.4.1-1. They consist of the solenoid-operated latching valves, the pressure transducers, and the temperature transducers.

The solenoid-operated latching valves use a three-pin Bendix PTIH-8-3P electrical connector, or equal for the three wires. The electrical schematic of the connector is shown in figure 13.5.10-1.

The pressure transducers use an electrical connector designated as HSC S7002-8-4P for four wires. The electrical wiring for this connector is shown in Figure 13.4.2-6.

The temperature transducers will operate across a

standard resistive telemetry circuit as shown in figure 13.5.12-1.

13.4.2 Mechanical

The propellant storage and distribution system is shown schematically in figures 13.3-1 and 13.3-2. The various components that make up this system are listed in table 13.4.2-1, along with other appropriate information.

The mercury tanks (fig 13.4.2-2) are suspended from the interface truss by eight 1-inch aluminum tubes which are attached to four mounting points at the tank flange using adapter fittings as described in section 10.3.2. The temperature transducer (fig 13.4.2-3) is threaded into a tapped hole located at the base of the mercury tank. The nitrogen fill valve (figs. 13.4.2-4 and 13.4.2-5) is welded into the nitrogen chamber on the top side of the mercury tank. A pressure transducer (fig. 13.4.2-6) is mounted in the common mercury line using a fitting similar to that shown in figure 13.4.2-7. The transducer is threaded into the fitting. The mercury lines are brazed into the fitting. The mercury fill and drain valves (figs. 13.4.2-8 and 13.4.2-9) are located at two points. One valve is in the main mercury feed line, the other is near the end of the main manifold (figure 13.4.2-10). The mercury lines are brazed into the valve flanges. There are two

solenoid latching valves (fig. 13.4.2-11) located between the mercury tanks and the main manifold. These valves use Resistoflex fittings to connect them to the mercury lines. The main manifold is shown in figure 13.4.2-10. All mercury lines are brazed into the manifold. A pressure transducer (Fig. 13.4.2-6) is threaded into one end of the manifold.

A solenoid latching valve (fig. 13.4.2-11) is used in the line to each thruster. The joints are Resistoflex fittings. A flexible gimbal line (fig. 13.4.2-12) is used to get the mercury across the gimbal joint. A "Y"-fitting (fig. 13.4.2-13) is used in each BIMOD to divide the mercury feedline to each thruster. The mercury lines are brazed into this Y-fitting. All of the field joints used in the PS&D system are Resistoflex fittings as shown in figures 13.4.2-14 and 13.4.2-15. The mercury lines are brazed into these fittings.

13.4.3 Thermal

The design temperature limits of the propellant storage and distribution system are $+80^{\circ}$C and -35° C.

The propellant tank is located in the controlled thermal environment of the interface module. Constant temperature control of the mercury is desirable.

13.5 Performance Description

13.5.1 Materials Compatibility

The materials used for the construction of the mercury

propellant tank and all components of the propellant storage and distribution system have been in constant use in the developmental testing of mercury ion propulsion systems by Hughes, NASA LeRC, and others, for over twenty years. The same materials have been flight qualified during the SERT II and the ion auxiliary propulsion system (IAPS) programs, and have been in functional use on the SERT II spacecraft for over nine years of space operation. During that period, there has been no evidence of stress corrosion, electrolyte attack, or other symptoms of material failuse or incompatibility.

A list of the materials that would be in contact with the mercury are:

1) 300 series stainless steel, primarily alloys 304 and 321
2) 17-4 PH stainless steel
3) Butyl rubber
4) Buna "N" O-ring material

13.5.2 Mercury Purity

There are two known basic concerns of mercury purity. First, non-volatiles, such as silver, gold, and copper, may cause mercury to wet the porous tungsten vaporizer and cause liquid mercury penetration of the pores. Second, gases absorbed in the mercury, such as O_2, H_2O, N_2, may be evolved through the vaporizer and cause

cathode insert contamination.

The required mercury purity was established during the SERT II flight program. This requirement is being used for the 8 cm thruster IAPS flight program. A LeRC specification for "Mercury, Standards for High-Purity" was written in 1965. It is included as applicable document No. 13.8-1. The required purity listed in this specification is too high, and was modified for the SERT II and 8 cm thruster programs.

The following revised mercury purity specification is recommended: The total non-volatile concentration shall be 1.5 ppm or less, and the maximum limit of any one element shall be 0.5 ppm or less.

For the IAPS flight program the absorbed gases in the mercury will be removed by the following handling procedure. Vacuum distillation of mercury directly into the propellant tanks allows volatile gases to be removed. The distillation also tends to further reduce any nonvolatile impurity. Another way to remove gases from mercury is to permit liquid mercury to splash over a series of baffles while the baffle region is being vacuum pumped. No known quantitative measurements are available from Hughes or Lewis for volatiles in liquid mercury, either before or after vacuum treatment. However, most mercury samples, when vacuum pumped, will "bump" or "gurgle" while releasing absorbed gases

Therefore, it is recommended that either vacuum distillation or vacuum splashing be used.

13.5.3 Mercury Slosh Dynamics

An important consideration in the use of a propellant tank of the SEP design is the evaluation of the liquid sloshing characteristics of the partially loaded flexible tank. A study was made to analytically determine the resonant frequencies of the tank system and compare them with the anticipated control natural frequency of a spacecraft. This work was accomplished in reference 13.1.1. The system studied was the 20-inch diameter tank.

For this system, the lowest natural frequency was found to be 0.593 hertz, which is higher than the lowest natural frequency of most proposed spacecraft. This lowest natural frequency was assumed to be at the root of the solar array (0.015 Hz).

13.5.4 Two Tank System

The only difference between the schematics shown in figures 13.3-1 and 13.3-2 is the number of storage tanks. The single tank system is lighter than a multiple tank system. The total weight of the support structure and tank system combined is lighter for the multiple tank system. Multiple tank loads are easier to distribute into the support structure and hard mounting points. Either system is acceptable.

Two tanks operate exactly like a single tank system after

they are filled. In order to expel mercury at an equal rate from both tanks, the tanks are pressurized with a common line. This filling procedure insures that the gas pressure is equal in both tanks, and mercury will be expelled at the same rate. Sloshing dynamic effects are different for a single tank than for a two tank system because mercury can flow from tank to tank. Although the calculations of this natural frequency have not been made, each tank should act as though it is somewhat isolated because the tubing acts as an orifice causing damping of the flow. If a two tank design is considered, natural frequency calculations should be made.

13.5.5 Off-Loading the Tank

A large increase in pressure of the propellant could cause intrusion (ie, liquid penetration) of the vaporizers. Since mercury is an incompressable fluid, and its thermal coefficient of expansion is greater than the stainless steel, the tank cannot be completely filled. If the tank were completely filled, a temperature rise would cause a large increase in pressure which would in turn cause intrusion of the vaporizers. In order to prevent intrusion the tank will be filled to something below its maximum capacity. Figure 13.5.5-1 shows fill fraction and reservoir pressure (both at 80° C) as a function of loading temperature for a tank fill fraction (initial) of 0.96 and a reservoir pressure (initial) of 50 psia. The 0.96 fill fraction was arbitrarily chosen for this

calculation. If the maximum temperature expected is $80^{o}C$, then a higher starting fill fraction could have been selected. The dynamic support of the mercury will be better if the fill fraction is as high as possible. It would be better to use a fill fraction of 0.99.

Figure 13.5.5-1 also shows the increase in pressure of the gas pressurant due to an increase in loading temperature. This increase is almost insignificant.

13.5.6 System Utilization

The BIMOD propellant storage and distribution system ideally is capable of 98.5% utilization. The residuals are caused by the bladder of the tank and by the flow volume of the components, primarily the tubing. Applicable document 13.8.3 (NASA Drawing CD-638484) shows the bladder rib pattern that is used to control the mercury to the tank outlet hole especially when the tank is almost empty.

A small amount of mercury will be trapped in the corners of the ribs. When the bladder is laying against the front hemisphere of the tank, it cannot displace mercury, and the amount of mercury trapped in the components and lines is not usable.

13.5.7 Tank Configuration

For a number of reasons, the best configuration for housing a heavy liquid such as mercury is a sphere. The shape of the gas pressurant volume can vary to suit the

packaging needs of the spacecraft. The original tank configuration as proposed by Electro Optical Systems had a cylindrical section and a hemisphere for the nitrogen gas volume. (fig. 13.5.7-1) This configuration is long. In order to reduce the package length, the gas volume was redesigned for SERT II (fig. 13.3.2-1).

By increasing the diameter, the length of the package was reduced. The back of the gas enclosure was designed as a constant stress membrane.

The tank shown in figures 13.4.2-2 and 13.3.2-2 has been designed for SEPS. The mercury is enclosed in a sphere. For load carrying capability the mounting flange of a large tank normally can be as heavy as the rest of the tank. The front part of the flange is designed as a part of the front hemisphere. It is designed as a hollow, high-torsion capability, lightweight section. The liner (bladder support) is welded to the other half of the flange that is used to clamp the bladder and seal the mercury and gas pressurant. The gas enclosure is welded to the front flange. This design double seals the mercury. The flange clamps the O-ring of the bladder. Then the gas enclosure, the flange, and the front hemisphere form a closed tank. This design allows the gas pressurant enclosure diameter to be as large as the flange diameter yielding a very compact configuration.

13.5.8 Tank Stress Calculations

A stress analysis of the 50.8-cm diameter tank shown in figures 13.3.2-2 and 13.4.2-2 was made by the Vehicle Structures Section of NASA LeRC using the following assumptions: (1) a factor of safety of 1.667 was used for burst pressure, (2) burst pressure - 1.667 X 50 psi = 83.3 psi, and (3) the flight design loads were: (a) operating pressure - 50 psi, (b) mercury weight = 936 kg, (c) inertia load factors: 10 g longitudinal and 6 g lateral.

A copy of the complete analysis is available in applicable document 13.8.2.

13.5.9 Fill Valves

The fill and drain valves shown in figures 13.4.2-4 and 13.4.2-5 were flown on SERT II and have been in space for over nine years. A valve similar to the SERT II valve was designed by Electro Optical Systems for the SERT application. The principle of the spring loaded plunger was retained, but the seat design was modified. The revised design allows the O-ring (fig. 13.4.2-4) to seat flat against the valve housing. A lock nut was added to the plunger to prevent the valve from vibrating open during the launch environment. The valve in the closed position (fig. 13.4.2-4) shows the plunger secured in place. The valve is double sealed by the O-ring seal that is designed into the cap. Referring to figure 13.4.2-5 (valve in the open position), the lock nut has been removed, and the cap has been replaced by a stem which automatically

depresses the plunger to open the valve. The stem is designed so that its O-ring is sealed before the plunger is disturbed during installation. The plunger is seated before the stem O-ring is disengaged during removal. This valve design was used for both the mercury and nitrogen pressurant.

Figures 13.4.2-8 and 13.4.2-9 show the same valve with a manifold type base. This design will be used for remote operation, where the base could be mounted to a structural member.

13.5.10 Solenoid Latching Valve

The solenoid latching valve or isolation valve is a Valcor Engineering Part No. V27200-578 (see fig. 13.4.2-11). The moving element is held in its open or closed position by a permanent magnet circuit that requires no holding power.

The solenoid latching valve has the following parameters:

Weight (estimated), lb	0.6
Operating pressure, psig (bidirectional)	30
Proof pressure, psig	50
Burst pressure, psig	120
Temperature (ambient and Fluid), ^{o}F	-36 to 176

The valve electrical parameters are:

Power at 22 Vdc, W	30
Voltage, Vdc	22 to 34
Duty cycle	Intermittent
Latching pulse (minimum), misc	50 to 100

The valve electrical connector is a 3-pin Bendix PTIH-8-3P, or equal. The electrical schematic of the connector is shown in figure 13.5.10-1.

The Valcor valve was selected over pyrotechnic-type valves after an extensive testing program. The information has been documented in a Hughes report, "Test Report, Mercury Shutoff Valves, Special Test" (see applicable document 13.8.4).

One of the anticipated problems of using an isolation valve is that when the valve is opened the dynamic effect of the mercury flow could cause intrusion of vaporizers. As a part of the 8-cm IAPS flight program Hughes tested the valve to determine what pressure surge could be identified at the vaporizer. The test setup is shown in figure 13.5.10-2. Mercury was loaded in the system up to the test valve. The line between the test valve and the high response pressure transducer was evacuated through valve V-4. The system was pressurized to 35 psia and the test valve opened. A plot of the pressure vs. time (fig. 13.5.10-3) shows that the surge was very low. The reason is the high impedance to flow was caused by the 1/16-inch-diameter tubing, and the simulated feed tube coil. The valve was also actuated with mercury in the system. There was no apparent pressure increase due to the actuation. The Valcor valve has no effect on the vaporizer operation.

13.5.11 Pressure Transducer

The pressure transducers are the same transducers that are used by Hughes for the IAPS program. The transducer (C.J. Enterprises Model CJSG-3101) has a range of 0 to 50 psia and has the following electrical parameters:

Current (maximum), mA.....15

Input voltage, Vdc.....28 ± 4

Output voltage, Vdc.....0 to 5

Limiting voltage, Vdc.....-1 and 7

Output impedance, ohm..... 100

Output noise, mVRMS (dc to 10 kHz)..... 10

Isolation resistance at 50 Vdc, Mohm.....100

The regulation of these transducers is ± 5 mV maximum change over the entire range of 28 ± 4 Vdc. The transducers electrical connectors are designated as HSC S 7002-8-4P and wired as:

Pin A is Pos. Exc.	Pin B is Pos. Out
Pin C is Neg. Out	Pin D is Neg. Exc.

As a part of the IAPS program, Hughes has written a test procedure and test report covering the propellant tankage, valves, and feed unit (applicable documents 13.8.5 and 13.8.6, respectively). The pressure transducer testing was included.

13.5.12 Temperature Transducer

The temperature transducer is a Fenwall Electronics, Inc. thermistor. The iso-curve thermistor is a CB34PM292 unit potted in a H3/ probe assembly.

The thermistor's electrical parameters are:

Input voltage, Vdc.....5

Output voltage, Vdc.....0 to 5

Resistance (R_o) at 77° F, Kohm.....4

Operating temperature range, ° F.....-50 to +350

The temperature transducer will operate across a standard resistive telemetry circuit as shown in figure 13.5.12-1.

13.5.13 Field Joint

The field joints all use Resistoflex fittings (shown in fig. 13.4.2-14 and 13.4.2-15). These fittings are all the same size except for the mounting hole for the mercury tubes. The design attributes of the Resistoflex fittings shown in figure 13.5.13-1 are listed below:

1) The beam portion of the shoulder continues to seal at its inner edge after tightening. The Belleville spring action serves as a lock for the entire union, preventing loosening. The forces built up in the union are parallel to the center line, which assures no deformation of the sealing interface or restriction of the fluid streams. This also permits each area to serve its own function without being dependent on any other function.
2) Resistoflex fittings are lighter than flared, modified flared and flareless fitting designs.
3) The protrusion of the tube shoulder into the connec-

tor is at a minimum. This facilitates installation of tubing particularly short runs and straight lengths.

4) Because the stress on sealing surfaces is controlled by the build-in dimensions, the Resistoflex fitting is not torque sensitive.

13.5.14 Fill and Drain Procedure

The actual fill and drain procedure has not been finalized for a SEPS size propellant tank. The proposed fill and drain procedures are similar to those used for SERT II (applicable document 13.8.7) and 8-cm IAPS (applicable document 13.8.5) programs.

The drain or removal of mercury has been considered by Hughes in two documents: (1) "Procedure for Removal of Mercury from Thruster-Gimbal Beam Shield Unit (TGBSU)" prepared by C.R. Dulgeroff (applicable document 13.8.8) and (2) "Special Procedure for Removal of Mercury from the Reservoir" (applicable document 13.8.9).

13.5.15 Cleaning Procedure

All of the stainless steel parts will be cleaned and passivated per finish no. 5.4.1 of MIL STD-171A. All parts will also be ultrasonic cleaned using freon. (applicable document 13.8.10) The "SERT II Process Spec, Ultrasonic Cleaning of SERT II Hardware" will be used as the basis for the freon cleaning.

13.6 Physical Characteristics and Constraints

Table 13.6-1 is a list of the weights of the components shown in the system schematics (figures 13.3-1 and 13.3-2).

The weight of the propellant tank will vary with the size. The mass fraction (tank weight divided by the weight of the mercury capacity of the tank) was calculated for a number of different tank sizes. Table 13.6-2 shows the weights and corresponding mass fraction.

It is obvious from table 13.6-2 that in the larger tank sizes, the mass fraction is close to 0.020. If the amount of mercury required for a particular mission is known, the weight of the tank can be found by interpolating table 13.6-2.

Table 13.6-3 gives a rough physical size of the three largest tanks shown in table 13.6-2.

R is the radius of the sphere of mercury. R' is the radius of the gas volume. L is the length of the straight section of the gas volume.

Referring to the dual tank system schematic of figure 13.3-1, a system weight breakdown would be as shown in table 13.6-4 assuming 1600 kg of mercury and eight thrusters.

13.7 Development History

In 1965 and 1966, a mercury propellant storage and distribution tank was designed and fabricated by the Electrical Optical Systems Company, under a NASA LeRC contract. The design consisted of a positive expulsion tank in which an elastomeric bladder separated the liquid mercury from

pressurant gas. Two fill and drain valves, one for the mercury and one for the gas were also included. The basic EOS design is shown in figure 13.5.7-1.

This design formed the basis for the SERT II flight tank (reference 13.1.2). The SERT II system utilized two tanks to supply mercury to each thruster, one for the main propellant and one for the neutralizer cathode. This was done to individually monitor the utilization of mercury to the thruster and the neutralizer. Two thruster systems were used on the SERT II spacecraft.

The SERT II spacecraft was launched February 3, 1970. The pressures of the two main propellant tanks have been monitored for the lifetime of the flight, most recently in March of 1979. The pressure is still directly related to the mercury utilization. The concept and the material selection have proven flight worthy. The two systems with two tanks each, have been successful for over nine years in space.

This same concept and materials selction have been adopted and flight qualified for the ion auxiliary propulsion system (IAPS). A photograph of the ion auxiliary propulsion system is shown in figure 13.7-1. An auxiliary propulsion system will be flow on the United States Air Force STP P80-1 flight in late 1981. The ion auxiliary propulsion system will consist of two 8 cm thruster systems and associated diagnostics.

Figure 13.7-1 shows the STP P80-1 engineering-model, qualification system. A solenoid latching valve, pressure transducer, and field joints have been added to the system and qualified for flight.

The SEP propellant storage and distribution system (shown in fig. 13.3-1) utilizes the same flight qualified and proven components, procedures, and materials as for the SERT II and P80-1 programs. The only new component is the manifold. It could be considered in the category of tubing hardware.

The propellant storage and distribution system is the most flight proven system of all the SEP systems.

13.8 Applicable Documents Enclosed

13.8.1 Mercury, Standards for High-Purity - NASA SPECIFICATION for NASA LeRC No. 101, 1965.

13.8.2 Edwards, R. C.; and Seeholzer, T. L.: Comet/Ion Drive Propellant Tank Stress Analysis. Dec. 1978.

13.8.3 Propellant Storage and Distribution System Drawing List.

13.8.4 Mercury Shutoff Valves Special Test. (Hughes Aircraft Co.; NASA Contract NAS3-21023.) June 1978.

13.8.5 Test Procedure, Peopellant Tankage, Valves, and Feed Unit (PTVFU). (TP-300, Hughes Aircraft Co.; NASA Contract NAS3-21023.) Jan. 1978.

13.8.6 Propellant Tankage, Valves, and Feed Unit - Design Verification Program. (TR-300, Hughes Aircraft Co.; NASA Contract NAS3-21023.) Aug. 1978.

13.8.7 Check Sheet 7 - Thruster Feed System Assembly Loading. (SERT II Ion Thruster System.)

13.8.8 Dulgeroff, C. R.: Procedure for Removal of Mercury from Thruster-Gimbal-Beam Shield Unit (TGBSU). (NASA Contract NAS3-21023.) March 1978.

13.8.9 Special Procedure for Removal of Mercury from the Reservoir. (Hughes Aircraft Co.; NASA Contract NAS3-21023.) March 1978.

13.8.10 SERT II PROCESS SPEC, Ultrasonic Cleaning of SERT II Hardware. Sept. 1968.

13.9 Ground Support Equipment

A fixture for vibration testing the tank, pressure and temperature transducers, fill valves, and solenoid latching valve, has been designed, and is being manufactured. Equipment for loading and unloading the system has been designed.

TABLE 13.4.2-1 PS&D System Components

COMPONENT	INTERFACES WITH	FIGURE	PART OR DWG. NUMBER
Mercury Tank (NASA -LeRC)	Interface Truss & Mercury Line	13.4.2-2	CD 638481 CF 638482 CD 638483 CD 638484 CC 638485
Temperature Transducer (Fenwall Electronics	Mercury Tank	13.4.2-3	H34
Nitrogen Fill Valve (NASA - LeRC)	Mercury Tank	13.4.2-4 13.4.2-5	CD 632178 CC 632179 CB 632180 CB 632181 CC 632182 CC 632183
Pressure Transducer (C.J. Enterprises)	Mercury Line & Mercury Manifold	13.4.2-6 13.4.2-7	CJSG-3101
Mercury Fill & Drain Valve (NASA-LeRC)	Mercury Line	13.4.2-8 13.4.2-9	CD 635902 CC 635903 CC 635904 CB 632180 CB 632181 CC 632182 CC 632183
Solenoid Latching Valve (Valcor Engineering Corp.)	Mercury Line	13.4.2-11	C96487-V27200-578
Manifold (NASA-LeRC)	Mercury Line	13.4.2-10	N.A.

TABLE 13.4.2-1 (Cont'd) PS&D System Components

COMPONENT	INTERFACES WITH	FIGURE	PART OR DWG. NUMBER
Flexible Gimbal Line (NASA-LeRC)	Thruster & Solenoid Latching Valve	13.4.2-12	CF 637903 Part #17
"Y" Fitting (NASA-LeRC)	Mercury Line	13.4.2-13	SKRIM-1
Field Joints (Resistoflex Corp.)	Mercury Line	13.4.2-14 13.4.2-15	50599-C-R44621 50599-C-R44620 50599-C-R44671 50599-C-R44672 50599-C-R44697 50599-C-R28722 50599-C-R44626
Tubing	All of above components		304 S.S. ASTM A269-65 -0.06250D x .0096 wall -0.0900D x .0125 wall -0.1250D x .018 wall

TABLE 13.6-1 COMPONENT WEIGHTS

COMPONENT	WEIGHT GRAMS
FILL VALVE	90.
PRESSURE TRANSDUCER	77.3
TEMPERATURE TRANSDUCER	1.3
SOLENOID LATCHING VALVE	181.
FIELD JOINT	9.4
TUBING W/FT. 1/8 DIA.	.006 #/FT
W/FT. 1/16 DIA.	.013 #/FT
MANIFOLD	100.
TUBING "Y"	12.5

TABLE 13.6-2 Tank Weight, Mercury Weight, Mass Fraction

	TANK WEIGHT Kg	MERCURY WEIGHT Kg	MASS FRACTION TANK WEIGHT/MERCURY
SERT II	1.3	14.5	.089
	3.7	120.	.031
	4.8	198.	.0243
	11.9	500.	.0238
	17.0	722.	.0235
	18.5	800.	.0231
	20.7	931.	.0222
	22.2	1000.	.0222
	26.2	1250.	.0210
	32.0	1600.	.0200

TABLE 13.6-3 Tank Size Versus Mercury Weight

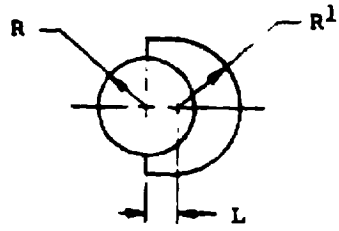

MERCURY (Kg)	R (INCHES)	R'(INCHES)	L (INCHES)
1000	10.25	11.37	2.92
1250	11.00	12.12	3.30
1600	12.00	13.12	3.35

TABLE 13.6-4 Dual Tank System Weight Breakdown

INTERFACE TRUSS

COMPONENTS		WEIGHT (Kg)
Tanks (2)		37.
Temp. Transducer (1)		.0013
Pressure Transducer (2)		.1446
Fill Valves (3)		.270
Solenoid Latching Valve (3)		.362
Manifold		.1
Tubing		.1
	TOTAL	37.9779

BIMOD SECTIONS

Field Joints (27)		.254
Solenoid Latching Valve (8)		1.448
Tubing "Y"		.050
Tubing		.18
	TOTAL	1.932
	TOTAL SYSTEM	39.9[illegible]

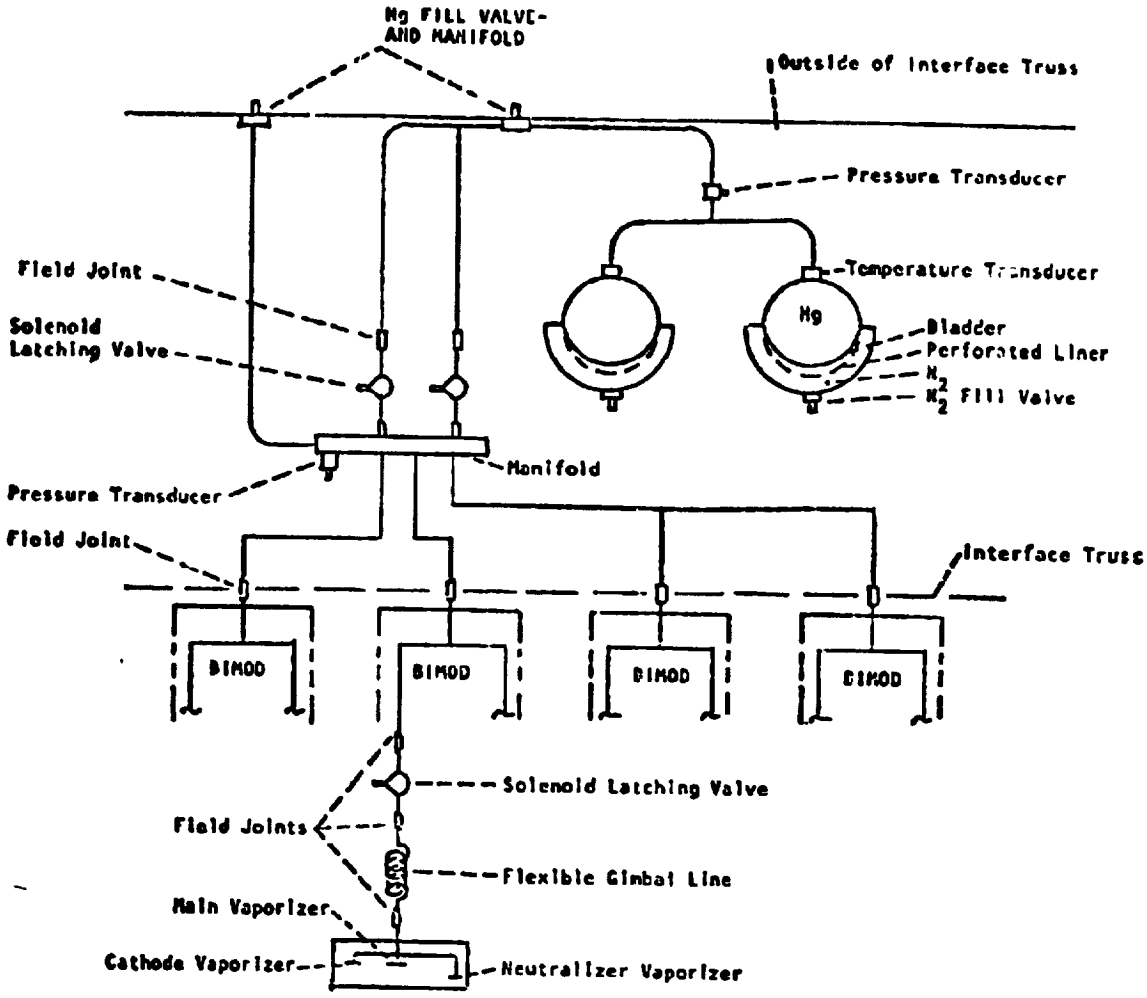

FIGURE 13.3-1 BIMOD, PSD, THRUSTER SYSTEM SCHEMATIC - DUAL TANK SYSTEM

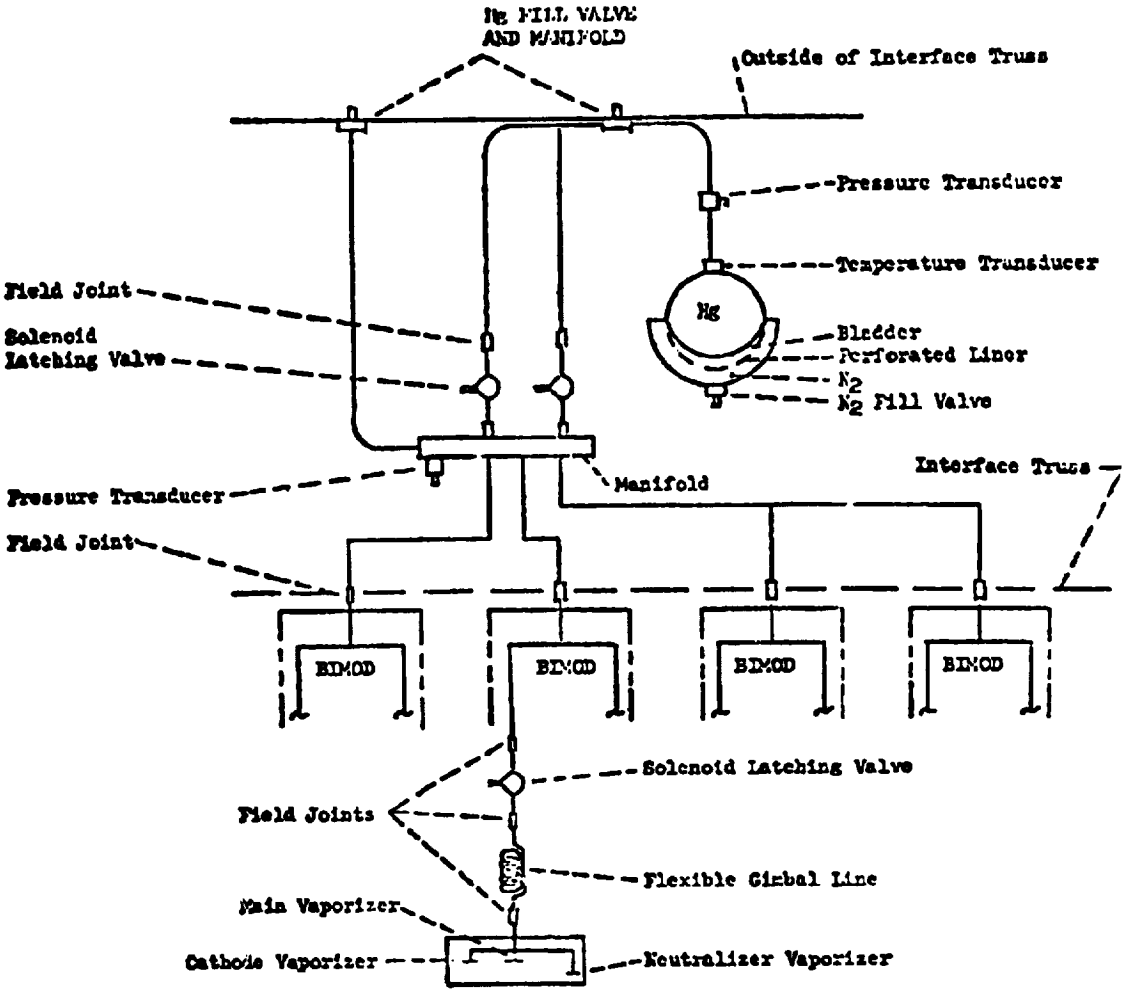

FIGURE 13.3-2 BIMOD, PSD, THRUSTER SYSTEM SCHEMATIC-SINGLE STORAGE TANK

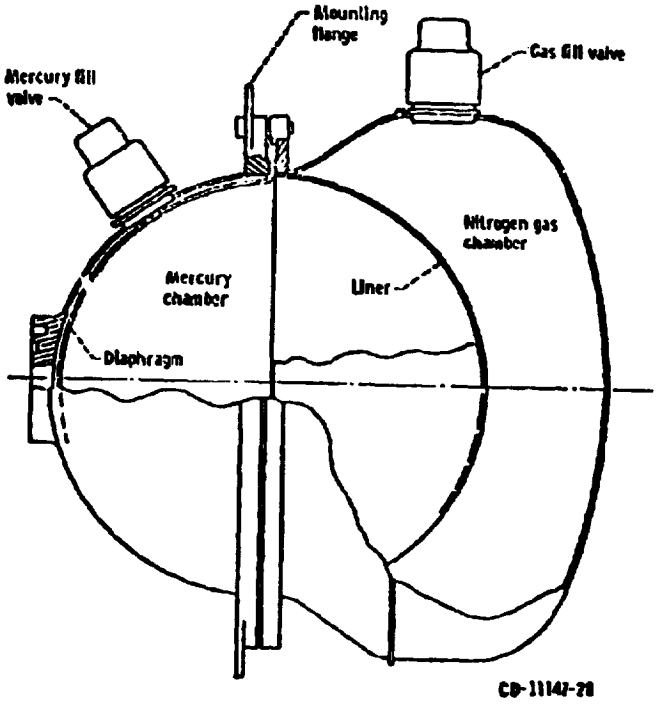

FIGURE 13.3.2-1 SERT II TANK DESIGN

FIGURE 13.3.2-2 91 Kg Mercury Capacity Propellant Tank

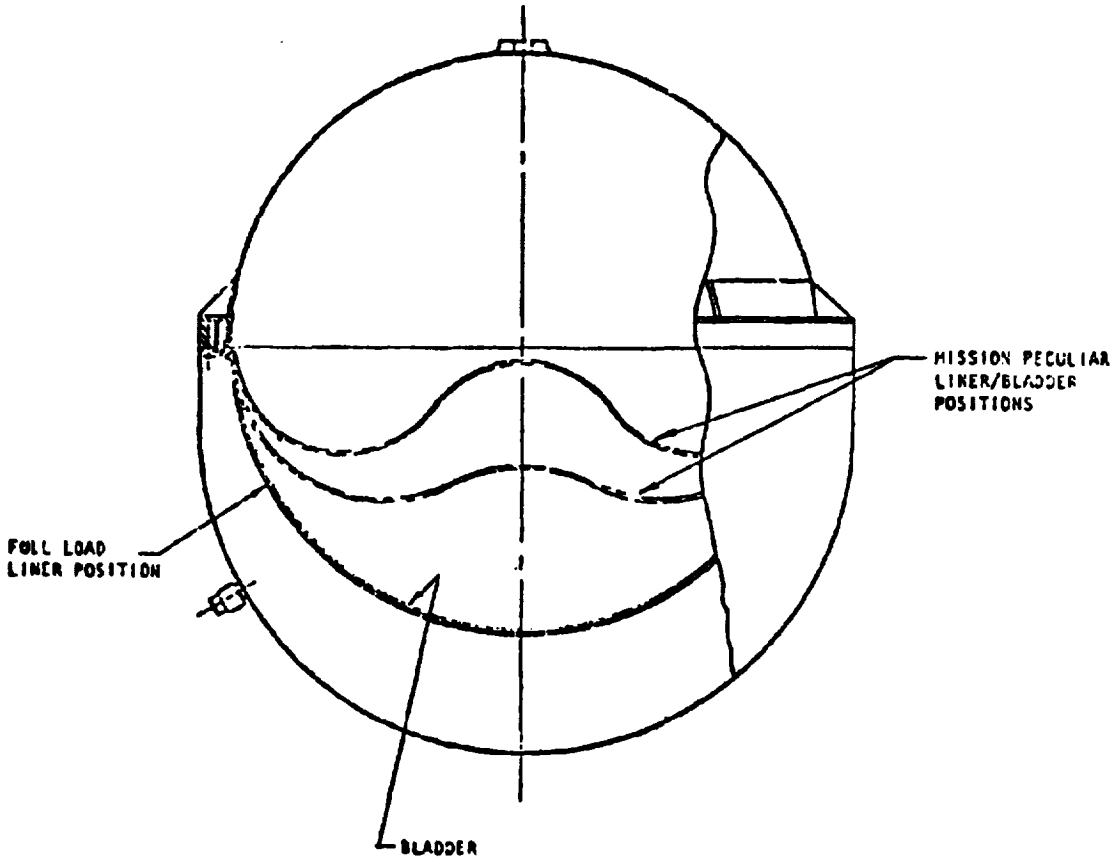

FIGURE 13.3.2-3 Mercury Propellant Tank

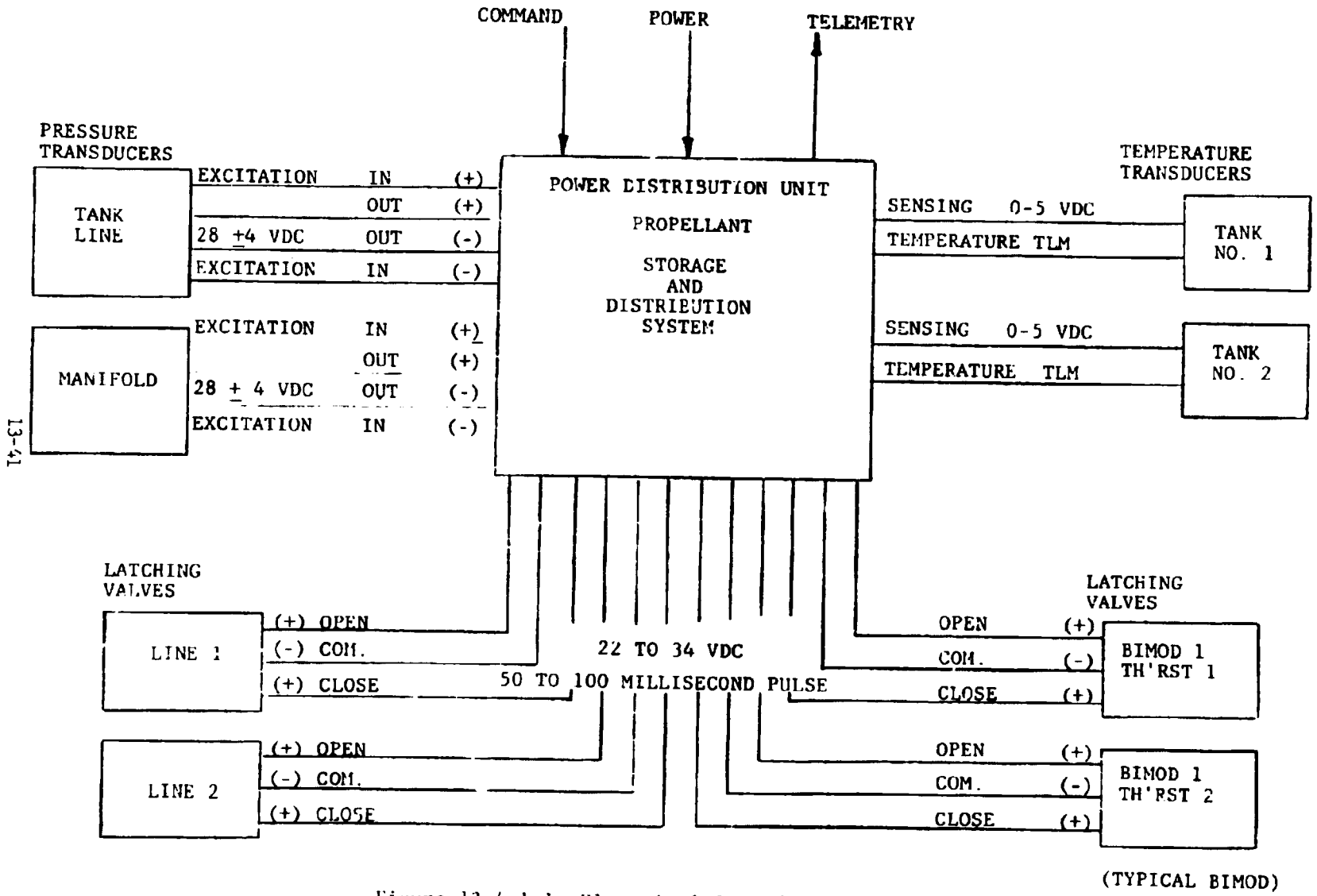

Figure 13.4.1-1 Electrical Interface Diagram

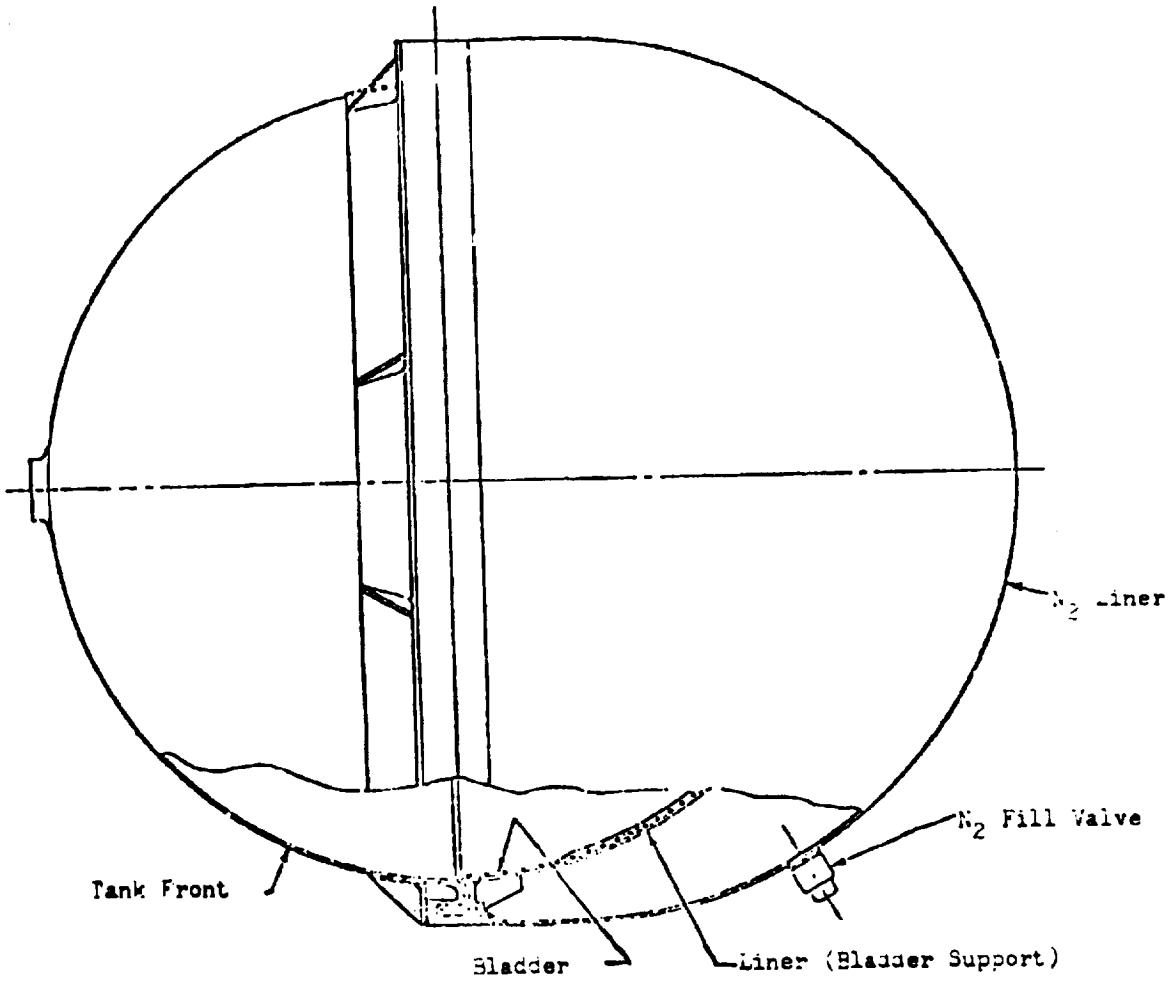

FIGURE 13.4.2-2 MERCURY STORAGE TANK

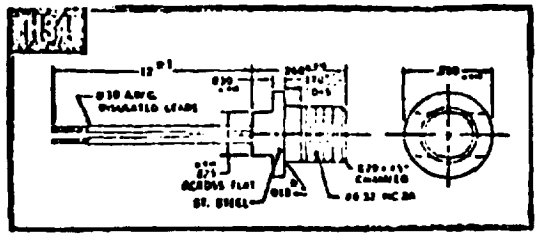

APPLICABLE THERMISTOR SENSORS	MAX. TEMP.	NOMINAL PRESSURE RATING	SHOCK RATING (MIL)	VIBRATION RATING (MIL)	ACCELERATION RATING (MIL)
1-2 beads	300°F [600°F] (Note 1)	—	50 G (Note 7)	50 G (Note 11)	100 G (Note 12)

FIGURE 13.4.2-3 TEMPERATURE TRANSDUCER

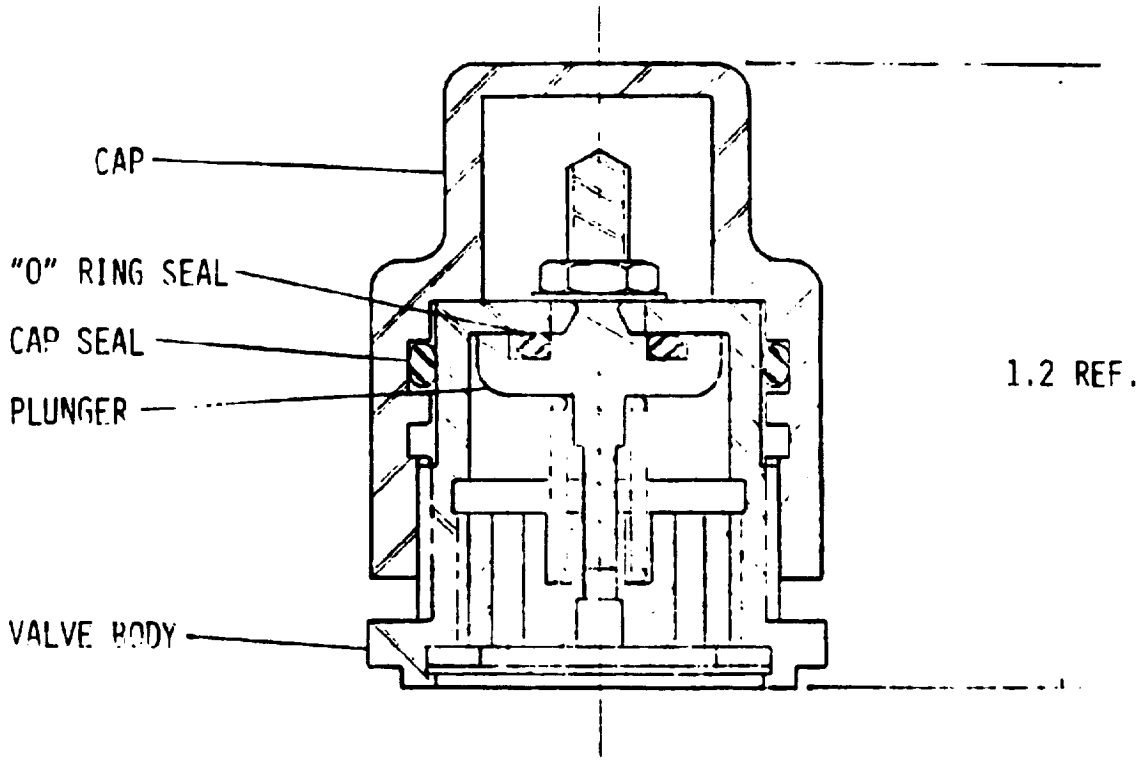

FIGURE 13.4.2-4 NITROGEN FILL VALVE (CLOSED)

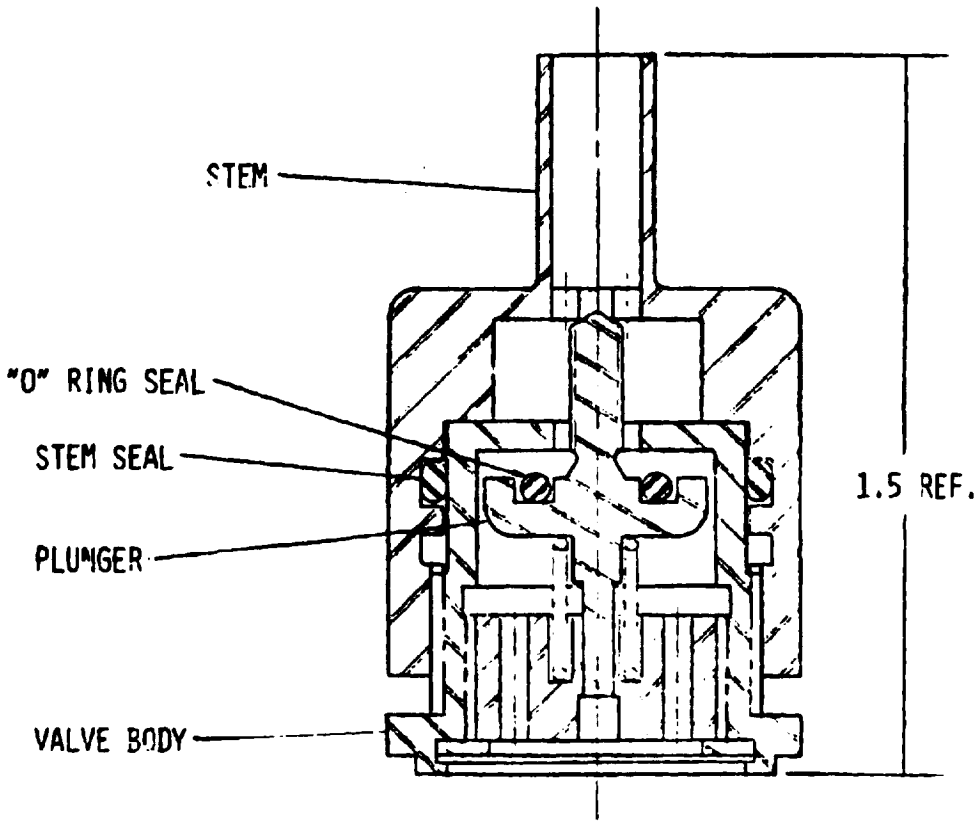

FIGURE 13.4.2-5 NITROGEN FILL VALVE (OPEN)

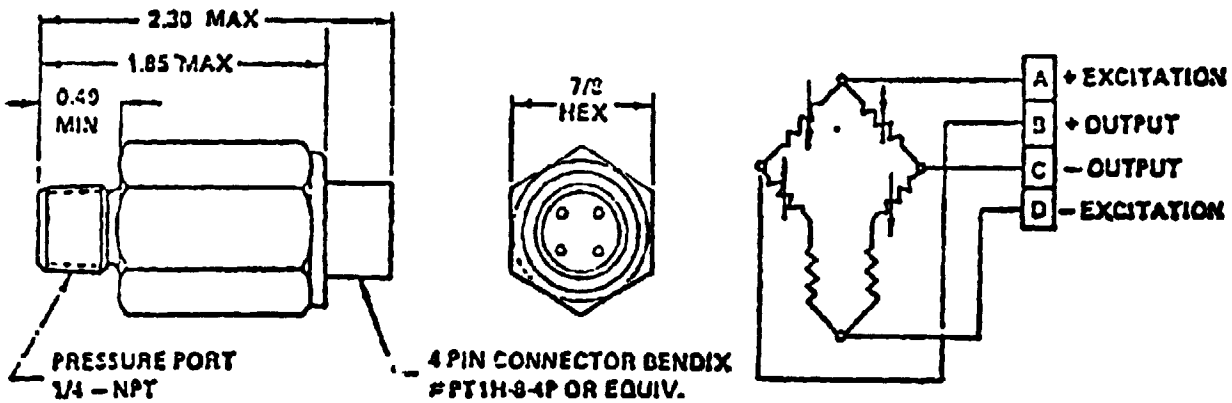

C. J. ENTERPRISES MODEL CJSG-3101

HUGHES P/N 3508634

FIGURE 13.4.2-6 PRESSURE TRANSDUCER

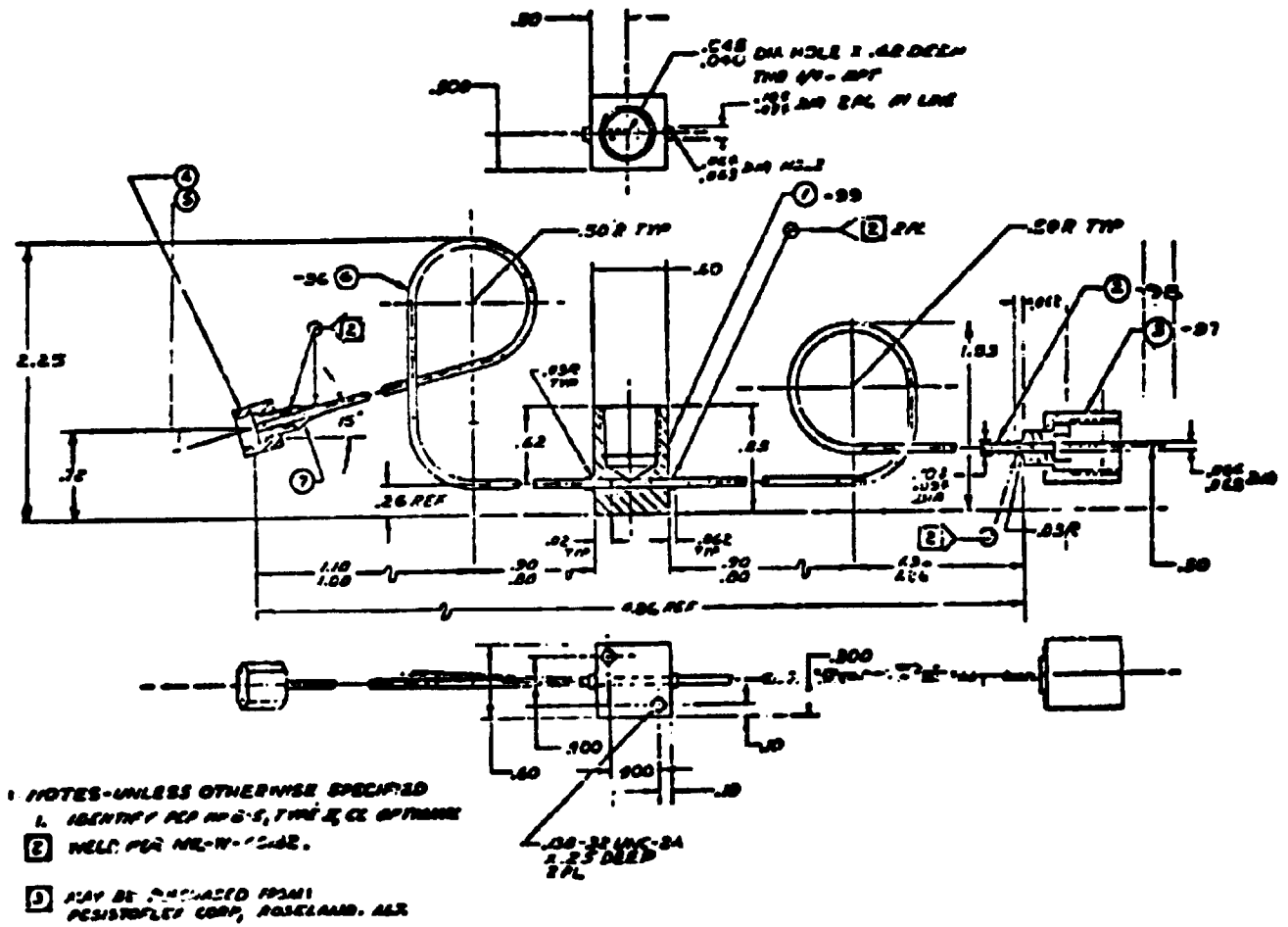

FIGURE 13.4.2-7 PRESSURE TRANSDUCER IN-LINE MOUNT

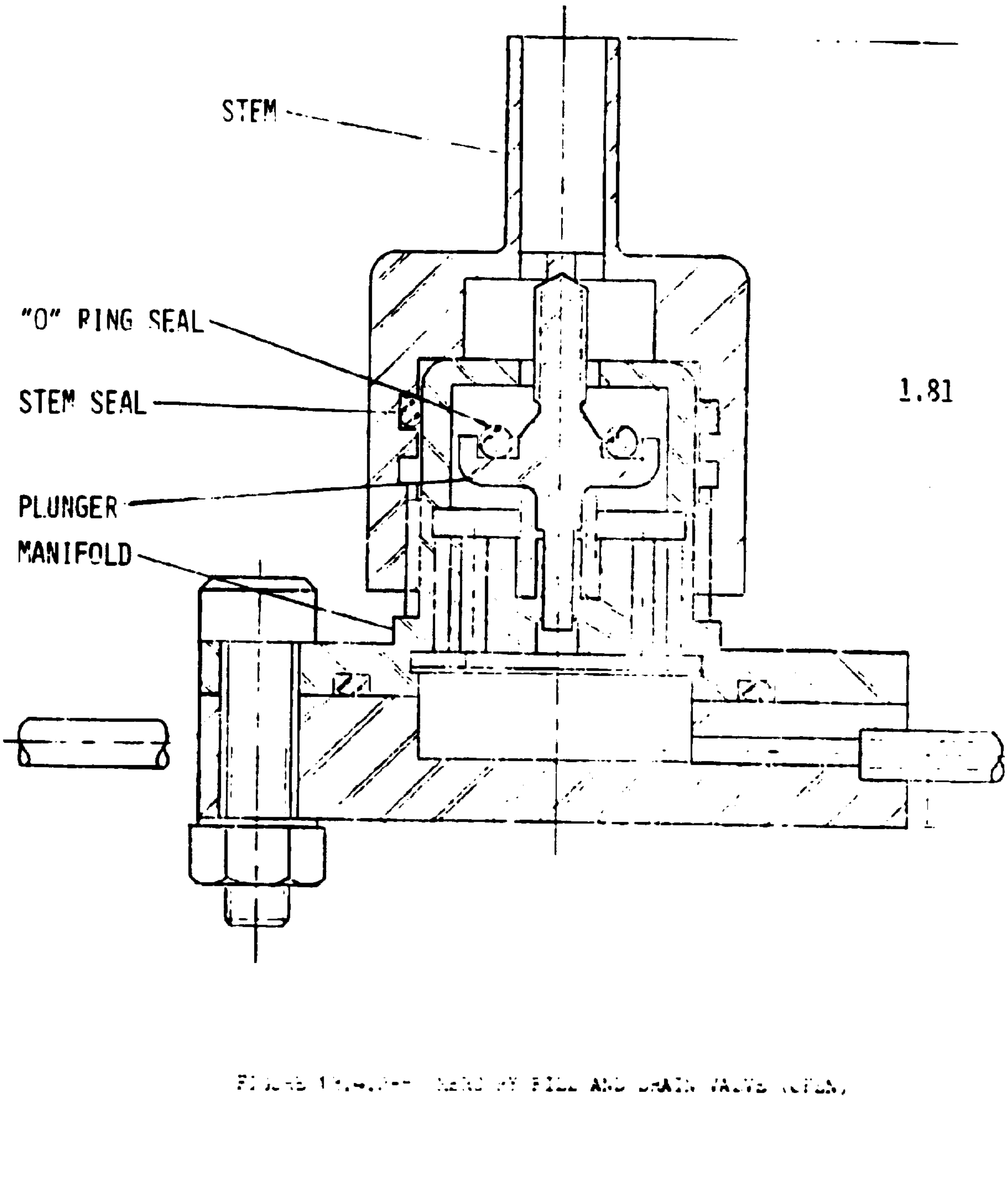

FIGURE [illegible] MERCURY FILL AND DRAIN VALVE (OPEN)

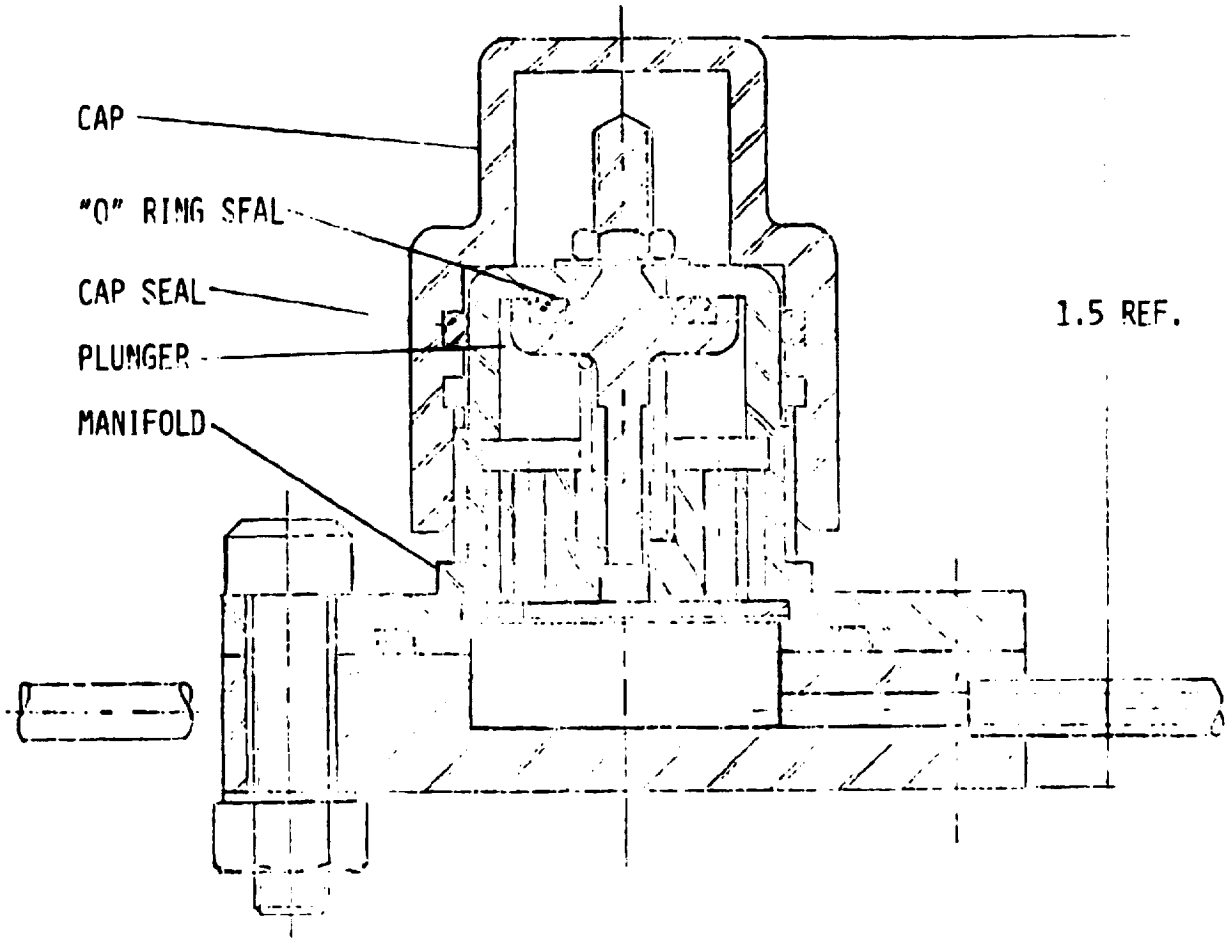

FIGURE 13.4.2-1 REPOSITORY FILL AND DRAIN VALVE (CLOSED)

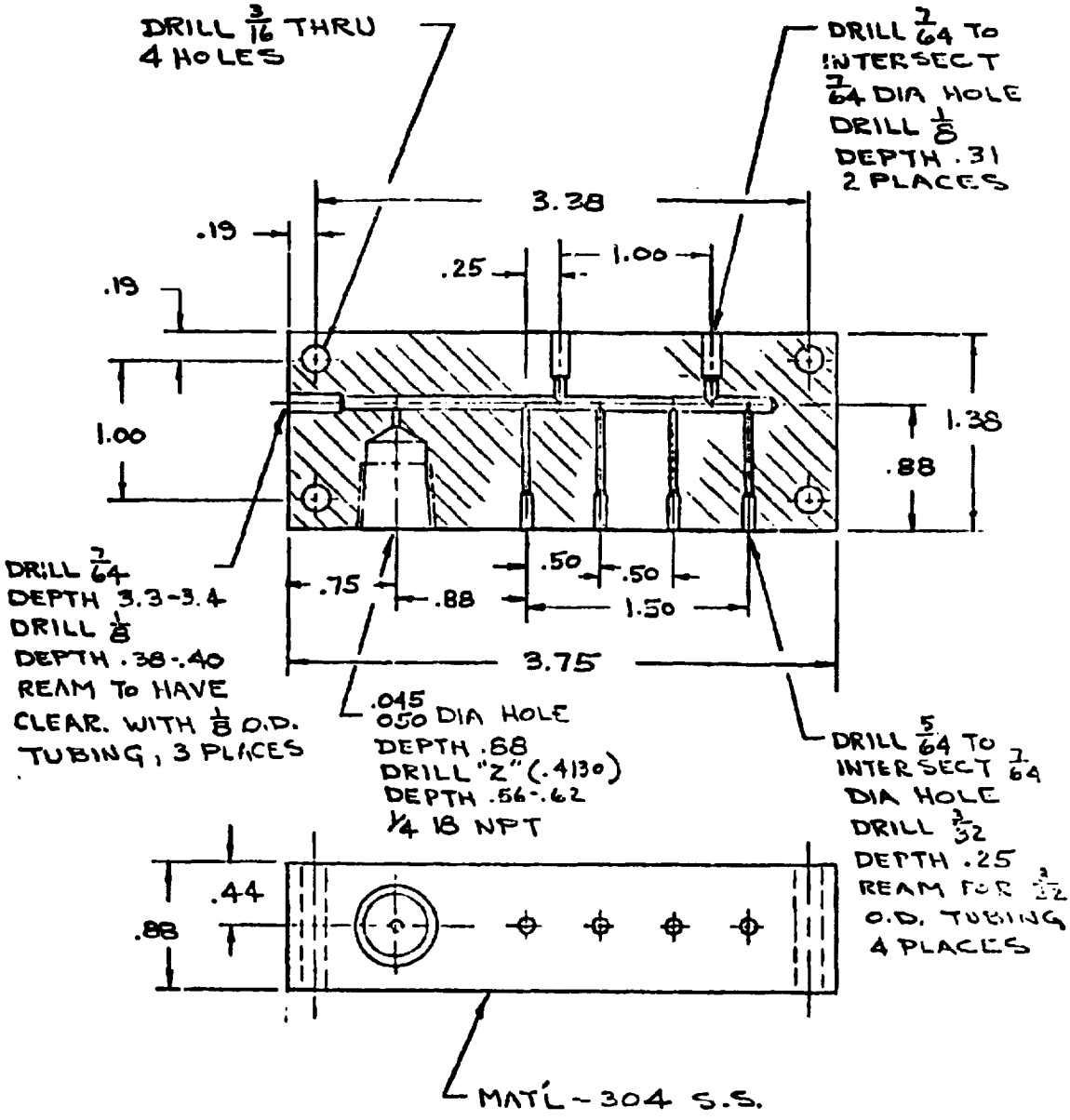

FIGURE 13.4.2-10 MAIN MANIFOLD

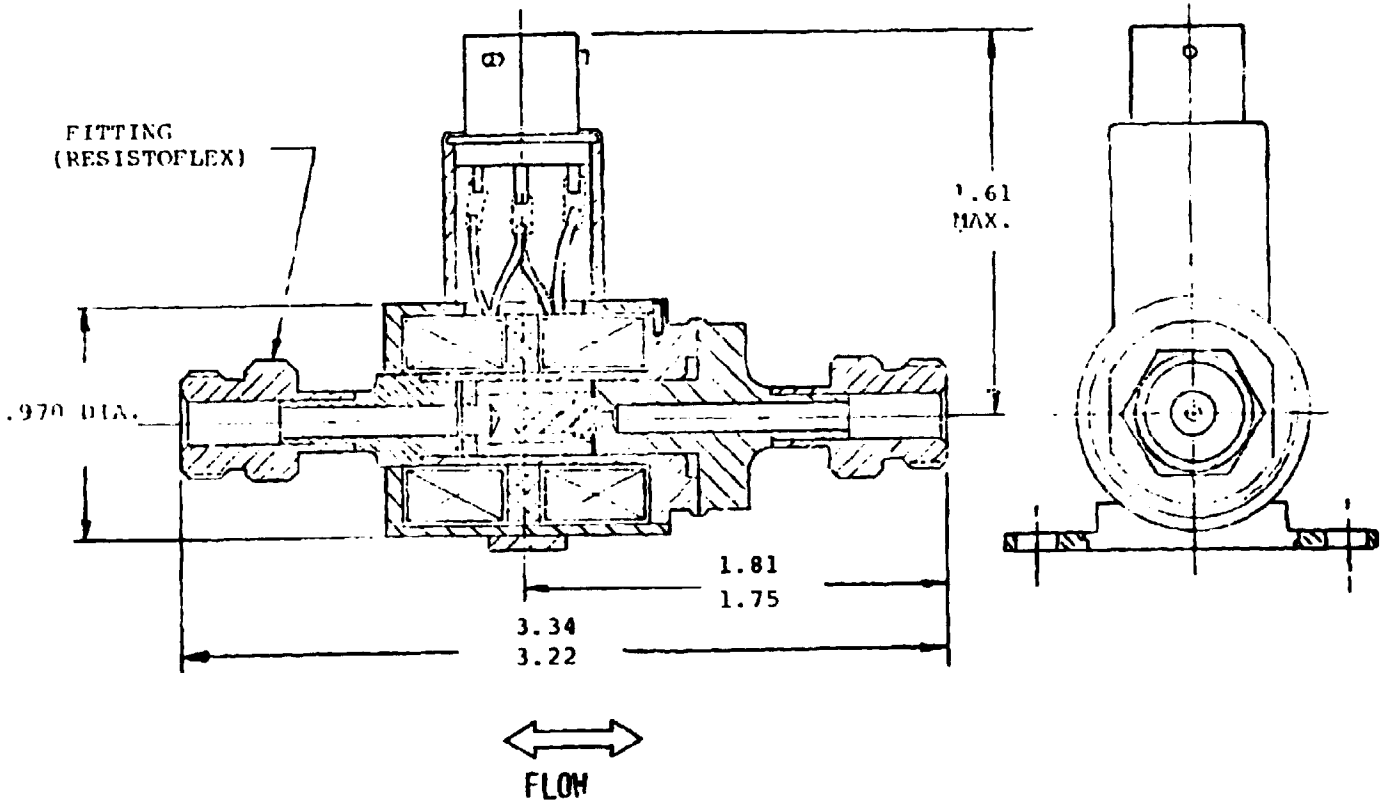

FIGURE 13.4.2-11 SOLENOID LATCHING VALVE

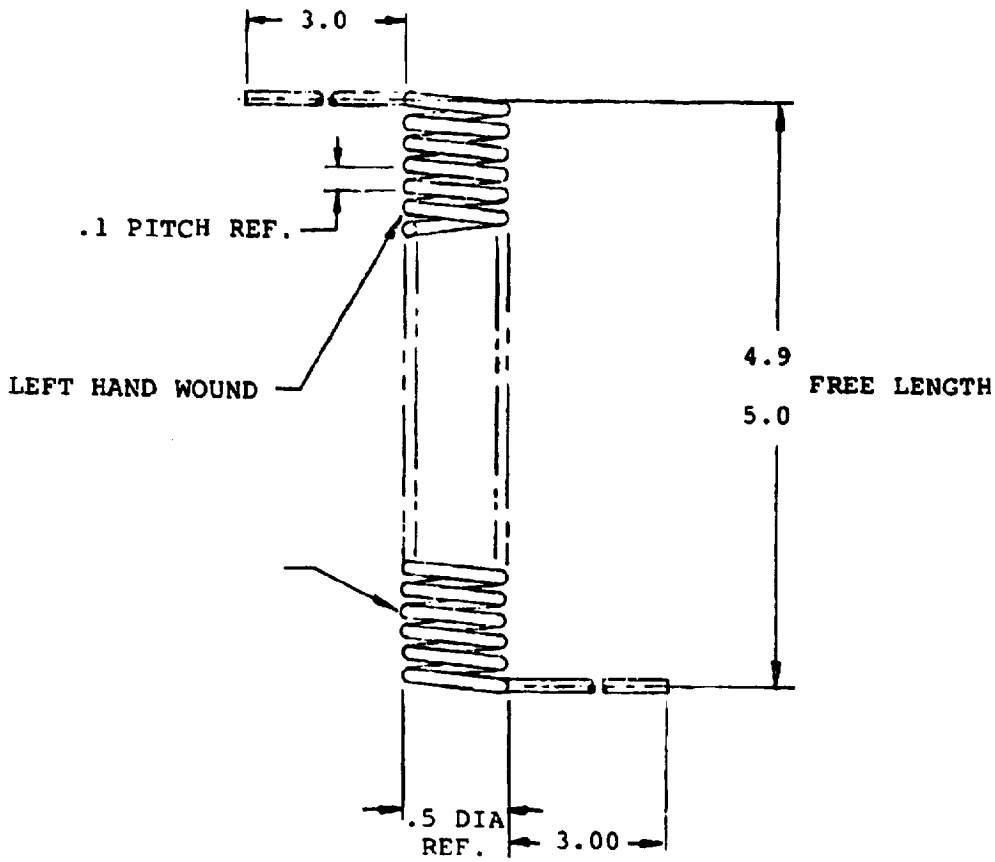

FIGURE 13.4.2-12 FLEXIBLE GIMBAL LINE

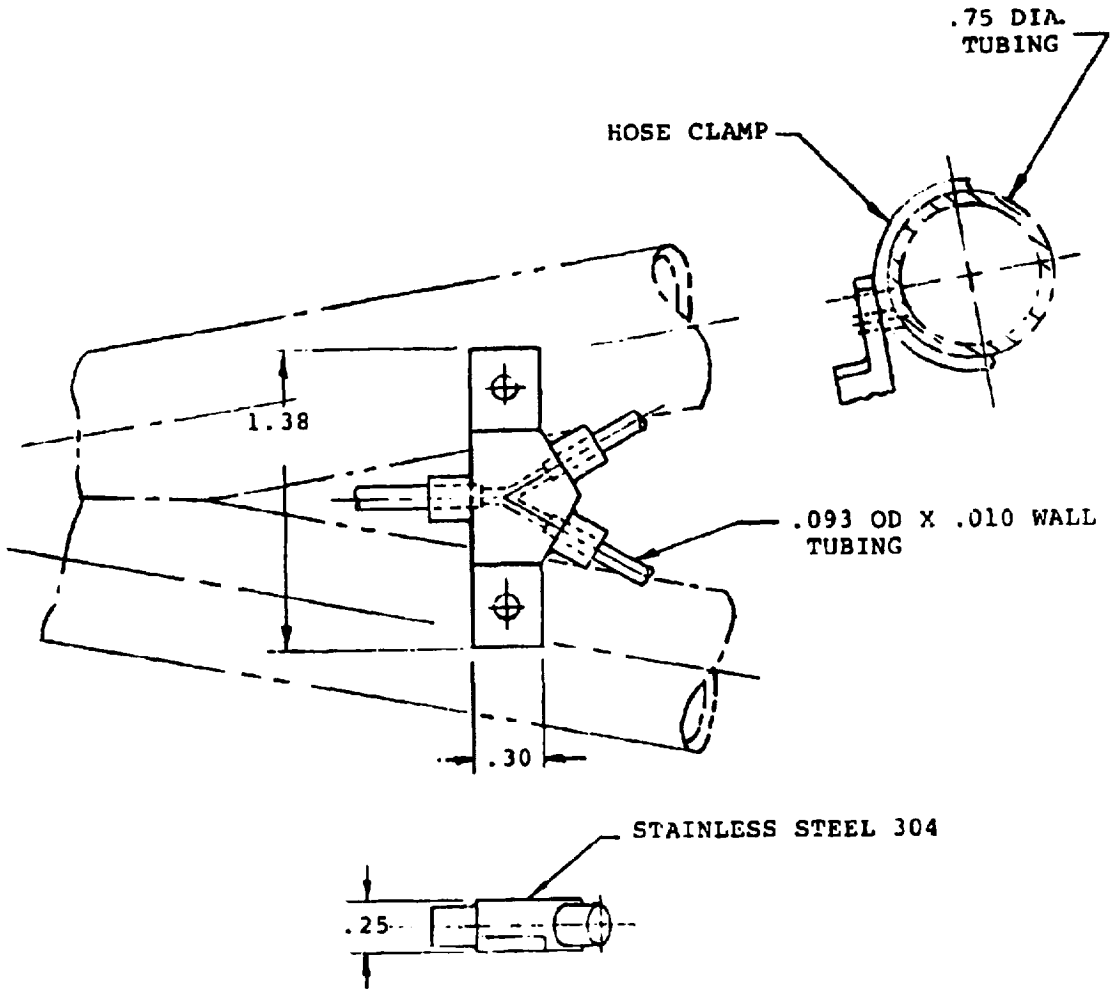

FIGURE 13.4.2-13 "Y" FITTING FOR MERCURY FEED LINE

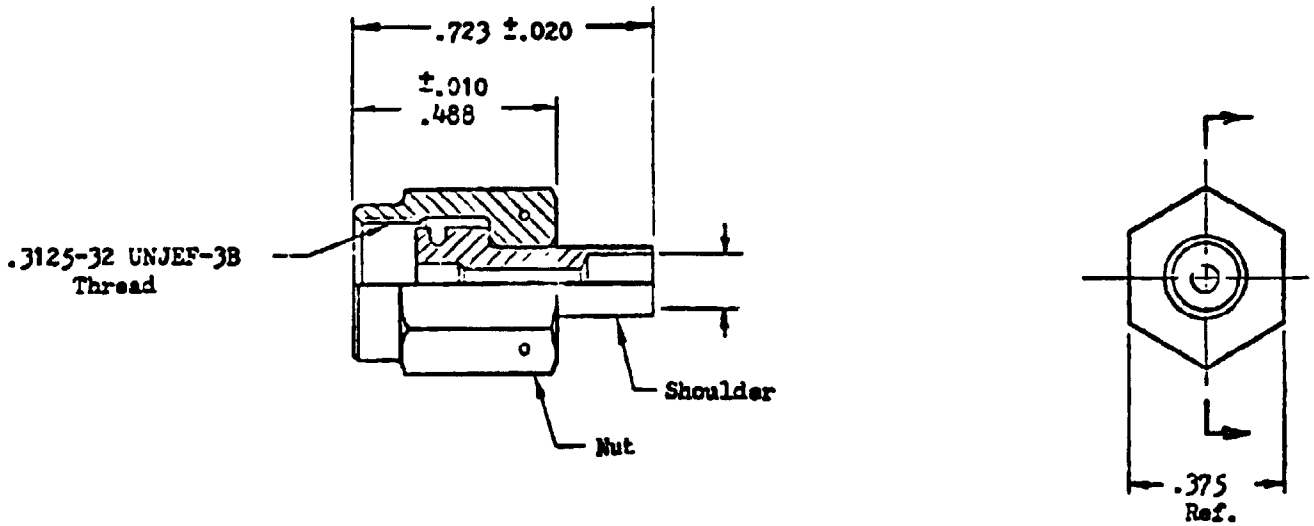

Dash No.	A
-01	.132 .130
-02	.098 .096

FIGURE 13.4.2-14 SHOULDER AND NUT (FIELD JOINT)

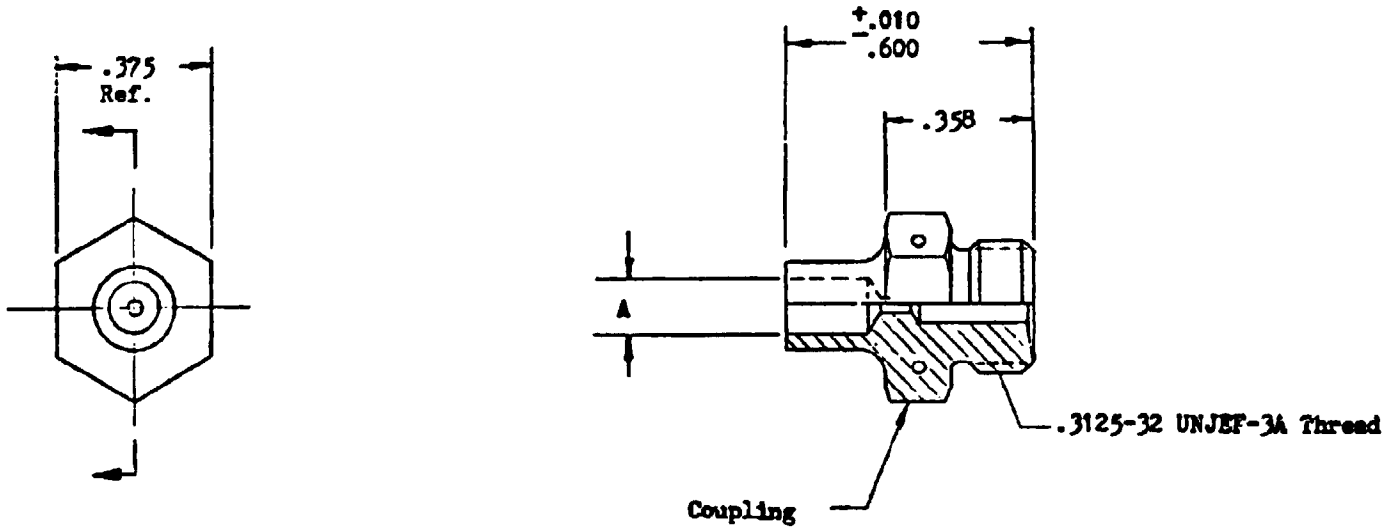

Dash No.	A
-01	.132 .130
-02	.098 .096

FIGURE 13.4.2-15 COUPLING (FIELD JOINT)

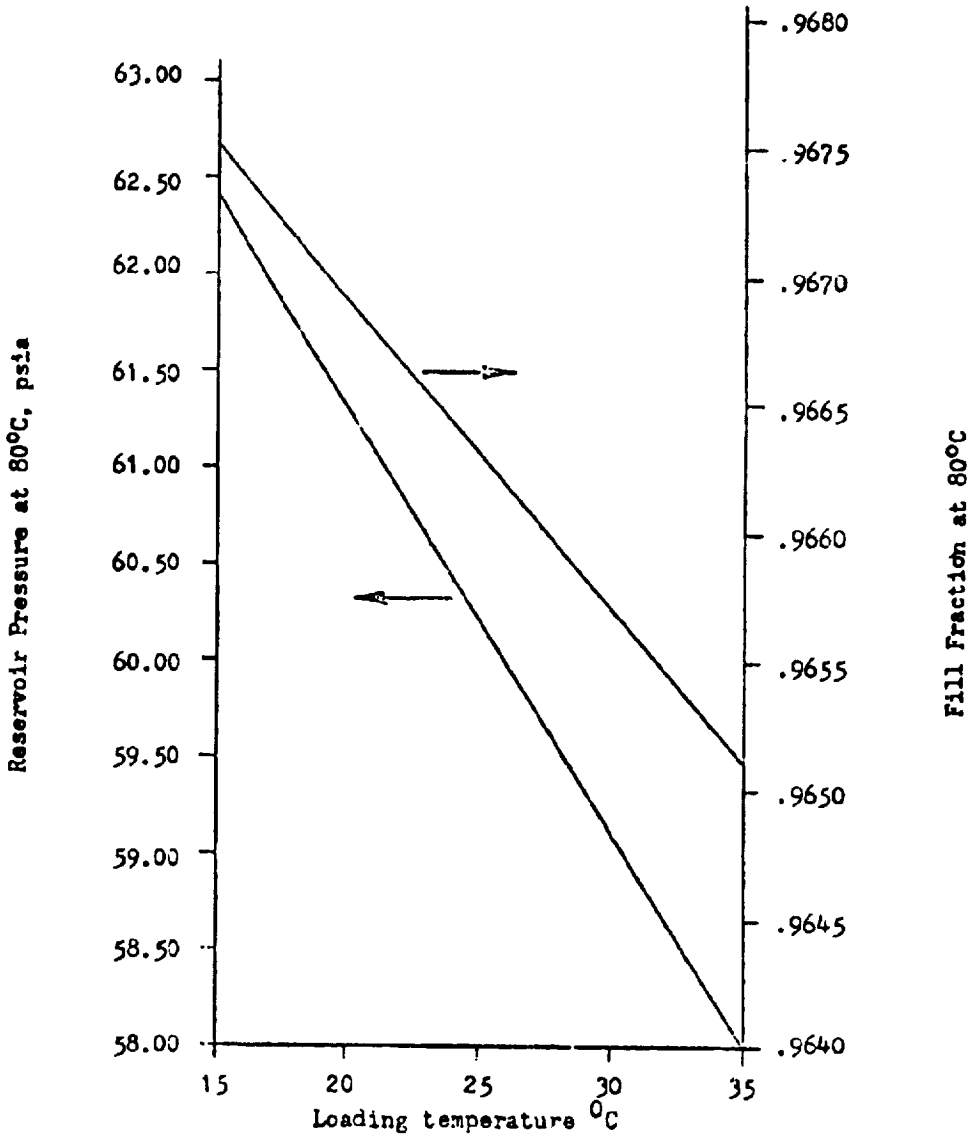

FIGURE 13.5.5-1 FILL FRACTION AND RESERVOIR PRESSURE AT 80°C vs. LOADING TEMPERATURE

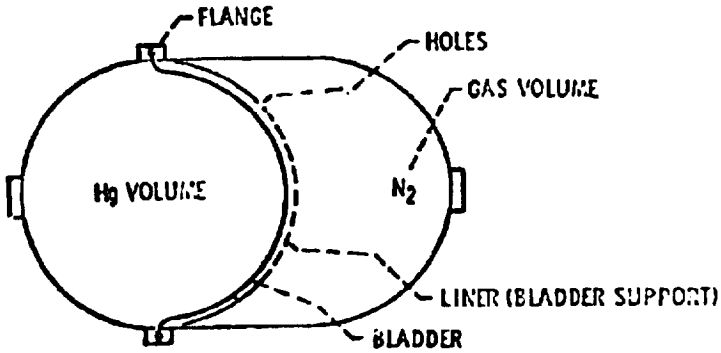

FIGURE 13.5.7-1 ELECTRO OPTICAL SYSTEMS TANK DESIGN

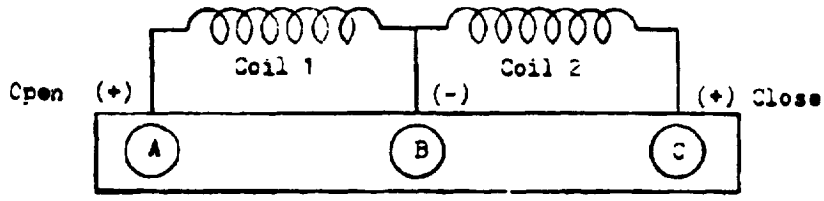

FIGURE 13.5.10-1 ELECTRICAL SCHEMATIC OF THE SOLENOID LATCHING VALVE CONNECTOR

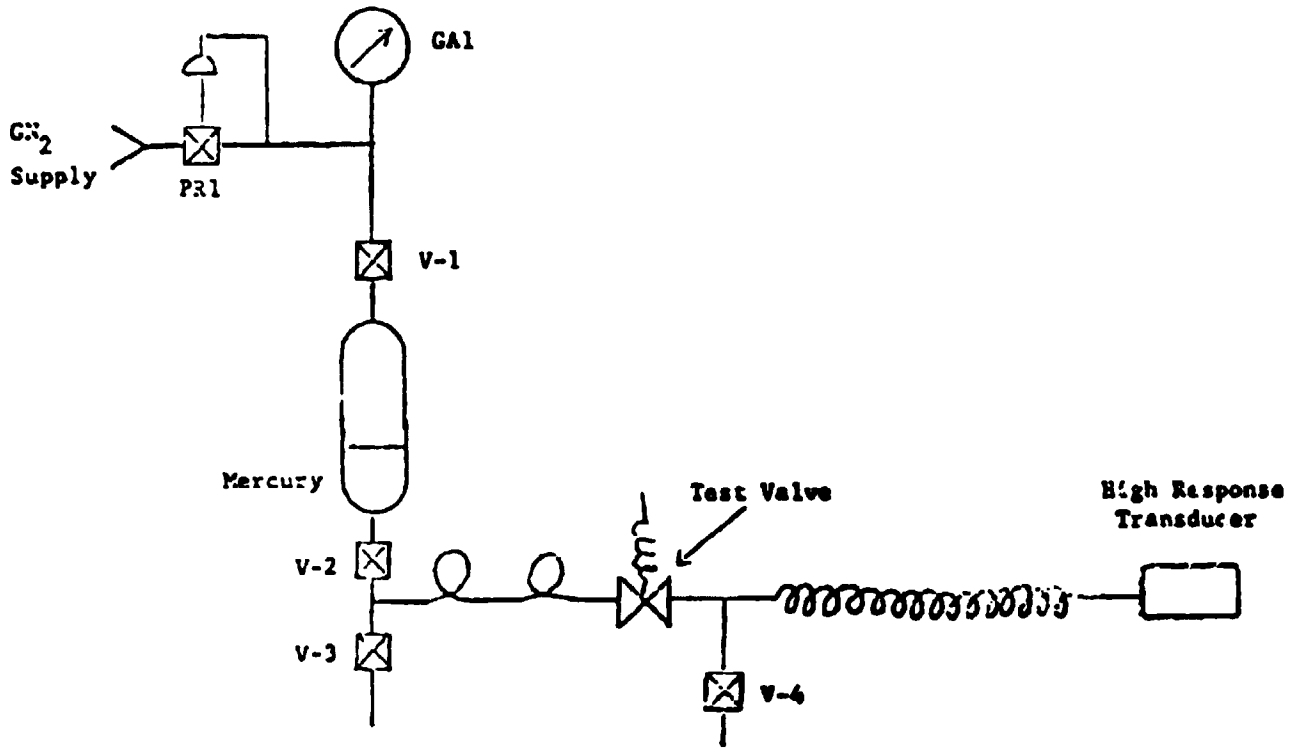

FIGURE 13.5.10-2 Mercury Control Valve Intrusion Test Configuration

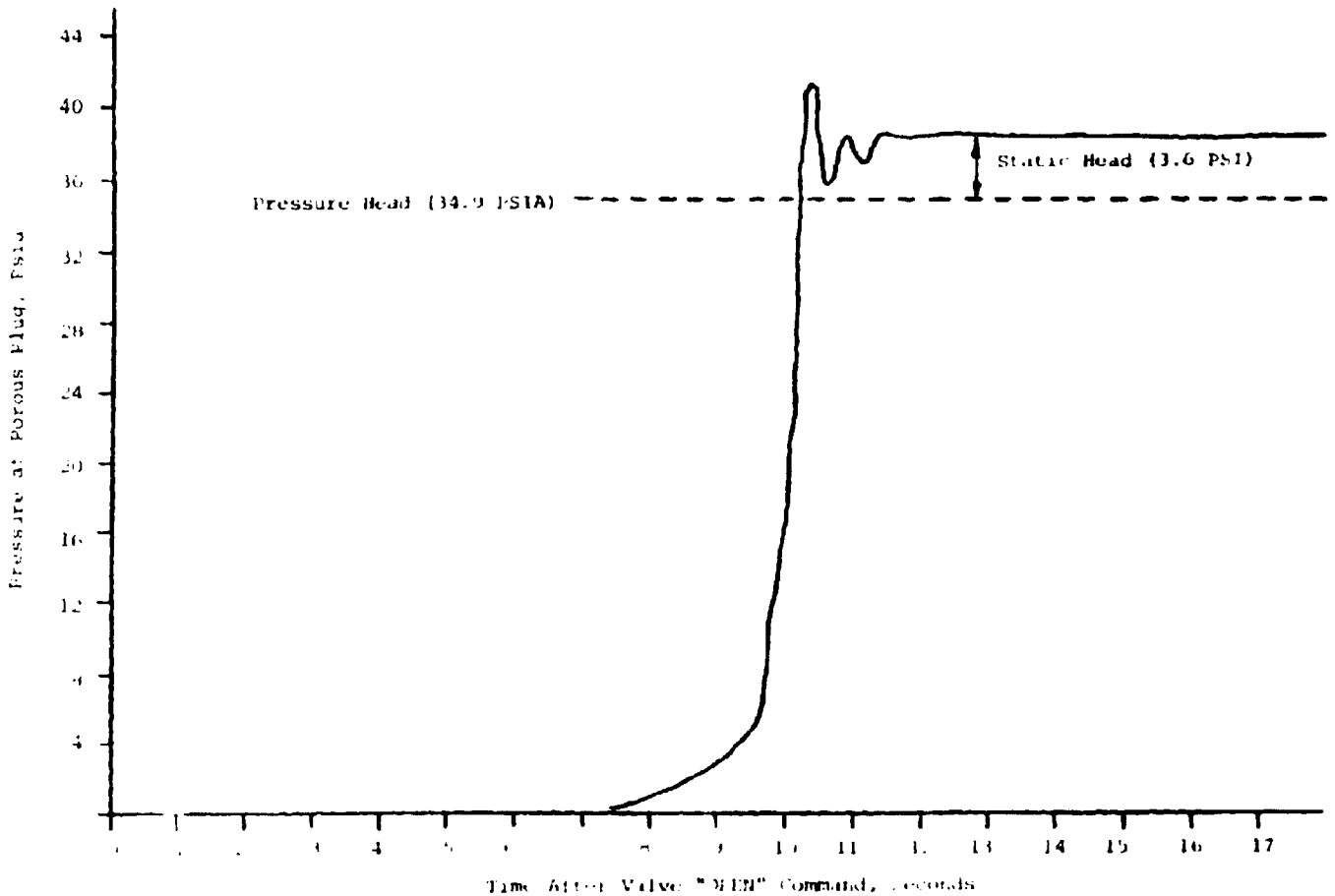

TABLE 13-6 LATCHING VALVE TEST RESULTS

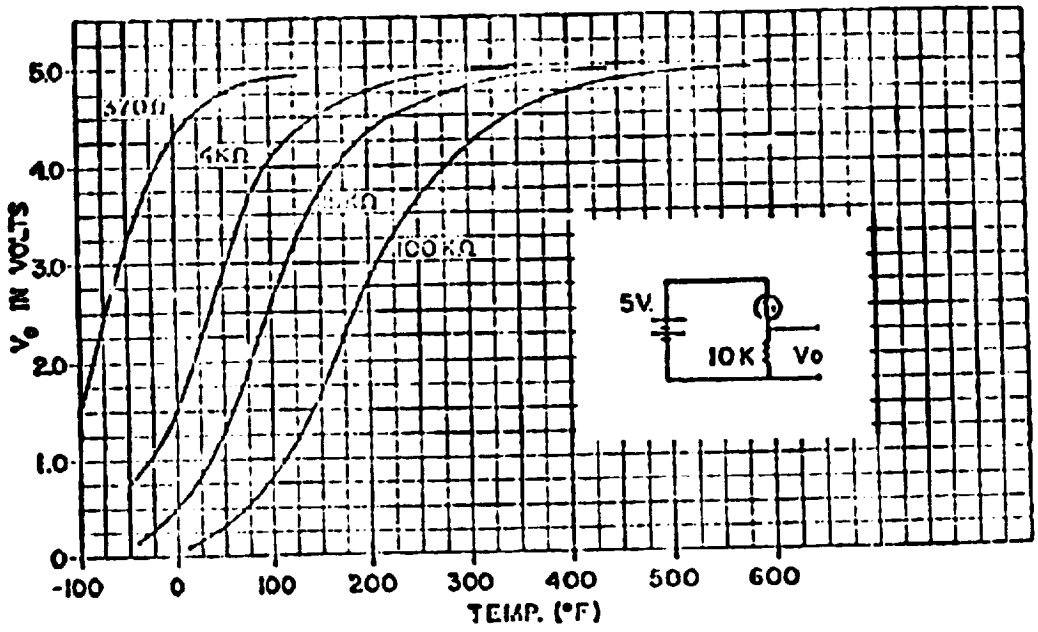

FIGURE 13.5.12-1 Half-bridge voltage output vs temperature for various ISO CURVE thermistors.

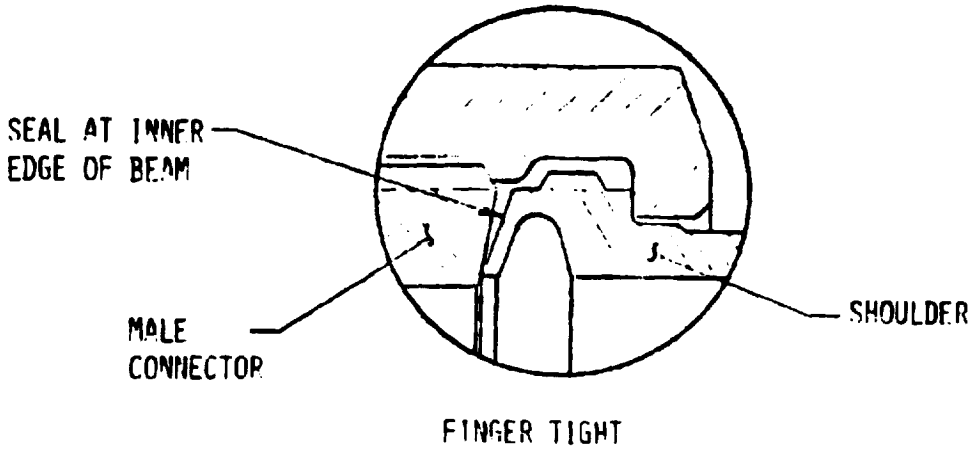

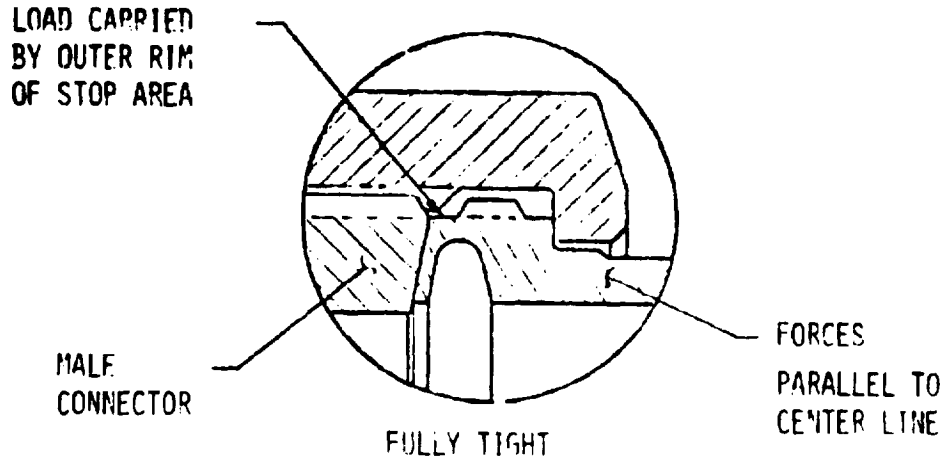

FIGURE 13.5.13-1 DESIGN ATTRIBUTES OF RESISTOFLEX FITTINGS

FIGURE 13.7-1 ION AUXILIARY PROPULSION SYSTEM

14.0

INTERFACE MODULE STRUCTURE/THERMAL CONTROL

Table of Contents

		Page
14.0	Interface Module Structure/Thermal Control. . . .	14-1
14.1	Reference Documents	14-2
14.2	Functional Requirements	14-2
14.3	Functional Description	14-2
14.3.1	Mechanical.	14-2
14.3.2	Thermal	14-3
14.4	Interface Definition.	14-4
14.4.1	Mechanical.	14-4
14.4.2	Thermal	14-4
14.5	Performance Description	14-5
14.6	Physical Characteristics and Constraints. . . .	14-5
14.7	Development History	14-5
14.8	Applicable Documents Enclosed	14-6
14.9	Ground Support Equipment.	14-6

FIGURE

14.3.1-1	Thrust Subsystem	14-7

14.0 Interface Module Structure/Thermal Control

14.1 Reference Documents

14.1.1 Space Shuttle Program, Space Shuttle System Payload Accommodations, Level II Program Definition and Requirements. NASA JSC 07700, Volume XIV, Revision F, June 1978, including Change No. 27, November 1978.

14.2 Functional Requirements

The primary function of the interface module is to provide a direct load path from the four BIMODs to the supporting Avionics Package while maintaining simple interfaces. In addition to this primary function, this module also serves to support the two propellant tanks and house the interface control electronics.

The structural requirements imposed on the design of the interface module consisted of quasi-static inertia loading conditions and minimum frequency conditions. The quasi-static loads were taken from reference 14.1.1 and applicable documents 14.8.1 and 14.8.2, with an appropriate factor to account for possible dynamic response of the SEP system mounted on the IUS interface (see Section 9.2). In order to minimize dynamic coupling with the STS/IUS/SEP system, a minimum cantilevered frequency of the TSS was taken as 10 Hz.

14.3 Functional Description

14.3.1 Mechanical

The interface module is an aluminum space frame type

structure with tubular structural members (fig. 14.3.1-1). Hard points are provided at the bottom and top of the frame for easy attachment of both the BIMODs and the Avionics Package. Each mercury tank is supported by eight struts which attach to the module at the top nodes. The vertical tank loads are transferred directly from these nodes into the Avionics Package while the in-plane tank loads (kick loads) are carried by the top chord members of the frame.

The BIMOD loads are transferred directly to the nodes at the bottom chord, travel through the planar truss, which forms the sides of the frame, and into the Avionics Package. The interface control electronics is housed on the interior of the frame; the exact nature of their supports will depend on its size and weight.

14.3.2 Thermal

As shown in figure 14.3.1-1, the interface module will be wrapped in MLI blankets. This MLI provides a thermal enclosure for the interface module equipment. The heat generated by the interface module electronics will be used to maintain the interface module components within their allowable temperature ranges. Since the ion drive controller dissipates 6 watts almost continually, a passive radiator (5.0 cm by 7.6 cm) with an emittance of 0.9 will be provided to reject the excess heat and maintain its temperature within the specified limits.

The MLI blanket on top of the interface module consists of the same materials as discussed in Section 9.3.2. In order to provide meteoroid and cometary dust particle protection, as well as preventing solar flux from impinging on the interior of the interface module, the MLI placed around the interface module will consist of the same materials as discussed in table 9.3.2-1 of Section 9.3.2

14.4 Interface Definition

14.4.1 Mechanical

The interface module interfaces with the Avionics Package and the BIMODs. The interfaces were purposely kept simple so that assembly and disassembly could be achieved with minimum effort. The top chord of the interface module contains 10 hard points (pads) which can be attached to the Avionics Package. The bottom chord has provisions for each BIMOD at four places. The outside envelope of the module forms a rectangular parallelepiped whose dimensions are approximately 0.75 m high by 2.6 m long by 0.96 m deep.

14.4.2 Thermal

The MLI blankets wrapped around the PPUs provide the thermal interface between the BIMOD thrust systems and the interface module and thermally isolate them from each other. Similarly, the MLI blanket across the top

of the interface module structure provides the thermal interface between the interface module and the Avionics Module and thermally isolates them from each other.

The MLI blanket around the space exposed surfaces provides the thermal interface between the interface module and the space environment.

14.5 Performance Description

To date no interface module hardware has been constructed. Therefore, there has been no hardware performance to describe. BIMOD structures are attached to the interface module. Section 9.5 is a performance description of the BIMOD structure.

14.6 Physical Characteristics and Constraints

The physical size of the interface module is approximately 0.75 m high by 2.6 m long by 0.96 m deep. A complete description of the envelope and protruding parts is TBD.

The overall mass of the interface module is TBD.

The interface module shall be designed to withstand the functional requirements outlined in Section 14.2.

14.7 Development History

The development history of the interface module has consisted primarily of configuration studies as outlined in Section 10.7. To date no hardware has been constructed. The actual fabrication and assembly of this module is

considered straightforward and no problems are envisioned.

14.8 Applicable Documents Enclosed

14.8.1 Trubert, M.; Bamford, R.: Limit Loads for Preliminary Design of the Galileo S/C and its Components. JPL Interoffice Memorandum, March 1978.

14.8.2 IUS/Spacecraft ICD Parametric Interface Requirements STS/Twin Stage IUS-NASA Generic, Boeing Company ICS-A-81225, July 1978.

14.9 Ground Support Equipment

Handling fixtures will be required. The exact nature of these fixtures is TBD. Vibration fixtures will also be necessary for vibration testing at both the component level (i.e., interface module with tanks and electronics) and the stage level (TSS).

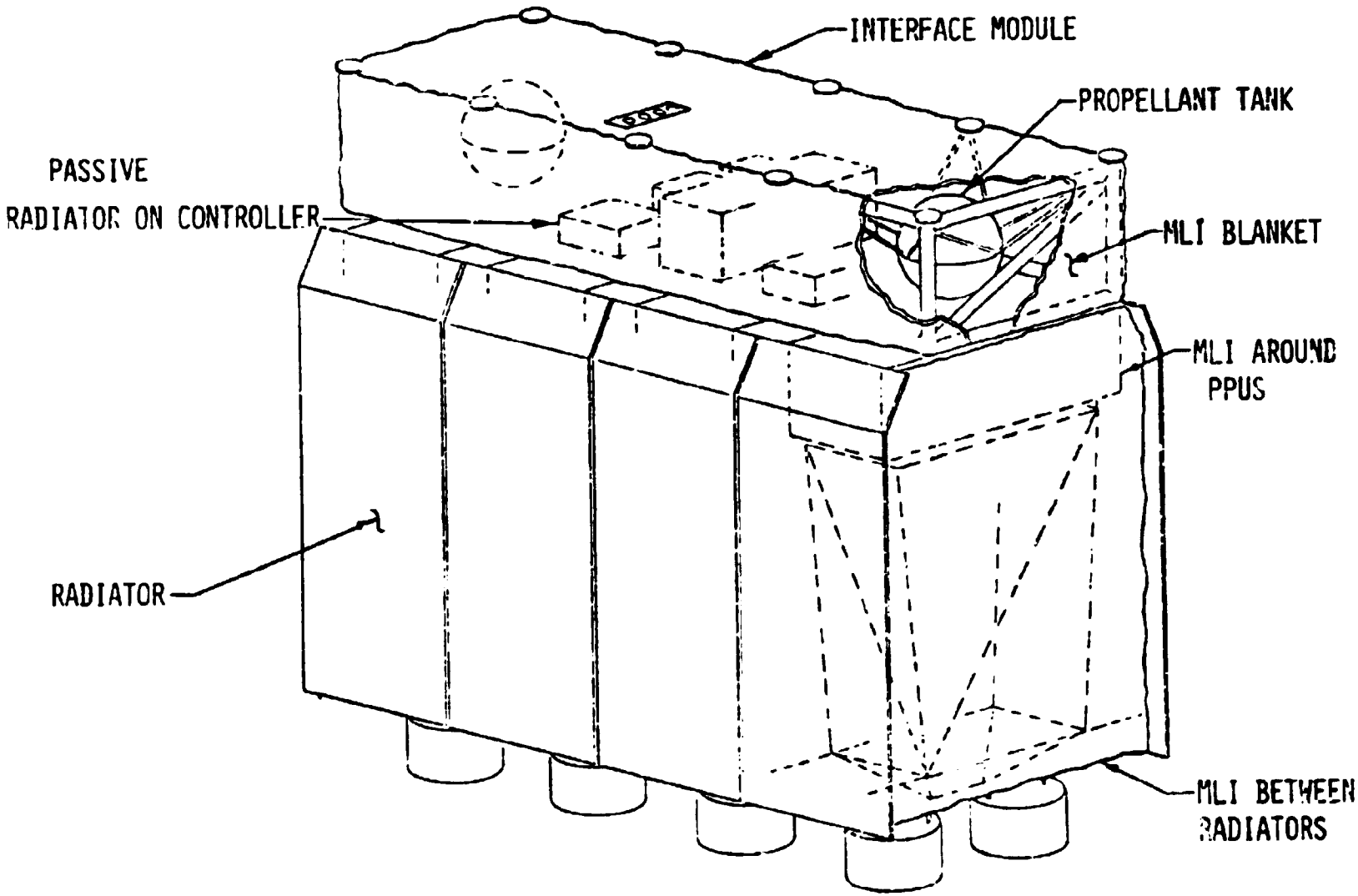
INTERFACE MODULE
PROPELLANT TANK
PASSIVE
RADIATOR ON CONTROLLER
MLI BLANKET
MLI AROUND
PPUS
RADIATOR
MLI BETWEEN
RADIATORS

NASA TM-79191		
30-CENTIMETER ION THRUST SUBSYSTEM DESIGN MANUAL		June 1979
		E-000
National Aeronautics and Space Administration Lewis Research Center Cleveland, Ohio 44135		
National Aeronautics and Space Administration Washington, D.C. 20546		Technical Memorandum

The principal characteristics of the 30-centimeter ion propulsion thrust subsystem technology that has been developed to satisfy the propulsion needs of future planetary and Earth orbital missions are described. The thrust subsystem defined herein was used to focus the thrust subsystem technology program performed for the NASA Office of Aeronautics and Space Technology by the NASA Lewis Research Center. Functional requirements and descriptions, interface and performance requirements, and physical characteristics of the hardware are described at the thrust subsystem, BIMOD engine system, and component level.

Solar electric propulsion Thrust subsystem BIMOD engine system Low thrust	Unclassified - unlimited STAR Category 20

Unclassified	Unclassified		